NATIONAL SYNCHROTRON LIGHT SOURCE

ACTIVITY REPORT 2006

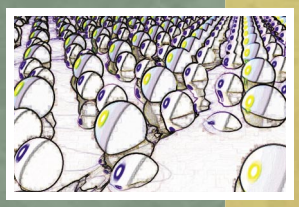

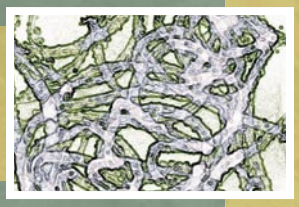

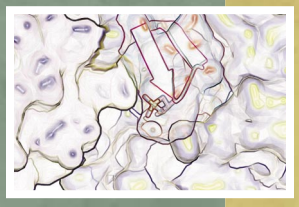

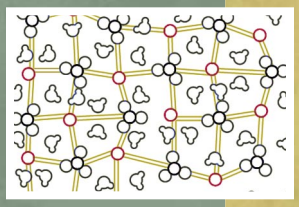

BNL-77450-2006
UC400
(General Energy Research)

Cover Images

1	*from Feature Highlight: "Liquid Alloy Shows Solid-Like Crystal Structure at Surface," page 2-24*
2	*from Science Highlight: "Characterizing the Surfaces of Carbon Nanotube Fuel Cell Catalysts," page 2-30*
3	*from Feature Highlight: "Plant Studies Reveal How, Where Seeds Store Iron," page 2-10*
4	*from Science Highlight: "Structural Insight into Antibiotic Fosfomycin Biosynthesis by a Mononuclear Iron Enzyme," page 2-68*
5	*from Science Highlight: "Effect of Te Precipitates on the Performance of CdZnTe (CZT) Detectors" page 2-94*
6	*from Feature Highlight: "Modeling Mineral Formation with X-rays," page 2-8*

Printed in the United States of America
Available from
National Technical Information Service
U.S. Department of Commerce
5285 Port Royal Road
Springfield, VA 22161

NATIONAL SYNCHROTRON LIGHT SOURCE
2006 ACTIVITY REPORT

Lisa M. Miller

managing editor

Kendra J. Snyder

science editor

Nancye A. Wright & Stephen A. Giordano

design & layout

The National Synchrotron Light Source Department is supported by the
Office of Basic Energy Sciences, United States Department of Energy, Washington, D.C.

Brookhaven National Laboratory, Brookhaven Science Associates, Inc., Upton, New York 11973
Under contract no. DE-AC02-98CH10886

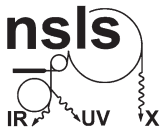

INTRODUCTION

SCIENCE HIGHLIGHTS

YEAR IN REVIEW

FACILITY REPORT

FACTS AND FIGURES

PUBLICATIONS

INTRODUCTION

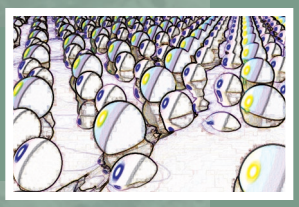

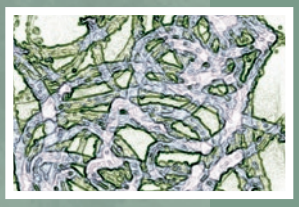

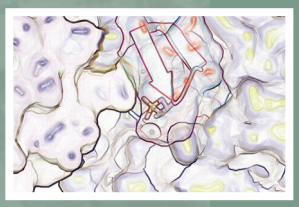

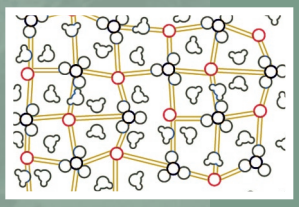

CHAIRMAN'S INTRODUCTION

Chi-Chang Kao
Chairman, National Synchrotron Light Source

As the NSLS continued its legacy of scientific excellence in 2006, I was honored to be named Chairman of the department after former Chair, Steve Dierker, stepped down to lead the development of NSLS-II. The NSLS is a very special place with a long and exemplary tradition of innovation in accelerator concepts and technology, as well as in the development of experimental techniques and applications of synchrotron radiation. Moreover, during the last quarter century, the NSLS has been one of the most widely used and productive scientific facilities in the world. The year 2006 was no exception, with a record-high 921 publications reported by our users and staff.

An impressive array of highlights is included in this Activity Report to illustrate this extraordinary productivity and its impact to science, technology, and society. For example, one user group investigated new materials for use in lithium-ion batteries, the most common type of battery found in portable electronics and the most promising type for hybrid cars. Another user group determined the atomic crystal structure and functional mechanism of an enzyme essential for eliminating unwanted, non-nutritional compounds such as drugs, industrial chemicals, and toxic compounds from the body. And in yet another interesting study, NSLS staff and users made improvements to microbeam radiation therapy, an experimental form of radiation therapy that has been under investigation for many years.

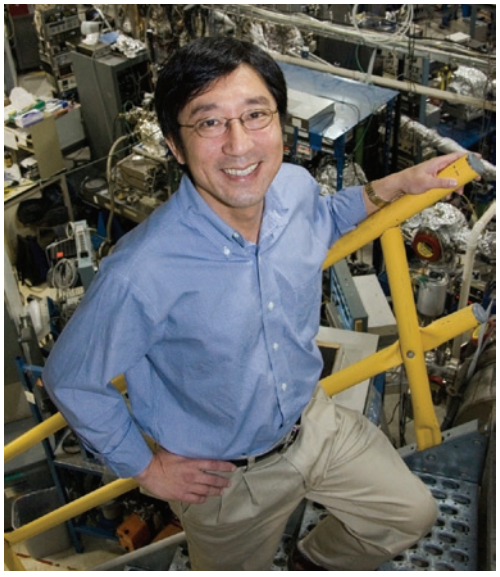

Chi-Chang Kao

As always, the success of these research projects depends on the performance of the facility. Thanks to the dedication and hard work of our staff, both storage rings were in top form again this year — reliability was 94.3 percent for the x-ray ring and 97 percent for the VUV-IR ring. In addition, we have made significant progress this year in improving machine performance and reliability, including klystron replacement, improving diagnostics in the injection system, conducting an orbit stability study, and commissioning the new X25 in-vacuum mini-gap undulator. Finally, to ensure the long-term reliability of the NSLS accelerator complex, Accelerator and Operation and Engineering Division staff were charged to assess the reliability risks and risk mitigation plans in preparation for an external review.

In the area of safety, I am very pleased that there were no reportable occurrences related to environmental, safety, or health issues in 2006. In addition, NSLS users and staff have worked more than 1,000 days without a lost-time injury, and counting. This is a remarkable record and we should all be proud of this accomplishment. But, we have to continue to be vigilant and make sure safety is integrated into everything that we do. A major safety initiative lunched this year was the implementation of an Electrical Equipment Inspection program at the NSLS. The goal of the program is to review and inspect all electrical equipment and installations to ensure they are free from electrical shock or fire.

Additionally, many beamline upgrade projects were initiated or completed this year. The most significant ones were the X25 beamline upgrade and the construction of the X9 small-angle x-ray scattering (SAXS) beamline. The X25 upgrade was critically important for the NSLS to meet the growing demand from the macromolecular crystallography user community for high-brightness beamlines, which are essential for tackling the most challenging scientific problems. X9 will be a new undulator-based beamline optimized to provide SAXS and grazing incidence SAXS capabilities for nano- and bioscience studies that require high flux and/or small beam. The beamline is a collaboration between the NSLS and Center for Functional Nanomaterials (CFN). In 2006, with the collaboration of the Case Center for Synchrotron Biosciences, the existing X9 beamlines were relocated to X3 to make room for the construction of the new X9 beamline.

In mid-May, the first joint NSLS-CFN Users' Meeting was carried out successfully, making way for close collaboration between the two facilities when the CFN opens next year. Progress on the NSLS-II also continues to press forward and we have begun to plan for the eventual transition to the new facility, which will provide x-rays more than 10,000 times brighter than those produced at the NSLS. Finally, with extensive input from the user community, NSLS staff, and Brookhaven research departments, we have developed a five-year strategic plan for the NSLS. The plan identifies a number of exciting scientific opportunities, improvements needed for better accelerator performance, and upgrades for beamlines, detectors, and infrastructure at the NSLS. We believe that this plan will keep scientific productivity up and grow new scientific communities at the NSLS, as well as allow us to smoothly transition the user scientific programs to the NSLS-II.

USERS' EXECUTIVE COMMITTEE REPORT

Chris Jacobsen
Stony Brook University

This past year has seen both challenges and fantastic new opportunities for the user community at the NSLS.

The fantastic new opportunities are clear and abundant. We now have a five-year strategic plan for new development and continued operation of the NSLS. The NSLS continues to be an extremely productive facility, and the UEC is delighted at how NSLS Chair Chi-Chang Kao has consulted widely within the user community to develop a five-year plan for strategic upgrades and continued operation of the facility. The NSLS-II project, led by Associate Lab Director Steve Dierker, has done very well in its Department of Energy (DOE) reviews and will hopefully soon receive Critical Decision-1 (CD-1) approval, which in DOE lingo gives a go-ahead to launch the detailed design of the facility.

We also held the first joint user meeting between the NSLS and Brookhaven's Center for Functional Nanomaterials (CFN), for which the building is near completion. The joint user meeting is an important step toward the close collaboration of the two facilities. The CFN, led by Emilio Mendez, promises to provide capabilities and research foci that are complementary to those at the NSLS.

Together, all of these developments give a clear path to an exciting future of synchrotron radiation research at Brookhaven!

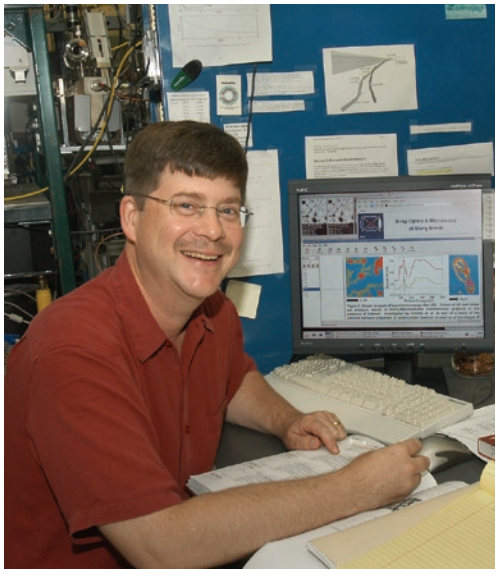

Chris Jacobsen

However, with opportunities come challenges! One of the largest of these faced in the past year involved congressional support for scientific research in general, and DOE user facilities in particular. As you likely know, Congress did not complete its usual budget process in 2006, with the exceptions of the departments of Defense and Homeland Security. This left science funding at the budget levels enacted in late 2005 for FY2006, and unfortunately, FY2006 was not a particularly memorable vintage for science support. The good news is that you, the user community, have spoken up with unprecedented vigor about this, and Congress appears to be listening. As we look at the FY2007 budget and the years to follow, we need to continue to educate our elected representatives about the benefits that are provided to our society and our economy by scientific investigation including research done at DOE user facilities like the NSLS.

We face another interesting challenge as the NSLS-II project progresses: the formation of scientific research teams associated with particular beamlines at the new facility. In early 2007, the final draft of the conceptual design report will be available, which will describe the projected capabilities of NSLS-II, and we can expect a workshop in mid-2007 to launch the process leading to letters of intent for beamlines. This process will include lots of discussion about access modes, as we seek ways to allow scientific and technical innovators from the user community to play significant roles at NSLS-II.

Let us rise to the challenges to fully realize the opportunities!

SCIENCE HIGHLIGHTS

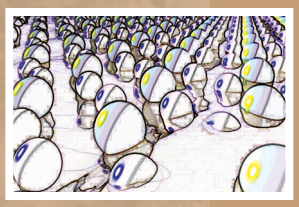

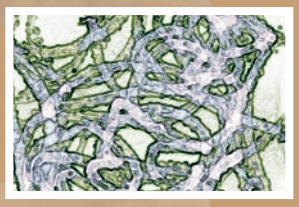

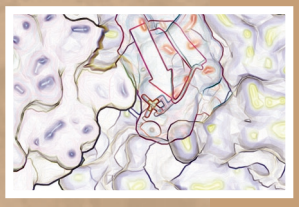

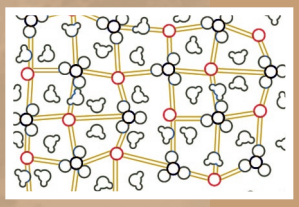

SCIENCE AT THE NSLS

Kendra Snyder
NSLS Science Writer

As the new science writer at the NSLS, I'm excited to introduce this year's Science Highlights and Feature Highlights sections.

Journalists are lifetime students; by 5 p.m. each day, they've become a sort of mini-expert in a topic that might have been completely foreign to them that morning. Being the NSLS science writer is no exception. Out of more than 800 articles published by NSLS users each year in peer-reviewed journals, about 50 are selected to appear on the NSLS homepage. I'm exposed to a number of those papers every month, and as a result, my knowledge of everything from nanoscience to condensed matter physics has greatly increased in the short time I've been here: I never thought I'd be writing about things like anisotropy, ferromagnetism, and biomineralization, let alone have those terms in my vocabulary.

Kendra Snyder

Yet, there's so much more out there. The most amazing part of this job is knowing that the highlights that appear on the following pages represent just a small fraction of the science performed at the NSLS in the chemical, material, environmental, physical, and life sciences. Keep that in mind as you read this year's Science Highlights – scientist-written summarized versions of published papers – and Feature Highlights, which are written by Brookhaven Lab science writers and targeted at a general audience.

Because I joined the NSLS in June 2006, I cannot take credit for all of the editing and writing involved in creating these sections. I would like to acknowledge Laura Mgrdichian, Lisa Miller, Karen McNulty Walsh, and Kay Cordtz for their work. And of course, thank you to all of the wonderful NSLS scientists and users who have welcomed me to this unique facility and helped me understand the even more unique work they accomplish.

I look forward to another great year of working with all of you.

SCIENCE HIGHLIGHTS

FEATURE HIGHLIGHTS

CHEMICAL SCIENCE

CONDENSED MATTER PHYSICS

GEOLOGY AND ENVIRONMENTAL SCIENCE

LIFE SCIENCE

MATERIALS SCIENCE

SOFT CONDENSED MATTER AND BIOPHYSICS

MODELING MINERAL FORMATION WITH X-RAYS

Some of the hardest and sturdiest materials aren't made in the factory; they're made inside the bodies of animals. Biominerals are commonly used for support and protection, forming in teeth, bones, and shells in animals ranging from humans to mollusks. The cells in an animal's body have special ways of controlling the sizes and shapes of these mineral compounds and incorporating organic materials into the mix, making many materials that are stronger, harder and more wear-resistant than rocks. The trick for scientists is to mimic these properties to repair bones and teeth and to find environmentally clean and strong materials for industrial uses. At the NSLS, a group of researchers from Brookhaven and the University of Florida are working toward that goal by studying the process of biomineralization.

"We're trying to understand how those minerals come to form," said NSLS physicist Elaine DiMasi. "They're literally as common as seashells on the beach, and the elements they're made from are very abundant, but synthetically, people have trouble making the particles small enough and getting control over the structure."

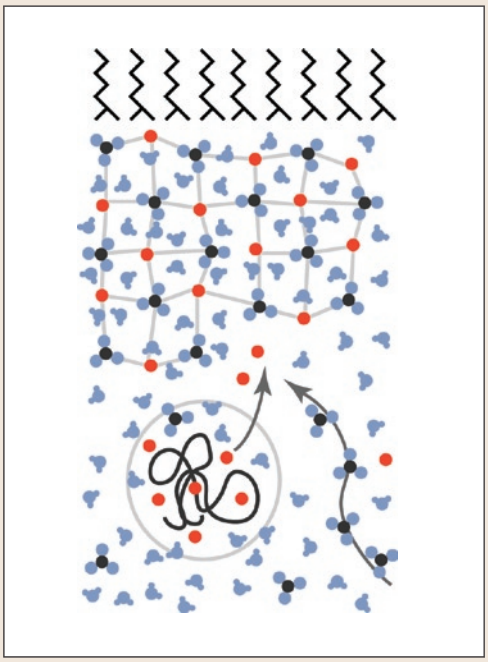

This image depicts the calcium carbonate biomineralization model studied by the research team. The black lines at the top represent the membrane, the network below it is the amorphous, hydrated mineral film and the squiggly black line in the circle is the PAA molecule with its collection of calcium cations (red balls), which get released by the film. The three-atom carbonates (black and blue balls) diffuse from the bottom right. Together, the calcium and carbonate form the mineral film.

The researchers studied the biomineralization of calcium carbonate by creating a model system with an organic layer to mimic a cell boundary and a liquid designed to precipitate the mineral. Using this model, which was set up in a water trough, the team focused on three factors that control calcium carbonate growth: the presence of magnesium, the presence of polyacrylic acid (PAA), and the escape rate of carbon dioxide.

These three factors were studied at beamline X22B using a special spectrometer that sends x-rays in at an angle and reflects them from different layers in the model system. This allowed the researchers to measure the thickness of the minerals as a function of time while alternating which controls are kept constant.

"We tried to clarify whether these things are all generically the same kind of calcium carbonate inhibitor, or whether they act differently from one another," DiMasi said. "What we discovered was each has a unique effect that we could differentiate quite clearly."

For example, the researchers found that PAA, which mimics the presence of proteins, stabilizes the calcium carbonate in the amorphous stage, a disordered phase that is incorporated with water. The amount of time before this calcium carbonate film thins out and dissolves is longest with large amounts of PAA and shortest when there's a small amount of the polymer in the system.

Another controlling factor, the carbon dioxide escape rate, was studied by altering the depth of the tray containing the model system. Carbon dioxide will diffuse from the system much more quickly with a shallow tray than a deeper one. The team found that this diffusion rate was the variable that controls mineral growth rate.

The final factor, the presence of magnesium, wasn't found to change the rate of growth as some expected. Instead, its presence causes a delay, in when the calcium carbonate film starts to grow.

Using what they discovered about these three factors, the researchers put together a model of the early formation of calcium carbonate. It goes something like this: PAA has many negative charges associated with it, which pull in positive calcium ions required for the amorphous film to form. Because the calcium is already collected and being held by PAA, the rate of growth depends on the amount of available carbonate, which is produced by the diffusion of carbon dioxide. The more shallow the tray, the quicker carbonate is available and the faster the calcium carbonate amorphous film

grows. The magnesium also is attracted to PAA because of its positive charge, and the ion fights against calcium for spots on the polymer. Calcium ultimately binds more strongly to PAA; however, the presence of magnesium in the system delays formation of the film as the two ions compete.

“Previously people thought that magnesium and PAA were both inhibitors, that they both stop calcite from crystallizing from the amporphous precursor phase,” DiMasi said. “Our results show that they do different things and this model shows why. PAA is not just defeating calcite crystal formation; it’s actually stabilizing the amorphous phase by adding cations. And the magnesium is not interfering with crystal formation; it’s interfering with this polymer-prepping action that happens.”

The time-resolved measurements, and small size of the biomineralization system itself, make this a unique study, DiMasi said.

“A lot of people in the field grow crystals and study them in great detail, but we’re looking at the stages before that,” DiMasi said. “Our film might be only 20 nanometers thick while we’re measuring it, and dissolve within 10 hours. If you gave our recipe to someone who needed to grow crystals big enough to look in a microscope, they would probably declare it a failure and rinse it down the sink.”

The group’s results were published in the July 27, 2006 edition of *Physical Review Letters*.

The research was funded by the U.S. Department of Energy, the National Science Foundation, and the National Institutes of Health.

For more information, see: E. DiMasi, S. Kwak, F. Amos, M. Olszta, D. Lush, and L. Gower, "Complementary Control by Additivies of the Kinetics of Amorphous $CaCO_3$ Mineralization at an Organic Interface: In-Situ Synchrotron X-ray Observations," Phys. Rev. Lett., ***97****, 045503 (2006).*

— Kendra Snyder

PLANT STUDIES REVEAL HOW, WHERE SEEDS STORE IRON

Dartmouth College issued the following press release detailing the storage of iron in plant seeds. These findings, which could lead to ways to prevent iron deficiency and malnutrition, were discovered at the National Synchrotron Light Source. At beamline X26A, researchers used fluorescence tomography, an x-ray imaging technique that allows scientists to "see" the distribution of elements inside the seeds without destroying them.

Dartmouth biologists are leading a research team

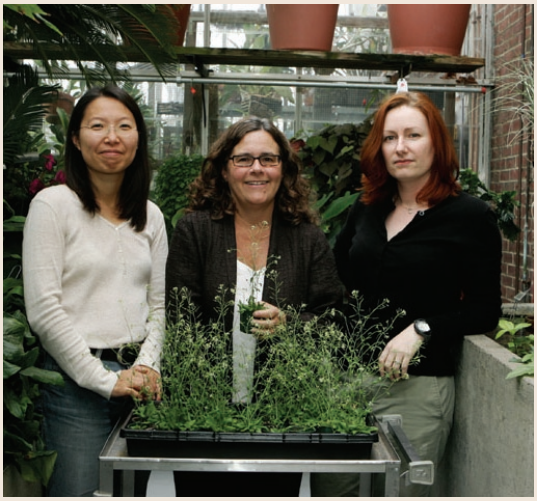

Dartmouth researchers Sun A. Kim, Mary Lou Guerinot, and Tracy Punshon (photo credit, Joseph Mehling, Dartmouth College).

that has learned where and how some plant seeds store iron, a valuable discovery for scientists working to improve the iron content of plants. This research helps address the worldwide issue of iron deficiency and malnutrition. Their findings were published in the November 24, 2006 edition of the journal *Science*.

The team found that iron is stored in the developing vascular system of the seed of Arabidopsis, a model plant used in research; in particular, iron is stored in the vacuole, a plant cell's central storage site. The researchers also learned that this localization is dependent on a protein called VIT1, shown to transport iron into the vacuole.

Dartmouth Professor of Biological Sciences Mary Lou Guerinot, the principal investigator on the study, says, "Iron deficiency is the most common human nutritional disorder in the world today, afflicting more than three billion people worldwide. Most of these people rely on plants for their dietary iron. However, plants are not high in iron, and the limited availability of iron in the soil can limit plant growth. Our study certainly suggests that iron storage in the vacuole is a promising and, before now, largely unexplored target for increasing the iron content of seeds. Such nutrient-rich seeds would benefit both human health and agricultural productivity."

The researchers combined traditional mutant analysis (turning on and off the VIT1 protein) with a powerful x-ray imaging technique to create a map of where iron is localized in the seed. Guerinot was surprised by the finding because most studies on iron storage focus on the protein ferritin. This paper reveals how important it is to look beyond ferritin to understand how iron is stored by plants. The researchers say their study suggests that the stored iron in the vacuole is an important source of iron for developing seedlings. Seedlings that do not express the VIT1 protein grow poorly when iron is limited.

"We have demonstrated the usefulness of synchrotron x-ray fluorescence microtomography to look inside a seed," says Guerinot. "This technique is noninvasive and requires no sample preparation. We think our work will open the way for many more biologists to use this technique to examine the spatial distribution of metals in samples of interest." The imaging was carried out at the Department of Energy's National Synchrotron Light Source at Brookhaven National Laboratory.

Other authors on the paper include Sun A. Kim and Tracy Punshon, both postdoctoral fellows at Dartmouth, Antonio Lanzirotti of the University of

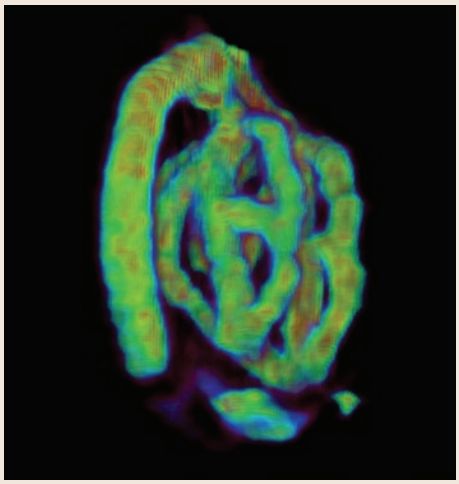

Rendered three-dimensional tomographic reconstruction of the iron (Fe) fluorescence from a wild type Arabidopsis thaliana seed (approx. 100 µm wide seed). In this seed, the tomographic reconstruction demonstrates that Fe is localized around the embryonic provasculature of the radicle and cotyledons. Using fluorescence microtomography, the research team demonstrated the vital role the gene vacuolar iron transporter 1 serves in controlling Fe homeostasis in plants.

Chicago, Liangtao Li and Jerry Kaplan from the University of Utah School of Medicine, José Alonso with North Carolina State University, and Joseph Ecker with the Salk Institute for Biological Studies.

This research was supported by grants from the National Science Foundation and the National Institutes of Health. Tracy Punshon was supported by a training fellowship provided by the National Institute of Environmental Health Sciences Superfund Basic Research Program Project through Dartmouth's Center for Environmental Health Sciences.

*For more information, see: S.A. Kim, T. Punshon, A. Lanzirotti, L. Li, J.M. Alonso, J.R. Ecker, J. Kaplan, and M.L. Guerinot, "Localization of Iron in Arabidopsis Seed Requires the Vacuolar Membrane Transporter VIT1," Science, **314**, 1295-1298 (2006).*

— Sue Knapp, Dartmouth University

A 'FERROELECTRIC' MATERIAL REVEALS UNEXPECTED, INTRIGUING BEHAVIOR

In electronics-based technologies, metal-oxide compounds known as “relaxor ferroelectrics” often make up key circuit components due to their unique electrical behavior. They are good insulators and can sustain large electric fields, making them excellent at storing electric charge. They can also turn a mechanical force, like squeezing, into electrical energy.

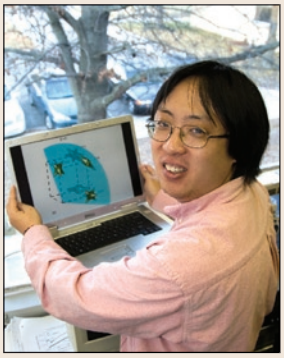

Guangyong Xu

Scientists at the Brookhaven National Laboratory investigated the poorly understood origin of these abilities — with surprising results. Their work, which may lead to new ways to use relaxor ferroelectric materials in electronic devices, was published in the February 2006 edition of *Nature Materials*.

The group studied a characteristic feature of relaxor ferroelectrics — billionth-of-a-meter-sized subregions that each carry a tiny electric field. These “polar nanoregions” (PNRs), embedded within the material’s crystal lattice, are thought to produce the materials’ intriguing electrical traits, but little is known about them. The Brookhaven researchers studied PNRs by subjecting a relaxor ferroelectric sample to a strong external electric field.

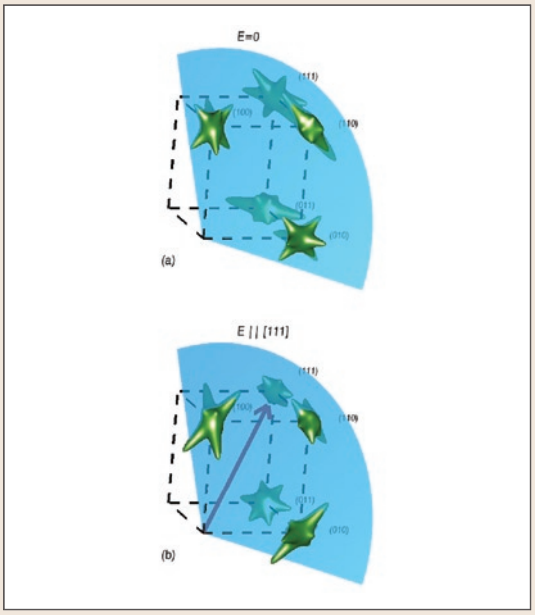

This sketch shows the distribution of three-dimensional x-ray scattering intensity patterns (green) in a relaxor ferroelectric material. This scattering pattern is due to the material’s polar nanoregions. The scattering was measured with an applied electric field (E) of (a) E = 0 and (b) E = 20 kV/cm, which is applied along the [111] direction. This external electric field causes the scattering pattern to redistribute, which is due to the redistribution of the polar nanoregions.

“We noticed that the weak PNR fields rotated spatially but resisted lining up with the powerful outside field,” said the study’s lead researcher, Brookhaven Lab physicist Guangyong Xu. “This is very surprising and extremely interesting, as we know of no other material in which this has been observed. This finding could lead to new uses for these materials, such as extremely sensitive transducer devices that convert mechanical or light energy into electrical energy.”

The group used NSLS beamline X17B1 to subject their sample to high-energy x-rays. They then analyzed the scattering patterns made as the x-rays passed through the sample, both before and after applying the electric field.

In the “before” case, the x-rays scattered about in many different directions, indicating that the PNR fields were oriented in many different ways. After applying the external field, the researchers expected a significant change in the x-ray patterns, showing that the PNR fields — somewhat like magnetic metal filings in a magnetic field — had neatly aligned with it. But the patterns changed in a different way than predicted. They indicated, instead, that the PNR fields preferred to line up *perpendicular* to the external field, even as the surrounding atomic lattice lined up along it.

“The reasons behind this behavior are not yet clear, but we plan to conduct further research that may help shed light on this interesting and rare situation,” said Xu. “For example, it is possible that an even stronger external field could suppress the PNRs, or that a different relaxor ferroelectric material could display different behavior.”

This work was funded by the Office of Basic Energy Sciences within the U.S. Department of Energy’s Office of Science, the U.S. Office of Naval Research, and the Natural Science and Research Council of Canada.

*For more information, see: G. Xu, Z. Zhong, Y. Bing, Z. Ye, and G. Shirane, "Electric-Field-Induced Redistribution of Polar Nano-Regions in a Relaxor Ferroelectric," Nat. Mater., **5**, 134-140 (2006).*

— Laura Mgrdichian

STRUCTURE OF AN E. COLI MEMBRANE PROTEIN

At the NSLS, a team of scientists from the University of Massachusetts Medical School and the University of Virginia have determined the molecular structure of a protein found in the outer membrane of the E. coli bacteria. Their work helps to explain how this protein is involved in the overall function of E. coli and may one day help in the creation of vaccines against pathogenic E. coli strains. The paper was featured as the cover article in the March 17, 2006 edition of the *Journal of Biological Chemistry*.

Cover of the March 17, 2006 edition of the *Journal of Biological Chemistry*

The protein they studied, known as "OmpW," is a member of a family of small proteins that are situated within the cell membranes of certain bacteria. Membrane proteins have many functions. For example, they are involved in the cell's metabolic processes, provide structural stability, aid in cell-to-cell adhesion, or can protect the cell from outside stresses. Many are also channel-like transport proteins, allowing molecules and ions to enter and exit the cell. However, the lack of good structural data on the OmpW proteins has left scientists uncertain of their particular role.

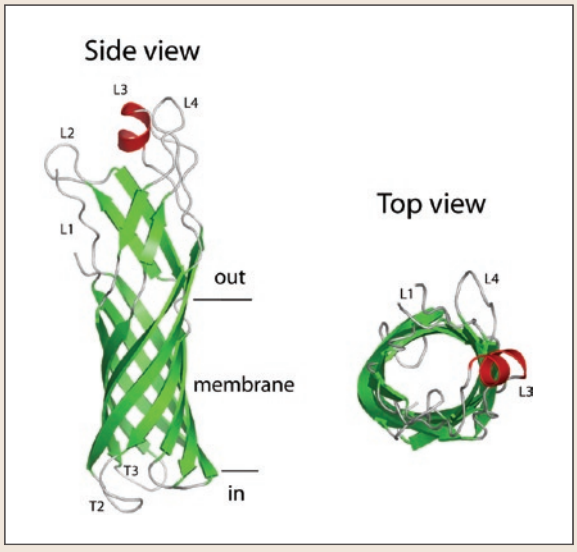

A side view and top view (from the outside of the cell) of the molecular backbone of OmpW, with the eight strands of the barrel shown in green and the loops (L1 to L4) connecting the strands in grey. The position of the membrane is indicated with horizontal lines.

"Previous crystal structures of proteins related to OmpW suggest that they have channels that are too narrow for them to function as transporters. However, our structure, along with other data, suggests that it can," said Bert van den Berg, a University of Massachusetts Medical School biologist involved in the study. "This helps us understand the role of OmpW with respect to the entire cell."

To obtain the structure, van den Berg and his colleagues worked at NSLS beamlines X25 and X6A. There, they aimed powerful x-ray beams at OmpW protein crystals and observed, using detectors and computers, how the x-rays were diffracted from the atoms in the samples. They then analyzed these diffraction patterns using computer software, which yielded a three-dimensional "snapshot" of the protein's molecular structure.

The structure shows that OmpW is a barrel-shaped protein formed by eight aligned molecular strands. The inside of the barrel forms a long and narrow channel, which is closed on one end. Interestingly, the channel is "hydrophobic," or water-repellent, suggesting that OmpW could form a channel for greasy, hydrophobic molecules.

To learn more about the protein's function, the scientists performed a series of "conductance experiments" on the protein. These tests, which are designed to determine if a membrane protein can form a channel for ions, revealed that OmpW does indeed form a channel. However, which types of ions and molecules are transported by OmpW in the bacterial cell is still unclear.

In future work, van den Berg and his colleagues plan to investigate which greasy molecules, referred to as substrates, are transported by OmpW proteins, and they hope to gain a better understanding as to how the transport process occurs.

For more information, see: H. Hong, D. Patel, L. Tamm, and B. van den Berg, "The Outer Membrane Protein OmpW Forms an Eight-Stranded β-Barrel with a Hydrophobic Channel," J. Biol. Chem., ***281****, 7568-7577 (2006).*

— Laura Mgrdichian

MEASURING SYNTHESIS INTERMEDIATES FOR BETTER MATERIALS

Involved in about 90 percent of all chemical processes and the creation of about 60 percent of the chemical products available on the market, catalysis is vital to American industries. Catalysis, the acceleration of a chemical reaction by means of a separate substance (the catalyst), benefits fields such as chemistry, petroleum production, environmental protection, pharmaceuticals, bioengineering, and the development of fuel cells. New

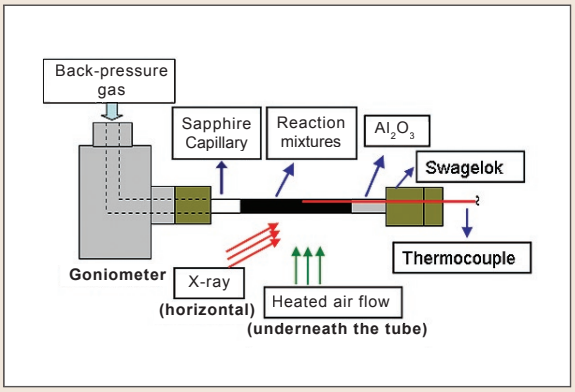

Schematic diagram of the tube reactor.

information about catalysis can lead to better and more efficient materials and processes such as oil refining and reducing harmful emissions in motor vehicles. But while catalysis might sound like it's all about the end product, Brookhaven National Laboratory and University of Connecticut researchers are focused on what happens in between.

The properties and activity of materials can vary significantly with different synthesis methods or at different conditions, such as temperature and time. Using x-rays at beamline X7B of the National Synchrotron Light Source, BNL and UConn researchers measured the changes catalyst materials go through during synthesis, showing that kinetic and mechanistic information about certain materials could allow for better synthesis control. "By understanding the intermediate, we can define the conditions whereby you get the product you want," said BNL chemist Jon Hanson, part of the group that performed the research.

The traditional way of making these observations is done outside of the reaction environment, termed ex-situ. During this method, target materials are separated from the reaction systems after different reaction times and then washed and dried before structural analysis. However, this process can alter materials from their original state in the reaction systems.

"You're probably going to change the material when you measure it," Hanson said. "You can't observe the characteristics under processed conditions."

Thanks to high-flux x-rays, scientists can avoid that alteration with a method called in-situ synchrotron x-ray diffraction. This process provides a real-time look at the phase transformations involved in the synthesis or catalysis without removing them from the reaction environment. At the NSLS, Hanson, along with Xiong-Fei Shen from Steven Suib's research group at the University of Connecticut used this mode to study structural changes during the synthesis of manganese oxide octahedral molecular sieves, a group of materials that have uses ranging from catalysts to gas sensors.

To find out details about manganese oxide synthesis, a different type of in-situ procedure was used. The majority of in-situ studies use the targeted material in a solid or gel form. BNL and UConn researchers, however, used hydrothermal synthesis, in which the material is in a heterogeneous liquid-solid form. Researchers heated a slurry of dried birnessite, a layered-structure manganese oxide, with HNO_3 solution. They then "watched" the effects of different temperatures on the mixture through x-ray diffraction and determined the conditions needed to obtain different structures of the compound. For example, after heating the mixture

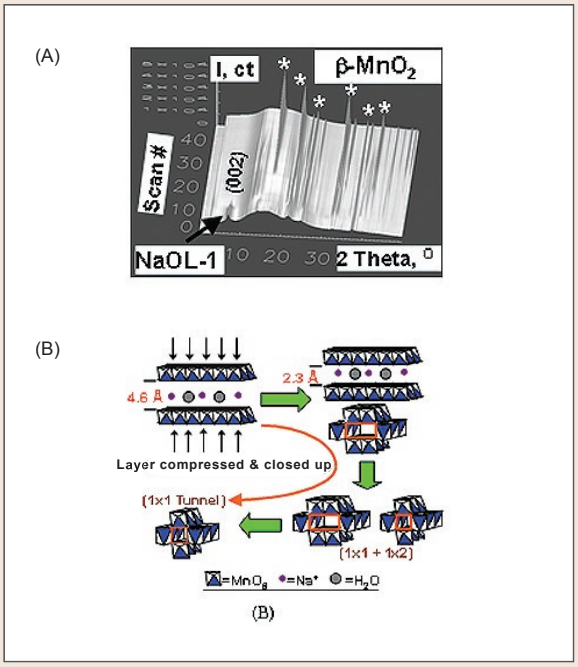

(A) In-Situ synchrotron XRD patterns for synthesis of a β-MnO_2 (1×1 tunnel structure) by hydrothermal treatment of a layered structure manganese oxide with 1 M HNO_3. The system was heated from 25 to 180 °C at 6.2 °C /min, and held at 180 °C. XRD patterns were collected continuously with 5 min/pattern. (B) Schematic to show transformation from layered structures to the final 1×1 tunnel structure.

for 15 minutes at 180 °C, a 1 x 2 tunnel structure of manganese oxide starts to form. Similar observations were performed with KOMS2, for which scientists determined the conditions needed to produce desired surface areas. Knowing basic characteristics, such as structure and surface area, as materials are synthesized can provide better control or “tuning” to get the catalytic properties scientists and industries want, Hanson said.

The results of their work were published in the April 12, 2006 edition of the *Journal of the American Chemical Society*. Other scientists involved in this research include Yun-Shuang Ding, and Mark Aindow (University of Connecticut). Funding was provided by the Office of Basic Energy Sciences within the U.S. Department of Energy’s Office of Science.

*For more information, see: X. Shen, Y. Ding, J. Hanson, M. Aindow, and S. Suib, "In Situ Synthesis of Mixed-Valent Manganese Oxide Nanocrystals: An In Situ Synchrotron X-ray Diffraction Study," J. Am. Chem. Soc., **128**, 4570 (2006).*

— Kendra Snyder

NEW X-RAY DELIVERY METHOD COULD IMPROVE RADIATION THERAPY

Researchers at Brookhaven National Laboratory and colleagues at Stony Brook University, the IRCCS NEUROMED Medical Center in Italy, and Georgetown University say improvements they have made to an experimental form of radiation therapy that has been under investigation for many years could make the technique more effective and eventually allow its use in hospitals. Results on the improved method, which was tested in rats, were published in the June 20, 2006 edition of the *Proceedings of the National Academy of Sciences*.

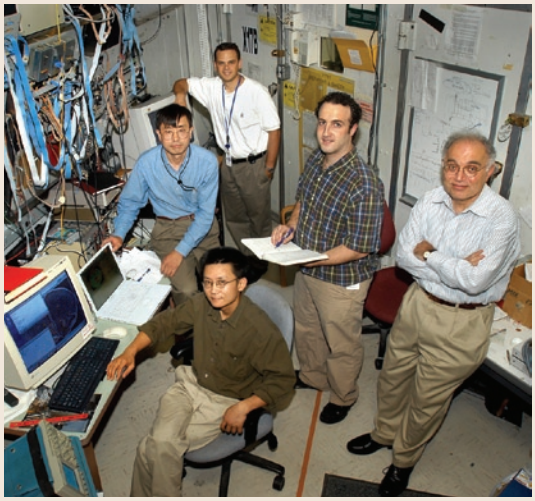

Authors (sitting) Zhong Zhong; (standing, from left) Ruiliang Wang, David Anschel, Jeremy Welwart, and Avraham Dilmanian

The technique, microbeam radiation therapy (MRT), previously used a high-intensity synchrotron x-ray source such as a superconducting wiggler at the NSLS to produce parallel arrays of very thin (25 to 90 micrometers) planar x-ray beams (picture the parallel panels of window blinds in the open position) instead of the unsegmented (solid), broad beams used in conventional radiation treatment. Previous studies conducted at Brookhaven and at the European Synchrotron Radiation Facility (ESRF) in Grenoble, France, demonstrated MRT's ability to control malignant tumors in animals with high radiation doses while subjecting adjacent normal tissue to little collateral damage.

But the technique has limitations. For one thing, only certain synchrotrons can generate its very thin beams at adequate intensity, and such facilities are available at only a few research centers around the world.

"The new development seeks a way out of this situation," explained Brookhaven scientist Avraham Dilmanian, lead author of the new study. In this paper, the scientists report results that demonstrate the potential efficacy of significantly thicker microbeams, as well as a way to "interlace" the beams within a well-defined "target" inside the subject to increase their killing potential there, while retaining the technique's hallmark feature of sparing healthy tissue outside that target.

First, using NSLS beamline X17B1, researchers exposed the spinal cords and brains of healthy rats to thicker (0.27 to 0.68 millimeter) microbeams at high doses of radiation and monitored the animals for signs of tissue damage. After seven months, animals exposed to beams as thick as 0.68 millimeter showed no or little damage to the nervous system.

"This demonstrates that the healthy-tissue-sparing nature of the technique stays strong at a beam thickness that is within a range that could be produced by specialized x-ray tubes of extremely high voltage and current," Dilmanian said. Such x-ray sources may become available sometime in the future and may allow the implementation of the method in hospitals.

Next, the scientists demonstrated the ability to "interlace" two parallel arrays of the thicker microbeams at a 90-degree angle to form a solid beam at a small target volume in the rats' brains, and measured the effects of varying doses of radiation on the targeted tissue volume and the surrounding tissue using magnetic resonance imaging (MRI) scans.

For interlacing, the gaps between the beams in each array were chosen to be the same as the thickness of each beam, so the beams from one array would fill the gaps in the other to produce the equivalent of an unsegmented beam in the target volume only.

"In this way we are effectively delivering an unsegmented broad beam type of dose to just the target region — which could be a tumor, or a non-tumerous target we want to ablate — while exposing the surrounding tissue to segmented radiation from which it can recover," Dilmanian said.

The MRI scans showed that at a particular dose of radiation, the new configuration could produce major damage to the target volume but virtually no damage beyond the target range. "The dose of radiation delivered to the target volume would have been enough to ablate a malignant tumor," Dilmanian said.

"These results show that thick microbeams generated by special x-ray tubes in hospitals could eventually be used to destroy selective targets while sparing healthy tissue," Dilmanian said.

Said collaborator Eliot Rosen, a radiation oncologist at Lombardi Comprehensive Cancer Center, Georgetown University, “This form of microbeam radiation therapy could improve the treatment of many forms of cancer now treated with radiation, because it can deliver a more lethal dose to the tumor while minimizing damage to surrounding healthy tissue. It may also extend the use of radiation to cases where it is now used only judiciously, such as brain cancer in patients under three years of age, because of the high sensitivity of young brain tissue to radiation.”

And according to collaborators David Anschel, a neurologist at Stony Brook University and Brookhaven Lab, and Pantaleo Romanelli, a neurosurgeon from NEUROMED Medical Center, the technique may also have applications in treating a wide range of benign and malignant brain tumors and other functional brain disorders such as epilepsy and Parkinson’s disease.

Background on MRT

MRT research was initiated by retired Brookhaven scientist Daniel Slatkin, the late Per Spanne, also from Brookhaven, Dilmanian, and others in the early 1990s at Brookhaven’s NSLS. Since the mid-1990s, the method has been under ongoing investigation also at ESRF.

It is not clear why high dose MRT is effective at killing tumor tissue while sparing healthy tissue. The researchers hypothesize that the normal tissue repairs itself, in part, as a result of the survival between the microbeams of the microvasculature’s angiogenic cells. This effect seems to occur more successfully in the normal tissue than in tumors, although other factors also seem to be involved.

Neither the original nor the improved MRT technique has been tested in humans.

The MRT research program at Brookhaven was funded in the past by Brookhaven’s Laboratory Directed Research and Development program, the Children’s Brain Tumor Foundation, the Office of Biological and Environmental Research within the U.S. Department of Energy’s Office of Science, and by the National Institutes of Health. The studies were carried out at the NSLS, which is supported by the Office of Basic Energy Sciences within DOE’s Office of Science.

*For more information, see: F. Dilimanian, Z. Zhong, T. Bacarian, H. Benveniste, P. Romanelli, R. Wang, J. Welwart, T. Yuasa, E. Rosen, and D. Anschel, "Interlaced X-ray Microplanar Beams: A Radiosurgery Approach with Clinical Potential," Proc. Natl. Acad. Sci. USA, **103**, 9709-9714 (2006).*

— Karen McNulty Walsh

THE UNUSUAL INSULATING PROPERTIES OF A SUPERCONDUCTOR

Since their discovery, high-temperature superconductors, a class of remarkable materials that conduct electricity with almost zero resistance, have perplexed scientists. Despite many, many studies, how these materials do what they do is still not well understood. At the NSLS, scientists have discovered a perhaps odd, yet important clue to the puzzle — that a common high-temperature superconductor actually has distinct *insulating* properties.

The superconductor is known as "LBCO," named for the elements it contains: lanthanum, barium, copper, and oxygen. LBCO is widely studied and, despite all there is yet to learn, researchers have learned some important things about it. For example, the barium atoms act as the material's sole electric carriers by introducing positively charged vacancies, called "holes," that electrons can jump to. Changing the amount of barium in LBCO thus changes its superconducting behavior. At a certain critical amount of barium — oddly enough — the superconductivity of LBCO disappears.

This disappearance of the superconductivity coincides with the formation of ribbon-like magnetic regions in the material, known as "stripes." Stripes were discovered by Brookhaven Lab physicist John Tranquada in 1995.

"What we were able to show is that the holes in LBCO are sandwiched between these magnetic stripes, forming ribbons of electric charge," said Abbamonte. "Significantly, we also found that the magnetic regions have insulating properties. Therefore, the material as a whole is neither a metal nor an insulator, since it retains characteristics of both."

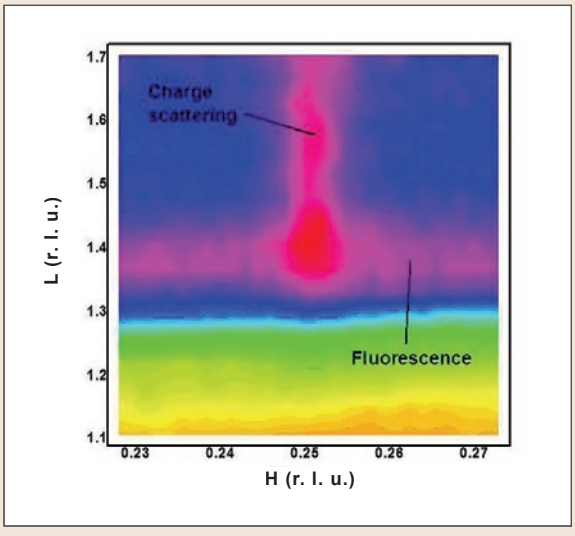

A "reciprocal space map" representation of the stripes in the copper-oxide layers of LBCO. "H" and "L" are measures of how often the ribbon-like stripes "wave." H corresponds to the a direction, and L corresponds to the c direction. Their reciprocals, 1/H and 1/L, are a measure of the stripes' wavelength. The red and pink vertical streak at H = 0.25 indicates that the stripes have a wavelength of four lattice parameters and are stacked along the c direction.

These findings are the result of work performed at NSLS beamline X1B, where the scientists studied LBCO using an x-ray technique called "resonant soft x-ray scattering." They aimed a beam of x-rays at an LBCO sample and used a detector to measure how the x-rays reflected away from the material. They then analyzed these reflections to reveal information about LBCO's electronic structure.

The results of this study are important because they support the theory that stripes are in some way related to superconductivity in high-temperature superconductors.

"Our results seem to support the stripe description of high-temperature superconductors. This is exciting, since it could mean that the scientific community may be very close to truly understanding how these materials perform," said Abbamonte.

The research was published in the December 2005 edition of *Nature Physics*. The paper's co-authors are Andrivo Rusydi (University of Hamburg), Serban Smadici (BNL/University of Illinois), Genda Gu (BNL), George Sawatzky (University of British Columbia and University of Groningen), and D.L. Feng (Fudan University). The work was supported by the U.S. Department of Energy, the Dutch Science Foundation, and the Netherlands Organization for Fundamental Research on Matter.

*For more information, see: P. Abbamonte, A. Rusydi, S. Smadici, G. Gu, G. Sawatzky, and D. Feng, "Spatially Modulated 'Mottness' in $La_{2-x}Ba_xCuO_4$," Nat. Phys., **1**, 155-158 (2005).*

— Laura Mgrdichian

AT THE NSLS, SCIENTISTS WORKING TOWARD BETTER BATTERIES

As more and more people rely on cell phones, laptop computers, personal organizers, and even hybrid electric-gas vehicles, scientists are working to develop rechargeable batteries that are ever smaller, cheaper, lighter, safer, and longer-lasting. At the NSLS, a collaboration of scientists is deeply involved in this effort. They are investigating a group of promising new materials for use in lithium-ion batteries, the most common type of battery found in portable electronics and the most promising type for hybrid cars.

Lithium-ion batteries work by shuttling positively charged lithium ions between the "cathode" (the battery's positive terminal) and "anode" (the negative terminal). As the battery is charged, lithium ions are forced out of the cathode and moved into to the anode through the "electrolyte," the solution inside the battery. When the battery is in use, the process reverses. The scientists are studying a group of new cathode compounds consisting of the elements lithium, cobalt, nickel, manganese, and oxygen.

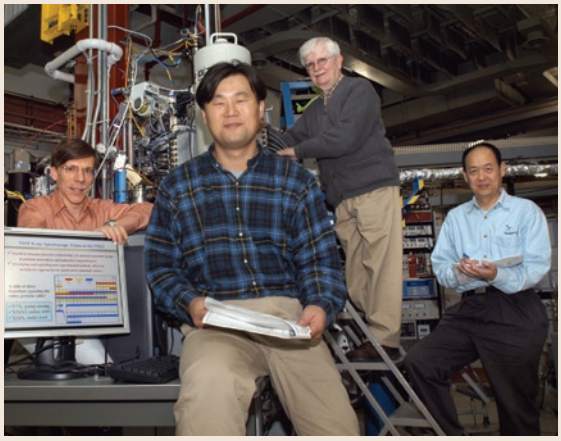

Authors (from left) Daniel Fischer, Won-Sub Yoon, James McBreen, and Xiao-Qing Yang

"Despite the wide use of lithium-ion batteries, there have been very few studies on exactly how the cathode material behaves in the charging process," said the study's lead researcher, Brookhaven chemist Won-Sub Yoon. "How are the oxygen atoms involved? What is the relationship between the oxygen atoms and the other metal atoms in the compound? To design a better cathode material, and thus a better battery, these questions must be answered. An in-depth understanding of these problems will provide a road map for the development of these new materials."

Using various x-ray techniques, Yoon and his colleagues have done just that. They discovered that as lithium ions leave the cathode material during the charging process, changes occur on the manganese and cobalt atoms that are quite different from those that occur on the nickel atoms. Specifically, the manganese and cobalt atoms do not lose electrons as the lithium ions are removed, while the nickel atoms, in contrast, do lose electrons. The group also learned more about how the cathode material compensates for the positive charge it loses as the lithium ions move to the anode. They found that empty regions with positive charge, called "holes," are created in the cathode. In addition, their x-ray data show just where these holes are located: within the electron orbitals of oxygen atoms that are bound to cobalt atoms.

Gathering these details on the cathode's electronic behavior is an important step in lithium-ion battery research. This new knowledge will help the material become a common component of a new series of better lithium-ion batteries. More detailed information on this research can be found in the group's scientific paper, which was published in the December 14, 2005 edition of the *Journal of the American Chemical Society*.

The other scientists involved in this research are Kyung Yoon Chung, Xiao-Qing Yang, and James McBreen (BNL Chemistry Department); Mahalingam Balasubramanian (Argonne National Laboratory); Clare Grey (Stony Brook University); and Daniel Fischer (National Institute of Standards and Technology).

*For more information, see: W. Yoon, M. Balasubramanian, K. Chung, X. Yang, J. McBreen, C. Grey, and D. Fischer, "Investigation of the Charge Compensation Mechanism on the Electrochemically Li-Ion Deintercalated $Li_{1-x}Co_{1/3}Ni_{1/3}Mn_{1/3}O_2$ Electrode System by Combination of Soft and Hard X-ray Absorption Spectroscopy," J. Am. Chem. Soc.. **127**, 17479-17487 (2005).*

— Laura Mgrdichian

STRUCTURE OF A MOLECULAR-SCALE CIRCUIT COMPONENT

Brookhaven National Laboratory researchers have determined the structure of an experimental, organic compound-based circuit component, called a "molecular electronic junction," that is only a few nanometers in dimension. This study may help scientists understand how the structure of molecular junctions relates to their performance and function and, in the longer term, may help incorporate these and other molecular-scale devices into a new generation of remarkably small electronics-based technologies.

The research is discussed in the February 21, 2006 edition of the *Proceedings of the National Academy of Sciences*.

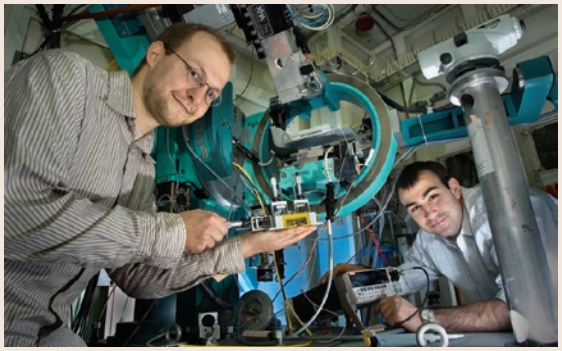

Authors (from left) Julian Baumert and Michael Lefenfeld

"Molecular electronics is a very exciting developing field, since these extremely small circuits, based on organic molecules rather than metal, have a potentially greater circuit density than conventional silicon-based technology. This means that more circuits could fit on one circuit board, leading to electronic devices that are much smaller than those currently produced," said one of the study's lead scientists, Brookhaven physicist Julian Baumert. "We're interested in the structure of the junction — how the molecules are oriented and packed together — because it is linked to the function and performance of the circuit."

In conventional circuits, junctions are commonly made of two different types of silicon that, when layered together, allow electric current to flow in one direction only. Here, the junction under study consists of two very thin layers of two different organic compounds — "alkyl-thiol" and "alkyl-silane." They are sandwiched on one side by a layer of solid silicon and on the other side by a layer of liquid mercury, which serve as electrodes. Alkyl-thiol and alkyl-silane molecules have simple structures and the potential to be good insulating materials.

The scientists created the junctions by filling a small container with a drop of liquid mercury and depositing a very small amount of alkyl-thiol onto the mercury surface. They then topped the alkyl-thiol layer with an alkyl-silane-coated silicon wafer. This method yielded a junction with just a five-nanometer-thick gap between the two electrodes.

"This technique is not limited to simple alkane molecules," said Columbia University graduate student Michael Lefenfeld, the study's second lead scientist. "Many other types of organic molecules could be used, such as semi-conducting and conducting molecules. These materials also have a structure and packing density that plays a large role in their electrical performance."

The research group studied the junction by aiming high-energy x-rays — energetic enough to penetrate the silicon wafer — at the junction from several incident angles and measured how the rays scattered off the organic molecules. Next, they attached electric contacts to the silicon and mercury electrodes and, for several different applied voltages, measured both the reflected x-ray signal and the electric current through the junction.

By analyzing the x-ray scattering data, the researchers discovered that the organic molecules are densely packed together, with most of the molecules positioned vertically. Further, the combination of the electric-current and x-ray measurements revealed that the current does not deform that structure, even when the applied voltage was very high. This implies that the molecular structure is quite stable.

"These are important details to know in order to fully understand the electronic properties of molecular-scale junctions," said Brookhaven physicist Benjamin Ocko, one of the paper's senior authors. "These investigation methods should be able to provide us with a better understanding of many other molecular junctions."

This research was supported by the Office of Basic Energy Sciences within the U.S. Department of Energy's Office of Science, the National Science Foundation, the New York State Office of Science, Technology, and Academic Research, and the German-Israeli Foundation.

*For more information, see: M. Lefenfeld, J. Baumert, E. Sloutskin, I. Kuzmenko, P. Pershan, M. Deutsch, C. Nuckolls, and B. Ocko, "Direct Structural Observation of a Molecular Junction by High-Energy X-ray Reflectometry," Proc. Natl. Acad. Sci. USA, **103**, 2541-2545 (2006).*

— Laura Mgrdichian

NANOPARTICLE ASSEMBLY ENTERS THE FAST LANE

The speed of nanoparticle assembly can be accelerated with the assistance of the molecule that carries life's genetic instructions, DNA, a team of researchers at Brookhaven National Laboratory recently found. Nanoparticles, particles with dimensions on the order of billionths of a meter, could potentially be used for more efficient energy generation and data storage, as well as improved methods for diagnosing and treating disease. Learning how to control and tailor the assembly of these miniscule particles into larger functional systems remains a major challenge for scientists. The Brookhaven results, published in the November 1, 2006 edition of the *Journal of the American Chemical Society*, are a step in that direction.

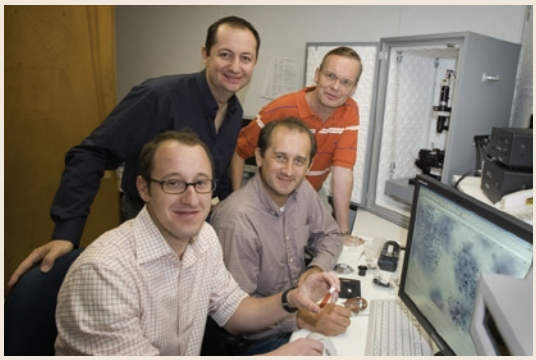

Authors standing (from left) Oleg Gang and Daniel van der Lelie sitting, (from left) Mathew Maye and Dmytro Nykypanchuk

"Understanding how to self-assemble these types of nanomaterials has applications in all areas of nanotechnology, from optics to electronics to magnetic materials," said the study's lead author Mathew Maye, a Brookhaven chemist. Maye is part of a team of interdisciplinary scientists from Brookhaven's new Center for Functional Nanomaterials (CFN) and the biology department. The researchers found a way to control the assembly of gold nanoparticles using rigid, double-stranded DNA. Their technique takes advantage of this molecule's natural tendency to pair up components called bases, known by the code letters A, T, G and C.

"In biology, DNA is mainly an informational material, while in nanoscience, DNA is an excellent structural material due to its natural ability to self-assemble according to well-specified programmable rules," said Oleg Gang, the Brookhaven physicist who leads the research team. "Using biological materials such as DNA, we are developing approaches to control the assembly of inorganic nano-objects. However, in order to really turn this attractive approach into nanotechnology, we have to understand the complexity of interaction in such hybrid systems."

The synthetic DNA used in the laboratory is capped onto individual gold nanoparticles and customized to recognize and bind to complementary DNA located on other particles. This process forms clusters, or aggregates, of gold particles.

"It's really by design," Maye said. "We can sit down with a piece of paper, write out a DNA sequence, and control how these nanoparticles will assemble."

One limitation to the assembly process is the use of single-stranded DNA, which can bend backward and attach to the particle's gold surface instead of binding with surrounding nanoparticles. This flexibility, along with the existence of multiple forms of single-stranded DNA, can greatly slow the assembly process. In the Brookhaven study, researchers introduced partially rigid, double-stranded DNA, which forces interacting linker segments of DNA to extend away from the gold surface, allowing for more efficient assembly.

"By using properties of DNA, we can increase assembly kinetics, or speed, by relatively simple means without a lot of synthetic steps," Maye said.

The research team probed the synthesized and assembled nanosystems with multiple imaging techniques, using beams of light and electrons as well as high-intensity x-rays at Brookhaven's National Synchrotron Light Source. The scientists look to further improve the controllability of the system, focusing next on the size of the nanoparticle clusters.

This research was funded by the Office of Basic Energy Sciences within the U.S. Department of Energy's Office of Science. The CFN at Brookhaven Lab is one of five Nanoscale Science Research Centers being constructed at national laboratories by the DOE's Office of Science to provide the nation with resources unmatched anywhere else in the world for synthesis, processing, fabrication, and analysis at the nanoscale.

*For more information, see: M. Maye, D. Nykypanchuk, D. van der Lelie, and O. Gang, "A Simple Method for Kinetic Control of DNA-Induced Nanoparticle Assembly," J. Am. Chem. Soc., **128**, 14020-14021 (2006).*

— Kendra Snyder

VISUALIZING THE IMMUNE SYSTEM'S MISSING LINK

Protecting us from diseases and infections, the immune system is traditionally divided into two parts: innate immunity, a nonspecific response to pathogens that cause disease; and adaptive immunity, which can specifically recognize a pathogen and to mount stronger attacks each time it is encountered. Some invertebrates only have innate immunity, which, at about one billion years old, is the more primitive of the two subsystems. It wasn't

Authors (from left) José Hernández Prada and David Ostrov

until many years later that adaptive immunity appeared along with innate immunity in jawed vertebrates. While much is known about the evolution of the immune system to the current two-part system found in lizards, humans, cats, and countless other organisms, details of its origin remain unknown. At the NSLS, a team of researchers looked for this missing link and unveiled valuable information that could be used in the medical community.

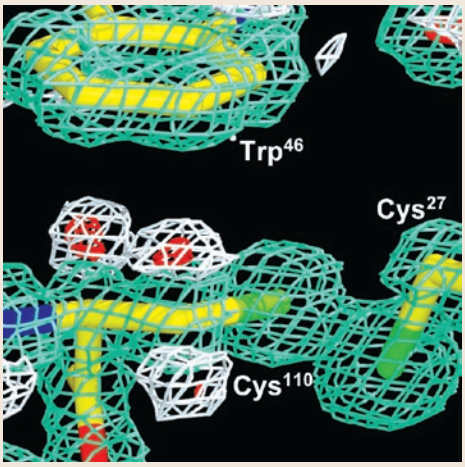

Non-canonical interactions in the core of VCBP3 V1 solved by MAD and refined to 1.15 Å. The side chain of Trp46 and the intrachain disulfide bond (Cys27-Cys110) are shown in the core of VCBP3 V1 (yellow for carbon, orange for sulfur, blue for nitrogen). Non-canonical interactions mediated by p electrons and H atoms apparent in the Fo-Fc electron density are shown at the 3s level (red), 2s level (white) and superimposed onto the final model (yellow for carbon, green for sulfur, blue for nitrogen, red for oxygen atoms). 2Fo-Fc electron density calculated from phases to 1.15 Å was contoured at the 2s level (colored in blue/green).

"In order to find something that represents the transition between the innate and adaptive immune systems, we needed to study an organism that was just below the level of jawed vertebrates on the evolutionary scale," said researcher David Ostrov, from the University of Florida College of Medicine.

The organism chosen was amphioxus, a small, jawless, invertebrate marine animal. The researchers focused on specific amphioxus V-type immunoglobulin domains, which are proteins used by the immune system to identify and neutralize foreign objects. Also used in antibodies, these V-type domains were studied on the structural level using x-ray crystallography at beamline X6A.

"We tried to answer the question, 'Does this protein resemble the types of proteins we use in our immune systems?' Ostrov said. "And the answer is clearly 'yes.' Even though the primitive immune response protein and the one seen in humans have very different sequences, at the structural level they're almost identical."

During their research, which was published in the August 2006 edition of *Nature Immunology*, the scientists ended up with something much more revealing than a simple answer. Using the multi-wavelength anomalous dispersion method (MAD), the researchers solved the structure of the immunoglobulin protein down to atomic resolution – the first V-type immunoglobulin structure ever solved to that level. "We could see structural details at the core of the domain that no one has ever seen," Ostrov said.

Learning the intricate details of this protein could allow scientists to generate more stable immune response proteins that might improve the treatment of cancers and immune diseases. "The problems with using antibodies as they exist is that they are susceptible to degradation," Ostrov said. "If we could learn how to stabilize antibodies, they could last longer in the bloodstream and be more useful clinically."

Other researchers involved in the study include José Hernández Prada, University of Florida College of Medicine; Robert Haire, University of South Florida College of Medicine; Marc Allaire, Jean Jakoncic, and Vivian Stojanoff, NSLS; John Cannon, University of South Florida College of Medicine and H. Lee Moffitt Cancer Center and Research Institute; and Gary Litman, University of Florida

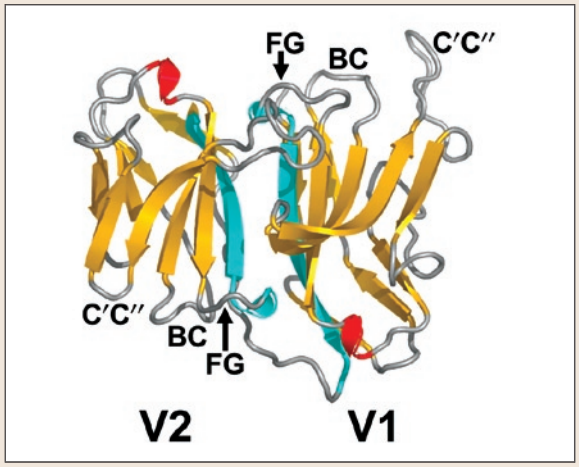

Crystal structure of VCBP3 V1V2 solved by SAD and refined to 1.85 Å. (a,b) Secondary structure is shown (Gold; ß-strands, gray; loop regions, red; helices). The G strand and FG loop encoded by a joining gene segment-like element is shown in cyan. The loops corresponding to CDR regions in T-cell receptor and Ig: BC loop, CDR1; C'C", CDR2; FG, CDR3.

College of Medicine, University of South Florida College of Medicine and All Children's Hospital. This research was funded by the National Institutes of Health, the Cure Autism Now Foundation, and the U.S. Department of Energy.

*For more information, see: J. Prada, R. Haire, M. Allaire, J. Jakoncic, V. Stojanoff, J. Cannon, G. Litman, and D. Ostrov, "Ancient Evolutionary Origin of Diversified Variable Regions Demonstrated by Crystal Structures of an Immune-Type Receptor in Amphioxus," Nat. Immunol., **7**, 875-882 (2006).*

— Kendra Snyder

LIQUID ALLOY SHOWS SOLID-LIKE CRYSTAL STRUCTURE AT SURFACE

Argonne National Laboratory issued the following press release describing research on the surface structure of a silicon and gold molten alloy. This research was conducted in part at beamline X22B of the National Synchrotron Light Source at DOE's Brookhaven National Laboratory by physicist Benjamin Ocko. Atoms are arranged randomly within the bulk of a liquid metal, but they form into discreet layers at the surface. This phenomenon, known as surface layering, was first discovered for mercury and gallium at Brookhaven in 1995. Continued research on the structure of liquid alloys is important for the metals industry and could lead to emerging nanotechnologies. The gold-silicon interconnect junction, for example, is one of the most common connections used in cell phones, computers and other devices.

A substance used in nanotechnology contains unusual structures at its surface, a team of researchers led by Oleg Shpyrko, Distinguished Postdoctoral Fellow at the U.S. Department of Energy's Argonne National Laboratory have learned. The research results, developed at the Center for Nanoscale Materials at Argonne, were published in the July 7, 2006 issue of *Science*.

The substance in question is a gold-silicon eutectic alloy, 82 percent gold and 18 percent silicon. The term eutectic means that the combination melts at a temperature lower than that of the melting temperature of either of its components. For most eutectic alloys, the difference between the melting point of the alloy and those of its pure components is about 100 °C; the gold-silicon eutectic alloy melts about 1,000 °C lower than either of its components, at 360 °C (680 °F).

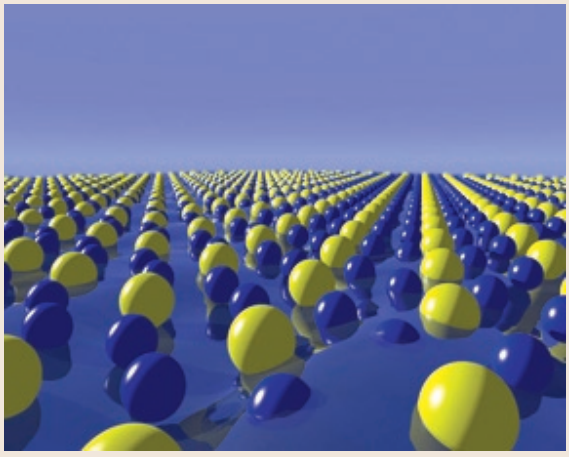

This image represents periodically ordered gold (yellow) and silicon (blue) atoms within the surface-frozen monolayer of liquid gold-silicon eutectic alloy. Research on this surface was conducted at both Brookhaven National Laboratory and Argonne National Laboratory.

But that's not the only unusual thing about the gold-silicon eutectic alloy. In a crystalline solid, atoms are arranged in an orderly, periodic fashion, and in a liquid, arrangements of atoms are disordered. It's been known for about 10 years that many metallic liquids show two or three distinct atomic layers near the surface, and usually there is no crystalline-like order within these layers. However, Shpyrko and his colleagues found that the gold-silicon eutectic alloy has seven or eight layers near its surface. In trying to understand this unexpected development, they found also that the top-most surface layer includes a crystal-like structure, similar to that normally found only in solid substances.

Understanding characteristics of novel surface phases like this surface-frozen monolayer is important for the growing realm of nanotechnology, in which the basic unit of measurement is a billionth of a meter.

"By the time you reduce the size of an object or device down to one nanometer, practically everything is surfaces and interfaces," Shpyrko said. "We need to understand what the new laws of physics and chemistry that govern the surface structures are." Gold and silicon are especially important to understand because they are used in computer technology. Gold is an oxide-resistant "noble" metal that is easily shaped into tiny computer chip interconnects, and silicon is the principal component of most semiconductor devices.

"If you think about it, you have gold and silicon in contact with each other in about every electronic device," Shpyrko said.

Shpyrko began the research as a doctoral student at Harvard University and finished it at Argonne. He used Argonne's Advanced Photon Source, which provides the most brilliant x-ray beams available in the Western Hemisphere, to perform several tests on the material: x-ray specular reflectivity, which provides information about atomic structure normal to the surface; x-ray grazing incidence diffraction, which provides information about in-plane structure; x-ray diffuse scattering, which provides information about waves and other dynamics at the surface; and x-ray crystal truncation rod, which measures thickness and structure of the crystalline surface layer.

Co-authors on the *Science* article were Reinhard Streitel, Venkatachalapathy S.K. Balagurusamy, Alexei Y. Grigoriev, and Peter S. Pershan of Harvard University; Moshe Deutsch of Bar-Ilan University in Israel; Benjamin M. Ocko of Brookhaven

National Laboratory; and Mati Meron and Binhua Lin of the University of Chicago.

This work was supported by the Department of Energy, through the Office of Science's Office of Basic Energy Sciences, and by the U.S.-Israel Binational Science Foundation, Jerusalem. Measurements at Brookhaven were also supported by the Office of Basic Energy Sciences.

For more information, see: O.G. Shpyrko, R. Streitel, V.S.K. Balagurusamy, A.Y. Grigoriev, M. Deutsch, B.M. Ocko, M. Meron, B. Lin, and P.S. Pershan, "Surface Crystallization in a Liquid AuSi Alloy," Science, ***313****, 77-80 (2006).*

— Eva Sylwester, Argonne National Laboratory

BREAKING THE BOUNDS OF PLASTICITY

In order to understand the planet we live on, it's crucial to understand the properties of the liquid- and plastic-like minerals flowing beneath the Earth's crust. The study of the deformation and flow of these minerals, along with many other natural and manmade materials, is known as rheology. Many of Earth's surface features, such as mountain belts, subduction zones, hot spots and seismic zones, are significantly affected by mantle rheology. To study these minerals, scientists mimic mantle conditions with high-pressure, laboratory-based experiments and modeling theories. But at the NSLS, a team from Stony Brook University found that a commonly used model in previous studies might be inaccurate.

The conventional method of modeling stress and strain propagation in materials uses two extreme bounds, called Reuss and Voigt bounds. The Reuss bound describes a condition where all the grains in a sample experience identical stress when forces are applied to the material. The Voigt

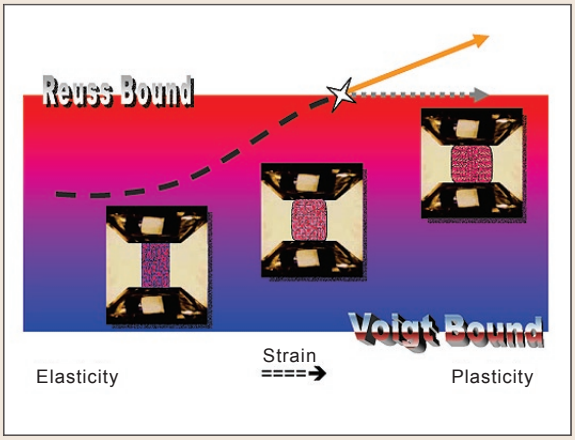

The research group experimentally determined that the stress propagation parameter went beyond the classic Reuss (isostress) bound at larger strains.

bound describes a condition where all the grains experience the same strain when the sample is deformed under stress. Intermediate conditions are described by combining the bounds to achieve a weight parameter between 0 and 1, with 0 representing the Voigt bound and 1 representing the Reuss bound.

Using a new technology at beamline X17B2, the Stony Brook team found that this parameter can actually exceed 1, the Reuss bound. This event occurs when a sample is pushed beyond its normal elastic state. Typically, when a force is applied and removed from a sample, the material will bounce back to its initial form. But if the force is greatly increased, the material will undergo an unrecoverable change, a characteristic known as plastic deformation. It's in this situation that the classic Reuss and Voigt model fails. "For the first time, we can quantitatively recognize that this parameter under plastic deformation can go beyond the boundary," said researcher Jiuhua Chen. "That means that this classic elastic model can no longer be applied in this situation."

The finding wouldn't have been possible without the development of a new type of x-ray diffraction experiment, Chen said. Traditionally, scientists have used one detector at a fixed angle to study materials under high pressure. But with the help of NSLS scientists Zhong Zhong and Chi-Chang Kao, the team developed a simultaneous multi-diffraction detection system that can detect x-ray diffraction along and normal to the applied principal stress.

"These techniques have offered means to reveal the information of material properties that was not obtainable before and have also enabled many reformations of traditional experiments," Chen said. "This technical development will really enable us to study the rheological properties of Earth's materials at a much higher pressure than before. And now we can explore the mantle at even deeper levels."

Other scientists involved in this study, which was published in the June 28, 2006 edition of the *Journal of Physics: Condensed Matter*, include Li Li, Tony Yu, Hongbo Long, Donald Weidner, Liping Wang, and Michael Vaughan, all from Stony Brook University. Funding was provided by the Consortium for Materials Properties Research in Earth Sciences and the National Science Foundation.

*For more information, see: J. Chen, L. Li, T. Yu, H. Long, D. Weidner, L. Wang, and M. Vaughan, "Do Reuss and Voigt Bounds Really Bound in High-Pressure Rheology Experiments?" J. Phys. Condens. Mat., **18**, S1049-1059 (2006).*

— Kendra Snyder

X-RAY ANALYSIS METHOD CRACKS THE 'LIPID PHASE PROBLEM'

Water-repellent lipids, such as fats and waxes, are a major class of molecules that form cell membranes and store energy, among other key functions. However, although these long chain molecules tend to form ordered crystal structures suitable for a common structural analysis method — x-ray diffraction — determining exactly how they pack together is difficult. This is due to a glitch in the diffraction method: the “phase problem.”

The phase problem exists because the diffraction pattern produced by the x-rays can only take into account the intensity of the x-rays used, not their phase (the particular position in time of the x-ray light waves). This limits the quality of the structural data that can be obtained. But recently at the NSLS, a research group learned how to use a common crystallographic method, called multi-wavelength anomalous dispersion (MAD), to determine the phases of diffraction from lipid structures. This important work may help elucidate many biological processes that involve lipids, particularly cell-to-cell fusion.

“Knowing just how lipid chains pack together is of considerable importance in biology,” said the study’s lead scientist, biophysicist Huey Huang of Rice University. “But the details of small-scale shape changes in these lipid structures are not well understood. We think that our work can help remedy this problem.”

Normally, how a molecular structure diffracts x-rays does not depend on the x-ray wavelength or energy. But this is not true when the structure contains atoms that have an absorption edge — a particular energy for which the x-rays are strongly absorbed — near the energy of the incident x-rays. These are called “anomalous” atoms. The MAD method makes use of this energy dependence to single out the contribution of the anomalous atoms in the overall diffraction behavior. This greatly simplifies the original phase problem. And once the phase problem is solved, the structure of the crystal can then be determined. MAD is routinely used to study protein structures, but, according to Huang and his group, this is the first time it has been used to solve a lipid crystal structure.

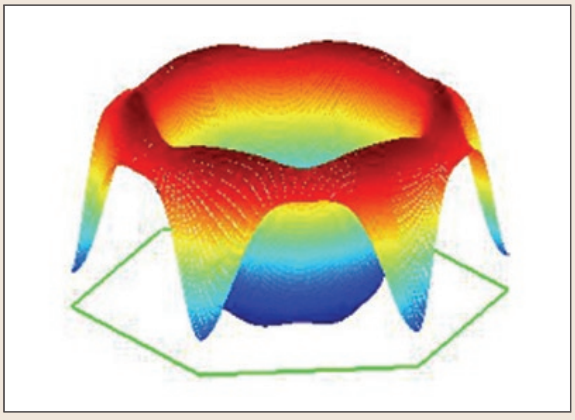

A three-dimensional view of the electron density distribution of bromine atoms in the hexagonal array of lipid cylinders.

One difference between lipids and proteins is that lipid samples take the form of thin films deposited on a substrate, such as a silicon wafer. These thin-film samples often do not have a uniform thicknesses, a technical problem that makes the standard method of MAD analysis difficult. Huang and his group developed a new way to analyze the thin film samples.

The lipid molecules they investigated are members of a lipid sub-class called phospholipids, which are a major component of cell membranes. The particular phospholipids used here were “labeled” with a bromine atom. Together, the molecules pack together such that they form cylinders arranged in a hexagonal array.

The Huang group’s analysis shows that the lipid chains pack together uniformly with each chain occupying the same volume, rather than one or two chains taking up more or less space than the others. Lipid chain volume has been assumed to be constant under configuration changes, but this is the first direct experimental proof.

The group is hoping, in particular, to shed light on “membrane fusion,” one step in the process by which two cells join to become a single cell. The membranes meet at one location and create a connection between the cells, allowing the exchange of molecules (this, for example, is how fertilization and viral infection can occur). Eventually, the membranes merge to create one larger membrane enveloping the contents of both cells. During all of this, the lipid layers in each membrane undergo a series of structural changes. Now, thanks to the work of Huang and his colleagues, scientists may be able to identify those changes to better understand membrane fusion.

This research was published in the March 22, 2006 edition of the *Journal of the American Chemical Society*. It was funded by the National Institutes of Health and the Robert A. Welch Foundation.

*For more information, see: D. Pan, W. Wang, W. Liu, L. Yang, and H. Huang, "Chain Packing in the Inverted Hexagonal Phase of Phospholipids: A Study by X-ray Anomalous Diffraction on Bromine-Labeled Chains," J. Am. Chem. Soc., **128**, 3800-3807 (2006).*

— Laura Mgrdichian

SCIENTISTS TAKE 'SNAPSHOTS' OF ENZYME ACTION

Scientists at Brookhaven National Laboratory, the New York Structural Biology Center, and SGX Pharmaceuticals, Inc., have determined the atomic crystal structure and functional mechanism of an enzyme essential for eliminating unwanted, non-nutritional compounds such as drugs, industrial chemicals, and toxic compounds from the body. The detailed mechanism of action will help scientists understand how these compounds are eliminated and what goes wrong in cases where normal metabolism fails. The research was published in the June 27, 2006 edition of the *Proceedings of the National Academy of Sciences.*

S. Swaminathan

According to Brookhaven biologists Eswaramoorthy Subramaniam, the lead author, and Subramanyam Swaminathan, who led the research, most non-nutritional, foreign substances such as drugs and industrial chemicals are insoluble in water. The body uses two main groups of enzymes — flavin-containing monooxygenases (FMOs) and cytochrome P450s — to convert these compounds to soluble forms that can be easily excreted.

"For FMOs, the end result — that an oxygen atom gets added to make these compounds soluble — is simple," Swaminathan says, "but the reactions require additional participants, or cofactors." In order to understand the molecular mechanism, the scientists used high-intensity x-ray beams at the NSLS to identify the positions of individual atoms and produce crystal structures of the enzyme, the enzyme plus its cofactor, and the enzyme plus the cofactor plus the compound to be oxidized (the substrate).

"These crystal structures give step-by-step snapshots of different stages of the catalytic action," Swaminathan says, "and reveal a mechanism that is different from what had been known about this process."

Previously, it had been believed that all the "players" — the enzyme, cofactor and substrate — came together at a particular time to perform the function of transferring an oxygen atom from the enzyme to the substrate. "Our finding shows that the substrate and cofactor are binding to the enzyme alternately, not together," Swaminathan says.

First, the cofactor (known as NADPH) binds to a molecule known as FAD, which is a coenzyme attached to the FMO, and transfers a hydride ion to it. That makes the FAD group capable of accepting molecular oxygen. Then, when the substrate arrives, the cofactor leaves so that the substrate can bind to the same site on the FAD group. At this moment an oxygen atom from molecular oxygen is attached to the substrate, and the hydride ion obtained from the cofactor combines with the other oxygen atom to form a water molecule, which is released. Once the substrate is oxygenated, it leaves

Figure 1

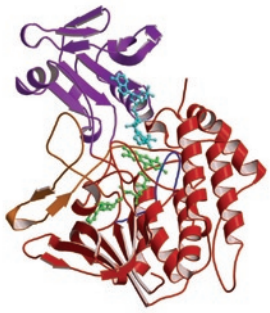

Figure 2

Figure 3

Snapshots of catalytic mechanism of FMO: The three stages in the mechanism of action of FMO are depicted here. The ribbon diagram represents the protein consisting of two domains with a long loop in the interface. The big and small domains are shown in red and purple with the interface in golden color. **Figure 1** represents the first stage with the coenzyme FAD (shown as a ball and stick model in green) bound to the enzyme. In the second stage (**Figure 2**), the cofactor NADPH (shown as a ball and stick model in cyan) approaches the enzyme and interacts with the coenzyme. In the third stage (**Figure 3**), the substrate (shown as a ball and stick model in cyan) displaces the cofactor and binds in the same place to get oxygenated. The molecular oxygen (shown as a dumbbell in red) is required for oxygenation of the substrate.

the enzyme and the cofactor binds again.

“With this back-and-forth, alternating binding, the process repeats over and over for continuous turnover of the product,” Swaminathan says.

The details of this process may help scientists understand what happens in cases where compounds are not properly metabolized, and possibly develop corrective measures. One example is a condition called trimethylaminuria, also known as “fish odor syndrome,” which results from defective FMOs. Affected individuals are unable to oxygenate trimethylamine, a byproduct of protein digestion released by bacteria living in the gut. People with the disorder release trimethylamine through breath, sweat, and urine, producing a fish-like odor that can be embarrassing and result in psychological effects such as withdrawal and depression.

People with defective FMOs might also suffer additional side effects from drugs, industrial compounds, or other chemicals.

This research was funded by the National Institutes of Health and was conducted at the National Synchrotron Light Source, supported by the Office of Basic Energy Sciences within the U.S. Department of Energy’s Office of Science.

*For more information, see: S. Eswaramoorthy, J. Bonanno, S. Burley, and S. Swaminathan, "Mechanism of Action of a Flavin-Containing Monooxygenase," Proc. Natl. Acad. Sci. USA, **103**, 9832-9837 (2006).*

— Karen McNulty Walsh

BEAMLINE
X18B

PUBLICATION
R.V. Hull, L. Li, Y. Xing and C.C. Chusuei, "Pt Nanoparticle Binding on Multiwalled Carbon Nanotubes," *Chem. Mater.*, **18,** 1780–1788 (2006).

FUNDING
American Chemical Society Petroleum Research Fund; Foundation for Chemical Research, Inc.; Missouri Research Board; UMR Intelligent Systems Center

FOR MORE INFORMATION
Charles C. Chusuei
Chemistry Department
University of Missouri-Rolla
chusuei@umr.edu

CHARACTERIZING THE SURFACES OF CARBON NANOTUBE FUEL CELL CATALYSTS

R.V. Hull[1], L. Li[2], Y. Xing[2], and C.C. Chusuei[1]

[1]Department of Chemistry and [2]Department of Chemical and Biological Engineering, University of Missouri-Rolla

Characterizing the surface structure of catalyst materials is important for the improvement of current fuel cell technology, which promises to deliver an environmentally benign means of energy production. Using x-rays produced at the National Synchrotron Light Source (NSLS), researchers at the University of Missouri-Rolla (UMR) were able to detect the presence of PtO_x at the outer-most perimeters of a potential catalyst: platinum nanoparticles tethered to carbon nanotubes. At the same time, they determined that its bulk composition was predominantly metallic.

Fuel cells are devices capable of generating electrical energy directly without involving a thermal cycle that typically releases greenhouse gases, such as CO and NO_x, into the atmosphere. Today, burning coal is still the primary and most efficient (with regard to power density) means of electrical energy production in the United States. New information obtained from a study performed at the NSLS may help catalyst researchers design improved fuel cell devices that can compete with current fossil fuel technology.

The active material on the carbon-nanotube supports consists of tiny platinum particles on the order of a few nanometers in diameter, which are deposited on the carbon surface. The deposition of these particles on the nanotubes has been found to enhance the electrocatalytic activity for direct methanol fuel cells (DMFCs) by as much as 48% relative to carbon black, but the underlying reasons for this observation have yet to be fully described. The exact relationship between the interfacial structure of these carbon-supported metal nanoparticles and their subsequent chemical activity has long mystified catalyst scientists.

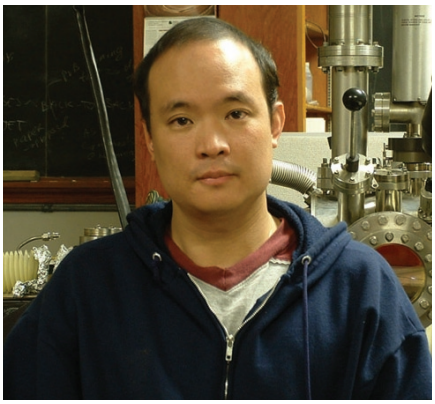

Charles Chusuei

Researchers from the University of Missouri-Rolla (UMR) used x-rays at NSLS beamline X18B to characterize the interfacial structure of platinum particles tethered to carbon-nanotube (CNT) catalyst surfaces. Graduate students Robert V. Hull and Liang Li and professors Charles C. Chusuei and Yangchuan Xing in the departments of Chemistry and Chemical and Biological Engineering at UMR collaborated on the study. The results of the work appear in the April 4, 2006 issue of *Chemistry of Materials*. The paper describes how the researchers used the extended x-ray absorption fine structure (EXAFS) technique in conjunction with x-ray photoelectron spectroscopy (XPS) (performed at UMR) to probe the surface and subsurface structures of the nanoparticles. They aimed to show evidence for the coordination of the platinum to oxygen atoms attached to the surface of the nanotubes (Pt-CNTs), which were functionalized with ketone, ester, and hydroxyl groups.

XPS is sensitive to probing approximately 50–100 Å deep while EXAFS is sensitive only to the first few atomic layers of the metal particles being probed. Comparisons of the two sets of spectra show that both metallic and oxidized platinum were present. It was discovered that the outermost structure of the particles consisted of an oxide, PtO_x, while the bulk of the nanoparticles was fully metallic. The XPS of the Pt 4f orbital showed a binding energy of 71.4 eV, indicative of the bulk metallic structure of the platinum nanopar-

ticles (**Figure 1**). The nearest-neighbor distances for the metal nanoparticle tethered to the nanotubes were observed at distances of ~1.78 Å — much too short for the expected ~2.77 Å distance between metallic platinum atoms (**Figure 2**), which signified Pt–O at the outermost perimeter of the clusters. This structure accompanied the increased DMFC activity observed. In addition to the dried powder catalyst materials, experiments were performed on the Pt-CNTs under aqueous solution environments to simulate the working conditions of the fuel cell, which exhibited the same surface structure as the dry powdered form.

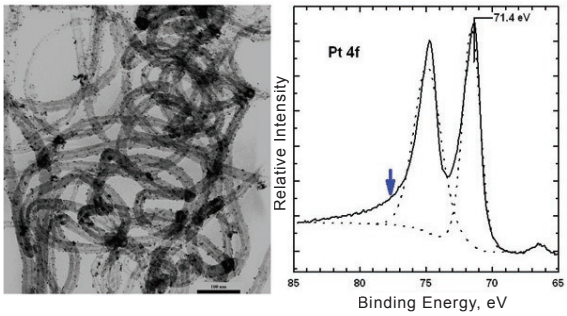

Figure 1. Pt 4f core level XPS spectrum (right panel) of nanoparticles tethered onto multiwalled carbon nanotubes; arrow denotes evidence for Pt(II/IV) oxidation state albeit small in amount. Left panel shows a transmission electron micrograph of Pt nanoparticles ~3.5 nm in diameter; the scale bar shown corresponds to 100 nm.

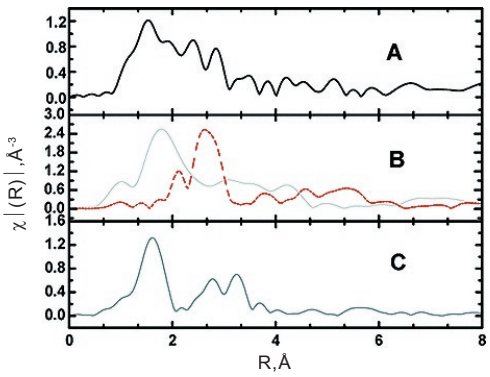

Figure 2. Pt L_3 edge EXAFS Fourier Transformations of (A) Pt-CNTs in an aqueous colloidal suspension; (B) Pt-CNTs in dry powder-like form (solid gray line; Pt foil scan shown as a dotted, orange spectral line); and (C) a PtO_2 standard.

BEAMLINE
X7B

PUBLICATION
J. Zhang, F. Lima, M. Shao, K. Sasaki, J. Wang, J. Hanson, and R. Adzic, "Platinum Monolayer on Nonnoble Metal-Nobel Metal Core-Shell Nanoparticle Electrocatalysts for O_2 Reduction," *J. Phys. Chem. B.*, **109**, 22701-22704 (2005).

FUNDING
U.S. Department of Energy; Stony Brook University; CAPES (Brazil)

FOR MORE INFORMATION
Radoslav Adzic
Department of Chemistry
Brookhaven National Laboratory
adzic@bnl.gov

PLATINUM MONOLAYER ON NON-NOBLE METAL - NOBLE METAL CORE-SHELL NANOPARTICLES ELECTRO-CATALYSTS FOR O_2 REDUCTION

J. Zhang[1], F.H.B. Lima[2], M.H. Shao[1], K. Sasaki[1], J.X. Wang[1], J. Hanson[1], and R.R. Adzic[1]

[1]Department of Chemistry, Brookhaven National Laboratory; [2]On leave from the University of São Paulo, Brazil

We synthesized a new class of O_2 electrocatalysts for fuel cell cathodes. They consist of a Pt monolayer deposited on carbon-supported nanoparticles that have non-noble-metal cores and noble-metal shells. These nanoparticles were formed from a mixture of noble and non-noble metals. At elevated temperatures, the noble metal moves to the surface, while the non-noble metal remains in the core. The Pt monolayer was deposited onto the nanoparticles by galvanically displacing an adsorbed Cu monolayer. The mass activity of these electrocatalysts is more than an order of magnitude higher than that of commercial Pt/C electrocatalysts. Strain in the Pt monolayer and the reduced coverage of the reaction inhibitor (PtOH), revealed by x-ray absorption spectroscopy data, are the origin of the enhanced catalytic activity.

As the interest in a "hydrogen-based economy" grows, research on its major elements — hydrogen production and storage, and energy conversion in fuel cells — is expanding. While fuel cells are expected to become a major source of clean energy, existing fuel-cell technology still has two drawbacks: energy conversion that is lower than the theoretical efficiency, and electrocatalysts with a high Pt content. Both problems are connected to the rather slow electrocatalytic O_2 reduction reaction (ORR).

Several approaches explored in the past to ameliorate this disadvantage have had limited success. We, however, have demonstrated a promising way to solve these problems. Our method involves electrocatalysts consisting of a Pt monolayer supported on suitable metal nanoparticles. These electrocatalysts have a very high activity and an ultra-low Pt content that promises to alleviate the above problems. Platinum is deposited in a monolayer amount on the surfaces of carbon-supported non-noble metal/noble metal core-shell nanoparticles (**Figure 1**). Using non-noble metals for the cores facilitates a further reduction of the content of the noble metal in the ORR electrocatalysts. In addition, by properly selecting the noble-metal shell, the activity of the Pt monolayer can be heightened through electronic and/or geometric effects. The choice of the metals constituting the shell and core is based on the segregation properties of the two metals, as well as their electronic and strain-inducing effects on the Pt monolayer. The nanoparticles were synthesized by segregating the atoms of the noble metal to the nanoparticle surface at elevated temperatures. A Pt monolayer was then deposited on the nanoparticles via the galvanic displacement by Pt of an adsorbed Cu monolayer.

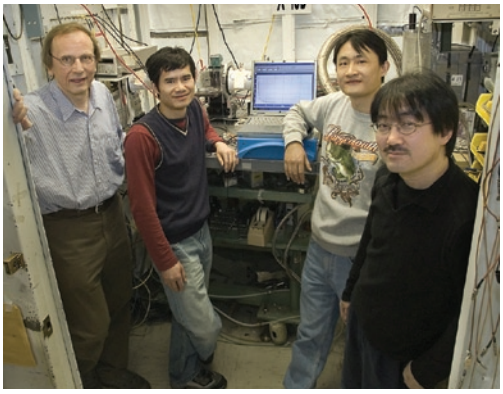

Authors (from left): Radoslav Adzic, Junliang Zhang, Minhua Shao, and Kotaro Sasaki

The noble-metal shell in the core-shell nanoparticle has two roles. First, it protects the non-noble core from contacting the acid electrolyte, i.e., it precludes its dissolution. Second, the proper shell can improve the catalytic properties of a Pt monolayer by affecting its electronic properties and/or by inducing strain in the monolayer, which increases its activity. A strong surface segregation of the noble metal component is the key feature of these systems. The surface segregation of Au, Pd, and Pt and their protection of the Ni or Co core from dissolution was verified by linear sweep voltammetry, underpotential deposition (UPD) of Cu, and x-ray diffraction techniques. The activity of these electrocatalysts, calculated as the current at 0.85 V divided by the mass of Pt, is about 20 times above that of commercial Pt/C electrocatalysts. If the total noble-metal mass is counted, the activity

is about four times larger. The very high activities appear to be a consequence of a strain that appears due to a mismatch in the lattice constants between the monolayers and these substrates, the changes in the d-band properties of the Pt monolayer itself (caused by its interaction with them), and the decreased PtOH coverage. These effects were observed by *in situ* synchrotron radiation techniques.

In conclusion, we demonstrated the synthesis of a new class of electrocatalysts consisting of a Pt monolayer deposited on non-noble metal/noble metal core-shell nanoparticles. We showed that it is possible to devise ORR electrocatalysts, with activity surpassing that of state-of-the-art carbon-supported Pt electrocatalysts, that contain only a fractional amount of Pt and a very small amount of another noble metal. Consequently, the cost of fuel cells could be lowered considerably. Further work on these systems will address the question of their long-term stability.

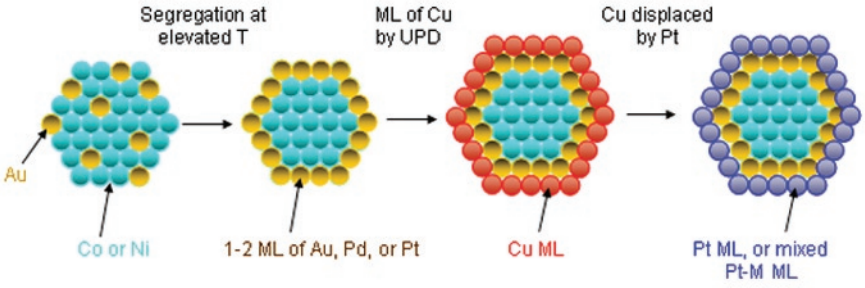

Figure 1. Model for the synthesis of Pt monolayer catalysts on non-noble metal-noble metal core-shell nanoparticles.

BEAMLINE
U12A

PUBLICATION
S.D. Senanayake, G.I.N. Waterhouse, H. Idriss, and T.E. Madey, "Coupling of Carbon Monoxide Molecules over Oxygen Defected UO_2 (111) Single Crystal and Thin Film Surfaces," *Langmuir*, **21**, 11141-11145 (2005).

FUNDING
Foundation for Research Science and Technology; U.S. Department of Energy

FOR MORE INFORMATION
H. Idriss
Department of Chemistry
The University of Auckland
h.idriss@auckland.ac.nz

REDUCTIVE COUPLING OF CARBON MONOXIDE MOLECULES OVER OXYGEN DEFECTED UO_2 (111) SINGLE CRYSTAL AND THIN FILM SURFACES

S.D. Senanayake[1,3], G.I.N. Waterhouse[1], H. Idriss[1], and T.E. Madey[2]

[1]Department of Chemistry, The University of Auckland, New Zealand; [2]Department of Physics and Astronomy, and Laboratory for Surface Modification, Rutgers, The State University of New Jersey; [3]Present address: Chemical Sciences Division, Oak Ridge National Labororatory

Coupling reactions of chemical compounds have a unique place in chemistry because they represent a key step in building complex molecules from simple ones. Solid catalysts are often used to accelerate the reaction rate by stabilizing the reaction intermediate, and can thus enhance or initiate a reaction that often could not be conducted in their absence. Among the most challenging coupling reactions is the selective coupling of two carbon monoxide molecules to C_2 compounds. This rare reaction, which has been previously observed in organometallic chemistry (solution chemistry), was successfully conducted on oxygen-defected uranium dioxide single crystal and thin-film surfaces. The oxidation/reduction reactions over the O-defected surfaces were studied using high-resolution x-ray photoelectron spectroscopy. This method revealed the reaction pathway.

The surface reaction of the oxide of actinides, such as uranium oxides, is one of the least studied, yet one of the most fascinating. Our interest in this surface reaction started a decade ago. The reaction represents one of the most challenging systems among all chemical reactions of solids. The *f*-orbitals of the actinide elements, because they differ in symmetry from the *d*-orbitals, can adsorb a reactant in a unique configuration and thus may orient to different chemical pathways not seen on the surfaces of early transition metals. In addition, relativistic effects, due to the large size of the nucleus, result in a wide range of oxidation states of metal cations, making them very active but also unstable. The observation of this reaction on a solid surface has allowed the use of x-ray photoelectron spectroscopy (XPS) (**Figure 1**). However, conventional XPS was not adequate to carry out accurate qualitative and quantitative investigations because of inevitable oxidations, over time, of the surface U atoms during data collection. By using the high-intensity, high-resolution (HR), and fast acquisition time available on NSLS beamline U12A, it was possible to study the mechanism of this reaction and outline quantitatively the changes in surface oxidation states before and after the reaction.

Authors (top) Hicham Idriss and Sanjaya Senanayake

Figure 2 shows the HRXPS spectra of the U4f and O1s lines of the clean oxygen-defected UO_2 thin-film surface, as well as the same surface upon exposure to carbon monoxide. The main lines at 380 and 391 eV are due to $U4f_{7/2,5/2}$ of U^{4+} while the shoulder at the low binding energy side of the $U4f_{7/2}$ is exclusively due to U cations in lower oxidation states than +4 (a detailed study of this region has been conducted in a separate work). Upon adsorption of carbon monoxide (b) the intensity of this shoulder decreases and becomes negligible at surface saturation (c and d). This is because CO has donated its oxygen atom to surface defects. A similar observation is seen in the O1s region. Detailed analysis of the C1s region has shown that the dissociation is not total. Parallel work has shown the formation of acetylene and ethylene as the end product at 550 K and above.

The above three observations — oxidation upon adsorption, partial dissociation at room temperature, and desorption of C_2 compounds at high temperature — can be explained in **Scheme 1**.

In **Scheme 1**, the η^2-η^2-bis-formyl species is proposed to be formed on a U surface; this could only be accommodated because of the particular symmetry of the fxy^2 orbitals. The bis-formyl species react at room temperature to give the pinacolates; this in turn gives C_2H_2/C_2H_4 at high temperatures.

Although the above reaction is not catalytic, its observation may open the routes for the design of new catalytic materials using uranium oxides or oxides of similar properties.

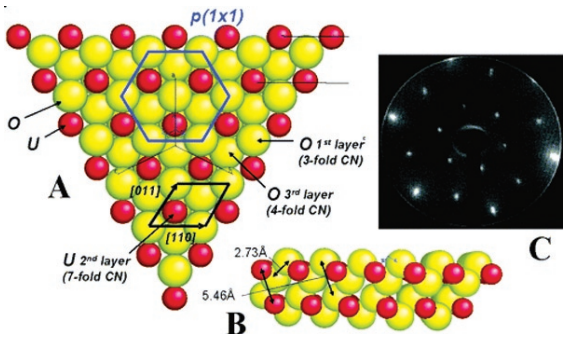

Figure 1. Ball model of the UO_2(111) surface showing the hexagonal arrangement of U and O atoms and lattice parameters. Red balls are U atoms and yellow balls are O atoms (A: top view, B: side view). C: Low Energy Electron Diffraction (LEED) of the UO_2(111) surface showing the extended order (131 eV). The surface is entirely composed of oxygen atoms. Their partial removal makes the U atoms (initially in the second layer) highly reactive for both reduction and coupling reactions.

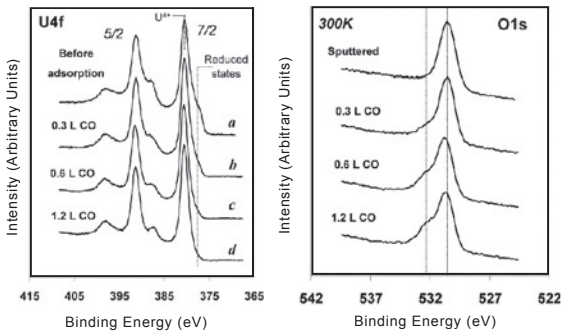

Figure 2. HRXPS U4f and O1s lines of Ar-ion sputtered UO_2 thin film before (a) and after (b, c, and d) reacting with CO at the indicated exposures in Langmuir (L = 10^{-6} torr s).

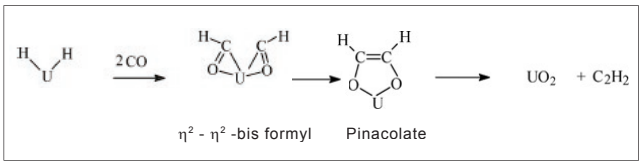

Scheme 1

BEAMLINES
X7B, X19A

PUBLICATION
D.H. Kim, J. Szanyi, J.H. Kwak, T. Szailer, J.C. Hanson, C. Wang, C.H.F. Peden, "Effect of Barium Loading on the Desulfation of Pt-BaO/Al_2O_3 Studied by H_2 TPRx, TEM, Sulfur K-edge XANES and *In-situ* TR-XRD," *J. Phys. Chem.*, **110**, 10441-10448 (2006).

FUNDING
U.S. Department of Energy

FOR MORE INFORMATION
Do Heui Kim
Institute for Interfacial Catalysis
Pacific Northwest National Lab
do.kim@pnl.gov

SULFUR K-EDGE XANES AND TR-XRD STUDIES OF Pt-BaO/Al_2O_3 LEAN NO_x TRAP CATALYSTS: EFFECTS OF BARIUM LOADING ON DESULFATION

D.H. Kim[1], J. Szanyi[1], J.H. Kwak[1], T. Szailer[1], J.C. Hanson[2], C. Wang[1], and C.H.F. Peden[1]

[1]Institute for Interfacial Catalysis, Pacific Northwest National Laboratory; [2]Chemistry Department, Brookhaven National Laboratory

Sulfur K-edge x-ray absorption near-edge spectroscopy (XANES) and in situ time-resolved x-ray diffraction (TR-XRD) are used to show that the removal of sulfur (in the form of $BaSO_4$) from Pt-BaO(x)/Al_2O_3 (x = wt% BaO) catalysts is strongly dependant on barium loading. Sulfated Pt-BaO(8)/Al_2O_3, consisting predominantly of monolayer BaO/$BaCO_3$ species, displays more facile desulfation by H_2 at lower temperatures than sulfated Pt-BaO(20)/Al_2O_3, a material containing primarily particulate BaO/$BaCO_3$ species. This suggests that the initial morphology differences between the two samples play a crucial role in determining the extent of desulfation and the temperature at which it occurs, a result that may be important in developing more sulfur-resistant LNT catalyst systems.

Internal combustion engines operating under lean-burn conditions, such as diesel engines, exhibit high fuel efficiency. Removal of harmful NO_x emissions from the exhaust in the presence of excess oxygen, however, presents a great challenge to the catalysis community because traditional three-way catalysts are ineffective under these conditions. Among the approaches being considered, urea and hydrocarbon selective catalytic reduction (SCR), and lean-NO_x traps (LNTs, aka NO_x storage/reduction (NSR) catalysts or NO_x adsorbers) are promising technologies. In LNT technology, an active oxide (alkali and/or alkaline earth) material takes up NO_x under lean engine operation conditions and stores them as nitrates. In a brief rich cycle, these nitrates are released from the active oxide catalyst component, and reduced to N_2 on the precious metal component of the catalyst.

Because even low concentrations of SO_2 in the emission gradually reduces the ability of the active phase to store NO_x, the resistance of the material to SO_2 poisoning remains a critical issue. Meanwhile, since we have shown that NO_x adsorption/desorption chemistry is strongly dependent on the loading of barium, an important question concerns the variation of the desulfation chemistry as a function of barium content in the LNT formulation. As such, we performed a multi-spectroscopy study to understand desulfation processes on Pt-BaO/Al_2O_3 LNT materials with varying barium loadings. In particular, we investigated the desulfation behavior of pre-sulfated Pt-BaO(8 or 20 wt%)/Al_2O_3 catalysts using H_2 temperature programmed reaction (TPRx). These two BaO loadings were chosen because we have previously shown that the Ba-phase morphologies are significantly different; notably, BaO consists of a monolayer "coating" on the alumina surface in Pt-BaO(8)/Al_2O_3, while this monolayer phase coexists with a "particulate" or bulk-like BaO phase in the Pt-BaO(20)/Al_2O_3 sample. Thus, we also followed the changes in catalyst morphology and sulfur oxidation states during desulfation processes using synchrotron time-resolved x-ray diffraction (TR-XRD) and sulfur K-edge x-ray absorption near-edge spectroscopy (XANES), which were performed on the NSLS beamlines X7B and X19A, respectively.

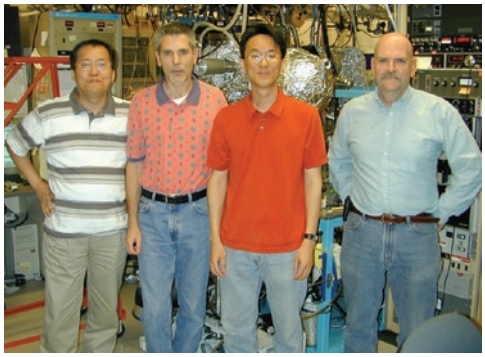

Authors (from left) Ja Hun Kwak, Janos Szanyi, Do Heui Kim, and Chuck Peden

Figure 1 shows the H_2 TPRx spectra of sulfated Pt-BaO(8)/Al_2O_3 and Pt-BaO(20)/Al_2O_3 samples, obtained by ramping the temperature of these samples in a H_2/He flow while continually monitoring the product gases with a mass spectrometer. H_2S is the primary product of the reaction between H_2 and sulfur species on the sample. H_2S is formed at higher temperature for the sample with higher barium loading, implying that the type

of barium sulfate species formed upon uptake of SO_2 is different depending on the loading of barium species – surface or 'monolayer' sulfates for Pt-BaO(8)/Al_2O_3, and 'bulk' $BaSO_4$ for the Pt-BaO(20)/Al_2O_3 sample. In addition, the amount of H_2S produced over Pt-BaO(8)/Al_2O_3 is two times larger than that of the sample with higher barium loadings, which suggests a more facile desulfation of 'monolayer' $BaSO_4$.

Sulfur K-edge XANES experiments were carried out to investigate changes in the oxidation states of sulfur as a function of H_2 reduction temperature. We collected samples after H_2 TPRx up to 553 K, 743 K and 1073 K (see arrows in **Figure 1**). After H_2 TPRx up to 553 K for the sulfated Pt-BaO(8)/Al_2O_3 sample, the spectrum in **Figure 2(A)** contains a small peak at 2472 eV, which can be assigned to a sulfide-like (S^{2-}) species, while the main sulfate (SO_4^{2-}) peak is unchanged. After H_2 TPRx up to 1073 K, the sulfate peak nearly disappears, while there is an increase in features from lower oxidation state sulfur species (sulfide-like and sulfite-like (SO_3^{2-})). The sulfated Pt-BaO(20)/Al_2O_3 sample shows qualitatively similar behavior as shown in **Figure 2(B)**. However, compared with the sample with lower barium loading, Pt-BaO(20)/Al_2O_3 contains a significantly larger amount of residual sulfur species of all types after H_2 TPRx up to 1073 K, which is consistent with the H_2 TPRx results.

Figure 3 shows a series of XRD patterns obtained during H_2 TPRx for the sulfated Pt-BaO(20)/Al_2O_3 sample. The room temperature XRD contains peaks assigned to $BaSO_4$. Up to about 773 K, the $BaSO_4$ phase is unchanged. However, above 773 K, diffraction peaks associated with BaS appear and continue to grow with increasing temperature, along with a corresponding drop in the intensities of the $BaSO_4$ peaks. Compared with the Pt-BaO(20)/Al_2O_3 sample, Pt-BaO(8)/Al_2O_3 contains much smaller amounts of BaS, confirming that residual sulfur species were present at much lower concentrations for the lower barium loading sample.

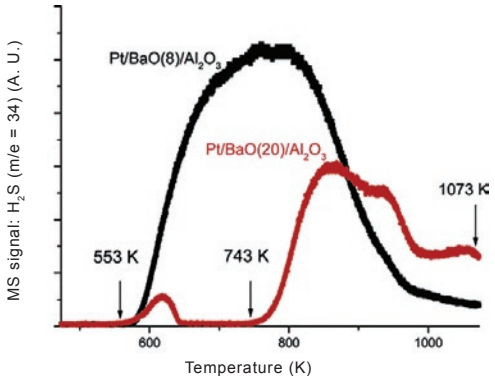

Figure 1. H_2 TPRx spectra for sulfated Pt-BaO(8)/Al_2O_3 and Pt-BaO(20)/Al_2O_3 samples.

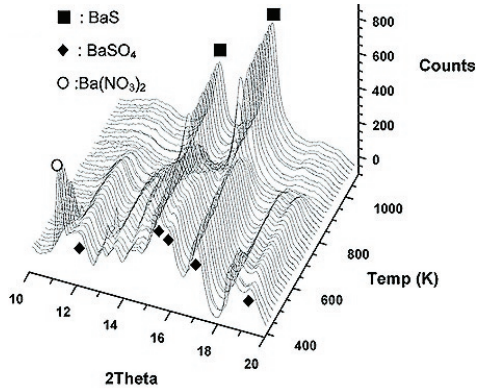

Figure 3. TR-XRD patterns collected during H_2 TPRx from a sulfated Pt-BaO(20)/Al_2O_3 sample.

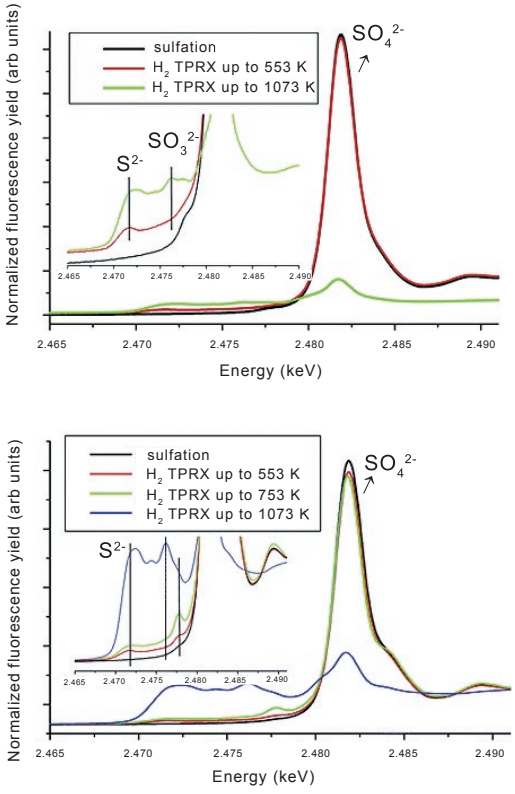

Figure 2. Sulfur K-edge XANES spectra of (A) sulfated Pt-BaO(8)/Al_2O_3, and (B) sulfated Pt-BaO(20)/Al_2O_3 samples.

BEAMLINES
U10A, U13UB

PUBLICATION
C.C. Homes, S.V. Dordevic, G. Gu, Q. Li, T. Valla and J.M. Tranquada, "Charge Order, Metallic Behavior, and Superconductivity in $La_{2-x}Ba_xCuO_4$ with x =1/8," *Phys. Rev. Letts.*, **96**, 257002 (2006).

FUNDING
U.S. Department of Energy

FOR MORE INFORMATION
Christopher Homes
Condensed Matter Physics & Materials Science Dept.
Brookhaven National Laboratory
homes@bnl.gov

CHARGE ORDER AND SUPERCONDUCTIVITY IN A HIGH-TEMPERATURE SUPERCONDUCTOR

C.C. Homes[1], S.V. Dordevic[1,2], G. Gu[1], Q. Li[1], T. Valla[1], and J.M. Tranquada[1]

[1]Condensed Matter Physics & Materials Science Department, Brookhaven National Laboratory; [2]Department of Physics, The University of Akron

Superconductivity at elevated temperature was originally discovered in the lanthanum barium copper oxide materials ($La_{2-x}Ba_xCuO_4$, or LBCO). However, because these materials were difficult to grow as single crystals, work quickly shifted to the analogous $La_{2-x}Sr_xCuO_4$ (LSCO) materials. Recently, large single crystals of LBCO have been grown that are suitable for optical studies. All high-temperature superconductors share the trait that the parent compounds are insulating, and that superconductivity is induced by chemical doping to produce a superconducting "dome;" LBCO is superconducting for Ba-dopings of about 0.05 to 0.23. Curiously, at the 1/8 doping, charge-order develops and superconductivity is destroyed, leading to an unusual electronic state.

In most cases, superconductivity develops from a metallic state, and is characterized by the formation of a superconducting energy gap at the Fermi surface. In metals and alloys, this gap is isotropic. However, a unique feature of the copper-oxide superconductors is that the gap is highly anisotropic, actually going to zero at some points on the Fermi surface (this is referred to as a *d*-wave gap). Optical studies allow the nature of both the metallic and superconducting states to be probed.

Single crystals of LBCO have been cleaved in air, revealing large, optically flat surfaces oriented parallel to the copper-oxygen planes where the superconductivity is thought to originate in these materials (**Figure 1**). The temperature dependence of the reflectance has been measured at a near-normal angle of incidence over a wide frequency range (about 2 meV to over 4 eV). The reflectance is in fact a complex quantity, consisting of an amplitude and a phase; in this case, only the amplitude is measured. However, if the reflectance is measured over a wide enough range (as is the case here), then the Kramers-Kronig relations may be used to determine the phase – once these two quantities are known, other quantities such as the optical conductivity may be calculated. The optical conductivity of LBCO at the 1/8 doping is shown in **Figure 2**. The conductivity of metals is often described by the simple Drude model, which may be described by a plasma frequency (a measure of the concentration of free carriers), and a scattering rate; the frequency response is a Lorentzian centered at the origin, and the width at half maximum is the scattering rate. This simple picture describes the optical conductivity of LBCO quite well, at least until about 60 K. However, for this particular doping, LBCO undergoes an orthorhombic to tetragonal transition at about 60 K, leading to formation of static charge stripes. Long-range charge order in a material often leads to the formation of a charge gap that destroys the conductivity in the material. However, as **Figure 2** clearly shows, while the response associated with the Drude component is shrinking, the conductivity remains metallic down to the lowest measured temperature. We interpret this response to indicate that the charge order is responsible for a partial gapping of the Fermi surface. Angle-resolved photoemission studies on this material do indeed detect a gap in this material below 60 K, but the gap is highly anisotropic and has a *d*-wave character; the metallic excitations are associated with the ungapped or nodal regions. This behavior is also

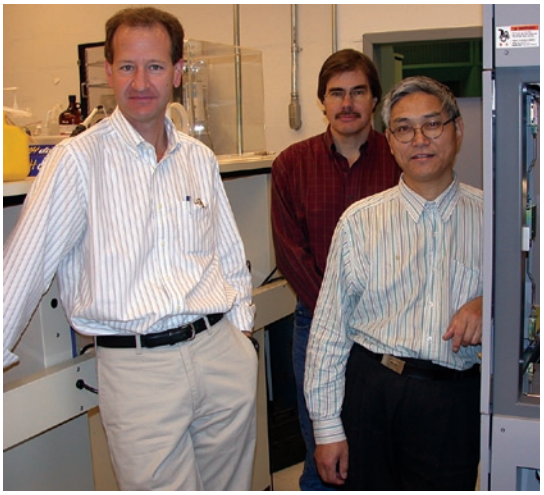

Authors (from left): Christopher Homes, John Tranquada, and Genda Gu.

observed in the normal-state of the underdoped copper-oxide materials, which are referred to as "nodal metals." It is tempting to associate this gap with a competing instability, such as a charge density wave. However, the fact that the superconductivity recovers quickly on either side of the 1/8 anomaly suggests that the gap we observe in the 1/8 material is in fact the superconducting gap, but with a near total absence of phase coherence.

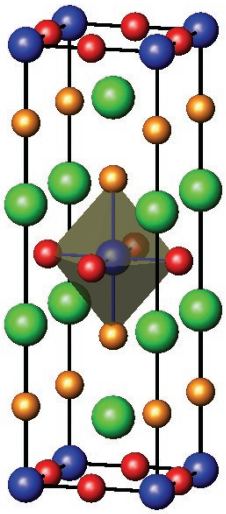

Figure 1. The unit cell of $(La,Ba)_2CuO_4$ [La, (Ba) – green, Cu – blue, O – red (sheet), orange (apical)] illustrating the copper-oxygen (*ab*) planes and bond coordination; the long axis is the *c* axis.

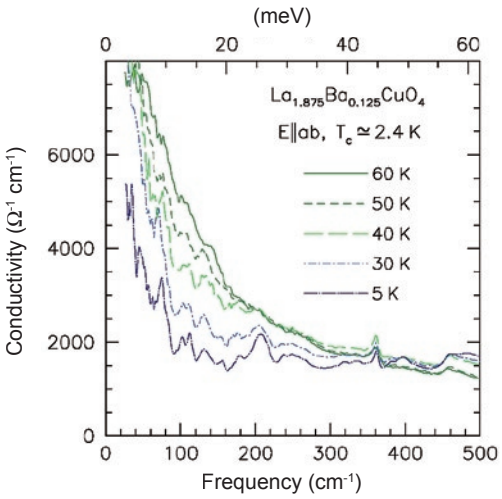

Figure 2. The *ab*-plane optical conductivity of LBCO for the 1/8 doping in the infrared region between 60 and about 5 K, showing a steady decrease and narrowing of the Drude-like component.

BEAMLINE
X13A

PUBLICATION
C. Sánchez-Hanke, R. Gonzalez-Arrabal, J. E. Prieto, E. Andrzejewska, N. Gordillo, D.O. Boerma, R. Loloee, J. Skuza, and R.A Lukaszew, "Observation of Nitrogen Polarization in Fe-N using Soft X-ray Magnetic Circular Dichroism," *J. Appl. Phys.*, **99**, 08B709 (2006).

FUNDING
U.S. Department of Energy; The "Ramon y Cajal" program of the Spanish Ministry of Education and Science

FOR MORE INFORMATION
Cecilia Sánchez-Hanke
NSLS-BNL
hanke@bnl.gov

OBSERVATION OF NITROGEN POLARIZATION IN Fe-N USING SOFT X-RAY MAGNETIC CIRCULAR DICHROISM

C. Sánchez-Hanke[1], R. Gonzalez-Arrabal[2], and R.A Lukaszew[3]

[1]National Synchrotron Light Source, Brookhaven National Laboratory; [2]Centro de Microanálisis de Materiales, University Autónoma of Madrid, Spain; [3]Physics and Astronomy Department, University of Toledo

Fe-nitrides together with transition metal oxides are part of a new generation of interesting magnetic materials extensively investigated because of their potential use in future magnetic devices. Fe-N is a complex system, with a rather complicated phase diagram containing multiple phases like γ'-Fe_4N, ε'-Fe_3N, ξ-Fe_2N and α"$Fe_{16}N_2$. The α" $Fe_{16}N_2$ phase is the most interesting phase, with a reported magnetic moment up to 4 times that of the Fe one. The fabrication of single-phase samples of Fe-N is currently a complicated task, especially for thin films of the α" phase. Our interest to study Fe-N thin films is driven by the search for a better understanding of nitrogen's role in the magnetic properties of this system. Previous structural reports place the N atoms in an interstitial position inside the Fe structure, suggesting rather weak interactions between Fe and N.

Using x-ray Magnetic Circular Dichroism (MCD), we studied a series of Fe-N thin films in a thickness range between 15 and 100 nm with predominantly γ'-Fe_4N phase. Prior to the MCD measurements, the samples were structurally characterized with x-ray diffraction (XRD) and magnetically characterized with a Superconducting Quantum Interference Device (SQUID), making use of the Polar Magneto-Kerr effect (MOKE) **(Figure 1)**. The P-MOKE data show an expected 4-fold symmetry as the Fe-N thin films were grown on a (001) FCC MgO substrate shown by the XRD measurements.

Authors (from top) Cecilia Sanchez-Hanke and Rosa Alejandra Lukaszew

MCD measurements were collected at the National Synchrotron Light Source beamline X13A. This beamline delivers modulated soft x-rays in an energy range between 200 and 1600 eV, switching between left and right polarization with frequencies close to 22 Hz. MCD, or the difference in the absorption signal of the sample collected with left and right elliptically polarized x-rays, provides a unique element-specific tool to study magnetic properties in magnetic materials. With the difference signal, the sum signal, and the help of the Sum Rules, it is possible to determine the spin and orbital magnetic moment associated with each of the elements present in the sample. Modulated x-rays switching at high frequencies allow the simultaneous collection of the absorption and MCD signal in a single energy scan. The modulation also increases the sensitivity in the detection of small magnetic signals as well as the collection of the MCD signals in highly diluted ferromagnetic materials. These characteristics made X13A an adequate choice to conduct the experiment in order to show the contribution of nitrogen to the Fe-N magnetic moment.

XMCD measurements were performed on Fe-N thin films at different incident angles, simultaneously collecting the reflectivity and the MCD spectra over the Fe L_{II} and L_{III} and the N K absorption edges **(Figure 2)**. The left panel of **Figure 2** shows the N polarization in the thin film with a small MCD signal, indicating that the experiment was successful. The detected MCD signal, in the range of 10^{-5}, is close to the beamline detection limit. On the right panel, the Fe reflectivity and MCD signal were collected at two different incident angles. The reflectivity spectra at the Fe edges show two different components at the L_{III} absorption edge. These signals can be enhanced independently depending on the angle of incidence. Comparing these spectra with a spectrum recorded on pure Fe relates the presence of the additional features in the spectra to different Fe sites in structure depending on the phase. The signal to noise ratio in the nitrogen MCD data was not good enough to try to apply the Sum Rules

and calculate the contribution to the magnetic moment of the sample. But the signal was sufficient to perform element specific hysteresis loops together with the Fe (**Figure 3**). Hysteresis loops were recorded for nitrogen and for each of the Fe components. The loops present the same shape as well as the same coercive field that shows the intimate relation between the N and the Fe signal.

We demonstrated that the nitrogen has some contribution to the magnetic moment of the sample, although small but detectable in the case we refer to here. Our data demonstrate an intricate Fe-N structure with the coexistence in the samples of multiple phases. We speculate that each feature or peak in the Fe spectra corresponds to Fe atoms occupying different sites inside the structure of the nitride. The complexity of the studied thin films does not allow us associate the Fe features to any specific phase, although we expect that an MCD study on single-phase samples, especially on the α" one, will help in the understanding of the contribution of the nitrogen, if any, to the total magnetic moment.

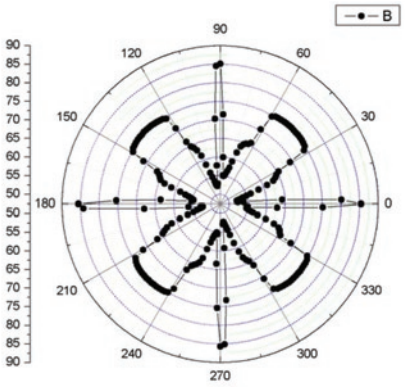

Figure 1. Azimuthal plot, Polar MOKE for a typical FeN sample. We noticed four-fold symmetry characteristic of (001) *fcc* structure. The vertical axis corresponds to coercive field (Oe).

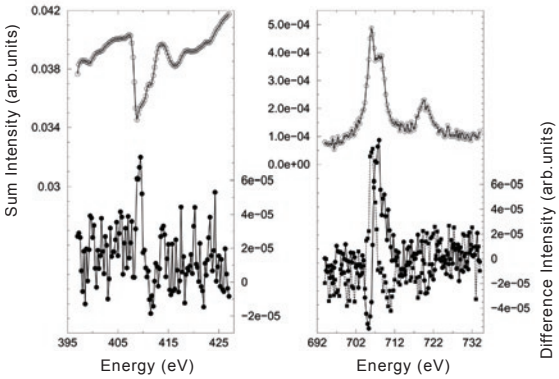

Figure 2. Fe and N reflectivity and XMCD spectra recorded at different angles. Fe spectra were obtained at 8 (dashed/dots) and 11 (continuous/squares) incident angle of the x-rays on the sample. Pure Fe signal (dashed/triangles) was also collected at 8 degrees.

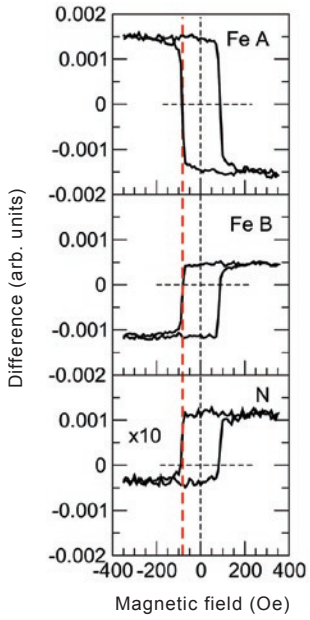

Figure 3. Hysteresis loops recorded at photon energies where the MCD signal presents a maximum. The N and Fe loops present the same coercive field.

BEAMLINE
U12IR

PUBLICATION
L. Mihály, B. Dóra, A. Ványolos, H. Berger, and L. Forró, "Spin-Lattice Interaction in the Quasi-One-Dimensional Helimagnet $LiCu_2O_2$," *Phys. Rev. Lett.*, **97**, 067206 (2006).

FUNDING
Hungarian Research Funds OTKA; Swiss National Science Foundation; U.S. Department of Energy

FOR MORE INFORMATION
László Mihály
Dept. of Physics and Astronomy
Stony Brook University
laszlo.mihaly@sunysb.edu

SPIN-LATTICE INTERACTION IN THE QUASI-ONE-DIMENSIONAL HELIMAGNET $LiCu_2O_2$

L. Mihály[1,2], B. Dóra[2], A. Ványolos[2], H. Berger[3], and L. Forró[3]

[1]Department of Physics and Astronomy, Stony Brook University; [2]Department of Physics, Budapest University of Technology and Economics, Hungary; [3]EPFL, Switzerland

We studied electron spin resonance (ESR) in $LiCu_2O_2$, using the far-infrared/high magnetic field instrumentation at U12IR. The electron spins in this quasi one-dimensional material develop a helical order at low temperature. The excitation of this spin chain results in a field- and frequency-dependent absorption feature in the IR spectrum. We compared the results to a theoretical analysis of the excitation, and we deduced the characteristic anisotropy energy of the spin system. In particular, we determined the interactions that keep the spins confined to a particular plane relative to the crystal.

Ferromagnets are all around us – in the seal on the door of the refrigerator, in the headset of the iPod, and in the computer's hard disk, to name a few examples. In ferromagnets, the interaction between the electrons makes the electron spins (and the associated magnetic moments) line up parallel to each other. What happens if the interaction is different, favoring spins in opposite directions? These materials, the so-called *antiferromagnets*, do not have widespread applications, but they are much less understood and the subject of intensive current research.

In this study we looked at the quasi one-dimensional antiferromagnet, $LiCu_2O_2$. The copper in this compound has two different ionization states. The Cu^{3+} ions are magnetically neutral, but the Cu^{2+} ions carry magnetic moments with spin ½. These ions form quasi one-dimensional chains with a zig-zag "ladders" along the b direction in the crystal (**Figure 1**).

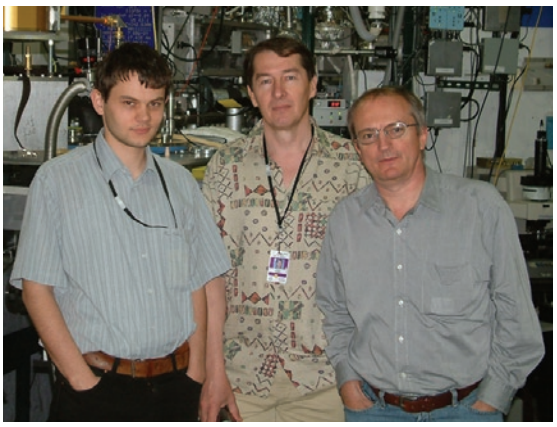

Authors (from left): Bálint Náfrádi, László Forró and László Mihály

In addition to its quasi one-dimensional structure, this material has two other interesting characteristics: The interaction between the moments goes beyond the first neighbors, and the structure has a triangular motif. In antiferromagnets both of these properties lead to *frustration*: it is impossible to find an arrangement of spins so that all interactions lead to a minimum of the energy. (For example, three spins on a triangle cannot all point opposite to each other.) Because of the absence of a simple classical ground state, quantum effects and fluctuations are expected to be important in this material. However, experiments, primarily NMR and neutron scattering, led to a somewhat disappointing conclusion. Instead of a fancy quantum state, the spins exhibit a helical order along the chains, with a wavevector *Q* incommensurate to the lattice. In zero external field all spins were found to be parallel to the ***a-b*** plane. (**Figure 2**) The intricate spin order was interpreted in terms of a classical interacting spin model, with no (or very little) quantum fluctuations. Why does this system of spin ½ electrons behave as if quantum mechanics did not exist? This was the principal question in our study.

We searched for the answer by trying to measure the energy gap in the excitation (magnon) spectrum, since the absence of low-energy excitations stabilizes the classical ground state. The main experimental results of the study are shown in the upper panel of **Figure 3**. There is a weak, but visible resonance at finite frequencies in zero external field. This is a direct measurement of the

energy gap, responsible for suppressing quantum fluctuations.

What is the source of the energy gap? And here is a related question: What makes the spins prefer the a-b plane instead of making a helical structure in some different planes? The anisotropy in interaction between the spins is needed to answer both of these questions. In this case the anisotropy is of the “easy plane” type: The interaction energies are larger for spins in the **a-b** plane than for spins in other directions. We performed theoretical modeling and, by fitting the resonance positions for all field, we determined a single anisotropy parameter for this system. The model also described the observed strong field dependence in the intensity of the resonance.

Interestingly, the model predicted two resonances at finite fields, but the other one (green line in **Figure 3**) was much weaker. We suspected that the instrument we used was not sensitive enough to see this other line, and we sent the sample back to EPFL, (Lausanne, Switzerland), where Bálint Náfrádi did more ESR measurements. The spectrometer in Lausanne operates at a few fixed frequencies, and it cannot be used to create a full two-dimensional map of absorption intensity seen in **Figure 3**, but it is much more sensitive than ours. The resonance line has been found at the predicted position, and we witnessed one of the rare cases when the theory not only interpreted the existing experimental data, but actually predicted the result of a new experiment.

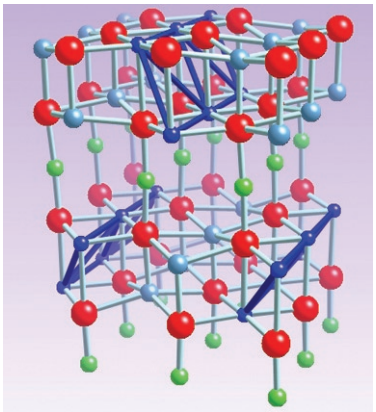

Figure 1. Crystal structure of $LiCu_2O_2$. The magnetic Cu^{2+} ions are dark blue, the non-magnetic copper is green, the lithium is light blue and the oxygen is red. The dark blue bonds emphasize the triangular spin ladder.

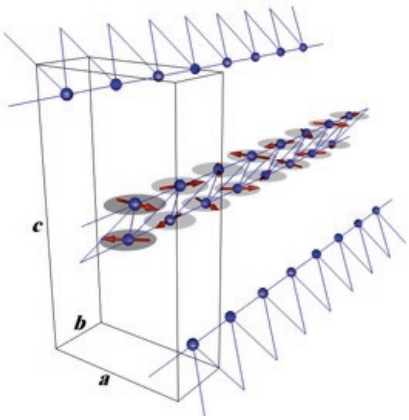

Figure 2. Helical spin order along a triangular ladder in $LiCu_2O_2$. All spin directions are parallel to the ***a-b*** plane, and subsequent spins on the same leg of the ladder make an angle slightly larger than 60°.

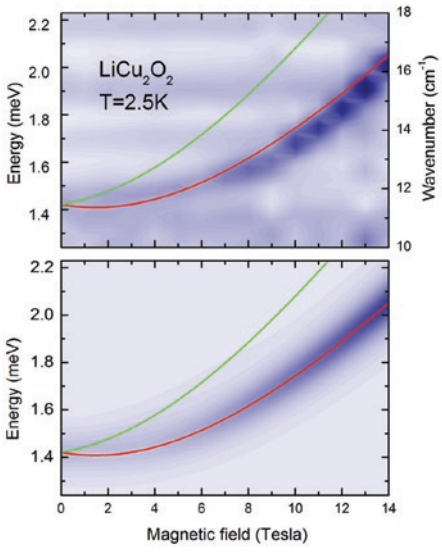

Figure 3. Upper panel: Absorption due to spin resonance as a function of field and frequency. Darker shades indicate stronger absorption. The red line is a theoretical fit to the line position. The green line is another resonance predicted by the theory. Lower panel: Simulated experimental results, based on the calculated intensity of the absorption.

BEAMLINE
X23B

PUBLICATION
X. Zuo, A. Yang, S. Yoon, J. Christodoulides, V.G. Harris, C. Vittoria, "Large Induced Magnetic Anisotropy in Manganese Spinel Ferrite Films," *Appl. Phys. Lett.*, **87**,152505 (2005).

FUNDING
National Science Foundation
Office of Naval Research

FOR MORE INFORMATION
Vincent Harris
Dept. of Electrical and Computer Engineering
Northeastern University
harris@ece.neu.edu

LARGE INDUCED MAGNETIC ANISOTROPY IN PULSED LASER DEPOSITED MANGANESE SPINEL FERRITE FILMS

X. Zuo[1], A. Yang[1], S.-D. Yoon[1], J.A. Christodoulides[2], J. Kirkland[3], V.G. Harris[1], and C. Vittoria[1]

[1]Department of Electrical and Computer Engineering, Northeastern University; [2]Naval Research Laboratory; [3]Sachs Freeman Associates

Here, we report the oxygen-pressure dependence of magnetic anisotropy in pulse laser deposited $MnFe_2O_4$ films. Magnetic anisotropy fields are shown to reach 5 kOe when the films are processed at oxygen pressures below 5 mTorr. The bulk values are around 200 Oe. Further, the preferred direction of magnetization can be aligned either along the film plane (p_{Ox}<8 mTorr), as is typical, or perpendicular to it (p_{Ox}>8 mTorr). The ability to induce large perpendicular magnetic anisotropy in spinel ferrites allows for new applications above S-band frequencies (i.e. phase shifters, filters, isolators, and circulators) to be considered.

Manganese ferrite ($MnFe_2O_4$) is a well-studied spinel ferrite that has low magnetic anisotropy (H_a) at room temperature (K_1 = -33×10^3 erg/cm^3 or $H_u = 2|K_1|/M_S$ = 175 Oe) arising from the low magnetocrystalline anisotropy energy common to cubic structures. This low H_u value limits the applications of this ferrite, or more generally, most cubic spinel ferrites, to frequencies at or below the S-band (1-5 GHz). To overcome this limitation, large magnetic fields are needed to achieve a high ferromagnetic resonance frequency and increase the bandwidth of these materials. These large magnetic fields do not allow for the miniaturization of such potential devices, however.

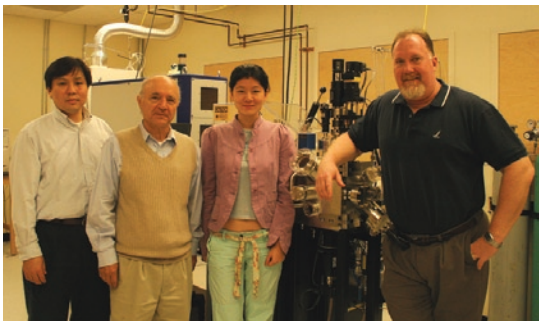

Authors (top, from left) Soack Dae Yoon, Carmine Vittoria, Aria Yang, and Vince Harris (bottom, from left) Joseph Christodoulides, Xu Zuo, and John Kirkland

The enhancement of the magnetic anisotropy in manganese ferrite is related to the oxygen processing pressure used in the pulsed laser deposition process (**Figure 1**). We measure a large growth-induced anisotropy for both low (H_u~5000 Oe) and high oxygen-processing pressures (~1500 Oe). The natures of these magnetic anisotropies are quite different. For example, at low oxygen-processing pressures the magnetization aligns in the film plane, as one might expect from the influence of the demagnetizing energy. However, at high pressures the anisotropy aligns perpendicular to the film plane.

One possible source of this magnetic anisotropy derives from the distribution of magnetic cations within the unit cell. In order to measure the cation distribution, select samples were subjected to EXAFS (extended x-ray absorption fine structure) measurements. Data collection was performed using beamline X23B at the National Synchrotron Light Source in fluorescence yield at room temperature. At the time data were collected, the storage-ring energy was 2.54 GeV and the ring current ranged from 180-250mA. Here, we applied a multi-edge refinement using Athena and Artemis codes of Ravel and Newville, respectively, to analyze the cation distribution of these samples, which were produced under different oxygen pressures. **Figure 2** is a plot of representative best-fit data for both Mn and Fe EXAFS.

With an increase in oxygen pressure used in processing, the octahedral site occupancy of the manganese ions increases, as measured using EXAFS, from 32% to greater than 50%. This is compared with the bulk equilibrium distribution of

20%. Correspondingly, the Fe octahedral occupation decreases from 84% to 75%. The difference in site distribution may be influenced by the difference in cation valence caused by the oxygen pressure, lattice strain from the mismatch in lattice constants and thermal expansion coefficients, or from the large effective quench rate.

As the oxygen pressure used in processing is increased from 1 to 50 mTorr there are significant changes in the physical state of the films. We envision that at low oxygen pressures (p<5 mTorr), anion defects arise from the incomplete oxidation of cations on the surface of the growing film. These defects lead to a greater occupation of Fe^{2+} on the octahedral sites, providing large contributions to the uniaxial anisotropy constant from a single ion anisotropy mechanism. At pressures greater than 8 mTorr, H_u becomes negative and the magnetization aligns perpendicular to the film plane. At higher pressures the ions in the ablated flux experience more collisions en route to the substrate, which reduces their kinetic energy and subsequently reduces their mobility on the surface of the growing film. This lack of mobility leads to the freezing in of cation disorder. In the case of $MnFe_2O_4$ this results in an increase in the inversion of Mn cations, that is, the distribution of Mn on the octahedral sublattice. Another interesting trend seen in the EXAFS analysis is the increase in the oxygen displacement parameter (commonly denoted by *u*). We speculate that this distortion is a direct consequence of the local strain resulting from the cation disorder and results in a tetragonal distortion of the unit cell. This breaking of the crystal symmetry leads to perpendicular anisotropy via a magnetocrystalline anisotropy mechanism.

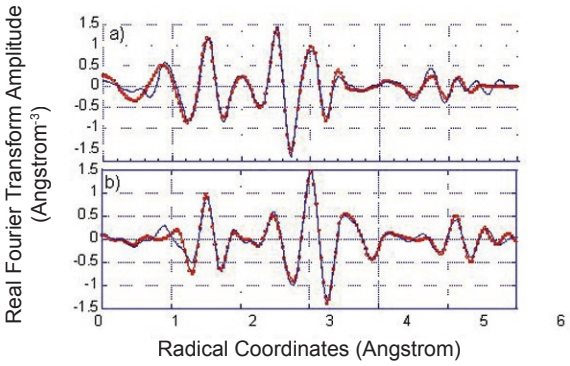

Figure 1. EXAFS data as the real part of the Fourier transform from Mn (a) and Fe (b) K-edge absorption (solid curve) with best fit data (symbols) for a $MnFe_2O_4$ film deposited on a (100) MgO substrate at an oxygen pressure of 1 mTorr.

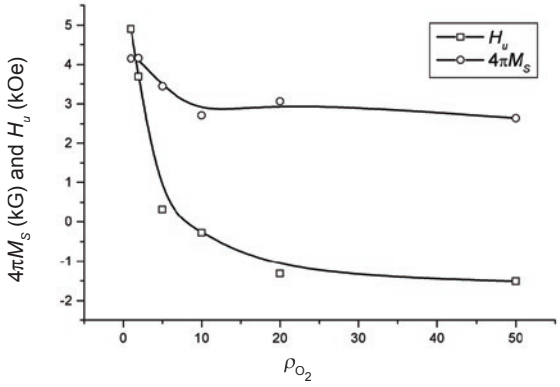

Figure 2. Uniaxial magnetic anisotropy field (H_u) and saturation magnetization ($4\pi M_S$) as functions of oxygen pressure used in PLD growth. M_e is the vector defining the magnetic easy axis.

BEAMLINE
X18A

PUBLICATION
H. Mo, G. Evmenenko, S. Kewalramani, K. Kim, S.N. Ehrlich, and P. Dutta, "Observation of Surface Layering in a Nonmetallic Liquid," *Phys. Rev. Letts.*, **96**, 096107 (2006).

FUNDING
National Science Foundation
U.S. Department of Energy

FOR MORE INFORMATION
Haiding Mo
Dept. of Physics and Astronomy
Northwestern University
mo@northwestern.edu

OBSERVATION OF SURFACE LAYERING IN A NONMETALLIC LIQUID

H. Mo[1], G. Evmenenko[1], S. Kewalramani[1], K. Kim[1], S.N. Ehrlich[2], and P. Dutta[1]

[1]Department of Physics & Astronomy, Northwestern University; [2]National Synchrotron Light Source, Brookhaven National Laboratory

It has previously been reported, on the basis of synchrotron x-ray scattering studies, that many liquid metals have oscillatory density profiles (i.e. smectic-like layering) at their free surfaces. On the other hand, previous x-ray studies of many nonmetallic isotropic liquids have detected no such surface ordering. Is this effect due to the electron gas and therefore unique to liquid metals? We used x-ray reflectivity to study a molecular liquid, tetrakis(2-ethylhexoxy)silane. When cooled to 227K and below, the bulk remains liquid but density oscillations appear at the surface. There is only short-range lateral order, just as in liquid metals and unlike surface freezing. Our results confirm theoretical predictions that a surface-layered state will appear in any liquid at sufficiently low temperatures, if not preempted by freezing.

The traditional picture of the free surface of a liquid is that the density changes monotonically from that of liquid bulk to that of the vapor. This picture describes dielectric liquid surfaces near room temperature quite well. However, x-ray scattering experiments have established that liquid metals and metallic alloy surfaces are layered.

Recently, Chacón *et al* concluded from simulations that surface layering will appear in any liquid below about $0.2T_c$, where T_c is the critical temperature, provided that it is not preempted by freezing. According to this theory, metallic liquid surfaces are found to be layered because they have high T_c values and so room temperature is below $T/T_c \sim 0.2$, while T_c is low for most dielectric liquids and so room temperature corresponds to $T/T_c \sim 0.4 - 0.5$. Many dielectric liquids will freeze above $T/T_c \sim 0.2$, making the necessary temperatures inaccessible. If one finds a dielectric liquid with relative high T_c and low melting point T_m, so that T_m/T_c is less than 0.2, one should be able to observe surface layering in this dielectric liquid.

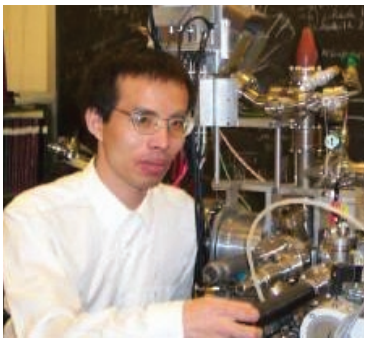

Haiding Mo

We have studied the surface of a molecular liquid, tetrakis(2-ethoxyhexoxy)-silane (TEHOS), using x-ray reflectivity and confirmed the prediction of Chacón. TEHOS is an isotropic (non-liquid-crystalline) dielectric liquid. The molecule consists of one Si and four O atoms in the center, surrounded by four saturated branched alkanes, forming a "wax coating" that makes the molecules nonreactive and roughly spherical. Viscosity measurements have shown that it is a fluid down to at least 219 K. Using x-ray scattering in transmission, and differential scanning calorimetry, we have found no evidence of a bulk phase transition down to 190 K. Its T_c is estimated to be ~950 K.

In order to easily cool the liquid, we prepared ~5000Å films of TEHOS supported on silicon substrates, which were formed by putting a few drops of liquid on the substrates, allowing the liquid to spread, and then draining the excess. There is no interference between the two interfaces of the films because the film thickness is much larger than the x-ray coherence length. To avoid seeing features in the reflectivity due to solid-liquid interface layering, we prepared and used substrates with RMS surface roughness >20Å. We have confirmed that the scattering features due to interfacial layers can no longer be seen when the substrate surface is rough.

Figure 1 shows the specular reflectivity R divided by the Fresnel reflectivity R_F at several temperatures. At 237 K (and at higher temperatures, not shown here), the scans are featureless, similar, to those from typical nonlayered dielectric liquids surfaces. At lower temperatures, distinct reflectivity oscillations are seen. A peak occurs at about 0.6 $Å^{-1}$, which matches precisely the peak position of the bulk scattering data, and signifies that the layering occurs at the surface. The temperature threshold corresponds to $T/T_c \approx 0.25$.

We fit the data in **Figure 1** by modifying the 'semi-infinite series of Gaussians' model frequently used to fit reflectivity data from liquid metal surfaces. Good fits were obtained as shown as solid curves in **Figure 1**. **Figure 2** shows the electron densities obtained from the fit. The dashed lines are the best-fit density functions; the solid lines are the same functions with the capillary width set to zero. In other words, the solid lines show what the surface profiles would look like if they had not been broadened by thermal capillary waves. The profiles show that at high temperature the density changes monotonically, but at low temperatures there are layers. The in-plane scattering data show only liquid-like order, just as at liquid metal surfaces.

Our results confirm the theoretical prediction that dielectric liquids will show layered structure at the surface if cooled down to sufficiently low temperature. In other words, the surface-layered state is a general property of the liquid phase, not one that is limited to liquid metals.

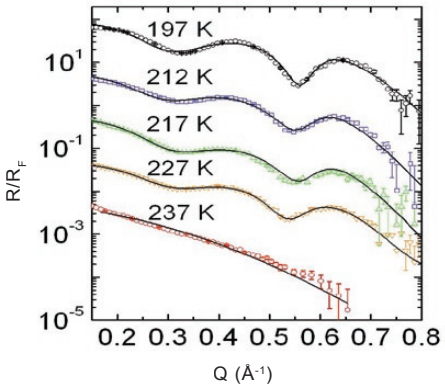

Figure 1. Normalized specular reflectivity for ~5000 Å TEHOS films on rough silicon wafers at different temperatures. Lines are best fits using the electron density profiles shown in Figure 2. The data are displaced vertically for clarity.

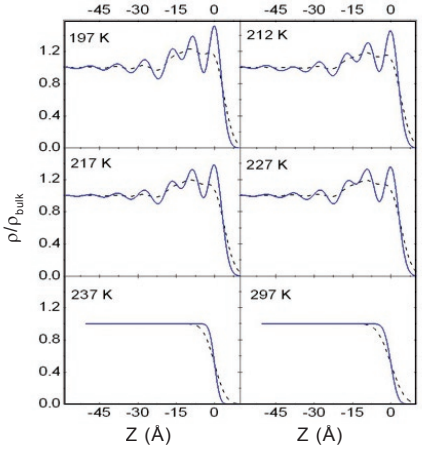

Figure 2. The dashed lines show best-fit electron densities as functions of distance from the surface for ~5000 Å TEHOS films at different temperatures. The solid lines show the density profiles with capillary broadening removed.

BEAMLINE
U12IR

PUBLICATION
F. Wang, D. Cheever, M. Farkhondeh, W. Franklin, E. Ihloff, J. van der Laan, B. McAllister, R. Milner, C. Tschalaer, D. Wang, D.F. Wang, A. Zolfaghari, T. Zwart, G.L. Carr, B. Podobedov, and F. Sannibale, "Coherent THz Synchrotron Radiation from a Storage Ring with High Frequency RF System," *Phys. Rev. Lett.*, **96**, 064801 (2006).

FUNDING
U.S. Department of Energy; Massachusetts Institute of Technology

FOR MORE INFORMATION
Fuhua Wang
MIT-Bates Linear Accel. Center
fwang@mit.edu

COHERENT THZ SYNCHROTRON RADIATION FROM A STORAGE RING WITH HIGH FREQUENCY RF SYSTEM

F. Wang[1], D. Cheever[1], M. Farkhondeh[1], W. Franklin[1], E. Ihloff[1], J. van der Laan[1], B. McAllister[1], R. Milner[1], C. Tschalaer[1], D. Wang[1], D.F. Wang[1], A. Zolfaghari[1], T. Zwart[1], G.L. Carr[2], B. Podobedov[2], and F. Sannibale[3]

[1]MIT-Bates Linear Accelerator Center; [2]National Synchrotron Light Source, Brookhaven National Laboratory; [3]Lawrence Berkeley National Laboratory

Coherent synchrotron radiation (CSR) generated in an electron storage ring is a promising source for stable, high-intensity terahertz (THz) radiation. The achievable CSR power and spectrum depend strongly on ring radiofrequency (RF) system parameters, mainly RF frequency and gap voltage. We report the initial results of CSR generation in the MIT-Bates South Hall storage ring (SHR), which is equipped with a unique high-frequency S-band RF system. The CSR enhancement is 10,000 times above background for wave numbers near 3 cm^{-1} with a bunch current of 1.1 μA. Suppressing beam instabilities emerged as the first challenge in pursuing a very brilliant ring-based THz source, with further investigations underway.

The THz region of the electromagnetic spectrum lies between the infrared and the microwave. Only over the past decade has this region become more available for scientific research and applications as moderate intensity sources have emerged. Accelerator-based CSR provides a category of broadband THz sources with much higher power. The stability of radiation flux, familiar to many synchrotron radiation users in synchrotron light sources, is also a distinguishing characteristic of the CSR obtained from a ring-based THz source.

Source research efforts in past years predict that the achievable stable CSR power and spectrum of a ring-based source are strongly dependent on ring RF frequency and gap voltage. At present, the RF frequencies employed in light-source storage rings are 500 MHz and below for practical reasons. For example, the BESSY II storage ring, at this frequency, has demonstrated CSR in the THz region. The MIT-Bates SHR is the only storage ring that is equipped with an S-band (2.856 GHz) RF system. The system was originally designed to facilitate uniform pulse stretching operation for nuclear physics. However, it has also been successfully operated in a storage mode for years with this RF system. This provides us with an excellent opportunity to investigate the potential of a ring-based source at its technical limits.

Authors (labeled 1-12, respectively): Fuhua Wang, Ernie Ihloff, Wilbur Franklin, Defa Wang, Larry Carr, Chris Tschalaer, Jan van der Lann, Boris Podobedov, Richard G. Milner, Abbi Zolfaghari, Manouchehr Farkhondeh, and Dong Wang

To attain short electron bunch length (~ 1 mm, rms), the SHR optics were turned into a low-momentum compaction (α) lattice, in which electrons with different momenta would have smaller path-length differences. As expected with the higher RF frequency, a bunch length of about 1mm rms was attained with a moderate α value of 0.0006, which is favorable for stable operation.

The CSR radiation was extracted through a 6-mm-thick fused quartz view port followed by two parabolic reflectors that collected the light and matched it to a spectrometer. The spectrometer was a modified commercial Nicolet Magna 860 Fourier Transform Infrared (FTIR) Spectroscopy interferometer with a liquid-helium-cooled silicon composite bolometer as the detector. The spectrometer could sense CSR to wave numbers as low as 1 cm^{-1}. The spectrometer assembly was carefully tuned and tested at the NSLS. Strong CSR signals were detected in the sub-THz region. The enhancement of CSR compared to the 300 K blackbody radiation background was 10,000 times, peaked near a wave number of 3 cm^{-1}, and had a very low electron bunch current of 1.1μA. Most

of the 1812 RF buckets of the ring were filled, as it was the only available SHR injection mode at the time. The signal of the incoherent THz radiation with a few mA circulating beam was below the detection limit. The coherency tests of the radiation included dependency of the spectrum intensity on the bunch current and bunch length. The CSR radiation spectra from electron bunches with different bunch lengths, and the quadratic dependency of intensity on bunch current, are shown in **Figure 1** and **Figure 2**.

Beam longitudinal instabilities were observed in both the radiation spectrum and time domain signals as well as in the beam longitudinal profile measurements. The instabilities limited the maximum bunch current that could be used for the tests and resulted in deteriorated radiation coherency at higher bunch intensities. Preparation for further tests is underway to address the technical challenges uncovered here.

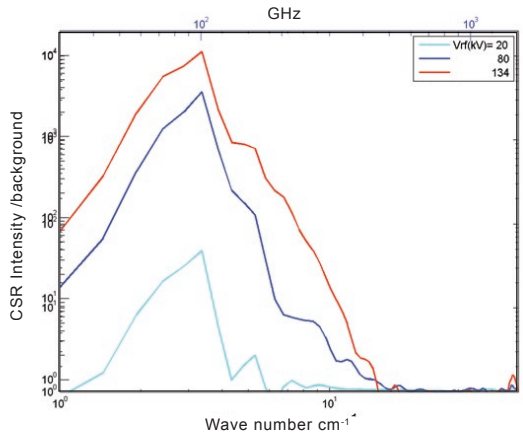

Figure 1. Intensity ratio of CSR to background for different bunch lengths. Total stored current I = 2 mA. Measured rms bunch length (ps): 7.6, 4.4, 4.0, corresponding to the RF peak voltage V_{RF} (kV) of 20, 80, and 134.

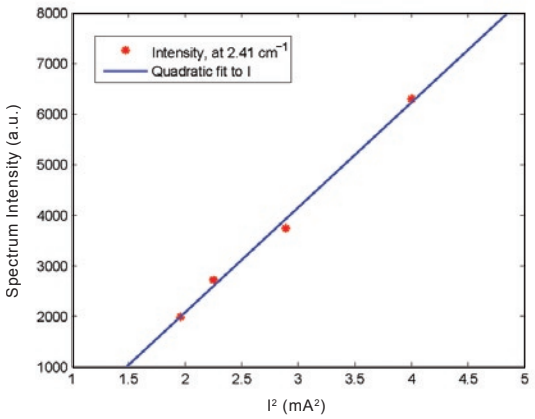

Figure 2. Quadratic dependency of spectrum intensity of CSR to beam current.

BEAMLINES
U12IR, U10A

PUBLICATION
R.P.S.M. Lobo, J.D. LaVeigne, D.H. Reitze, D.B. Tanner, Z.H. Barber, E. Jacques, P. Bosland, M.J. Burns, and G.L. Carr, "Photoinduced Time-resolved Electrodynamics of Superconducting Metals and Alloys," *Phys. Rev. B*, **72**, 024510-10 (2005).

FUNDING
U.S Department of Energy; Centre National de la Recherche Scientifique (France); City of Paris

FOR MORE INFORMATION
Ricardo Lobo
LPS-ESPCI and CNRS
lobo@espci.fr

DISTURBING SUPERCONDUCTIVITY WITH LIGHT

R.P.S.M. Lobo[1], D.B. Tanner[2], and G.L. Carr[3]

[1]CNRS and ESPCI, France; [2]Department of Physics, University of Florida; [3]National Synchrotron Light Source, Brookhaven National Laboratory

Superconductors can be sent out of equilibrium by using light to break Cooper pairs. Using a pump-probe setup, we studied the time-dependent behavior of thus depleted superconductivity. Laser pulses were utilized to break pairs and synchrotron far-infrared (a.k.a. terahertz) pulses measured the spectra as a function of time in the sub-nanosecond scale. This measurement allowed us to determine how electrons recombine into pairs, bringing the system back to equilibrium. The direct observation of the superconducting gap diminution, expected for an excited superconductor, was measured for the first time.

The Bardeen, Cooper, and Schrieffer (BCS) theory of superconductivity showed that, in a classical superconductor, zero electrical resistance is a consequence of electrons pairing themselves. These "Cooper pairs" have a typical binding energy (2Δ) that leads to a gap for unpaired electrons at the Fermi energy. However, Cooper pairs can be broken into two electrons if they are given an energy larger than the gap. One of such possible processes is the absorption of a photon of energy greater than 2Δ. As Cooper pairs are energetically more favorable than electrons, the electrons eventually reform the pair. The full relaxation process is a bit more complex, as shown in **Figure 1**. In equilibrium, all the electrons in a superconductor should form pairs below the Fermi level (**Figure 1A**). The absorption of a photon will excite pairs across the gap and produce electrons above the Fermi energy (**Figure 1B**). We then reach a situation where the "unstable" excited electrons want to recombine into a pair. Energy conservation imposes that the energy gain occurring when electrons form a pair must be emitted, usually as a crystal lattice vibration (phonon). Nevertheless, phonons can also break pairs; therefore, the emitted phonon is able to produce two new excited electrons. This subtle competition between electrons willing to recombine and phonons trying to break pairs only ends because, eventually, phonons become unavailable by either relaxing to very low energies or simply escaping the material. The whole process of relaxation is schematized in **Figure 1C**.

Ricardo Lobo

A collaboration between the University of Florida and the NSLS built a pump-probe setup to study systems out of equilibrium. The facility consists of a Ti:Sapphire pulsed laser synchronized with the electron bunches of the VUV-IR ring. We utilized the laser pulses to break pairs (pump) in several conventional superconductors, including Pb, Nb, and NbN, and the far-infrared light from beamlines U12IR and U10A to probe the changes in the optical response of the superconductor, which strongly depends on the number of Cooper pairs. By delaying the laser pulses with respect to the synchrotron bunches, we can obtain the time-dependent optical response for the specimen.

Figure 2 shows the integrated far-infrared transmission for several out-of-equilibrium superconductors as a function of time and temperature. At zero delay, both the laser and synchrotron pulses arrive at the sample at the same time and the changes in the optical transmission are maximum. As we push the synchrotron pulses further away

from the laser, we allow enough time for some pairs to recombine and the optical transmission to recover its equilibrium value. Finally, we obtained the measurement of the non-equilibrium infrared spectrum (**Figure 3**), which is the first direct determination of the superconducting gap shrinkage expected for superconductors with excess unpaired electrons.

This technique is now being used to analyze more complex superconductors such as the cuprate high critical-temperature materials and the "two-superconductors-in-one" material MgB_2.

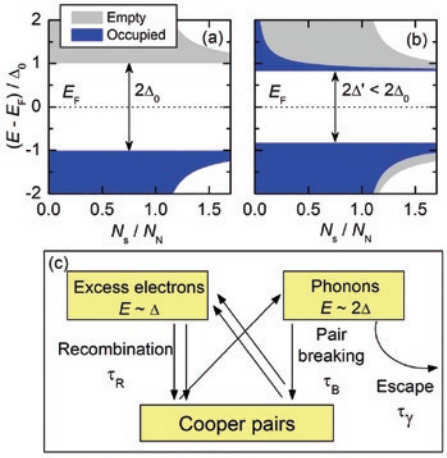

Figure 1. Density of states for a BCS superconductor (A) in equilibrium and (B) where pairs were broken into electrons. Panel (C) shows schematically the processes involved when the system relaxes back to equilibrium. Each process (recombination, pair breaking, and phonon escape) is characterized by a different time scale.

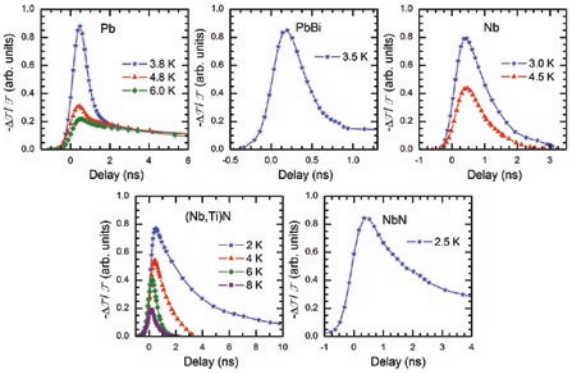

Figure 2. Relative variation in the far-infrared transmission of several classical superconductors as a function of temperature and time.

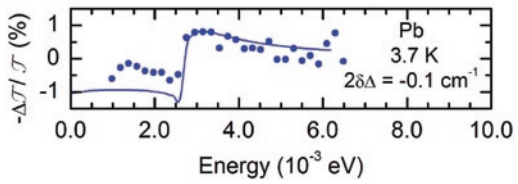

Figure 3. Non-equilibrium far-infrared spectrum for superconducting lead (dots) and expected response from BCS theory (line). The jump in the curve is a direct measurement of the superconducting gap shrinkage expected for a superconductor with excess unpaired electrons.

BEAMLINE
X18B

PUBLICATION
S. Choi, P.A. O'Day, N.A. Rivera, K.T. Mueller, M.A. Vairavamurthy, S. Seraphin, and J. Chorover, "Strontium Speciation During Reaction of Kaolinite with Simulated Tank-waste leachate: Bulk and Microfocused EXAFS Analysis," *Environ. Sci. and Technol.*, **40**, 2608-2614 (2006).

FUNDING
U.S. Department of Energy

FOR MORE INFORMATION
Peggy A. O'Day
School of Natural Sciences
University of California
poday@ucmerced.edu

STRONTIUM SPECIATION DURING REACTION OF KAOLINITE WITH SIMULATED TANK-WASTE LEACHATE: BULK AND MICROFOCUSED EXAFS ANALYSIS

S. Choi[1,2], P.A. O'Day[2], N.A. Rivera[2], K.T. Mueller[3], M.A. Vairavamurthy[4], S. Seraphin[5], and J. Chorover[1]

[1]Dept. of Soil, Water and Environmental Science, Univ. of Arizona; [2]School of Natural Sciences, Univ. of California; [3]Dept. of Chemistry, The Pennsylvania State Univ.; [4]Brookhaven National Laboratory; [5]Dept. of Materials Science and Engineering, Univ. of Arizona

Radioactive strontium (^{90}Sr) is an important constituent of complex wastes produced from past nuclear weapons production and stored in underground tanks at DOE sites (e.g., Hanford, WA). Using bulk and microfocused EXAFS spectroscopy, we examined temporal changes in solid phase Sr speciation in kaolinite samples reacted for 1 to 369 days with high-pH, high ionic strength synthetic tank-waste leachate containing Sr^{2+} and Cs^{+}. Our results and supporting characterizations show that Sr forms a transient carbonate phase at early reaction times that is replaced by incorporation into neoformed, cage-type feldspathoid aluminosilicate minerals, with Sr becoming dehydrated and non-extractable with longer reaction times. Formation of feldspathoid minerals as products of sediment alteration may help sequester contaminants at sites such as Hanford.

The remediation of radioactive contamination at former weapons testing and production sites is a costly and protracted legacy of the U.S. post-WWII military industrial complex. ^{90}Sr and ^{137}Cs are important contaminants at a number of Department of Energy (DOE) sites, and particularly at the Hanford (WA) site, because their half-lives fall within human timescales (29 and 30 years, respectively), they are potentially mobile in groundwater, and they are bioavailable substituents for Ca^{2+} and K^{+}, respectively, in organisms. Large volumes of high-level radioactive waste and contaminant metals were generated from plutonium production and separation processes, much of which was stored in underground tanks. At least 67 single-shell tanks containing high-level wastes are known to have leaked into vadose zone sediments, where caustic fluids have reacted with sediment minerals and groundwater to generate a complex history of mineral alteration, fluid evolution, and waste dispersal.

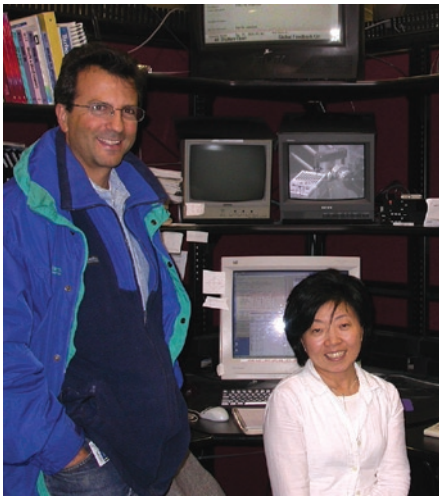

Authors Jon Chorover and Sunkyung Choi

Our research team has examined the reaction of high-pH, high ionic strength synthetic tank-waste leachate (STWL) with model clay minerals and Hanford sediments in the laboratory to unravel the geochemical processes that control subsurface contaminant uptake or release. Our approach is to link quantitative macroscopic measures of contaminant partitioning to the molecular-scale mechanisms that mediate the process, particularly those that may lead to irreversible sequestration of contaminants into a solid phase. This study examined temporal changes in solid-phase Sr speciation using bulk and microfocused EXAFS analyses in samples of STWL containing Sr^{2+} and Cs^{+} (at 10^{-3} m) reacted with the clay mineral kaolinite from 1 to 369 days. Bulk EXAFS spectral analyses showed that Sr initially forms a precipitate by 7 days with a local structure similar to $SrCO_3$(s). At 33 days, the bulk sample spectrum showed few features beyond the first shell of oxygen atoms, but microfocused EXAFS of three individual particles in the same sample indicated distinct differences **(Figure 1)**. Quantitative analyses revealed a mixture of hydrated and dehydrated Sr associated with neoformed sodalite-type (feldspathoid) phases. At aging times of 93 days and longer, bulk EXAFS spectra and supporting characterization methods indicated an increasing fraction of non-exchangeable Sr with a local structure consistent with incorporation into increasingly crystalline aluminosilicate particles, particularly sodalite **(Figure 2)**. A combination of spectro-

scopic and microscopic characterization studies by our group, including NMR, XRD, SEM/TEM, and FTIR, indicated the formation of both sodalite and cancrinite, with cancrinite forming at the expense of sodalite for reaction times longer than 93 days. The Sr-EXAFS analysis uniquely identified the stronger association of Sr with sodalite-type cage structures, rather than cancrinite-type structures, in these samples and showed that local dehydration of Sr within the neoformed phases was associated with increasingly irreversible sequestration. Although this experimental system is greatly simplified from field conditions, an important observation is that trapping of radionuclides can occur if they are present as cage-structure aluminosilicates form and age as alteration products of local Si-bearing sediment minerals. Sequestration of radionuclides by feldspathoid mineral trapping may be an important mechanism for retardation near waste sources because re-release to solution requires mineral dissolution rather than ion exchange.

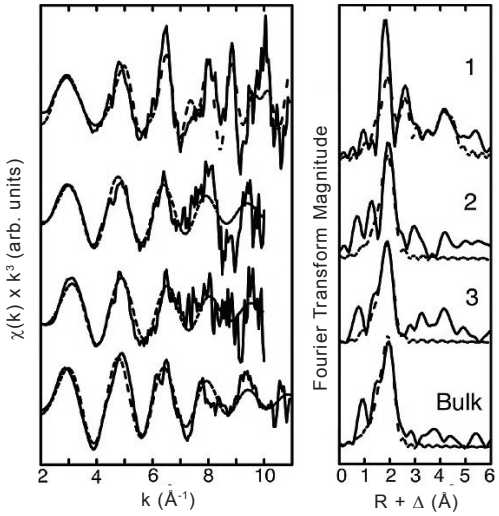

Figure 1. From left: SEM images, synchrotron Sr x-ray microprobe maps, and microfocused Sr K-edge EXAFS of three neoformed particles from a kaolinite sample reacted for 33 days with synthetic tank-waste leachate. A bulk EXAFS spectrum of the sample is shown for comparison. The bulk spectrum was collected at the NSLS (beamline X18B) and the microfocused spectra were collected at the APS (GSECARS beamline 13-ID-C). Particles were dispersed on carbon tape and imaged with SEM to identify isolated Sr-bearing particles prior to synchrotron analyses. X-ray element maps were made prior to EXAFS data collection in order to re-locate the Sr-bearing particles.

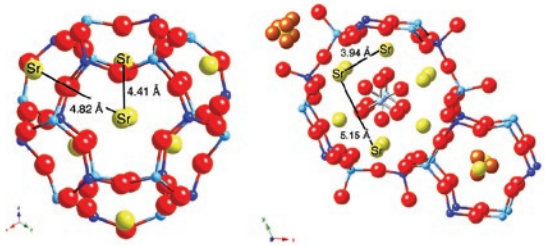

(A) basic sodalite (B) nitrate cancrinite

Figure 2. (A) Atomic structure of basic sodalite, which has a single cage and cation site. Sr (yellow atoms) occupies the Na site; surrounding anions and water within cages are omitted for clarity; (B) Nitrate cancrinite has two distinct cation sites in large (sodalite-type) and small (cancrinite-type) cages; Sr is shown occupying Na sites within the sodalite cage, nitrate groups occupy the counter-anion position in the center of the cage, and Na and water are shown in the cancrinite cage. Nearest interatomic cation-cation positions in the ideal structures are indicated.

BEAMLINE
X19A

PUBLICATION
G. Toevs, M.J. Morra, M.L. Polizzotto, D.G. Strawn, B.C. Bostick, and S. Fendorf, "Metal(loid) Diagenesis in Mine-impacted Sediments of Lake Coeur d'Alene, Idaho," *Environ. Sci. Technol.*, **40**, 2537-2543 (2006).

FUNDING
Idaho Water Resources Research Institute; Idaho Agricultural Experiment Station; Inland Northwest Research Alliance; EPA-STAR Fellowship Program; NSF-Environmental Molecular Science Institute

FOR MORE INFORMATION
Michael J. Morra
Soil & Land Resources Division
University of Idaho
mmorra@uidaho.edu

METAL(LOID) DIAGENESIS IN MINE-IMPACTED SEDIMENTS OF LAKE COEUR D'ALENE, IDAHO

G.R. Toevs[1], M.J. Morra[1], M.L. Polizzotto[2], D.G. Strawn[1], B.C. Bostick[2,3], and S. Fendorf[2]

[1]Soil & Land Resources Division, University of Idaho; [2]Department of Geological and Environmental Sciences, Stanford University; [3]Department of Earth Sciences, Dartmouth College

Mining operations in northern Idaho have resulted in Pb, As, Hg, Cd, and Zn contamination of Lake Coeur d'Alene. Unfortunately, limited knowledge of sediment biogeochemistry precludes accurate modeling of metal(loid) flux to the water. We characterized the sediments to elucidate diagenetic processes potentially controlling contaminant release, showing that flood events bury ferric oxides present at the sediment-water interface, transitioning them to an anoxic zone where reductive dissolution occurs. Insufficient sulfur limits sulfidic mineral formation, but high carbonate concentrations promote siderite formation. Metal(loid) sorption and release is thus a dynamic process intimately tied to reactions involving iron minerals within the sediments.

Lake Coeur d'Alene (CDA) is a natural lake of glacial origin located in northern Idaho. As a result of mining activity within the region, mine tailings and mill slurries contaminated with Pb, As, Cd, Zn and other metal(loid)s have accumulated in the sediments of Lake CDA. Prior research to characterize sediment geochemistry has produced inconsistent and contradictory results. Our objective was to characterize Lake CDA sediments using spectroscopic techniques combined with *in situ* interstitial water data, thereby identifying the dominant solid-phase minerals and diagenetic processes controlling interstitial water metal(loid) concentrations. Ultimately, our results will facilitate the prediction of contaminant release from the sediments to the overlying water column.

Two sample sites, Harlow Point (HP) and Peaceful Point (PP), were located in the southern portion of Lake CDA in an area highly impacted by metal(loid)s. An uncontaminated control site, St. Joe (SJ), was also established. Interstitial water was collected *in situ* utilizing Plexiglas equilibrium, dialysis samplers (peepers) and cores collected in polycarbonate tubes.

Gordon Toevs

Sulfur x-ray absorption near-edge structure (XANES) spectroscopy analyses were conducted at the National Synchrotron Light Source on beamline X19A. Iron XANES and extended x-ray absorption fine structure (EXAFS) spectroscopy analyses were conducted at the Stanford Synchrotron Radiation Laboratory on beamline 4-3.

Sediment sulfur was speciated in an attempt to identify specific components of the sediment solid phase that potentially participate in metal(loid) retention. XANES data clearly indicate that pyrite was the principle S mineral detected at the contaminated sites **(Figure 1)**. Ester-bound sulfate decreased with depth at all sites **(Figure 1)**. Increased pyrite percentages with depth are consistently accompanied by a corresponding decrease in organic ester sulfate species. Thus, diagenetic alteration of ester-bound sulfate is likely important in the generation of pyrite in these sediments. However, metal(loid) partitioning into and on sulfidic minerals in Lake CDA sediments must be re-evaluated given the high Fe to S ratios of the sediments.

The speciation of sedimentary iron, achieved with XAS spectra, offers additional evidence for the diagenesis of sedimentary Fe and S. Contaminated sites show an obvious trend in the speciation of solid-phase Fe that reflects changes in sediment redox potentials with depth, with both sites displaying a decrease in Fe(III) minerals below the

suboxic boundary and a concomitant increase in Fe(II)-containing solids **(Figure 2)**.

Linear combination of Fe-EXAFS spectra indicated the majority of the Fe(II) increase was in the form of siderite. Thus, a cycle of Fe-diagenesis is established where Fe(III) minerals buried by depositional events undergo reductive dissolution in the suboxic and anoxic sediments, forming Fe(II) that precipitates as siderite or diffuses to the oxic zone and reprecipitates as an Fe(III) mineral.

Ferric (hydr)oxides at the sediment-water interface restrict contaminant migration, but diagenetic reactions that occur during sediment burial and exposure to reducing conditions release metal(loid)s into the interstitial water. Metal(loid) cycling between the solid and aqueous phases in Lake CDA is thus a dynamic process intimately tied to diagenetic reactions involving Fe minerals within the sediments.

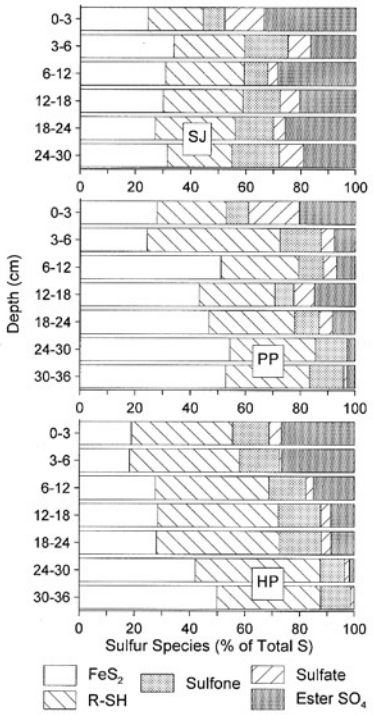

Figure 1. Comparison of S species as determined by S-XANES analyses of Lake Coeur d'Alene sediments at the contaminated sites (PP and HP) and the control site (SJ). Data shown for each depth are an average of two spectra from adjacent cores collected in May 2002 and have a fitting accuracy of ±5%. Maximum total sulfur within all sediments was less than 0.5% by weight.

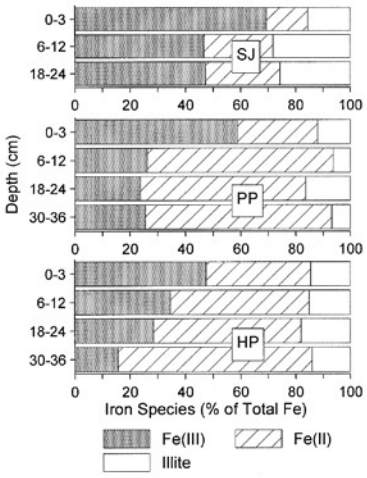

Figure 2. Iron XANES analyses of Lake Coeur d'Alene sediments as determined from linear combination fittings of Fe(II) and Fe(III) proxies and illite. Data are from cores collected in May 2002 at the control site (SJ) and two contaminated sites (PP and HP) and have a fitting accuracy of ±5%. Iron comprised up to 10% of the sample by weight at the contaminated sites.

BEAMLINE
X19A

PUBLICATION
S. Sato, D. Solomon, C. Hyland, Q.M. Ketterings, and J. Lehmann, "Phosphorus Speciation in Manure and Manure-Amended Soils Using XANES Spectroscopy," *Environ. Sci. Technol.*, **39**, 7485–7491 (2005).

FUNDING
U.S. Department of Agriculture; N.Y. Department of Agriculture and Markets

FOR MORE INFORMATION
Shinjiro Sato
Dept. of Crop and Soil Sciences
Cornell University
shinjiro@ifas.ufl.edu

PHOSPHORUS SPECIATION IN MANURE AND MANURE-AMENDED SOILS USING XANES SPECTROSCOPY

S. Sato, D. Solomon, C. Hyland, Q.M. Ketterings, and J. Lehmann

Department of Crop and Soil Sciences, Cornell University

It is important to know what inorganic phosphorus (P) species are being formed in soils subjected to high, long-term poultry-manure application in order to understand P accumulation and release patterns. Phosphorus K-edge XANES spectra of fresh manure showed no evidence of crystalline P minerals, but did exhibit a dominance of soluble calcium phosphates (CaP) and free and weakly bound phosphates. Soils with a short-term manure history contained both Fe-associated phosphates and soluble CaP. Long-term application resulted in a dominance of CaP and a transformation from soluble to more stable CaP species. However, none of the amended soils showed the presence of crystalline CaP. Maintaining a high pH is therefore an important strategy that can be used to minimize P leaching in these soils.

Poultry manure is frequently applied to agricultural fields to supply essential nutrients to crops, subsequently increasing yields. However, apart from plant uptake, manure P can be lost as the result of surface erosion and/or leaching. Such losses have resulted in the eutrophication of watersheds in the past. Soil pH plays a critical role in P retention in soils by, for instance, changing the solubility of secondary Fe, Al, and CaP minerals in soils. Manure is a well-known liming material; however, it is unknown how manure application impacts the solubility and transformation of these secondary P compounds. Our previous studies suggest an increase in the proportion of CaP in the total P pool in soils with long-term manure application. Using P K-edge XANES, this study aims to assess the CaP species formed in an originally acidic soil in response to high and long-term (up to 25 years) manure applications.

We measured standards of inorganic phosphate forms for comparison with spectra of the investigated soils (**Figure 1**). Both the spectra of the Fe-oxide strengite (STR) and the Al-oxide variscite (VAR) featured a peak at 2156 eV (**Figure 1e**), but were distinguished by the presence and absence of a peak at 2146 eV (**Figure 1a**) for STR and VAR, respectively. The most characteristic feature for all of the CaP species was a peak at 2159 eV (**Figure 1f**) and a shoulder between 2151 eV (**Figure 1c**) and 2152 eV (**Figure 1d**). A closer observation of the shoulder (**Figure 1c-1d**) revealed this shoulder to be better expressed for CaP species with decreasing solubility. The solubilities of these CaP species generally decrease as follows: dibasic calcium phosphate dehydrate (DCPD) > dibasic calcium phosphate (DCP) > amorphous calcium phosphate (ACP) ≈ *β*-tricalcium phosphate (TCP) > octacalcium phosphate (OCP) > hydroxyapatite (HAP).

Authors (from left) Shinjiro Sato, Johannes Lehmann, and Dawit Solomon

The manure spectrum showed only two small shoulders that are characteristic of CaP species (**Figure 2Ac-d and 2Af**), but the overall spectra rather resembled that for Aq-PO_4. The linear combination fitting result showed that this manure contained 18% DCP, 35% ACP1, and 47% Aq-PO_4. Aq-PO_4 in the fitting results is considered a group of “free and weakly bound (adsorbed) phosphates,” since it is not possible to use XANES alone to quantitatively distinguish Aq-PO_4 from phosphate adsorbed on minerals. The forest soil spectrum showed a shoulder (**Figure 2Aa**) that is indicative of FeP but was significantly widened compared to STR, suggesting the presence of a combination of phosphates in strengite and phosphates adsorbed to the surfaces of various Fe-oxides. The linear combination fitting resulted in 38% ACP1, 32% STR, and 30% Aq-PO_4 in the forest soil. Spectra of the manure-applied soils showed a decrease and disappearance of the FeP shoulder (**Figure 2A-2Ca**) and an increase in the

intensity of the CaP shoulder (**Figure 2A-2Cc**) and the CaP peak (**Figure 2A-2Cf**) as the application history increased. In fact, the linear combination fitting suggested that long-term manure application resulted in the transformation of relatively soluble CaP species (**Figure 2A**, S2 soil: 8% DCP and 19% ACP1) into more crystalline CaP species (**Figure 2C**, L1 soil: 13% ACP1 and 43% TCP) in soils over time. Yet, the most crystalline and therefore least soluble CaP form, such as HAP, was not found in the studied soils. Since CaP minerals are least soluble at high pH, maintaining a high pH may be an important strategy for minimizing P leaching in these soils.

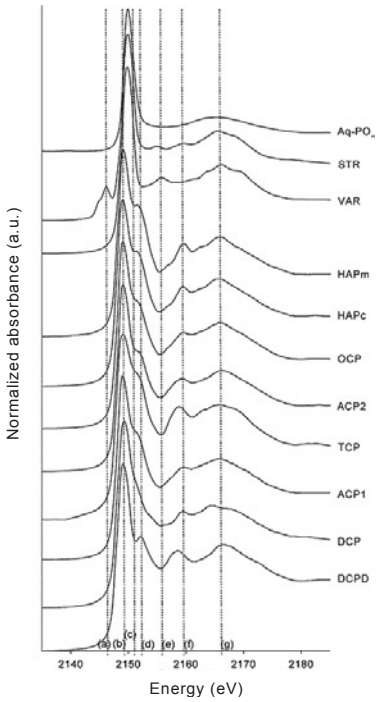

Figure 1. Phosphorus K-edge XANES spectra for different inorganic phosphate standard species. The dashed lines show energy levels of importance to indicate unique spectra features for different species: (a) STR; (b) absorption edge (white line); (c)–(d) CaP species related to their solubility; (e) STR and VAR; (f) CaP species; (g) oxygen oscillation. Aq-PO_4 is $H_2PO_4^-$ species in 0.1 M NaCl solution. STR: strengite, VAR: variscite, HAP: hydroxyapatite, OCP: octacalcium phosphate, ACP: amorphous calcium phosphate (phase 1 and 2), TCP: β-tricalcium phosphate, DCP: dibasic calcium phosphate, and DCPD: dibasic calcium phosphate dehydrate.

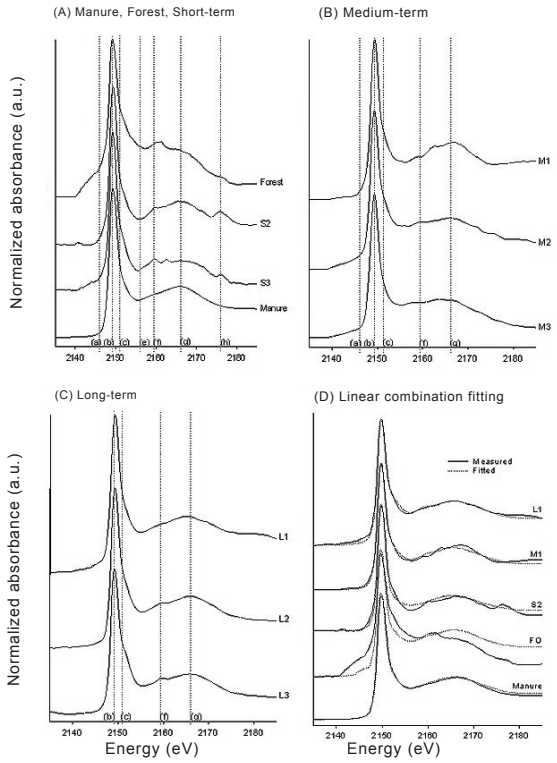

Figure 2. Phosphorus K-edge XANES spectra for poultry manure, forest, and manure-applied soils with different histories of application: (A) manure, forest, and short-term; (B) medium-term; (C) long-term; and (D) linear combination fits of selected spectra. The dashed lines in (A), (B), and (C) correspond to those in Figure 1. The dotted lines in (D) represent the best fitted result to respective spectra by linear combination fitting.

BEAMLINES
X11A, X26A

PUBLICATION
Y. Arai, A. Lanzirotti, S. Sutton, M. Newville, J. Dyer, and D. Sparks, "Spatial and Temporal Variability of Arsenic Solid-State Speciation in Historically Lead Arsenate Contaminated Soils," *Environ. Sci. Tech.*, **40**, 673-679 (2006).

FUNDING
U.S. Department of Agriculture

FOR MORE INFORMATION
Yuji Arai
Dept. of Plant and Soil Sciences
University of Delaware
yarai@usgs.gov

SPATIAL AND TEMPORAL VARIABILITY OF ARSENIC SOLID-STATE SPECIATION IN HISTORICALLY LEAD ARSENATE CONTAMINATED SOILS

Y. Arai[1], A. Lanzirotti[2], S.R. Sutton[3], M. Newville[2], J. Dyer[1], and D.L. Sparks[1]

[1]Department of Plant and Soil Sciences, University of Delaware; [2]Consortium for Advanced Radiation Sources, University of Chicago; [3]Department of Geophysical Sciences, University of Chicago

We investigated aging effects on As retention mechanisms in historically lead-arsenate contaminated urban soils using synchrotron-based microfocused (μ) XRD, μ-XRF, and μ- and bulk-XAS analyses. Whereas As is predominantly present as As(V) adsorbed onto amorphous iron oxyhydroxides with a residue of schultenite ($PbHAsO_4$) at an oxic site, there is no trace of schultenite from a semi-reduced site. Instead, adsorbed As(V) phases on amorphous iron oxyhydroxide, amorphous orpiment, and As(V)-Ca co-precipitates were identified. This study shows that aging effects can significantly alter the original chemical constituent in soils, resulting in multi and site-specific As solid-state speciation.

Arsenic (As) solid-state speciation is one of the most important factors controlling dissolved As concentrations at As-contaminated sites. In this case study, we utilized a combination of *in situ* bulk- and μ-XAS, *in situ* μ-XRF, and μ-XRD to investigate As solid-state speciation in aged As-contaminated urban soils in the northeastern United States. The origin of As in the soils (predominantly lead arsenate) is the disposal of former commodity, specialty, and agricultural chemicals. There are two distinct sites with average redox potential values of approximately 33 and 275 mV in the top 4 meters. Subsurface samples at 2-4 m depths from a semi-reduced site A and an oxic site B (thereafter sample A and B), where total As was most concentrated (80 and 284 ppm, respectively), were chosen for detailed spectroscopic investigation.

In situ μ-SXRF analyses indicated that elevated As counts (regions 1, 2, 4, and 6 in **Figures 1A and 1B**) are similarly distributed with Ba, Ca, and Fe in sample A and with Fe in sample B (XRF maps of the metals are not shown). Regions 2, 3, and 5 (**Figures 1A and 1B**), where the As concentrations are not elevated, do not seem to be co-distributed with elements such as Cu, Ni, Zn, Mn, and Ca. The μXANES analyses show 1) a predominant As(V) oxidation state at regions 1, 2, 4 and 5; and 2) regions 3 and 6 contain As(III)-S and As(III), respectively (**Figure 2A**). Selected diffractograms of the μ-XRD measurements on sample B (**Figure 2B**) show the presence of calcite, rutile, and quartz in all 26 diffractograms, and schultenite ($PbHAsO_4$) in about half of the diffractograms.

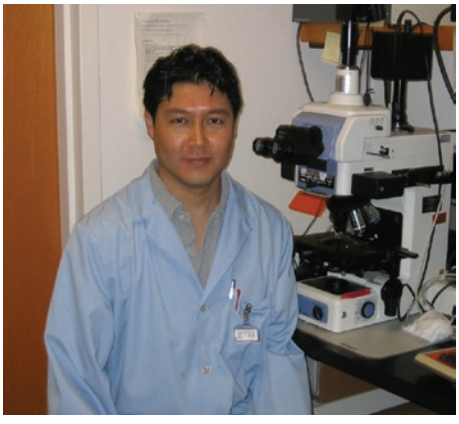

Yuji Arai

In the bulk EXAFS analyses, results from μ-XRF, -XRD and -XANES analyses were considered, and coordination numbers of species at low R were correlated with the expected proportions of the species at high R (e.g., an As-Ca shell with an As-As shell). **Figures 2C and 2D** shows the least-square fits of samples A and B. The CN (±30%) and R (±0.03Å) of the first and second shells (As-O: 4.3 and 1.7 Å, As-S: 3 and 2.27 Å, As-Fe: 2 and 3.3 Å, As-Ca: 2 and 4.06 Å, As-Pb: 2 and 3.9 Å and As-As: 1.5 and 4.09 Å) in each sample correspond to surface species that consist of approximately 25% amorphous orpiment (As_2S_3), 28% adsorbed As(V) on iron oxyhydroxide, 46% of Ca-As(V) coprecipitates and/or substitution of arsenate into gypsum in sample A, and approximately 71% As(V) adsorbed species on iron oxyhydroxide with approximately 29% residual schultenite.

In this study, multi-scale spectroscopic techniques (μ-XANES, -XRF, and -XRD and bulk-XAS) were

effectively combined to elucidate As solid-state speciation in lead-arsenate contaminated soils. Decades of contamination and weathering resulted in an alternation of the original As contaminant source (lead arsenate). Traditional bulk chemical digestion and the leachate test could possibly overestimate the site-specific As solid-state species that significantly control the bioavailability of As in soil solutions. The variability in spatial and temporal scale may be important in assessing the environmental risk and in developing in-situ remediation technologies.

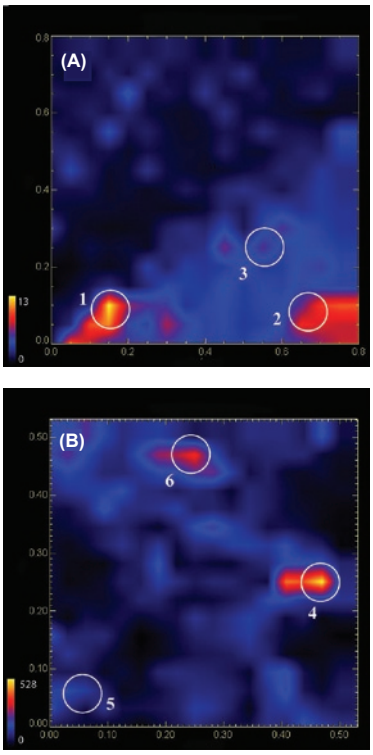

Figure 1. In situ As Kα and Kβ μ-x-ray fluorescence maps of sample A and B, respectively. Scale of maps in x- and y-axis is in mm. Fluorescence counts of each element are indicated by color contour bars on the left side of each map, and the intensity of each color is proportional to the amount of the corresponding element. Regions 1, 2, 3, 4, 5, and 6 indicate the area where μ-XANES spectra were taken.

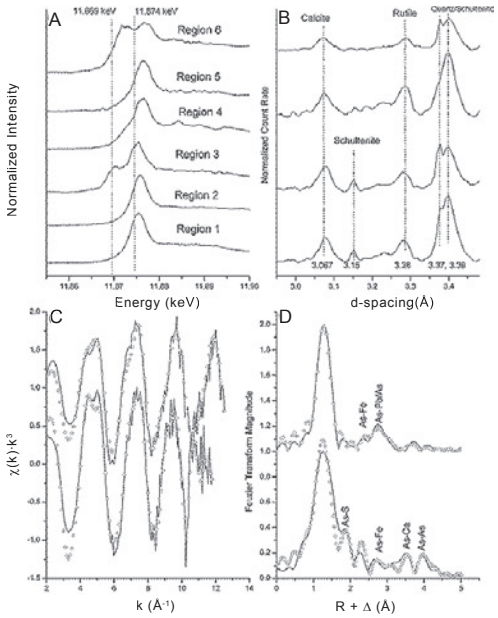

Figure 2. (A) Microfocused XANES spectra at regions 1-6 of selected areas of the As fluorescence maps shown in Figure 1. (B) Microfocused SXRD patterns (λ=0.7598 Å) of As concentrated areas of sample B. Selected diffractograms show 2.8 Å < d-spacing <3.6 Å. (C) Non-linear least-square fits to normalized k^3-weighted EXAFS spectra of the reference compounds and samples A and B. Raw data and fits are shown by solid lines and open circles, respectively. (D) Non-linear least-square fits to Fourier transforms of the reference compounds and samples A (bottom) and B (top). Raw data and fits are shown in solid lines and open circles, respectively.

BEAMLINES
X19A, X26A, X23A2

PUBLICATION
A. Leri, M. Hay, A. Lanzirotti, W. Rao, and S. Myneni. "Quantitative Determination of Absolute Organohalogen Concentrations in Environmental Samples by X-ray Absorption Spectroscopy," *Anal. Chem.*, **78**, 5711-5718 (2006).

FUNDING
U.S. Department of Energy; National Science Foundation (NSF); NSF Graduate Research Fellowships

FOR MORE INFORMATION
Alessandra Leri
Department of Geosciences
Princeton University
aleri@princeton.edu

QUANTITATIVE DETERMINATION OF ABSOLUTE ORGANOHALOGEN CONCENTRATIONS IN ENVIRONMENTAL SAMPLES BY X-RAY ABSORPTION SPECTROSCOPY

A.C. Leri[1], M.B. Hay[2], A. Lanzirotti[3], W. Rao[4], and S.C.B. Myneni[5,6]

[1]Department of Chemistry, Princeton University; [2]Department of Civil and Environmental Engineering, Princeton University; [3]Consortium for Advanced Radiation Sources, The University of Chicago; [4]Savannah River Ecology Laboratory, University of Georgia; [5]Department of Geosciences, Princeton University; [6]Earth Sciences Division, Lawrence Berkeley National Laboratory

A method for quantification of organic and inorganic halogen concentrations in environmental samples using x-ray absorption spectroscopy has been developed. Organochlorine (Cl_{org}) and inorganic chloride (Cl_{inorg}) concentrations are determined from Cl 1s XANES spectra. The absolute fluorescence intensity of these spectra is linearly dependent on Cl concentration. Calibration curves are obtained from NaCl standards in a matrix of uniform bulk density, and Cl concentration in natural samples is estimated from these curves with high precision. The fractions of Cl_{inorg} and aliphatic/aromatic Cl_{org} contributing to the total Cl 1s XANES signal are computed through least-squares spectral fitting with representative model compounds. Concentrations of organic and inorganic Br (Br_{org} and Br_{inorg}) in sediment samples are also measured using a combination of XRF and Br 1s XANES spectroscopy.

Halogens undergo complex biogeochemical transformations in terrestrial systems, cycling between organic and inorganic forms. Naturally produced organohalogens include a diverse array of relatively low molecular weight molecules, as well as macromolecules of indeterminate structure. Despite the ubiquity of natural organohalogens, the processes associated with their formation and degradation in the environment remain poorly understood, largely due to the inadequacy of available techniques to account for the myriad halogen species in heterogeneous soil, sediment, plant, and aqueous samples. Established quantitative methods require chemical isolation of organohalogen fractions from natural samples and are prone to partial recoveries and/or chemical alterations of halogens. We have applied synchrotron-based x-ray fluorescence (XRF) and x-ray absorption near-edge structure (XANES) spectroscopy to the *in situ* determination of Cl_{org} and Br_{org} concentrations in natural samples.

Authors Alessandra Leri and Michael Hay

Quantification of Cl relies on the absolute fluorescence intensity of Cl 1*s* XANES spectra (acquired at beamline X19A) determined at 2850.8 eV, an energy ~20 eV above the Cl K-absorption edge (**Figure 1A**). By this energy, the near-edge oscillations are attenuated and absorption intensity is independent of Cl speciation. Polyacrylic acid-based NaCl standards yield calibration curves with a strong linear relationship between Cl concentration and absolute Cl fluorescence intensity (**Figure 1B**). X-ray beam absorption and scattering by polyacrylic acid-based standards and natural organic matter (NOM) are comparable, allowing for direct measurement of Cl concentrations in homogenized NOM sample pellets, which minimizes matrix effects.

Unnormalized Cl 1*s* XANES spectra of oak leaf NOM at progressive stages of decay are shown in **Figure 2A** (a = least degraded; c = most degraded). Comparison of the absolute Cl fluorescence intensity values of these spectra with standard curves (as in **Figure 1B**) yields the following total Cl concentrations: a, 364 ppm; b, 141 ppm; c, 70 ppm. The decreasing trend in Cl concentration is consistent with leaching of soluble forms of Cl from the mulch material as part of the degradation process.

In addition to providing Cl concentration measurements, Cl 1*s* XANES spectra illuminate the chemical forms of Cl present in a sample. Cl_{inorg} exhibits a broad absorption maximum (**Figure 2B,** x) higher in energy than the more intense maxima characteristic of Cl_{org} compounds. These sharp peaks denote 1s → π^* or σ^* transitions and differ in energy depending on C-Cl bond length, as

becomes evident through comparison of aliphatic and aromatic Cl_{org} spectra **(Figure 2B,** y-z**)**. The substantial variations in spectral features depending on the coordination environment of Cl allow percentage estimates of Cl_{inorg} and aliphatic and aromatic Cl_{org} in natural samples to be ascertained via least-squares fitting of normalized sample spectra with spectra of representative model compounds (**Figure 2B**). Combination of these proportions with total Cl concentrations yields the concentrations of Cl_{inorg}, aromatic Cl_{org}, and aliphatic Cl_{org} in NOM samples.

Total Br concentrations in environmental samples have been determined via XRF analysis for decades. The novelty of our application lies in the combination of quantitative information from XRF (acquired at beamline X26A) with Br speciation information from Br 1*s* XANES spectra (acquired at beamline X23A2) to determine absolute concentrations of Br_{org} and Br_{inorg} in chemically heterogeneous sediments.

This method provides a rigorous new approach to the determination of organohalogen concentrations in complex natural samples *in situ*. Robust, quantitative information about organohalogen fluxes in soil and sediment systems will help complete the description of natural halogen cycles, potentially illuminating the sources and sinks of naturally and industrially produced organohalogens in the environment.

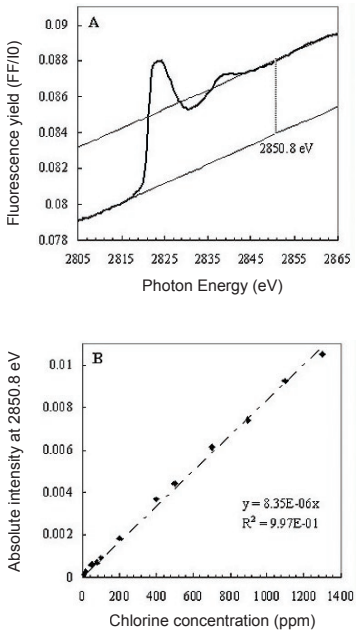

Figure 1. Quantification of Cl concentration from Cl 1*s* XANES spectra. (A) Unnormalized Cl 1*s* XANES spectrum of NaCl standard in PAA matrix (200 ppm Cl). The difference at 2850.8 eV between splines through the pre-edge and post-edge regions is used as a measure of absolute Cl fluorescence intensity. (B) Relationship between Cl concentration in PAA-based NaCl standards and absolute Cl fluorescence intensity. Dashed line, equation, and R^2 value represent linear fits to the data.

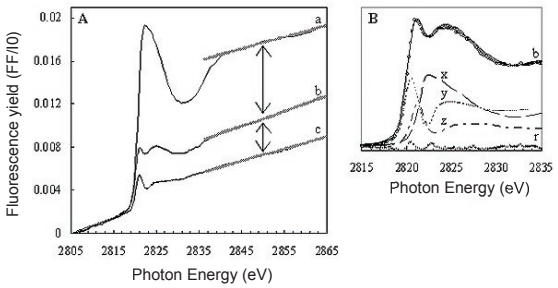

Figure 2. Determination of Cl speciation and concentration in NOM samples from Cl 1*s* XANES spectra. (A) Unnormalized Cl 1*s* XANES spectra of pulverized oak leaves at different stages of decay (a = least degraded; b = more degraded; c = most degraded). Arrows illustrate the differences in absolute Cl fluorescence intensity among the spectra. (B) Least-squares fit of background-subtracted, normalized spectrum b with representative inorganic (x, glycine-HCl), aliphatic (y, chlorodecane), and aromatic (z, chlorophenol red) Cl model compounds. Spectrum b data are represented by circles and fit by the solid line; r is the residual after the fit. Estimated Cl speciation by least-squares fitting: a, 78% inorganic (284 ppm), 16% aromatic (58 ppm), 6% aliphatic (22 ppm); b, 40% inorganic (56 ppm), 20% aromatic (29 ppm), 40% aliphatic (56 ppm); c, 16% inorganic (12 ppm), 42% aromatic (29 ppm), 42% aliphatic (29 ppm).

BEAMLINES
X6A, X29

PUBLICATION
P.D. Pawelek, N. Croteau, C. Ng-Thow-Hing, C.M. Khursigara, N. Moiseeva, M. Allaire, and J.W. Coulton, "Structure of TonB in Complex with FhuA, E. coli Outer Membrane Receptor," *Science*, **312**, 1399-1402 (2006).

FUNDING
Canadian Institutes of Health Research

FOR MORE INFORMATION
James W. Coulton
Department of Microbiology and Immunology
McGill University
james.coulton@mcgill.ca

STRUCTURE OF TonB IN COMPLEX WITH FhuA, E. COLI OUTER MEMBRANE RECEPTOR

P.D. Pawelek[1], N. Croteau[1], C. Ng-Thow-Hing[1], C.M. Khursigara[1], N. Moiseeva[2], M. Allaire[2], and J.W. Coulton[1]

[1]Department of Microbiology and Immunology, McGill University, Canada; [2]National Synchrotron Light Source, Brookhaven National Laboratory

Iron, an essential element for most living organisms, is highly insoluble at physiological pH, making it difficult for bacteria to acquire. In order to obtain sufficient amounts of iron, bacteria have developed high affinity uptake systems. For the first time, interactions between two proteins of the ferric hydroxymate uptake (Fhu) system are seen at atomic resolution. Crystals of a complex of outer membrane receptor FhuA and its energizing partner, TonB, give us insights into the mechanism by which E.coli acquires iron. Learning about this mechanism could help in the development of targeted antibiotics.

Bacteria, like most living organisms, need iron to survive. Because of the low bioavailability of iron, bacteria synthesize high-affinity, iron-chelating low molecular weight compounds called siderophores that form metal:siderophore conjugates.

The size of a metal:siderophore conjugate like ferrichrome prohibits entry into the bacteria via simple diffusion through porin-like channels. Alternatively, bacteria have developed uptake systems for these conjugates. We study the Ferric Hydroxymate Uptake system (Fhu) that works as follows (**Figure 1**): The outer membrane receptor FhuA, a 22-strand β-barrel protein with a cork domain, binds iron-bound ferrichrome. TonB that has been energized by the ExbB/D cytoplasmic membrane complex comes into contact with FhuA and allows ferrichrome to pass into the periplasmic space. Once in that space, ferrichrome binds to the protein FhuD that brings it to the FhuB/C complex, an ABC transporter that finally transports it into the cytoplasm.

Authors (from left) Natalia Moiseeva, Marc Allaire, Nathalie Croteau, and Peter Pawelek

We first showed that upon binding of the ferrichrome-iron conjugate, a conformational change is transmitted to the periplasmic side of FhuA, resulting in the unwinding of a switch helix, thus signaling the ligand-loaded status of the receptor (**Figure 2A,B**). The next step involves the binding of TonB to the FhuA receptor; however the molecular mechanism whereby this occurs was unknown. By obtaining diffraction-quality crystals of a 1:1 FhuA:TonB complex and the use of synchrotron radiation, we have been able to shed light on how ferrichrome enters the periplasmic space.

The resulting crystal structure of this complex reveals that residues from the FhuA Ton box form a parallel β-interaction with the β3-strand of the central β-sheet of the C-terminal domain of TonB (**Figure 2C**). This interaction positions the highly conserved TonB residue, Arg166, to contact FhuA residue Glu56, which is also located in a conserved motif. From this we are able to predict the functional importance of this FhuA-TonB ionic interaction.

What does the crystal structure of the FhuA-TonB complex tell us about interactions of TonB with a cognate OM receptor and the transport of metal-chelated siderophore? From our structural data combined with findings from previous studies, we propose that the interprotein β-sheet formed between the receptor Ton box, and the C-terminal domain of TonB is required to position the TonB helix close to the receptor cork domain. In the FhuA-TonB structure, this results in TonB Arg166

forming an electrostatic interaction with FhuA cork residue Glu56. It was recently proposed that hydration of the cork domain may render it prone to disruption by TonB through transmission of a relatively small force perpendicularly applied to it.

Given its position proximal to the FhuA cork domain, TonB Arg166 is positioned to mediate such a mechanical shearing or pulling force to the cork domain. This may result in cork disruption, allowing siderophore translocation into the periplasm.

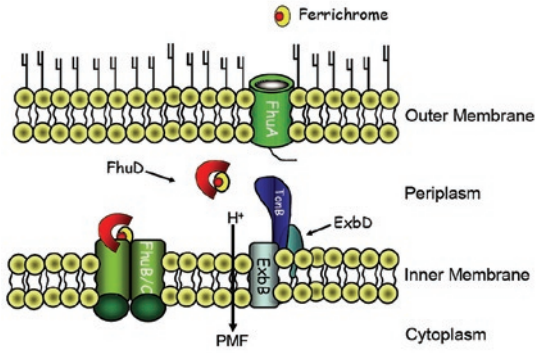

Figure 1. The Ferric Hydroxymate Uptake system (Fhu)

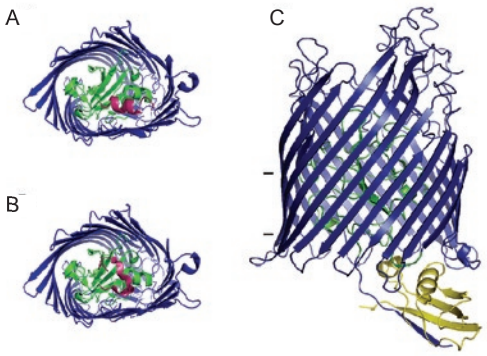

Figure 2. Changes occurring at the periplasmic side of FhuA. (A) Prior to iron-ferrichrome conjugate binding on the FhuA receptor. (B) Unwinding of the switch helix upon iron-ferrichrome conjugate binding. (C) Binding of the C-Terminal domain of TonB to the FhuA conserved Ton box.

BEAMLINE
X6A

PUBLICATION
T. Kajander, A.L. Cortajarena, E.R.G. Main, S.G.J. Mochrie, and L. Regan, "A New Folding Paradigm for Repeat Proteins," *J. Am. Chem. Soc.*, **127**(29), 10188-10190 (2005).

FUNDING
Helsingin Sanomat Centennial Foundation (Finland) postdoctoral fellowship; Spanish Ministry of Culture, Education and Sports postdoctoral fellowship

FOR MORE INFORMATION
Simon Mochrie
Departments of Physics and Applied Physics
Yale University
simon.mochrie@yale.edu

A NEW FOLDING PARADIGM FOR REPEAT PROTEINS

T. Kajander[1], A.L. Cortajarena[1], E.R.G. Main[2], S.G.J. Mochrie[3], and L. Regan[2,4]

[1]Department of Molecular Biophysics and Biochemistry, Yale University; [2]Department of Chemistry, University of Sussex, UK; [3]Departments of Physics and Applied Physics, Yale University; [4]Department of Chemistry, Yale University

Determining how a protein's amino acid sequence specifies its structure and properties is a grand challenge for biology in the post-genomic era. Repeat proteins, composed of tandem arrays of a basic structural motif, account for more than 5% of metazoan proteins in the Swiss-Prot database. It is therefore surprising that the folding of repeat proteins has been little studied, especially because their modular structures promise a more tractable folding problem than globular proteins. Our approach has been to design a consensus tetratricopeptide repeat (CTPRa) and from this construct a series of proteins that contain from two to 20 tandem copies of this repeat. We have shown that the folding of this family of TPR proteins can be described and predicted by the classical one-dimensional Ising model of statistical mechanics, which thus represents a new folding paradigm for repeat proteins.

We solved the x-ray crystal structure of the repeat protein CTPRa8, which contains eight identical TPR repeats, at 2.05Å resolution, using single wavelength anomalous diffraction data from cadmium. The structure of CTPRa8 (**Figure 1**) reveals that each repeat is comprised of two helices, which are arrayed to form a super helix. A key feature of CTPRa8, and of repeat proteins in general, is that, in contrast to globular proteins, there are no sequentially distant amino acid contacts. This pattern of local contacts suggests that a theoretical description based on the classical one-dimensional Ising model might be an appropriate way to understand the folding/unfolding behavior of repeat proteins, with the repeating units cast as Ising spins.

How can we test this hypothesis? Because the variation in behavior for different numbers of coupled subunits is a textbook signature of collective effects, the possibility of creating CTPRs in any multiplicity desired renders them an ideal system in which to test this model of repeat protein stability. Accordingly, we synthesized a series of CTPRs, for which the number of helices varied from 5 to 21. The stability of these proteins as a function of guanidine hydrochloride (GuHCl) concentration (GuHCl is an agent used to induce protein unfolding) is shown in **Figure 2**. The rapid change in each profile with increasing GuHCl concentration corresponds to the transition from the folded to the unfolded state. The best fits of the Ising model to these data are shown as the solid lines in **Figure 2**. Clearly, the model provides an excellent description of the folding/unfolding for all of the proteins studied.

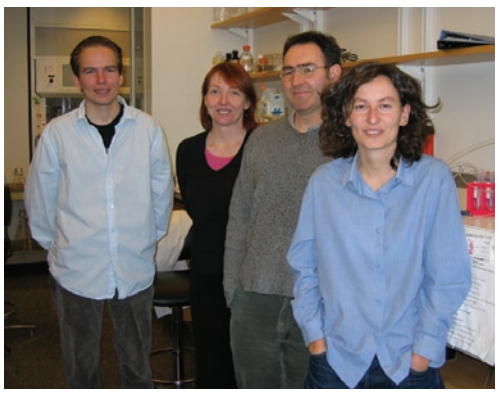

Authors (from left) Tommi Kajander, Lynne Regan, Simon Mochrie, and Aitziber Cortajarena

We believe that several aspects of this work are particularly exciting. First, the Ising model is predictive: Because thermodynamic data from just two different CTPRs in a series are sufficient to predict the behavior of all additional CTPRs in that series, we may view four of the model profiles in **Figure 2** as predictions. These are the first examples of successfully predicting the stabilities of proteins and the shapes of their unfolding curves.

Second, the Ising model requires a new microscopic picture: In the usual two-state transition, a protein is essentially always completely folded or completely unfolded with only brief transient behavior. In contrast, the Ising description implies that near the transition midpoint, partially folded configurations occur with significant probability.

Finally, the structure of CTPRa8 reveals both of the atomic details of an individual repeat, and the arrangement of repeats in the superhelix, and thus

promises the possibility of being able to assign the Ising model parameters to specific structural elements. Re-designs are in progress to test such ideas.

In a more general sense, beyond repeat proteins, does the behavior of the CTPRa series tell us anything about the folding of *globular* proteins? The folding of several small, single-domain globular proteins has been well-studied. As for individual repeat proteins, their thermodynamic behavior can usually be well-described by the traditional two-state model. However, in many cases, hydrogen-exchange measurements reveal a richer free-energy landscape than simply two free-energy minima, hinting that it may be sensible to envision each element of secondary structure itself as a degree of freedom that can be either folded or unfolded, *i.e.* as an Ising spin. Such observations suggest important similarities between the thermodynamics of repeat proteins and globular proteins.

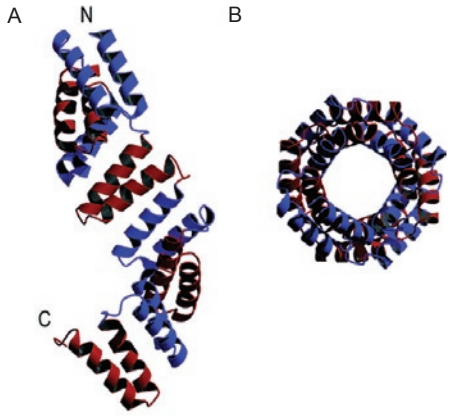

Figure 1. Crystal structure of CTPRa8. (A) View perpendicular to the superhelical axis. Each TPR repeat is colored either red or blue. (B) View along the superhelical axis.

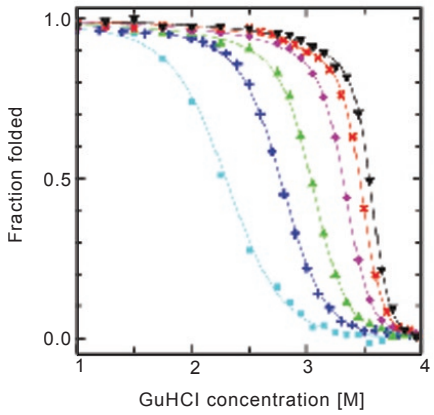

Figure 2. Thermodynamics of CTPRa unfolding. Fraction folded *vs.* [GuHCl] for CTPRa2 (squares), CTPRa3 (crosses), CTPRa4 (triangles), CTPRa6 (diamonds), CTPRa8 (crosses), CTPRa10 (inverted triangles) in 50 mM sodium phosphate, pH 6.5, 150 mM sodium chloride, at -25 °C. Root-mean-square errors of 0.8 millidegrees are smaller than the plotting symbols, except (when transformed) for the fraction folded of CTPRa2 in (B). Solid lines correspond to the best-fits to the predictions of the one-dimensional *N*-spin Ising model. Analogously to the Ising-Zimm-Bragg treatment of the polypeptide helix-coil transition, our model ascribes a reduced stability to the endmost helices, relative to those not at the end, by incorporating interactions with ficticious down spins at position 0 and *N*+1.

BEAMLINE
X25

PUBLICATION
A. Serganov, A. Polonskaia, A.-T. Phan, R.R. Breaker, and D.J. Patel, "Structural Basis for Gene Regulation by a Thiamine Pyrophosphate-Sensing Riboswitch," *Nature*, **441**, 1167-1171 (2006).

FUNDING
National Institutes of Health

FOR MORE INFORMATION
Alexander Serganov
Structural Biology Program
Memorial Sloan-Kettering Cancer Center
serganoa@mskcc.org

STRUCTURAL BASIS FOR GENE REGULATION BY A THIAMINE PYROPHOSPHATE-SENSING RIBOSWITCH

A. Serganov[1], A. Polonskaia[1], A. Tuân Phan[1], R.R. Breaker[2], and D.J. Patel[1]

[1]Structural Biology Program, Memorial Sloan-Kettering Cancer Center; [2]Department of Molecular, Cellular and Developmental Biology and Howard Hughes Medical Institute, Yale University

Genes are commonly turned on or off by protein factors that respond to cellular signals. The recent discovery of riboswitches proved that RNA molecules also control genes by directly sensing the presence of essential cellular metabolites. We determined the three-dimensional structure of the most widespread riboswitch class bound to its target, thiamine pyrophosphate, a co-enzyme derived from vitamin B1. These findings reveal how riboswitch RNA folds to form a precise pocket for its target and how a drug that kills bacteria tricks the riboswitch and starves disease-causing organisms of this essential compound.

RNA molecules, traditionally viewed as passive messengers of genetic information, have surprised researchers every few years with the discovery of novel functions that they perform. Recent studies have shown that some mRNAs - termed riboswitches - can sense changes in the levels of cellular metabolites and activate or repress genes involved in the biosynthesis and transport of these metabolites. Riboswitches are now recognized as one of the major metabolite-controlling systems that account for about 2% of genetic regulation in bacteria and that respond to various metabolites including co-enzymes, sugars, nucleotide bases, amino acids, and cations.

Riboswitches typically consist of two parts: a sensing region recognizing metabolites and an expression platform carrying gene-expression signals. Metabolite binding causes alternative folding in the sensing domain followed by conformational changes in the adjoining expression platform. This structural re-organization of the riboswitch results in the formation of specific structures that can terminate mRNA synthesis or prevent protein biosynthesis **(Figure 1)**. Remarkably, riboswitches do not need protein co-factors for recognition of their targets or for RNA folding. Though riboswitches are made of only 4 nucleotides instead of 20 different amino acids building the proteins, riboswitches can choose their target molecules among very similar metabolites as well as proteins do.

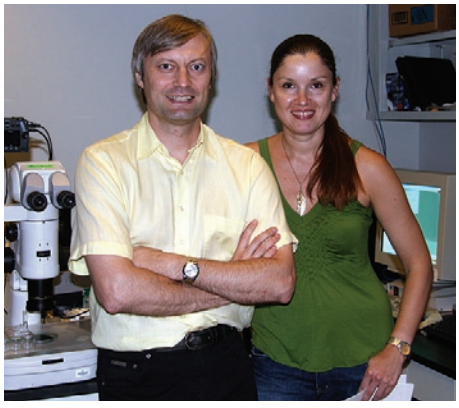

Authors Alexander Serganov and Anna Polonskaia

In order to understand how riboswitches recognize their metabolite targets and regulate gene expression, we have determined the three-dimensional structure of the complex between thiamine pyrophosphate (TPP) and its cognate *E.coli* riboswitch at 2.05 Å resolution. The TPP riboswitches are the most widespread class of metabolite-sensing RNAs and the only riboswitches found in all three kingdoms of life. The structure shows that the riboswitch consists of two large helical domains and a short helix P1 connected by a junction **(Figure 2)**. The helical domains are parallel and contact each other by long-range tertiary interactions. TPP binds the riboswitch in an extended conformation and positions itself between and perpendicular to the helical domains such that opposite ends of TPP are bound to a specific RNA pocket. Notably, TPP carries negatively charged phosphate groups and the structure shows how RNA recruits positively charged metal ions to mediate otherwise unfavorable electrostatic interactions. Similar to purine riboswitches, TPP is largely enveloped in the structure of the complex and, in agreement with biochemical experiments, the TPP riboswitch folds upon binding to TPP. However, discrimination

between TPP and related compounds is achieved using a principle that is different from purine riboswitches. Purine riboswitches distinguish between adenine and guanine ligands via formation of Watson-Crick base pairs with either uridine or cytosine nucleotides located in strategic positions in the riboswitch. The TPP riboswitch, on the other hand, can be considered as a molecular ruler measuring the length of the ligand. Analogs of TPP lacking one or both phosphates cannot reach well into both binding pockets of the riboswitch. According to biochemical experiments, they cannot stabilize the metabolite-bound architecture of the riboswitch, including the key helix P1, and cannot effectively control gene expression. The central part of TPP is not specifically recognized by the riboswitch, and this observation explains how the man-made TPP-like drug pyrithiamine pyrophosphate, which differs from TPP in the middle part, targets the riboswitch and down-regulates expression of thiamine-related genes, thus starving microbes of TPP. Given the important role of riboswitches in various microorganisms and the fact that riboswitches have not yet been detected in the human genome, riboswitch structures should enable researchers to employ rational drug discovery strategies to create novel classes of antimicrobial compounds that specifically target riboswitches.

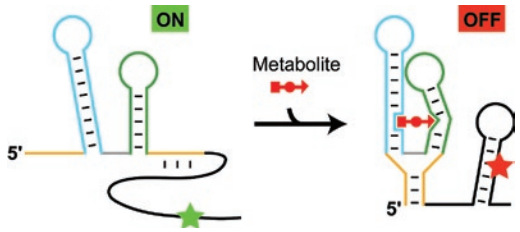

Figure 1. Schematic representation of the riboswitch's function exemplified by the thiamine pyrophosphate - specific riboswitch, which represses the initiation of protein biosynthesis in the presence of metabolite. The structural elements of the metabolite-sensing domain are colored in yellow, blue, green, and gray, and the expression platform is in black. In the absence of metabolite, the metabolite-sensing domain folds into the structure, which exposes the initiation signal of protein synthesis (green asterisk), thereby turning gene expression 'ON'. In the presence of metabolite (shown in red), the sensing domain folds into an alternative structure and causes the formation of the hairpin in the expression platform. As a result, the initiation signal becomes engaged in base pairing (red asterisk) and cannot function anymore, thereby shutting down gene expression, and acting as an 'OFF' switch.

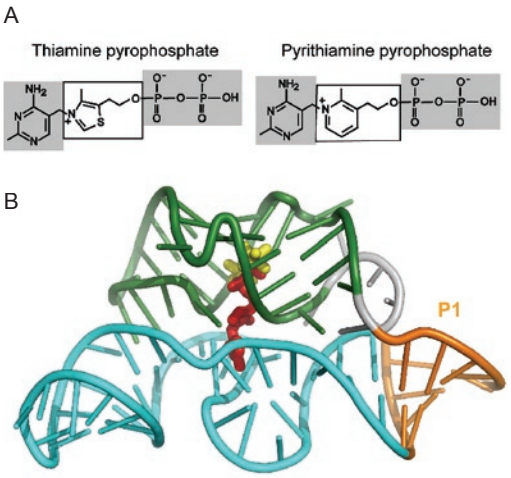

Figure 2. Structural models of a TPP riboswitch and its ligands. (A) Chemical structures of the natural metabolite TPP and the antimicrobial compound pyrithiamine pyrophosphate; (B) Crystal structure of the TPP-bound sensing domain from E.coli thiM gene in a ribbon representation. Structural elements of riboswitch are colored according to Figure 1: major helical domains are in green and blue, helix P1 in orange and three-way junction in gray. TPP and hydrated Mg cations are shown in red and yellow, respectively.

BEAMLINE
X26C

PUBLICATION
L.J. Higgins, F. Yan, P. Liu, H.-W. Liu, and C.L. Drennan, "Structural Insight into Antibiotic Fosfomycin Biosynthesis by a Mononuclear Iron Enzyme," *Nature*, **437**, 838-844 (2005).

FUNDING
National Institutes of Health; National Institute of Environmental Health Sciences; Searle Scholars Program; Alfred P. Sloan Foundation; A Lester Wolfe Predoctoral Fellowship

FOR MORE INFORMATION
Catherine L. Drennan
Department of Chemistry
Massachusetts Institute of Technology
cdrennan@mit.edu

STRUCTURAL INSIGHT INTO ANTIBIOTIC FOSFOMYCIN BIOSYNTHESIS BY A MONONUCLEAR IRON ENZYME

L.J. Higgins[1*], F. Yan[2], P. Liu[2], H.-W. Liu[2], and C.L. Drennan[1]

[1]Department of Chemistry, Massachusetts Institute of Technology; [2]Department of Chemistry and Biochemistry, University of Texas at Austin; * Currently a Harvard Medical School Fellow

The mononuclear iron enzyme S-(2)-hydroxypropylphosphonic acid epoxidase (HppE), from Streptomyces wedmorensis, uses O_2 to catalyze the formation of the broad-spectrum antibiotic fosfomycin (which inhibits bacterial cell-wall peptidoglycan biosynthesis) from S-(2)-hydroxypropylphosphonic acid (S-HPP). The reaction is a two-electron oxidation and is mechanistically atypical because it is independent of any cofactor or co-substrate and results in the incorporation of the hydroxyl oxygen of the substrate, rather than an atom of O_2, into the epoxide ring. The x-ray crystal structures of six forms of HppE — apo-HppE, Fe(II)-HppE, tris(hydroxymethyl)amino methane-Co(II)-HppE complex, S-HPP-Co(II)-HppE complex, and two S-HPP-Fe(II)-HppE complexes — were solved using data collected in part at the NSLS. The purpose was to gain insight into the mechanism of this unique enzyme.

Mononuclear non-heme iron enzymes use their metal cofactor to activate dioxygen (O_2) for difficult redox processes. One of these enzymes, *S*-(2)-Hydroxypropylphosphonic acid epoxidase (HppE), from *Streptomyces wedmorensis* (**Figure 1**, overall structure), employs its mononuclear iron center and molecular oxygen for the two-electron oxidation of *S*-(2)-hydroxypropylphosphonic acid (*S*-HPP) to catalyze the formation of the antibiotic (1R,2S)-(1,2-epoxypropyl)phosphonic acid (fosfomycin). This reaction is essentially a dehydrogenation reaction (loss of hydrogen). In order to balance the four-electron reduction of oxygen to water, we have proposed a putative two-electron reductant (or reductase). Fosfomycin is an unusual C-P-bond-containing epoxide that covalently modifies UDP-GlcNAc enolpyruvyl transferase, consequently inhibiting bacterial cell-wall peptidoglycan biosynthesis and bacterial growth. Since it accumulates in the kidneys and bladder, fosfomycin has been used clinically for the treatment of lower-urinary-tract infections. The structures of the apo-HppE (metal-free), native Fe(II)-HppE, tris(hydroxymethyl)aminomethane (Tris)-Co(II)-HppE complex, *S*-HPP-Co(II)-HppE complex, and two *S*-HPP-Fe(II)-HppE complexes (form 1 and form 2) were solved in order to better understand the epoxidation mechanism of this enzyme. It is interesting to note that the Tris molecules in the Tris-Co(II)-HppE structure result from the Tris buffer used in the crystallization solution.


Authors Catherine Drennan and Luke Higgins

Selenomethionine (SeMet) derivatization was used to obtain phase information for these protein structures. Initial experimental phases were determined from an x-ray dataset of Tris-Co(II)-SeMet-HppE collected at the wavelength for the Se absorption peak (0.9791 Å) on NSLS beamline X26C. This dataset was refined to 2.5 Å in space group $P6_522$ and the resulting model was further refined against a 1.8 Å native Tris-Co(II)-HppE dataset that was obtained at 0.9791 Å on Advanced Photon Source beamline 8BM. All subsequent structures were determined from these initial models.

The structures of *S*-HPP-Fe(II)-HppE complexes (form 1 and form 2) confirm the direct binding of the substrate, *S*-HPP, to the iron and show the existence of two binding modes, a monodentate mode and a bidentate mode. These two modes are explained by a two-step binding process: (i) *S*-HPP first binds in a monodentate fashion via the oxygen atom of the phosphonic acid group, resulting in displacement of a water molecule; (ii) The subsequent rotation of the substrate allows for bidentate coordination of *S*-HPP to Fe(II). A β-hairpin-like structure, formed by β-strands 2 and 3, acts as a cantilever that responds to the bidentate positioning of the substrate and adopts a closed catalytic conformation to cover the hydrophobic portion of the substrate bound in the active site

(**Figure 2**). The negative charge on the substrate is expected to enhance the reactivity of the diiron center toward oxygen, a role that co-substrates play in other mononuclear iron proteins. The addition of oxygen to the only open coordination site on Fe(II) of the bidentate-S-HPP complex appears to occur through a very small channel created at the interface of the α- and β- domains. Once O_2 is bound, abstraction of the C1 hydrogen atom could occur by a Fe(IV)-oxo intermediate (**Scheme 1, pathway A**) or by a Fe(III)-hydroperoxide intermediate (**Scheme 1, pathway B**). This results in the formation of a transient-substrate radical intermediate that undergoes cyclization to yield fosfomycin.

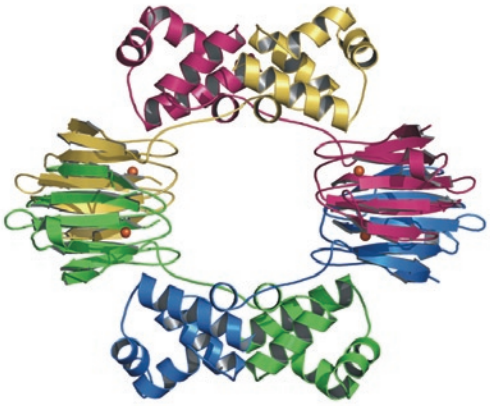

Figure 1. Tetrameric structure of HppE.

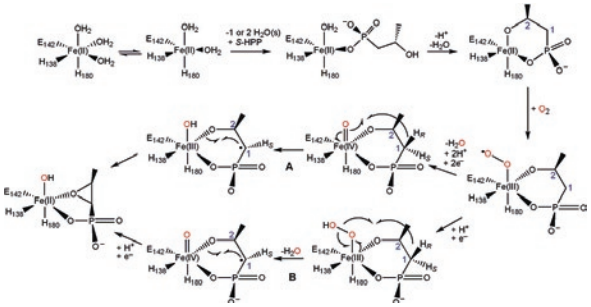

Scheme 1. Possible reaction mechanisms for HppE.

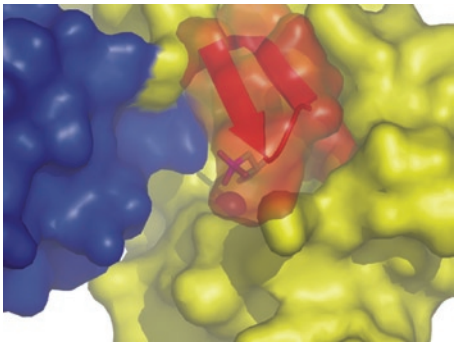

Figure 2. A portion of the structure called the cantilever (red) closes over the active site iron (brown) and substrate (ball-and-stick).

BEAMLINES
U10B, X26A

PUBLICATION
L.M. Miller, Q. Wang, T.P. Telivala, R.J. Smith, A. Lanzirotti, and J. Miklossy, "Synchrotron-based Infrared and X-ray Imaging Shows Focalized Accumulation of Cu and Zn Co-localized with β-amyloid Deposits in Alzheimer's Disease," *J. Struct. Biol.*, **155**(1), 30-3 (2006).

FUNDING
National Institutes of Health

FOR MORE INFORMATION
Lisa M. Miller
Brookhaven National Laboratory
NSLS
lmiller@bnl.gov

CO-LOCALIZATION OF β-AMYLOID DEPOSITS AND METAL ACCUMULATION IN ALZHEIMER'S DISEASE

Q. Wang[1], T.P. Telivala[1], R.J. Smith[1], A. Lanzirotti[2], J. Miklossy[3], and L.M. Miller[1]

[1]National Synchrotron Light Source, Brookhaven National Laboratory; [2]Consortium for Advanced Radiation Sources, University of Chicago; [3]Kinsmen Laboratory of Neurological Research, University of British Columbia

Alzheimer's disease (AD) is the most common age-related neurodegenerative disease. It is characterized by the misfolding and plaque-like accumulation of a naturally occurring protein, amyloid beta (Aβ) in the brain. This misfolding process has been associated with the binding of metal ions such as Fe, Cu, and Zn in vitro. In this work, the secondary structure of the amyloid plaques in human AD brain tissue was imaged in situ using synchrotron Fourier transform infrared microspectroscopy (FTIRM). The results were correlated spatially with the metal ion distribution in the identical tissue, as determined using synchrotron x-ray fluorescence (XRF) microprobe. Results revealed "hot spots" of accumulated Zn and Cu ions that were co-localized with the elevated regions of β-sheet protein, suggesting that metal ions may play a role in amyloid plaque formation in human Alzheimer's disease.

Alzheimer's disease (AD) is a progressive brain disorder that gradually destroys a person's memory, ability to learn, reason, make judgments, communicate, and carry out daily activities. The brain in AD is characterized by the presence of amyloid plaques, which consist of small deposits of a peptide called amyloid β (Aβ). *In vitro* evidence suggests that metal ions such as Cu, Zn, Fe, and Mn may play a role in the misfolding of Aβ in AD. However, the functions of these metal ions and Aβ misfolding in the disease process are not well understood. The overall aim of this research is to obtain an *in situ* structural and mechanistic picture of how metal ions in the brain are involved in Aβ formation and plaque aggregation in AD.

In this work, thin cryosections (~10 μm) of brain tissue from patients with neuropathologically confirmed AD were studied. The locations of the amyloid plaques were visualized by green fluorescence using Thioflavin S staining and epifluorescence microscopy (**Figure 1B**). FTIRM carried out at NSLS beamline U10B showed that the amyloid plaques had elevated β-sheet content, as demonstrated by a strong Amide I absorbance at 1625 cm^{-1}, which was different from the FTIR spectrum of Aβ *in vitro* (**Figure 2A**). The correlation image generated based on peak height ratio of 1625 / 1657 cm^{-1} (**Figure 1C**) revealed that regions of elevated β-sheet content in the AD tissue corresponded well with amyloid deposits as identified by Thioflavin staining.

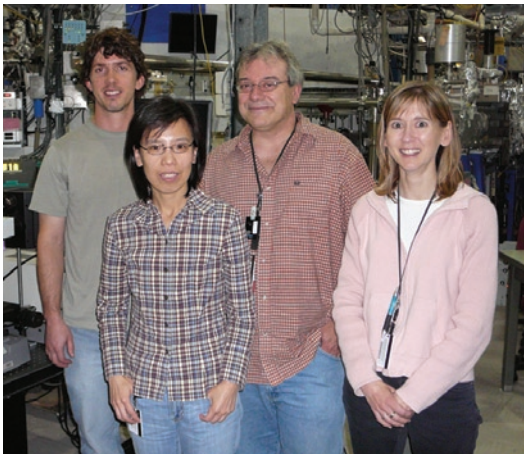

Authors (From left) Randy Smith, Adele Qi Wang, Antonio Lanzirotti, and Lisa Miller

Using XRF microprobe at NSLS beamline X26A and Advanced Photon Source beamline 13-ID, we found that the background content of Ca, Fe, Cu, and Zn in AD *vs*. control tissue were similar; however the metal distribution in AD tissue was not uniform. Specifically, "hot spots" of accumulated Ca, Fe, Cu, and Zn ions were observed. The SXRF images of Zn and Cu can be seen in **Figure 1D and 1E**, respectively. A strong spatial correlation (r^2 = 0.97) was found between the locations of the Cu and Zn ions. The elevated Zn and Cu in the "hot spot" is also evident in representative XRF spectra (**Figure 2B**).

In order to correlate the misfolded amyloid protein and metal distribution in the tissue, an RGB image was generated with Zn content in red channel, β-sheet protein content in the green channel, and Cu content in the blue channel. Results revealed the co-localization of Cu, Zn, and β-sheet protein in the amyloid plaques in AD human tissue (**Figure 1F**). Neither plaques nor accumulated metal hot

spots were observed in control brain tissue.

In summary, these results provide increasing evidence that the formation of amyloid plaques from the Aβ peptide is associated with metal ions in the brain. Here we show for the first time a direct strong spatial correlation between AD plaques and metal ions in the brain, emphasizing the role of metal ions in AD etiology. In the future, exploring earlier stages of disease and *in-situ* probing metal-protein binding will be of interest for understanding the disease pathogenesis and mechanism.

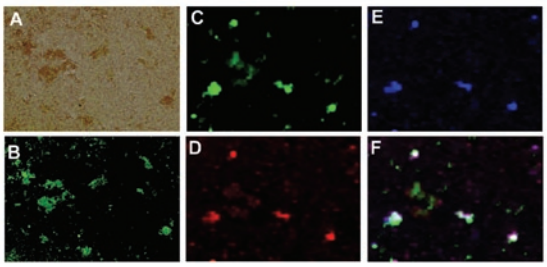

Figure 1. (A) Bright field and (B) Epifluorescence image of human AD tissue stained with Thioflavin S. (C) Single channel color FTIR correlation image of β-sheet protein (green). (D) Single channel color SXRF microprobe image of Zn (red). (E) Single channel color SXRF microprobe image of Cu (blue). (F) The RGB correlation image.

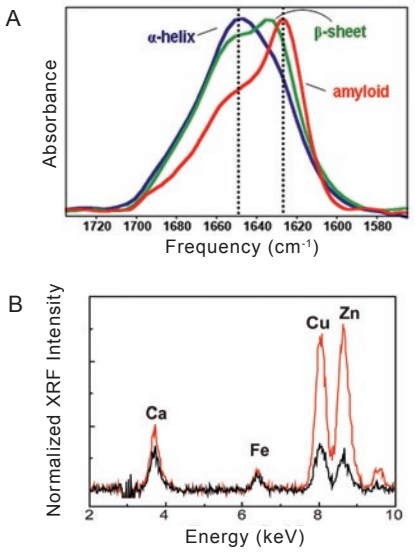

Figure 2. (A) Infrared spectra of Thioflavin-positive area (red) and Thioflavin-negative area (blue) of AD tissue. For comparison, the FTIR spectrum of purified Aβ peptide in vitro is shown (green). (B) SXRF microprobe spectra from Thioflavin-positive area (red) and Thioflavin-negative area (black).

BEAMLINES
X26C, X25

PUBLICATION
N.H. Tolia, E.J. Enemark, B.K.L. Sim, and L. Joshua-Tor, "Structural Basis for the EBA-175 Erythrocyte Invasion Pathway of the Malaria Parasite Plasmodium Falciparum," *Cell,* **122**(2),183-93 (2005).

FUNDING
Watson School of Biological Sciences Leslie C. Quick Jr. Predoctoral Fellowship; Louis Morin Charitable Trust; Department of Defense Small Business Innovation Research

FOR MORE INFORMATION
Leemor Joshua-Tor
W.M. Keck Structural Biology Laboratory
Cold Spring Harbor Lab
leemor@cshl.edu

STRUCTURAL BASIS FOR THE EBA-175 ERYTHROCYTE INVASION PATHWAY OF THE MALARIA PARASITE *PLASMODIUM FALCIPARUM*

N.H. Tolia[1,2], E.J. Enemark[2], B. Kim Lee Sim[3], and L. Joshua-Tor[1,2]

[1]Watson School of Biological Sciences and [2]Keck Structural Biology Laboratory, Cold Spring Harbor Laboratory; [3]Protein Potential

Invasion of red blood cells by the malaria parasite Plasmodium falciparum marks the commencement of the clinical manifestation of the disease. During invasion, erythrocyte binding antigen 175 (EBA-175), a protein on the surface of the parasite, binds to glycophorin A (GpA) on red blood cells. Of the several domains in EBA-175, region II (RII) is necessary and sufficient for binding to GpA. We have solved the crystal structures of RII and RII in complex with a sugar that contains the essential components required for the binding of EBA-175 to GpA. This study provides insight into the mechanism of erythrocyte binding and invasion by the malaria parasite, and understanding this interaction will aid in the development of drugs and vaccines.

Malaria causes an estimated 300-500 million cases and 1-3 million deaths annually, 80% of which are in children under the age of five. There are four species of malaria parasite, of which *Plasmodium falciparum* is responsible for the majority of deaths associated with the disease. Within 9-14 days after an organism is infected (via a mosquito bite) the parasite has invaded the red blood cells, breaking them down and resulting in the clinical symptoms of the disease. Therefore, preventing binding and invasion of the red blood cells by the parasite would be critical in either preventing malaria (through vaccine design) or treating it (through drug design).

Binding of the parasite to the red blood cells requires the interaction between erythrocyte binding antigen 175 (EBA-175), a protein on the surface of the parasite, and the sugars of glycophorin A (GpA) on the red blood cell. One domain of EBA-175, region II, has been found to be the essential component of the parasite required to bind GpA. The structure of RII shows that it is a dimer, and that the two molecules interact extensively with one another in an anti-parallel fashion resembling a handshake. The dimer results in the formation of two channels in the center of the molecule (**Figure 1**).

Authors (from left) Eric Enemark, Leemor Joshua-Tor, and Niraj Tolia

To examine the binding interaction of RII to GpA, we cocrystallized RII with the sugar α-2,3-sialyllactose, which contains the essential components of GpA required for binding to RII. We found six binding sites for the sugar to the RII dimer, all of which were located at the dimer interface (**Figure 1**). Using a cell-based binding assay, we mutated RII at residues required for dimerization or the observed sugar binding sites to confirm that dimerization and sugar/RII binding are essential for red blood cell binding. These mutations were expressed on the surface of COS cells (monkey test cells) and we assayed for their ability to bind normal human erythrocytes. All dimerization and glycan-binding mutants had impaired erythrocyte-binding ability, demonstrating the importance of dimerization in erythrocyte binding and validating the glycan binding sites.

Together these results allowed us to propose a model for RII binding to GpA (**Figure 2**). We propose that the RII domain of EBA-175, which is present on the surface of the parasite, might assemble around the GpA extracellular domains of the red blood cells and that dimerization of EBA-175 would occur upon receptor binding. The GpA extracellular domains may either bind within the channels or dock on the outer surface of RII, feeding sugars into the channels. Binding of the

malaria parasite to the red blood cell triggers many signaling pathways within the red blood cell. Therefore, we propose that RII-mediated dimerization of EBA-175 may be the trigger for signaling during invasion.

These structures have broad implications in helping to model other erythrocyte-binding-like (EBL) family members required for binding between the parasite and red blood cells. Of particular interest is the homologous protein PfEMP-1 that is responsible for cytoadherence of the parasitized red blood cells to the endothelium, resulting in the most fatal form of malaria. Perhaps most importantly, the structure, along with the functional analysis, presents possibilities for drug and vaccine design.

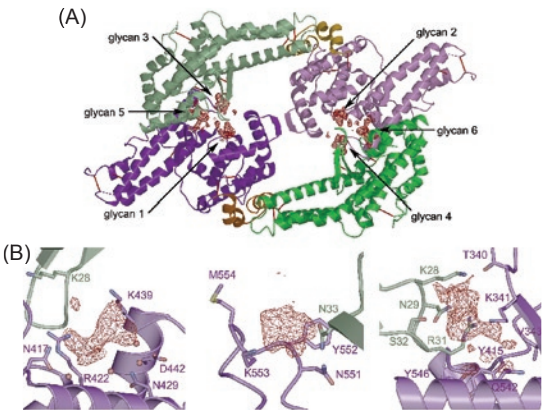

Figure 1. Crystal structure of RII with sialyllactose. (A) A ribbon representation of the dimeric structure of RII. The monomers are shaded in different intensities and are composed of two subdomains (green and purple), F1 and F2. Two channels are created in the center of the molecule. Glycan positions are shown in $F_o - F_c$ electron density in red. (B) Close-up views of three of the glycan binding sites – 1, 3 and 5, from left to right. Residues from both monomers contact each glycan.

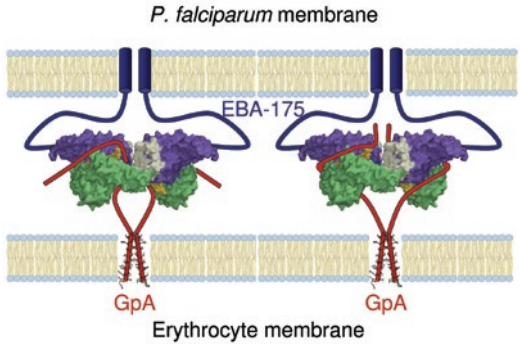

Figure 2. The P. *falciparum* membrane is shown on the top and the erythrocyte membrane on the bottom. The receptor binding domain of EBA-175, RII, is shown as a surface representation (green/purple denotes each sub-domain). Blue lines represent portions of EBA-175 backbone not included in the crystal structure. The receptor Glycophorin A (GpA) is shown in red with the membrane-spanning region in detail using the NMR structure and the extracellular domain is drawn as a schematic flexible line. The glycans of GpA, modeled based on the position of sialyllactose, are shown as space-filling models in gold. In the left panel, the RII dimer assembles around the GpA dimer, with GpA binding within the channels. An alternative model is shown on the right, where the GpA monomers dock on the outer surface of the protein, feeding glycans into the channels.

BEAMLINES
X25

PUBLICATION
A. Banerjee, W. Santos and G.L. Verdine, "Structure of a DNA Glycosylase Searching for Lesions," *Science*, **311**, 1153-1157 (2006).

FUNDING
National Institutes of Health

FOR MORE INFORMATION
Gregory L. Verdine
Department of Chemistry
Harvard University
gregory_verdine@harvard.edu

DISULFIDE TRAPPED STRUCTURE OF A REPAIR ENZYME INTERROGATING UNDAMAGED DNA SHEDS LIGHT ON DAMAGED DNA RECOGNITION

A. Banerjee[1,3], W. Santos[1], and G.L. Verdine[1,2]

[1]Departments of Chemistry and Chemical Biology and [2]Molecular and Cellular Biology, Harvard University; [3]Current address: Rockefeller University

Spontaneous changes to the covalent structure of DNA are a threat that living systems battle constantly. Repair of the resulting lesions is initiated by enzymes known as DNA glycosylase enzymes, which extrude damaged nucleosides from the helical stack, insert them into an extrahelical active site pocket, and catalyze cleavage of their glycosidic bond. It is poorly understood how DNA glycosylases search the genome to locate the exceeding rare sites of damage embedded in a vast excess of normal DNA. Through the use of intermolecular disulfide crosslinking and x-ray crystallography, we have trapped and characterized in atomic detail the initial complex formed between a bacterial 8-oxoguanine (oxoG) DNA glycosylase, MutM, and undamaged DNA. The structures represent the earliest stage of DNA interrogation by a DNA glycosylase and suggest a kinetic mode of discriminating normal nucleobases from damaged ones.

The oxidation of guanine by escaped intermediates in aerobic respiration generates 8-oxoguanine, a potent endogenous mutagen that causes G:C to T:A transversion mutations. Repairing this lesion is initiated by the 8-oxoguanine DNA glycosylase, MutM in bacteria, and the structurally unrelated OGG1 in eukaryotes. The mechanistic and structural details of oxoG recognition by MutM and human OGG1 (hOGG1) have been studied exhaustively. Both enzymes bend DNA drastically at the site of damage and extrude the substrate oxoG from the helix into the extrahelical enzyme active site; a similar strategy is used by DNA glycosylases. In previous work, we reported the use of intermolecular disulfide crosslinking (DXL) to trap and then characterize a complex in which hOGG1 was interrogating an undamaged extrahelical guanine nucleobase in DNA. Here we extend DXL technology to include crosslink attachment to the DNA backbone, and we use this chemistry to trap complexes of MutM with undamaged DNA having no extrahelical nucleobase. The trapping chemistry is based on proximity-directed disulfide bond formation between backbone-modified DNA containing a disulfide linker attached via a phosphoramidite linkage and a cysteine residue engineered into the protein. Of the three different positions we tested on MutM and DNA for crosslinking, the Q166C/p6 combination emerged as the one that underwent the most efficient crosslinking, hence we chose this position for further structural work. By varying the sequence of DNA and the position of crosslinking, we solved the structures of three different complexes of MutM crosslinked to undamaged DNA, namely interrogation complexes 1, 2, and 3 (IC1, IC2, and IC3, **Figures 1, 2**). The structures of all the complexes reveal, for the first time, a DNA glycosylase interrogating a fully intrahelical base-paired duplex for damaged sites. Although the base-pairing in the duplex is intact, MutM severely bends the DNA and actively distorts the interrogated base-pair (also referred to as the sampled register) by inserting the aromatic ring of Phe114 in the duplex, thereby severely buckling the base-pair in question.

Authors (from left) Webster Santos, Gregory L. Verdine, and Anirban Banerjee

The sequence of the DNA in IC1 was designed to unravel the details of MutM interrogating a G:C base pair being crosslinked to p6. However, when we solved the structure of IC1, it became clear that instead of sampling the G:C base pair at position 8 (the +2 register), MutM jumps by one base-pair position along the duplex and instead samples the A:T base pair at position 9 (register +3), evincing enough flexibility allowed by the disulfide crosslink to allow MutM to adopt the position of choice (**Figure 1**). In an attempt to coax MutM to sample a G:C base pair, we moved the crosslinking position from p6 to p5. However, the structure

of the resulting complex revealed that MutM continues to sample the A:T base pair at position 9 at the cost of inducing a pronounced distortion in the DNA helical structure (not described in this work). Next, by keeping the crosslinking position fixed at p5 and switching bp8 to an A:T, the resulting complex IC2 was found to adopt the same overall conformation seen in IC1, except now sampling the A:T base pair at position 8 (**Figure 1**). Thus, MutM prefers to sample an A:T base pair over G:C and the +3 sampling register over +2 or +4.

In IC1, IC2, and IC3, the target base pair is intact but severely buckled, with Phe114 inserted deeply into the helical stack on the 3'-side of the nucleobase targeted for extrusion. The structure differs in other significant ways from that of MutM bound to an extrahelical oxoG lesion (lesion-recognition complex, or LRC). In the LRC, Arg112 occupies part of the space vacated by the extruded oxoG and makes specific interactions with the partner C (**Figure 2B**). In the ICs, Arg112 curls down and makes non-specific backbone contacts with the DNA (**Figure 2B**). MutM makes numerous direct contacts to the DNA phosphate backbone in the LRC and a number of these contacts are replaced by water-mediated contacts in the ICs. It has now been shown by single-molecule studies that both MutM and hOGG1 rapidly slide along DNA with a low overall barrier for translocation from one base pair to the next. Presumably these water molecules play the role of "lubricating" the protein-DNA interface to allow fast translocation of MutM along undamaged DNA, as is required by a fast search process. The fast search process coupled to the severe distortion caused by the probe residue, Phe114 (**Figure 2B**), suggests a kinetic mode of discrimination between normal and damaged base pairs where the distortion serves as a means for enhancing selective extrusion of damaged bases. Although structures of other DNA glycosylases with undamaged DNA are not available, a survey of existing structures of LRCs reveal a similar probe residue, mostly aromatic in nature, involved in severe local distortion of DNA by the disruption of local helical π-stacking. Thus, DNA interrogation by an intercalating probe residue akin to Phe114 may be a general strategy employed by diverse DNA glycosylases in their search for lesions in the genome.

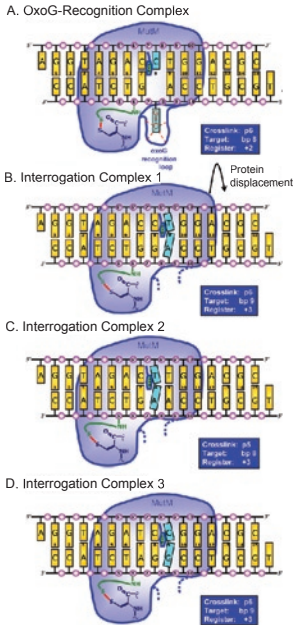

Figure 1. Schematic representation of Q166C MutM-DNA complexes. (A) The MutM lesion-recognition complex (LRC) used as the basis for the design of the crosslinking system. (B – D) Interrogation complexes showing the positioning of MutM over the DNA duplex, with the target base-pair in aqua. The side-chain of the helix-probe residue Phe114 is indicated. The numbering system for the base-pairs and backbone phosphates is as indicated. The curved green line denotes the thiol-bearing tether engaged in a crosslink to Cys^{166}. Each blue box indicates the site of tether attachment to DNA, the position of the target base-pair, and the separation between them, here referred to as the register. Dashed blue lines indicate the lack of order in the oxoG-recognition loop.

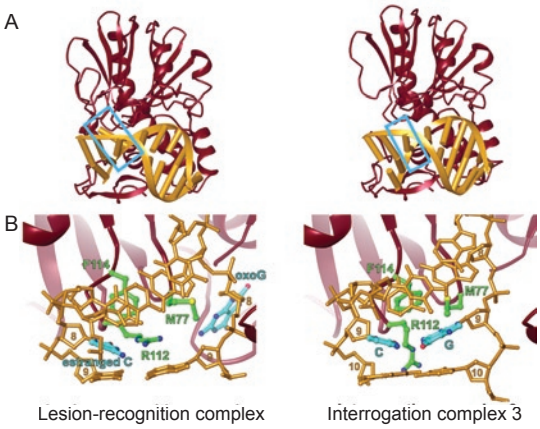

Figure 2. Comparison of the lesion recognition complex with interrogation complex 3. (A) Overall structures of the complexes. (B) Close-up view of key interactions between the target base-pair and MutM. The protein backbone is in a crimson ribbon representation, with the side-chain of key residues shown in green. The DNA is in gold. The target base-pair is shown with a box in (A) and is colored aqua in (B)

BEAMLINE
X6A

PUBLICATION
M. Nadella, M.A. Bianchet, S.B. Gabelli, J. Barrila, and L.M. Amzel, "Structure and Activity of the Axon Guidance Protein MICAL," *Proc. Natl. Acad. Sci. USA*, **102**(46),16830-5 (2005).

FUNDING
National Institutes of Health

MORE INFORMATION
L.M. Amzel
Department of Biophysics and Biophysical Chemistry
Johns Hopkins University School of Medicine
mario@neruda.med.jhmi.edu

A REDOX REACTION IN AXON GUIDANCE: STRUCTURE AND ENZYMATIC ACTIVITY OF MICAL

M. Nadella, M.A. Bianchet, S.B. Gabelli, and L.M. Amzel

Department of Biophysics and Biophysical Chemistry, Johns Hopkins University School of Medicine

During development, neurons are guided to their final targets by external cues. MICAL, a large multidomain cytosolic protein, is a downstream signaling molecule required for repulsive axon guidance. We have determined the structure of the N-terminal FAD-binding domain of MICAL to 2.0 Å resolution. This structure shows that $MICAL_{fd}$ is structurally similar to aromatic hydroxylases and amine oxidases. We obtained biochemical data that show that $MICAL_{fd}$ is a flavoenzyme that, in the presence of NADPH, reduces molecular oxygen to H_2O_2. We propose that the H_2O_2 produced by this reaction may be one of the signaling molecules involved in axon guidance by MICAL.

Neurons are required to make path-finding decisions throughout their development and are guided to their final targets by a variety of environmental cues. Semaphorins are a family of guidance molecules that act as repellents in a variety of axon development processes. Repulsive guidance by Semaphorins is mediated through their interaction with Plexins, a family of transmembrane receptors. Biochemical and genetic analysis indicates that a large multi-domain cytosolic protein, MICAL (Molecule Interacting with CasL), is required for the repulsive axon guidance mediated by the interaction of Semaphorins and Plexins. MICAL proteins contain a large amino-terminal FAD-binding domain ($MICAL_{fd}$), followed by a series of protein-protein binding domains. $MICAL_{fd}$ is of great interest since it offers a novel link between redox reactions and an axon guidance response. Using x-ray crystallography, we determined the structure of murine MICAL1 FAD-binding domain, $MICAL_{fd}$ **(Figure 1)**.

Authors (from left) L.M. Amzel, S.B. Gabelli, M.A. Bianchet, and M. Nadella

$MICAL_{fd}$ is a mixed α/β globular protein that contains a Rossmann β-α-β fold, two conserved FAD-binding motifs, and a third conserved sequence motif. The first conserved GXGXXG dinucleotide binding motif resides within the Rossman fold. The second conserved GD motif has been observed in flavoprotein hydroxylases and forms part of a strand and a helix. A search of known structures reveals that the $MICAL_{fd}$ protein is most similar to aromatic hydroxylases, especially the *p*-hydroxybenzoate hydroxylase (pHBH) from *P. fluorescens* (rms 1.79 Å for 199 out of 484 aligned α-Carbons). The strong structural similarity of $MICAL_{fd}$ to PHBH suggests that the two proteins might have similar enzymatic activities. Since purified $MICAL_{fd}$ contains oxidized FAD, reduction of the cofactor was tested using either NADH (nicotinamide adenine dinucleotide) or NADPH (nicotinamide adenine dinucleotide phosphate). Although no net reduction of the FAD was detected, a steady, time-dependent oxidation of reduced nicotinamide dinucleotide was observed **(Figure 2)**. This observation suggested that enzyme-bound $FADH_2$ was formed but was then reoxidized by oxygen. The resulting production of H_2O_2 was confirmed by monitoring its formation with horseradish peroxidase in a coupled spectrophotometric assay **(Figure 2)**. The rate of the reaction is over 10 times faster with 200 μM NADPH than with 200 μM NADH, suggesting that MICAL is probably an NADPH-dependent enzyme.

The observation of this enzymatic activity can be explained by one of three cases. First, H_2O_2 is the physiological product of the enzyme and is a component of the avoidance signal. Second, as with other FAD hydroxylases, in the absence of

substrate the hydroperoxide form of the enzyme (the $MICAL_{fd}$-FADH-O_2H intermediate) decomposes, producing hydrogen peroxide and oxidized enzyme-bound FAD (**Scheme 1**).

Third, the enzyme may actually be an amine oxidase in which the $FADH_2$ is reoxidized by molecular oxygen, and the reduction by NADPH is a fortuitous, non-specific reaction. Although this last case is unlikely, discrimination among these possibilities requires further experimentation.

The synthesis of a specific metabolite and the production of reactive oxygen species have been previously proposed as possible mechanisms of MICAL signaling. We have shown here that the FAD-binding domain of MICAL can generate at least the second kind of signals: MICAL reduces molecular oxygen using NADPH to produce H_2O_2.

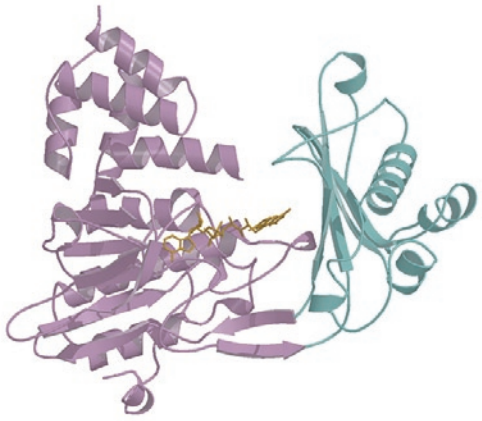

Figure 1. Ribbon representation of the tertiary structure of $MICAL_{fd}$. $MICAL_{fd}$ is a mixed α/β globular protein composed of two sub-domains of different sizes linked by two β-strands. Subdomain-1 is colored in magenta and subdomain-2 is colored in light blue. The observed FAD molecule is colored in yellow. The large sub-domain (subdomain-1; residues 1 to 226 and 373 to 484) contains the two known FAD sequence motifs (residues 84 to 114 and 386 to 416) and a third conserved motif typically found in hydroxylases (residues 212 to 225). The first motif is part of a Rossmann β-α-β fold (β1-α5-β2 in $MICAL_{fd}$). This is a sequence commonly found in FAD and NAD(P)H-dependent oxidoreductases. The second motif, which contains a conserved GD sequence in hydroxylases, forms part of a strand and a helix. In $MICAL_{fd}$ this second conserved sequence makes contacts with the ribose moiety of FAD.

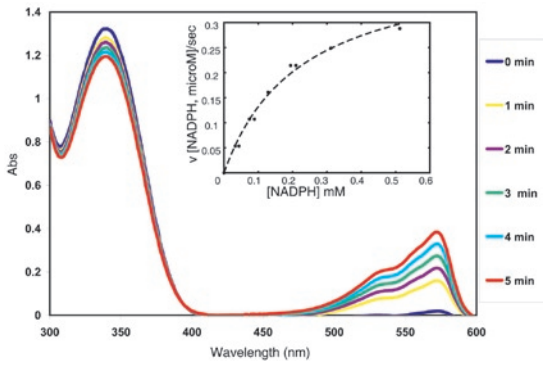

Figure 2. Kinetics of NADPH oxidation and H_2O_2 production. The absorbance peak at 340 nm is characteristic of reduced NAPDH and the peak at 560 nm the concentration of H_2O_2. The experiment ran for five minutes after the addition of the enzyme. The inset shows the initial rates as a function of NADPH concentration.

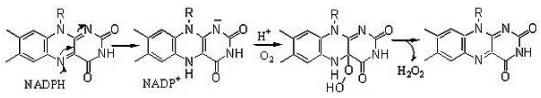

Scheme 1

BEAMLINE
X4A

PUBLICATION
B. Yu, W.C. Edstrom, J. Benach, Y. Hamuro, P.C. Weber, B.R. Gibney, and J.F. Hunt, "Crystal Structures of Catalytic Complexes of the Oxidative DNA/RNA Repair Enzyme AlkB," *Nature*, **439**, 879-884 (2006).

FUNDING
National Institutes of Health
American Heart Association

FOR MORE INFORMATION
John F. Hunt
Department of Biological Sciences and Northeast Structural Genomics Consortium
Columbia University
jfhunt@biology.columbia.edu

CRYSTAL STRUCTURES OF CATALYTIC COMPLEXES OF THE OXIDATIVE DNA/RNA REPAIR ENZYME AlkB

B. Yu[1], W.C. Edstrom[1], J. Benach[1], Y. Hamuro[2], P.C. Weber[2], B.R. Gibney[3], and J.F. Hunt[1]

[1]Department of Biological Sciences and Northeast Structural Genomics Consortium, Columbia University; [2]ExSAR Corporation; [3]Department of Chemistry, Columbia University

AlkB is a protein whose role in DNA repair has only recently been elucidated. Identified as a member of the Fe(II)-2-oxoglutarate-dependent digoxygease superfamily, AlkB directly converts alkylated DNA and RNA bases back into their original form. The preferred substrates of AlkB are based-modified by Sn2-type alkylating agents, like busulfan, an anti-cancer drug widely used in the treatment of chronic myelogenous leukemia. Here we describe the crystal structure of substrate and product complexes of E. coli AlkB. Anaerobic crystallization conditions were used to obtain structures from a protein construct optimized for crystallization based on high-resolution backbone amide $^{1}H/^{2}H$ exchange measurements.

Enzymes in the Fe(II)-2-oxoglutarate-dependant digoxygenase superfamily use molecular oxygen, Fe(II), and the decarboxylation of 2-oxoglutarate (2OG) to generate succinate and CO_2 while oxidizing organic substrates. This superfamily makes up the largest class of non-heme iron-containing enzymes and is responsible for such diverse biological reactions as the synthesis of some antibiotics and plant metabolites, the hydroxylation of collagen, and the regulation of hypoxia. In the reaction catalyzed by AlkB, a methyl adduct on a nucleotide base is converted to an unstable hydroxymethyl moiety that is spontaneously released as formaldehyde to regenerate the original unmethylated base. Several AlkB substrates have been identified: 1-methyladenine, 3-methylcytosine, 1-methylguanine, and 3-methylthymine. *E. coli* AlkB has also been demonstrated to remove ethyl, propyl, and exocyclic etheno adducts. The substrates for AlkB are generated by S_N2 (substitution, nucleophilic, bimolecular) alkylating reagents preferentially in single-stranded DNA and RNA. However, AlkB has been shown to demethylate these bases in both single-stranded and double-stranded nucleic acid polymers as well as in DNA/RNA hybrids.

Authors John Hunt and Bomina Yu

The accumulation of DNA lesions caused by alkyl modifications to nucleic acids is associated with the development of aging, cancer, and neurodegenerative diseases. However, these same DNA modifiers are widely used as chemotherapeutic drugs for the treatment of cancer. Consequently, a thorough knowledge of how DNA repair mechanisms work could benefit both cancer therapy and prevention. Understanding how AlkB repairs different nucleic acid bases requires the detailed characterization of how substrates are recognized and bound in the active site. However, initial attempts to crystallize full-length *E. coli* AlkB proved unsuccessful. High-resolution backbone amide $^{1}H/^{2}H$ (H/D) exchange measurements showed that the N-terminus of *E. coli* AlkB is conformationally flexible. When repeated in the presence of iron and substrates, other internal regions of the protein backbone became significantly more protected against H/D exchange, implying that the presence of the ligands stabilized the structure. A new construct lacking the first 11 amino acids (AlkB-ΔN11) was created. Crystallization trials were performed in the presence of Fe(II), 2OG, and a model methylated trimer [dT-(1-me-dA)-dT] under anaerobic conditions since the presence of oxygen would cause enzyme turnover. This new N-terminally truncated AlkB produced high-quality crystals under these conditions. Crystals obtained anaerobically were exposed to atmospheric oxygen over a number of days to capture the enzymatic reaction in progress.

The resulting crystal structures of *E. coli* AlkB offer insights into the DNA repair mechanism catalyzed not only by AlkB but by Fe-2OG dioxygenases in general. Although the Fe-2OG dioxygenase core

of AlkB-ΔN11 matches that in other superfamily members, a unique, conformationally flexible subdomain holds a methylated trinucleotide substrate into the active site. This subdomain corresponds to that region protected by H/D exchange in the presence of ligands. The flexibility of this "lid" may enable docking of diverse alkylated nucleotide substrates into the active site. The observed open and closed states of a tunnel (**Figure 1**) in different crystal structures provide further evidence for a putative O_2 diffusion pathway that has been suggested for other superfamily members. Furthermore, we found that exposing crystals of the anaerobic Michaelis complex to air yields partial oxidation of 2OG to succinate (**Figure 2**), supporting the theory that oxygen binds to the iron ion, which then moves or rotates to catalyze the dealkylation reaction.

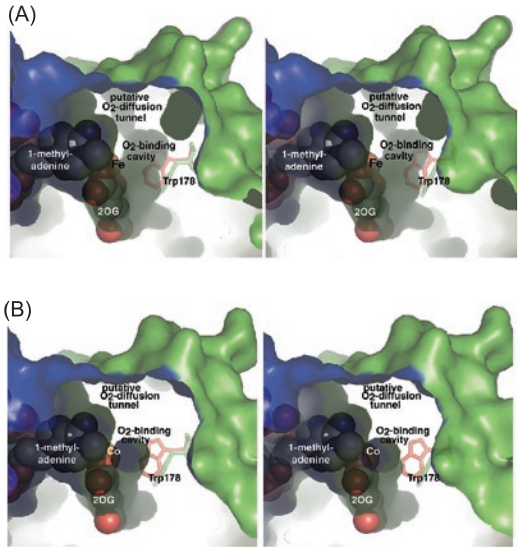

Figure 1. Stereo pairs showing cavities near the active site in (A) the structure of the anaerobic Michaelis complex after 2 h of exposure to air and (B) the substrate complex with Fe(II) replaced by Co(II) and in which the putative O_2-diffusion tunnel is closed. The molecular surface of the protein is colored according to the subdomain of origin (with the nucleotide-recognition lid in blue and the catalytic core in green). The sidechain of trp-178 is shown in the different conformations observed in these two structures, which exhibit the greatest variation in the structure of the O_2-diffusion tunnel among the 7 crystal structures reported in our paper. Trp-178 has been reported to be hydroxylated by AlkB in the absence of nucleotide substrate, although no evidence of this modification is observed in the any of these refined crystal structures.

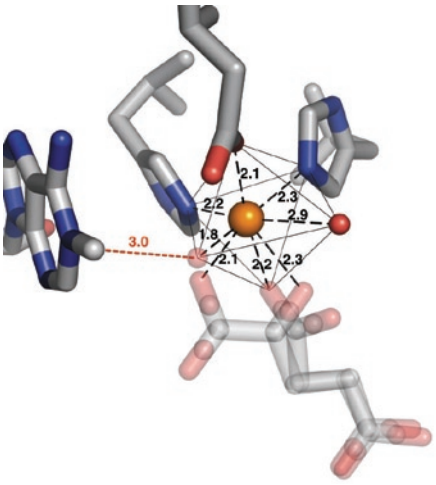

Figure 2. Stereo pair showing active site stereochemistry in the crystal structure in which the anaerobic Micheaelis complex was exposed to oxygen for 2 h. Unbiased electron density maps support the conclusion that a significant amount of the 2OG has been oxidized to succinate but that the adenine base remains largely methylated after short-term *in situ* oxidation. The alternative ligands are shown in semi-transparent rendering with the degree of transparency scaled according to refined occupancy.

BEAMLINE
X12B

PUBLICATION
L. Di Costanzo, G. Sabio, A. Mora, P.C. Rodriguez, A.C. Ochoa, F. Centeno, and D.W. Christianson, "Crystal Structure of Human Arginase I at 1.29 Å Resolution and Exploration of Inhibition in the Immune Response," *Proc. Natl. Acad. Sci. USA*, **102**(37), 13058-13063 (2005).

FUNDING
National Institutes of Health

FOR MORE INFORMATION
David W. Christianson
Department of Chemistry
University of Pennsylvania
chris@sas.upenn.edu

CRYSTAL STRUCTURE OF HUMAN ARGINASE I AT 1.29 Å RESOLUTION AND EXPLORATION OF INHIBITION IN THE IMMUNE RESPONSE

L. Di Costanzo[1], G. Sabio[2], A. Mora[2], P.C. Rodriguez[3], A.C. Ochoa[3], F. Centeno[2], and D.W. Christianson[1]

[1]Roy and Diana Vagelos Laboratories, Department of Chemistry, University of Pennsylvania; [2]Department de Bioquímica y Biología Molecular, Facultad de Veterinaria, Universidad de Extremadura, Spain; [3]Tumor Immunology Program, Stanley S. Scott Cancer Center and Department of Pediatrics, Lousiana State University

Human arginase I, an enzyme critical to the urea cycle, is a potential drug target for diseases linked to compromised L-arginine homeostasis. Here, we report high-affinity binding of the boronic acid-based inhibitors "ABH" and "BEC" to human arginase I. The 1.29 Å resolution structure of the complex with ABH yields an unprecedented view of arginase I's binuclear manganese cluster and illuminates the structural basis for nanomolar enzyme-inhibitor affinity. This work serves as a foundation for studying the structural and chemical biology of arginase I in the immune response, and we demonstrate the inhibition of arginase activity by ABH in human and murine myeloid cells (blood cells).

Arginase is a trimeric binuclear manganese metalloenzyme that catalyzes the hydrolysis of the amino acid L-arginine to form L-ornithine and urea. Two arginase isozymes have been identified in mammals: cytosolic arginase I, which is responsible for the nitrogen-elimination step of the urea cycle, and mitochondrial arginase II, which functions in L-arginine homeostasis. Significantly, arginase inhibitors can enhance NO-dependent biological processes such as smooth muscle relaxation, so arginase is a potential drug target for diseases characterized by insufficient NO flux in biological signaling pathways. Most recently, our laboratory has determined that arginase is a potential drug target for the treatment of male and female sexual arousal disorders. Arginase also plays a role in mediating the effects of nitric oxide in the immune response. Notably, macrophage arginase I and NO synthase are reciprocally regulated at the level of transcription: NO synthase is induced by TH1 cytokines, and arginase I is induced by TH2 cytokines. As a modulator of NO-dependent macrophage cytotoxicity, arginase I is implicated in the suppression of the tumoricidal activity of macrophages and T cells. In a murine model of multiple sclerosis, arginase I expression is up-regulated approximately 300-fold. Administration of the arginase inhibitor ABH improves the symptoms of the disease.

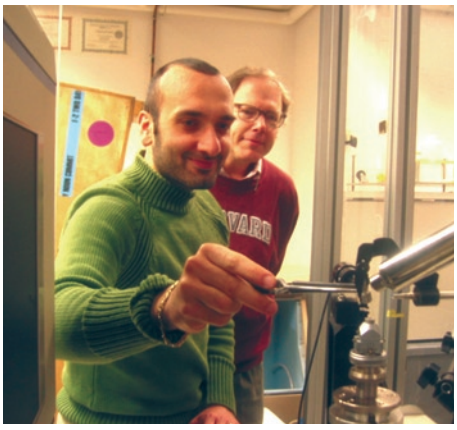

Authors Luigi Di Constanzo and David Christianson

In the current study, we demonstrate that the boronic acid substrate analogues ABH and BEC (**Figure 1**) are highly potent inhibitors of human arginase I, with K_d values of 5 and 270 nM, respectively. Therefore, ABH and BEC may be potentially useful for blocking tumor-cell growth or treating multiple sclerosis in humans. Analysis of the high-resolution structures of human arginase I complexed with ABH and BEC reveals that the boronic acid moiety of each inhibitor undergoes a nucleophilic attack to bind as tetrahedral boronate anion (**Figure 2**). This binding mode mimics that expected for the actual tetrahedral intermediate and its flanking transition states in catalysis. Thus, boronic acid inhibitors such as ABH and BEC are reactive substrate analogues that are chemically transformed into transition state analogues in the enzyme active site. Such reactive substrate analogues are informally known as "reaction coordinate analogues."

Nanomolar affinity is a consequence of strong boronate-manganese coordination interactions as well as hydrogen-bond networks between the enzyme and the α-carboxylate and α-amino groups of the inhibitor, as illustrated for BEC in

Figure 3. In catalysis, this array of intermolecular interactions ensures specificity for L-arginine and disfavors binding and catalysis for L-arginine analogues bearing modified α-substituents. These structure-affinity relationships are important to consider as arginase I is explored as a potential target for new therapies directed toward inflammatory and immunological disorders, and especially so as boronic acid-based inhibitors ultimately join the growing family of enzyme-targeted drugs.

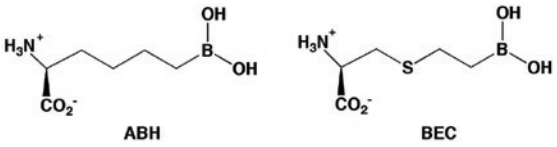

Figure 1. Human arginase inhibitors S-(2-boronethyl)-L-cysteine (BEC, K_d = 270 nM) and 2(*S*)-amino-6-boronhexanoic acid (ABH, K_d = 5.0 nM).

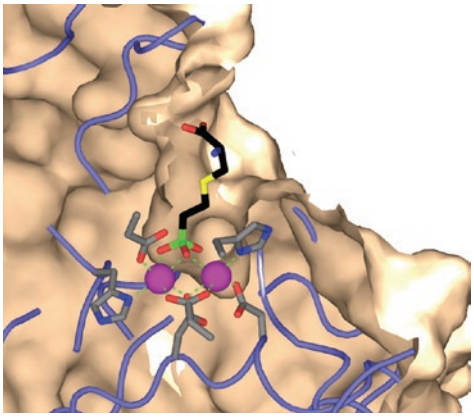

Figure 2. Complex between human arginase I and the reactive substrate analogue inhibitor *S*-(2-boronethyl)-L-cysteine (BEC). The inhibitor binds as the tetrahedral boronate anion (green). Coordination interactions with the binuclear manganese cluster (magenta) spheres are indicated by green dotted lines.

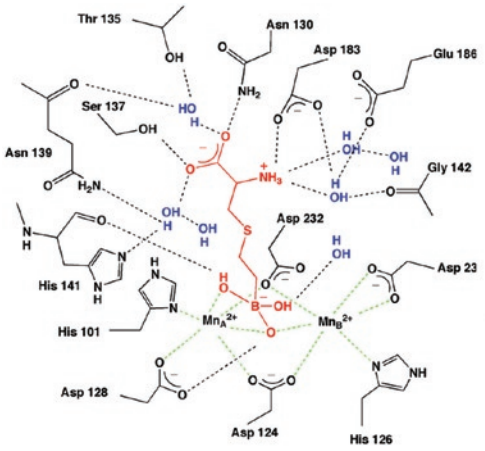

Figure 3. Summary of intermolecular interactions in the human arginase I-BEC complex.

BEAMLINE
X4A

PUBLICATION
P. Bachhawat, G.V.T. Swapna, T. Montelione, and A.M. Stock, "Mechanism of Activation for Transcription Factor PhoB Suggested by Different Modes of Dimerization in the Inactive and Active States," *Structure*, **13**, 1353-1363 (2005).

FUNDING
National Institutes of Health
Cancer Institute of New Jersey

FOR MORE INFORMATION
Ann M. Stock
Department of Molecular Biology and Biochemistry
Rutgers University
stock@cabm.rutgers.edu

MECHANISM OF ACTIVATION FOR TRANSCRIPTION FACTOR PhoB SUGGESTED BY DIFFERENT MODES OF DIMERIZATION IN THE INACTIVE AND ACTIVE STATES

P. Bachawat[1,2], G.V.T. Swapna[1,3,5], G.T. Montelione[1,2,3,4,5], and A.M. Stock[1,2,5]

[1]Center for Advanced Biotechnology and Medicine; [2]Department of Biochemistry, Robert Wood Johnson Medical School, University of Medicine and Dentistry of New Jersey; [3]Department of Molecular Biology and Biochemistry, Rutgers University; [4]Northeast Structural Genomics Consortium; [5]Howard Hughes Medical Institute

We have determined the crystal structures of the regulatory domain of response regulator PhoB ($PhoB_N$) in its inactive and active forms, which suggest its mechanism of phosphorylation-mediated regulation. The structure of active $PhoB_N$, together with the structure of the effector domain bound to DNA, define the conformation of the active transcription factor in which the regulatory domains dimerize using rotational symmetry while the effector domains bind to DNA tandemly, implying a lack of intra-molecular interactions. While this active DNA-bound state seems common to all members of the family, the mode of dimerization in the inactive state seems specific to PhoB.

Response regulators function within two-component systems, signal transduction pathways that are highly prevalent in bacteria. They are modular switches typically comprised of a conserved regulatory domain that regulates the activities of an associated effector domain in a phosphorylation-dependent manner. They confer virulence and antibiotic resistance in several pathogenic bacteria, making them attractive drug targets. The majority of response regulators function as transcription factors, and the OmpR/PhoB family is the largest among them.

Phosphorylation at the active-site aspartate residue in the regulatory domain leads to a propagated conformational change from the active site to a distant "functional face" of the protein through the concerted reorientation of a few key residues. How this conformational change in the regulatory domain affects the activity of the effector domain in the OmpR/PhoB family is unknown. In the two published structures of full-length family members DrrB and DrrD, the recognition helix is completely exposed, unhindered by the regulatory domain, suggesting that the mechanism of activation is not intra-molecular relief of steric inhibition. We present crystallographic and solution NMR data that suggest a mechanism of activation for PhoB, and we extend it to other members of the family.

Authors (from left) Gaetano T. Montelione, Priti Bachhawat, Ann M. Stock, and G.V.T. Swapna

The regulatory domain of PhoB shows distinct rotationally symmetric dimers in the inactive and active states when crystallized under identical conditions. In the inactive state, $PhoB_N$ crystallizes as a two-fold symmetric dimer using the $\alpha1$-$\alpha5$ interface. The symmetry was confirmed in solution using NMR. Concentration-dependent shifts of resonances in NMR experiments and analytical ultracentrifugation studies show that inactive $PhoB_N$ exists in equilibrium between a monomer and a dimer in solution. When the structure of the effector domain is docked on the structure of the inactive $PhoB_N$ dimer using either DrrD or DrrB as a model, the effector domains project in opposite directions, in an orientation incompatible with tandem binding to direct repeat DNA sequences. This alternate dimer is not observed for any other OmpR/PhoB family member and may be a specific feature of PhoB that provides an additional means of regulation.

$PhoB_N$ was also crystallized in the active state using the non-covalent beryllium fluoride (BeF_3^-) complex as a phosphoryl analog. In the active state, $PhoB_N$ forms a two-fold symmetric dimer using the $\alpha4$-$\beta5$-$\alpha5$ interface. The symmetry was confirmed in solution using NMR. The dimer interface is composed of highly conserved residues

that form a central hydrophobic patch surrounded by salt-bridges. The structure of active $PhoB_N$, together with the previously solved structure of the effector domain bound to DNA, provides a model of the active transcription factor in which the regulatory domains dimerize with rotational symmetry while the effector domains bind to DNA using tandem symmetry (**Figure 1**). The different symmetries adopted by the regulatory and effector domains suggest that activation causes a loss of intra-molecular orientational constraints on the effector domains. The high degree of conservation of the α4-β5-α5 interface and a number of other similar structures from this family suggest that this mode of dimerization is common to all members of the OmpR/PhoB family.

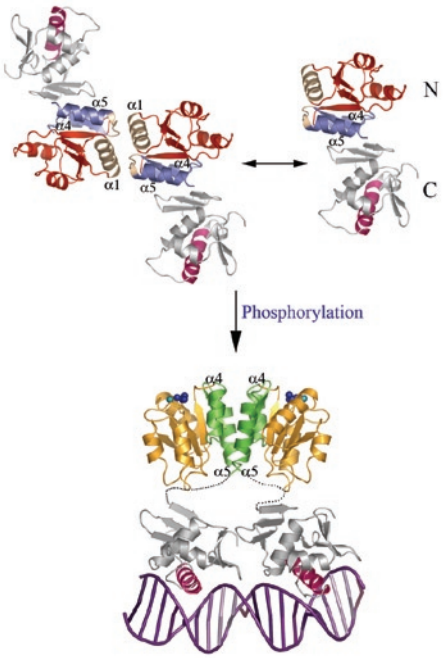

Figure 1. Model of phosphorylation-mediated activation for transcription factor PhoB

BEAMLINE
X12C

PUBLICATION
K. Ye and D.J. Patel, "RNA Silencing Suppressor p21 of Beet Yellows Virus Forms an RNA Binding Octameric Ring Structure," *Structure*, **13**, 1375–1384 (2005).

FUNDING
The Abby Rockefeller Mauze Trust; The Dewitt Wallace and Maloris Foundations

FOR MORE INFORMATION
Keqiong Ye
National Institute of Biological Sciences, Beijing
yekeqiong@nibs.ac.cnio@nerud

RNA SILENCING SUPPRESSOR P21 ADOPTS AN UNUSUAL siRNA-BINDING OCTAMERIC RING ARCHITECTURE

K. Ye and D.J. Patel

Structural Biology Program, Memorial Sloan-Kettering Cancer Center

In plants, RNA silencing functions as an innate defense mechanism against virus infection, where viral RNA strands are degraded by an RNA-guided mechanism. Many plant viruses counter-attack by expressing proteins to inhibit this defense pathway. The p21 protein, a RNA silencing suppressor in Beet yellows virus, seems to function by binding siRNAs, a critical mediator in the process. The crystal structure of p21 reveals an octameric ring architecture involving a new mode of protein oligomerization. Putative RNA binding sites inside the ring are suggested by the structure. In addition, biochemical assays show that p21 binds various RNAs besides the siRNA duplex, suggesting the existence of an alternative suppression mechanism.

Unlike animals, plants have no immune system, yet they are still able to recover from virus infection and even acquire resistance. This is because plants have other innate defense mechanisms. RNA silencing, one of the available plant defense mechanisms, targets viral RNA for destruction. Double-stranded RNAs generated during viral replication can be perceived as a signal of virus infection by the plant host and diced into smaller fragments, called small interfering RNAs (siRNAs). These siRNAs, consisting of duplexes of 21 nucleotides in length, are critical mediators in the silencing process. The siRNAs assemble with effector nucleases and instruct them to specifically cleave viral RNAs, thereby thwarting the proliferation and propagation of the virus. On the other hand, viruses need to evade or suppress this defense in order to survive and propagate. Studies have shown that many plant viruses do possess evolved weapons for counter-defense. The p21 protein is an RNA silencing suppressor recently discovered in Beet yellows virus. Because of its siRNA binding ability, p21 is thought to inhibit the silencing process by inactivating siRNA. To understand the function and mechanism of p21, we have determined its crystal structure in its free state, thereby revealing a surprising viral-engineered scaffold used in binding siRNA.

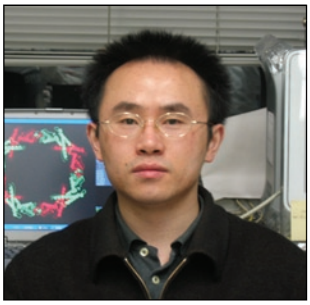

Keqiong Ye

The structure of the p21 monomer is comprised entirely of α-helices and folded into amino-terminal (NTD) and carboxy-terminal (CTD) domains (**Figure 1B**). But at the higher structural level, p21 forms an octameric ring, which adopts a previously unknown topology (**Figure 1A**). Normally, protein ring structures are formed by a single type of asymmetric (involving a different part of the protein, head-to-tail) association process between adjacent subunits. In stark contrast, the eight p21 monomer subunits associate through two types of symmetric alignments, namely via a head-to-head (NTD-NTD) and tail-to-tail (CTD-CTD) association. This structure represents a new theme in the cyclic oligomerization of proteins. **Figure 1C** compares the topology of p21 and other common ring structures.

To search for the RNA binding site, we noticed that several basic residues, exposed within the inner surface of the ring, are highly conserved among p21 homologs, suggesting that they might be involved in RNA binding through electrostatic interactions with negatively charged phosphates in RNA (**Figure 2**). In addition, the large inner cavity of the ring (~90 Å in diameter) provides enough space for RNA binding.

The structure of p21 differs significantly from a previously characterized suppressor, p19 from tombusvirus, which is dimeric and strictly recognizes an siRNA duplex of specific length. These

structural differences suggest that their RNA binding mechanisms might also be different. Indeed, biochemical analysis showed that p21 is a general nucleic acid binding protein, interacting with 21-nt or longer single- and double-stranded RNAs (**Figure 3**). Because RNA silencing involves various types of RNA, it is possible that p21 might suppress RNA silencing by interacting with RNAs besides siRNA.

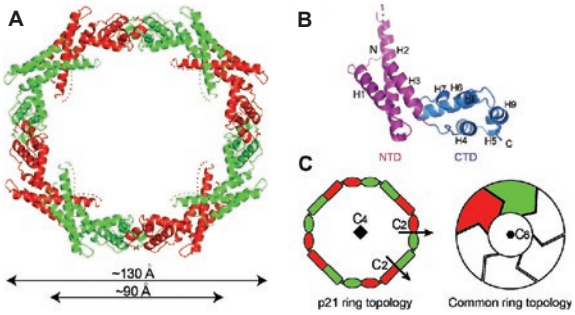

Figure 1. Crystal structure of p21. (A) The entire octameric ring. Neighboring monomers are alternatively colored with green and red. (B) Structure of the p21 monomer, which consists of two domains. (C) Ring topology of p21 (left panel) compared with other common hexameric ring scaffolds as an example (right panel). Each p21 monomer, colored the same as in (A), is represented by a rectangle (NTD) and an ellipse (CTD).

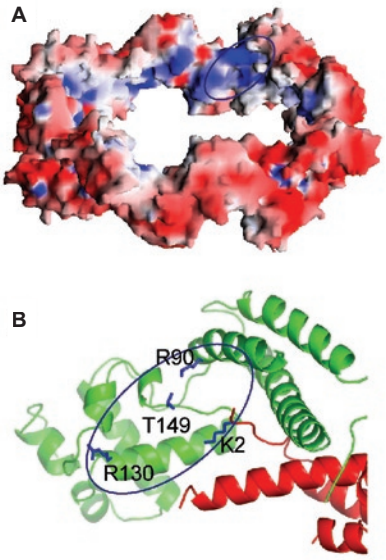

Figure 2. A putative RNA-binding surface inside the ring, which is (A) positively charged and (B) clustered with several conserved residues.

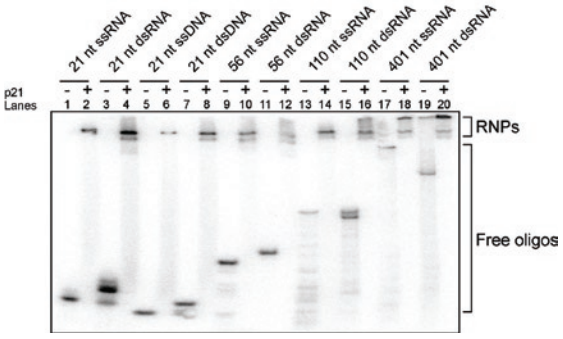

Figure 3. RNA-binding assay of p21 showing that p21 forms complexes with various RNAs. Individual RNAs migrate slower in the native gel after forming protein complex (RNP).

BEAMLINE
X26C, X29

PUBLICATION
E.J. Enemark and L. Joshua-Tor, "Mechanism of DNA Translocation in a Replicative Hexameric Helicase," *Nature*, **442**, 270-275 (2006).

FUNDING
The National Institutes of Health

FOR MORE INFORMATION
Leemor Joshua-Tor
Cold Spring Harbor Laboratory
leemor@cshl.edu

MECHANISM OF DNA TRANSLOCATION IN A REPLICATIVE HEXAMERIC HELICASE

E.J. Enemark[1] and L. Joshua-Tor[1]

[1]W.M. Keck Structural Biology Laboratory, Cold Spring Harbor Laboratory

During DNA replication, two complementary DNA strands are separated and each becomes a template for the synthesis of a new complementary strand. Strand separation is mediated by a helicase enzyme, a molecular machine that uses the energy derived from ATP-hydrolysis to separate DNA strands while moving along the DNA. We determined a crystal structure of a viral replicative helicase bound to single-stranded DNA and nucleotide molecules at the ATP-binding sites. This structure demonstrates that a single strand of DNA passes through the hexamer channel and that the DNA-binding hairpins of each subunit collectively form a spiral staircase that sequentially tracks the DNA backbone. It also demonstrates a correlation between the height of each DNA-binding hairpin in the staircase and the ATP-binding configuration, suggesting a straightforward mechanism for DNA translocation.

Papillomaviruses are tumor viruses that cause benign and cancerous lesions in their host. Replication of papillomaviral DNA within a host cell requires the viral E1 protein, a multifunctional protein. E1 initially participates in recognizing a specific replication origin DNA sequence as a dimer with E2, another viral protein. Subsequently, further E1 molecules are assembled at the replication origin until two hexamers are established. These hexamers are the active helicases that operate bidirectionally in the replication of the viral DNA. In order to unwind DNA, helicases must separate the two strands while moving along, or translocating on the DNA. Based on structures of the DNA-binding domain of E1 bound to DNA that we determined a few years ago, we suggested a mechanism for DNA strand separation. However, the mechanism that couples the ATP cycle to DNA translocation has been unclear. The E1 hexameric helicase adopts a ring shape with a prominent central channel that has been presumed to encircle substrate DNA during the unwinding process, but the atomic details of this binding have been uncertain, including whether the ring encircles one or both strands of DNA during unwinding.

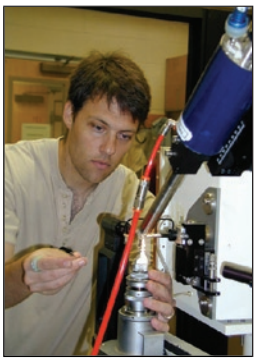

Authors (from left) Leemor Joshua-Tor and Eric Enemark

Our crystal structure of the E1 hexameric helicase bound to single-stranded DNA (**Figure 1**) demonstrates that only one strand of DNA passes through the central channel and reveals the details of the non-specific binding (**Figure 2**). The β-hairpins (DNA-binding hairpins) of each subunit sequentially track the sugar-phosphate backbone of the DNA in a one nucleotide per subunit increment. This configuration resembles a spiral staircase (**Figure 2**).

ATP-binding (and hydrolysis) sites are located at the subunit interfaces, and multiple configurations are observed within the hexamer. These have been assigned as ATP-type, ADP-type, and apo-type. The configuration of the site for a given subunit correlates with the relative height of its DNA-binding hairpin in the staircase arrangement. The subunits that adopt an ATP-type configuration place their hairpins at the top of the staircase while the hairpins of apo-type subunits occupy the bottom positions of the staircase. The hairpins of the ADP-type subunits are placed at intermediate positions.

A straightforward "coordinated escort" DNA-translocation mechanism is inferred from the staircased DNA-binding and its correlation with the configuration at the ATP-binding sites. Each DNA-binding hairpin maintains continuous contact with one unique nucleotide of ssDNA and migrates downward via ATP-hydrolysis and subsequent ADP-release at the subunit interfaces. ATP-hydrolysis

occurs between subunits located toward the top of the staircase, while ADP-release occurs between subunits located toward the bottom of the staircase. The hairpin at the bottom of the staircase releases its associated ssDNA phosphate to conclude its voyage through the hexameric channel. Upon binding a new ATP molecule, this subunit moves to the top of the staircase to pick up the next available ssDNA phosphate, initiating its escorted journey through the channel and repeating the process. For one full cycle of the hexamer, each subunit hydrolyzes one ATP molecule, releases one ADP molecule, and translocates one nucleotide of DNA through the interior channel. A full cycle, therefore, translocates 6 nucleotides with associated hydrolysis of 6 ATPs and release of 6 ADPs.

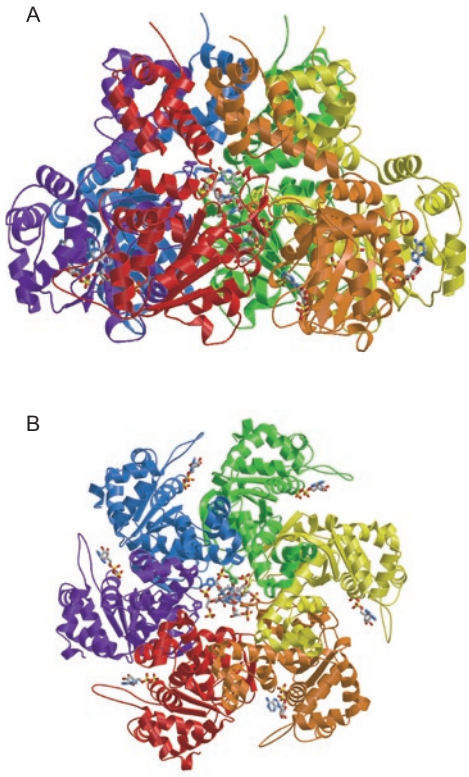

Figure 1. Views of the E1 hexamer parallel and perpendicular to the central channel with indidual subunits are color-coded. Single-stranded DNA is bound discretely within the chanel, and nucleotides are present at the subunit interfaces.

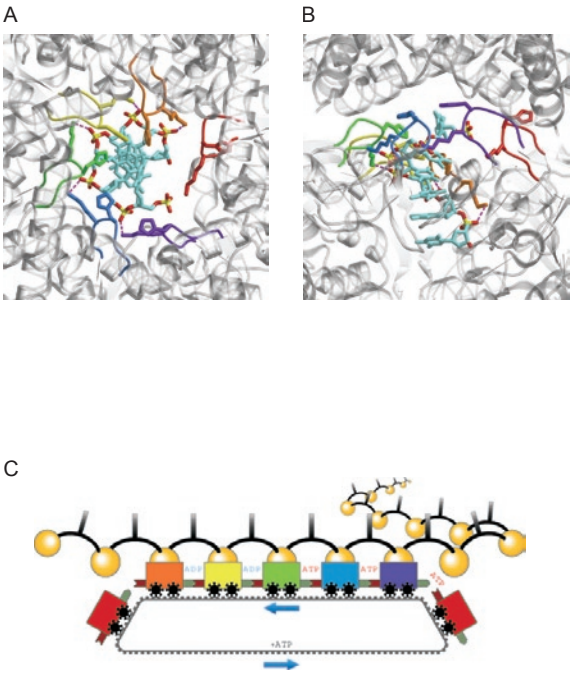

Figure 2. Details of DNA coordination viewed (A) parallel and (B) perpendicular to the hexamer channel and (C) a cartoon depicting the “coordinated escort” mechanism for DNA translocation.

PHASE STABILITY IN CERIA-ZIRCONIA BINARY OXIDE NANOPARTICLES

F. Zhang[1], C.-H. Chen[1], J.M. Raitano[1], R.D. Robinson[1], I.P. Herman[1], J.C. Hanson[2], W.A. Caliebe[2], S. Khalid[2], and S.-W. Chan[1]

[1]Department of Applied Physics and Applied Mathematics, Materials Research Science and Engineering Center, Columbia University; [2]Brookhaven National Laboratory

Cerium oxide has been widely investigated as a key component in catalysts and as an electrolyte for solid oxide fuel cells because of its ability to release or store oxygen when in its cubic fluorite structure. This property, which is the alleged source of the oxygen storage capacity (OSC) of ceria, is much enhanced by a large surface area and a small particle size. However, at high temperatures, ceria particles are coarsened, resulting in a smaller total surface area and a lower catalytic efficiency. Alloying with other metal oxides, particularly zirconia, can halt this coarsening process. However, the zirconia content for most effective catalysis will cause the binary oxide in micron-sized particles to contain a substantial amount of tetragonal phase that does not have the OSC properties, In our study, nanoparticles of ceria-zirconia were found to have a stable cubic fluorite phase despite what was predicted by the normal "bulk" phase diagram. Furthermore, we proved that a reducing environment stabilizes the cubic phase to 90% zirconia.

BEAMLINES
X7B, X18B, X19A

PUBLICATION
F. Zhang, J.M. Raitano, C. Chen, J.C. Hanson, W. Caliebe, S. Khalid, and S. Chan, "Phase Stability in Ceria-Zirconia Binary Oxide (1-x)$CeO_{2-x}ZrO_2$ Nanoparticles: The Effect of Ce^{3+} Concentration and the Redox Envirnment," *J. of Appl. Phys.*, **99**, 0843131-0843138 (2006).

FUNDING
U.S. Department of Energy
National Science Foundation

FOR MORE INFORMATION
Siu-Wai Chan
Dept. of Applied Physics and Applied Mathematics
Columbia University
sc174@columbia.edu

Cerium oxide in the cubic fluorite structure has been widely investigated because of its multiple applications, such as catalyst and electrolyte material of solid oxide fuel cells. In particular, the structural properties of binary oxide system of ceria and zirconia (CeO_2–ZrO_2) are extensively studied because it retains the superb redox and oxygen storage capacity (OSC) properties, and prevents thermal instability against coarsening of CeO_2. However, its various phases have not been discussed in detail, particularly with crystallite size. In this study, we aimed to investigate the structural properties of its nanoparticles for phase information. Specifically, we aimed to address two areas: First, we looked for methods that can stabilize the c' phase for a higher zirconia concentration to lessen particle coarsening. Second, we ascertained the extent to which particle size affects phase stability. This has a significant impact on catalysis.

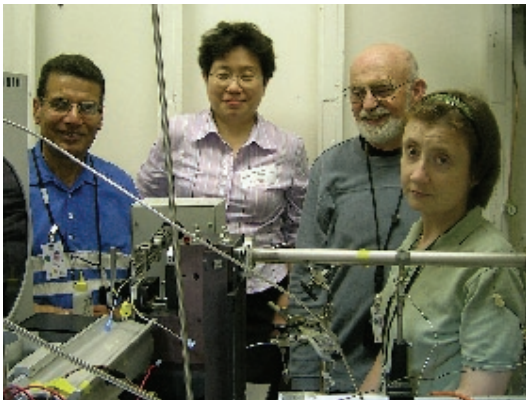

Authors (from left) Syed Khalid, Siu-Wai Chan, Jonathan C. Hanson, and Joan M. Raitano

Phase information of ceria–zirconia nanoparticles observed in air is studied by x-ray diffraction, transmission electron microscopy, and Raman spectroscopy. Particle size and composition are varied. Both the metastable tetragonal t' phase and the monoclinic m phase are not observed. The nanoscale of the particles likely stabilizes the tetragonal t phase against the formation of the monoclinic phase even at 100% zirconia. As the particle size decreases, both the c–t" and the c'–t phase boundaries shift to higher zirconia concentrations. The zirconia solubility limit increases with decreasing particle size such that the c and t" phases can be sustained at higher concentrations of zirconia before the corresponding formation of the t" and t phases. Raman scattering and XRD results are consistent in determining the emerging compositions of the t phase in the 1200° and the 800°C samples. The nanoparticles show different phases from those of the bulk in the CeO_2–ZrO_2 binary system. Nanoparticles of 20 nm and smaller having 35%–40% zirconia in ceria are 100% c' and stable against coarsening. The t" phase also likely contributes to OSC. This shows that the range of c' phase can be extended to high ZrO_2 concentrations by decreasing the c' crystallite size alone.

We observed that the range of the c' phase can extend to high ZrO_2 concentrations by decreasing the c' crystallite size alone. Earlier, we used x-ray absorption near edge spectroscopy (XANES) to demonstrate that the Ce^{3+} concentration in ceria nanoparticles increases with a decreasing crystallite size. Here, we investigated the valence state of Ce with varying ZrO_2 concentration and annealing atmosphere to better understand the phase stability in this nanocrystalline binary oxide system.

We used x-ray absorption near edge spectroscopy (XANES), time-resolved high temperature x-ray diffraction (XRD), and room temperature XRD to study the stability of the cubic phase (c') of $Ce_{1-x}Zr_xO_{2-y}$ nanoparticles. Results from XANES at the Ce L_{III} edge and the Zr L_{III} edge indicate the same phase transition point of c'-t for samples prepared in air. This is consistent with earlier results of XRD and Raman spectroscopy. The results show that the stability of the c' phase is directly related to the Ce^{3+} concentration. The percentage of the 3+ oxidation state of cerium was measured from the relative Ce^{3+} peak intensity at the Ce L_{III} edge in XANES. An 11% concentration of the larger Ce^{3+} ions, coupled with the smaller particle size, helps in releasing the local stress induced by the smaller Zr^{4+} ions and stabilizes the c' phase even under high zirconia concentrations of 40%–60%. XANES results at the Zr L_{III} edge supported the cubic phase stabilization. Under a reducing environment instead of in air, when the homogenization anneal was performed, the solubility limit of the cubic phase $Ce_{1-x}Zr_xO_{2-y}$ was extended to above 90% zirconia. The Ce^{3+} concentration increased, reaching 94% in $Ce_{0.1}Zr_{0.9}O_{2-y}$. Thus, the stability of c' phase is extended to higher ZrO_2 concentrations not by finer crystallite size alone but, more significantly, by a reducing environment.

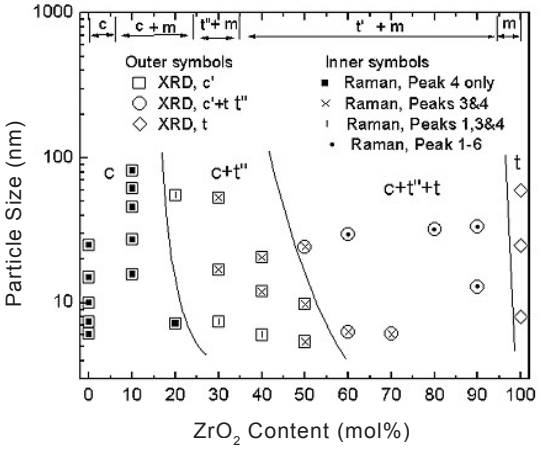

Figure 1. Phase stability diagram of $(1-x)CeO_{2-x}ZrO_2$ samples with various crystal size of the c' phase. There are overlapping symbols to denote XRD and Raman techniques in phase identification. Open symbols are from the XRD results and the inside symbols are from Raman scattering. Open squares (□): 100% c' phase present from XRD, circles (○): t phase present from XRD, diamonds (◊): only t phase present from XRD. Inner symbols, solid squares (■): only Raman peak 4 is present; vertical line (|): only Raman peaks 3 and 4 are present; crosses (×): only Raman peaks 1, 3 and 4 are present; dots (•): all Raman peaks 1-6 are present. At the top of the diagram are the phase fields identified at 800°C from reduced-quench-re-oxidized bulk/micron-size samples.

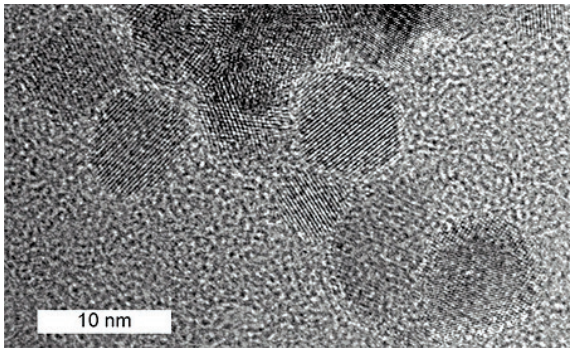

Figure 2. TEM lattice image of $Ce_{0.8}Zr_{0.2}O_{2-y}$ nanoparticles annealed previously at 900 °C.

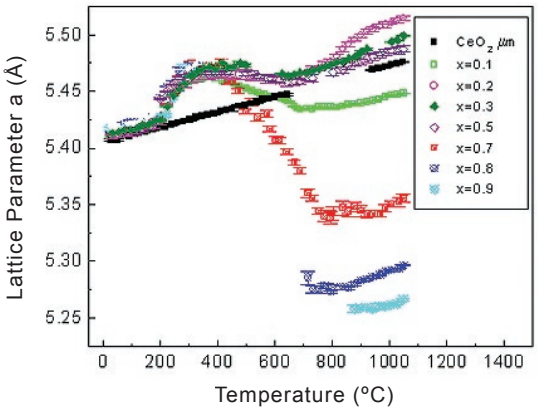

Figure 3. Lattice parameter study from in-situ XRD of as-prepared $(1-x)CeO_{2-x}ZrO_2$ in a reducing atmosphere as temperature increases. Each composition shown exhibits the cubic phase, c'.

BEAMLINE
X16C

PUBLICATION
A.I. Frenkel, S. Nemzer, I. Pister, L. Soussan, T. Harris, Y. Sun, and M.H. Rafailovich, "Size-controlled Synthesis and Characterization of Thiol-stabilized Gold Nanoparticles," *J. Chem. Phys.*, **123**, 184701 (2005).

FUNDING
U.S. Department of Energy; NSLS Faculty/Student Research Support Program

FOR MORE INFORMATION
Anatoly I. Frenkel
Physics Department
Yeshiva University
Anatoly.Frenkel@yu.edu

SIZE-CONTROLLED SYNTHESIS AND CHARACTERIZATION OF THIOL-STABILIZED GOLD NANOPARTICLES

A.I. Frenkel[1], S. Nemzer[1], I. Pister[1], L. Soussan[1], T. Harris[1], Y. Sun[1], and M.H. Rafailovich[2]

[1]Yeshiva University; [2]Stony Brook University

We synthesized thiol-protected gold nanoparticles by varying just one parameter: the gold-thiol ratio (ξ), within the range from 6:1 to 1:6. Their size and structure were analyzed self-consistently using transmission electron microscopy to measure their size distribution and EXAFS to measure their coordination numbers and nearest-neighbor distances. Surface tension in the framework of the spherical drop model was used to interpret apparent bond length shortening as ξ decreased. The smallest of such particles (16 Å in diameter) were obtained for ξ = 1:1 and the average size did not change as ξ was lowered to 1:6. We interpret this behavior in terms of surfactant-mediated stabilization of the particle size.

Size-controlled synthesis of nanoparticles less than a few nanometers in diameter is a challenge due to the spatial resolution limit of most scattering and imaging techniques used for their structural characterization. We present a self-consistent analysis of the extended x-ray absorption fine-structure (EXAFS) spectroscopy data of ligand-stabilized metal nanoclusters. Our method employs the measurement of the coordination numbers and metal-metal bond-length decrease that can be correlated with the average diameter and structure of the nanoparticles in the framework of the surface tension model and different structural motifs. To test the method, we synthesized and analyzed a series of dodecanethiol-stabilized gold nanoparticles where the only control parameter was the gold/thiol ratio ξ, varied between 6:1 and 1:6.

The dodecanethiolate gold nanoparticles were synthesized by the Brust method at the undergraduate chemistry laboratory of Yeshiva University's Stern College for Women. They were analyzed by transmission electron microscopy at the National Science Foundation Garcia Materials Research Science and Engineering Center at Stony Brook University. EXAFS data were collected at NSLS beamline X16C. It is evident that the particle size is reduced by lowering the Au/thiol ratio as inferred from the visible changes in the relative contributions of Au-Au and Au-S bonds to the Au L_3 EXAFS (**Figure 1A**). The contributions of the Au-Au or Au-S interactions to EXAFS progressively become less important, or more important, respectively, as ξ decreases. Indeed, the particle size decrease lowers the amplitude of Au-Au EXAFS oscillations due to the truncation effect (atoms on the surface of the particle are surrounded by fewer neighbors than those in the bulk and, hence, the average coordination numbers of Au-Au decrease) and enhances the amplitude of Au-S EXAFS due to the larger surface/bulk ratio.

Authors (from left) M. Rafailovich, A. Frenkel, I. Pister, L. Soussan, S. Nemzer, and T. Harris

EXAFS data were analyzed by fitting FEFF6 paths to Au-S and Au-Au shells. The particle diameters can be estimated, among other methods, by assuming specific polyhedral shapes that Au nanoparticles can adopt: The icosahedral, cuboctahedral, and truncated octahedral are among the most commonly discussed geometries. In our case, the cuboctahedral fcc model was chosen due to the similarity between the nanoparticles data and bulk Au data (**Figure 1A**) for all ξ. The particle diameters were obtained from their Au-Au coordination numbers (**Figure 2**).

For all samples, the second quantity, $\Delta R(\xi) = R_0 - R(\xi)$, where R_0 = 2.88 Å in bulk gold and $R(\xi)$ is the bond length measured at the certain ξ, mono-

tonically as ξ increases (**Figure 1B**). Such 1NN distance shortening at smaller sizes has a familiar ring from the lattice contraction of closely packed nanoparticles that has been previously interpreted in terms of surface stress by Mays, et al. (1968) using electron microscopy. We relate the particle diameter *d* to the relative lattice contraction $\alpha = \Delta R/R$ via the surface stress and compressibility *K*:

$$d = \frac{4}{3}\frac{f_{rr} K}{\alpha}$$

Using our EXAFS measurements of ΔR (**Figure 1b**) as well as the experimentally determined values for *K* and f_{rr}, we obtained the particle diameters for all ξ (**Figure 2**). The fact that both (independent) techniques of EXAFS data analysis that we employed for the particle diameter determination (by using the coordination numbers and the distance contraction) obtain very similar results (**Figure 2**) characterizes these results as highly reliable.

Our results for the gold-core sizes obtained by the new EXAFS analysis procedure are in good agreement with Scherrer analysis and statistical thermodynamic calculations by Leff, et al., which find that the thiol-capped gold nanoparticles should reach the minimum size of 14.7 ± 3.7 Å for a certain Au/thiol ratio (ξ_0) beyond which, for $\xi < \xi_0$, the thiols will be present in solution as monomers instead of assembling on the nanoparticle surface. In our work, a similar result (the gold-core size stabilizes at its minimum value of 16 ± 2 Å at $\xi_0 \approx$ 1:1) was obtained by two independent methods of EXAFS analysis: the coordination number method and the surface tension method in the framework of the spherical drop model.

In summary, the size and structure of thiol-coated gold nanoparticles can be controlled by a single parameter: the Au/thiol ratio. We demonstrated that their lattice contraction follows the simplified spherical drop model and their size stabilization at the lowest Au/thiol ratio can be explained by the interplay between Au-thiol and thiol-thiol interactions.

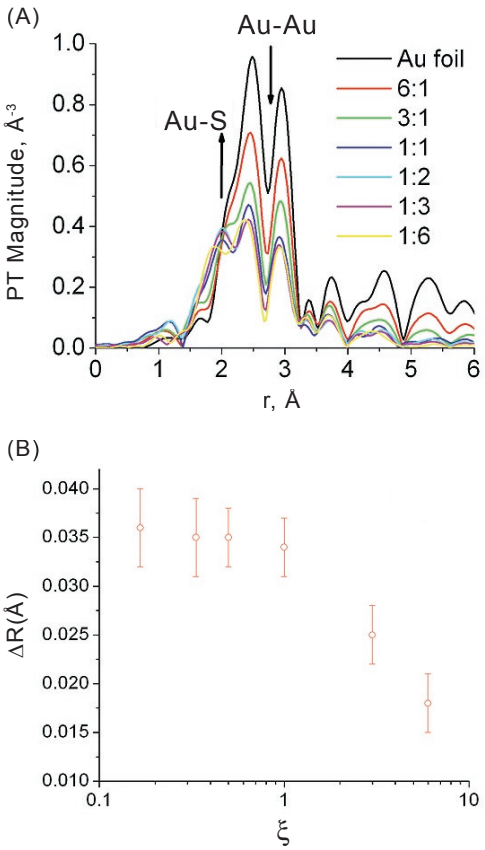

Figure 1. Particle size decrease and saturation is evidenced in EXAFS data of the samples prepared by the two-phase method. (A) The coordination numbers of the Au-Au bonds decrease and for Au-S increase as ξ decreases. (B) Size-dependence of the average Au-Au distances (relative to the bulk) for the samples prepared by the two-phase method.

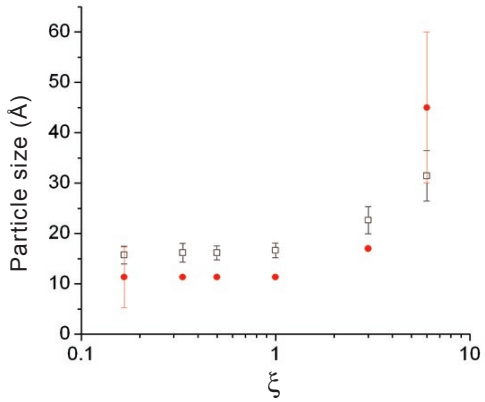

Figure 2. Particle sizes for the samples prepared by the Brust methods. The sizes were obtained by EXAFS using two analysis techniques: empty squares indicate the surface tension technique and filled circles were obtained from the coordination numbers characteristic for the cuboctahedral *fcc* packing.

BEAMLINE
X15A

PUBLICATION
Z. Zhang, et al., "Structure of Hydrated Zn^{2+} at the Rutile TiO_2 (110)–Aqueous Solution Interface: Comparison of X-Ray Standing Wave, X-ray Absorption Spectroscopy and Density Functional Theory Results," *Geochim. et Cosmochim. Acta*, **70**, 4039 (2006).

FUNDING
U.S. DOE; Materials Simulation Center, a Penn State MRSEC facility; U.S. NSF/DOE Environmental Molecular Sciences Inst., Center for Environmental Kinetics Analysis

FOR MORE INFORMATION
Zhan Zhang
X-ray Science Division
Argonne National Laboratory
zhanzhang@anl.gov

STRUCTURE OF HYDRATED Zn^{2+} AT THE RUTILE TiO_2 (110) – AQUEOUS SOLUTION INTERFACE: COMPARISON OF X-RAY STANDING WAVE, X-RAY ABSORPTION SPECTROSCOPY AND DENSITY FUNCTIONAL THEORY RESULTS

Z. Zhang[1], P. Fenter[1], S.D. Kelly[1], J.G. Catalano[1], A.V. Bandura[2], J.D. Kubicki[2], J.O. Sofo[3], D.J. Wesolowski[4], M.L. Machesky[5], N.C. Sturchio[6], and M.J. Bedzyk[1,7]

[1]Argonne National Laboratory; [2]St. Petersburg State University, Russia; [3]Pennsylvania State University; [4]Oak Ridge National Laboratory; [5]Illinois State Water Survey; [6]University of Illinois at Chicago; [7]Northwestern University

Adsorption of Zn^{2+} at the rutile TiO_2 (110)-aqueous interface was studied with x-ray standing waves, surface x-ray absorption spectroscopy, and density functional theory calculations to understand the interrelated issues of adsorption site, occupancy, ion coordination geometry, and hydrolysis. At pH 8, Zn^{2+} was found to adsorb as an inner-sphere complex at two different sites. A 4- or 5-fold first shell coordination environment was observed for adsorbed Zn^{2+} instead of the 6-fold coordination found for aqueous species at this pH. DFT calculations confirmed the energetic stability of a lower coordination environment and revealed that such change is correlated with the hydrolysis of adsorbed Zn^{2+}.

Ion adsorption and electrical double layer (EDL) formation at the oxide-aqueous solution interface are fundamental to a number of processes, including contaminant transport in the subsurface, mineral dissolution and precipitation rates and mechanisms, bioavailability of trace metals, incorporation of trace metals into growing crystals, and heterogeneous catalysis. While there have been extensive studies of EDL phenomena over the past decades, the connection between molecular-scale processes and their macroscopic manifestations remains elusive. Recent experimental and computational studies led to new insights concerning the adsorption of various mono- di- and tri-valent cations at the rutile (α-TiO_2) (110)-aqueous interface with excellent consistency between studies ranging from macroscopic observations to microscopic structures and processes. While these previous studies clearly demonstrated that the Zn^{2+} adsorbs in a manner that was distinct from other cations, discrepancies between the predicted and observed behavior of Zn^{2+} suggested that its interaction at the rutile-water interface was poorly understood. To resolve this gap, we used a combination of Bragg-reflection x-ray standing waves (XSW), surface x-ray absorption spectroscopy and density functional theory (DFT) to understand the adsorption of Zn^{2+} at the rutile (α-TiO_2) (110)–aqueous interface.

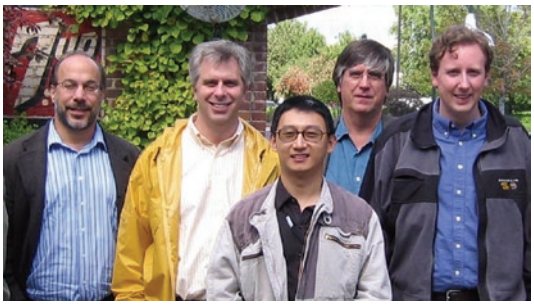

Authors (from left) Neil Sturchio, Paul Fenter, Zhan Zhang, Michael Bedzyk, and Jeffrey Catalano

In the current study, we first confirmed with XSW imaging that Zn^{2+} ions adsorbed at two distinct surface sites at pH 8, i.e., monodentate above the bridging oxygen (BO) site, and bidentate between two terminal oxygen (TO) sites **(Figure 1)**, with however, a coverage and partitioning of Zn^{2+} ions between the two sites that was found to be sensitive to solution pH. Polarization-dependent surface extended x-ray absorption fine structure (EXAFS) spectroscopy results revealed a reduced (i.e., 4- or 5-fold) first shell coordination environment for adsorbed Zn^{2+} with respect to the 6-fold coordination found for aqueous species at pH 8. Octahedral to tetrahedral coordination geometry changes have previously been observed for adsorbed Zn^{2+} ions, although this was not well understood. It could, for instance, be due to the interfacial charge distribution and reduced interfacial dielectric constant, which might be significant enough to overcome the relatively small energy differences between the ion's two coordination environments. DFT calculations revealed that this transformation was favored energetically and was directly coupled to surface induced hydrolysis of the hydrated Zn^{2+} cation. Very good agreement between all experimental and computational results is achieved when comparing the predicted and observed Zn^{2+} adsorption structures and coverage. Ball-and-stick models for the two adsorption geometries based on the DFT results are shown in **Figure 2**.

These results demonstrated that a multi-technique approach, including structural and spectroscopic measurements and high-level DFT theory, allow for a complete characterization of the adsorption of ions at the oxide-water interface, even when the actual structure involves numerous complexities, including multiple adsorption sites, changes in the ion hydration shell structure, as well as hydrolysis of the adsorbed species. Comparison of such results with macroscopic pH-titration/adsorption studies of powder suspensions and large-scale molecular dynamics simulations leads to definitive information on the molecular structure of sorbed species at the oxide-water interface, as well as realistic models to rationalize and accurately predict the macroscopic manifestations of ion adsorption phenomena.

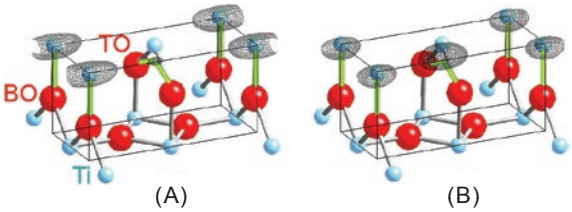

Figure 1. XSW generated 3D iso-density contour surfaces for Zn^{2+} cations at (A) pH 8, and (B) pH 6. The iso-density contour surfaces at 65% of the peak element density are plotted overlapping with the reference ball-and-stick model of a half rutile surface unit cell terminated at the Ti-O basal plane.

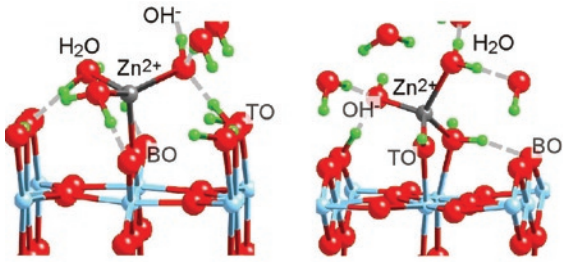

Figure 2. Adsorption geometry of adsorbed Zn^{2+} cations at the TiO_2 rutile (110)-aqueous interface. Two distinct adsorption geometries are observed: (A) monodentate above the bridging oxygen and (B) bidentate between terminal oxygens. Hydrogen bonds are represented with dashed lines.

BEAMLINE
X12A

PUBLICATION
G.A. Carini, A.E. Bolotnikov, G. S. Camarda, G.W. Wright, L. Li, and R.B. James, "Effect of Te Precipitates on the Performance of CdZnTe (CZT) Detectors," *Appl. Phys. Lett.*, **88**, 143515 (2006).

FUNDING
U.S. Department of Energy

FOR MORE INFORMATION
Gabriella Carini
Dept. of Nonproliferation and National Security
Brookhaven National Laboratory
carini@bnl.gov

EFFECT OF TE PRECIPITATES ON THE PERFORMANCE OF CDZNTE (CZT) DETECTORS

G.A. Carini[1], A.E. Bolotnikov[1], G.S. Camarda[1], G.W. Wright[1], L. Li[2], and R.B. James[1]

[1]Department of Nonproliferation and National Security, Brookhaven National Laboratory; [2]Yinnel Tech, Inc.

Measurements taken at the National Synchrotron Light Source allowed us to make detailed comparisons of the microscale responses and infrared (IR) microscopy images of CdZnTe Frisch-ring x-ray and gamma-detectors. The data conclusively showed that local deteriorations of electron-charge collection and the device's response to x-rays fully correlate with the presence of Te precipitates as revealed in the IR images. These data offer the first experimental evidence of the material property limiting the energy resolution of CZT gamma-ray detectors.

$Cd_{1-x}Zn_xTe$ is an attractive material for fabricating crystals for x- and gamma-ray detectors. With its large band-gap (i.e., the energy gap determines its leakage current), detectors produced from the material function well at room temperature, while the high atomic numbers of its elements impart high quantum efficiency (i.e., sensitivity). In principle, detectors are simple devices that directly convert the charge pairs generated by ionizing- and gamma-radiation into electrical signals. These advantages, combined with very good resolution, make CZT detectors suitable for a wide range of purposes, such as imaging devices for nuclear medical imaging, detectors for measuring the movement of radioactive materials, monitors to prevent the diversion of stored nuclear weapons and components, and applications in astronomy.

Authors (from left) Giuseppe Camarda, Gabriella Carini, and Aleksey Bolotnikov

Unfortunately, structural defects, such as twins, dislocations, inclusions, grain- and tilt-boundaries result in crystals of low quality, which severely limit the detectors' performances. Several groups have characterized CZT detectors at the microscale, thereby allowing detailed investigations of their spatial responses. These measurements delineated the detrimental effects of grain boundaries and twins, but were unable to describe the physical mechanisms responsible for the carrier trapping. Further, the role of dispersed Te inclusions and precipitates within the single-crystal CZT volumes remained unclear. Recently, by developing a unique measurement facility affording an order-of-magnitude improvement in spatial resolution, we obtained unequivocal evidence correlating regions where the detector's performance was degraded with the presence of dispersed Te-rich inclusions.

This correlation between Te precipitates, visible in the IR images of crystals, and the deterioration of the devices' responses was measured for several 1-mm thick planar CZT detectors. The original CZT crystals, grown by the Modified Vertical Bridgman method, were supplied by Yinnel Tech., Inc. To obtain the measurements, the detectors were mounted inside a standard eV-Products device holder and irradiated from the cathode side. The output signals were readout and processed using standard spectroscopy electronics, including a charge-sensitive preamplifier, a shaper, and a MCA card to collect pulse-height spectra. To study local variations in the device's response, x-ray scans were performed at the NSLS X12A beamline employing beams of different sizes; the smallest was slightly less than 10x10 μm^2. For each X-Y

position of the x-ray beam, pulse-height spectra were collected, and the peak positions, which are proportional to the total collected charge, were evaluated using a Gaussian fit. We plotted the findings from the scans as two-dimensional maps of the devices' responses (**Figure 1**)

Comparing the IR micrographs and x-ray scans (**Figure 2**), the Te precipitates in the IR images clearly correspond to the dark spots in the x-ray maps where the device's response drops off by up to 50% of its average value. Furthermore, several similar measurements for different thin devices fabricated from CZT crystals grown by different techniques showed, for the first time, a 100% correlation between the locations of the precipitates and the areas of the detector with poor performance.

In contrast to randomly distributed single-level traps, precipitates can be considered as extended local defects with a very high local concentration of trapping centers. In this case, an unpredictable number of charges will be trapped, and the amount of trapping cannot be corrected with current techniques. Here, the fluctuations in charge loss are proportional to the total number of such defects encountered by the electron cloud. Moreover, any electric-field distortions around these defects also can contribute to dispersing the collected charges and to degrading the spectroscopic performance.

In the past, CZT detectors underwent x-ray, gamma-ray, and alpha-particle scans to investigate the uniformity of their responses; the sizes of the beams used in those measurements were 100 μm or larger. This investigation clarified that the size of the x-ray beam used for the scans is an important factor in determining the ability to spatially resolve the effects of isolated Te-rich precipitates. **Figure 3** presents four maps of the same area on a device evaluated with different spatial resolutions to simulate different beam sizes. The original x-ray map, measured with 10 μm steps in both directions with a beam of 10x10 μm^2 unambiguously shows the degraded regions due to 10-20 μm diameter Te inclusions. They are not as clear in the 20x20 μm map. No precipitates were observed with a 100x100 μm^2 beam, and the crystal seems fairly uniform in the 200x200 μm^2 map. The earlier mapping measurements obtained by many groups using larger beams led the CZT detector community to incorrectly assume that isolated Te precipitates did not adversely affect a detector's quality. Our new measurements, offered in this paper, allow researchers to easily discern the effects of precipitates on electron trapping, and they highlight the critical need to address the presence of isolated Te precipitates and aggregates of them within single-crystal CZT detectors.

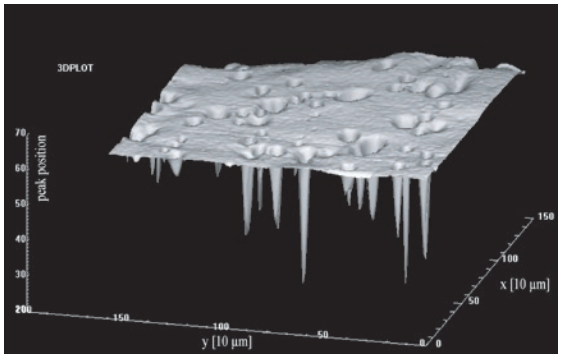

Figure 1. Three-dimensional view of an x-ray map. The scan was performed by using a 10x10 μm^2 sized, 30 keV beam.

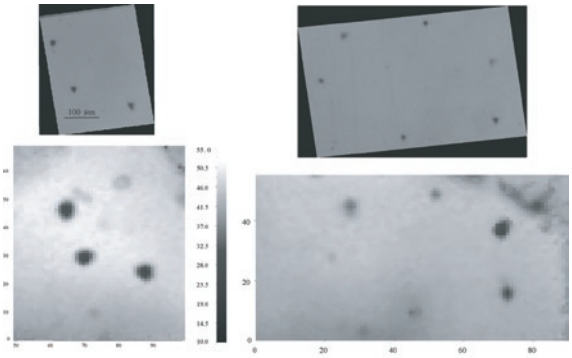

Figure 3. X-ray maps from the same area of the device evaluated with different spatial resolutions: 10x10 μm^2, 20x20 μm^2, 100x100 μm^2, and 200x200 μm^2.

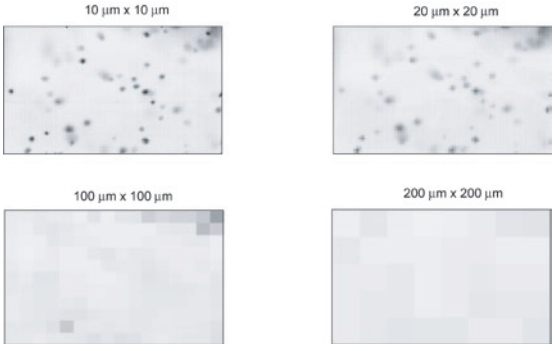

Figure. 2. Examples of correlations between x-ray and IR transmission maps measured for a 1 mm thick CZT planar device. The scans were performed by using a 10x10 μm^2 sized, 85 keV x-ray beam. In some cases, the typical triangular shapes of precipitates are recognizable in the x-ray maps.

BEAMLINE
X7B

PUBLICATION
J.D. Martin, C.L. Keary, T.A. Thornton, M.P. Novotnak, J.W. Knutson, and J.C.W. Folmer, "Metallotropic Liquid Crystals: Surfactant Induced Order in Molten Metal Halides," *Nat. Mater.*, **5**, 271-275 (2006).

FUNDING
The National Science Foundation
Research Corporation-Cottrell Scholar

FOR MORE INFORMATION
James D. Martin
Department of Chemistry
North Carolina State University
Jim_Martin@ncsu.edu

METALLOTROPIC LIQUID CRYSTALS: SURFACTANT INDUCED ORDER IN MOLTEN METAL HALIDES

J.D. Martin, C.L. Keary, T.A. Thornton, M.P. Novotnak, J.W. Knutson, and J.C.W. Folmer

Department of Chemistry, North Carolina State University

Liquid crystals consist of anisotropic molecular units, the majority of which are organic molecules. More recently, liquid crystals incorporating metals into anisotropic molecules have been prepared. Generally these require at least two long-chain organic ligands per metal center. In order to create liquid crystals with high metal content we have investigated the surfactant templated design of anisotropic structure in molten inorganic networks. Variable temperature x-ray diffraction (VTXRD) in conjunction with differential scanning calorimetery (DSC) and polarized light optical microscopy (POM) were used to determine the structural variation in metallotropic liquid crystals as the relative volume fraction of the inorganic block was increased from 33 to 80 mole percent.

Using the cationic surfactants C_nTACl (C_n = alkyl chain with n = 8 to 18, TA = trimethylammonium) and divalent metal-halides (including Zn, Cd, Cu, Ni, Co, Fe, and Mn) we have found a rich variety of liquid crystalline phases. The amphiphilic character of the inorganic/organic hybrid and the respective tunability of charge density of the inorganic anions are responsible for the observed variation in structure. Amphiphilic molecules and salts, as well as many diblock copolymers are well known to exhibit molecular scale phase segregation that results in the formation of lamellar, cubic, hexagonal columnar, and spherical micellar structural organizations depending on the nature and volume fraction of each block of the amphiphile. The majority of literature reports of $[Surfactant]_2MCl_4$ salts exhibit a lamellar crystalline structure. However, reducing the relative volume of the organic block by reducing the length of the surfactant tail to only an eight-carbon chain affords significantly increased curvature to the interface between the organic and inorganic blocks resulting in the columnar crystalline structure shown in **Figure 1A** for $[C_8TA]_2ZnCl_4$. In this work, we have also demonstrated that it is possible to control structural organization by variation of the volume fraction, and thus charge density, of the inorganic polar-block. The metal-halide fraction of these materials may consist of discrete molecular anions such as the relatively high charge density $[MCl_4]^{2-}$ or low charge density oligomeric anionic networks, $[M_nCl_{2n+m}]^{m-}$, depending on the relative concentration of the inorganic component. An early stage of such oligomerization is observed in the crystal structure of $[C_{16}TA]_2Zn_2Cl_6$ shown in **Figure 1B**, for which the low charge density of the inorganic anion requires a severe canting of the surfactant chains. Any further decrease in the charge density of the inorganic anion requires a structure with a greater curvature than can be afforded by a lamellar structure.

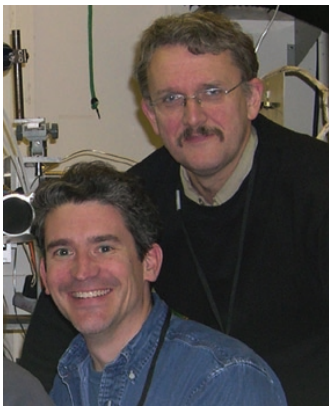

Authors (from left) Jim Martin and Jaap Folmer

Each of the divalent metal halide systems studied exhibit relatively low melting points (below 100°C). Furthermore, upon melting systems with surfactant chain lengths greater than C_{10} exhibit classic smectic, bicontinuous cubic, hexagonal columnar or spherical cubic liquid crystalline textures as observed by both x-ray diffraction, **Figure 2A**, and polarized optical microscopy (see the journal cover below). Because of the polymorphic nature of the parent binary metal halide, a greater structural diversity is observed for the zinc systems than any of the other transition metals. The phase diagram shown in **Figure 2B**, compiled by VTXRD, DSC and POM measurements demonstrates the diversity of structure based on the molecular scale segregation of surfactant and inorganic blocks of this hybrid system. Most of the crystalline phases melt congruently and have a relatively narrow homogeneity range. However, for compositions intermediate between crystalline phases, single homogeneous liquid crystalline phases with broad homo-

geneity ranges are observed with no evidence of immiscible liquid crystalline phases except at compositions loaded as close to the phase boundary as possible. While the copper (II) system, for example, yields somewhat less structural diversity than that of the zinc (II) system, the liquid crystalline organization of a relatively high concentration of d^9 metals in C_{16}TA-CuCl-60 give evidence of ferromagnetic coupling between metal centers.

This demonstration of templating anisotropic structure into liquid metal-halides, with length scales of organization sufficient to exhibit classic liquid crystalline birefringent optical textures, is a significant advance in the emerging field of amorphous materials engineering. The high metal content of these liquid crystalline systems significantly advances the field of metallomesogens, which seeks to combine magnetic, electronic, optical, redox and catalytic properties common to inorganic materials, with fluid properties of liquid crystals.

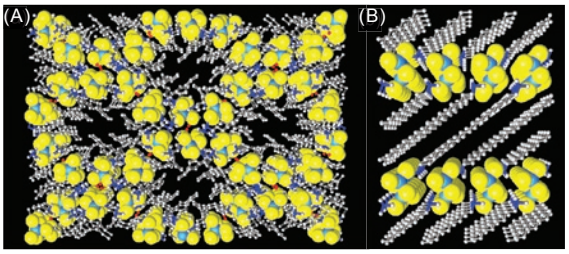

Figure 1. Drawing of the crystal structures of (A) $[C_8TA]_2ZnCl_4$, and (B) $[C_{16}TA]_2Zn_2Cl_6$, showing columnar and lamellar organization, respectively.

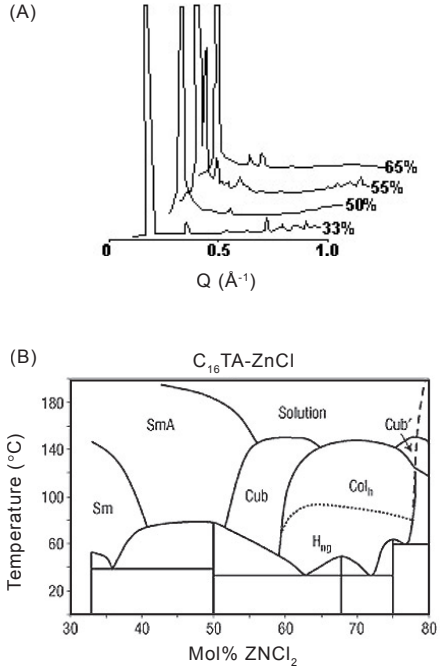

Figure 2. (A) XRD patterns for liquid crystalline C_{16}TA-ZnCl-# (# is the mole % $ZnCl_2$) recorded at approximately 100 °C. Each pattern is offset by 0.1Å^{-1} for clarity. The 33% and 50% compositions exhibit lamellar structures, the 55% composition indexes to a Ia3d bi-continuous cubic phase, and the 65% composition indexes as a hexagonal columnar structure. (B) Phase diagram of the C_{16}TAC/$ZnCl_2$ system. Crystalline phases are identified by solid vertical lines. Liquid crystalline phases include lamellar (SmA) (also crystal smectic (Sm)), Ia3d bi-continuous cubic (Cub), hexagonal non-geometric (H_{ng}), hexagonal columnar (Col_h) and cubic micelle (Cub'). Dashed lines represent the composition boundary above which crystals of $ZnCl_2$ are observed. The dotted line indicates the temperature of the H_{ng}-Col_h transition that is only observed by a change in the optical texture upon heating.

BEAMLINE
U7A

PUBLICATION
S. Krishnan, R. Ayothi, A. Hexemer, J.A. Finlay, K.E. Sohn, R. Perry, C.K. Ober, E.J. Kramer, M.E. Callow, J.A. Callow, and D.A. Fischer, "Anti-biofouling Properties of Comblike Block Copolymers with Amphiphilic Side Chains," *Langmuir*, **22**, 5075-5086 (2006).

FUNDING
Office of Naval Research
National Science Foundation

FOR MORE INFORMATION
Christopher K. Ober
Department of Materials Science and Engineering
Cornell University
cober@ccmr.cornell.edu

ANTI-BIOFOULING PROPERTIES OF COMBLIKE BLOCK COPOLYMERS WITH AMPHIPHILIC SIDE CHAINS

S. Krishnan[1], R. Ayothi[1], A. Hexemer[2], J.A. Finlay[4], K.E. Sohn[2], R. Perry[4], C.K. Ober[1], E.J. Kramer[2,3], M.E. Callow[4], J.A. Callow[4], and D.A. Fischer[5]

[1]Department of Materials Science and Engineering, Cornell University; [2]Department of Materials and [3]Department of Chemical Engineering, University of California at Santa Barbara; [4]School of Biosciences, The University of Birmingham; [5]National Institute of Standards and Technology

Novel polystyrene block copolymers with amphiphilic side chains were synthesized and evaluated for their anti-biofouling surface characteristics. The side chain consisted of a hydrophilic poly(ethylene glycol) (PEG) segment capped with a hydrophobic perfluoroalkyl segment. Surfaces prepared using these polymers showed a depth-dependent composition profile that was characterized using NEXAFS at the NSLS beamline U7A. The angle between the surface-normal and an in-plane electron detector was varied and partial electron yield NEXAFS spectra were acquired at each angle. An analytical framework to extract composition profile from the angle-dependent variations in Auger electron intensity was developed. The block copolymer surfaces, which showed surface segregation of the higher surface-energy PEG groups, were found to have promising fouling release properties when evaluated against the marine macroalga Ulva and the diatom Navicula.

Marine biofouling refers to the unwanted accumulation of marine organisms on an underwater surface. An environmentally benign strategy to tackle marine biofouling is the use of non-toxic polymer coatings that can resist bioaccumulation. Poly(dimethyl siloxane) (PDMS) elastomers are widely used as "fouling release" surfaces because they enable easy release of colonizing organisms.

Authors (from left) John Finlay, Ramakrishnan Ayothi, and lead researcher Sitaraman Krishnan

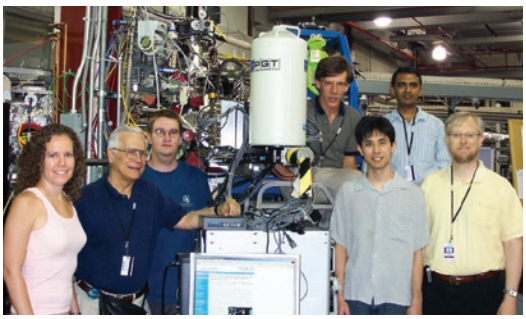

Authors (from left) Karen Sohn, Edward Kramer, Alex Hexemer, Dan Fischer, Marvin Paik, Sitaraman Krishnan, and Christopher Ober

While PDMS surfaces are quite efficient in the release of *Ulva*, they are ineffective against diatom fouling. The green macroalga *Ulva* and unicellular diatoms are the commonly found algae in marine biofilms. Their attachment to surfaces is achieved through secretion of adhesive glycoproteins, polysaccharides or proteoglycans. The attachment strength is determined by molecular interaction of these adhesives with the surface. Previous studies had shown that diatoms attached strongly to hydrophobic PDMS and weakly to hydrophilic glass surfaces, while *Ulva* exhibited an exactly opposite behavior. Our goal was to prepare biomaterial surfaces that minimized adhesion of extracellular adhesive matrices of a wide range of organisms.

Toward this goal, we attached PEGylated fluoroalkyl groups to a polystyrene-*block*-poly(acrylic acid) copolymer synthesized by ATRP. The amphiphilic polymers were expected to undergo an environment-dependent reconstruction as shown in **Figure 1**. Despite a slightly higher surface energy than polystyrene, we expected the PEG groups to segregate to the air-polymer interface because they were anchored to the low-energy perfluoroalkyl groups. Surface segregation of the PEGylated side chains was confirmed by NEXAFS. **Figure 2** shows the normalized partial electron yield NEXAFS spectra for four representative emission angles, ϕ. The sampling depth is proportional to $\cos\phi$. Hence, a higher emission angle implies that a thinner surface layer is being probed. The intensity of the C1s$\rightarrow\pi^*_{\Phi}$ resonance corresponding to the polystyrene block was found to be lower at a higher ϕ **(Figure 2)**. Conversely, the C1s$\rightarrow\sigma^*_{C-F}$ resonance intensity was higher at higher ϕ. Therefore, the polymer surface was enriched in the

PEGylated fluoroalkyl side chains relative to the polystyrene phenyl rings.

We have shown that the normalized intensity of the π^*_Φ resonance at a given emission angle, $I_\Phi(\phi)$, is proportional to the Laplace-transform of the concentration profile, $f_\Phi(z)$, of the phenyl-ring carbon atoms. Thus, $f_\Phi(z)$ could be determined from the experimental intensity versus emission angle data. Due to surface segregation of the amphiphilic block, only about 25% of the carbon atoms at the surface were from polystyrene, a concentration that was significantly lower than the value expected based on the block copolymer structure (~60%). The surface concentration of polystyrene decreased further upon water-immersion. The surface was immersed in water and the contact angle of an air bubble was measured over a period of 2 weeks. The captive-bubble contact angle decreased from 55° immediately after immersion to 31° after 2 weeks. The equilibrium contact angle was close to that of a pure PEG surface.

The amphiphilic surfaces showed a higher removal of both *Ulva* and *Navicula* compared to PDMS **(Figure 3)**. It remains to be determined whether these surfaces show similar fouling release properties against invertebrate larvae and other marine organisms.

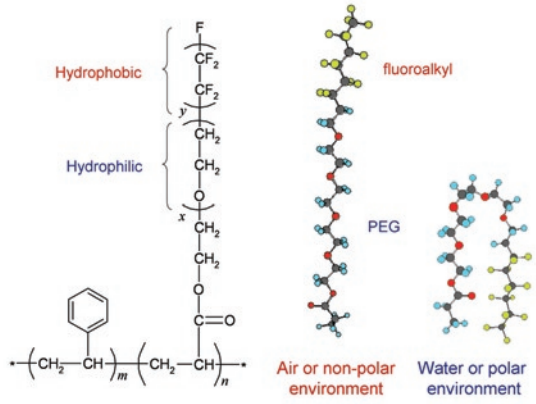

Figure 1. The left-hand side of this figure shows the chemical structure of the surface active block copolymer and its amphiphilic side group. In an air or non-polar environment, the fluoroalkyl group is exposed, but in water or polar environment, the polar PEG group occupies the surface.

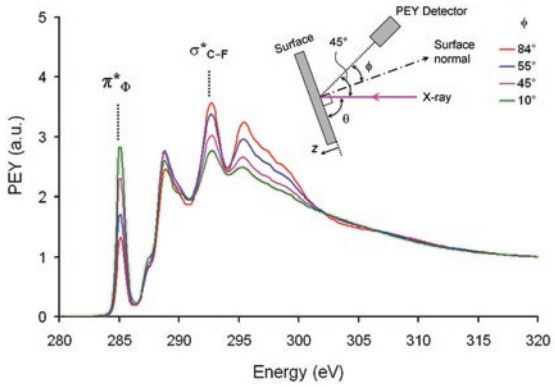

Figure 2. Normalized partial electron yield (PEY) NEXAFS spectra at different emission angles, ϕ, between the surface normal and the partial electron yield detector.

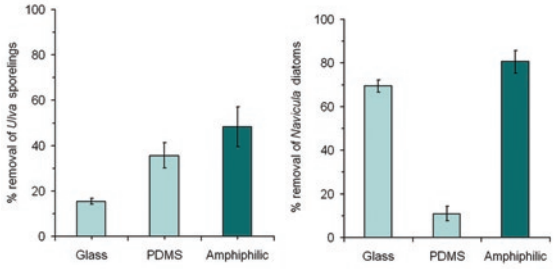

Figure 3. The left-hand side shows removal of Ulva sporelings (small, multicelled pregenitors to seaweed) and demonstrates that they are most easily removed from our new amphiphilic coating compared to PDMS (silicone rubber) or even glass. The right-hand side shows that Navicula diatoms are also very easily removed from the amphiphilic surface as well as glass whereas they adhere very strongly to silicone rubber.

BEAMLINE
X10B

PUBLICATION
S.E. Harton, T. Koga, F.A. Stevie, T. Araki, and H. Ade, "Investigation of Blend Miscibility of a Ternary PS/PCHMA/PMMA System using SIMS and Mean-Field Theory," *Macromolecules,* **38**, 10511-10515 (2005).

FUNDING
National Science Foundation
U. S. Department of Energy

FOR MORE INFORMATION
Harald Ade
Department of Physics
North Carolina State University
harald_ade@ncsu.edu

MISCIBILITY IN A TERNARY POLYMER SYSTEM

S.E. Harton[1], T. Koga[2], F.A. Stevie[3], T. Araki[4], and H. Ade[4]

[1]Department of Materials Science & Engineering, North Carolina State University; [2]Department of Materials Science & Engineering, Stony Brook University; [3]Analytical Instrumentation Facility, North Carolina State University; [4]Department of Physics, North Carolina State University

The polymers poly(cyclohexyl methacrylate) (PCHMA) and polystyrene (PS) are miscible with each other, but each is highly immiscible with poly(methyl methacrylate) (PMMA). Due to their similar glass transition temperatures and the ability of PS and PCHMA to be controllably synthesized with a narrow molecular-weight distribution, we anticipate this blend to be a model system for future investigations of certain phenomena, such as diffusion in miscible blends and diffusion near surfaces and interfaces. As a first step, we have investigated the segregation of deuterated PS (dPS) from a miscible blend with PCHMA to a dPS: PCHMA/PMMA interface. We achieved this by recording real-space depth profiles of dPS with secondary ion mass spectrometry (SIMS). X-ray reflectometry was used to determine the interfacial roughness between PCHMA and PMMA.

Miscible polymer blends have been model systems for investigations of polymer dynamics and equilibrium segregation at polymer surfaces and polymer/polymer interfaces. They are often composed of polymer pairs that have an apparent exothermic enthalpy of mixing. Previously investigated miscible blends have included polystyrene (PS) in combination with poly(xylenyl ether) (PXE), poly(vinylmethyl ether) (PVME), or tetramethylbisphenol-A polycarbonate (TMPC). These systems have constituents with highly different glass transition temperatures (T_gs). These asymmetries can lead to spatially varying T_gs, making accurate decoupling of various phenomena difficult. The need for a model miscible blend involving polymers with similar T_gs and well-defined thermodynamic parameters has motivated this investigation.

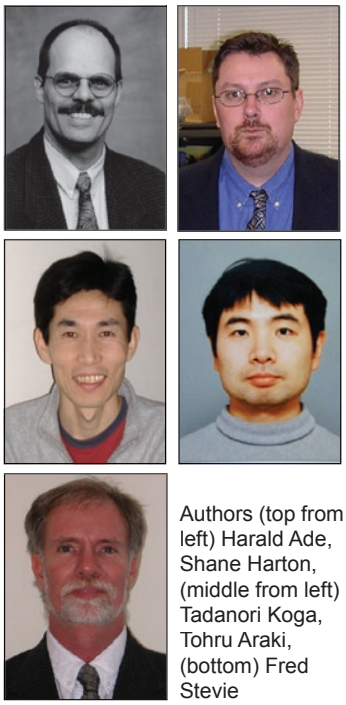

Authors (top from left) Harald Ade, Shane Harton, (middle from left) Tadanori Koga, Tohru Araki, (bottom) Fred Stevie

To analyze the PCHMA/PMMA bilayers with x-ray specular reflectometry (XR), single layers of PCHMA and PMMA were used at NSLS beamline X10B to individually measure the dispersion, δ, of the two polymers. In the case of XR analysis of polymer bilayer systems, difficulties often arise in obtaining details regarding polymer-polymer interfaces due to the small x-ray contrast, $\Delta\delta/\delta$, between the individual polymers, which is typically less than 10% for most polymer pairs. In order to overcome this difficulty, we used a Fourier transformation (FT) analysis method developed previously. A four-layer model (a silicon substrate, a native oxide layer, a PMMA layer, and a PCHMA layer) was used to fit the XR data. Using the measured values for δ, the PCHMA/PMMA bilayers were analyzed using the FT method, as shown in **Figure 1**, and the interfacial roughness (Gaussian) was determined to be 0.6 nm. It should be noted that the x-ray contrast between PCHMA and PMMA is quite small (< 3%), and that this value is considered a lower limit.

In order to investigate segregation, deuterium depth profiles were acquired using a CAMECA IMS-6f magnetic sector secondary ion mass spectrometer (SIMS) with a 15 nA Cs^+ primary beam (6.0 keV impact energy) rastered over a 200 μm x 200 μm area, with detection of negative secondary ions from a 60 μm diameter circle at the center. The analysis conditions used provided a nominal depth resolution (full width at half maximum) of 8 to 10 nm. From the phase behavior of the three polymer pairs, it is known that PS and PCHMA are completely miscible with each other, yet PS and PCHMA are completely immiscible with PMMA under the conditions implemented here. Taking advantage of these asymmetries in the thermodynamic interactions between dPS:PMMA and PCHMA:PMMA, dPS has been driven to the

interface by annealing bilayer films at 150°C for 42 hours. Using SIMS, the depth profiles were measured for initial dPS concentrations of 5, 10, and 20% (v/v) in PCHMA, as shown in **Figure 2**. Because of the low interfacial excess (segregated dPS at the dPS:PCHMA/PMMA interface) observed, previously implemented techniques used to measure these depth profiles, such as forward recoil spectrometry or nuclear reaction analysis, would not be able to resolve the segregation of dPS to the dPS:PCHMA/PMMA interfaces, as their depth resolutions range from approximately 30 to 80 nm. Even with the relatively high depth resolution attainable using SIMS, it is difficult, if not impossible, to measure the interfacial roughness for highly immiscible polymer bilayers. In contrast, XR can accomplish that, and SIMS and XR are excellent complementary tools.

Our work confirmed that PCHMA and PMMA are highly immiscible. Prior literature on the degree of miscibility of PS/PCHMA was inconsistent and large differences are reported for the interaction parameter that governs miscibility. Our segregation data agrees with the more highly miscible value, indicating that the PS/PCHMA system might be indeed an ideal model system for highly miscible polymers.

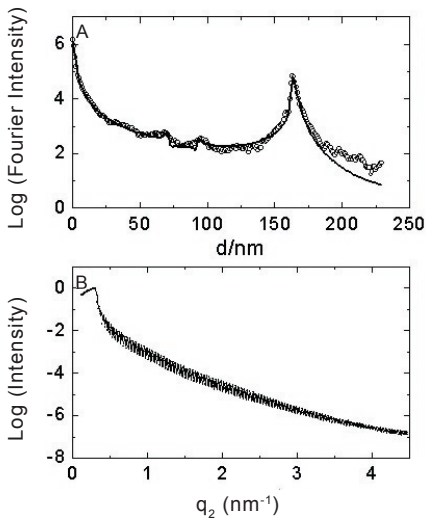

Figure 1. XR of PCHMA/PMMA bilayers. (A) The Fourier method was used to determine the interfacial roughness of this low contrast system. (B) The low contrast is clearly observed in the reflectivity profile.

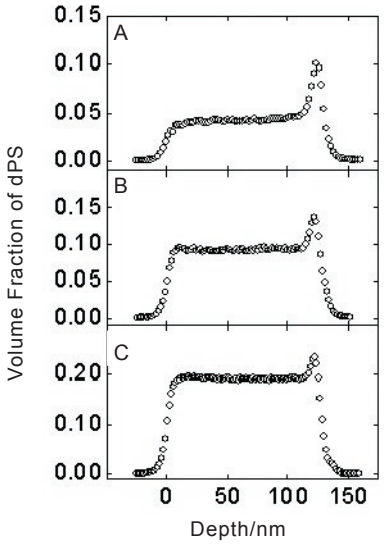

Figure 2. SIMS profiles for bilayers of dPS in PCHMA on PMMA with (A) 5, (B) 10, and (C) 20% (v/v) initial concentrations of dPS. After depletion of dPS due to segregation to the interface during the 42-hour anneal at 150 °C, the bulk concentration away from the interface was reduced to (A) 4.3, (B) 9.2, and (C) 19.2%.

BEAMLINE
U10B

PUBLICATION
J. Torre, M. Cortázar, M.A. Gómez, C. Marco, G. Ellis, C. Riekel, P. Dumas, "Nature of the Crystalline Interphase in Sheared iPP / Vectra Fiber Model Composites by Microfocus X-ray Diffraction and IR Microspectroscopy using Synchrotron Radiation," *Macromolecules*, **39**, 5564-5568 (2006).

FUNDING
Spanish Ministry of Education and Science; European Synchrotron Research Facility

FOR MORE INFORMATION
Gary Ellis
Department of Polymer Physics and Engineering
Inst. of Polymer Science and Technology
gary@ictp.csic.es

STUDY OF THE MICROSTRUCTURE OF POLYMORPHIC INTERPHASES IN FIBER REINFORCED POLYPROPYLENE COMPOSITES BY SYNCHROTRON IR MICROSPECTROSCOPY AND X-RAY MICRODIFFRACTION

G. Ellis[1], M.A. Gómez[1], C. Marco[1], J. Torre[2], M. Cortázar[2], C. Riekel[3] and P. Dumas[4]

[1]Dpto. Física e Ingeniería, Instituto de Ciencia y Tecnología de Polímeros (CSIC), Spain; [2]Dpto. Ciencia y Tecnología de Polímeros, Facultad de Química, Universidad del País Vasco UPV/EHU, Spain; [3]European Synchrotron Radiation Facility, France; [4]Synchrotron SOLEIL, France

The nature of the fiber-matrix interphase conditions the final properties of fiber-reinforced semicrystalline polymers. Heterogeneous nucleation at the fiber surface can alter the properties of the matrix, thus the understanding and control of the crystalline morphology and microstructure of the interphase is fundamental. Spatially resolved information was obtained from an LCP fiber reinforced isotactic polypropylene model composite using two synchrotron-based methods; infrared microspectroscopy and microfocus x-ray diffraction. The combination of IR microspectroscopy with spatially resolved crystallographic information, obtained for the first time from a polymorphic fiber–matrix interphase, confirms a generally accepted model based on morphological evidence.

Fiber-reinforcement is one of the most important strategies to improve the application properties of both commodity and engineering polymers. With an annual production of more than 2.5 billion pounds, and a spectacular growth rate, the U.S. fiber-reinforced polymer (FRP) market is expected to surpass the $6-billion mark in the next few years. Many everyday items employ FRPs, from automobiles, boats, and sports goods to civil engineering structures and biomedical devices. While glass fiber thermosets occupy more than 60 percent of the market, one of the main growth areas is thermoplastic resins, including polypropylene, and the use of alternative fiber types for reinforcement. Thermotropic liquid crystal polymer (LCP) fibers are interesting because of their superior mechanical properties, excellent melt flow properties, reduced machine wear and processing costs, good recyclability, and low density almost half that of glass fibers. This is important for the design of strong, lightweight components.

Gary Ellis

LCP fibers can induce heterogeneous nucleation in isotactic polypropylene (iPP) with a high density of nucleation sites at the fiber surface, and the habitual three-dimensional spherulitic growth is impeded due to overcrowding. Crystalline growth takes place perpendicular to the fiber surface generating a *transcrystalline* (*TC*) layer around the fiber, in which both the elastic and tensile moduli are improved. Various crystalline polymorphs can be observed in iPP; the thermodynamically more stable monoclinic α-modification predominates, whereas crystallization of the less stable trigonal β-modification requires specific conditions such as thermal gradients, shear stresses, or the presence of specific β nucleating agents. Generally when fiber-reinforcement generates a *TC* morphology, the α-form of iPP is observed, and the *TC* β-phase is rare. However, there is much interest in the mechanical properties of the β-phase, particularly improved toughness and impact strength, although the mechanisms that generate the β-phase and the exact relationship between the presence of *TC* morphologies and the final properties of the material are still much debated issues.

Shear stress can also generate β-phase *TC-like* iPP around fibers, and a *cylindritic* crystalline superstructure is developed, differentiating it from *TC* structures. The most important evidence for this comes from polarized thermo-optical light microscopy that, along with morphological data from SEM and AFM, support the Varga and Karger-Kocsis model: shear produced in the melt by fiber-pulling generates extended chain geometries that give rise to series of α-row nuclei along the fiber surface. At the interface of this thin layer of oriented α-crystals a transition from the α- to the

β-phase takes place, giving rise to the formation of the β-cylindritic crystalline superstructure.

Our main goal was to obtain direct structural information from the fiber-matrix interphase. We have studied samples where fiber-pulling at 140 ºC generated shear in the polymer melt, and after isothermal crystallization and subsequent cooling to room temperature, selected regions of the samples were examined using both infrared microspectroscopy and wide-angle x-ray microdiffraction.

Mapping relative IR band intensities at specific sampling geometries in the highly polarized synchrotron beam allows us to differentiate between the two crystalline polymorphs (**Figure 1**), and a false-color image of the marked area clearly shows evidence of a layer of α-phase iPP around the fiber. Unequivocal identification depends on the relative orientation of the polymer chains with respect to the polarization axis of the synchrotron beam.

This is confirmed with wide-angle x-ray microdiffraction experiments (**Figure 2**). A 3 μm diameter x-ray beam was scanned through the interphase region perpendicular to the fiber axis in 5 μm steps. The observation of the β-cylindritic layer and a highly ordered α-phase iPP close to the fiber **(Figure 2C)** confirms the spectroscopic evidence.

The presence of a thin layer close to the sheared fiber corresponding to the α-phase has been unequivocally confirmed by both synchrotron IR microspectroscopy and x-ray microdiffraction. We hope further high spatial resolution studies of the chain geometry in the transition zone will provide more information on the mechanisms involved in the formation of the highly ordered β-phase.

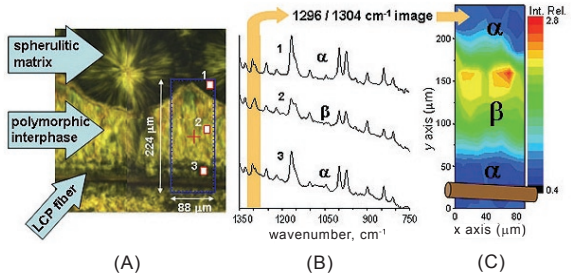

Figure 1. Synchrotron infrared microspectroscopy. (A) Polarized light microscopy of polymorphic iPP interphase, (B) IR spectra recorded through an 8 μm aperture at positions marked, and (C) false-color IR imaging of the interphase region using relative band intensities indicated. The LCP fiber position is also shown.

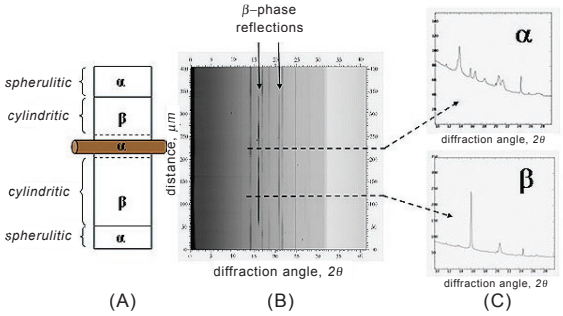

Figure 2. Synchrotron x-ray microdiffraction. (A) Schematic of sampled region showing original position of LCP fiber, (B) integrated intensities of x-ray patterns obtained from a 400 μm line-scan, and (C) diffraction patterns from positions marked.

BEAMLINE
X21

PUBLICATION
A. Sehgal, Y. Lalatonne, J.-F. Berret and M. Morvan, "Precipitation-Redispersion (P-R) of Cerium Oxide Nanoparticles with Poly(Acrylic Acid) : Towards Stable Dispersions," *Langmuir*, **21**(20), 9359 (2005).

FUNDING
U.S. Department of Energy

FOR MORE INFORMATION
Jean-Francois Berret
Matière et Systèmes Complexes
Université Denis Diderot Paris-VII
jean-francois.berret@ccr.jussieu.fr

NANOPARTICLE-POLYMER COMPLEXATION: ELECTROSTATIC SELF-ASSEMBLY AS A ROUTE TO STABLE DISPERSIONS OF HYBRID NANOCOLLOIDS

A. Sehgal[1], Y. Lalatonne[1], J.-F. Berret[2], and M. Morvan[1]

[1]Complex Fluids Laboratory, CNRS - Cranbury Research Center Rhodia Inc; [2]Matière et Systèmes Complexes,Université Denis Diderot Paris-VII, France

The inherent instability of inorganic nanoparticle sols may be resolved by complexation with ion-containing polymers at the particle interface. We exploit a precipitation-redispersion (P-R) mechanism to achieve the complexation of short chain polyelectrolytes with cerium oxide nanoparticles in order to extend their stability over a wide pH range. Small-angle x-ray scattering in conjunction with static and dynamic light scattering reveals that P-R may yield hybrid nanocolloidal complexes with a single inorganic core-charged corona structure. The electrostatic self-assembly of ionic stickers anchors the chains onto the surface, resulting in a polymeric brush that provides steric and electrostatic stabilization. This simple strategy to achieve stable dispersions surmounts the critical limitation in the use of nanoparticles, allowing a facile means to translate the intrinsic properties of mineral oxide nanoparticles to a range of novel applications.

Emerging nanomaterials utilize not only the chemical composition but also the size, shape and surface-dependent properties of nanoparticles in applications with remarkable performance characteristics. As synthesized, aqueous dispersions of metal-oxide nanoparticles (e.g. oxides of cerium, iron, or zirconium) exhibit some common properties: *i)* the particles have crystalline structure, *ii)* the sols are typically synthesized in extremely acidic (or basic) conditions, and *iii)* the particles are stabilized by electrostatics and are extremely sensitive to perturbations in pH, ionic strength, and concentration. In order to translate the intrinsic properties of nanoparticles to industrially relevant uses there is a need for a robust means to stabilize nanoparticle dispersions in aqueous media for a variety of processing conditions.

This instability of inorganic nanoparticle sols was resolved by complexation with charged ion-containing polymers. To achieve the goal, we have developed a two-step process, defined as the precipitation-redispersion (P-R) process. In this study we address the issue of the adsorption and of the complexation between cerium oxide nanoparticles and short poly(acrylic acid) (PAA) chains (molecular weight, M_w=2000 g·mol^{-1}). We demonstrate that we may considerably extend the range of pH and concentration stability of cerium nanosols by irreversibly adsorbing weak polyelectrolytes on the surface. This process does not require mechanical stimulation.

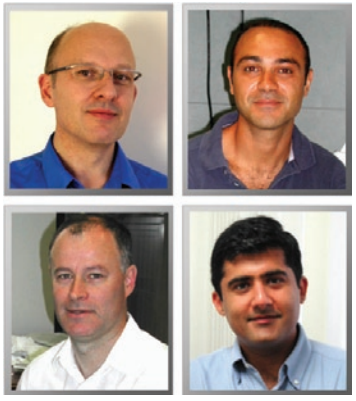

Authors (clockwise from left) J.-F. Berret, Y. Lalatonne, M. Morvan, and A. Sehgal

As synthesized, cerium oxide sols at pH 1.4 consist of monodisperse cationic nanocrystalline particles with a hydrodynamic diameter D_H = 10 nm. Interparticle interactions in the form of strong van der Waals attraction, electrostatic repulsion, and surface chemistry act in concert to make the charged nanosol highly sensitive to the electrostatic environment. Any perturbation in pH (>3) results in aggregation and macroscopic precipitation of the nanoparticle suspension, severely limiting the utility of nanoceria.

Figure 1 shows that when cerium oxide sols are mixed with poly(acrylic acid) solutions (with the same concentration *c* and pH 1.4), the solution undergoes an instantaneous and macroscopic precipitation. The mixing is characterized by $X_{Mix}=V_{CeO_2}/V_{PAA_{2K}}$, where V_{CeO_2} and $V_{PAA_{2K}}$ are the respective volumes of the cerium and polymer solutions. Sedimentation or centrifugation gave two distinctly separated phases. Complexation of the polymer chains with several particles results in precipitation due to colloidal bridging, which is reminiscent of classical associative phase separation. As the pH is progressively increased, the suspension spontaneously redisperses into a clear solution. This evolution of the CeO_2-PAA_{2K} solutions at X=1 and c = 1 wt. % is illustrated in **Figure 1A** for the pH range 1.4-10. The precipitation-redis-

persion was followed by static and dynamic light scattering experiments. D_H was found to decrease progressively from 18 nm at pH 7.5 to 12.5 ± 1 nm at pH 10 (**Figure 2B**). This latter value is approximately 3 nm larger than the diameter of the bare particles (D_H = 9.8 nm), suggesting that the nanoceria are now coated by a PAA corona.

Figure 2 illustrates the SAXS intensity profiles performed on both bare and PAA_{2K}-coated nanoparticles. At low concentration (c < 0.5 wt. % and X = 1), where no structure factor is apparent, the scattered intensity is proportional to the concentration and the q-dependence of the intensity reflects the form factor of the aggregates. The form factors for the bare and coated CeO_2-nanoparticles have been shifted vertically so as to superimpose the scattering cross-sections at high wave-vectors (**Figure 2**). This result indicates that on a local scale (*i.e.* below 5 nm) both particles have the same structure. A slight deviation below 0.03 $Å^{-1}$ is ascribed to the PAA corona surrounding the particles. This is also illustrated in the inset (**Figure 2**) as intensities in a Guinier representation. The logarithm of the intensity decreases linearly with q^2 and from the straight lines we deduce a radius of gyration R_G = 3.52 ± 0.02 nm for the bare particles and R_G = 4.8 ± 0.02 for the coated CeO_2-PAA_{2K} particles. As q → 0, the intensity of the coated particles is 1.4 times that of the bare nanoceriums. This value can be used to estimate the number of adsorbed polymers. We assume that a coated nanoparticle is of the core-shell type, having electronic densities ρ_{CeO2} and ρ_{PAA}. The excess of intensity as q → 0, due to the PAA shell with respect to that of the bare particles, may be estimated:

$$\left.\frac{I_{CeO2\text{-}PAA}}{I_{CeO2}}\right|_{q\to 0} = \left(1+n_{ads}\,\frac{\rho_{PAA}-\rho_s}{\rho_{CeO2}-\rho_s}\,\frac{V_{PAA}}{V_{CeO2}}\right)^2$$

where ρ_S is the electronic scattering density of the solvent, V_{PAA} is the molar volume of poly(ammonium acrylate) polymer, and V_{CeO2} is that of the bare particle. We calculate the number of adsorbed polymers n_{ads} = 34 ± 6. This was corroborated by static light scattering and total organic carbon measurements. The final amount of 40 – 50 polymers per particle corresponds to 1/5 of the total weight of the coated particles.

An insight into the conformation of the adsorbed polymeric corona is obtained. With 50 chains per particle and a monomer molar volume v_0 = 54.8 $Å^3$, the radius of the polymer nanoparticles would be increased by 0.4 nm. With a fully extended polyelectrolyte corona the hybrid nanocolloid would result in D_H = 18 nm. With the intermediate redispersed D_H ~ 13 nm, the PAA conformation may be described as multisite adsorption of –COOH moieties along the contour length with the remainder constituting a solvated polyelectrolyte brush.

The P-R process is a simple route to obtain single nanoparticles irreversibly coated with PAA chains. With a 2 – 3 nm polyelectrolyte brush surrounding the particles, the cerium sols are stable over a broad range of pH values and concentrations. The process described could easily be extended to other nanoparticle systems. This opens new opportunities with electrostatic self assembly as a means to dramatically improve the stability of inorganic nanosols.

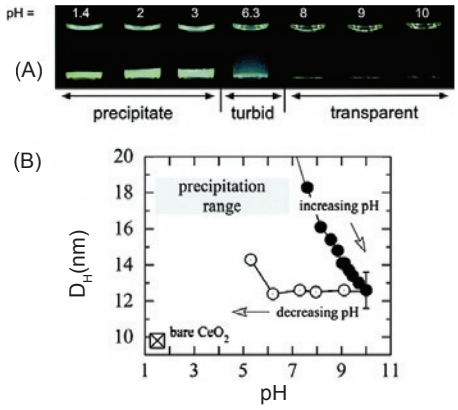

Figure 1. (A) Series of CeO_2-PAA_{2K} solutions prepared at different pH. The mixing of the polymer and cerium solutions was made at pH 1.4, and the pH was further adjusted with NH_4OH. Above pH 7, the precipitate is redispersed. (B) Hydrodynamic diameters measured by dynamic light scattering on CeO_2-PAA_{2K} solutions during the P-R (close symbols). At pH 10, the PAA_{2K}-coated cerium sol is stable and it can be brought back to pH 6 without noticing any change in the dispersion (empty symbols). Below pH 6, the nanoparticles start to aggregate.

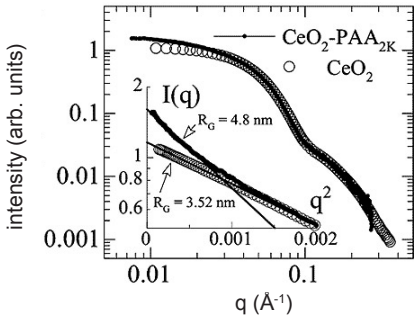

Figure 2. X-ray scattering intensity for bare and PAA_{2K}-coated nanoparticles in double logarithmic scale. The concentrations are in the two cases c = 0.5 wt. %. At such low concentrations, the intensities represent the form factors of the particles. The deviation below 0.03 $Å^{-1}$ is due to the PAA corona surrounding the particles. Inset: Guinier representation of the intensity for the same samples (I(q) versus q^2). From the straight line, the radius of gyration R_G of the nanoceria (= 3.52 ± 0.02 nm) can be calculated.

YEAR IN REVIEW

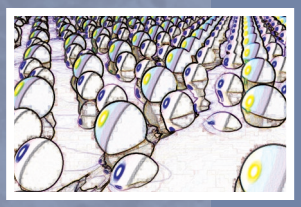

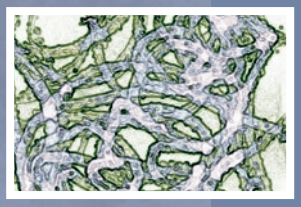

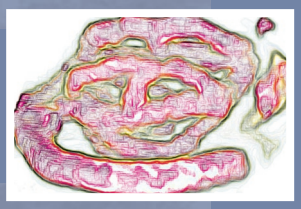

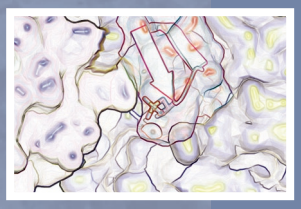

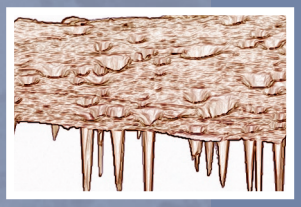

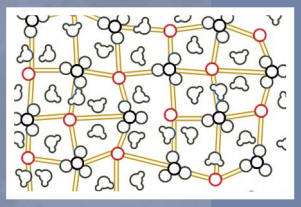

411TH BROOKHAVEN LECTURE 'SHINING LIGHT ON THE CAUSE OF ALZHEIMER'S DISEASE'

January 18, 2006

Alzheimer's disease is a progressive brain disorder that gradually destroys a person's memory and ability to learn, reason, communicate, and carry out daily activities. An estimated 4.5 million Americans have it, a number that is expected to triple over the next 50 years. Today, one in ten people aged 65 and half of people over 85 are affected.

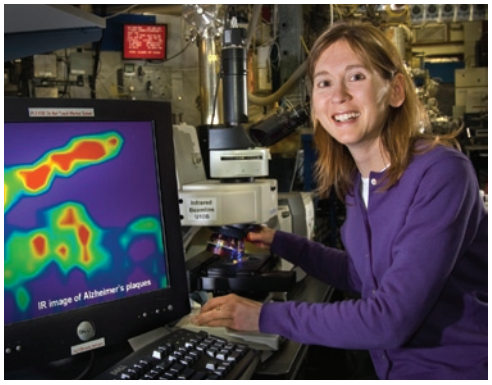

Lisa Miller

The cause of Alzheimer's disease is thought to involve the formation of "plaques" — tiny aggregates of a naturally occurring, but misfolded or misshapen protein — in the brain. Recently, the formation of these plaques has been associated with the binding of metal ions such as iron, copper, and zinc. Yet the function of these metal ions and the misfolded proteins in the disease process is not well understood.

Now, synchrotron infrared and x-ray microscopes are used to image the protein structure and metal content in the Alzheimer's-affected brain tissue, providing a better understanding of how the disease occurs and potential ways of preventing it in the future.

Biophysical chemist Lisa Miller of the National Synchrotron Light Source Department (NSLS) gave the 411th Brookhaven Lecture on this research in her talk "Shining Light on the Cause of Alzheimer's Disease," on January 18, 2006 in Berkner Hall.

Lisa Miller obtained her B.S. in chemistry from John Carroll University in 1989, her M.S. degree in chemistry from Georgetown University in 1992, and her Ph.D. in biophysics from the Albert Einstein College of Medicine in 1995. Rejoining Albert Einstein in a faculty position, she worked with BNL scientists to develop new tools using synchrotron light to study biological and medical problems.

She joined the NSLS in 1999 and uses x-ray and infrared imaging to study diseases such as osteoarthritis, osteoporosis, and Alzheimer's. She is also an adjunct Assistant Professor in the Department of Biomedical Engineering at Stony Brook University, and she heads the NSLS Information & Outreach Office, which communicates NSLS science to other scientists, government officials, and the community.

— Liz Seubert

NSLS ONE OF 10 BNL ORGANIZATIONS TO ACHIEVE OHSAS 18001 REGISTRATION

January 19, 2006

Lab Director Praveen Chaudhari and Safety & Health Services Division Manager Pat Williams held a celebration on January 19, 2006 to show BNL's appreciation to the many dedicated employees who worked for 12 months to prepare seven organizations — the Superconducting Magnet Division (SMD), Basic Energy Sciences (BES) Directorate, Instrumentation Division, Physics Department, National Synchrotron Light Source (NSLS), Environmental & Waste Management Services (EWMS) Division, and Staff Services (SS) Division — for successful registration of their occupational safety management systems to Occupational Health & Safety Assessment Series (OHSAS) 18001.

OHSAS 18001 is widely acknowledged as offering one of the best guidelines available for safety

Among those who celebrated the successful registration of seven more BNL organizations to the OHSAS 18001 safety management standard are hosts Praveen Chaudhari (front, second from left) and Pat Williams (front, second from right); and, between them, from left: BNL organization representatives Tom Kirk, Sally Dawson, John Taylor, Robert Casey, Michael Clancy, and Veljko Radeka, with Jeff Swenson (front, left).

management systems and it is a significant enhancement of the Integrated Safety Management System that was already in place on site. In addition to the certificates of appreciation presented to all those in attendance, framed OHSAS 18001 Certificates of Registration were presented to Chaudhari as representing BNL, and to Tom Kirk for SMD, John Taylor for BES, Veljko Radeka for Instrumentation, Sally Dawson for Physics, Robert Casey for NSLS, Michael Clancy for EWMS, and Jeff Swenson for SS.

Together with the three pilot organizations that were successfully registered in September 2004 — the Central Fabrication Services Division, Collider-Accelerator Department, and Plant Engineering Division — BNL now has a total of 10 organizations' occupational safety management systems that have achieved OHSAS 18001 registration.

Regarding future plans for the Lab, Jim Tarpinian, Assistant Laboratory Director for Environment, Safety, Health, & Quality, explains, "In 2006, we will expand the OHSAS 18001 registration to include the balance of BNL organizations. The important thing for BNL is not the registration itself, but the processes of job-risk assessments, employee involvement, goals and objectives, management review, and continual improvement. OHSAS 18001 is a significant enhancement to our Integrated Safety Management System."

— Maria Beckman

JOINT PHOTON SCIENCES INSTITUTE ESTABLISHED

January 23, 2006

A new initiative in photon sciences will capitalize on the unique capabilities of NSLS-II.

A partnership between the DOE and New York State, the Joint Photon Sciences Institute (JPSI), will serve as an intellectual center for development and application of the photon sciences and as a gateway for NSLS-II users. It will enhance scientific programs that use the powerful photon beams by cultivating and fostering collaborative, interdisciplinary R&D.

New York State Governor George Pataki recently committed to providing $30 million for the JPSI building, which will be located next to NSLS-II and provide office space, meeting areas, and specialized state-of-the-art laboratories. The operating expenses of the institute and its research programs will be covered by funding from the federal government, including the Department of Energy,

New York State Capitol Building, Albany

the National Institutes of Health, the Department of Defense, and others. Research will be focused around several multi-year scientifically and technologically relevant research initiatives.

Over the past few decades, the power of photon sources has increased dramatically, and they are now used for a broad spectrum of research. Modern research increasingly requires interdisciplinary work that either spans multiple scientific disciplines or falls at the boundaries between them. JPSI will be an interdisciplinary institute devoted to basic research in areas of the physical sciences, engineering, and the life sciences that are united in employing synchrotron-based methods. JPSI will also develop new methods and applications that exploit the unique capabilities of NSLS-II.

JPSI will have great flexibility in making scientific appointments, encompassing both Brookhaven scientists and faculty from universities. Junior and senior fellowships and sabbatical programs will draw the best photon scientists from institutions worldwide for interactions with the resident staff and user communities. An important element of the institute's mission will be training new researchers and enabling established researchers to embark on new directions in interdisciplinary research. JPSI will also host interdisciplinary workshops that highlight new opportunities, foster new collaborations, and promote JPSI initiatives in emerging areas of photon science.

— Steve Dierker

NSLS EXAMINES PIECES OF STAR DUST

January 25, 2006

Launched on February 7, 1999, Stardust's mission was to collect dust and carbon-based compounds from a passing comet, as well as tiny amounts of interstellar dust streaming toward Earth from deep

space. Its delivery of this material marks the first time since Apollo 17 that a NASA spacecraft has successfully brought back a space-matter sample.

At the NSLS and other synchrotron facilities, portions of that teaspoonful-sized amount of comet and star dust was studied to determine its composition and properties. The variety of research techniques available at the NSLS allowed researchers to maximize the amount and type of information learned about the dust particles. The information scientists gather could help answer some very important, very fundamental questions about the formation of the solar system and the Earth in particular.

The initial analysis of these samples, known as the Preliminary Examination Period, began in the Stardust Laboratory at NASA's Johnson Space Center. Following these first studies, the samples were divided, prepared, and distributed to qualified investigators, including those at the NSLS, for more intensive studies. These scientists are members of the Stardust Preliminary Exam Team.

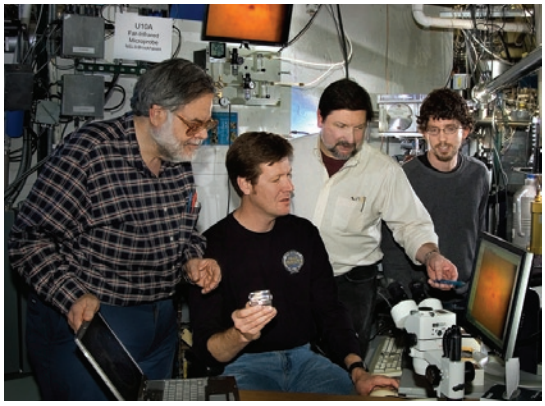

(From left) George Flynn (SUNY Plattsburgh), Lindsay Keller (NASA), Larry Carr (NSLS), and Randy Smith (NSLS) examine samples from the Stardust mission at beamline U10A.

At the NSLS, analyses took place at beamline X26A, led by physicist and Stardust co-investigator George Flynn (SUNY Plattsburgh). Flynn is leading a worldwide group of scientists who will perform chemical composition measurements on the comet samples collected by Stardust. The extremely tiny and bright x-ray beams produced at beamline X26A are an excellent tool for analyzing the particles, which are just 10-20 millionths of a meter in diameter (so small that five particles fit across the width of a single human hair). Using these capabilities, the X26A scientists were able to extract chemical and mineralogical information from the sample without the need to remove the dust particles from the "aerogel" substance used to capture them in space.

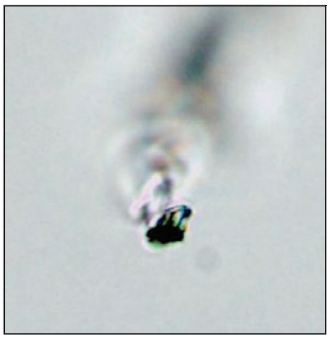

Stardust particle (crystalline object with dark borders), embedded in the aerogel collector. (Photo courtesy of NASA)

After the particles were extracted from the aerogel, they were analyzed at other beamlines using both x-rays (X1A1), and infrared light (U10A and U10B). At beamline X1A1, a powerful imaging device called a scanning transmission x-ray microprobe (STXM) was used to collect detailed images of the particles. The STXM employs a technique known as x-ray absorption near-edge structure (XANES) to gather information about the elemental makeup of the particles, especially the carbon found in organic compounds. Flynn's studies using the STXM can identify organic compounds within some of the smallest Stardust particles - compounds that may have formed at the birth of our solar system.

In a concurrent set of studies, Flynn and Stardust co-investigator Lindsay Keller used infrared light to identify specific minerals within the dust particles. Keller, who leads the group of scientists who will perform optical studies of the Stardust samples, is a lunar and planetary scientist with NASA's Johnson Space Center. The far-infrared microscope at beamline U10A, which can sense the unique vibrations of atoms in crystalline solids, is an excellent tool for identifying specific minerals within the Stardust sample. The mid-infrared light produced at beamline U10B was also used to characterize any organic material found in the particles. Unlike x-ray methods, the information collected using these infrared techniques can be compared with the astronomical observations of distant interstellar dust clouds, including those involved with the formation of planetary systems like ours.

— Laura Mgrdichian

TWO NSLS STAFF MEMBERS AWARDED FOR JOBS WELL DONE

February 2, 2006

Congratulations are due to Peter Siddons and Nick Gmur, who, respectively, recently were honored with a Science & Technology Award and a Brookhaven Award at the Fiscal Year 2006 BNL Employee Recognition Award Ceremony on February 2.

Peter Siddons

Siddons, a physicist at the NSLS, was cited for his outstanding contributions to developing detectors for use in synchrotron sources. His ideas were recognized as innovative and original, resulting in new and unique detectors that make new experiments feasible. He is a strong advocate and leader in the U.S. for detector development and has made significant advances possible despite the lack of funding in this area. Over the last several years, Siddons has directed the NSLS detector and control group and, in collaboration with BNL's Instrumentation Division, has developed a suite of detectors. These included fast photon counting detectors for different energy ranges and applications, linear array detectors, and two-dimensional detectors. The detectors have been delivered to users with great success, and have made significant impact on scientific programs at the NSLS and elsewhere. Also, the detector group under Siddons' direction has gained worldwide recognition for the NSLS and BNL. For example, recently BNL was awarded a multi-year project to construct two imaging detectors for the Linear Coherent Light Source project at Stanford Linear Accelerator Center. Facilities in England, Australia and Taiwan as well as at Argonne National Laboratory are

Peter Siddons (second from left) at the BNL Employee Recognition Award Ceremony with the other Science & Technology Award winners. They are Stephen Schwartz of the Environmental Sciences Department (far left), James Alessi of the Collider-Accelerator Department (second from right), and Peter Vanier of the Nonproliferation & National Security Department (far right). Not pictured: Alexei Tsvelik of the Condensed Matter Physics & Materials Science Department.

interested in or already actively collaborating with Siddons' group. He received his Ph.D. in physics at Kings College, London, and joined BNL in 1985.

The Science & Technology Award (presented by Peter Bond, Deputy Interim Director for Science & Technology) recognizes distinguished contributions to BNL's science and technology mission over one or more years. Nominations for the Science & Technology Award are made by organization heads. The three criteria considered for this award are the exceptional nature of the employee's contributions, their level of difficulty, and their benefit to BNL.

Nick Gmur

Gmur was cited for his outstanding work as the NSLS Environmental Safety & Health (ESH) Coordinator. In this role, he is involved in many activities within the department that carry into almost every part of all programs. He has been a key contributor to challenging ESH issues at the NSLS that include implementing requirements for

Brookhaven Award winner Nick Gmur (second from left) at the awards ceremony with the other Brookhaven award winners. Also presented with Brookhaven awards were (from left) John DiNicola (Plant Engineering Division), Raymond Karol (Collider-Accelerator Department), Gerard Shepherd (Safety & Health Services Division), and Peter Stelmaschuk (Plant Engineering).

BNL's Integrated Safety Management program and the internationally recognized ISO 14001 and OHSAS 18001 programs. Other major achievements included writing, conducting, and coordinating reviews and implementing the accelerator authorization basis documents for the Deep-Ultraviolet-Free Electron Laser, the NSLS and Accelerator Test Facility, and the NSLS Environmental Assessment required by the National Environmental Policy Act. In addition, Gmur resolves many smaller issues daily. He is recognized for his leadership, for bringing great attention to quality and detail, and for always getting the job done on schedule. He is widely respected throughout BNL for his efforts and is an excellent representative of the NSLS. Gmur, who came to BNL in December 1975, has a B.S. in zoology and chemistry from McGill University and an M.S. in biology from the University of Michigan.

Presented by Laboratory Director Praveen Chaudhari, the Brookhaven Award recognizes key contributors in support functions whose performance and achievements represent outstanding service to the Laboratory. Nominees for the Brookhaven Award are evaluated by the exceptional nature and difficulty level of the contributions, their benefit to the Laboratory, and the length of time over which the contributions were made.

— Laura Mgrdichian

NSLS RESEARCHERS PRODUCE A PRAISEWORTHY POSTER

March 1, 2006

At the Materials Research Society semi-annual meeting, an NSLS research group received a special honor. Its meeting poster, one of hundreds, was chosen as one of only six to receive a "best poster" award.

Elaine DiMasi (left) and poster presenter Karthikeyan Subburaman.

The group, which includes scientists from Stony Brook University, Brookhaven National Laboratory, and the City University of New York, is studying "biomineralization," the process by which organisms create mineralized tissues, such as bones, teeth, and shells. The collaboration includes NSLS scientist Elaine DiMasi, as well as Karthikeyan Subburaman (SBU), Nadine Pernodet (SBU), Seo-Young Kwak (BNL), Shouren Ge (SBU), Nan-Loh Yang (CUNY), and Miriam Rafailovich (SBU). They presented their poster at the MRS Fall 2005 meeting, held November 27 through December 1 in Boston, Massachusetts.

Biominerals are interesting, in part, because they are typically much stronger than ordinary minerals. As such, they may one day be used to create a new class of nanoscale composite materials. First, however, the underlying mechanisms of biomineral formation and structure must be better understood.

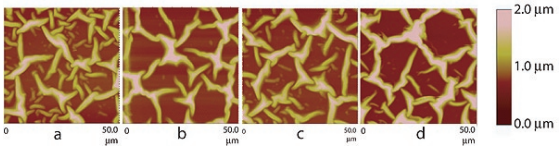

Elastin protein networks imaged by AFM (a) before mineralization and after (b) 30, (c) 60, or (d) 120 minutes of exposure to mineral. The fibrous parts of the protein become thicker and stiffer as they induce calcium carbonate mineralization.

The group's winning poster is a summary of their research on eggshell protein mineralization. They use this as a model to study biomineralization in general, since the formation of an eggshell can be thought of as a process that includes a series of steps. First, the shell's support membrane is formed and proteins are deposited onto it. Then, the minerals that make up the shell begin to form and grow, using the protein deposits as nucleation points. Finally, the mineral forms a crystal structure on top of the protein-fiber network.

The researchers studied this process using real "extracellular matrix proteins" — the type of proteins that make up skin tissue, for example. They used networks of these proteins as the basis of the mineralization process and then studied the mineralized proteins using a powerful imaging device called an atomic force microscope (AFM).

As described in their poster, their results show that, at the eggshell's early growth stages, only the fibrous portions of the proteins accepted calcium carbonate, the mineral. The fibers became thicker as the calcium was incorporated and, ultimately, large mineral crystals appeared. The group hopes to build on these results by learning exactly how the proteins induce the mineralization process.

— Laura Mgrdichian

GENERAL BARRY MCCAFFREY TOURS THE NSLS

March 1, 2006

During a visit to BNL on March 1, Barry McCaffrey, a retired four-star general from the U.S. Army, toured the NSLS.

McCaffrey came to BNL with a view to using his specialized experience to help the Laboratory focus on ideas to increase its sponsorship in areas related to homeland security and the understanding and treatment of drug addiction.

At the NSLS, he was guided on a tour of the beamline floor by NSLS scientist Peter Siddons, who explained how the facility works and gave an overview of the science done. McCaffrey expressed interest in the range of scientific research that is performed at the NSLS, the type of users (academic, industry, etc.), and how the NSLS facility is organized.

McCaffrey's visit also included tours of the Positron Emission Tomography imaging facility, the Radiation Detector Testing and Evaluation Facility, and labs developing nuclear-detector instrumenta-

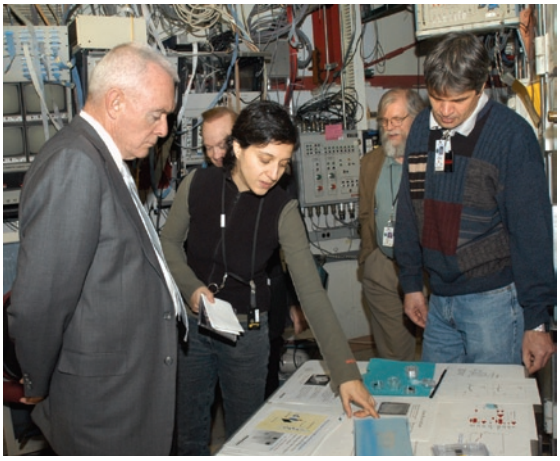

From left, General Barry McCaffrey, Ralph James (BNL-EENS), Gabriella Carini (BNL-EENS), Peter Siddons (BNL-NSLS), and Alexey Bolotnikov (BNL-EENS).

tion. This gave him first-hand contact with several BNL scientists and an opportunity to learn more about some of the Lab's research and development programs.

McCaffrey, who served as the Commander in-Chief of the U.S. Armed Forces Southern Command, coordinating all national security operations in Latin America, also served as the Director for Strategic Plans and Policy on the Joint Chiefs of Staff. In addition, he followed this distinguished record by serving as Director of the Office of National Drug Control Policy under President Bill Clinton from 1996-2001.

— Laura Mgrdichian

NSLS STUDENT-RESEARCHER TALKS AT THE MARCH APS MEETING

March 13-16, 2006

Each year, the NSLS hosts several high school and college students, who come to the facility to perform research using its bright beams of x-ray, ultraviolet, and infrared light. This year, four of these students presented the results of their research at the March meeting of the American Physical Society (APS) in Baltimore, Maryland.

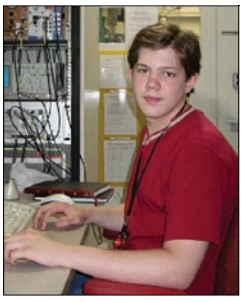

Michael DiBiccari

Michael DiBiccari, a senior at Hauppauge High School in Hauppauge, New York, worked with NSLS biophysicist Elaine DiMasi. His project was part of a wider research effort on the study of biomineralization, the process by which living organisms produce minerals, such as shell and bone. He studied diatoms — single-celled algae with outer shells composed of biosilica, a type of biomineral. DiBiccari used x-rays to identify the atomic structure of the biosilica, which he then compared to the structure of synthetic silica. His results showed that the structures of both materials were identical. He discussed this research and its implications on March 16, 2006, at 1:15 p.m. in Room 323 of the Baltimore Convention Center.

Kathryn Krycka

Two graduate students working at the NSLS also gave talks on their research. **Kathryn Krycka**, from Stony Brook University, works with NSLS scientist and chair Chi-Chang Kao and Professor Sara Majetich of Carnegie Mellon University. Using an x-ray technique known as small-angle resonant x-ray scattering, she studied the size and internal structure of magnetic nanoparticles, which often consist of metal-only cores surrounded by thin metal-oxide shells. This work is important for understanding the magnetic properties of nanoparticle systems. In her talk, on March 14, 2006 at 9:24 a.m. in Room 319 of the Baltimore Convention Center, she discussed her recent work on cobalt-oxide nanoparticles.

Raji Sundaramoorthy

Raji Sundaramoorthy, a student of NSLS user scientist and collaborator Alex Weiss from the University of Texas at Arlington, worked with NSLS scientist Steve Hulbert. She studied photon-stimulated "Auger" decays in solids, a type of multi-electron decay. In this process, an incoming x-ray photon creates a "hole," or positively charged electron vacancy, in one of the atom's core levels. The hole then is filled by an electron that jumps down from a higher electron orbital, which in turn causes an electron (the Auger electron) to be ejected from the solid. An Auger decay often results in a cascade of additional decays, leaving the atom ionized. At the NSLS, Sundaramoorthy closely studied this process in the compound manganese oxide, and compared her results to that of silver and palladium. Her talk took place at 10:12 a.m. on March 13 in Baltimore Convention Center Room 311.

Samantha Palmaccio, another high school student working with DiMasi, attends Sachem High School

in Farmingville, New York. She investigated the biomineralization of protein fibers, which is one step in the process by which many organisms form shells. Recently, she studied the "growth" of the mineral calcium carbonate on a protein-fiber network. Her results show that the strength of the mineral increases over time as it covers the fibers. This is unlike stand-alone calcium carbonate. Additionally, using a powerful microscope, she was able to study the crystal structure formed by the mineral. Palmaccio presented her results on March 13, 2006, at 8:24 a.m. in Room 326 of the Baltimore Convention Center.

"The NSLS considers education to be an important part of its scientific program and mission," said Kao. "As is also evident by these talks, students at the NSLS are working on a wide range of exciting research topics."

— Laura Mgrdichian

NEW WRINKLE IN THE MYSTERY OF HIGH-T_C SUPERCONDUCTORS

March 13-16, 2006

In the 20 years since the discovery of high-temperature (Tc) superconductors, scientists have been trying to understand the mechanism by which electrons pair up and move coherently to carry electrical current with no resistance. "We are still at the beginning," says Tonica Valla of the Condensed Matter Physics & Materials Science Department (CMPMS), who gave a talk on his group's latest results at the March American Physical Society meeting in Baltimore, Maryland. "If anything," he adds, "it looks as if the story is getting more complicated."

The research of Valla and his group, which includes Alexei Fedorov, now of Lawrence Berkeley National Laboratory's Advanced Light Source, and Peter Johnson and Genda Gu, both of CMPMS, was funded by the Office of Basic Energy Sciences within DOE's Office of Science. In 1999, Valla's group was the first to observe a "kink" in the energy level of electrons in high-Tc superconductors just as they went through the transition temperature from their normal to superconducting state. The kink was the first clue to explaining what the mechanism of electron pairing might be. "The kink gave us the hope that we could identify the interaction that was responsible for the electron pairing," Valla said. Some groups hold that the mechanism is the same as in conventional superconductors — that is, that phonons, or vibrations in the crystal lattice, are responsible for electron pairing.

Other scientists believe that changes in the spin alignment, or magnetic polarity, of adjacent electrons — known as magnons — are responsible. "The problem is that there are both phonons and magnons in the crystal with the energy where we see the kink, so it is still not clear," Valla says.

The latest wrinkle uncovered by Valla's group is the observation of similar energy scales and gaps in a material that is not a superconductor. The material is a special form of a compound made of lanthanum, barium, copper, and oxygen, where there is exactly one barium atom for every eight copper atoms. With less or more barium, the material acts as a high-Tc superconductor (in fact, this was the very first high-Tc superconductor discovered). But at the 1:8 ratio, the material momentarily loses its superconductivity.

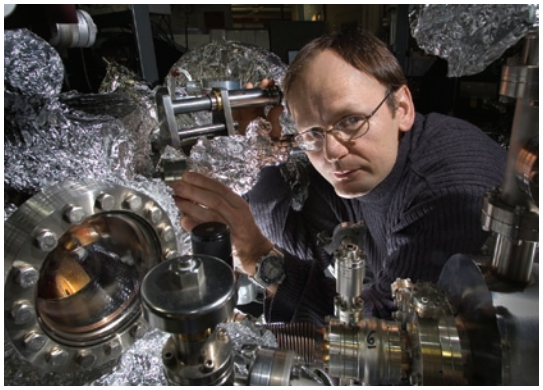

Tonica Valla

"The fact that this system, which is not a superconductor, has similar properties to the superconducting system is not helping to solve the mystery," Valla says. But then he notes that 20 years since the discovery of high-Tc superconductors is still not that long. "For conventional superconductors," he says, "it took about 50 years to come up with a good explanation for the behavior.

"Valla's talk was part of a session on the use of angle-resolved photoemission spectroscopy in the study of high-Tc superconductors. It included a discussion of advances in this technique. His group uses bright beams of ultraviolet light at beamline U13UB at BNL's National Synchrotron Light Source to emit electrons from the samples they are studying. Using high-resolution spectrometers, the scientists measure the energy and the angle at which the electrons exit the crystal, allowing them to reconstruct the electrons' state while in the crystal — their energy level and whether they had any interactions with phonons and/or magnons.

— Karen McNulty Walsh

CERIUM OXIDE NANOTUBES GET NOTICED

March 28, 2006

Chemists and materials scientists often study "nanotubes" — capsule-shaped molecules only a few billionths of a meter (nanometers) in width. In nanotube form, many materials take on useful, unique properties, such as physical strength and excellent conductivity. Carbon nanotubes are the most widely investigated variety. Now, in pioneering research, scientists at Brookhaven National Laboratory have created and investigated the properties of nanotubes made of a different, yet equally interesting material: cerium oxide.

"Cerium oxide nanotubes have potential applications as catalysts in vehicle emission-control systems and even fuel cells," says Brookhaven chemist Wei-Qiang Han, the lead scientist involved in the work. "But until very recently, they haven't been studied."

Han and his colleagues are in the midst of ongoing research into the structure and properties of cerium oxide nanotubes. As part of this, they have devised a method to synthesize cerium oxide nanotubes of high quality. First, they allow the compounds cerium nitrate and ammonia hydroxide to chemically react. Initially, this reaction forms "one-dimensional" nanostructures, such as rods and sheets, made of the intermediate product cerium hydroxide. The intermediate product is then quickly cooled to zero degrees Celsius, which freezes those structures into place. By letting the chemical reaction proceed over a long period of time, a process called "aging," the hydrogen is eventually removed from the intermediate product and a large quantity of the desired end product — cerium oxide nanotubes — is formed.

Han discussed this synthesis method at the American Chemical Society National Meeting in Atlanta, Georgia. During his talk, Han also discussed his group's recent study — how cerium oxide nanotubes release oxygen ions when immersed in a low-oxygen environment, a process that is critical to the nanotubes' effectiveness as catalysts. To do this, the researchers used several techniques. These include "transmission electron microscopy," a very powerful imaging technique, and two x-ray techniques, which they performed at NSLS beamline X19A.

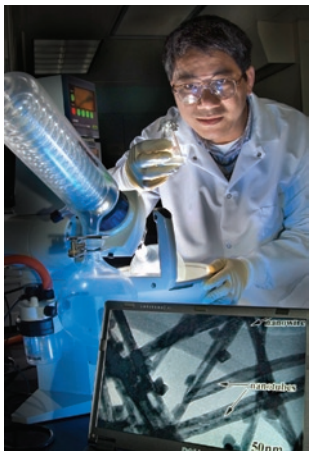

Wei-Qiang Han

"We're interested in studying oxygen-atom vacancies in cerium oxide nanotubes because, when combined with their other surface features, these vacancies may make them more functional and effective in the applications mentioned," Han said.

This work was funded by the Office of Basic Energy Sciences within the U.S. Department of Energy's Office of Science.

— Laura Mgrdichian

FUTURE CRYSTALLOGRAPHERS ATTEND RAPIDATA 2006 AT NSLS

April 23-28, 2006

Once again, 48 future crystallographers from around the world gathered at BNL for RapiData 2006. This week-long course is designed to introduce students to the best and latest equipment and techniques. The students also get to meet and learn from the leading developers of software for macromolecular x-ray crystallography.

The students and instructors, RapiData class of 2006

The course has been offered annually since 1998 by BNL's Biology and National Synchrotron Light Source (NSLS) departments. It reflects the educational component of the PXRR (Macromolecular Crystallography Research Resource), funded jointly by the National Center for Research Resources — a branch of the National Institutes of Health (NIH) — and DOE's Office for Biological & Environmental Research. The course's usefulness to the nearly 400 participants since its inception is apparent from the constant numbers of new students who sign up each year. Many of these budding crystallographers are now becoming experts in the field and sending others from their institutions to BNL to learn the initial steps of this highly specialized area of interest.

This year's course, which ran from April 23-28,

began with three days of lectures and tutorials taught by scientists from BNL, industry, academia, and other national labs. Then the beamline staff and other teachers guided the students through a marathon, 60-hour data-collection session, which eventually employed six NSLS beamlines for the whole time, and three others to help out as needed. At the same time, nine different tutorials were underway. As usual, half of the students came with their own specimens to analyze, while the other half learned as observers.

Said Bob Sweet of Biology, who, with Denise Robertson and Alex Soares, primarily organized the course, "This program excites both the students and the teachers by providing a short 'total immersion' in this technology. Students learn how to obtain and process real data, learning how to locate and fix problems as they arise. It's a gripping experience. About half a dozen of the students left with potentially publishable results. This is inspiring to everyone in the course.

"The students find that there is always a hands-on scientific supervisor available to give expert help, so they can set up experiments in the optimal way, or find out the next step without wasting time," continued Sweet. "We depend on so many team members for the program's success: many members of the PXRR (the Biology and NSLS Macromolecular Crystallography Research Resource), NSLS staff members, and about 18 outside teachers."

In addition to the DOE and NIH funding, a special grant was provided by the International Union for Crystallography and the US National Committee for Crystallography to assist half a dozen Latin American students in attending the course. Additional support is provided by Brookhaven Science Associates, the NSLS, and several very generous equipment vendors and drug companies.

— Liz Seubert

STUDENTS EXPERIENCE THE NSLS VIA WEBCAST

April 25, 2006

More than 20 chemistry and earth-science students from Sayville High School participated in a unique data-analysis project at NSLS beamline X15B — without ever entering the NSLS. Via webcast, they watched as their teachers, assisted by scientists from Stony Brook University's (SBU) Geosciences Department and Brookhaven Lab's Environmental Sciences Department, analyzed soil samples from a creek near the school. This arrangement, which could become a model for other schools nationwide, allowed an entire classroom

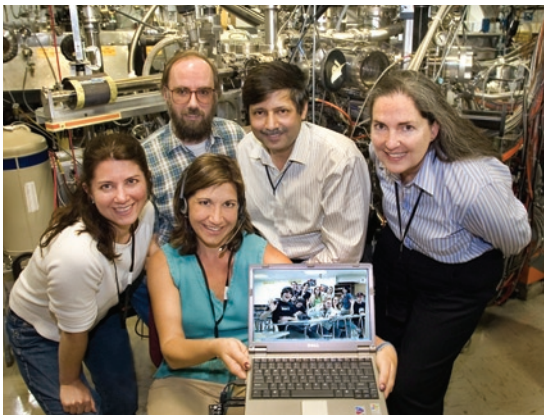

Participants in the X15B webcast, from left: Janet Kaczmarek, Paul Northrup, Adriana Adler, Mirza Beg, and Jen Clodius.

of students to remotely observe and interact with their teachers in real time. Thus, they were able to share in the research experience without being present.

The soil samples were taken from various locations along the creek, from wetlands to uplands, and from various depths. The students have studied water and soil samples from the creek in past work, but this exercise provided the first molecular-scale information about the soils.

On April 25, as the students watched over the web (using VRVS, the Virtual Room Videoconferencing System), teachers Adriana Adler and Janet Kaczmarek analyzed the samples at the NSLS to determine what types of sulfur compounds were present in the soils, and in what amounts. Adler and Kaczmarek (who teach chemistry and earth science, respectively) mounted the samples into the "hutch box" located at the beamline and scanned each sample with a beam of x-rays. This resulted in a set of x-ray absorption "spectra" for sulfur — measurements that show how the sulfur compounds in the soils absorbed the x-rays. Since every compound absorbs x-rays differently, this analysis uncovered the identity and relative amount of each sulfur compound present. The proportions of these compounds reveal important information about the soil samples and the wetlands ecosystem, such as how organic matter decays in soils at different depths and under different conditions. The sulfur compounds can also indicate how environmental contaminants will behave in the wetlands.

As Adler and Kaczmarek worked at the beamline, they were able to see their students. Simultaneously, their students could see them. Thus, the webcast provided valuable two-way interaction.

"The webcast was a fantastic experience for students," said Adler. "We attempt to provide many opportunities for hands-on laboratory exercises for our students. Bringing the NSLS beamline 'into the

classroom' and allowing students to direct experiments at the NSLS from the classroom opened a valuable teaching tool for us at Sayville High School."

Kaczmarek commented, "This was an invaluable experience both for myself and the high school students involved with the webcast. I don't think many high school students can say that they were part of an experiment run at world-known BNL. I see much potential with this type of educational outreach and the benefits to all parties involved. It is all very exciting."

The webcast stems from a Research Experience for Teachers (RET) project called "High School Teacher Training in an EMSI: Bringing First-Hand Research Experiences from the Lab to the Classroom," which is being conducted at the Center for Environmental Molecular Science (CEMS) at SBU. This project is a collaboration between CEMS and an initiative within the Brookhaven Lab Office of Educational Programs (OEP) called "Building Leadership to Expand Participation in Environmental Molecular Science." Both programs are funded through National Science Foundation (NSF) supplements to CEMS, which is a collaboration between SBU Geosciences and BNL Environmental Sciences departments and is co-funded by the NSF and the U.S. Department of Energy. As part of the RET program, both Adler and Kaczmarek have undergone research training at CEMS, focused on the integration of molecular-scale approaches for studies of environmental chemistry. Both teachers also attended an NSLS-sponsored introductory seminar on x-ray absorption spectroscopy applications.

The CEMS personnel who enabled this project include Richard Reeder (Director of CEMS and Professor of Geoscience at SBU), Mirza Beg (Environmental Education Specialist at CEMS), Paul Northrup (CEMS Principal Investigator from BNL's Environmental Sciences Department), and Marianna Kissell (a CEMS graduate student conducting research at NSLS beamline X15B). The project was also enabled by OEP personnel, including Ken White (OEP Manager), Jen Clodius (Senior Educational Programs Representative), and Scott Bronson (Educational Programs Administrator). OEP provided guidance on the use of the VRVS technology and made the broadcast successful. Clodius coordinated the webcast at the beamline, while Bronson managed it at the school.

Students tune in to the X15B webcast.

Northrup, a beamline scientist for X15B, devoted beam time, as well as his own time and expertise, to the project. His efforts were critical to the project's success. Northrup, along with Kissell, also provided scientific support to the teachers. Administrative support was provided by the chair of the Science Department at the Sayville High School, Brian Vorwald. Mike Tabor, head of the school's Technology Department, provided computer and network support.

The outcome of the webcast was very positive. It generated considerable interest among the students. During the experiment they asked questions about x-ray absorption spectroscopy, beamline operation and safety procedures, the results of the analysis, and the NSLS in general. The organizers of the webcast are hopeful that this event could serve as a pilot for other scientific facilities and schools across the country.

Northrup and beamline X15B are supported by the Office of Biological and Environmental Research (Environmental Remediation Sciences Division) within the U.S. Department of Energy's Office of Science, through the BNL EnviroSuite initiative.

— Laura Mgrdichian

NSLS' YOUNGEST SCIENTISTS LEARN FROM LIGHT ON 'TAKE OUR DAUGHTERS AND SONS TO WORK' DAY

April 27, 2006

On April 27, more than 30 daughters and sons of NSLS users and staff learned about some of the scientific programs at the NSLS, and even performed their own scientific experiments. The one-day visit was part of the national "Take Our Daughters and Sons to Work Day."

Upon arriving at the NSLS, the children learned that the facility produces many types of light, from microwaves to x-rays, and that this light has many applications in many fields, including electronics, catalysis, microscopes, and medicine. Then the fun started!

This year's program focused on liquid nitrogen, which is used by most scientists at the NSLS. The children were taken down to the NSLS experimental floor, where they were given 30 minutes

Participants in the 2006 "Take our Daughters and Sons to Work Day" at the NSLS

to count the number of beamlines that used liquid nitrogen. They questioned beamline scientists and learned that liquid nitrogen is used for cooling samples, detectors, magnets, and monochromators. Upon summing the beamlines at the end of the tour, the children were amazed to find that more than 40 beamlines use liquid nitrogen on a daily basis.

Next, the children experienced the wonders of liquid nitrogen first-hand. By immersing an inflated balloon in liquid nitrogen, they discovered that the air inside of the balloon contracts, and then re-expands when warmed up. The children also learned that a tiny pinhole in a ping pong ball will cause the ball to spin wildly after being removed from liquid nitrogen. Other experiments included making a liquid nitrogen banana-hammer and an "ice egg" with a water balloon. They also listened to a "boiling" tea kettle and learned about the wonders of superconductivity, a phenomenon that becomes possible when certain materials are cooled to very low temperatures using liquid nitrogen.

But perhaps the most memorable experiment was the "grand finale": The students mixed cream, sugar, and strawberries with liquid nitrogen to make the fastest (and perhaps tastiest) ice cream ever.

— Laura Mgrdichian

NSLS BIOPHYSICIST LISA MILLER AWARDED TENURE

May 1, 2006

Brookhaven Science Associates (BSA) granted tenure effective May 1 to six BNL scientists: Wolfram Fischer, Collider-Accelerator Department; Frithjof Karsch, Physics Department; Lisa Miller, National Synchrotron Light Source Department; Peter Steinberg, Chemistry Department; Daniel van der Lelie, Biology Department; and Vitaly Yakimenko, Physics.

At the NSLS, Miller was awarded tenure for her outstanding research in the application of spectroscopic synchrotron imaging probes in the biomedical field, her leadership in building a new synchrotron user community, and her extensive outreach activities.

Miller earned her Ph.D. in biophysics from the Albert Einstein College of Medicine, where she is still a visiting assistant professor in the Department of Medicine. She joined the NSLS as an assistant biophysicist in 1999, rising to biophysicist by 2003. Since then, she has most fully developed her research in the areas of mineralization in bone and aberrant protein folding, which are of central importance respectively in osteoporosis and in neurological diseases such as Alzheimer's and scrapie. Concerning the scientific impact of her bone research, for example, she is recognized as having provided unique insights into the site-specific chemical composition of bone that are important for both industrial and academic researchers.

Said NSLS Chair Chi-Chang Kao, "Lisa has made major contributions to research in bone and protein-folding diseases and to the development of synchrotron-based biomedical imaging techniques.

Lisa Miller

She is widely recognized for the creativity and originality of her work, which has resulted in a superb record of publications, invited talks, and funded proposals. The very active user program in biomedical imaging that she has developed at infrared beamline U10B is being emulated at other facilities. Her leadership, educational supervision, and outreach activities are outstanding, and she is truly a valuable member of the NSLS staff."

Miller was honored in 2002 with a DOE Outstanding Mentor Award and in 2005 by Brookhaven Town for outstanding contributions to science and the community. She is also an adjunct assistant professor in the Department of Biomedical Engineering at Stony Brook University.

— Liz Seubert

QUITE A REMARKABLE SPRING: NOTES FROM THE 2006 NSLS-CFN JOINT USERS' MEETING

May 15-17, 2006

A rosy future was forecast for Brookhaven's user facilities at the first-ever joint meeting of the user communities for the National Synchrotron Light Source (NSLS) and the Center for Functional Nanomaterials (CFN), held May 15-17, 2006.

2006 NSLS UEC Members and SpIG Representatives stand with DOE and BNL management.

At the main meeting on May 16, held in BNL's Berkner Hall, officials from the Laboratory, the Department of Energy's (DOE) Office of Science, and the New York State congressional delegation painted an optimistic picture for an audience of several hundred current and prospective users of Brookhaven's cutting-edge science facilities – those that are currently in operation, planned and under construction, or eagerly anticipated. The Laboratory's interim director, Sam Aronson, welcomed the participants and outlined Brookhaven's "extremely strong science agenda in terms of ongoing research and new facilities that will maintain Brookhaven as a leader in world science." He said meetings like this are important places in which to foster new research collaborations and get updated on the status of work at the Lab. He said that the Laboratory's highest priority is the design and construction of the NSLS-II, which, along with the CFN, will give Brookhaven a powerful combination of cutting-edge research tools.

Sam Aronson

Last fall, the DOE granted "Critical Decision Zero (CD-0) status to National Synchrotron Light Source-II (NSLS-II), the planned world-leading successor to the NSLS. soon, Critical Decision One (CD-1) will yield a construction plan and a site decision will be made.

Robert McGrath

"The NSLS-II will allow our science to continue to flourish and expand, and keep the United States in the forefront of light-source science," Aronson said. Citing Brookhaven's expected contribution to energy research, Aronson said that work here "will be vital to that effort for the U.S. economy and energy security." He said that the DOE's forward-looking investments in user facilities "will eventually change the face of the Laboratory. The completion and operation of the CFN and NSLS-II will profoundly change the balance of research here."

Following Aronson, Stony Brook University provost Bob McGrath gave an update on the search for a new Laboratory director. The search committee has created a list of potential candidates and is contacting key individuals of interest. McGrath said that the committee has a list of 40 people and will begin serious interviews with 10 of those candidates. The committee expects to have a recommendation to Brookhaven Science Associates in September.

The American Competitiveness Initiative

Pat Dehmer, director of DOE's Office of Basic Energy Sciences, outlined the chain of events that led to the Laboratory's bright future outlook, which she termed "a quite remarkable spring." Focusing on the rollout of the American Competitiveness Initiative (ACI) which she called "great news for the physical sciences," Dehmer explained that the ACI doubles funding for DOE's Office Science over the next 10 years. One of the ACI's focus areas is the tools of science, described as "unique, expensive, large-scale tools beyond the means of a single organization."

Pat Dehmer

Dehmer said that she had anticipated that funding for Office of Science programs would be flat or would decline slightly, but that when the ACI was announced during the President's State of the Union speech in January, "a miracle occurred." Projected funding for the Office of Basic Energy Sciences has increased by 25 percent, in large part because the Office's work "aligns almost 100 percent with the ACI goals."

While Dehmer was optimistic about the construction of the NSLS-II, she cautioned that the project would have a long construction life, which will be filled with unanticipated challenges.

"You are embarking on a wonderful journey," she said. "You should be euphoric...and frightened. And you will vacillate between the two."

She concluded her remarks by urging employees and users to contact their congressional representatives to thank them for the support that resulted in this "completely unexpected" funding picture.

"You must realize how difficult it was to make that happen," she said, citing the war, last fall's hurricanes and other budgetary pressures. "Politicians are people, too. They deserve your thanks, and they need to hear from you."


Tim Bishop

Speaking after Dehmer, Congressman Tim Bishop said that he is "so proud of this Lab, the people who work here, and the work that's moving America forward in so many different ways." To see the administration's proposed investments in science is "encouraging indeed," he said. Citing the FY06 budget language stating that it is the "sense of the Congress" that NSLS-II be built at Brookhaven, Bishop pledged to continue pushing for that result.

Bishop said the full funding of the CFN is also a testament to the faith that the Office of Science has in Brookhaven, as well as to the "strenuous advocacy" of the New York congressional delegation.

"We speak with one voice on the importance of this Lab," he said, and urged attendees to stay in touch with their representatives.

"Be forceful in your advocacy," he said. "We value your professional expertise, and these are important issues."

NSLS-II Update

The morning's next speaker, Steve Dierker, BNL Associate Director for Light Sources, is leading the effort to bring the NSLS-II to BNL. Noting that "the CFN will be producing materials that will be crying out to be characterized," he said that development of nanoscale materials will be critical for the development of future energy technologies.

"NSLS-II will be brighter than any existing light source. None of today's light sources were designed to probe materials with one-nanometer spatial resolution and 0.1 meV energy resolution," he said. "The changes that NSLS-II brings will be transformative."


Steve Dierker

Dierker briefly described plans for the Joint Photon Sciences Institute (JPSI), intended to foster development of new techniques and capabilities. He thanked Stony Brook's Bob McGrath for helping to secure a $30 million commitment from New York State for a building to house the proposed institute.

"JPSI will serve as an intellectual center for development and application of the photon sciences and as a gateway for NSLS-II users," he said.

Dierker showed new drawings depicting the proposed facilities, and noted that there have been some changes in the design, in particular, the substitution of a full-energy booster for a full-energy linac injector. He said that 99 people are currently working on NSLS-II, and predicted that the programs would overlap for less than one year before both will be fully and independently staffed.

"The NSLS-II will be essential for energy security, and important for U.S. industry, "he concluded. "It will enable 'grand challenge' science in many diverse fields."

The Center for Functional Nanomaterials

Doon Gibbs, Associate Laboratory Director for Basic Energy Sciences and Interim Director of the CFN, said that an active search is underway for a permanent CFN director, and he urged attendees to bring promising candidates to the attention of the search committee. He said a broader search effort will begin this fall, with an eye to have a permanent director on board by October 2007. Gibbs observed that the CFN building's structural shell is complete, and that more than half of the Center's equipment will be ordered by the end of May.


Doon Gibbs

The CFN, whose focus will be energy security, has added nine new scientific and technical staff members, bringing the total fulltime staff total to over 20. He added that the staff is becoming more collaborative and using bigger teams.

Gibbs said that along with NSLS-II, the CFN will "enable the nanoscience revolution," and he said that the joint user meetings should take place every year or two.

"It is very significant and gratifying that so many users have come here from all over," he said. "We should continue to have such joint workshops because they perform a valuable service and bring us together."

"It really has been fun being interim director," he said. "It's an exciting time to lead this project."

NSLS Update

An update on the work of the NSLS was given by Chi-Chang Kao, Interim NSLS Chairman. He said that FY06 was a "tough year," but observed that no layoffs were necessary, and he said that funding prospects for FY07 remain very good.

Chi-Chang Kao

Kao said the NSLS continues to serve some 2,300 users per year, and announced plans for a BNL User Center to give users "one-stop shopping," for functions including check-in, badging, and housing. The user center will also have extended hours on nights and weekends. He said the NSLS hopes to continue to add more staff on the floor, which he termed important for both science and safety.

"More staff, then more beamlines," he said.

Kao addressed the issue of orbit stability at the facility, noting that the staff running the 65 operating beamlines is not the same staff that built them.

"There has been some lack of understanding of the sensitivity of beamline optics to electron beam motion," he said. "The beamlines need regular alignment and performance calibration."

Along with its usual complement of materials science users, Kao noted an "up tick" in the number of biomedical imaging users. A technique called Diffraction Enhanced Imaging or DEI has been developed to image soft tissue samples and delivers 8 to 33 times greater contrast than digital mammograms.

"This could eventually have a very wide impact in the health industry," he said.

In conclusion, Kao promised both an aggressive upgrade plan for the facility and close NSLS-CFN coordination.

Building Safe Nanomaterials

As science ventures into the nanoworld, concerns will arise over the potential risks involved in producing and working with materials with properties that may not have previously been observed. Vicki Colvin, a chemistry professor from Rice University, spoke about developing nanomaterials with low environmental impacts.

The future of nanotechnology promises answers to key questions in science, she said. Of particular interest to Long Islanders and others in the northeast United States is a technology to remove arsenic from water efficiently and in large quantities. But in considering such advances in technology, scientists must deal with what Colvin termed the "Wow to Yuck Trajectory," in which the environmental impacts of new technology are only revealed after the technology is in wide use. Examples include DDT, which cured malaria but endangered birds, and refrigerants, which cooled our houses but led to a hole in the ozone layer.

"Early examination of nanomaterials' effects will create a responsible technology," Colvin said. "Scientific data and analysis should take the debate about the risks of nanotechnology to the highest possible technical level."

Colvin illustrated some of the challenges inherent in attempting to answer questions of risk by considering the question: Are single-walled carbon nanotubes (SWNTs) toxic? She pointed out that there are 20 major types of SWNTs, and four manufacturing types. All of these types have different lengths, different purification methods, and 10 possible surface coatings, for a possible 50,000 SWNT samples.

"It will be necessary to map out basic structure-function relationships for nanomaterials and biological impacts," she said. "Fundamental nanostructure will include both chemical and physical properties."

NSLS User Science Talks

Following a lunch break, users heard from several scientists who have conducted research at the NSLS.

Henry Chapman, a staff scientist at Lawrence Livermore National Laboratory, spoke on "Ultrafast Coherent Diffraction Imaging with a Soft X-Ray Free-Electron Laser." This vacuum ultra-violet free-electron laser is located at the Deutsches Elektronen-Synchrotron (DESY) in Hamburg, Germany. It generates pulses just 25 femtoseconds in duration with more than a trillion photons per pulse, and is the first free-electron laser to produce soft x-rays. It is ideal for high-resolution holography and imaging, Chapman said, and he showed this by displaying diffraction images and measurements.

Next, a talk on the “Engineering of Carbon Nanotube Structures” was presented by Pulickel M. Ajayan from the Department of Materials Science and Engineering at Rensselaer Polytechnic Institute. His talk focused on recent developments in his laboratory to fabricate carbon-nanotube-based structures that are tailored for various applications. Specifically, he discussed how he and his group create branched nanotube and nanotube-hybrid structures for applications such as sensors, electrical interconnects, and filters.

Before the afternoon break, Lawrence Shapiro, an associate professor at Columbia University, spoke on “Decoding Cell Adhesion with Protein Crystallography.” Cell adhesion – connections that allow cells to stick together – is critical to the formation of tissues and complex cellular networks, such as those that make up the nervous system. These connections are made possible by a few cell-surface protein families. Shapiro discussed how, at the NSLS and other synchrotrons, high-resolution protein-crystal structures are beginning to reveal the atomic-level mechanisms of cell adhesion.

Other Notables
Each year, the NSLS Users’ Executive Committee (UEC) presents one user with the UEC Community Service Award, which honors hard work and dedication toward bettering the experience of users and the user community. At the main meeting, UEC Chair Peter Stephens presented this year’s award to Bob Sweet (BNL-Biology). More details on this year’s award can be found in the following article.

At the conclusion of the main meeting, participants attended the annual poster session and vendor exhibition. Hors d'oeuvres were served as attendees mingled and talked, making for a lively, enjoyable event. Awards were presented to the top student and postdoc posters, which were on display in the NSLS lobby during the month of June. The winners were: Elena Loginova (Rutgers University), Seo-Young Kwak (BNL-NSLS), Shuguo Ma (BNL-Chemistry), Minhua Shao (Stony Brook University), Jae-Hyuk Her (Stony Brook University), and Ariane Kretlow (Robert Koch Institute, Germany). Each winner received a BNL certificate and a $50 American Express gift certificate. Additionally, the Synchrotron Catalysis Consortium gave out two poster prizes of its own. First prize went to Shao, and second prize was awarded to Wen Wen (BNL-Chemistry).

During the two days after the main meeting, workshops were held at locations across the Laboratory. They were *"Synchrotron Catalysis Consortium: New Opportunities for in-situ XAFS Studies of Nanocatalysis,"* organized by Simon Bare (UOP) and Anatoly Frenkel (Yeshiva University); *"Soft Matter and Biomolecular Materials: X-ray Scattering Enabled by High Brightness Beamlines,"* organized by Ben Hsiao (Stony Brook University), Lin Yang (BNL-NSLS), Elaine DiMasi (BNL-NSLS), and Ron Pindak (BNL-NSLS); *"Nanoscale Correlations Heterostructures,"* organized by Jim Misewich (BNL-Material Sciences) and Tony Heinz (Columbia University); *“Chemical and Biological Applications of X-ray Emission Spectroscopy,"* organized by James Penner-Hahn (University of Michigan) and Trevor Tyson (New Jersey Institute of Technology); *"Platforms for the Integration of Biological Systems into Nanomaterials and Interfaces,"* organized by Oleg Gang (BNL-CFN), Daniel Van Der Lelie (BNL-Biology), and Molly Frame (Stony Brook University); and *"VUV Radiometry,"* organized by Jeff Keister (SFA, Inc).

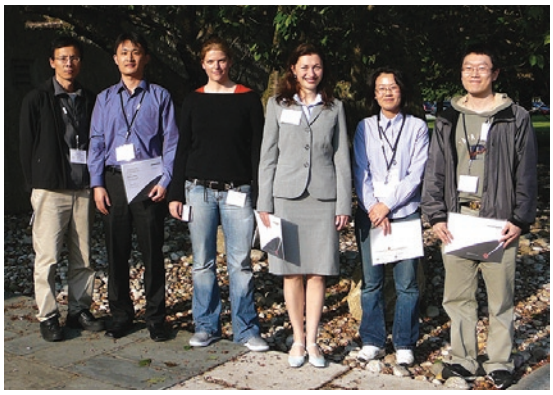

Poster winners (from left) Shuguo Ma, Minhua Shao, Ariane Kretlow, Elena Loginova, Seo-Young Kwak, and Jae-Hyuk Her.

— Kay Cordtz and Laura Mgrdichian

BOB SWEET, THE 2006 UEC COMMUNITY SERVICE AWARD RECIPIENT

May 16, 2006

For his extraordinary service, the NSLS Users' Executive Committee chose Robert M. Sweet for the UEC Community Service Award.

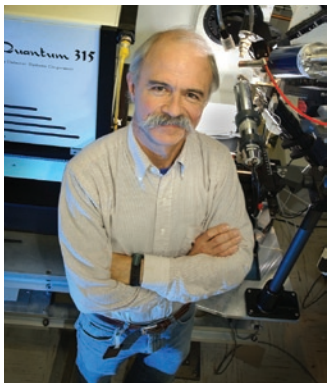

Bob Sweet

Biological crystallography has emerged as an extremely high-profile research area with synchrotron radiation, and Bob has made numerous contributions to create and sustain a vibrant community of users at the NSLS. Bob is the Principal Investigator of the Macro-

molecular Crystallography Research Resource (PXRR), which provides facilities and support at the NSLS for the benefit of outside and in-house investigators. The PXRR is supported by the NIH's National Center for Research Resources and the DOE Office of Biological and Environmental Research in its mission to create optimal facilities and environments for macromolecular structure determination by synchrotron x-ray diffraction. With a staff of about 24, the PXRR innovates new access modes such as FedEx crystallography, builds new facilities, develops remote participation software, collaborates with outside groups, teaches novice users, and supports visiting investigators with seven-day, 20-hour staff coverage.

The PXRR includes six beamlines at X8C, X12B, X12C, X25, X26C, and X29. Bob's work on developing macromolecular crystallography at the NSLS helped in a continual push toward improved performance for NSLS beamlines. The X25 wiggler provided an early demonstration of the potential for insertion devices at NSLS, and the mini-gap undulator at X29 has added to that innovation, and inspired upgrades to mini-gap undulators for other beamlines, notably X25.

Bob's efforts have led to the development of sample-loading automation techniques at the NSLS, software that enables easy user experimental interaction, and the scope of the PXRR has established standardization across many NSLS beamlines, enabling users to move easily from one beamline to the next.

Bob is warm, easy to talk to, and accessible to regular users in the community. Through all his efforts, Bob has likely been the single most important factor in keeping the NSLS on the cutting edge of macromolecular synchrotron crystallography.

It is thus with great pleasure that Bob Sweet was given the NSLS Community Service Award for 2006.

ENERGY SECRETARY, UNDER SECRETARY FOR ENERGY TOUR NSLS

June 2, 2006

On June 2, BNL welcomed Energy Secretary Samuel Bodman and Raymond Orbach, newly named Under Secretary for Science at the Energy Department.

During a whirlwind visit, the Secretary and Under Secretary met researchers at the NSLS, where they talked about current and future research. While discussing applications of synchrotron soft x-rays, NIST physicist, Dan Fischer, gave Bodman and Orbach a tour of beamline U7A. NSLS biophysical chemist, Lisa Miller, showed the Secretary and Under Secretary infrared beamline U10B and described her group's work on skin melanoma while Steve Dierker, Associate Laboratory Director for Light Sources, highlighted the prospects for NSLS-II.

ALD for Light Sources Steve Dierker shows Energy Secretary Samuel Bodman and Under Secretary Raymond Orbach posters in the NSLS lobby.

Bodman and Orbach also met researchers at the Relativistic Heavy Ion Collider's (RHIC) PHENIX and STAR detectors and the molecular beam epitaxy system laboratory, where they heard about the Lab's nanoscience efforts.

Later, the Secretary gave a standing-room-only talk in Berkner Hall to an audience of employees and other guests, including Shirley Strum Kenny, President of Stony Brook University and Chair of the Brookhaven Science Associates (BSA) Board; Carl Kohrt, Battelle President, CEO, and BSA Vice-Chair; and other members of the Board. His purpose in coming to the Lab, the Secretary said, was to support the same level of quality in BNL's future work as that of the greatness of its past — ensuring that "from RHIC to the new Center for Functional Nanomaterials to the preferred siting for the NSLS-II, history will be repeated at the Lab."

DOE/BNL Partnership Requires Safety and Science

In committing to maintaining that tradition, DOE "requires a partnership between you and us," Bodman said. "We look to this laboratory for excellence in management as well as science."

"The most important asset the Department has here . . . is all of you," he continued. "The personal safety of all departmental employees and contractors is a top priority for me." The Secretary emphasized that Brookhaven can be proud of its

Energy Secretary Samuel Bodman (front, middle) stands at beamline U7A with (from left) NIST physicist Dan Fischer, Under Secretary Raymond Orbach, Battelle President and CEO Carl Kohrt, Associate Laboratory Director for Light Sources Steve Dierker, BNL Interim Director Sam Aronson, and scientists Faisal Alamgir and Sharadha Sambasivan.

history of scientific achievement and contributions in many fields, "But, in my judgment, your safety record requires improvement," he said. "We ask you to take care of each other and think of yourselves. Small accidents are the precursors to serious accidents."

Investing in Science

The President understands that we must make investments to ensure that America retains its world pre-eminence in science, Bodman said. "That is why he has proposed the American Competitiveness Initiative (ACI), the Alternative Energy Initiative, and the Global Nuclear Energy Partnership (GNEP). The Energy Department has a major role in all three programs."

Through the ACI, the Office of Science budget is expected to increase by 14 percent in 2007, to $4.1 billion. This initiative is especially important to the NSLS, as the Office of Science will direct additional funds to sectors promising breakthroughs, including supercomputers, nanotechnology, energy from biomass, nuclear fusion, and high-intensity light sources like the NSLS.

Another reflection of Washington's growing awareness of the importance of science, the Secretary pointed out, is Congress' recent confirmation of Ray Orbach as "the first Under Secretary for Science in the history of our Department. The symbolism involved expresses a role for science in our country's government that it has never had before, and we will take maximum advantage of it." Over the next 10 years, even more funding will come from the ACI — $136-plus billion — to invest in research and development, improved math and science education, and incentives to encourage entrepreneurship and innovation, Bodman said.

NSLS scientist Lisa Miller shows Energy Secretary Samuel Bodman infrared beamline U10B.

GNEP, meanwhile, is a collaboration among several countries, Bodman said. The aim is to develop new technologies to recycle spent nuclear fuel in a way that cuts proliferation risks while reducing the volume of waste for disposal. Nine DOE labs, including Brookhaven, are playing a role in this program.

The Alternative Energy Program is also focused on developing new technology. With a 22 percent increase for FY07, this will translate into more support for work on cellulosic ethanol, lithium ion batteries for hybrid vehicles, and hydrogen fuel cells.

All this effort depends on people, Bodman said, and pointed to the ACI call for $380 million to improve mathematics, science, and technical education in U.S. elementary and high schools. He cited the work being done by BNL's Office of Educational Programs as an example of the type of program needed to "assure that future generations of scientists and engineers will step forward to carry on the work that all of you are doing so ably here today." In conclusion, the Secretary reiterated the "tremendous respect" he had for BNL's achievements and what he expected the Lab to achieve in the future. He ended his formal comments by urging Lab employees to e-mail him with their concerns at any time.

— Liz Seubert with Peter Genzer and Kendra Snyder

CRYSTAL GROWTH WORKSHOP HAS CRYSTALLIZING RESULTS

June 12-15, 2006

Hailing from as far as Australia, 40 researchers shared the complexity of the protein crystal growth process with leaders in the field at the "Crystallization: Focus on Optimization and High Throughput Techniques" workshop. The fourth annual course took place at the NSLS from June 12-15, 2006. Organized by Vivian Stojanoff (NSLS) and Naomi Chayen (Imperial College London), with help from

scientists Fabiano Yokaichiya (NSLS) and Jean Jakoncic (NSLS), East Coast NIGMS Structural Biology Research Facility, and Stony Brook intern Matthew Worth, the workshop included a record-number of 11 hands-on tutorials for participants to choose from.

The purpose of the three-day course was to help researchers obtain high-quality protein crystals through both conventional and non-conventional methods including the use of oils, novel nucleating agents, detergents, crystallization in lipid cubic phase, crystallization with gels and high throughput techniques. Participants were divided into groups of three or four, according to their main interests, and followed practical sessions during the course. Researchers chose seven of the 11 sessions to attend, whereas last year's course offered eight sessions.

The participants of the 2006 Crystallization workshop

"What's unique about this course is that it is a real hands-on experience," Stojanoff said. "You really get to try these things out yourself." This unique aspect inspired about a third of the participants to bring their own proteins on which they tried different methods. A few participants actually produced crystals from the proteins they brought, which were screened on beamline X6A on the last day of the workshop.

Experts in the academic and industrial crystallization field gave a series of talks and tutorials. Neer Asherie (Yeshiva University) discussed "Understanding Protein Phase Behavior," Marie-Claude Marchand (Qiagen Inc.) discussed "The Vapor Diffusion Method and Optimization," Gwen Nneji (Imperial College of London) discussed "Non-standard Crystallization Techniques," Pat Loll (Drexel University) discussed "Membrane Proteins and Detergents," Peter Nollert (Emerald BioSystems) discussed "Micro Crystallization using the Lipidic Cubic Phase Methodology," Ingo Grotjohann (Arizona State University) discussed "The Role of the Phase Diagram in the Crystallization of PSI and PSII," and Abel Moreno (Universidad Nacional Autonoma de Mexico) discussed "Gels and Fields: What Can They Say About the Phase Diagram?"

Practical sessions also included talks by Troy Burke (GE Healthcare), Marcia Armstrong (Qiagen Inc.), Trevor Harvard (Precision Detectors), Craig Sterling (Emerald BioSystems), Chris Gawronski (Fluidigm), and NSLS Interim Chairman Chi-Chang Kao, who gave participants an introduction to the light source facility.

In addition, by request of last year's participants, a special session on cryogenic protection and quality assessment of crystals was conducted at beamline X6A on the last day of the workshop. Seetharaman Jayaraman (Columbia Universtiy) introduced the topic and conducted demonstrations in the New York Structural Biology Center Laboratory.

The course attracted researchers with all levels of crystallization experience, including current NSLS users who have previously encountered problems with their crystals. "The course brings new people and awareness to companies about the NSLS and mutual benefits we can have," Stojanoff said.

One participant commented on the course survey: "It is better than a conference. In a conference, people present results, but in this workshop, we are shown how to get results."

Stojanoff stressed her appreciation to the following groups that allowed the use of their labs and time: New York Structural Biology Center, Case Center for Proteomics, the X19C PRT, X17 PRT, X19A PRT, NSLS staff, NSLS User Administration, and the NSLS Outreach Office. Major sponsors included GE HealthCare, Qiagen, Precision Detectors, Emerald Biosystems, and Fluidigm. Additional support was provided by Hampton Research, Douglas Instruments, Anatrace, Millipore, Eppendorf, and New York New Jersey Scientific.

— Kendra Snyder

FUTURE 'POETS,' STUDENTS LEARN ABOUT NANOSCIENCE AT BNL

June 19, 2006

Whether they want to be speech therapists or chemists, all students can benefit from learning about nanoscience. That's the mantra of National Synchrotron Light Source user Anatoly Frenkel, who taught two courses on the subject this summer leading up to a week of hands-on research at BNL for eight students and eight research assistants from Yeshiva University.

The six-week courses, "Discover Nanoscience" and "Nanoscience for Poets" attracted students

with majors ranging from history to computer science. “We want them to become aware of the most important problems in modern science,” said Frenkel, who taught the courses along with fellow Yeshiva professors Gabriel Cwilich and Fredy Zypman.

Participants in the Yeshiva University nanoscience courses at the NSLS

The students worked in teams on the design, synthesis, manipulation, and characterization of nanoparticle catalysts, which are key components of hydrogen fuel cells. “We designed the course around some activities that students could do from beginning to end,” Frenkel said.

The courses began in late May with introductory lectures and labs at the Yeshiva campus, in New York City, in order to get participants up to speed with the concepts of nanoscience and nanotechnology. Students then prepared thiol-stabilized Pd nanoparticles for their research.

The focal point of both courses was a weeklong stay at Brookhaven, which started on June 19. On NSLS beamline X11A, students analyzed their samples using x-ray absorption fine structure (XAFS) spectroscopy. Short trips also were made to Stony Brook University, where students characterized their nanoparticles with electron microscopy and atomic force microscopy.

The efficiency of hydrogen fuel cells correlates with the ability of their catalysts to absorb and/or adsorb hydrogen. The students studied the effect of hydrogenation of fuel cell performance by changing the size of their Pd samples. One of the most exciting parts of the courses is that actual data was collected, Frenkel said. A mini conference with presentations served as the final exam for the students, and their results will be presented in Boston this November at the annual meeting of the Materials Research Society.

Frenkel held a similar course in 2003 on experiments in modern physics and plans to expand the nanotechnology courses in future years.

“Some students go into sciences without knowing too much what the day-to-day research is like because they didn’t have any opportunity to learn how serious research is different from undergraduate work. And then they’re disappointed and find out later in their lives that research is not what they wanted to do,” Frenkel said. “We can help show them what it’s like and help them make a decision, no matter what that decision is.”

— Kendra Snyder

IN MEMORIAM: DAVID MURRAY ZEHNER

June 19, 2006

David Murray Zehner, who helped develop beamline U12B at the NSLS, died on June 19, 2006. He was 62.

David Zehner

A native of Philadelphia, Zehner received his B.A. at Drexel University and his Ph.D. in physics from Brown University. Zehner was a research scientist for more than 30 years in the Solid State and Condensed Matter Physics Divisions at Oak Ridge National Laboratory, where he served as group leader and section head for many years.

He completed his thesis at Brown under famed physicist Harrison E. Farnsworth, one of the first to use low-energy electron diffraction to study metal crystal surfaces. Described by colleagues as an “old-school physicist,” Zehner was greatly influenced by his mentor and focused most of his research on elemental and alloy metal surfaces.

Doon Gibbs, BNL’s Associate Laboratory Director for Basic Energy Sciences, first worked with Zehner in the late 70s and early 80s on experiments focused on the structure and phase behavior of gold surfaces. Prior to completion of the NSLS, Gibbs’ group used a rotating anode source in the Physics Department and the Cornell High Energy Synchrotron Source (CHESS) to carry out the experiments. After the start-up of the NSLS, they transferred their studies to beamline X22C and added platinum and iridium surfaces to their research. Zehner also conducted research at beamline X20.

"David was brutally honest and he liked to do things right," Gibbs said. "He was very precise about the little details, from doing the experiment to writing the papers. But he also was a lot of fun and cared a lot about what people thought and how they were doing."

Zehner helped develop beamline U12B at the NSLS in the early 80s along with Ward Plummer, now a Distinguished Scientist at Oak Ridge and a Distinguished Professor of physics at the University of Tennessee. As a collaboration between Oak Ridge and the University of Pennsylvania, beamline U12B researchers used electron scattering to determine and understand the structure and chemistry of surfaces. "He was emphatic that he had to do it right and he would do it over and over again until it was," said Plummer, who published some 15 papers with Zehner during their time together at the beamline. "That led to a lot of late nights at Brookhaven."

Colleagues say Zehner's compassion was evident by the way he mentored the graduate students and postdoctoral researchers who worked on his experiments. "He followed their career with every step they made," Plummer said. "He really cared about people. He joked that with his affinity for people, he probably missed his calling and should have become a real doctor."

One of those young researchers who Zehner took under his wing was Art Baddorf, now a senior research staff member at Oak Ridge who worked with Zehner and Gibbs at Brookhaven in the 1990s. "I learned a lot from him," Baddorf said. "He was a lot of fun to be around and he was interested in what everyone else was doing and how they were doing it."

Zehner enjoyed windsurfing, sports, and music, and was a member of the American Vacuum Society and the American Physical Society. A resident of Lenoir City, TN, Zehner is survived by close friend, Donna Watson; and former wife, Theodora Zehner.

— Kendra Snyder

IN MEMORIAM: JULIAN DAVID BAUMERT

June 24, 2006

Julian David Baumert, a Brookhaven physicist working on the cutting edge of research on liquid surfaces and thin organic films, died of melanoma on June 24, 2006. He was 31.

Described as dedicated, bright and caring,

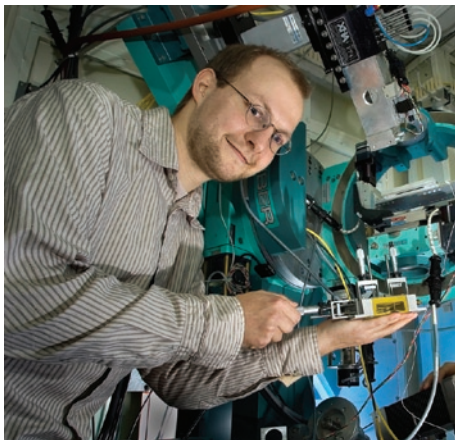

Julian Baumert

Baumert was a relatively new research associate in the Soft Matter and X-ray groups in the Condensed Matter Physics and Materials Science Department at BNL. "Julian was an exceptionally talented, hard-working young researcher, who loved his work," said colleague John Hill. "He understood his research at a deep level and it was always a pleasure to ask him what he was working on and hear his clear, precise, and enthusiastic explanations of his latest results and what they meant. It is such a tragedy to lose him so early in his life and in his career. We will all miss him immensely."

A native of Molfsee, Germany, Baumert was educated at the Institute of Experimental and Applied Physics (IEAP) at the University of Kiel and the Institute Laue-Langevin (ILL) in Grenoble, France, where he studied a compound known as methane hydrate, which is found naturally on the sea floor and is a major worldwide energy resource. His thesis focused on the structure and dynamics of this compound using neutron and x-ray scattering techniques and numerical simulations. Baumert obtained his Ph.D. from the University of Kiel in February 2004, receiving the prestigious "Familie-Schindler Foerderungs-Preis" of the Faculty of Science in Kiel.

"He was a very cheerful person," said colleague Oleg Gang. "We deal with so many difficult and complicated things here, but he created this atmosphere around him where everything was positive."

Baumert came to BNL in July 2004 and conducted his research at beamline X22 of the National Synchrotron Light Source, where he was part of a team of scientists learning to make smaller and more powerful molecular-scale circuit components that could someday make electronic devices more efficient. He was the principal investigator on a paper published in February 2006 in the Proceedings of the National Academy of Sciences that

described the first measurements of the structure of a molecular junction at buried interfaces. He was working to elucidate how the structural and electrical properties of these molecular junctions depend on the molecular coverage.

"He had such great promise to be an extremely successful scientist," said Ben Ocko, who hired Baumert into his research group. "He was easy-going and friendly, and exhibited a high level of creativity, great skills as an experimentalist, and the ability to explain complex phenomena in simple and elegant terms. He had such a bright future ahead of him."

In the past year, Baumert was diagnosed as having skin cancer and underwent extensive treatment. That didn't stop him from continuing his research at Brookhaven. "Even when his health deteriorated, he continued to come to the Lab daily to work on experiments and to discuss science with his colleagues," Ocko said. After an operation last summer, Baumert continued his scientific research including travel to the Advanced Photon Source last December to investigate how "surface freezing" modifies the capillary wave spectrum at the surface of long-chain alkane molecules using a technique called x-ray photon correlation spectroscopy.

"It was really amazing how he dealt with it," said Baumert's office mate and colleague Masa Fukuto. "He must have known the odds were against him, but he was courageous to the very last minute. He never lost hope."

A resident of Sound Beach, Julian Baumert is survived by his wife, Maren; his parents, Ingrid and Jürgen; and his sisters, Anna and Sophia.

— Kendra Snyder

IN MEMORIAM: ELIZABETH A. HICKS

July 12, 2006

Elizabeth "Liz" A. Hicks, a Brookhaven systems analyst for more than 14 years, died on July 12, 2006. She was 41.

A native of Syosset, Hicks received a B.S. in computer science from Stony Brook University. She joined BNL in May 1990 as a Database Administrator at the National Synchrotron Light Source and later became an applications engineer. Hicks maintained and developed numerous employee databases, assisted the NSLS User Administration Office, helped develop the NSLS stockroom database, and provided general support for sections throughout the department.

Liz Hicks with sons Christopher and Adam

"She was very competent and very good at what she did," said NSLS Business Operations Manager Frank Terrano. "She loved her work, she loved to work, and she never shied away from putting in extra hours. She had a huge effect across the entire department."

When last-minute jobs came in, Hicks was ready to work, said colleague Mary Anne Corwin. "She was always there and always helpful," Corwin said. "She was so friendly and really focused on doing things the right way."

Hicks battled multiple illnesses during her time at Brookhaven, but she didn't let that affect her spirits. "She was so strong-willed and optimistic," said colleague Donna Buckley, who worked with Liz to develop the NSLS stock room database. "She was such a happy person. I don't think I ever saw her angry in all of the days I worked with her."

Described as daring, humorous, and without a "mean bone in her body," Hicks enjoyed skiing, sailing and the annual Mattituck Strawberry Festival, which she attended for the last time with her two sons in June. Hicks left the lab on long-term disability in July 2004, partly to spend as much time as possible with her children, friends said. "She knew she wasn't going to make it to a ripe old age," said colleague Wendy Morrin. "She lived for her boys. She was a really good mom."

Hicks also loved to sing, dance and play the piano. The clanking sound of tap shoes ringing down the NSLS hallways could be pinpointed to Hicks' office, where she and Morrin practiced routines during lunchtime for their dance classes.

"It was always great to see Liz," Morrin said. "She was always cheerful and smiling. She had so much against her health-wise, but she never let it show. She lived every day to its fullest. She was just a truly beautiful person."

A resident of Mattituck, Hicks is survived by her husband, Eugene; her sons, Christopher and Adam; her parents, Holmes and Lucy; her brothers, Gary and Kenneth; and her sister, Lee.

— Kendra Snyder

JEAN JAKONCIC WINS ESTEEMED STUDENT LECTURER AWARD

July 22-27, 2006

National Synchrotron Light Source student researcher Jean Jakoncic won the prestigious Margaret C. Etter Student Lecturer Award for researching the use of high-energy x-rays to prevent crystal damage in diffraction studies.

Jean Jakoncic

He received the award at the American Crystallographic Association national meeting, held in Honolulu, Hawaii, on July 22-27, where he also gave a talk on the subject. The Etter award, given out just once a year, recognizes achievement and future potential for scientists at an early stage in their independent careers.

Jakoncic, a graduate student from Joseph Fourier University working toward his Ph.D. in structural biology, came to the NSLS four years ago. Conducting research primarily at NSLS beamline X6A (under the supervision of Vivian Stojanoff), in addition to X17B1 and the European Synchrotron Radiation Facility (ESRF) beamline ID15B, Jakoncic helped to show that high-energy x-rays could be an option for the structural determination of radiation-sensitive proteins. In addition to Stojanoff, he worked with NSLS scientist Zhong Zhong and ESRF scientists Marco Di Michiel and Veijo Honkimaki.

“Traditionally, people use medium- and low-energy x-rays for diffraction studies of protein samples,” Jakoncic said. “At these energies, there is a significant amount of energy deposited in the crystal and substantially there is radiation damage. We propose to use higher energies, where the energy deposition is about 10 to 15 times less than at lower-energy x-rays.”

To visualize radiation damage, the group exposed lyzozyme crystals, which are standard test protein crystals, to high-energy and low-energy x-rays and compared the results. “With the same resolution limit, we didn’t see any radiation damage at 55 keV, the high-energy data, while we observed radiation damage at 12 keV,” Jakoncic said, adding that plans for additional testing with crystals from different proteins are underway. “This is the first step,” he said.

Jakoncic describes his efforts associated with the high-energy x-ray research as a “satellite project” in relation to his other scientific interests. His core research at the NSLS focuses on enzymes involved in the degradation of toxic compounds, in particular polycyclic aromatic hydrocarbons (PAH).

— Kendra Snyder

NSLS SUMMER SUNDAY DRAWS 650 VISITORS TO FACILITY

July 30, 2006

Using gumdrops and toothpicks to illustrate molecular crystals and Marshmallow Peeps to demonstrate the power of a vacuum, about 650 community members had a sweet time at the NSLS Summer Sunday on July 30, 2006.

For eight consecutive Sundays each summer, the Brookhaven National Laboratory Summer Sunday program invites the public to see the popular Whiz-Bang Science Show and showcases a different BNL facility every week.

Visitors who came to the event began their tours in Berkner Hall, where Marc Allaire, Lisa Miller,

A steady stream of visitors filled the NSLS Lobby

Visitors gather around the liquid nitrogen display outside the NSLS

Steve Hulbert, Tony Lanzirotti, and Andrew Ackerman explained the concept of a light source and gave more detailed information about the facility and its research goals. Before boarding a bus for the quick drive to the NSLS, visitors learned more about nanoscience research at a display set up by the Center for Functional Nanomaterials, and roamed among several other hands-on exhibits.

Once at the NSLS, visitors crowded the lobby, seminar room, and front patio, where 14 hands-on displays were set up to demonstrate how the light source works and teach visitors about the science performed there. Learning about science topics ranging from diffraction to liquid nitrogen, the NSLS guests floated from display to display, asking questions and collecting some goodies along the way.

At the "Crystals: Unlocking the Secrets of Life" display, many kids, and some adults, assembled "crystals" from toothpicks and gumdrops. Another popular display was "Sounds of Silence," where guests watched how a vacuum pump caused a balloon to expand and the sound of a ringing bell to considerably fade. Display volunteers also exposed Marshmallow Peeps to the vacuum, which expanded the Peeps when turned on and shriveled them down to a smaller size when turned off. Visitors then performed a science experiment of their own by popping the de-puffed Peeps in their mouths. Their findings: The vacuum didn't make the candies any less tasty.

At "See the Light," visitors could observe actual synchrotron light, guided to the lobby from the experimental floor by a fiber-optic. And by using a Skee Ball-type backboard and rubber bouncy balls, the "Electron Catapult" display showed visitors how different amounts of energy are required to propel an electron from an atom's "ground state" level to higher levels.

Standing at the lobby and second-floor viewing windows overlooking the experimental floor were scientists Steve Bennett, John Dabrowski, Susila Ramamoorthy, Gary Weiner, and Ray Raynis. The volunteers pointed out various components of the light source to visitors, using large neon numbers as reference points.

The excitement also carried over to the outside, where every half hour visitors gathered around the building's front windows or on the patio to watch a special water rocket launch in the parking lot across the street by Matt Engel, John Kuczewski, and Steve Ehrlich.

Upon entering the building, each guest received a quiz with questions that could be answered by visiting each display. Every finished quiz was handed in and redeemed for an NSLS orange frisbee, to match the volunteers' orange shirts. In addition, one person was selected raffle-style every half hour by the enthusiastic MC Gerry Van Derlaske to receive one of two prizes – a BNL T-shirt or a tour of the experimental floor. This is the first year that floor tours were offered during the event, and visitors were excited to see the actual piping, foil and wires of the NSLS up close.

Summer Sunday visitors look at displays in the seminar room

The rest of the more than 40 NSLS volunteers that made the event possible included: Kimone Antoine, Al Borrelli, Jonathan Cheung, Mary Anne Corwin, Angelo Dragone, Steve Giordano, Sarah Heins, Madeline Hughes, Steve Hulbert, Syed Khalid, Steve Kramer, Ariane Kretlow, Tony Kuczewski, Brian Kushner, Andreana Leskovjan, Sean McCorkle, Corinne Messana, Eileen Morello, Payman Mortazavi, Shirin Mortazavi, Kathy Nasta, Kumi Pandya, Meghan Ruppel, Cecilia Sanchez Hanke, Lenny Santangelo, Yusuf Siddiqui, Randy Smith, Kendra Snyder, Marie Van Buren, Adele Wang, Matt Worth, Nancye Wright, and numerous NSLS family members.

— Kendra Snyder

1,000 INJURY-FREE DAYS... AND COUNTING

August 14, 2006

NSLS users and staff have worked more than 1,000 days without a lost-time injury. This significant safety milestone was reached on Monday, August 14, 2006 as the tally in the NSLS lobby jumped into the quadruple digits. The number means that almost three years has passed without a person working at the NSLS losing work time or incurring restricted duties as the result of an injury or exposure on the job.

The milestone is a major accomplishment for the NSLS, considering the complicated work environment and the hundreds of people working within the building 24 hours a day, said Bob Casey, the NSLS Associate Chair for Environment, Safety, Health, and Quality. “This success is the result of many people taking care to plan their work and making sure that hazards are identified and controlled,” Casey said. “A safe work environment is good for each of us personally, and it is good for the NSLS. I tip my hat to everyone for their efforts to keep our workplace safe.”

— Kendra Snyder

HATS OFF TO THE 2006 NSLS SUMMER STUDENTS

September 1, 2006

Eighteen high school and college students performed summer research projects at the NSLS this year, working with scientists and engineers from the department in research fields ranging from medical sciences to electrical and mechanical engineering. In addition to their research projects, students had the opportunity to attend scientific lectures, tour BNL research facilities, and participate in numerous social activities.


Kimone Antoine

Interested students apply to these programs in the spring and the programs range from six to 10 weeks long. Here’s an idea of what they did during the summer:

Kimone Antoine worked with Lisa Miller to analyze differences in the chemical composition between children’s and adults’ fingerprints using infrared microspectroscopy. Her objective was to reveal why children’s fingerprints disappear faster than those of adults. Antoine received her Associate’s degree in mathematics and natural science from Lehigh Carbon Community College in Pennsylvania and attends classes at Hiram College.


Kobbina Awuah

Kobbina Awuah worked with John Skaritka as part of the Science Undergraduate Laboratory Internship (SULI) program at BNL. They designed a 2-in-1 cryogenic permanent magnetic undulator (CPMU) and a superconducting undulator (SCU). The design will help reduce project costs associated with switching from one kind of undulator to the other (i.e. CPMU to SCU and vice versa). Awuah is a junior at Cornell University.


Jonathan Cheung

Jonathan Cheung worked at the NSLS with Syed Khalid and Vivian Stojanoff on a project related to the origin of color from natural pigments. Cheung collected different materials that were dyed using pigments from vegetables, tree bark, and flowers. This dying process involves some natural mordants (fixers) such as iron, copper, and aluminum. Using spectroscopy, he found the color of the finished sample to be dependent on the type of material and mordant used. Cheung is a senior at Syosset High School.

Sarah Heins spent most of her time was observing administrative staff and scientists while they worked on everything from completing travel authorization forms to determining the structure and magnetism of certain elements. She worked with Stony Brook University graduate student Kathryn Krycka to learn how much time and effort is needed in order to conduct experiments, write a thesis and earn a


Sarah Heins

high-level degree in the physics field. She also spent a small portion of her time researching physical concepts and past experiments done at the NSLS. In her spare time, Heins helped the secretarial staff to learn about the administrative aspects of scientific research. Heins is a freshman at Syracuse University.

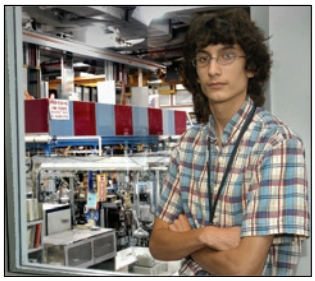
John Kuczewski

John Kuczewski worked with Peter Siddons at the NSLS as part of the High School Summer Research Program. He developed a graphical user interface for the Thorlabs OPTODC Servo Motor System under the GNU/Linux platform. Modeled from Siddon's driver and kernel patch, Kuczewski's software package for this motor system was programmed using the C programming language and the GTK+2.0 libraries for the Debian GNU/Linux operating system. GNU/Linux based systems are used at the light source for beamline controls and this new software package will integrate seamlessly into the present control systems. Kuczewski is a sophomore at Shoreham-Wading River High School.


Elhag Shaban, Marcus Mason and Eric Huey

Marcus Mason and Eric Huey worked with Peter Siddons and Elhag Shaban at the NSLS as part of the Faculty and Student Team (FaST) program. Mason and Huey studied the processes involved in the development of a Bulk MicroMegas Detector. They characterized the detector using extended x-ray absorption fine structure (EXAFS) methodology at beamline X12A They also attempted to reproduce stable gains and excellent resolutions as studied in previous detectors. They both are juniors at Southern University at Baton Rouge.


Shirin Mortazavi

Shirin Mortazavi participated in BNL's High School Research Program. Under the guidance of Lisa Miller, Mortazavi studied the chemical composition of children's and adults' fingerprints using infrared microspectroscopy at beamline U10B. The difference between the chemical make-ups should explain why the fingerprints of children disappear before those of adults. Mortazavi is a junior at Bellport High School.

Saka Okyere-Asiedu and Christopher Dixon worked under the mentorship of Delaware Materials Science Professor Robert Opila and NSLS staff scientist Steve Hulbert at the NSLS as part of the Faculty and Student Team (FaST) program. They used ultraviolet photoelectron spectroscopy at beamline U4A to determine how the chemical bonding of materials affects the electrical performance of materials. They investigated how the valence bands of silicon determine the conductivity of photovoltaics. The team also used the system to test for electrical properties of material with a high dielectric constant for application in Si circuits. Their results will help maximize the efficiency of solar cells and help determine which metal and dielectric are used in the future generation of very highly integrated circuits. Okyere-Asiedu and Dixon are undergraduate students at the University of Delaware.


Saka Okyere-Asiedu, Christopher Dixon and Robert Opila

Dylan Roden participated in the Science Undergraduate Laboratory Internship (SULI) program at the NSLS under Lisa Miller. Dylan worked with photodynamic therapy treatment of human melanoma cells in an effort to discover an effective treatment for the disease. He also uses Fourier Transform Infrared (FTIR) analysis to assess chemical changes within the melanoma cells as a function of treatment method. Roden is an undergraduate student at the Massachusetts Institute of Technology pursuing a bachelor's degree in biological engineering with hopes to continue his education in medical school.

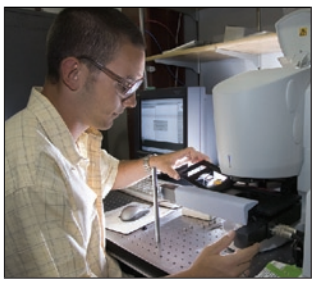
Dylan Roden

Yusuf Siddiqui worked with Syed Khalid and Vivian Stojanoff as part of the Community Summer Science Pro-


Yusuf Siddiqui

gram at the NSLS. Siddiqui searched for the chemical composition of the active site of ferritin – a protein used in anemia prevention and early haemochromatosis detection. Ferritin contains a hollow shell that can contain a significant amount of iron and is therefore of great use to doctors treating iron deficiency disorders. Small amounts of cadmium, a toxic transition metal found to be in ferritin, could shed light on the plausibility of ferritin usage as a medical treatment, therefore contributing to further research into new treatments for iron deficiency disorders. For these experiments Siddiqui used extended x-ray absorption fine structure spectroscopy (EXAFS). Siddiqui said he hopes that the work done during his internship will contribute to expand general scientific knowledge. He is a junior at Boston University Academy.


Rodney Snow

Rodney Snow worked with Peter Siddons at the NSLS as a GEM National Consortium intern. Snow was engaged with many assignments simultaneously, but his main project was assembling, testing, and characterizing a spin polarization detection chamber. This chamber will be used to detect the ballistic transport of low-energy electrons through ultra-thin films with a thickness on the order of 20 to 100 nm. This study can ultimately realize a new generation of electronics called spin-based electronics. Snow is a second-year graduate student at Michigan Technological University.

Weisha Zhu worked with Babu Manjasetty of the Case Center for Synchrotron Biosciences as a Science Undergraduate Laboratory Intern. Their project studied the complex structures of Escherichia coli L-Arabinose isomerse, an enzyme with potential use for tagatose (low-calorie natural sugar) production. By co-crystallizing the enzyme in complex with co-factor metal ions and candidate substrates/inhibitors, they were able to understand structure-function interactions important for the enzyme's biological mechanism. Crystals of different complexes were grown and several diffraction datasets were collected at NSLS-X4C and X6A beamlines. Comparison studies between the native and complex forms of crystal structures will provide valuable biological information in designing new pathways to increase tagatose production. Zhu is an undergraduate student at Cornell University.

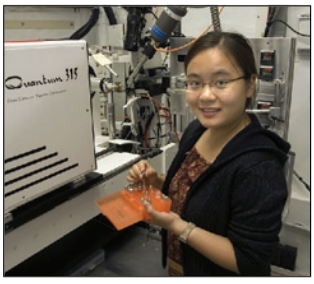
Weisha Zhu

— Kendra Snyder

NSLS, NSLS-II STAFF CELEBRATE AT PICNIC AND SERVICE AWARDS

September 21, 2006

Pushed back a week because of rain, the 2006 Light Source Directorate Picnic took place on September 21 with beautiful weather. For the first time, the annual end-of-year celebration was held for both NSLS and NSLS-II employees, hosted by NSLS Chair Chi-Chang Kao and Steve Dierker, Associate Laboratory Director for Light Sources. In addition to the vast amounts of meat, cheese, pasta salads and candy, Kao presented a cake to celebrate 1,000 injury-free days at the NSLS. The cake was cut – carefully – by Jim Tarpinian, Assistant Laboratory Director for Environment, Safety, Health and Quality, after he congratulated employees on the significant safety milestone.

Service Awards

Michael Caruso, Richard Freudenberg, Richard Heese and Pooran (Boyzie) Singh were honored for 25 years of service at Brookhaven Lab, and 20-year awards went to Scott Buda, Shuchen Kate Feng, and Michael Fulkerson. In the 10-year category were G. Lawrence Carr, Elaine DiMasi, Joan Marshall, Cheo Teng, and John Vaughn III. And although it isn't an officially recognized BNL milestone, John Dabrowski was acknowledged for an impressive 45 years of service at the Lab.


NSLS and NSLS-II staff enjoy the food at the annual picnic.

Spotlight Awards
The Spotlight awards are tributes to NSLS staff members who have shown exceptional dedication to their jobs during the year. This year, the winners were:


NSLS Chair Chi-Chang Kao

Walter DeBoer: The vendor contracted to build the X25 undulator could not deliver the completed device on schedule, so the burden of completing and testing the device fell onto the NSLS technical staff. From August 2005 through February 2006, DeBoer took on a great amount of that responsibility, traveling twice to Lansing, NY, to assemble, bake, and vacuum-test the undulator. Working unpaid hours on long days and weekends both in Lansing and at BNL, DeBoer is a big reason why the undulator was installed successfully during the winter shutdown.

David Harder: The original schedule for X25 undulator development included at least one and a half months for magnetic measurement and shimming of the device. However, the delivery was delayed because of the vendor, and as a result, less than two weeks were left to spend on these steps. Harder, whose careful examination of the Hall probe scanning system enabled a precise characterization of the undulator's magnetic field, spent seven days a week for two months on the project to compensate for the lost time.


ALD for Light Sources Steve Dierker

Mike Lehecka: Lehecka also worked seven days a week for two months to make up for lost time on the magnetic measurement and shimming aspect of the X25 undulator installation. Lehecka, who runs the pulsed wire bench for the NSLS magnetic measurement laboratory, does both mechanical and intricate vacuum-related work. He is an expert in setting up pulsed wire measurement systems, which vendors don't have the capability to do. Without his effort, the X-25 undulator measurements couldn't have been finished in such a short amount of time.

Ed Losee: In the effort to produce superconducting undulators for the NSLS and NSLS-II, Losee undertook the responsibility for prototype undulator magnet fabrication and assembly. The process requires special skills and equipment, and such devices had never been built in the United States. With minimal direction, Losee taught himself how to use a complex turntable device to fabricate the magnet, and using it, he then produced several prototypes. The NSLS can now produce and test superconducting magnets and other complex components in-house with Losee's assistance and skills. Losee also provided significant support on the X17 superconducting wiggler during the winter 2005-06 shutdown.

Philip Marino and Tom McDonald: Marino and McDonald won this shared Spotlight Award for upgrading the NSLS beamline safety checklists, which were old, difficult to use, and didn't have a system in place to assure periodic review and update. Beginning in 2003, Marino and McDonald approached each beamline to identify the critical components, meeting with the local contacts to assure minimal interruption to operation. They then made and connected all the needed labels and photos and assembled the new checklists in a standard format. The NSLS relies on this system for radiological safety, and Marino and McDonald spent considerable effort and time completing the upgrade.

Paul Montanez: Montanez served as an engineer, supervisor and coordinator during the relocation of beamlines X9A and X9B to X3. The series of moves was planned and coordinated in a way that needed no additional shutdown time for the machine and minimized the total disruption to the X9 program. The originally proposed spring shutdown schedule was cut in half because Montanez figured out ways to do more preparation and minimize work. He put in extra hours to ensure this relocation was successful while still completing projects with beamline X25 and NSLS-II.

Charlie Nielson and Wayne Rambo: The NSLS Controls and Diagnostics groups were tasked with integrating the X25 MGU control system, designed by an outside contractor, into the NSLS Controls System. At the end of 2005 and early part of 2006, Rambo and Nielson both put in overtime hours and extraordinary effort to accomplish the system pretesting, installation and commissioning within the tight schedule. Both men made trips to Advanced Design Consulting in Lansing, NY, to check on the project's progress and work around problems as they came up during testing and commissioning.

Mihai Radulescu: The bellows on the VUV-IR injection shutter failed during operations in July

2006. A previous failure of this same assembly required complete removal and rebuilding of the shutter, and fortunately, the about two-week repair process happened near a major maintenance time. This recent instance, however, would have resulted in major downtime if it weren't thanks to Radulescu. He developed a method for removing the actuator while leaving the shutter block in place. This whole process was completed in less than 60 hours from the time it was discovered.

— Kendra Snyder

CHI-CHANG KAO NAMED CHAIR OF THE NSLS

October 1, 2006

Chi-Chang Kao, a physicist and leader in synchrotron light research, was named Chair of the NSLS Department, effective October 1. Kao served as interim NSLS Chair since mid-January 2006, after Steve Dierker stepped down to lead the development of the NSLS-II.

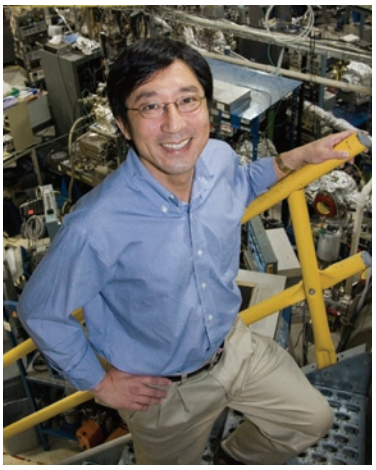

Chi-Chang Kao

"Chi-Chang is an internationally recognized scientist with a remarkable talent for bringing people together and growing scientific programs," said Dierker, who is the current Associate Laboratory Director for Light Sources. "I can think of no better choice than Chi-Chang to lead the NSLS forward."

As Interim Chair, Kao produced a five-year plan for the future development of the NSLS. With input from the user community, NSLS staff, and Brookhaven researchers, the plan identifies a number of exciting scientific opportunities, improvements needed for better accelerator operation, and upgrades for beamlines, detectors, and infrastructure. As the new NSLS Chair, Kao wants to ensure that these initiatives are implemented.

"The next five years will be a very important time for the NSLS, because if NSLS-II gets approval, we will transition into the new light source at the end of that period," Kao said. "We have developed a very aggressive strategic plan that will help keep scientific productivity up and also grow new scientific communities at the NSLS. In particular, we want to grow in a way that will allow us to smoothly transition the user scientific program to the NSLS-II."

Additionally, Kao wants to encourage closer interaction between the NSLS, Brookhaven's research departments, industry, and universities, as well as emphasize research related to nanoscience and energy. "There are many ways that synchrotron research can make significant contributions to solve the energy problems the world is facing today," Kao said. "Using light, we can study and make advances in the fields of catalysis, energy storage, fuel cells, and solar energy."

Kao earned a B.S. degree in chemical engineering in 1980 from National Taiwan University and a Ph.D in chemical engineering from Cornell University in 1988. Shortly after, he joined BNL as a postdoctoral research assistant at the NSLS. His research focuses on the development of new experimental techniques using synchrotron radiation, and their applications to condensed matter physics and material sciences.

He received tenure as a Brookhaven physicist in 1997 and served as the NSLS high-energy program coordinator from 1998 to 2001. He was promoted to senior physicist in 2001 and was named NSLS Deputy Chairman in 2005. Kao also is the Associate Chairman for User Science and an adjunct professor in the Department of Physics and Astronomy at Stony Brook University. He is a member of the American Physical Society and the American Association for the Advancement of Science.

— Kendra Snyder

UPDATE ON THE X27A MICRO-SPECTROSCOPY FACILITY BEAMLINE

October 1, 2006

In 2006, NSLS hard x-ray micro-spectroscopy facility beamline X27A became fully operational. A smooth transition from commissioning to operations during the fall of 2005 provided immediate implementation of a wide and diverse research program involving an extensive range of institutions: Stony Brook University, Rutgers University, BNL Environmental Sciences Department, Miami University, Institute of Nuclear Physics (PAN) Poland, University of Western Ontario, Natural Resources Canada and IMEC of Belgium. Ongoing research areas include the study of manganese and arsenic speciation/distribution in a range of environmental sensitive samples; the nature of

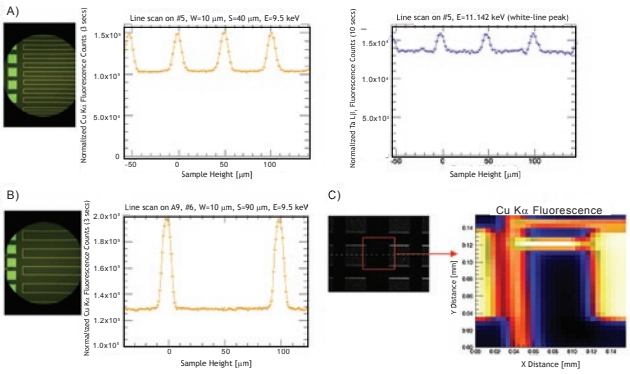

Figure 1. X-ray fluorescence line scans across 10 um-wide copper interconnects spaced at (A) 40 um and (B) 90 um. (C) Cu Kd fluorescence image of a pad structure.

titanium incorporation through applied creams into human skin layers; plutonium and uranium distribution/speciation in contaminated soils; polarization dependent thorium EXAFS measurements on small apatite single-crystals; understanding strontium incorporation in osteoporotic bone; and determining trace-metal distribution in diseased brain tissue. The success of implementing these research areas, and the high-quality data being collected at this facility, is largely due to the good stability of the NSLS x-ray ring, which is especially important for microprobe beamlines.

An example of an area of research initiated at X27A is the investigation of tantalum and tungsten thin-film diffusion barriers that are used in copper interconnect technology. Using the x-ray microbeam, buried thin-film layers beneath copper are investigated using fluorescence x-ray absorption spectroscopy. The ability to characterize these films, which are often amorphous and cannot be studied using x-ray micro-diffraction, is an important area of applied research within the semiconductor industry. Currently, preliminary experiments on thin-film interconnect test structures have been conducted and analyzed, and these encouraging results have initialized the fabrication of 'real' systems for future in-situ measurements. Preliminary measurements on passivated 10 μm wide, 120 nm thick Cu interconnects, separated by 40 μm and 90 μm 'field' regions, and with a 4 nm thin ALD Ta_3N_4 barrier layer have been performed. Cu Kα fluorescence recorded at an incident x-ray energy of 9.5 keV, and Ta $L\beta_1$ fluorescence recorded at the peak of the Ta white-line at ~11.142 keV, are shown in **Figure 1**. The Ta L_2 XANES on a PVD Ta_2N (5 nm)/Ta (20 nm) blanket film and a 4nm ALD Ta_3N_4 barrier used in a copper interconnect test structure are shown in **Figure 2**. As can be seen, the nitrogen content within the Ta_2N barriers is clearly evidenced by the spectral signature of the near-edge region and the shift in the absorption edge towards higher x-ray energies, compared to the Ta_2N (5 nm)/Ta(20 nm) blanket film, which is of predominantly Ta character.

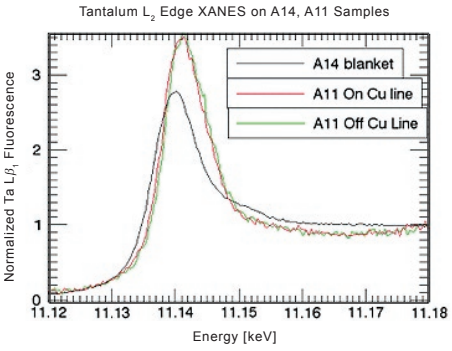

Figure 2. Ta L_2 absorption-edge XANES on Ta_2N (5 nm)/Ta (20 nm) blanket film and the Ta_2N barrier on a Cu interconnect patterned sample, both on and off the interconnect lines.

— James M. Ablett

RICHARD BISCARDI WINS SITEWIDE SAFETY STEWARD AWARD

October 16, 2006

NSLS chief electrical engineer Richard Biscardi was one of four BNL employees to win a Sitewide Safety Steward (S3) Award as part of a new employee recognition program for safety awareness.

The S3 program recognizes outstanding awareness and implementation of health and safety improvements and corrective actions. Biscardi was nominated for the award based on his initiative in reducing electrical hazards, an important area of risk for the NSLS.

Erik Johnson, Biscardi's supervisor, noted that his job requires him to be more attuned to electrical hazards than most staff members, but he has built upon his heightened awareness and shared his expertise broadly throughout BNL, primarily as a member of the Lab's electrical safety committee.

"His work has led to the identification of hazards and non-compliances as well as possible methodologies for their mitigation that are now being employed across the Laboratory," Johnson said. "He has truly adopted a stewardship role in promoting electrical safety for the NSLS and BNL."

Of particular note is his effort in providing pathways to compliance with the requirements of two safety codes: National Fire Protection Association (NFPA) 70E, which describes standards for electrical safety in the workplace; and 10CFR851, a worker health and safety program.

At the presentation of the Sitewide Safety Stewardship (S3) Award, the winners were: (from left) Richard Biscardi, National Synchrotron Light Source Department; Cheryl Conrad, Energy Sciences & Technology Department; and (right) Richard Scheidet, Plant Engineering Division. The fourth award winner, Jeff Gillow, Environmental Sciences Department, was not present. A team award was also presented to: (third from left) Adele Billups, Laura Thompson, and Peter Guida, all of the Medical Department.

On very short notice, Biscardi worked with staff across the department to develop a protocol for the NSLS to come into compliance with the personal protection equipment requirements of 70E. He also established an equipment inspection program to assure the electrical equipment used by staff, vendors, and visitors either meets Nationally Recognized Testing Laboratory (NRTL) requirements or has been properly inspected and tagged. This program is being emulated across the Laboratory.

Biscardi also formed a team to investigate equipment compliance with the requirements of 10CFR851. This working group's findings and recommendations are at the heart of the NSLS program to come into compliance with 10CFR851.

Biscardi, along with the other S3 award winners, runner-ups, and nominees, was recognized in a BNL ceremony on October 16.

— Kendra Snyder

418TH BROOKHAVEN LECTURE 'BRIGHT PHOTON BEAMS: DEVELOPING NEW LIGHT SOURCES'

October 18, 2006

A world-leading brightness of intense x-ray light is needed for scientists to make the next generation of discoveries in a wide range of disciplines, from structural biology to nanoscience, from the structure and dynamics of disordered materials to properties of materials under extreme conditions — and more.

To provide this bright light, BNL proposed and the DOE approved the National Synchrotron Light Source II (NSLS-II), a state-of-the-art medium energy machine designed to produce x-rays more than 10,000 times brighter than those produced at the current NSLS. These powerful beams and the advanced instrumentation at NSLS-II will be able to probe samples of materials in a wide range of sizes and conditions, giving information that could lead to advances, for example, in clean and affordable energy, molecular electronics, and the self-assembly of nanomaterials into useful devices.

Developing the machine and its instrumentation is not easy, however. Achieving and maintaining the needed level of intensity will involve tightly focusing the electron beam, providing the optimally matched insertion devices, and achieving and maintaining a high electron current. At BNL, research and development are ongoing on these and other challenges.

Timur Shaftan

Timur Shaftan, a scientist in the NSLS Department, gave the 418th Brookhaven Lecture on this work on October 18, 2006 during his talk "Bright Photon Beams: Developing New Light Sources."

In his talk, Shaftan discussed various sub-systems of NSLS-II and the requirements and key elements of their design. He also explained how scientists at the NSLS developed a prototype of a light source of a different kind — a short-wavelength free electron laser — and reviewed the development of new concepts in the physics of bright electron beams in this facility.

Timur Shaftan, who earned his Ph.D. in physics at the Budker Institute of Nuclear Physics, Russia, in 1997, joined BNL in February 2000. Since 2003, he has been involved in many areas of the NSLS-II project, including lattice design, insertion devices, and the design of the injection system. He currently leads the group working on Conceptual Design of the NSLS-II injection system. Involved in collaborations with a few accelerator facilities worldwide, he also serves as a reviewer in Nuclear Instruments and Methods in Physics Research journal.

— Liz Seubert and Kendra Snyder

BNL WINS R&D 100 AWARD FOR X-RAY FOCUSING DEVICE

October 19, 2006

Brookhaven National Laboratory has won a 2006 R&D 100 award for developing the first device able to focus a large spread of high-energy x-rays. The device, called a Sagittal Focusing Laue Monochromator, could be used in about 100 beamline facilities around the world to conduct scientific research in physics, biology, nanotechnology, and numerous other fields.

R&D 100 Awards are given annually by R&D Magazine to the top 100 technological achievements of the year. Typically, these are innovations that transform basic science into useful products. The awards were presented in Chicago on October 19.

NSLS physicist Zhong Zhong led the development of the focusing device with help from BNL scientists Chi-Chang Kao, Peter Siddons, Hui Zhong, Jonathan Hanson, Steven Hulbert, Dean Connor and Christopher Parham; BNL technicians Anthony Lenhard, Shu Cheung, and Richard Greene; and former BNL scientist Jerome Hastings, who is now working at the Stanford Linear Accelerator Center.

"I congratulate the researchers who have won this award, which highlights the power and promise of DOE's investments in science and technology," Secretary of Energy Samuel W. Bodman said about the BNL team. "Through the efforts of dedicated and innovative scientists and engineers at our national laboratories, DOE is helping to enhance our nation's energy, economic and national security."

As x-rays are produced at light sources, they spread out, or diverge. X-rays produced by a beamline with a 5 milliradian divergence, for example, will spread to 5 millimeters (mm) by the time they are 1 meter away from their source, and to 50 mm when 10 meters away. This is a problem for light source scientists, who want the highest possible x-ray flux on a small spot, which requires a well-focused beam.

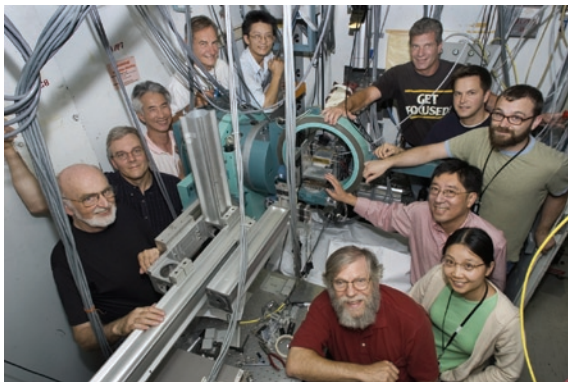

On the left, from front to back: Jonathan Hanson, Steven Hulbert, Shu Cheung, Anthony Lenhard, and Zhong Zhong. On the right, from front to back: Peter Siddons, Hui Zhong, Chi-Chang Kao, Dean Connor, Christopher Parham, and Richard Greene. Not pictured: Jerome Hastings.

Previous x-ray focusing technologies relied on mirror-like surface reflections, but this required large surfaces and caused technical difficulties in error control and limitations on the energy of the x-rays that could be focused. The device developed by Zhong's team, however, doesn't rely on a crystal surface to reflect the beam. Instead, it sends the x-rays directly through a set of silicon Laue crystals, named for German physicist Max von Laue. The result is a 1,000-fold increase in beam intensity, as well as high-energy resolution, reduced costs and ease of operation, Zhong said.

The device consists of two thin bent crystals mounted on a slide, with the first one diffracting upward and the second one diffracting downward to focus the beam horizontally. It is the first device that can focus a large divergence of high-energy x-rays, handling a beamline with a divergence as great as 20 milliradian.

"This is a very elegant solution to an existing problem," said Zhong, who started working on the project in 2001. The first version of the device is installed at the NSLS beamline X17B1 and is gaining interest from members of other Brookhaven beamlines and scientists at light sources around the world. Development of the award-winning device was supported by the Office of Basic Energy Sciences within the U.S. Department of Energy's Office of Science.

— Kendra Snyder

SHORT COURSE: XAFS STUDIES OF NANOCATALYSIS AND CHEMICAL TRANSFORMATIONS

October 19-21, 2006

The short course in x-ray absorption fine-structure (XAFS) analysis, emphasizing problem-solving methods in typical catalysis applications, was offered on October 19-21 at the NSLS. It continued the annual NSLS tradition of gathering a group of scientists, active in the field, who share their expertise with those interested in learning about the possible use of XAFS in their research as well as with those who are relatively advanced. The latest two courses were organized and co-sponsored by the U.S. Department of Energy's Synchrotron Catalysis Consortium (SCC) and the NSLS. The theme of the latest course was tailored to users

Participants in the XAFS Studies of Nanocatalysis and Chemical Transformations Short Course

of the SCC who have recently collected data in systems of relevance for catalysis applications: nanoparticles- mono- and bimetallic (including core-shell), supported on different surfaces, studied ex situ or in situ. The latter included real-time reactions studied at the SCC facilities by XAFS.

The course was organized by Anatoly Frenkel (Yeshiva University), Syed Khalid (NSLS), and Faisal Alamgir (NIST). The format of the course consisted of lectures in the morning and data analysis sessions in the afternoon. Most lectures were designed as tutorials on different aspects of XAFS analysis, such as the "Theory of XANES" and "Theory of EXAFS" (Josh Kas, University of Washington), advanced data analysis methods (Principal Component Analysis, by Stephen Wasserman, SGX Pharmaceuticals), and the basics of EXAFS data processing and fitting (Scott Calvin, Sarah Lawrence College). In addition, lecture topics included the "Concepts of advanced EXAFS data modeling" (Anatoly Frenkel), "In situ XAFS studies of fuel cell catalysts" (Carlo Segre, IIT), "XAFS studies of battery materials" (Faisal Alamgir), and "New opportunities with Quick XAFS at the NSLS" (Syed Khalid).

There were 26 registered participants from academia, industry, and national laboratories, as well as 5-10 graduate students from Stony Brook University and Yeshiva University who audited the course. The lecturers were also the data analysis session instructors. During the data analysis session, participants were trained in using the XAFS analysis packages IFEFFIT (authors: M. Newville and B. Ravel), FEFF8 (authors: J. Rehr, et al) and PCA software (author: S. Wasserman).

Most of the course participants brought their own data they recently collected at the NSLS or other synchrotrons. The analysis sessions were organized by matching instructors to the problems. Instructors rotated between sessions, thus sharing their expertise with more than one group of participants. For example, all groups benefited from Steve Wasserman's tutorials on the use of his Principal Component Analysis program and Josh Kas' tutorials of modeling in-situ XANES data in nanoparticles with FEFF8. Scott Calvin, Faisal Alamgir, and Carlo Segre advised all those interested in adaptation of IFEFFIT programs to advanced modeling methods. Anatoly Frenkel helped those studying monometallic and bimetallic, including core/shell, nanoparticles.

All course members thoroughly enjoyed friendly and professional logistical support by the NSLS Users Administration Office: Gretchen Cisco, Liz Flynn, Kathy Nasta, and Mercy Baez.

— Anatoly Frenkel

NSLS USERS RECOGNIZED

October 25, 2006

Each year, a number of NSLS users win prestigious awards in their field of scientific research. The following represent a collection of some of the 2006 awards:

2006 Alvin Van Valkenburg award

Li Li

NSLS user Li Li was the 2006 recipient of the Alvin Van Valkenburg award. This international award is given every second year in the name of physicist Alvin Van Valkenburg, co-inventor of the diamond anvil cell, to honor a young scientist whose research involves high pressure.

Li received her Ph.D. in geophysics from Stony Brook University in 2003 and is an adjunct research assistant professor at the Stony Brook Mineral Physics Institute. She started using beamline X17B2 as a graduate student in 1998 to study the rheology of minerals at high pressures and temperatures.

Rheological properties of materials at high pressure are valuable in many scientific fields, including geoscience, which is Li's concentration. Geoscientists obtain insight about the dynamics of the earth by deforming minerals at mantle conditions. Li probes these properties in-situ using synchrotron x-rays. She also performs theoretical calculations in collaboration with the University College London.

The Van Valkenburg award was presented at the 2006 High Pressure Gordon Conference in Biddeford, Maine, on June 29, 2006.

2005 Hans-Jürgen Engell Prize

Dev Chidambaram

The International Society of Electrochemistry (ISE) awarded the 2005 Hans-Jürgen Engell Prize to NSLS user Dev Chidambaram in recognition of his scientific work and publications in the field of electrochemistry.

The ISE is a professional organization for electrochemists, with 1,400 members from more than 60 countries. Chidambaram received his prize, consisting of a plaque and 500 euros, at the organization's 2006 annual meeting, held in Edinburgh, Scotland. Chidambaram delivered a keynote lecture on September 1, 2006.

Chidambaram joined Brookhaven Lab in 2004 as a Goldhaber Distinguished Fellow. His research focuses on protecting metals from corrosion and remediating toxic metals and radionuclides in the environment. In a project funded by the U.S. Air Force, Chidambaram found that molybdenum may be a viable replacement for chromate coatings, which are used to coat metals to prevent corrosion but are carcinogenic. Later, this result was used as a starting point for a program funded by the U.S. Army. Working with a team from Stony Brook University, Chidambaram has developed a new molybdate-based coating to prevent the deterioration of depleted uranium. Both programs extensively used the analytical techniques at the NSLS to study the materials.

Best Paper Award at 2006 EPCOS

Simone Raoux

Jean Jordan-Sweet

NSLS users Simone Raoux and Jean Jordan-Sweet won one of three "best paper" awards given annually at the European Symposium on Phase Change and Ovonic Science (EPCOS) for work done in part at NSLS beamline X20C.

The award was presented in May at the 2006 EPCOS in Grenoble, France, for the paper "Scaling properties of phase change nanostructures and thin films."

Using time-resolved x-ray diffraction (XRD), the researchers studied the thickness and size-dependent behavior of ultra-thin films and nanostructures, which are important for their applications in solid-state memory devices that could one day replace digital camera flash cards. The goal, Raoux said, is to find a small-scale phase change material that would allow for faster and cheaper technology.

Raoux, from the IBM Almaden Research Center, and Jordan-Sweet, from the IBM T.J. Watson Research Center, started working on the project at the NSLS more than two years ago. Other companies involved in the research included Infineon Technologies and Macronix International Co.

2006 Gregori Aminoff prize

Stephen Harrison

Stephen Harrison, a former NSLS user, was awarded the 2006 Gregori Aminoff Prize in Crystallography by the Royal Swedish Academy of Sciences. Harrison received the prestigious award along with Oxford University professor David Stuart, "for their remarkable contributions in virus crystallography."

The Aminoff prize is given out annually to scientists or research groups who have made a major contribution to the field of crystallography. It consists of a gold medal, a diploma, and a cash award, and is named after Swedish crystallographer Gregori Aminoff, the first scientist to introduce crystallography to Sweden.

Harrison was a regular NSLS user from the mid 80s through the end of the 90s. He worked mainly on beamline X25, studying the structure of DNA protein complexes, in particular, those that control the process of transcription. He also served on the NSLS Science Advisory Committee, which advises the NSLS Chair and the Associate Laboratory Director for Light Sources on scientific, technical, and policy issues related to the optimization of the scientific productivity of the NSLS. Harrison, a Harvard Medical School professor, used the Cornell High Energy Synchrotron Source (CHESS) to conduct most of his research in virus crystallography.

The prize was presented at the Royal Swedish Academy of Sciences in Stockholm on June 7, 2006. A two-day symposium illuminating the latest developments and results in the field of structural work on viruses was organized to honor the prize-winners.

— Kendra Snyder

NANOSCIENCE SAFETY HIGHLIGHTED

December 1, 2006

Nanoscience safety requirements at the NSLS tightened in 2006, in an effort to ensure that there are no harmful health effects from the study and handling of nanomaterials.

The properties of nanoscale materials are known to differ from those observed for the same materials in bulk or even microscale configuration, and those differences result in uncertainty about the potential health effects and environmental concerns these materials could present.

Studies are showing that nanoscale particulates can pass through intact skin, are more likely to reach the air exchange portion of the lungs when inhaled, and can migrate in the body through compartments, along nerve pathways, and through epithelial barriers. The acute and chronic effects of exposure are not yet defined and, until researchers are able to develop a technical basis for exposure standards and for assessment of the risks presented, nanomaterial work conducted at Brookhaven National Laboratory must include conservative controls.

The U.S. Department of Energy (DOE) and BNL policy is to use these materials with care and to minimize personnel exposures and environmental releases. Environmental, Safety and Health (ESH) staff working at each of the five DOE nanocenters developed a set of nanoscience safe work practices that is posted on the BNL Standards Based Management System (SBMS) website: *https://sbms.bnl.gov/sbmsearch/subjarea/105/3836d011.pdf*. Everyone working with these materials is expected to know and meet the requirements outlined in that document.

The work practices apply to all nanomaterial handling, but focus on control of "free" nano-particulate work as that presents greater risk of exposure or release. Included are requirements for working in hoods, encapsulating samples, scrubbing gasses that flow over particulates, labeling, transport packaging, and waste handling.

— Andrew Ackerman

CHI-CHANG KAO AMONG FIVE NAMED APS FELLOWS

December 28, 2006

Five scientists at BNL – Tim Hallman, Chi-Chang Kao, Dmitri Kharzeev, William Morse, and Yimei Zhu – were named Fellows of the American Physical Society (APS), a professional organization with more than 45,000 members. Election to APS Fellowship is limited to no more than one half of one percent of its membership in a given year, and election for this honor indicates recognition by scientific peers for outstanding contributions to physics. The Brookhaven scientists were among 212 Fellows elected in 2006.

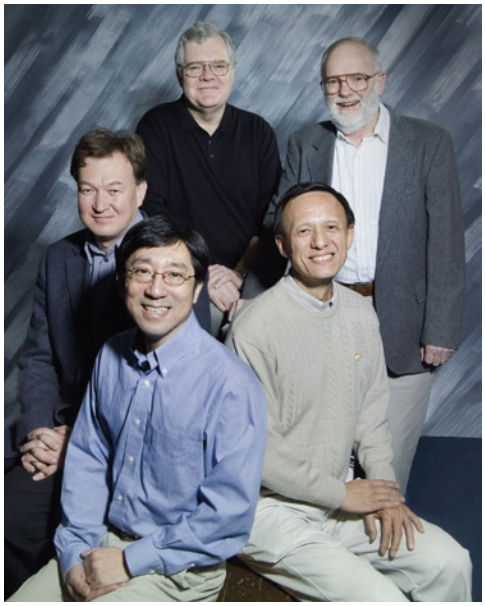

Clockwise from left, Dmitri Kharzeev, Tim Hallman, William Morse, Yimei Zhu, and Chi-Chang Kao

Kao, Chair of the NSLS, was recognized “For his many contributions to resonant elastic and inelastic x-ray scattering techniques and their application to materials physics.” During his research at the NSLS, Kao has developed new x-ray scattering techniques to study the electronic and magnetic properties of magnetic and strongly correlated materials. These techniques have led to better understanding of the Earth’s interior and materials properties under extreme conditions.

Kao earned his Ph.D. in chemical engineering from Cornell University in 1988. Shortly after, he joined BNL as a postdoctoral research assistant at the NSLS. He was promoted to senior physicist in 2001. Kao is also an adjunct professor in the Department of Physics and Astronomy at Stony Brook University.

— Kendra Snyder

2006 NSLS TOURS

1/4/2006	Karen Agostisi, Congressman Steve Israel's Washington Legislative Aide
1/24/2006	Alain E. Kaloyeros, Executive Dir., NYS Center for Advanced Technology, Albany NanoTech
2/3/2006	New York Institute of Technology, IEEE Club
2/23/2006	New York City Biology Teachers Association
2/28/2006	Suffolk County Economic Development Agency
3/1/2006	Retired U.S. Army General Barry McCaffrey, President of B.R. McCaffrey Associates, LLC
3/2/2006	The National Institute for Occupational Safety and Health Data Capture Team
3/8/2006	Communications Trust Advisory Panel Committee
3/14/2006	Polytechnic University of Brooklyn
3/15/2006	American Society of Metals/Materials-Long Island Chapter
3/17/2006	City College of New York
3/21/2006	John J. Grossenbacher, Director of Idaho National Laboratory
3/22/2006	Charterhouse School
3/24/2006	York College of CUNY
3/24/2006	National Research Council of Canada, Infotonics of Rochester and Javelin Assoc. Directors
3/27/2006	Stony Brook University - Graduate Students
3/28/2006	Wildlife Genetics Conference
3/29/2006	University of Montenegro and State Department
3/30/2006	Stars Program and Japanese Exchange Team
3/31/2006	Smithtown Science Teachers - Staff Development Day
4/11/2006	ASHRAE: American Society of Heating, Refrigeration and Air-Conditioning Engineers
4/18/2006	Renaissance Technologies Corporation
4/28/2006	Muhlenberg College
4/28/2006	Nassau Community College - Radiation Therapy Program
5/4/2006	Queens College of CUNY
5/16/2006	Department of Energy Budget Officers
5/18/2006	Brigham Young University
6/2/2006	Stony Brook University - Summer Undergraduate Program
6/2/2006	U.S. Secretary of Energy Samuel Bodman
6/19/2006	Nuclear Chemistry Summer School
6/22/2006	Sheryl Silberman, Special Assistant to the Director, Idaho National Laboratory
7/11/2006	Columbia University REU Students
7/12/2006	Dr. Mitchell Shapiro - Overview of BNL
7/13/2006	Laser Safety Officer Conference
7/14/2006	Morgan State University
7/14/2006	Queens Hall of Science Ham Radio Club
7/14/2006	Southern University of New Orleans

2006 NSLS TOURS

7/20/2006	Columbia University - Summer Chemistry Program
7/27/2006	Jose Antonio Brum, Brazilian Synchrotron Light Source Director
7/27/2006	Stony Brook University - REU Chemistry Program
7/31/2006	Stony Brook University - REU Physics Program
8/7/2006	Lauren Hill, Long Island Alliance
8/9/2006	Research Library General Laboratory Tour
8/9/2006	Stony Brook University - Brookhaven Women in Science
8/10/2006	New York State Business Council's Committee on Education
8/11/2006	Dongwha Kum, Korean Institute of Science & Technology (KIST) President
8/22/2006	Northrop Grumman Corporation
8/24/2006	Long Island Chapter of Oil and Heating Service Managers
8/28/2006	Rocky Point Rotary Club
9/8/2006	John Ryan, State University of New York Chancellor
9/21/2006	Brookhaven Women in Science
9/26/2006	Hofstra University
9/28/2006	New York University Graduate School of Journalism Science and Environmental Reporting
9/29/2006	Wayne Horsley, Chair of Suffolk County Legislature-Committee for Economic Development, Higher Education & Energy
10/2/2006	University of Palermo
10/11/2006	DOE - Library Operations Working Group
10/12/2006	Battelle Commercialization Managers
10/13/2006	Half Hollow Hills School District
10/16/2006	BNL ESHQ Directors
10/18/2006	United States Merchant Marine Academy
10/18/2006	Brian Foley, Brookhaven Town Supervisor
10/20/2006	City College of New York
10/20/2006	Korean Institute of Science and Technology for the Center for Nanomaterial Technology
10/20/2006	Borough of Manhatten Community College
10/24/2006	Hofstra University
10/24/2006	Adelphi University
10/27/2006	Eastport Manorville School District
11/1/2006	Fordham University-Society of Physics Students Club
11/3/2006	Steven H. Stern, Suffolk County Legislator, 16th District
11/15/2006	Edo Corporation
11/16/2006	Sarah Lawrence University
12/4/2006	Suffolk County Community College
12/8/2006	Suffolk County BOCES Staff Workers

2006 NSLS SEMINARS

1/11/2006	Interim Controls Upgrade for Measuring Noise and Detecting Glitches in Magnet Power Supplies at the APS Storage Ring *Surajit Sarkar, Massachusetts General Hospital*
1/13/2006	Control and Noise Immunity for High-Resolution Experiments *Jinyang Liu, University of New Mexico*
1/17/2006	Resonant X-ray Magnetic Scattering from Nanoscale Magnetic Materials *Richard M. Osgood, III, Lincoln Laboratory, Massachusetts Institute of Technology*
1/18/2006	Shining Light on the Cause of Alzheimer's Disease *Lisa M. Miller, NSLS-BNL*
1/30/2006	Synchrotrons Helping Solve the Magnetic Oxide Semiconductor Puzzle *Ives U. Idzerda, Montana State University*
1/31/2006	Atomic Design and Engineering of Spinel Ferrites for RF and Microwave Device Applications *Vincent Harris, Northeastern University*
3/10/2006	Progress in the Development of New Optics for Very High Resolution Inelastic X-ray Scattering Spectroscopy. *Yuri Shvyd'ko, Argonne National Laboratory*
3/13/2006	Adsorption of Protein GlnB of Herbaspirilum Seropedicae on Silicon Using Spin-Coating Technique *Adriana Lubambo, Universidade Federal do Parna, Curitiba, Brazil*
3/14/2006	New Insights on the Formation of Bone by Synchrotron X-ray Scattering *Christian Burger, Stony Brook University*
3/14/2006	High-Throughput Crystallography for Drug Discovery - In Practice *Gyorgy Snell, Syrrx/Takeda, San Diego*
3/21/2006	High-Speed Semiconductor Detectors for the Synchrotron Experiments at LCLS and XFEL *Lothar Strüder, Max-Planck-Institut and University of Siegen, Germany*
3/21/2006	Subgrain Size, Planar Defects, and Vacancies from X-ray Line Profile Analysis Tamas Ungar, *Eötvös University, Hungary*
3/28/2006	The Art of Scientific Project Management - An LBNL Perspective Kem Robinson, *Lawrence Berkeley National Laboratory*
3/28/2006	NSLS-II: Challenges and Opportunities *Steve Dierker, Brookhaven National Laboratory*
3/28/2006	An Introduction to X-ray Absorption Spectroscopy in Enviro-, Geo-, and Biosciences *Paul Northrup, Brookhaven National Laboratory*
3/29/2006	Superconducting Undulator Development *Kem Robinson, Lawrence Berkeley National Laboratory*
4/4/2006	Biological Applications of Bench-top and Synchrotron-based Micro-Computed Tomography: PIRL's Twelve-Year Experience *Steve Jorgensen, Mayo Clinic College of Medicine*

2006 NSLS SEMINARS

4/4/2006	The Generation of Short Electron Bunches and Coherent Synchrotron Radiation in the BESSY Storage Ring *Godehard Wuestefeld, BESSY, Germany*
4/17/2006	Observation of Surface Layering in a Normal Dielectric Liquid *Haiding Mo, Northwestern University*
4/20/2006	Imaging Magnetic Nanostructures via Resonant Soft X-ray Spectro Holography *Olav Hellwig, Hitachi Global Storage Technologies*
4/20/2006	Interpretation of Complex Images in Coherent X-ray Diffraction *Ian Robinson, University College, London, United Kingdom*
4/24/2006	Perspectives in meV Resolved Inelastic X-Ray Scattering *Alfred Baron, Harima RIKEN and SPring-8/JASRI, Japan*
4/25/2006	Nonintercepting, Time-resolved Imaging Diagnostics for Multi-GeV Beams *Alex Lumpkin, Argonne National Laboratory*
4/26/2006	X-ray Imaging at a 3rd Generation Synchrotron *Qun Shen, Argonne National Laboratory*
4/27/2006	Status of High Energy X-ray Microfocusing at the ESRF: Pathways for Nanofocusing *Anatoly Snigirev, ESRF, France*
5/2/2006	Resonant Soft X-ray Scattering and Resonant Soft X-ray Reflectivity: New Tools for the Characterization of Organic Materials *Harald Ade, North Carolina State University*
5/4/2006	Calculation of Beam Impedance for Long Tapers and Short Bunches *Gennady Stupakov, SSRL, SLAC*
5/19/2006	Si-Ge Thin Film Engineering *J. Burnette, North Carolina State University*
5/23/2006	Liquid Crystals in Random Environments *Dennis Liang, Johns Hopkins University*
5/31/2006	Multilayer Laue Lenses - a Path Towards Nanometer Focusing of X-rays *Jorg Maser, Argonne National Laboratory*
6/8/2006	Current State and Fundamental Limitations of Focusing Hard X-rays with Refractive Optics *Christian Schroer, Institute of Structural Physics Dresden, Germany*
6/14/2006	Accelerator Physics Aspects of Crab-Cavity-Based Production of Picosecond X-ray Pulses *Michael Borland, Argonne National Laboratory*
6/15/2006	The New PEEM at the Swiss Light Source *Christoff Quitmann, Swiss Light Source, Switzerland*
6/21/2006	Surface and Interface Studies Using High Energy X-rays *Harald Reichert, Max Planck Institute, Germany*
6/22/2006	Tailoring the Self-assembly of Small Molecules in Complex Structures in Bulk and at Interfaces *Raluca I. Gearba, Institut de Chimie des Surfaces et Interfaces (ICSI), France*

2006 NSLS SEMINARS

6/22/2006	Strategy Towards Nanometer Size Beams with Reflective Optics *Olilvier Hignette, ESRF, France*
6/27/2006	Hierarchical Self-assembly of Plant Viruses for Materials Development *Qian Wang, University of South Carolina*
7/7/2006	New Generation of Instruments for Spin Polarized Electron Spectroscopy: Ultrafast Compact Classical Mott Polarimeter *V.N. Petrov, St. Petersburg State Polytechnical University, Russia*
7/10/2006	Upgrading and Improving the HERA ep Collider *Ferdinand Willeke, DESY, Germany*
7/11/2006	The Effect of Alloying Ru into Pt on Bonding Electronics of CO on Pt *Eugene Smotkin, University of Puerto Rico*
7/25/2006	The Sub-Picosecond Pulse Source: A Retrospective *Dr. Jerome Hastings, SSRL/SLAC*
8/1/2006	CAMD Light Source: Recent Challenges and Improvements *Mikhail Fedurin, Louisiana State University*
8/4/2006	Dynamical Theory for X-ray Diffraction and Photonic Crystal Diffraction *Xianrong Huang, Stony Brook University*
8/4/2006	Blazed Gratings and Minimal Zone Plates *Li Jiang, Louisana State University*
9/5/2006	Femtosecond Electron Diffraction: Probing Structural Dynamics on the Fundamental Timescale *Jianming Cao, Florida State University*
9/7/2006	Micro-diffraction and Other Novel Probes of Charge Density Wave Transport and Dynamics *Abdel Isakovic, Cornell University*
9/7/2006	Implementation and Performance Overview of Orbit Feedback Systems at APS *Om Singh, Argonne National Laboratory*
9/8/2006	The Short Bunches for CSR at MIT-Bates Ring *Dong Wang, Massachusetts Institute of Technology*
10/6/2006	A Stroboscopic View Inside High-speed Magnetic Materials *William Bailey, Columbia University*
10/10/2006	GM/CA CAT Beamline Control System for Protein Crystallography at the APS *Sergey Stepanov, Argonne National Laboratory*
10/18/2006	Bright Photon Beams: Developing New Light Sources *Timur Shaftan, NSLS-BNL*
11/16/2006	Flexoelectricity in Nematics and Chiral Nematics: Symmetry, Geometry, and Devices *Robert B. Meyer, Brandeis University*
11/27/2006	Studying the Short and Medium Range Order in Amorphous Metal Systems *Stephan Hruszkewycz, Johns Hopkins University*

2006 NSLS SEMINARS

11/29/2006	The Linac System at LSU CAMD *Yanshan Wang, Louisana State University*
11/30/2006	Electronic Reconstruction of the $LaMnO_3$-$SrMnO_3$ Interface *Peter Abbamonte, University of Illinois*
12/5/2006	Advanced Accelerator R&D at the A0 Photoinjector *Raymond Fliller, Fermilab*
12/14/2006	High Pressure Electronic Properties Investigated by RIXS: From Magnetic Collapse to Quantum Criticality *Jean-Pascal Rueff, CNRS / Synchrotron SOLEIL, France*
12/19/2006	X-ray Fluorescence Microscopy of Saccharomyces Cerevisiae *Matthew Kidd, University of Michigan*

2006 NSLS WORKSHOPS

4/4/2006	X6A Workbench: Advanced Tools for Structural Biology
4/23/2006	RapiData 2006
5/16/2006	Synchrotron Catalysis Consortium: New Opportunities for *in situ* XAFS Studies of Nanocatalysis
5/16/2006	Soft Matter and Biomolecular Materials: X-ray Scattering Enabled by High Brightness Beamlines
5/16/2006	Nanoscale Correlations Heterostructures
5/17/2006	Chemical and Biological Applications of X-ray Emission Spectroscopy
5/17/2006	Platforms for the Integration of Biological Systems into Nanomaterials and Interfaces
5/17/2006	Vacuum Ultraviolet Radiometry
6/12/2006	Crystallization: Focus on Optimization and High Throughput Techniques
6/19/2006	Discover Nanoscience and Nanoscience for Poets
10/19/2006	Short Course: XAFS Studies of Nanocatalysis and Chemical Transformations

FACILITY REPORT

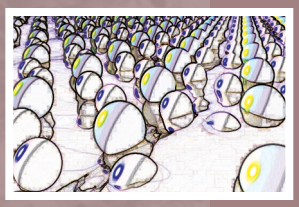

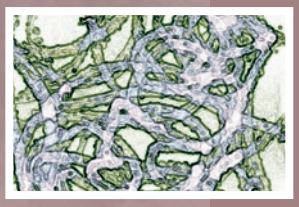

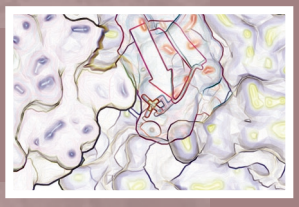

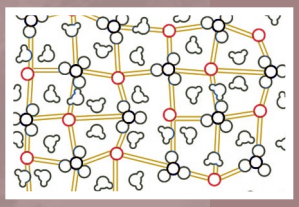

NATIONAL SYNCHROTRON LIGHT SOURCE ORGANIZATION

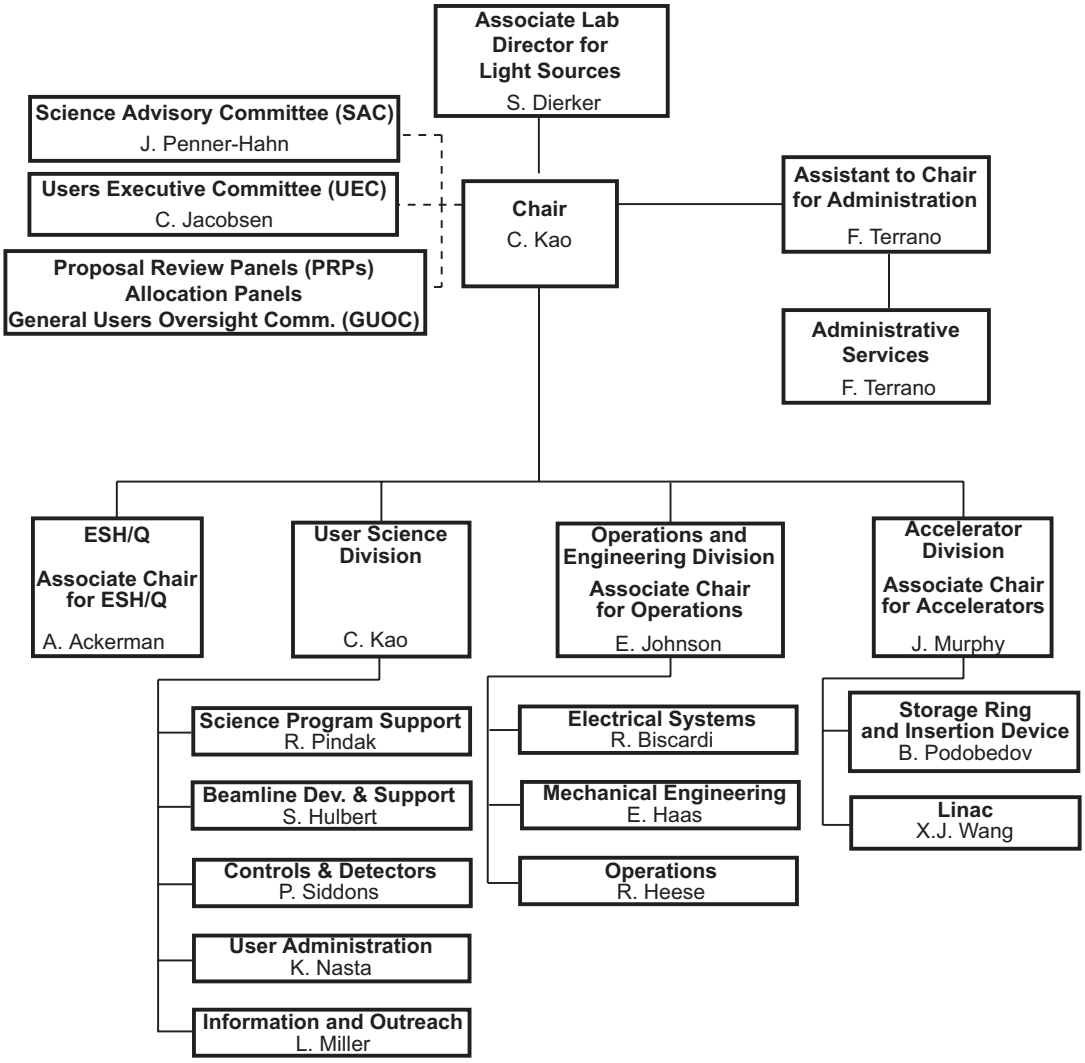

NSLS and NSLS-II Staff

NSLS ADVISORY COMMITTEES

Users' Executive Committee

The Users Executive Committee (UEC) provides for organized discussions among the user community, NSLS administration, and laboratory directorate. It aims to communicate current and future needs, concerns, and trends within the user community to NSLS staff and management, and to disseminate to the users information about the NSLS and BNL plans.

Chair
Chris Jacobsen, Stony Brook Univ.

Vice Chair
Daniel Fischer, NIST

Past Chair
Peter Stephens, Stony Brook Univ.

Member
Steve Almo, AECOM

Member
Chris Cahill, George Washington Univ.

Member
Chris Dvorak, Montana State Univ.

Member
Howard Robinson, BNL-Biology

Ex-Officio
Chi-Chang Kao, NSLS User Science Division

Ex-Officio
Kathy Nasta, User Administration Office

Ex-Officio
Lisa Miller, NSLS Information and Outreach Office

Special Interest Group Representatives

Special Interest Groups in areas of common concern communicate with NSLS management through the UEC.

Bio. Scattering and Diffraction
Alexei Soares, BNL-Environ. Sci.

High Pressure
Jiuhua Chen, Stony Brook Univ.

Imaging
Jeff Gillow, BNL-Environ. Sci.

Industrial Users
Simon Bare, UOP LLC

Infrared Users
Jiufeng Tu, City College of NY

NSLS-II
Paul Evans, Univ. Wisconsin-Madison

Nuclear Physics
Mahbub Khandaker, TJNL

Students and Post Docs
Dean Connor, Jr., BNL-NSLS

Time Resolved Spectroscopy
John Sutherland, BNL-Biology

Topography
Michael Dudley, Stony Brook Univ.

UV Photoemission and Surface Science
Jeff Keister, SFA, Inc.

XAFS
Paul Northrup, BNL-Environ. Sci.

X-ray Scattering and Crystallography
Cecilia Sanchez-Hanke, BNL-NSLS

Science Advisory Committee

The Science Advisory committee (SAC) evaluates science programs at the NSLS and makes recommendations to the Chairman.

Simon Bare, UOP LLC

Joel Brock, Cornell Univ.

Robert Hettel, SSRL/SLAC

Eric D. Isaacs, ANL

Leemor Joshua-Tor, Cold Spring Harbor

Edward Kramer, Univ. of California

Simon Mochrie, Yale Univ.

James Penner-Hahn (Chair), Univ. of Michigan

William Thomlinson, CLS

Chris Jacobsen (UEC Chair), Stony Brook Univ.

UEC members and SpIG representatives: (Standing from left): Chi-Chang Kao (BNL-NSLS), Dean Connor, Jr. (BNL-NSLS), Jiuhua Chen (Stony Brook U.), Mahbub Khandaker (TJLab), Jiufeng Tu (City College of NY), Jeff Keister (SFA, Inc.), Paul Evans (Univ. Wisconsin-Madison), Paul Northrup (BNL-Env. Sci.), Jeff Gillow (BNL-Env. Sci.), Michael Dudley (Stony Brook Univ.), Cecilia Sanchez-Hanke (BNL-NSLS), Kathy Nasta (BNL-NSLS), and Lisa Miller (BNL-NSLS). (Sitting from left): John Sutherland (BNL-Biology), Chris Jacobsen (Stony Brook University), Joe Dvorak (Montana State U.), Howard Robinson (BNL-Biology), Chris Cahill (George Washington Univ.), and Dan Fischer (NIST). Missing from photo: Peter Stephens (Stony Brook Univ.), Steve Almo (AECOM), Alexei Soares (BNL-Envi. Sci.), and Simon Bare (UOP LLC).

NSLS ADVISORY COMMITTEES

General User Proposal Review Panel

The Proposal Review Panel (PRP) reviews and rates General User Proposals. Members are drawn from the scientific community and generally serve a two-year term.

Imaging and Microprobes: Biological and Medical

Leroy Chapman, Univ. of Sask.
Max Diem, City Univ. of New York
Paul Dumas, Soleil
Kathleen Gough, Univ. of Manitoba
Barry Lai, ANL
Irit Sagi, Weizmann Institute of Sci.

Imaging and Microprobes: Chemical and Materials Sciences

Harald Ade, N.C. State Univ.
David Black, NIST
Gene Ice, ORNL
Qun Shen, ANL
Nobumichi Tamara, LBNL

Imaging and Microprobes: Environmental and Geosciences

Don Baker, McGill Univ.
David Black, NIST
George Flynn, SUNY @ Plattsburgh
Kenneth Kemner, ANL

IR/UV/Soft X-ray Spectroscopy: Chemical Sciences/Soft Matter/ Biophysics

Jingguang Chen, Univ. of Delaware
Daniel Fischer, NIST
Jan Genzer, N.C. State Univ.
David Mullins, ORNL
Michael White, BNL-Chemistry

IR/UV/Soft X-ray Spectroscopy: Magnetism/Strongly Correlated Electrons/Surfaces

Robert Bartynski, Rutgers Univ.
Di-Jing Huang, SRRC
Alexander Moewes, Univ. of Sask.
Boris Sinkovic, Univ. of Connecticut
Jiufeng Tu, CUNY
Tonica Valla, BNL-Physics

Methods and Instrumentation

Leroy Chapman, Univ. of Sask.
Kenneth Finkelstein, Cornell Univ.
Ralf-Hendrik Menk, Sincrotrone Trieste
Peter Takacs, BNL-Instrumentation

SAC Committee members (standing, from left) Robert Hettel, Leemor Joshua-Tor, and Eric Isaacs. Sitting (from left) Simon Mochrie, Edward Kramer, James Penner-Hahn, and Bill Thomlinson. Missing from photo: Simon Bare, Joel Brock, and Chris Jacobsen.

Macromolecular Crystallography

Alex Bohm, Tufts Univ.
Daniel Leahy, John Hopkins Univ.
Brenda Schulman, St. Jude Hospital
Da Neng Wang, New York Univ.
Joshua Warren, Duke Univ.

Powder/Single Crystal Crystallography

Simon Billinge, Michigan State Univ.
Thomas Duffy, Princeton Univ.
Andrew Fitch, ESRF
Joseph Hrilijac, Univ. of Birmingham
Stefan Kycia, Univ. of Guelph
Peter Lee, ANL
Peter Stephens, Stony Brook Univ.

X-ray Scattering: Magnetism/ Strongly Correlated Electrons/ Surface

Kenneth Finkelstein, Cornell Univ.
Peter Hatton, Univ. of Durham
Valery Kiryukhin, Rutgers Univ.
Karl Ludwig, Boston Univ.
George Srajer, ANL
Trevor Tyson, NJIT

X-ray Scattering: Soft Matter and Biophysics

Ben Hsiao, Stony Brook Univ.
Huey Huang, Rice Univ.
H. Miriam Rafailovich, Stony Brook Univ.
Detlef Smilgies, Cornell Univ.
Helmut Strey, Stony Brook Univ.

X-ray Spectroscopy: Biological, Environmental, and Geosciences

Martine Duff, Westinghouse Savannah River
Douglas Hunter, Univ. of Georgia
Kenneth Kemner, ANL
Satish Myneni, Princeton Univ.

X-ray Spectroscopy: Chemical and Material Sciences

Simon Bare, UOP LLC
Uwe Bergmann, SLAC
Anatoly Frenkel, Yeshiva Univ.
Steven Heald, ANL
Jean-Pascal Rueff, Jussieu
Tsun Sham, Univ. of Western Ontario
Trevor Tyson, NJIT

Allocation Panel

The Allocation Panel allocates general user beam time to both new proposals and beam time requests based on ratings provided by the Proposal Study Panels. Members are drawn from the scientific community and generally serve a two-year term.

Biology-PX

Marc Allaire, BNL-NSLS
Annie Heroux, BNL-Biology

EXAFS

Jeffrey Fitts, BNL-Environ. Sci.
Syed Khalid, BNL-NSLS

Imaging and Microprobes

James Ablett, BNL-NSLS
Kenneth Evans-Lutterodt, BNL-NSLS
Antonio Lanzirotti, Univ. of Chicago
Lisa Miller, BNL-NSLS

IR/UV/Soft X-Ray

Larry Carr, BNL-NSLS

VUV Allocations

Elio Vescovo, BNL-NSLS

Powder/Single Crystal/HiPress/Optics

Zhong Zhong, BNL-NSLS

Scattering

Elaine DiMasi, BNL-NSLS
Cecilia Sanchez-Hanke, BNL-NSLS
Jean Jordan-Sweet, IBM
Christie Nelson, BNL-NSLS
Lin Yang, BNL-NSLS

ACCELERATOR DIVISION REPORT

James B. Murphy
Associate Chair for Accelerators

Organization and Mission
The NSLS Accelerator Division (AD), headed by James B. Murphy, is organized into two sections: the Storage Ring & Insertion Device Section (SR&ID), headed by Boris Podobedov, and the Linear Accelerator (Linac) Section, headed by Xijie Wang. In addition to the NSLS accelerator complex, the AD staff operates the Magnetic Measurements Laboratory (MML) and the Source Development Laboratory (SDL), which are led by Toshiya Tanabe and Xijie Wang, respectively.

The NSLS Accelerator Division has a four-part mission:

- To ensure the quality of the electron beam in the existing NSLS booster, linear accelerator, and x-ray & vacuum ultraviolet storage rings
- To participate in the NSLS-II project, in particular the design of the storage ring and injection system
- To operate the MML and the SDL
- To perform fundamental research and development in accelerator and free-electron laser physics.

2006 Activities

NSLS Accelerator Complex
The AD staff performed studies to improve the efficiency and diagnostics of the NSLS injection system. The studies resulted in identifying a loss region near the extraction septum in the booster and led to a better understanding of the injection system performance. Improvements in the diagnostics and controls of the injection system provided for measurement of the electron beam position in the booster at anytime during the booster ramp. During the NSLS May shutdown, the AD staff assisted the Operations and Engineering Division (OED) staff in replacing a 40-year-old klystron with a rebuilt tube resulting in a significant improvement in the reliability of the NSLS linac system.


James Murphy

Close cooperation of all the NSLS divisions contributed to the successful commissioning of the new X25 mini-gap undulator (MGU) after its installation in the winter shutdown. The commissioning included establishing the correct undulator elevation, calculation of the proper trip points for the active interlock system, and assessing the impact of the new insertion device on the beam dynamics and lifetime of the X-ray ring.

The Task Force on Orbit Stability generated its final report and concluded that no major problems were identified. The feed forward system to compensate for the elliptically polarized wiggler (EPW) was significantly improved by the OED staff. A procedure to regularly check the performance of the beam position monitoring (BPM) receivers with an RF calibrator is being explored.

Development of the Middle Layer Toolkit for studying the properties of the VUV and X-ray storage rings continued to make progress. Automated scripts for the evaluation of accelerator parameters were deployed. The scripts provide for calibration of the correctors and BPMs, restoration of the lattice symmetry broken by gradient errors in the sextupoles, and estimation of the quadrupole gradients in the sextupoles due to closed orbit shifts. Studies to determine the minimum emittance coupling in the X-ray ring were very successful, and it was shown that the coupling ratio could be reduced to 0.3%. An improved characterization of the X-ray ring lattice at injection energy (750 MeV) will be launched in the near future.

NSLS-II Project
The accelerator physics staff of the AD provided the core team for the design of the NSLS-II accelerator complex, including the ultra-high brightness storage ring and the top-off booster injection system. A conceptual design report was prepared as part of the qualification process to achieve Critical Decision One (CD-1) approval from the Department of Energy for the NSLS-II project.

While the primary emphasis of the NSLS-II project is the production of ultra-high brightness x-rays, it is highly desirable to continue to provide for state-of-the-art capabilities in the VUV and IR as well. For the IR region in particular, several options

were explored, including upgrading the existing VUV ring with a superconducting RF system to provide short bunches for a coherent mode of operation.

Magnet Measurement Laboratory (MML)
The AD staff worked in collaboration with the OED, the User Science Division and an outside vendor to design, construct, and measure the new X25 cryo-ready MGU. The team completed the iterative process of magnetic measurements, shimming, and optimization in time for the December 2005 installation. Magnetic measurements before and after baking at 90°C, as well as before cool down to –120°C and after warm-up to room temperature, confirmed that the high field quality and very low phase error (2.5° RMS) were preserved through the thermal cycling. Also proven were the mechanical design features for accommodating differential expansion and contraction during the extreme temperature excursions, as were the Keyence optical micrometers monitoring the actual magnet gap. Commissioning took place in February 2006. **Figure 1A** shows the measured brightness spectrum at the minimum gap of 5.6 mm, and the theoretical spectrum computed by the SPECTRA code (from SPRING-8) for an ideal undulator; there is excellent agreement between the two results. **Figure 1B** shows the measured tuning curves for the 3rd through 9th harmonics over the normal range of magnetic gap operation. (Figures courtesy of J. Ablett & L. Berman, NSLS)

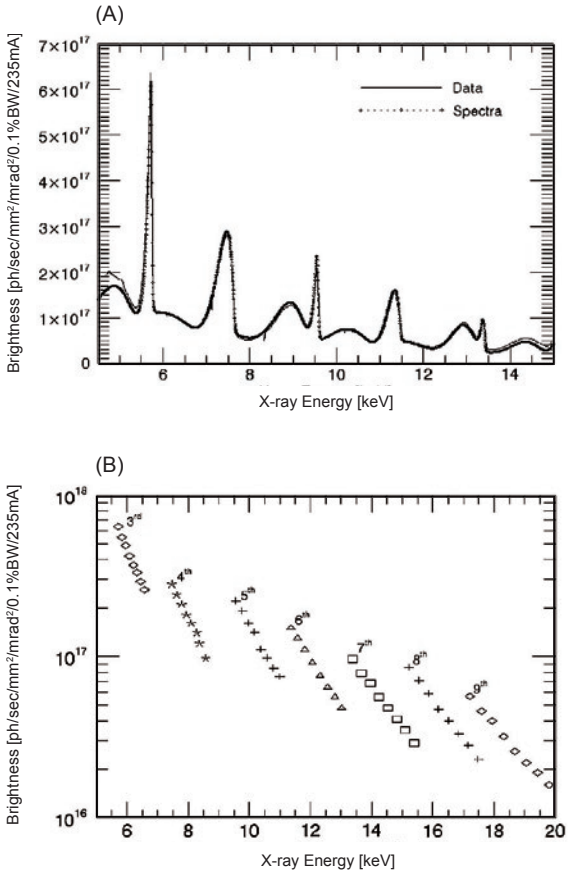

Figure 1. (A) Measured (solid curve) and predicted (dotted curve) brightness spectra of X25 MGU at minimum magnetic gap of 5.6 mm. (B) Measured tuning curves for the 3rd through 9th harmonics.

The X25 MGU is operating presently with water-cooling only. Cryogenic operation at 150K could extend the tuning range of each harmonic downward by about 10%. Potential benefits of the extended tuning are being weighed against the cost of the refrigeration system and the lack of magnetic measurements at cryogenic temperatures.

The BNL Cryogenic Safety Committee approved the Phase I configuration of the superconducting (SC) undulator Vertical Test Facility (VTF), permitting operation with liquid helium in the pool-boiling mode. For the commissioning test, a SC Helmholtz coil (for in-situ Hall probe calibration) and a refurbished pair of legacy SC mini-undulator sections with 8.8 mm period were used. Field scans were taken over a range of currents from 25 to 150 A. **Figure 2** shows the on-axis field map of the Helmholtz coil and the test SCU at a current of 150 A in both devices. The commissioning run successfully demonstrated the operation of the cryogenic Hall probe mapper and the in-situ calibrator.

In collaboration with BNL Superconducting Magnet Division and HTS110, Inc., the MML staff embarked on a technical study of using high-temperature superconductor (HTS) coils to replace the existing copper coils used in VUV dipoles. Three identifiable benefits from an HTS retrofit are: a significant reduction in electrical power requirements to run the dipoles, a simpler and cheaper current supply, and an increased aperture for beam extraction.

As an LDRD project, the development of cryo-coil packs for an X-ray ring sextupole magnet has been conducted. Fabrication of the cryo-coil packs has been undertaken and a prototype will be tested by the end of FY07.

The 2-meter long strong focusing VISA undulator magnet was completed and measured as part of the Office of Naval Research-funded Free Electron Laser program at the SDL.

Source Development Laboratory (SDL)
The SDL is an ideal platform to conduct R&D on high-brightness electron beams and laser-seeded free electron lasers (FEL). The SDL consists of a Titanium-Sapphire laser, a photoinjector, a 300-MeV linac and a 10-meter undulator. A second year of funding was obtained from the Joint Technology Office (JTO) and the Office of Naval Research (ONR) to pursue high-gain free electron laser amplifier experiments in the infrared wave-

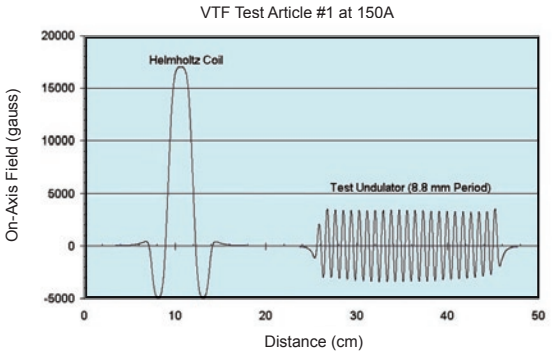

Figure 2. VTF commissioning run with Helmholtz coil and legacy 8.8 mm period SC undulator immersed in LHe. Helmholtz coil provides cold Hall probe calibration up to 1.7 Tesla at 150 A.

length regime. The JTO/ONR-sponsored program included experiments on optical guiding, efficiency enhancement and the first observation of super-radiance in an FEL.

In addition to the work in the infrared regime, new short-wavelength milestones in the ultraviolet region (UV) were also established. UV light at 190 nm was generated by operating the FEL in the Self Amplified Spontaneous Emission mode and the first lasing of the High Gain Harmonic Generation (HGHG) scheme in 4th harmonic mode at 199 nm was achieved. Preliminary results on operating the SDL FEL in the Enhanced Self Amplified Spontaneous Emission mode (E-SASE) were also obtained.

The SDL has the ability to generate very short electron pulses (1 ps FWHM) with high charge (~ 1 nC), which is ideal for the generation of copious quantities of coherent terahertz radiation (THz). The AD worked in collaboration with the NSLS User Science Division and the BNL Instrumentation Division to characterize the high intensity (~ 100 μJ/pulse) single cycle THz radiation. The high-intensity pulses allowed BNL researchers to explore new phenomena such as nonlinear cross-phase modulation (XPM) in electro-optic crystals and preliminary ideas on using the THz as a pump in pump-probe experiments on high-temperature superconductors. The development of an ultra-fast electron diffraction source based on the SDL photoinjector technology is also being considered.

OPERATIONS AND ENGINEERING DIVISION

Erik D. Johnson
Associate Chair for Operations and Engineering

Organization and Mission

The Operations and Engineering Division (OED) has three sections: Operations, which is led by Richard Heese; Electrical Systems, led by Richard Biscardi; and Mechanical Engineering, led by Ed Haas. To serve the NSLS User community, our mission falls into three main areas:

- Operation of the NSLS 24 hours a day, 7 days a week, on average 44 weeks a year
- Design, fabrication, and maintenance of the NSLS accelerators, infrastructure, and instru ments, including upgrades, modifications, and proposal development
- Engineering and technical support for other NSLS divisions and the NSLS user community

The OED staff includes one scientist, 17 engineers, and 53 technicians, making it the largest of the NSLS divisions. In addition to its own staff, the division coordinates the activities of five full-time skilled tradesmen from the Laboratory, as well as shops and trades assigned for specific jobs. The breadth of our mission requires us to draw on the capabilities of the other NSLS divisions for support, and in turn, provide specialized support for their activities.

2006 Activities

An overview of machine performance summarized for calendar year 2006 is provided in Section 5, “Facility Facts and Figures.” For Fiscal Year 2006, which is the DOE reporting period, overall reliability was 94% for the X-ray ring and 97% for the VUV ring. As in previous years, a comparatively small number of disruptions longer than four hours in duration account for much of the down time. For

Erik Johnson

FY06 Summary Fault Analysis

Group / Area/System	Number of Faults Total	X- DT	U- DT	Downtime [hr] X-ray	UV
Total Charges to Down Time					
Controls and Diagnostics	140	44	5	61.6	6.9
Power Systems	235	112	27	139.8	74.0
Utilities	80	36	30	53.3	95.1
Miscellaneous	64	42	5	35.7	4.7
	519	234	67	290.3	180.7
Significant Disruptions					
VUV Transport line shutter					67.2
Modulator 3 Core Bias				54.1	48.7
XRF Micro				20.2	
Electron Gun Replacement					15.3
LBQ9 Short				11.5	4.2
BXESH1				6.8	
Modulator 3 Thyratron Replacement				6.7	
Water Fitting fail at X18/19 Sawtooth				6.1	6.5
XRF 2B 3 kW Amplifier				5.6	
UV Trim Micro					5.6
X1 Active Interlock PS				5.1	
X25 MGU Cooling				5.1	
UV Interlock Security System					4.4
X29 Active Interlock				4.3	
X13/14 Water Interlock				4.1	
URF Interlocks					4.0
				129.5	155.8
Balance to 'Routine' Faults					
				160.8	24.9

FY 2006, almost half of the x-ray downtime came from only 11 events, and on the UV ring, only eight faults accounted for more than 80% of the down time. This distribution is a continuing indication of an effective maintenance program in action; the majority of the faults are small and quickly recoverable and many potential “big” events are avoided through preventative maintenance.

The single largest down-time event in 2006 was the failure of the bellows on the UV transport line shutter. The shutter assembly is actually welded into the transport line, so the decision was made to replace the failed actuator without removing the shutter housing. This is not as easy as it sounds because of mechanical interferences, but the innovative approach that made it possible kept the down time to less than three days, from failure to return to operations. On the one hand, it is heartening that the institutional knowledge and creativity are still there to respond so effectively to a problem of this kind. A “traditional” repair, which would have cut out the shutter and welded in the spare, could have resulted in more than a week of down time. However, it is a concern that we may be beginning to see more “age-related” failures in NSLS equipment.

The NSLS has an aggressive preventive maintenance program, which has been effective in mitigating the effects of normal "wear and tear" on machine down time. The system stewards have also identified elements of the machine operations where failures are deemed to be most likely or to have the greatest impact. In those cases, plans for spares, upgrades, or replacements have been developed. To help validate the planning assumptions, a Machine Operations Reliability Evaluation (MORE) was held in 2006. This review was conducted by an external committee that was charged to evaluate our allocation of resources and plans to secure reliable operations to the 2012 to 2014 time frame.

Overall, the committee gave kudos to the NSLS staff members and their contributions to delivering high levels of machine availability and performance, and found that "the analysis of machine support and development needs is very good and that the mechanisms for project planning and prioritization are in place and appear to be effective." However, the committee also expressed the same kinds of concerns raised by the staff regarding threats to continued reliable operations. These included:

- Aging instrumentation, components, and infra structure
- The possibility of a major breach in security and/or safety
- A flat budget in out years
- Staff recruiting, retention, and knowledge transfer.

The committee also noted that staffing is a critical concern with the ramp-up of NSLS-II. These issues are being factored into the near-term planning for the facility as are the initiatives outlined in the NSLS Five Year Plan.

One of the new initiatives described in the plan is the construction of a new insertion device beamline at X9. As noted in the 2005 Activity Report, initial preparations for this construction began at the end of 2005. During 2006, the move of the Case Center for Synchrotron Biosciences beamlines from X9 to X3 was successfully completed. Preparations are underway for the construction and installation of the new insertion device-based Small Angle X-ray Scattering (SAXS) beamline to support research for the Center for Functional Nanomaterials. During the winter 2006 shutdown, the original "phase I" storage ring vacuum chamber for the X9/10 dipole and all of the old X9 bending magnet front-end components were removed. A new dipole vacuum chamber with a zero-degree output port compatible with the new X9 insertion device was installed. The design of a new Mini-Gap Undulator (MGU) and new front-end components compatible with the X9 MGU started in FY06 and will continue into FY07.

The old phase I chamber removed during the winter shutdown, and the chamber that replaced it being prepared in the lab prior to its installation.

Fabrication efforts for many components of the new X9 MGU insertion device have already begun, as has layout and fabrication of the new hutch for X9 (the largest ever at the NSLS!). During 2007, beamline design is to be completed, and the installation of the front end and insertion device are planned for the winter 2007 shutdown.

With many years of NSLS operations ahead, continuous maintenance and upgrades of the facility will be vital to ensure that a robust research community is ready to exploit the exciting new capabilities of NSLS-II when it comes online. The OED will continue its work to advance the initiatives in the NSLS strategic plan to keep our user community one of the most productive anywhere.

USER SCIENCE DIVISION REPORT

Chi-Chang Kao
Associate Chair for User Science

Organization and Mission
The User Science Division (USD) coordinates major facility activities related to users so that we can be more effective in communicating with the user community, strengthening existing scientific programs, fostering the growth of new scientific programs, and raising the visibility of the exciting science produced by our users both inside and outside the scientific community. The division consists of five sections: User Administration (Kathy Nasta), Information and Outreach (Lisa Miller), Beamline Development and Support (Steve Hulbert), Scientific Program Support (Ron Pindak), and Detectors and Controls (Peter Siddons). The major initiatives and accomplishments of the User Science Division and the NSLS user community for 2006 are summarized below.

2006 Activities

NSLS Five-Year Plan
The most important activity of the USD in 2006 was the development of the NSLS Five-Year Strategic Plan. We worked closely with the user community and the NSLS Science Advisory Committee (SAC) to identify future scientific opportunities, as well as beamline and infrastructure upgrades needed to exploit those opportunities. A more detailed plan, which includes the resources required, funding sources, and schedule to implement these upgrades, also was developed.

Contributing User Proposals
With the assistance from the SAC, the first set of nine Contributing User (CU) proposals was approved. The approved CUs include two research resources: COMPRES (a National Science Foundation-funded research resource for earth sciences) and PXRR (a National Institutes of Health and DOE Office of Biological and Environmental Research-funded resource for macromolecular crystallography), as well as several groups of researchers who bring significant new instrumentation to the NSLS. Although these CU programs have only been in operation for a relatively short time, they have already made a significant impact to the NSLS user science program.

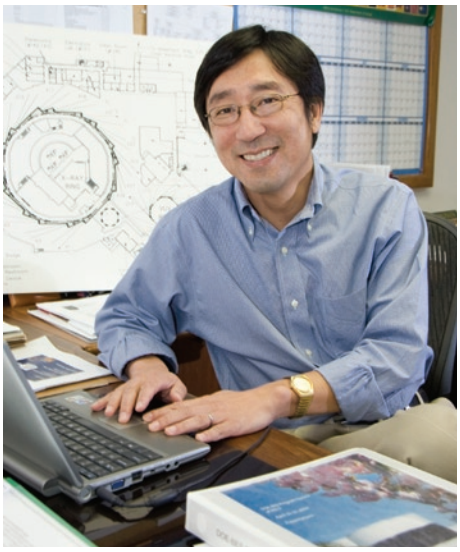
Chi-Chang Kao

Funding Renewed for X6A
On the scientific program front, we are delighted that funding for the East Coast Structural Biology Facility, beamline X6A, has been renewed by the National Institute of General Medical Sciences (NIGMS). X6A is funded for macromolecular crystallography and, in particular, to provide beam time access to young scientists in the process of establishing research groups whose primary interest is not x-ray crystallography. This grant from NIGMS has enabled the NSLS to significantly expand its structural biology program, as well as to develop a rapid access and remote user program.

NSLS, BNL to Build Linac Coherent Light Source Detectors
The NSLS and Brookhaven's Instrumentation Division were awarded a multi-year project to construct detectors for the Linac Coherent Light Source (LCLS) project at the Stanford Linear Accelerator Center (SLAC). This is a very challenging project and an important milestone for the detector development effort at the NSLS. It will significantly expand the expertise of the detector and control group at the NSLS, led by Peter Siddons, which has successfully delivered a wide range of detectors to users over the last several years, including fast photon counting detectors and linear array detectors. The detectors developed for the LCLS will also benefit many scientific programs at the NSLS.

Education and Outreach
We continue to put a large focus on user education, training, and outreach at the NSLS. In the area of user training, our annual XAFS short course was held in October 2006, with the title "Short Course: XAFS Studies of Nanocatalysis and Chemical Transformations." In addition, two macromolecular crystallography courses, "RapiData 2006," and the "X6A Workbench: Advanced Tools for Structural Biology," continued to attract a large number of users. We also worked closely with users to organize additional focused scien-

tific workshops, including “Synchrotron Catalysis Consortium: New Opportunities for in situ XAFS Studies of Catalysis,” a workshop on “Soft Matter and Biomolecular Materials: X-ray Scattering Enabled by High Brightness Beamlines,” the “Nanoscale Correlations Heterostructures” workshop, a workshop on “Chemical and Biological Applications of X-ray Emission Spectroscopy,” a workshop on “Platforms for the Integration of Biological Systems into Nanomaterials and Interfaces,” a “Vacuum Ultraviolet Radiometry” workshop, and the workshop “Crystallization: Focus on Optimization and High Throughput Techniques.” These short courses and workshops were very effective in introducing the use of synchrotron techniques in a particular area of science to non-synchrotron users. Many new research opportunities and collaborations have resulted from them. Additionally, we’ve continued our effort this year to coordinate closely with the Center for Functional Nanomaterials in order to reach out to nanoscience researchers through joint seminars, workshops, and visits to interested universities and institutions.

Beamline Upgrades and Performance Improvements

We initiated a program this year to characterize beamline performance, including flux, energy resolution, and focal spot size, on a regular basis, led by Lonny Berman. The goal is to establish a performance baseline for all NSLS facility beamlines, and identify areas that need improvement. In addition, the three major upgrade projects initiated and completed this year by the NSLS and PRTs were at X18, X25, and X9. Details are described below:

X18B Beamline Upgrade for Quick-EXAFS

A new monochromator drive and data-collection scheme have been developed for beamline X18B to allow quick measurements of x-ray absorption spectra (QEXAFS). The micrometer on the standard NSLS tangent-arm driven monochromator has been replaced with a cam, which continuously changes the Bragg-angle of the monochromator with a simple rotation of a motor. Different positions in the cam result in different angular ranges over which the monochromator is rotated, which translates into different energy ranges for the scans. This allows the user to concentrate on either the near-edge structure (XANES), or the extended fine structure (EXAFS). The data are collected using an analog-to-digital converter, which digitizes the voltage from the current amplifier directly.

During 2006, the QEXAFS setup was used by three groups. Switching the X18B monochromator control system from conventional EXAFS to QEXAFS mode takes only minutes. The graphical user interface (GUI) for QEXAFS data collection is now capable of continuous operation with data collection duration of one or five minutes, each with many cycles. In fast mode, a full EXAFS scan with good signal to noise ratio can be collected in 200 milliseconds. This new capability will enable the use of x-ray absorption spectroscopy for fast in-situ kinetic measurements, e.g., for catalysis and fuel cell research.

X25 Cryo-Capable Mini-Gap In-Vacuum Undulator Installed in the X-Ray Ring

At the start of 2004, beamline X25’s programmatic focus shifted completely to monochromatic macromolecular crystallography, following 14 years of operation as a mixed-use high-brightness beamline. Thus, the NSLS was presented with an opportunity to renovate the beamline, as well as the radiation source, to optimize them for a dedicated macromolecular crystallography program. To this end, the BNL Macromolecular Crystallography Research Resource (PXRR), a collaboration between the BNL Biology Department and the NSLS, submitted a funding request in late 2002 as part of its proposal to the National Institutes of Health’s National Center for Research Resources and the Department of Energy’s Office of Biological and Environmental Research (DOE BER) to renew its five-year grant. The proposal was well received, and $2.2M in funds was awarded by DOE BER beginning in late 2003, to be dispensed over the course of three fiscal years.

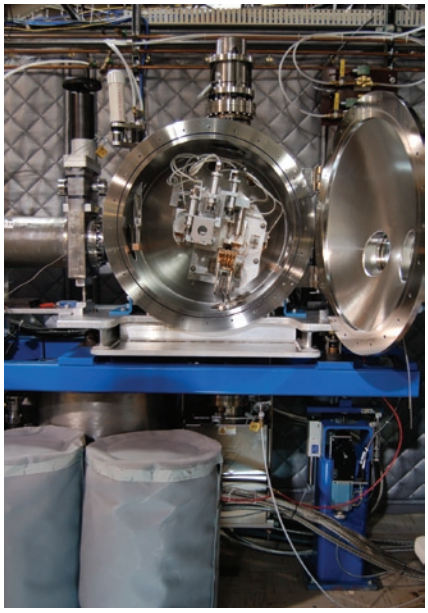

The newly installed double crystal monochromator at beamline X25 is shown, with its vacuum chamber open. The white beam enters from the right and the diffracted beam emerges to the left. The first silicon crystal is mounted on a copper support that can be cooled to cryogenic temperature, and the second crystal is mounted in a bender that can curve the crystal sagittally in order to focus the beam horizontally. Directly beneath the monochromator is the cryocooler and heat exchanger assembly which forms part of the new cryogenic refrigerator for cooling the first crystal.

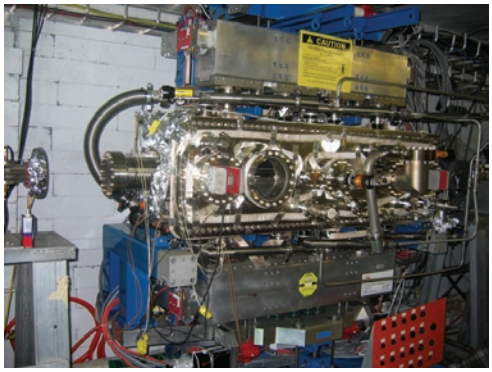

The new X25 MGU installed in the NSLS x-ray ring.

During the December 2005 shutdown, the original hybrid wiggler, which served as the radiation source for beamline X25 since its inception in 1990, was replaced by a custom-designed in-vacuum miniature-gap hybrid undulator. At a photon energy of 6.3 keV, the new radiation source will be 15 times brighter than the old one, and will be six times brighter at a photon energy of 10.5 keV. Its design consists of 0.99 meter-long planar hybrid magnet arrays with a period length of 18 mm (55 periods total) and a minimum attainable gap of 5.6 mm, with a corresponding maximum deflection parameter, K, of 1.5. The NdFeB-type permanent magnet material, which has been used in this insertion device, can have a higher magnetic field and a higher radiation resistance simply by cooling: Operation at 150K will likely produce a 13-14% higher magnetic field (and higher K), resulting in a larger photon energy tuning range. Therefore, this undulator design also incorporates a provision for cryogenic operation, which might be pursued in the future. Unlike previous miniature-gap undulator designs in use at the NSLS, the one now implemented for X25 will be continuously tunable from 2 to 20 keV by employing all harmonics up through the 9th. The undulator vacuum and gap separation system was manufactured by Advanced Design Consulting of Lansing, NY. In conjunction with the installation of the undulator, certain components in the front end of the beamline, and the active interlock system that protects the x-ray ring exit chamber, were upgraded in order to cope with the much higher power density of the undulator beam.

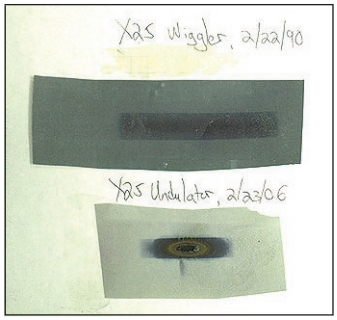

X-ray burns taken using original wiggler (top) and the new undulator (bottom), in the same location, show that the undulator beam is much smaller than the wiggler beam, as expected.

In addition to the new radiation source, upgrades to the beamline optics also were implemented in order to exploit the properties of the new source. The current double crystal monochromator was replaced by one that incorporates cryogenic cooling of the first crystal and sagittal bending of the second crystal to permit horizontal focusing. It was followed by the installation of a new bendable mirror, containing multiple coating stripes, to permit vertical focusing. The completion of the X25 upgrade, expected in FY07, is essential to the macromolecular crystallography program at the NSLS.

X9 to X3 Beamline Relocation Complete

In October 2006, beamlines X3A and X3B began operating without restrictions after being transferred from X9 in just four and a half months. The relocation of the two beamlines was completed in advance of original estimates, with deconstruction of X9A and X9B beginning in early May and the first commissioning beams at X3A and X3B running in late August and early September.

The Case Center for Synchrotron Biosciences, which utilized the former X9 beamlines, moved to X3 to make room for a new undulator-based beamline at X9. The X9 straight section is cur-

Beamline X3 before

Beamline X3 after

rently the last one available in the x-ray ring. It will be used for a small-angle x-ray scattering Facility Beamline with BNL's Center for Functional Nanomaterials as a Contributing User. The new X9 beamline is expected to be operational in 2008, with commissioning completed during the first cycle of the year and full operations starting in May or June.

Although performed quickly, the relocation from X9 to X3 wasn't an easy process. First, the X16C beamline was renovated to accept the experimental program that was operating at beamline X3B1. Next, the former X3 beamlines and experimental equipment were completely removed from the X3 floor space. Then, planning, surveying, and engineering and design for the relocation of the two X9 bending magnet beamlines to counterpart locations at X3 were undertaken and the necessary reviews were completed. The X9A hutch was modified and re-built in its new location at X3A, a new hutch for X3B was constructed, and associated utilities and interlocks were installed. The beam pipes for both beamlines, which penetrate the shield wall and connect them with the front end, were moved from X9 to X3, and the shield wall and neighboring lead shields were re-built accordingly. All experimental equipment and controls for these beamlines also were moved to their new locations at X3.

All of the equipment was in place at X3 by August, with the first commissioning beams running shortly after. Re-commissioning was completed around the end of the 2006 fiscal year. In addition to hosting Participating Research Team (PRT) experiments, both beamlines also are accepting General Users.

NSLS-II REPORT

Steven Dierker
Associate Laboratory Director for Light Sources
NSLS-II Project Director

Introduction
NSLS-II is a proposed new state-of-the-art medium energy storage ring designed to deliver world leading brightness and flux with top-off operation for constant output. The facility will replace the NSLS, producing x-rays more than 10,000 times brighter than those produced at the NSLS today. The design and engineering is expected to begin in 2007, construction in 2009, and operations in 2014.

The superlative character and combination of capabilities will have broad impact on a wide range of disciplines and scientific initiatives in the coming decades, including new studies of small crystals in structural biology, a wide range of nanometer-resolution probes for nanoscience, coherent imaging of the structure and dynamics of disordered materials, greatly increased applicability of inelastic x-ray scattering, and properties of materials under extreme conditions.

2006 Activities
2006 was an extraordinary year for the NSLS-II Project – challenging, exciting, and full of change and accomplishment.

The NSLS-II Project organization, which was created in January 2006, grew rapidly and by the end of the year a true team of about 100 people were working on the project. Jim Yeck, as Deputy Project Director, brings a wealth of prior experience with large DOE and NSF construction projects. We are also very fortunate to have the able leadership of Satoshi Ozaki, John Hill, Marty Fallier, and Diane Hatton, who as Directors of the Accelerator Systems, Experimental Facilities, Conventional Facilities, and Project Support Divisions, respectively, have guided their development. We are also delighted that Ferdinand Willeke, formerly head of the complex HERA facility at DESY, will be joining the project this coming July to succeed Satoshi Ozaki.

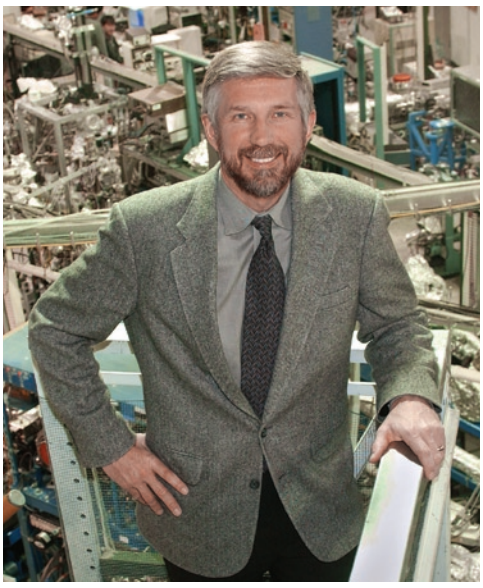

Steve Dierker

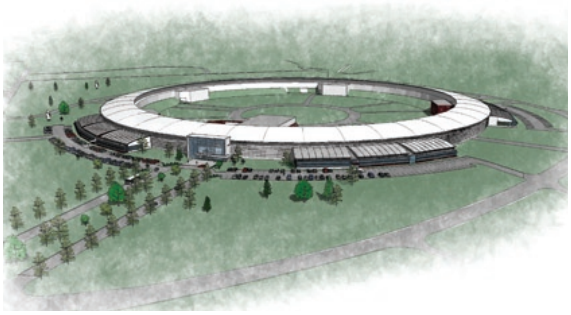

Latest NSLS-II rendering

In testimony to BNL's strength as a first-class accelerator laboratory, we have been able to draw on expertise from throughout the laboratory, with staff from NSLS, CAD, SMD, and many other departments contributing to the project. The full-time NSLS-II staff took up residence in the new NSLS-II Project Site Office, Buildings 817 and 830M. These buildings are now full, and we will be expanding into a new building, 817M, in the coming months.

The project also benefited from the continued involvement of the scientific community by hosting visits of from 1 day to several weeks of more than 70 international experts in a variety of disciplines. Additional community involvement occurred through the formation of four external NSLS-II advisory committees, created to guide, and provide oversight to, the project. Altogether, we hosted more than 10 reviews or workshops on a wide range of topics during 2006.

The culmination of these efforts was expressed in the NSLS-II Conceptual Design Report, available on the NSLS-II website, which presents the conceptual design of a world leading facility that will enable the study of material properties and

functions, particularly at the nanoscale, at a level of detail and precision never before possible.

In December, 2006 the project underwent a very successful DOE ("Lehman") Review. Overall, the committee judged the project team to be strong and to have the full support of BNL and the design as likely to achieve the technical goals.

2007 promises to be equally challenging. In addition to ramping up our R&D program, our current schedule calls for completing Title I, or preliminary engineering, design by the end of this year.

In summary, through the hard work and dedication of an extremely talented community, both inside and outside BNL, we have gotten off to a great start. I look forward to continued future success.

USER ADMINISTRATION REPORT

Kathleen Nasta
User Administrator

The User Administration Office at the NSLS coordinates site access for all of our users, covering everything from processing appointments to ensuring safety compliance and issuing badges. We also facilitate the general user proposal program, maintain beamline agreements and data, record and interpret statistical data, and plan and organize meetings and workshops, including the annual Users' Meeting.

2006 Activities

User Statistics

During Fiscal Year 2006, 2105 users performed experiments at the NSLS. **Figures 1 and 2** detail the affiliations of our users and their areas of scientific research, respectively. There were 656 new users that joined us in 2006, indicating that the NSLS user community continues to be very dynamic. Roughly half of our users are U.S. citizens, and about 75% are male. A little more than half of the users from the 399 unique institutions came from U.S. universities. Other institutional categories included foreign, academic, BNL (non-NSLS), U.S. industry, U.S. laboratories, federally funded institutions (non-DOE), non-federally funded institutions, foreign national laboratories, and others. About two-thirds of the users came from institutions located in the northeastern United States, and one third of those were located in New York (**Figure 3**). Scientists, faculty members, and professional staff made up 44% of those users performing experiments, while 37% were graduate students and 13% were postdoctoral students.

Kathy Nasta

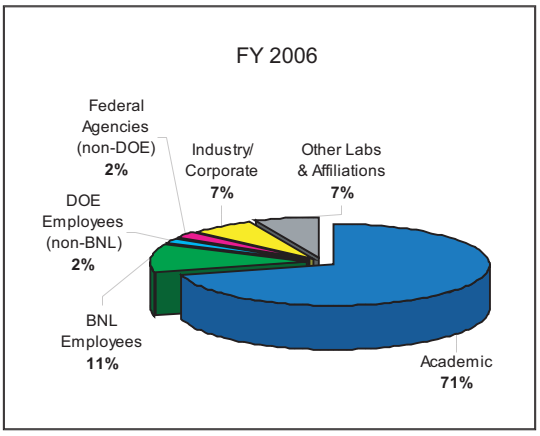

Figure 1. NSLS users by affiliation

Four percent were undergraduate-level students. Reviewing users' fields of research, almost half (45%) perform experiments in the life sciences area. The next largest group, at 29%, lists materials science as their research area, and 13% of the users are in the environmental and geosciences fields.

User Access Procedures

The web-based Proposal, Allocation, Safety and Scheduling (PASS) system was used for the first time for the fall 2004 operations cycle. PASS allows numerous actions to be taken care of in one system, including creating and submitting proposals, conducting feasibility and peer reviews, allocating and scheduling beam time, performing safety reviews, and maintaining beamline information.

During 2006, work began on prerequisites to create a framework for developing a system for Rapid Access to beamtime. A Principal Investigator (PI) can now name a delegate for a PASS form (for example, a professor can name a student). This delegate is another PASS user and s/he can prepare, submit, and receive status updates. In addition, a system of Envelope Safety Approval Forms (SAFs) was established. At this time, Macromolecular Crystallography users are asked specific questions prior to a full SAF. If answers indicate the experiment meets the criteria of a predefined Safety Envelope, no further SAF information will be required, and approval of the SAF is greatly expedited. Several meetings were held to gather input on the design and flow of the Rapid Access system, and it is expected that during FY 2007 the system will be operational.

A new Proposal Oversight Panel (POP) group was established prior to the Fall 2006 beamtime cycle. The POP is comprised of a small number of scientific personnel with broad subject-matter expertise. The first face-to-face meeting of the group was held in order to address any general user proposal

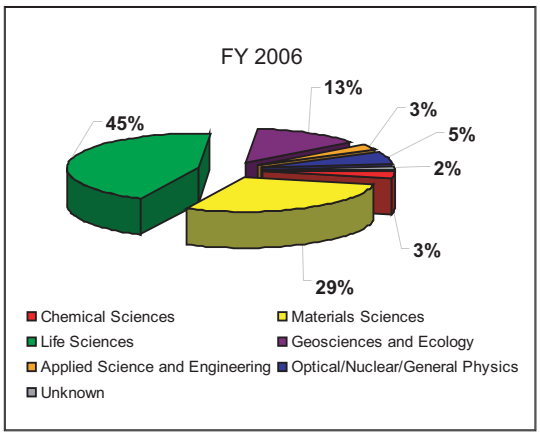

Figure 2. NSLS users by field of research

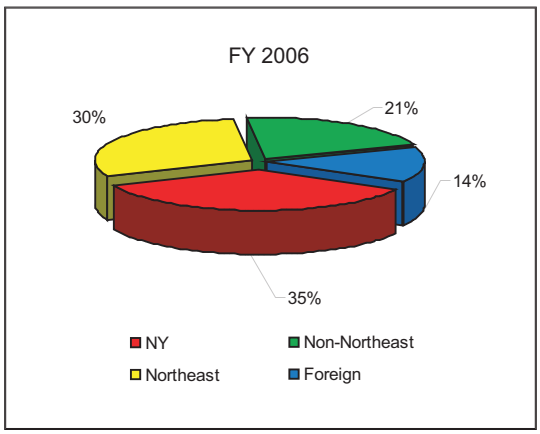

Figure 3. NSLS geographical user distribution

issues, such as appeals based on score differentials resulting from the initial peer review. Work is continuing to develop and streamline the role, responsibilities, and reporting of the POP. Related to this initiative was initial planning to adjust the current guidelines for rating proposals in an attempt to create a more efficient, more quantifiable way of scoring.

User Satisfaction Survey

The Department of Energy requests that all users complete a user satisfaction survey at the close of each experimental run. At the NSLS, this is called our End-of-Run survey. These surveys revealed that more than half of the respondents would communicate their research results through publishing in peer-reviewed open literature. About half said they would present findings at a professional society meeting, and three users indicated they would acquire a patent. Additional benefits gained according to feedback from most of our users included:

- obtained access to unique facilities
- facilitated collaborative interactions (such as stimulated new ideas for future experi ments, increased multidisciplinary work, or enabled a new approach)
- created an opportunity to train students (un dergraduate through postdoctoral fellows)

The End-of-Run survey form was revised during 2006, and is now available online. Changes were made to limit the number of questions and simplify the information gathered so that users can complete the survey more quickly. Further changes are planned to allow access for particular beamline staff, through the PASS system, to view the responses to the survey directly and as often as they wish. Further, a tracking system will be created so that users can view the issues brought out through End-of-Run surveys, and what is being done to resolve the issues. It is anticipated that this will ensure more timely feedback and/or resolution for problems identified. The survey will continue to remain anonymous, unless a user wishes to provide an email address for an individual follow-up response.

BNL Research Support Building

In 2006, plans were created to provide a more convenient and simpler check-in process for the users and guests of all facilities on the BNL site. These plans included moving all users' services to the new Research Support Building. Located on Brookhaven Avenue diagonally across from Berkner Cafeteria, the Research Support Building opened in October 2006 and currently provides part of the envisioned "one-stop shopping" model for visiting scientists and guests. The housing, travel, rental car, and transportation offices as well as the Ronkonkoma Train Station Shuttle and Teachers Federal Credit Union are already functioning in the new location.

Currently, NSLS users still need to check in at the User Administration Office on the second floor of the NSLS upon arrival at BNL. But in 2007, the new Guests, Users, and Visitors' (GUV) Center will also open in the Research Support Building, eliminating the need for NSLS users to visit two buildings upon their arrival on site. When the new GUV Center becomes operational, it will allow all guests, visitors, and scientists (not including contractors) to complete their physical check-in process and fulfill other needs, such as picking up a key for an on-site dorm room, in one location. The hope is to provide weekday coverage from 7 a.m. to 7 p.m. with some later hours on weekdays and Sundays to accommodate users and guests who cannot arrive during normal working days and hours. Once the GUV Center is open, NSLS users

The User Administration Group (from left) Kathy Nasta, Gretchen Cisco, Mercy Baez, and Liz Flynn

will be able to go there to complete the check-in tasks that would normally be done at the NSLS User Administration registration desk. After this transition, the NSLS User Administration Office will remain in place to pre-process registrations prior to physical check-in, and for other user functions as mentioned at the beginning of this article.

Meetings and Workshops

The User Administration office has taken a more active role in the past year to help plan and organize major meetings and workshops at the NSLS, such as the RapiData course held every April and the Crystallization workshop, which is held in June. Of course, our largest effort in this area is the annual Users' Meeting, which in May 2006, was the first held jointly with BNL's Center for Functional Nanomaterials (CFN). Although there are always improvements to be made, most of the 416 participants of the meeting were pleased with the joining of the two user communities, the main meeting and workshop programs, and logistical arrangements. There were six workshops offered: two concentrated on NSLS user interest, two focused on CFN interest, and the remaining two workshops were of interest to both communities. There were 34 vendors in exhibition and 47 posters displayed. New ideas brought out by participants that we hope to implement for the 2007 meeting include holding workshops and/or special times for NSLS/CFN technical staff to meet with vendors for product discussions, and holding a working luncheon to gather Proposal Review Panel members.

SAFETY REPORT

Andrew Ackerman
ESH&Q Manager

Organization and Mission
The NSLS Environment, Safety, Health, and Quality Division is managed by Andrew Ackerman and includes contributions from a mixture of department and assigned Laboratory personnel. The group includes nine professional staff, two administrative assistants, and one technician whose combined efforts amount to about seven full-time equivalent positions. These personnel manage the various ESH, Quality Assurance, and Training issues presented by facility and experiment operations.

There is a continued emphasis on integration of ESH&Q principles into all work at BNL and the NSLS. Laboratory initiatives for 2006 included a focus on electrical safety, implementation of the DOE Integrated Safety Management (ISM) principles, assurance of worker qualification, and control of workplace injury. The NSLS ESH&Q Division is committed to advancing those programs and managing the risks presented to personnel and the environment in support of the department's scientific program.

2006 Activities
Everyone was busy in 2006 and there was considerable ESH&Q activity throughout the department. A few highlights pertinent to the user community are as follows:

- The NSLS completed independent registration with the Occupational Health and Safety Assessment Series (OHSAS) management system, an important goal for the Laboratory.

Andrew Ackerman

- The definition of worker qualification through training and experience was advanced, allowing improved work planning and a better understanding of worker skills.
- Configuration control and equipment identification on the beamlines were improved with better checklists, labeling, and photographs.
- Inspection of electrical equipment for compliance with Nationally Recognized Testing Laboratory (NRTL) requirements was implemented for user equipment.
- Electrical safety and Lock Out/Tag Out (LOTO) training requirements were redefined for beamline staff, resulting in a lowered training burden and the assignment of courses that are most applicable to the work performed.
- Personnel lead exposure resulting from shielding movement was well characterized and shown to be low and controlled with existing practices.

Several performance measures are tracked to follow the effectiveness of the ESH&Q programs. Performance in 2006 was excellent.

- There were no "Days Away, Restricted, Transferred" (DART) cases during 2006 or 2005. That means no injuries or illnesses resulted in lost or restricted work time. There were some minor injuries, but nothing severe enough to require personnel to miss time at the Laboratory. The significance of this result is obvious to those who work at the NSLS and is an important parameter as these values are reported to and tracked carefully by the DOE as a key indicator of safety performance.
- There were two incidents that met the criteria for reporting within the Occurrence Reporting and Processing System (ORPS) – another parameter tracked closely by the DOE. One involved a chemical spill and the second a mistake in cutting an electrically energized wire. Neither resulted in injury or significant environmental insult. Both were carefully investigated and yielded some valuable lessons that were disseminated throughout the community.
- Training compliance was excellent and improved from last year.
- Routine workplace inspections yielded fewer findings per inspection and correction time was short.
- Numerous internal and external audits resulted in few findings, and the department response was timely and organized.

- Waste generation continues to be low and well managed. The department's mercury inventory has been significantly reduced through the replacement of mercury switches with solid-state devices and the elimination of mercury thermometer use. That effort resulted in some extra waste, but also virtually eliminated the risk of a significant environ mental mercury release and helped us meet an important DOE initiative.
- Radiation exposure remains very low; the measured collective dose this year was less than 50 mRem for some 3,000 personnel who were monitored.

There is more to report, but the summaries above provide an overall picture of the department's activity and performance in ESH&Q for 2006. The NSLS programs are acknowledged throughout the Laboratory and by the DOE area office as excellent and there is much reason for pride in staff and user attention to safety and in keeping the facility a safe place to work. Good performance indicators and well-managed programs are important, but what is most important is that we completed an enormous amount of science last year without significant injuries or environmental insults.

2007 ESH&Q Initiatives

All that was completed last year must continue, and we must seek to improve. A brief summary of three important initiatives for 2007 is as follows:

Integrated Safety Management (ISM)

The DOE Integrated Safety Management program is aimed at assuring that work is planned, risks are controlled, and personnel are qualified. These principles are well implemented at the NSLS. Worker qualification is assured through training and experience, and all work at the facility is planned with attention to scoping and evaluating tasks, identifying and implementing pertinent controls, and providing feedback mechanisms for improvement.

Evaluation of the program in 2006 confirmed that overall implementation is good and that improvement efforts should focus on enhancing feedback mechanisms and personnel awareness to the application of ISM. That has begun and will continue into the next year with an emphasis on completing "End of Run" forms to collect better feedback, and with continued discussion of the ISM principles to assure that everyone understands how they apply to work at the NSLS.

10 CFR Part 851

"10 CFR Part 851" refers to a section in the federal code rules that incorporates many ESH standards into federal law applicable to the DOE. The incorporated rules include OSHA requirements and various health and safety "consensus" standards that cover many topics including electrical, fire, laser, pressure, chemical, biological, and nano-material safety. Evaluation of this new rule has begun. It has uncovered areas where improvements can be made and will likely result in requirement changes for the upcoming year.

Event and Issues Management

It is valuable to investigate and understand minor occurrences and learn from them with the hope to avoid a more significant event. That is the basis for a renewed focus on event management and emphasis on reporting all occurrences and investigating even those that are minor. Everyone is asked to help identify issues and resolve concerns before they become troublesome by reporting unexpected occurrences to the NSLS Operations staff. The approach of finding leading indicators to more significant events will be emphasized next year.

Summary

A continued focus on ESH&Q has obvious importance to everyone. 2006 was a great year and everyone's involvement and commitment to safety is much appreciated. That success can continue in 2007 if we remain vigilant. There will be program challenges as we seek to meet new requirements and improve on the old. The ESH&Q Division will work to assure that changes fit NSLS operations and are well communicated. The focus for the New Year will be, as always, safe science. Help us achieve that by knowing requirements, continuing to generate great science, and assuring that all the work we do includes evaluation and control of risks.

BUILDING ADMINISTRATION REPORT

Bob Kiss
NSLS Building Manager

Organization and Mission
The NSLS Building Manager, Bob Kiss, coordinates the activities of BNL Plant Engineering departments involved in operating and maintaining the building to ensure that the integration and execution of facility work is efficiently and effectively managed and controlled, providing a safe, comfortable and hazard free environment for the NSLS staff and users. He is supported by Plant Engineering Trades Staff Supervisors in the maintenance and housekeeping of the NSLS Complex.

The Mission of the Building Administration consists of multiple disciplines:

- To maintain the housekeeping and ES&H of the facilities in a showcase condition
- To ensure the general maintenance of all building systems
- To oversee the construction and installation of new equipment or facilities
- To ensure the maintenance and function of all security systems
- To promote energy awareness and conservation
- To function as the Work Control Coordinator for all building systems
- To comply with the Emergency Preparedness Program

2006 Activities

Change of Building Managers
2006 has been more than a busy and positive "business-as-usual" year for the NSLS. With the NSLS-II project in the spotlight, the NSLS has seen many changes in staff. Many of our valued staff members are now doing double duty, continuing to provide support to our current facility while giving their expertise to the new and bright future of the NSLS-II. Several buildings were acquired for the NSLS-II to accommodate the transfer of staff into a central, convenient location. Gerry Van Derlaske has stepped up and become the Facility Manager for the NSLS-II and as such has played a major role in setting up the new facilities. During the past year, this had taken up the majority of Gerry's time, leaving the day-to-day care of the NSLS to me, first as the Alternate Building Manager and then as the permanent Building Manager when Gerry officially became the NSLS-II Facility Manager at the end of 2006. We thank Gerry for his many years of leadership in this position and wish him well.

Bob Kiss

Work Planning and Controls
With the emphasis on safety and work planning by DOE and OSHA, the NSLS has become an excellent example of Work Planning and Controls. Al Boerner, the NSLS Work Control Manager, has continued to ensure that all work is completed in a safe and complete manner. Under Al's guidance, the number of work permits for tasks completed at the NSLS has grown to about 65 Work Permits for 2006. These permits range in complexity from a simple permit to ensure the safety of a contract vendor repairing a copy machine, to a complex permit coordinating the tasks of many BNL trades and NSLS staff for the installation of RF Cavities. With attention to safety, work planning and work controls, we have maintained our safety record of no lost workdays for more than three years.

Machine Shop Operations
Machine Shop Safety was an area that received extensive attention during 2006. BNL issued a new SBMS, detailing the updated requirements for the training, safe operation, maintenance, and inspections of all machine shops. As the NSLS User Machine Shop Manager, I was a member of the SBMS review committee and was able to provide NSLS Machine Shop Program policies for the SBMS. This resulted in the review and changes of the training requirements for anyone authorized to use the NSLS User Machine Shop and the NSLS Tech Shops. Major changes include required periodic retraining and review of all authorized users, monthly and yearly inspections of the shop by the shop manager, and restricting access to all machines to only those individuals fully trained for the

particular machine. The NSLS User Machine Shop was referred to as a prime example of a well-run and maintained facility. This past year has seen a change in management of the User Machine Shop. Since becoming a member of the NSLS in 2000, I had been the Shop Manager. With the many staffing changes at the NSLS, the responsibility of the NSLS User Machine has now been turned over to Dennis Carlson. Dennis has many years of machine shop experience, having been a member of the NSLS Beamline Development and Support group for many years. His experience and knowledge of the workings of the NSLS beamlines is a very valuable asset for the users of the machine shop.

High Sensitivity Smoke Detector (HSSD)
In early 2006, at the end of last year's winter maintenance period, the new HSSD was fine-tuned and tested. Having met and passed all the expected requirements and tests, the system was placed into full service. The testing of the system included simulation of various possible maintenance tasks that may trigger the alarms. These tasks included the bake-out of a cavity, soldering of large pipes, and the idling of a truck outside the area roll-up door. The system consists of a system of special PVC piping and nozzles located directly above the critical equipment in the NSLS power supply area. It is a continuous sampling system that pulls air samples through the nozzles and piping to a computer analyzer, providing early detection of any smoke or fire in the area well before it becomes a major issue. This early detection provides the operations coordinators with valuable extra time to investigate and shut down any equipment necessary to prevent a major incident.

X9-X3 Transfer
The x-ray experimental floor received a major change with groups working together to "Green Field" the X3 beamline in 2005. With that portion of the project completed, the next phase of the project was to modify and relocate the X9 experimental end station enclosure (EESE) to X3. This was a major undertaking since the original EESE was too tall to fit at X3. The lead-lined panels were transported to the Central Fabrication Facility to be modified and then transported back and re-assembled in place at the X3 beamline. All the X9 beamline components were painstakingly removed and re-assembled at the new X3 location.

Green Field of X9
With the completion of the X9 to X3 beamline, preparations for the new X9 beamline were begun. The most visible aspect of this task was to "Green Field" the area beginning with the removal and disposal of the old EESE. With the help of Plant Engineering Carpenter and Riggers, and thorough work planning using the BNL Work Permit program, the removal of the EESE was completed quickly and safely. Once the EESE was removed, work continued to remove all remaining excess equipment, clean, and make necessary repairs to the floor to prepare for the planning and installation of the new line later this year.

Library Renovations
After many years of use, the NSLS Chasman-Green Library was remodeled. With the assistance of Plant Engineering, the old carpet and platform was removed and new carpets installed. New ceiling tiles were installed and the walls received a fresh coat of paint. Bookcases were rearranged, excess file cabinets removed, old periodicals were scanned to computer files, and many volumes of reference books were placed into storage until the renovations were complete.

The renovated Green-Chasman Library

In 2007, the reference books will be sorted and arranged for easy access and plans for new furniture will be finalized. Plans also include the installation of a retractable projection screen in the ceiling to allow the library to be used as a conference room. A small area will be set up and equipped with a computer station, and a fax/copy machine for use by visiting users. These renovations will result in a warm, quiet, and friendly atmosphere to gather and relax or just get away from the busy life of running an experiment.

Behind-the-Scenes Accomplishments
Many times during the year there are tasks and jobs completed that go unnoticed by the majority of staff and users. Most times these are tasks that do not affect the everyday workings of the NSLS, but once completed, they make life a little safer or comfortable for everyone. Most of these do not take much effort on the part of the NSLS, but require much coordination between building management, Plant Engineering, contractors and other BNL departments. Some of this year's behind-the-scenes accomplishments include for following:

- Parking lots outside the east side of the build-

ing were cleaned, repaired, and painted.

- A ramp was installed outside the east roll-up door entrance to eliminate the curb to the bicycle rack storage area. This also allows an electric vehicle to be parked under the over hang and charged overnight. This was completed with funding from the BNL Safety Solutions (S2) project.
- The NSLS User Administration Office, along with several other offices and the Chasman-Green Library received new carpets.
- The LEGS Helium trailer was removed to create space for an LN2 to N2 heat exchanger. Removal of the trailer eliminated the need to install another concrete pad to the system.
- The XLS trailer was emptied and disconnected in preparation for removal.

Conclusion

Year after year, thousands of people come to the NSLS, some to use the facility for research, some to attend research conferences and training courses, and others to tour our facility just to find out "what do they do there." Whoever they are, no matter where they come from, it is wonderful to know that they leave with a better understanding and appreciation of science. A large part of their appreciation must go to the talented support staff that keeps the NSLS facility up and running, and showcases the research community.

FACTS AND FIGURES

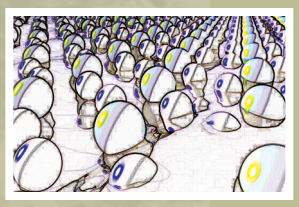

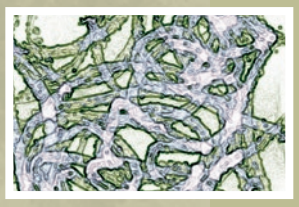

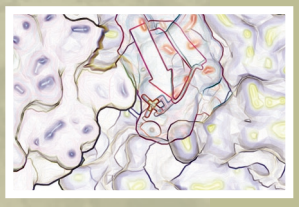

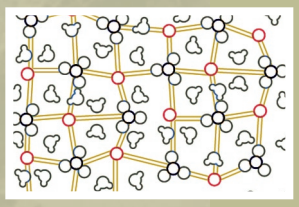

FACILITY FACTS & FIGURES

The National Synchrotron Light Source (NSLS) is a national user research facility funded by the U.S. Department of Energy's Office of Basic Energy Science. The NSLS operates two electron storage rings: an x-ray ring (2.8 GeV, 300 mA) and a vacuum ultraviolet (VUV) ring (800 meV, 1.0 A), which provide intense light spanning the electromagnet spectrum from the infrared through x-rays. The properties of this light, and the specially designed experimental stations, called beamlines, allow scientists in many fields of research to perform experiments not otherwise possible at their own laboratories.

Over 2,100 scientists representing almost 400 institutions, 47 of them corporations, come to Brookhaven National Laboratory annually to conduct research at the NSLS. The facility operates seven days a week, 24 hours a day throughout the year, except during periods of maintenance and studies.

As a national user facility, the NSLS does not charge for its beamtime, provided that the research results are published in the open literature. Proprietary research is conducted on a full cost recovery basis. The primary way to obtain beamtime at the NSLS is through the General User program. General Users are independent investigators interested in using the NSLS for their research. Access is gained through a peer-reviewed proposal system.

The NSLS currently has 51 x-ray and 14 VUV-IR operational beamlines available to users for performing a wide range of experiments. There are two types of beamlines at the NSLS: Facility Beamlines (FBs) and Participating Research Team (PRT) beamlines. In 2006, the NSLS had 18 FBs and 47 PRT beamlines. FBs are operated by the NSLS and reserve at least 50% of their beamtime for General Users. Some FBs host contributing users (CUs), who enhance the endstation capabilities and provide specialized user support. PRT beamlines are operated by user groups with related interests from one or more institutions. PRT beamlines reserve 25% of their beamtime for General Users. Membership in a PRT or CU program is open to all members of the scientific community who can contribute significantly to the program of the beamline, (i.e., funding, contribution of equipment, scientific program, design and engineering, operations manpower, etc).

The following pages list the operational beamlines at the NSLS and their unique characteristics.

BEAMLINE GUIDE ABBREVIATIONS

ARPES
UV photoelectron spectroscopy, angle-resolved

DAFS
X-ray diffraction anomalous fine structure

DEI
Diffraction-enhanced imaging

EXAFS
X-ray absorption spectroscopy, extended fine structure

GISAXS
Grazing incidence small angle x-ray scattering

HARMST
High aspect ratio microsystems technology

IRMS
Infrared microspectroscopy

MAD
Multi-Wavelength anomolous dispersion

MCD
Magnetic circular dichroism

NEXAFS
Near edge x-ray absorption spectroscopy

PEEM
Photo emission electron microscopy

SAXS
Small angle x-ray scattering

STXM
Scanning transmission x-ray microscopy

UPS
UV photoelectron spectroscopy

UV-CD
Ultraviolet circular dichroism

WAXD
Wide-angle x-ray diffraction

WAXS
Wide-angle x-ray scattering

XAS
X-ray absorption spectroscopy

XPS
X-ray photoelectron spectroscopy

XRD
X-ray diffraction

XSW
X-ray diffraction, standing waves

VUV-IR BEAMLINES

Beamline	Source	Technique	Energy Range	Type	Organization
U1A	Bend	XAS EXAFS NEXAFS	270-900 eV	PRT	ExxonMobil Research and Engineering Co.
U2A	Bend	IRMS High Pressure Research IR spectroscopy	30-8000 cm-1	FB	BNL-NSLS Carnegie Institution of Washington COMPRES
U2B	Bend	IRMS IR spectroscopy	50-4000 cm-1	PRT	Case Western Reserve University
U3C	Bend	Metrology	50-1000 eV	PRT	Bechtel Nevada Lawrence Livermore National Laboratory Los Alamos National Laboratory Sandia National Laboratory
U4A	Bend	UPS	10-250 eV	PRT	Army Research Laboratory North Carolina State University Rutgers University University of North Carolina
U4B	Bend	X-ray scattering, resonant MCD UPS X-ray fluorescence spectroscopy XPS	20-1200 eV	PRT	Montana State University Northeastern University
U5UA	Insertion Device	ARPES UPS, spin-resolved PEEM	15-150 eV	FB	BNL-CFN
U7A	Bend	NEXAFS XPS	180-1200 eV	PRT	BNL-Chemistry Dow Chemical Company NIST University of Michigan
U9B	Bend	UV-CD UV florescence spectroscopy	0.8 - 8.0 eV	PRT	BNL-Biology
U10B	Bend	IRMS	500-4000 cm-1	FB	BNL-NSLS
U11	Bend	UV-CD	3-10 eV	PRT	BNL-Biology
U12A	Bend	XAS XPS	100-800 eV	PRT	Oak Ridge National Laboratory
U12IR	Bend	IR spectroscopy THz / mm wave spectroscopy Time-resolved spectroscopy	6-600 cm-1	FB	BNL-NSLS

Beamline	Source	Technique	Energy Range	Type	Organization
U13UB	Insertion Device	UPS ARPES	3-30 eV	PRT	Boston College Boston University BNL-Physics Columbia University

X-RAY BEAMLINES

X1A1	Insertion Device	STXM	0.25-0.50 keV	PRT	BNL-Environmental Science ExxonMobil Research and Engineering Co. SUNY @ Plattsburgh Stony Brook University University of Texas @ Houston
X1A2	Insertion Device	STXM	0.25-1 keV	PRT	Stony Brook University
X1B	Insertion Device	X-ray scattering, coherent XAS X-ray fluorescence spectroscopy XPS	0.2-1.6 keV	PRT	Boston University Thomas Jefferson National Accelerator Facility University of Illinois
X2B	Bend	X-ray microtomography	8-35 keV	PRT	ExxonMobil Research and Engineering Co.
X3A	Bend	MAD Macromolecular crystallography	5-15 keV	PRT	Albert Einstein College of Medicine Case Western Reserve University Rockefeller University Sloan-Kettering Institute
X3B	Bend	XAS EXAFS	5-15 keV	PRT	Case Western Reserve University
X4A	Bend	MAD Macromolecular crystallography	3.5-20 keV	PRT	Albert Einstein College of Medicine City University of New York (CUNY) Columbia University Cornell University Mount Sinai School of Medicine New York Structural Biology Center New York University SUNY @ Buffalo Sloan-Kettering Institute Wadsworth Center
X4C	Bend	MAD Macromolecular crystallography	7-20 keV	PRT	Albert Einstein College of Medicine City University of New York (CUNY) Columbia University Cornell University Mount Sinai School of Medicine New York Structural Biology Center New York University Rockefeller University SUNY @ Buffalo Sloan-Kettering Institute Wadsworth Center

Beamline	Source	Technique	Energy Range	Type	Organization
X5A	Bend	Laser backscattering	150-420 MeV	PRT	BNL-Physics Forschungszentrum Juelich (KFA) James Madison University Norfolk State University Ohio University University of Rome II University of South Carolina University of Virginia Virginia Polytechnic Inst. and State University
X6A	Bend	MAD Macromolecular crystallography	6.0-23 keV	FB	BNL-NSLS
X6B	Bend	XRD, surface WAXD X-ray reflectivity SAXS GISAXS	6.5-19 keV	FB	BNL-CFN BNL-NSLS
X7B	Bend	XRD, single crystal XRD, time resolved WAXD WAXS	5-21 keV	PRT	BNL-Chemistry General Electric
X8A	Bend	Metrology	1.0-5.9 keV	PRT	Bechtel Nevada Lawrence Livermore National Laboratory Los Alamos National Laboratory Sandia National Laboratory
X8C	Bend	MAD Macromolecular crystallography	5-19 keV	PRT	Biogen Incorporated Biotechnology Research Institute Hoffmann-La Roche National Institutes of Health
X10A	Bend	XRD, powder WAXD SAXS WAXS	8-11 keV	PRT	ExxonMobil Research and Engineering Co.
X10B	Bend	XRD, powder XRD, surface WAXD X-ray reflectivity X-ray scattering, surface WAXS	14 keV	PRT	ExxonMobil Research and Engineering Co.
X10C	Bend	XAS EXAFS NEXAFS	4-24 keV	PRT	ExxonMobil Research and Engineering Co.
X11A	Bend	DAFS XAS EXAFS NEXAFS	4.5-35 keV	PRT	BNL-Material Science BNL-Environmental Science Canadian Light Source ETH Labs - Zuerich Natural Resources Canada Naval Research Laboratory (NRL) Naval Surface Warfare Center New Jersey Institute of Technology North Carolina State University Stony Brook University Sarah Lawrence College

Beamline	Source	Technique	Energy Range	Type	Organization
X11B	Bend	XAS EXAFS NEXAFS	5.0-23 keV	PRT	BNL-Environmental Science BNL-Material Science Canadian Light Source ETH Labs - Zuerich Natural Resources Canada Naval Research Laboratory (NRL) Naval Surface Warfare Center New Jersey Institute of Technology North Carolina State University Stony Brook University Sarah Lawrence College
X12B	Bend	MAD Macromolecular crystallography	5-20 keV	PRT	BNL-Biology
X12C	Bend	MAD Macromolecular crystallography	5.5-20.0 keV	PRT	BNL-Biology
X13A	Insertion Device	X-ray scattering, resonant MCD	0.2-1.6 keV	FB	BNL-NSLS
X13B	Insertion Device	Microdiffraction Imaging	4-16 KeV	FB	BNL-NSLS BNL-CFN Columbia University IBM
X14A	Bend	MAD XRD, powder XRD, single crystal XRD, time resolved WAXD X-ray reflectivity	5-26 keV	PRT	Oak Ridge National Laboratory Tennessee Technological University University of Tennessee
X15A	Bend	XSW DEI	3-25 keV XSW 10-60 keV DEI	FB	BNL-NSLS Northwestern University
X15B	Bend	XAS EXAFS NEXAFS	0.8-15 keV	PRT	BNL-Environmental Science Lucent Technologies, Inc. Stony Brook University Temple University University of Texas @ Austin
X16C	Bend	XRD, powder	4.5-25 keV	PRT	Stony Brook University
X17B1	Insertion Device	XRD, powder	55-80 keV mono 20-150 keV white	FB	BNL-NSLS Rutgers University
X17B2	Insertion Device	XRD, powder XRD, time resolved High pressure research	20-130 keV	FB	BNL-NSLS COMPRES Stony Brook University
X17B3	Insertion Device	XRD, powder XRD, single crystal High pressure research	5-80 keV	FB	BNL-NSLS COMPRES University of Chicago

Beamline	Source	Technique	Energy Range	Type	Organization
X17C	Insertion Device	XRD, powder XRD, single crystal High pressure research	5-80 keV	FB	COMPRES University of Chicago
X18A	Bend	XRD, powder XRD, single crystal XRD, surface WAXD X-ray reflectivity X-ray scattering, surface WAXS	4-19 keV	PRT	BNL-Chemistry Indiana University @ Bloomington Pennsylvania State University Purdue University Stony Brook University University of Missouri @ Columbia
X18B	Bend	XAS EXAFS NEXAFS	4.8-40 keV	FB	BNL-Chemistry BNL-Electrochemistry BNL-NSLS ORNL University of Delaware UOP LLC Yeshiva University
X19A	Bend	X-ray scattering, resonant XAS EXAFS NEXAFS	2.1-17 keV	FB	BNL-Chemistry BNL-Electrochemistry BNL-NSLS ORNL University of Delaware UOP LLC Yeshiva University
X19C	Bend	XRD, surface X-ray topography X-ray reflectivity X-ray scattering, liquid X-ray scattering, surface	6-17 keV	PRT	Arizona State University Fairfield Crystal Technology, LLC Kansas State University Kyushu University SUNY @ Albany Stony Brook University University of Illinois @ Chicago
X20A	Bend	XRD, single crystal Microdiffraction Imaging X-ray reflectivity X-ray scattering, surface	4.5-13 keV	PRT	IBM Research Division
X20C	Bend	XRD, single crystal XRD, surface XRD, time resolved X-ray reflectivity X-ray scattering, surface	4-11 keV	PRT	IBM Research Division
X21	Insertion Device	XRD, single crystal XRD, surface X-ray scattering, magnetic X-ray scattering, resonant X-ray scattering, surface SAXS	5-15 keV	FB	BNL-NSLS Boston University University of Vermont
X22A	Bend	XRD, single crystal XRD, surface WAXD X-ray reflectivity X-ray scattering, surface WAXS	10.7 keV 32 keV	PRT	BNL-CMPMSD BNL-Chemistry

Beamline	Source	Technique	Energy Range	Type	Organization
X22B	Bend	X-ray scattering, liquid X-ray scattering, surface	6.5-10 keV	PRT	Bar-Ilan University BNL-CMPMSD BNL-CFN Harvard University
X22C	Bend	XRD, single crystal XRD, surface X-ray reflectivity X-ray scattering, magnetic X-ray scattering, surface	3-12 keV	PRT	BNL-CMPMSD Massachusetts Institute of Technology Rutgers University
X23A2	Bend	XRD, powder DAFS XAS EXAFS NEXAFS	4.7-30 keV	PRT	NIST
X23B	Bend	XRD, powder XAS EXAFS NEXAFS	4-10.5 keV	PRT	Hunter College Montana State University Naval Research Laboratory (NRL) New Jersey Institute of Technology Sarah Lawrence College
X24A	Bend	XSW Auger spectroscopy EXAFS X-ray fluorescence spectroscopy XPS	1.8-5 keV	PRT	NIST
X24C	Bend	X-ray reflectivity UV photoabsorption spectroscopy UPS XAS	0.006-1.8 keV	PRT	Naval Research Laboratory (NRL) Universities Space Research Association
X25	Insertion Device	MAD Macromolecular crystallography	3-28 keV	FB	BNL-Biology BNL-NSLS
X26A	Bend	Microdiffraction Imaging X-ray microprobe	3-30 keV	PRT	BNL-Environmental Science University of Chicago University of Georgia
X26C	Bend	MAD Macromolecular crystallography	5-20 keV	PRT	BNL-Biology Cold Spring Harbor Laboratory Stony Brook University
X27A	Bend	X-ray microprobe	4.5-20 keV	FB	BNL-Environmental Science BNL-NSLS Stony Brook University
X27B	Bend	HARMST	8-40 keV	PRT	BNL-Nonproliferation & National Security
X27C	Bend	XRD, time resolved WAXD SAXS WAXS	9 KeV	PRT	Air Force Research Laboratory Dow Chemical Company National Institutes of Health Naval Surface Warfare Center Stony Brook University

Beamline	Source	Technique	Energy Range	Type	Organization
X28C	Bend	X-ray footprinting	White Beam	PRT	Case Western Reserve University
X29A	Insertion Device	MAD Macromolecular crystallography	6-15keV	PRT	BNL-Biology Case Western Reserve University

NSLS LINAC PARAMETERS AS OF DECEMBER 2006

Injection Energy	100 keV
Final Energy	120 MeV
Number of Sections	3
Number of Klystrons	3
Frequency	2856 MHz

NSLS BOOSTER PARAMETERS

Booster Injection Energy	120 MeV
Booster Extraction Energy	736 MeV
Circumference	28.35 m
Number of Superperiods	4
Dipole Bend Radius	1.91 m
Nominal Horizontal Tune	2.42
Nominal Vertical Tune	1.37
Maximum Horizontal Beta Function	8.63 m
Minimum Horizontal Beta Function	1.01 m
Maximum Vertical Beta Function	5.26 m
Minimum Vertical Beta Function	1.73 m
Maximum Dispersion Function	1.21 m
Minimum Dispersion Function	0.41 m
Momentum Compaction	0.106
RF Frequency	52.88 MHz
RF Peak Voltage	25 kV
Momentum Acceptance	±0.0025

BOOSTER MAGNETIC ELEMENTS (FIELDS AT 750 MEV)

Name	Type	Quantity	B (kG)	B' (kG/m)	B" (kG/m)	Effective Length (m)
BB	Dipole	8	13.099	-7.97	-125	1.5
Q1	Quadrupole	4		68.82		0.3
Q2	Quadrupole	4		93.60		0.3
SF	Sextupole	4			1223.7	0.2

VUV STORAGE RING PARAMETERS AS OF DECEMBER 2006

Stored Electron Beam Energy	0.808 GeV
Injected Current	1.0 amp (1.06 x 10^{12}e-)
Lifetime @ 200 mA unstretched (stretched)	~6 (9.8) hr
Circumference	51.0 meters

PHOTON CRITICAL WAVELENGTH (ENERGY)

Dipole Source 1.41 T $\lambda_c(E_c)$	19.9 Å (622 eV)

LATTICE STRUCTURE (CHASMAN-GREEN) SEPARATED FUNCTION, QUAD DOUBLETS

Number of Superperiods (N_s)	4
Magnet Complement	{ 8 Bending Magnets (1.5 meters each) 24 Quadrupole (0.3 meters each) 12 Sextupole in two families (0.2 meters each)

STORAGE RING CHARACTERISTICS

Number of Dipole Ports	18
Number of Insertion Device Straight Sections	2
Maximum Length of Insertion Devices	2.25 meters
Radiated Power	20.4 kW/amp of beam
Power per Horizontal Milliradian (@ 1A)	3.2 W
RF Frequency (f_{rf})	52.887 MHz
B(ρ)	1.41 Tesla (1.91 meters)
Electron Orbital Period	170.2 nanoseconds
Number of RF Buckets	9
Typical Bunch Mode	7
Damping Times	τ_x=τ_y= 13 msec; τ_ε = 7 msec
Nominal Tunes (ν_x,ν_y)	3.14, 1.26
Momentum Compaction	0.0235
RF Peak Voltage with 52 MHz (with 211 MHz) (V_{rf})	80 kV (20 kV)
Design RF Power with 52 MHz (with 211 MHz)	50 kW (10 kW)
Synchrotron Tune (ν_s)	0.0018
Natural Energy Spread (σ_e/E)	5.0 x 10^{-4} (I_b< 20 mA)
Bunch Length (2σ)	10 cm (I_b< 20 mA)
(2σ with 211 MHZ Bunch Lengthening)	38 cm
Horizontal Damped Emittance (ε_x)	1.60 nm-rad
Vertical Damped Emittance (ε_y)	≥ 0.35 nm-rad (4nm-rad in normal ops.)*

ARC SOURCE PARAMETERS

Betatron Function (β_x,β_y)	1.18 to 2.25 m, 10.26 to 14.21 m
Dispersion Function (η_x,η'_x)	0.500 to 0.062 m, 0.743 to 0.093 m
$\alpha_{x,y}$ = -$\beta'_{x,y}$/2	-0.046 to 1.087, 3.18 to -0.96
$\gamma_{x,y}$ =(1 +$\alpha^2_{x,y}$)/$\beta_{x,y}$	0.738 to 0.970 m^{-1}, 1.083 to 0.135 m^{-1}
Source Size (σ_x,σ_y)	536 to 568 µm, >60 to >70 µm (170-200 µm in normal ops.)*
Source Divergence (σ'_x,σ'_y)	686 to 373 µrad, 19.5 to 6.9 µrad (55-20 µrad in normal ops.)*

INSERTION DEVICE PARAMETERS

Betatron Function (β_x,β_y)	11.1 m, 5.84 m
Source Size (σ_x,σ_y)	1240 µm, >45 µm (220 µm in normal ops.)*
Source Divergence (σ'_x, σ'_y)	112 µrad, >7.7 µrad (22 µrad in normal ops.)*

* ε_x is adjustable

X-RAY STORAGE RING PARAMETERS AS OF DECEMBER 2006

Stored Electron Beam Energy	2.800 GeV
Maximum Operating Current	300 mA
Lifetime	~20 hours
Circumference	170.08 meters

PHOTON CRITICAL WAVELENGTH (ENERGY)

$\lambda_c(E_c)$ 1.36 T	1.75 Å (7.1 keV)
$\lambda_c(E_c)$ at 5.0 T (W)	0.48 Å (26.1 keV)

LATTICE STRUCTURE (CHASMAN-GREEN) SEPARATED FUNCTION, QUAD TRIPLETS

Number of Superperiods	8
Magnet Complement	16 Bending (2.70 meters each) 40 Quadrupole (0.45 meters each) 16 Quadrupole (0.80 meters each) 32 Sextupole (0.20 meters each)

STORAGE RING CHARACTERISTICS

Number Beam Port on Dipoles	30
Number of Insertion Device Straight Sections	6
Maximum Length of Insertion Devices	< 4.50 meters
Dipole Bend Radius	6.875 meters
Radiated Bending Magnet Power (1=0.25A)	198 kW
Electron Orbital Period	567.2 nanoseconds
$B(\rho)$	1.36 Tesla (6.875 meters)
Damping Times	$\tau_x=\tau_y$= 4 msec; τ_ε = 2 msec
Nominal Tunes (ν_x,ν_y)	9.8, 5.7
Momentum Compaction	4.10^{-3}
RF Frequency (f_{rf})	52.88 MHz
Radiated Power for Bending Magnets	237 kW (300 mA)
RF Peak Voltage	1120 kV
Design RF Power	450 kW
Synchrotron Tune (ν_s)	0.0023
Natural Energy Spread ($\sigma E/E$)	9.2×10^{-4}
Natural Bunch Length (2σ)	87 mm
Number of RF Buckets	30
Typical Bunch Mode (filled buckets)	25
Horizontal Damped Emittance (ε_x)	6.2×10^{-8} m-rad
Vertical Damped Emittance (ε_y)	3.4×10^{-10} m-rad
Power per Horizontal Milliradian (0.3A)	38 W

ARC SOURCE PARAMETERS

Betatron Function (β_x,β_y)	1.0 to 3.5 m, 11.4 to 23.6 m
Dispersion Function (η_x,η'_x)	0.03 to 0.25, -0.25 to 0.08
$\alpha_{x,y} = -\beta'_{x,y}/2$	0.38 to 1.65, -2.3 to 3.6
$\gamma_{x,y} = (1+\alpha^2_{x,y})/\beta_{x,y}$	1.073 to 1.133 m^{-1}, 0.54 to 0.58 m^{-1}
Source Size (σ_x,σ_y)	260 to 464 µm, 62 to 90 µm
Source Divergence (σ_x',σ_y')	261 to 352 µrad, 13.5 to 14.1 µrad

INSERTION DEVICE PARAMETERS

Betatron Function (β_x, β_y)	1.16 m, 0.33 m
Source Size (σ_x,σ_y)	307 µm, 11 µm
Source Divergence (σ_x', σ_y')	231 µrad, 32 µrad

CALENDAR YEAR 2006 NSLS MACHINE ACTIVITIES

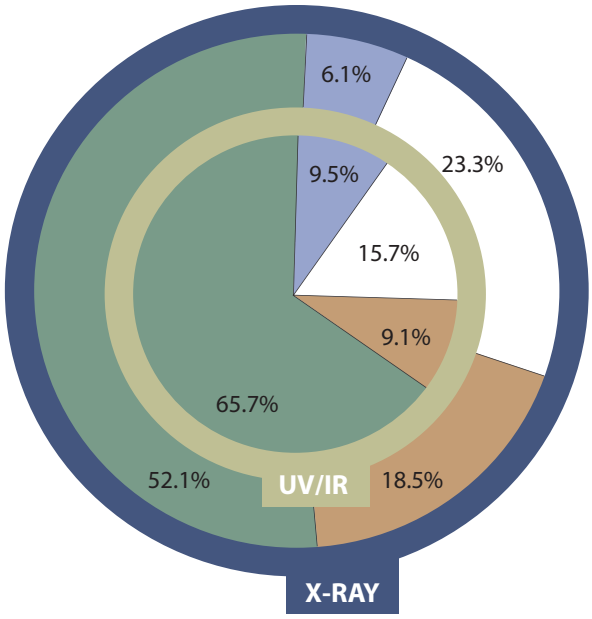

Key
Scheduled Operations
Unscheduled Operations
Maintenance
Other

Other Activities	UV/IR	X-ray
Studies	1.0%	4.4%
Comm/Cond.	2.5%	5.7%
Holiday	2.4%	2.4%
Injection	1.1%	2.1%
Unscheduled Downtime	2.1%	3.4%
Interlock	0.0%	0.6%

CALENDAR YEAR 2006

	VUV ACTUAL CY 06			X-RAY ACTUAL CY 06		
Month	Planned Hours	Reliability[1]	Availability[2]	Planned Hours	Reliability[1]	Availability[2]
January	419	98.4%	118.0%	0	-	-
February	570	98.6%	108.4%	372	91.8%	100.9%
March	615	99.2%	111.9%	588	98.1%	106.8%
April	597	99.4%	111.1%	557	94.9%	105.9%
May	420	99.8%	121.7%	275	96.7%	106.1%
June	596	98.3%	110.9%	555	89.6%	98.1%
July	467	86.9%	109.6%	428	95.6%	116.5%
August	613	98.5%	111.2%	565	93.8%	106.5%
September	599	90.8%	101.9%	577	86.4%	-
October	571	98.9%	114.4%	563	96.5%	108.1%
November	470	96.6%	105.3%	382	97.3%	103.5%
December	0	-	-	0	-	-
	5937			**4862**		
Calendar 2006 Delivered	5756	97.0%	110.9%	4562	93.8%	104.9%

Note: Delivered hours are only those accumulated during scheduled operations. Unscheduled operations do not contribute to this total.

[1] Operations during scheduled time
[2] Operations compared to total scheduled time

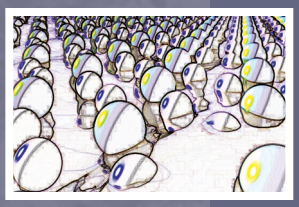

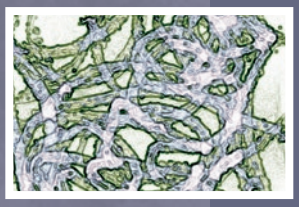

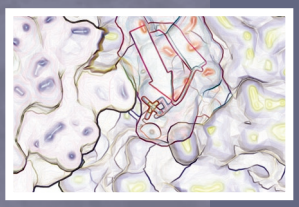

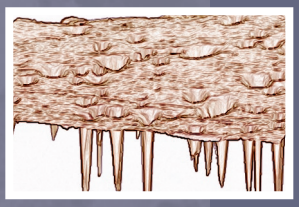

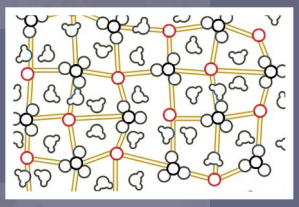

PUBLICATIONS

PUBLICATIONS

The following pages list all papers published in the 2006 calendar year as reported to the NSLS by February 28, 2007. Citations are listed in order of beamline number and then alphabetically by the last name of the first author. This list contains reported citations for journal articles, published conference proceedings, books, chapters in books, formal reports, informal reports, technical reports, theses, dissertations, and patents. For citation submissions where research was performed on more than one beamline, the citation is listed under each beamline. However, each citation was only counted once.

The first column in the table lists the number of publications reported to the NSLS during the 2006 fiscal year (Oct. 1, 2005 – Sept. 30, 2006) and published between 2003 and 2006. Although some of these publications were published earlier than FY 2006, they were not reported to the NSLS until this fiscal year. Thus, they have not been counted in prior years' activity reports.

The second column in the table lists the number of publications published in the 2006 calendar year and reported to the NSLS as of February 28, 2007. These numbers are slightly lower than the fiscal year values because they contain only publications from 2006 and it often takes many months or years to account for user and staff publications.

	Reported in Fiscal Year 2006*	**Published in Calendar Year 2006****
Journals, peer-reviewed, premier	228	199
Journals, other peer-reviewed	532	489
Journals, non peer-reviewed	33	28
Total Journals and Magazines	**793**	**716**
Books/Chapters in Books	4	4
Published Conference Proceedings	79	40
Reports: Technical, Formal, Informal	1	0
Theses/Dissertations	33	25
Patents	11	1
Total Misc. Publications	**128**	**70**
Total Publications	**921**	**786**
NSLS VUV User Publications	**87**	**67**
NSLS X-Ray User Publications	**734**	**627**
NSLS Staff Publications	**100**	**92**
	921	**786**

** Publications reported to the NSLS from Oct 1, 2005 – Sept. 30, 2006 and published between 2003 – 2006.*
*** Publications published in 2006 as reported to the NSLS by Feb. 28, 2007.*

Several types of journal articles are reported in this list, including premier journals, peer-reviewed journals, and a few that are not peer-reviewed. A publication is considered premier if the journal has an impact factor of 6 or greater (from Journal Citation Report 2003, Thomson Institute for Scientific Information). These journals represent approximately the top 3% of all journals.

For calendar years 2003-2006, the NSLS users and staff published in 40 premier journals. These premier journals are: Accounts of Chemical Research, Advanced Materials, Angewandte Chemie, Annual Review of Biophysics and Biomolecular Structure, Annual Review of Genomics and Human Genetics, Applied Physics Letters, Cancer Cell, Cell, Chemical Reviews, Chemistry and Biology, Current Biology, Current Opinion in Chemical Biology, Current Opinion in Structural Biology, EMBO Journal, Faseb Journal, Genes and Development, Genome Research, Human Molecular Genetics, Immunity, Journal of Biological Chemistry, Journal of Experimental Medicine, Journal of Immunology, Journal of Neuroscience, Journal of the American Chemical Society, Molecular and Cellular Biology, Molecular and Cellular Proteomics, Molecular Cell, Nano Letters, Nature, Nature Immunology, Nature Materials, Nature Structural & Molecular Biology, Neuron, Nucleic Acids Research, Physical Review Letters, PNAS, Reports on Progress in Physics, Science, Structure, Trends in Biochemical Sciences, and Trends in Neurosciences. Two additional journals are included in the premier list, Applied Physics Letters (impact factor 4.0) and Environmental Sciences and Technology (impact factor 3.6), because these journals represent the "best in class" for the NSLS industrial and environmental science users, even though their impact factors are less than 6.

In FY 2006, NSLS users and staff had 921 publications – a record high for the facility. Moreover, 228 papers were published in premier journals, representing 25% of the total publications from the facility, and demonstrating the high impact of NSLS science.

NSLS USERS

Beamline U1A

S Buzby, M Barakat, H Lin, C Ni, S Rykov, J Chen, S Shah, Visible Light Photocatalysis with Nitrogen-Doped Titanium Dioxide Nanoparticles Prepared by Plasma Assisted Chemical Vapor Deposition, *J. Vac. Sci. Technol., B*, **24** (3), 1210 (2006).

G Liu, K Rider, W Nam, S Fonash, S Kim, Dendritic Aggregation of Oligothiophene During Desorption of 2,5-Diiodothiophene Multilayer and Topography-Induced Alignment of Oligothiophene Nanofibers, *J. Phys. Chem. B*, **110**, 20197-20201 (2006).

M Smith, R Lobo, The Local and Surface Structure of Ordered Mesoporous Carbons from Nitrogen Sorption, NEXAFS and Synchrotron Radiation Studies, *Microporous Mesoporous Mater.*, **92** (1-3), 81-93 (2006).

Beamline U2A

J Ciezak, T Jenkins, Z Liu, R Hemley, High Pressure Vibrational Spectroscopy of Energetic Materials: Hexahydro-1,3,5-trinitro-1,3,5-triazine, *J. Phys. Chem. A*, **59-63**, 5 (2006).

L Dobrzhinetskaya, Z Liu, P Cartigny, J Zhang, D Tchkhetia, R Hemley, H Green, Synchrotron infrared and Raman spectroscopy of microdiamonds from Erzgebirge, Germany, *Earth Planet Sci. Lett.*, **248**, 325-334 (2006).

S Ho, C Yan, Z Liu, H Mao, R Hemley, Prospects for Large Single Crystal CVD Diamonds, *Ind. Diamond Rev.*, **66**, 28-32 (2006).

G Iezzi, Z Liu, G Ventura, Synchrotron Infrared SpectroscopyofSyntheticNa(NaMg)Mg5Si8O22(OH)2 up to 30 GPa: Insight on a New High-Pressure Amphibole Polymorph, *Am. Mineral.*, **91**, 479-482 (2006).

D Klug, J Tse, Z Liu, R Hemley, Hydrogen-bond Dynamics and Fermi Resonance in High-pressure Methane Filled Ice, *Chem. Phys.*, **125**, 154509 (2006).

J Smedley, I Ben-Zvi, A Burrill, X Chang, J Grimes, T Rao, Z Segalov, Q Wu, Electron Amplification in Diamond, *2006 Workshop on Advanced Accelerator Concepts (AAC06)*, Vol 887, p. 672-4, sponsored by Argonne National Laboratory (2006).

H Zhang, B Chen, B Gilbert, J Banfield, Kinetically Controlled Formation of a Novel Nanoparticulate ZnS with Mixed Cubic and Hexagonal Stacking, *J Mater. Chem.*, **16** (3), 249-254 (2006).

Beamline U2B

K Jones, H Feng, E Stern, U Neuhausler, J Osan, N Marinkovic, Z Song, Properties of New York/New Jersey Harbor Sediments, *Acta Phys. Pol. A*, **109** (3), 279-286 (2006).

J Smedley, I Ben-Zvi, A Burrill, X Chang, J Grimes, T Rao, Z Segalov, Q Wu, Electron Amplification in Diamond, *2006 Workshop on Advanced Accelerator Concepts (AAC06)*, Vol 887, p. 672-4, sponsored by Argonne National Laboratory (2006).

P Yu, An Emerging Method for Rapid Characterization of Feed Structures and Feed Component Matrix at a Cellular Level and Relation to Feed Quality and Nutritive Value, *Arch. Anim. Nutr.*, **60**, 229-244 (2006).

Beamline U3C

G Rochau, J Bailey, G Chandler, T Nash, D Nielsen, G Dunham, O Garcia, N Joseph, J Keister, et al., Energy Dependent Sensitivity of Microchannel Plate Detectors, *Rev. Sci. Instrum.*, **77**, 10E323 (2006).

C Sorce, J Schein, F weber, K Widmann, K Campbell, E Dewald, R Turner, O Landen, K Jacoby, et al., Soft X-ray Power Diagnostic Improvements at the Omega Laser Facility, *Rev. Sci. Instrum.*, **77**, 10E518 (2006).

Beamline U4A

T Ellis, K Park, M Ulrich, S Hulbert, J Rowe, Interaction of Metallophthalocyanines (Mpc, M=Co, Ni) on Au(001): Ultraviolet Photoemission Spectroscopy and Low Energy Electron Diffraction Study, *J. Appl. Phys.*, **100**, 093515-10 (2006).

A Mathew, Study of Interfacila Phenomena in Thin Films using Photoelectron Spectroscopy, M.S. Thesis, University of Delaware, Newark (2006).

E Nemanick, P Hurley, L Webb, D Knapp, D Michalak, B Brunschwig, N Lewis, Chemical and Electrical Passivation of Single-Crystal Silicon(100) Surfaces Through a Two-Step Chlorination/Alkylation Process, *J. Phys. Chem. B*, **110**, 14770-14778 (2006).

R O'Connor, G Hughes, P Glans, T Learmonth, K Smith, X-ray Photoemission and X-ray Absorption Studies of Hf-silicate Dielectric Layers, *Appl. Surf. Sci.*, **253** (5), 2770-2775 (2006).

R O'Connor, S McDonnell, G Hughes, K Smith, Photoemission Studies of Pulsed-RF Plasma Nitrided Ultra-thin SiON Dielectric Layers, *Surf. Sci.*, **600**, 532-536 (2006).

M Traub, J Biteen, D Michalak, L Webb, B Brunschwig, N Lewis, High-Resolution X-ray Photoelectron Spectroscopy of Chlorine-Terminated GaAs(111)A Surfaces, *J. Phys. Chem. B*, **110**, 15641-15644 (2006).

M Ulrich, J Rowe, J Keister, H Niimi, L Fleming, G Lucovsky, Comparison of Ultrathin SiO2/Si(100) and SiO2/Si(111) Interfaces from Soft X-ray Photoelectron Spectroscopy, *J. Vac. Sci. Technol., B*, **24**, 2132 (2006).

Beamline U4B

D Hill, D Arena, R Bartynski, P Wu, G Saraf, Y Lu, I Wielunski, R Gateau, J Dvorak, et al., Room Temperature Ferromagnetism in MN Ion Implanted Epitaxial ZnO Films, *Phys. Status Solidi (a)*, **203** (15), 3836-3843 (2006).

C Kinane, A Suszka, C Marrows, B Hickey, D Arena, J Dvorak, T Charlton, S Langridge, Soft x-ray resonant magnetic scattering from an imprinted magnetic domain pattern , *Appl. Phys. Lett.*, **89**, 092507 (2006).

E Negusse, J Holroyd, M Liberati, J Dvorak, Y Idzerda, T Santos, J Moodera, E Arenholz, Effect of Electrode and EuO Thickness on EuO-Electrode Interface in Tunneling Spin Filter, *J. Appl. Phys.*, **99**, 08E507 (2006).

K Neupane, J Shearer, Influence of Amide/Amine vs Nis-Amide Coordination in Nickel Superoxide Dismutase, *Inorg. Chem.*, **45**, 10552-10566 (2006).
H Noh, S Yeo, J Kang, C Zhang, S Cheong, S Oh, P Johnson, Jahn-Teller Effect in Spinel Manganites Probed by Soft X-ray Absorption Spectroscopy, *Appl. Phys. Lett.*, **88**, 081911 (2006).
P Wu, G Saraf, Y Lu, D Hill, R Gateau, L Wielunski, R Bartynski, D Arena, J Dvorak, et al., Ferromagnetism in Fe-Implanted a-plane ZnO Films, *Appl. Phys. Lett.*, **89**, 012508 (2006).
S Yoon, Y Chen, A Yang, T Goodrich, X Zuo, D Arena, K Ziemer, C Vittoria, V Harris, Oxygen-defect-induced Magnetism to 880 K in Semiconducting Anatase TiO2-delta Films, *J. Phys.: Condens. Matter*, **18** (27), L355-L361 (2006).

Beamline U4IR

H Liu, M Quijada, D Romero, D Tanner, A Zibold, G Carr, H Berger, L Forro, L Mihaly, et al., Drude Behavior in the Far-Infrared Conductivity of Cuprate Superconductors, *Ann. Phys.*, **15** (7), 606-618 (2006).

Beamline U5UA

I Baek, W Kim, E Vescovo, H Lee, Effect of Ni Concentration on Quantum-well States of the Alloy System Ag/Fe1-xNix: A Spin- and angle-Resolved Photoemission Study, *Phys. Rev. B*, **74**, 113302 (2006).
L Colakerol, T Veal, H Jeong, L Plucinski, A DeMasi, T Learmonth, P Glans, S Wang, Y Zhang, et al., Quantized Electron Accumulation States in Indium Nitride Studied by Angle-Resolved Photoemission Spectroscopy, *Phys. Rev. Lett.*, **97**, 237601 (2006).
H Lee, I Baek, S Kim, E Vescovo, Electronic and Magnetic Properties in Fe-Based Fe1-xNix, Fe1-xCox, and Fe1-xVx Films on W(110), *Surf. Sci.*, **600**, 4137-4142 (2006).
H Lee, I Baek, E Vescovo, Spin Reorientation Transition in Fe-Rich Alloy Films on W(110): The Role of Magnetoelastic Anisotropy and Structural Transition, *Appl. Phys. Lett.*, **89**, 112516 (2006).
E Vescovo, Reply to “Comment on `Oxidation of the Fe(110) surface: An Fe3O4(111)/Fe(110) bilayer’ “, *Phys. Rev. B: Condens. Matter*, **74**, 26406 (2006).
E Vescovo, Spin-Resolved Photoemission Studies of Magnetic Films, *Modern Techniques for Characterizing Magnetic Materials* , p. 600, Kluwer Academic Pub, New York (2006).

Beamline U7A

B Clare, K Efimenko, D Fischer, J Genzer, N Abbott, Orientations of Liquid Crystals in Contact with Surfaces that Present Continuous Gradients of Chemical Functionality, *Chem. Mater.*, **18**, 2357-2363 (2006).
D DeLongchamp, Y Jung, D Fischer, E Lin, P Chang, V Subramanian, A Murphy, J Frechet, Correlating Molecular Design to Microstructure in Thermally Convertible Oligothiophenes: The Effect of Branched Versus Linear End Groups, *J. Phys. Chem. B*, **110**, 10645-10650 (2006).
D DeLongchamp, M Ling, Y Jung, D Fischer, M Roberts, E Lin, Z Bao, Thickness Dependence of Microstructure in Semiconducting films of an Oligofluorene Derivative, *J. Am. Chem. Soc.*, **128**, 16579-16586 (2006).

D Fischer, A Moodenbaugh, Q Li, G Gu, Y Zhu, J Davenport, D Welch, Soft X-ray Absorption Spectroscopy of the MgB2 Boron K Edge in an MgB2/Mg Composite, *Mod. Phys. Lett. B*, **20** (19), 1207-1216 (2006).
J Genzer, K Efimenko, D Fischer, Formation Mechanisms and Properties of Semifluorinated Molecular Gradients on Silica Surfaces, *Langmuir*, **22**, 8532-8541 (2006).
B Haines, Catalytic Hydrodechlorination of Chlorinated Aromatics on the Pt(111) Surface, Ph.D. Thesis, University of Michigan, Ann Arbor (2006).
T Hemraj-Benny, S Banerjee, S Sambasivan, M Balasubramanian, D Fischer, D Lowndes, W Han, J Misewich, S Wong, et al., Near-Edge X-ray Absorption Fine Structure Spectroscopy as a Tool for Investigating Nanomaterials, *Small*, **2** (1), 26-35 (2006).
T Hemraj-Benny, Investigating the Structural and Electronic Properties of Carbon Nanotubes upon Chemical Functionalization and Purification, Ph.D. Thesis, Stony Brook University, Stony Brook (2006).
A Hexemer, Order and Disorder of Block Copolymers and Particles on Surfaces with Topology, PhD Thesis, UCSB, Santa Barbara (2006).
D Krapchetov, H Ma, A Jen, D Fischer, Y Loo, High-Sensitivity Transmission IR Spectroscopy for the Chemical Identification and Structural Analysis of Conjugated Molecules on Gallium Arsenide Surfaces, *Langmuir*, **22**, 9491-9494 (2006).
S Krishnan, R Ward, A Hexemer, K Sohn, K Lee, E Angert, D Fischer, E Kramer, C Ober, Surfaces of Fluorinated Pyridinium Block Copolymers with Enhanced Antibacterial Activity, *Langmuir*, **22** (26), 11255-11266 (2006).
S Krishnan, R Ayothi, A Hexemer, J Finlay, K Sohn, R Perry, C Ober, E Kramer, M Callow, et al., Anti-Biofouling Properties of Comblike Block Copolymers with Amphiphilic Side Chains, *Langmuir*, **22** (11), 5075-5086 (2006).
S Krishnan, N Wang, C Ober, J Finlay, M Callow, J Callow, A Hexemer, K Sohn, E Kramer, D Fischer, Comparison of the Fouling Release Properties of Hydrophobic Fluorinated and Hydrophilic PEGylated Block Copolymer Surfaces, *Biomacromolecules*, **7** (5), 1449-1462 (2006).
S Krishnan, C Ober, A Hexemer, E Kramer, D Fischer, Compositional Depth Profiling of Block Copolymer Surfaces using NEXAFS, *Polym. Mater. Sci. Eng.*, **94**, 672-673 (2006).
C Lee, P Gong, G Harbers, D Grainger, D Castner, L Gamble, Surface Coverage and Structure of Mixed DNA/Alkylthiol Monolayers on Gold: Characterization by XPS, NEXAFS, and Fluorescence Intensity Measurements, *Anal. Chem.*, **78**, 3316-3325 (2006).
C Lee, L Gamble, D Grainger, D Castner, Mixed DNA/Oligo(ethylene glycol) Functionalized Gold Surface Improve DNA Hybridization in Complex Media, *Biointerphases*, **1**, 82-92 (2006).
L Lewis, D Yoder, A Moodenbaugh, D Fischer, M Yu, Magnetism and the Defect state in the Magnetocaloric Antiperovskite Mn3GaC1-ä, *J. Phys.: Condens. Matter*, **18**, 1677-1686 (2006).

A Nambu, J Graciani, J Rodriguez, Q Wu, E Fujita, J Fdez Sanz , N Doping of TiO2(110): Photoemission and Density-Functional Studies, *J. Chem. Phys.*, **125**, 094706 (2006).

L Pattison, A Hexemer, P Petroff, E Kramer, D Fischer, NEXAFS Determination of the Orientation of a Conjugated Liquid Crystalline Polymer Film on a Rubbed Polyimide Alignment Layer, *Polym. Mater. Sci. Eng.*, **94**, 216-217 (2006).

L Pattison, A Hexemer, E Kramer, S Krishnan, P Petroff, D Fischer, Probing the Ordering of Semiconducting Fluorene-Thiophene Copolymer Surfaces on Rubbed Polyimide Substrates by Near-Edge X-ray Absorption Fine Structure, *Macromolecules*, **39**, 2225-2231 (2006).

V Prabhu, S Sambasivan, D Fischer, L Sunberg, R Allen, Quantitative Depth Profiling of Photoacid Generators in Photoresist Materials by Near-edge X-ray Absorption Fine Structure Spectroscopy, *Appl. Surf. Sci.*, **253**, 1010-1014 (2006).

S Rendon, Processing, Structure, and Property Relationships in Commercial Thermotropic Liquid Crystalline Polymers, Ph. D. Thesis, Northwestern University, Evanston (2006).

S Sambasivan, S Shieh, D Fischer, S Hsu, Effect of Self-Assembled Monolayer Film Order on Nanofriction, *J. Vac. Sci. Technol., A*, **24** (4), 1484 (2006).

N Samuel, C Lee, L Gamble, D Fischer, D Castner, NEXAFS Characterization of DNA Components and Molecular-Orientation of Surface-Bound DNA Oligomers, *J. Electron. Spectrosc. Relat. Phenom.*, **152**, 134-142 (2006).

M Smith, J Tong, J Genzer, D Fischer, P Kilpatrick, Effects of Synthetic Amphiphilic alpha-Helical Peptides on the Electrochemical and Structural Properties of Supported Hybrid Bilayers on Gold, *Langmuir*, **22** (4), 1919-1927 (2006).

C Xu, S Barnes, T Wu, D Fischer, D DeLongchamp, J Batteas, K Beers, Solution and Surface Composition Gradients via Microfluidic Confinement: Fabrication of a Statistical-Copolymer-Brush Composition Gradient, *Advanced Materials*, **18** (11), 1427-1430 (2006).

X Zhao, J Rodriguez, Photoemission Study of Glycine Adsorption on Cu/Au (111) Interfaces, *Surf. Sci.*, **600** (10), 2113-2121 (2006).

Beamline U8B

T Owens, K Nicholson, D Fosnancht, B Orr, M Banaszak Holl, Formation of Mixed Monolayers of Silsesquioxanes and Alkylsilanes on Gold, *Langmuir*, **22**, 9619-9622 (2006).

Beamline U9B

Y Nie, J Hobbs, S Vigues, W Olson, G Conn, S Munger, Expression and Purification of Functional Ligand-binding Domains of T1R3 Taste Receptors, *Chem. Senses*, **31**, 505-513 (2006).

Beamline U10A

C Homes, S Dordevic, G Gu, Q Li, T Valla, J Tranquada, Charge Order, Metallic Behavior, and Superconductivity in La{2-x}Ba{x}CuO{4} with x = 1/8, *Phys. Rev. Lett.*, **96**, 257002 (2006).

Beamline U10B

M Gallant, M Rak, A Szeghalmi, M Del Bigio, D Westaway, J Yang, R Julian, K Gough, Focally Elevated Creatine Detected in Amyloid Precursor Protein (APP) Transgenic Mice and Alzheimer Disease Brain Tissue, *J. Biol. Chem.*, **281** (1), 5-8 (2006).

A Kretlow, Q Wang, J Kneipp, P Lasch, M Beekes, L Miller, D Naumann, FTIR-Microspectroscopy of Prion-Infected Nervous Tissue, *Biochim Biophys Acta*, **1758**, 948-959 (2006).

J Miklossy, A Kis, A Radenovic, L Miller, L Forro, R Martins, K Reiss, N Darbinian, P Darekar, et al., Beta-Amyloid Deposition and Alzheimer's Type Changes Induced by Borrelia Spirochetes, *Neurobiol. Aging*, **27**, 228-236 (2006).

L Miller, P Dumas, Chemical Imaging of Biological Tissue with Synchrotron Infrared Light, *Biochim Biophys Acta*, **1758** (7), 846-57 (2006).

L Miller, Q Wang, T Telivala, R Smith, A Lanzirotti, J Miklossy, Synchrotron-based Infrared and X-ray Imaging Shows Focalized Accumulation of Cu and Zn Co-localized With Beta-amyloid Deposits in Alzheimer's Disease, *J. Struct. Biol.*, **155** (1), 30-37 (2006).

P Ramasamy, Interactions of Proteins in Gels, Solutions and on Surfaces, Ph.D. Thesis, State University of Newyork at Stony Brook, Stony Brook (2006).

M Ruppel, D Burr, L Miller, Chemical Makeup of Microdamaged Bone Differs from Undamaged Bone, *Bone*, **39** (2), 318-324 (2006).

S Sandford, J Aleon, C Alexander, T Araki, S Bajt, G Baratts, J Borg, J Bradley, D Brownlee, et al., Organics Captured from Comet 81P/Wild2 by the Stardust Spacecraft, *Science*, **314** (5806), 1720-1724 (2006).

S Seaman, E Helfrich, M Dyar, The Role of Water in the Growth and Texture of Spherulites in Rhyolitic Lava Flows, *Geological Society of America Annual Meeting*, Vol 38, p. 167, sponsored by Geological Society of America (2006).

S Seaman, M Dyar, N Marinkovic, N Dunbar, An FTIR Study of Hydrogen in Anorthosite and Associated Melt Inclusions, *Am. Mineral.*, **91** (1), 12-20 (2006).

F Serrano, L Lopez, M Jadraque, M Koper, G Ellis, P Cano, M Martin, L Garrido, A Nd:YAG Laser-microperforated poly(3-hydroxybutyrate-co-3-hydroxyvalerate)-basal Membrane Matrix Composite film as Substrate for Keratinocytes, *Biomaterials*, **28** (4), 650-660 (2006).

J Torre, M Cortazar, M Gomez, C Marco, G Ellis, C Rickel, P Dumas, Nature of the Crystalline Interphase in Sheared IPP/Vectra Fiber Model Composites by Microfocus X-ray Diffraction and IR Microspectroscopy using Synchrotron Radiation, *Macromolecules*, **39**, 5564-5568 (2006).

L Xie, J Jacobsen, B Busa, L Donahue, L Miller, C Rubin, S Judex, Low-Level Mechanical Vibrations can Reduce Bone Resorption and Enhance Bone Formation in the Growing Skeleton, *Bone*, **39** (5), 1059-1056 (2006).

P Yu, An Emerging Method for Rapid Characterization of Feed Structures and Feed Component Matrix at a Cellular Level and Relation to Feed Quality and Nutritive Value, *Arch. Anim. Nutr.*, **60**, 229-244 (2006).

Beamline U11

Y Nie, J Hobbs, S Vigues, W Olson, G Conn, S Munger, Expression and Purification of Functional Ligand-binding Domains of T1R3 Taste Receptors, *Chem. Senses*, **31**, 505-513 (2006).

Beamline U12A

D Mullins, M Robbins, J Zhou, Adsorption and Reaction of Methanol on Thin-film Cerium Oxide, *Surf. Sci.*, **600**, 1547-1558 (2006).

D Mullins, Adsorption of CO and C2H4 and Rh-loaded Thin-film Dysprosium Oxide, *Surf. Sci.*, **600** (13), 2718-2725 (2006).

S Senanayake, H Idriss, Photocatalysis and the Origin of Life: Synthesis of Nucleoside Bases from Formamide on TiO2(001) Single Surfaces, *Proc Natl Acad Sci USA*, **103** (5), 1194-1198 (2006).

J Zhou, D Mullins, Adsorption and Reaction of Formaldehyde on Thin-film Cerium Oxide, *Surf. Sci.*, **600**, 1540-1546 (2006).

J Zhou, D Mullins, Rh-Promoted Methanol Decomposition on Cerium Oxide Thin Films, *J. Phys. Chem. B*, **110**, 15994-16002 (2006).

Beamline U12IR

L Mihaly, B Dora, A Vanyolos, H Berger, L Forro, Spin-Lattice Interaction in the Quasi-One-Dimensional Helimagnet LiCu2O2, *Phys. Rev. Lett.*, **97**, 067206 (2006).

S Washburn, Novel Polymer Nanofilms from a Topochemical Deposition/Polymerization Process, Ph.D. Thesis, University of Delaware, Newark (2006).

Beamline U13UB

T Valla, T Kidd, J Rameau, H Noh, G Gu, P Johnson, H Yang, H Ding, Fine Details of the Nodal Electronic Excitations in Bi2Sr2CaCu2O8+gamma, *Phys. Rev. B*, **73**, 184518 (2006).

Beamline X1A1

M Anderson, T Haraszti, G Peterson, S Wirick, C Jacobsen, S John, M Grunze, Scanning Tranmission X-ray Microscopic Analysis of Purifed Melanosomes of the Mouse Iris, *Micron*, **37** (8), 689-698 (2006).

A Braun, S Wirick, A Kubatova, B Mun, F Huggins, Photochemically Induced Decarboxylation in Diesel Soot Extracts, *Atmos. Environ.*, **40** (30), 5837-5844 (2006).

D Brownlee, P Tsou, J Aléon, C Alexander, T Araki, S Bajt, G Baratta, R Bastien, P Bland, et al., Comet 81P/Wild 2 Under a Microscope, *Science*, **314** (5806), 1711 - 1716 (2006).

B DeGregorio, Structure, Bonding and Composition of Carbonaceous Material in Precambrian Cherts, Ph.D Thesis, Arizon State University, Tempe (2006).

M Denecke, P Panak, M Plaschke, J Rothe, M Weigl, Spectroscopic Actinide Speciation for Nuclear Waste Disposal, *Recent Advances in Actinide Science (ACTINIDES 2005)*, Vol 305, p. 673-679, (2006).

M Denecke, Actinide Speciation using X-ray Spectroscopic Methods, *Coordin. Chem. Rev.*, **250**, 730-754 (2006).

M Feser, B Hornberger, C Jacobsen, G De Geronimo, P Rehak, P Holl, L Struder, Integrating Silicon Detector with Segmentation for Scanning Transmission X-ray Microscopy, *Nucl. Instrum. Meth. A*, **565**, 841-854 (2006).

P Haberstroh, J Brandes, Y Gelinas, A Dickens, S Wirick, G Cody, Chemical Composition of the Graphitic Black Carbon Fraction in Riverine and Marine Sediments at Submicron Scales using Carbon X-ray Spectromicroscopy, *Geochim. Cosmochim. Acta*, **70** (6), 1483-1494 (2006).

B Hornberger, M Feser, C Jacobsen, S Vogt, D Legnini, D Paterson, P Rehak, G De Geronimo, B Palmer, Combined Fluorescence and Phase Contrast Imaging at the Advanced Photon Source, *8th International Conference on X-ray Microscopy*, Vol IPAP Conference Series 7, p. 396-398, sponsored by S Aoki et al. (2006).

J Kinyangi, D Solomon, B Liang, M Lerotic, S Wirick, J Lehmann, Nanoscale Biogeocomplexity of the Organomineral Assemblage in Soil: Application of STXM Microscopy and C 1s-NEXAFS Spectroscopy, *Soil Sci. Soc. Am. J.*, **70** (5), 1708-1718 (2006).

B Liang, J Lehmann, D Solomon, J Kinyangi, J Grossman, B O'Neill, J Skjemstad, J Thies, F Luizão, et al., Black Carbon Increases Cation Exchange Capcity in Soils, *Soil Sci. Soc. Am. J.*, **70**, 1719-1730 (2006).

M Lu, Nanofabrication of Fresnel zone plates for soft X-ray imaging at carbon edge, Ph.D Thesis, SUNY at StonyBrook, StonyBrook (2006).

M Lu, D Tennant, C Jacobsen, Orientation Dependence of Linewidth Variation in sub-50-nm Gaussian e-beam Lithography and its Correction, *J. Vac. Sci. Technol., B*, **24** (6), 2881 (2006).

L Lucai, H Nanko, A Rudie, D Mancosky, S Wirick, The Use of C-near Edge X-ray Absorption Fine Structure Spectroscopy for the Elaboration of Chemistry in Lignocellulosics, *2006 TAPPI International Conference on Nanotechnology*, Vol 2006, p. 8, sponsored by TAPPI (2006).

A Naber, M Plaschke, J Rothe, H Hofmann, T Fanghänel, Scanning Transmission X-ray and Laser Scanning Luminescence Microscopy of the Carboxyl Group and Eu(III) Distribution in Humic Acid Aggregates, *J. Electron. Spectrosc. Relat. Phenom.*, **153**, 71-74 (2006).

S Sandford, J Aleon, C Alexander, T Araki, S Bajt, G Baratts, J Borg, J Bradley, D Brownlee, et al., Organics Captured from Comet 81P/Wild2 by the Stardust Spacecraft, *Science*, **314** (5806), 1720-1724 (2006).

M Schumacher, I Christl, R Vogt, K Barmettler, C Jacobsen, R Kretzschmar, Chemical Composition of Aquatic Dissolved Organic Matter in Five Boreal Forest Catchments Sampled in Spring and Fall Seasons, *Biogeochemistry*, **80**, 263-275 (2006).

J Steinbrener, Scanning luminesence X-ray microscopy exploring the use of quantum dot nanocrystals as high spatial resolution biological labels, MS Thesis, Stony Brook University, StonyBrook (2006).

M Zolensky, T Zega, H Yano, S Wirick, A Westphal, M Weisberg, I Weber, J Warren, M Velbel, et al., Mineralogy and Petrology of Comet 81P/Wild 2 Nucleus Samples, *Science*, **314** (5806), 1735 - 1739 (2006).

Beamline X1A2

M Feser, B Hornberger, C Jacobsen, G De Geronimo, P Rehak, P Holl, L Struder, Integrating Silicon Detector with Segmentation for Scanning Transmission X-ray Microscopy, *Nucl. Instrum. Meth. A*, **565**, 841-854 (2006).

B Hornberger, M Feser, C Jacobsen, S Vogt, D Legnini, D Paterson, P Rehak, G De Geronimo, B Palmer, Combined Fluorescence and Phase Contrast Imaging at the Advanced Photon Source, *8th International Conference on X-ray Microscopy*, Vol IPAP Conference Series 7, p. 396-398, sponsored by S Aoki et al. (2006).

M Lu, Nanofabrication of Fresnel zone plates for soft X-ray imaging at carbon edge, Ph.D Thesis, SUNY at StonyBrook, StonyBrook (2006).

M Lu, D Tennant, C Jacobsen, Orientation Dependence of Linewidth Variation in sub-50-nm Gaussian e-beam Lithography and its Correction, *J. Vac. Sci. Technol., B*, **24** (6), 2881 (2006).

J Steinbrener, Scanning luminesence X-ray microscopy exploring the use of quantum dot nanocrystals as high spatial resolution biological labels, MS Thesis, Stony Brook University, StonyBrook (2006).

Beamline X1B

P Abbamonte, Charge Modulations Versus Strain Waves in Resonant X-ray Scattering, *Phys. Rev. B*, **74**, 195113 (2006).

A Rusydi, P Abbamonte, H Eisaki, Y Fujimaki, G Blumberg, S Uchida, G Sawatzky, Quantum Melting of the Hole Crystal in the Spin Ladder of Sr14-xCaxCu24O41, *Phys. Rev. Lett.*, **97**, 016403 (2006).

H Tian, C Reece, M Kelley, S Wang, L Plucinski, K Smith, M Nowell, Surface Studies of Niobium Chemically Polished Under Conditions for Superconducting Radio Frequency (SRF) Cavity Production, *Appl. Surf. Sci.*, **253** (3), 1236-1242 (2006).

S Wilkins, N Stojic, T Beale, N Binggeli, P Hatton, P Bencock, S Stanescu, J Mitchell, P Abbamonte, M Altarelli, Separating the Causes of Orbital Ordering in LaSr2Mn2O7 using Resonant Soft X-ray Diffraction, *J. Phys.: Condens. Matter*, **18** (24), L323-L329 (2006).

Y Zhang, J Downes, S Wang, T Learmonth, L Plucinski, A Matsuura, C McGuinness, P Glans, S Bernardis, et al., Electronic Structure in Thin Film Organic Semiconductors Studied using Soft X-ray Emission and Resonant Inelastic X-ray Scattering, *Thin Solid Films*, **515**, 394-400 (2006).

Beamline X2B

B Borah, T Dufresne, E Ritman, S Jorgensen, S Liu, P Chmielewski, R Phipps, X Zhou, J Sibonga, R Turner, Long-term Risedronate Treatment Normalizes Mineralization and Continues to Preserve Trabecular Architecture: Sequential Triple Biopsy Studies with Micro-Computed Tomography, *Bone*, **39** (2), 345-352 (2006).

S Erdo, Determination of Aggregate Shape Properties Using X-Ray Tomographic Methods and the Effect of Shape on Concrete Rheology, Ph.D Thesis, The University of Texas, Austin (2006).

S Jorgensen, D Eaker, A Vercnocke, E Ritman, Reproducibility of 3D Micro-CT Gray-Scale and Structural Dimension Dte in Longitudinal Studies, *Medical Imaging 2006: Physiology, Function, and Structure from Medical Images*, Vol 6143 ll, p. 61433, sponsored by SPIE (2006).

M Prodanovic, W Lindquist, R Seright, Porous Structure and Fluid Partitioning in Polyethylene Cores from 3D X-ray Microtomographic Imaging, *J. Colloid Interface Sci.*, **298** (1), 282-297 (2006).

M Taylor, E Garboczi, S Erdoğan, D Fowler, Some Properties of Irregular 3-D Particles, *Powder Technol.*, **162** (1), 1-15 (2006).

Beamline X3A

B Manjasetty, A Turnbull, K Bussow, M Chance, Recent Advances in Protein Structure Analysis , *Recent Research Developments in Biochemistry*, p. 47-71, Transworld Research Network, Trivandrum (2006).

Beamline X3A1

S Park, H Boysen, J Parise, Structural Disorder of a New Zeolite-like Lithosilicate, K2.6Li5.4[Li4Si16O38]4.3H2O, *Acta Cryst. B*, **62**, 42-51 (2006).

Beamline X3B

A Huq, P Stephens, Crystal Structure of Rb4C60 Under Pressure: X-ray Diffraction Experiments, *Phys. Rev. B*, **74**, 075424 (2006).

J Majzlan, B Kiefer, An X-ray and Neutron Diffraction and Ab-initio Study of the Crystal Structure of Ferricopiapite, Fe14/3(SO4)6(OH)2(H2O)20, *Can. Mineral*, **44**, 1227-1237 (2006).

D Orosel, R Dinnebeier, M Jansen, High-Pressure Synthesis and Structure Determination of K6(SeO4)(SeO5), The First Potassium Orthoselenate(VI), *Inorg. Chem.*, **45**, 10947-10950 (2006).

Y Soo, W Sun, S Weng, Y Lin, S Chang, L Jang, X Wu, Y Yan, Local Environment sSrrounding S and Cd in CdS:O Thin Film Photovoltaic Materials Probed by X-ray Absorption Fine Structures, *Appl. Phys. Lett.*, **89**, 131908 (2006).

K Sugimoto, R Dinnebier, T Schlecht, Chlorartinite, A Volcanic Exhalation Product Also Found in Industrial Magnesia Screed, *J. Appl. Cryst.*, **39**, 739-744 (2006).

S Ziemniak, M Hanson, Zinc Treatment Effects on Corrision Behavior of 302 Stainless Steel in High Temperature, Hydrogenated Water, *Corros. Sci.*, **48** (9), 2525-2546 (2006).

S Ziemniak, M Hanson, Corrosion Behavior of NiCrFe Alloy 600 in High Temperature, Hydrogenated Water, *Corros. Sci.*, **48**, 498-521 (2006).

Beamline X3B1

R Bune, M Lobanov, G Popov, M Greenblatt, C Botez, P Stephens, M Croft, J Hadermann, G Van Tendeloo, Crystal Structure and Properties of Ru-Stoichiometric LaSrMnRuO6, *Chem. Mater.*, **18**, 2611-2617 (2006).

J Burley, J van de Streek, P Stephens, Ampicillin Trihydrate from Synchrotron Powder Diffraction Data, *Acta Cryst. E*, **62**, o797-o700 (2006).

R Dinnebier, N Sofina, L Hildebrandt, M Jansen, Crystal Structures of the Trifluoromethyl Sulfonates M(SO3CF3)2 (M = Mg, Ca, Ba, Zn, Cu) from Synchrotron X-ray Powder Diffraction Data, *Acta Cryst. B*, **62**, 467-473 (2006).

J Gubicza, T Ungar, Y Wang, G Voronin, C Pantea, T Zerda, Microstructure of Diamond-SiC Nanocomposites Determined by X-ray Line Profile Analysis, *Diamond Relat. Mater.*, **15** (9), 1452-1456 (2006).

A Huq, P Stephens, N Ayed, H Binous, L Burgio, R Clark, E Pantos, Combined Technique Analysis of Punic Make-up Materials, *Appl. Phys. A*, **83**, 253-256 (2006).

A Huq, J Mitchell, H Zheng, L Chapon, P Radaelli, K Knight, P Stephens, Structural and Magnetic Properties of the Kagome Antiferromagnet YbBaCo4O7, *J. Solid State Chem.*, **179** (4), 1136-1145 (2006).

J Majzlan, A Navrotsky, B McCleskey, C Alpers, Thermodynamic Properties and Crystal Structure Refinement of Ferricopiapite, Coquimbite, Rhomboclase, and Fe3(SO4)2(H2O)5, *Eur. J. Mineral.*, **18**, 175-186 (2006).

S McLain, M Dolgos, D Tennant, J Turner, T Barnes, T Proffen, B Sales, R Bewley, Magnetic Behaviour of Layered Ag(II) Fluorides, *Nat. Mater.*, **5**, 561 (2006).

M Rajeswaran, T Blanton, D Giesen, D Whitcomb, N Zumbulyadis, B Antalek, M Neumann, S Misture, Azine Bridged Silver Coordination Polymers: Powder X-ray Diffraction Route to Crystal Structure Determination of Silver Benzotriazole, *J. Solid State Chem.*, **179** (4), 1053-1059 (2006).

E Sileo, L Rodenas, C Paiva-Santos, P Stephens, P Morando, M Blesa, Correlation of Reactivity with Structural Factors in a Series of Fe(II) Substituted Cobalt Ferrites, *J. Solid State Chem.*, **179** (7), 2237-2244 (2006).

M Sun, A Nelson, J Adjaye, Examination of Spinel and Nonspinel Structural Models for gamma-Al2O3 by DFT and Rietveld Refinement Simulations, *J. Phys. Chem. B*, **110** (5), 2310-2317 (2006).

L Whaley, M Lobanov, D Sehptyakov, M Croft, K Ramanujachary, S Lofland, P Stephens, J Her, G Van Tendeloo, et al., Sr3Fe5/4Mo3/4O6.9, an n = 2 Ruddlesen-Popper Phase: Synthesis and Properties, *Chem. Mater.*, **18**, 3448-3457 (2006).

S Wishkerman, J Bernstein, P Stephens, Polymorphism in 4-Methoxy-3-nitrobenzaldehyde, *Cryst. Growth Des.*, **6** (6), 1366-1373 (2006).

Beamline X4A

J Akana, A Federov, E Federov, W Novak, P Babbitt, S Almo, J Gerlt, D-Ribulose 5-Phosphate 3-Epimerase: Functional and Structural Relationships to Members of the Ribulose-Phosphate Binding (beta/alpha)8-Barrel Superfamily, *Biochemistry*, **45**, 2493-2503 (2006).

N Armstrong, J Jasti, M Beich-Frandsen, E Gouaux, Measurement of Conformational Changes Accompanying Desensitization in an Ionotropic Glutamate Receptor, *Cell*, **127** (1), 85-97 (2006).

E Bergamin, J Wu, S Hubbard, Structural Basis for Phosphotyrosine Recognition by Suppressor of Cytokine Signaling-3, *Structure*, **14**, 1285-1292 (2006).

J Cordero-Morales, L Cuello, Y Zhao, V Jogini, D Cortes, B Roux, E Perozo, Molecular Determinants of Gating at the Potassium-Channel Selectivity Filter, *Nat. Struct. Mol. Biol.*, **13** (4), 311 (2006).

M Cosgrove, K Bever, J Avalos, S Muhammad, X Zhang, C Wolberger, The Structural Basis of Sirtuin Substrate Affinity, *Biochemistry*, **45**, 7511-7521 (2006).

Y Deng, J Liu, Q Zheng, W Yong, M Lu, Structures and Polymorphic Interactions of Two Heptad-Repeat Regions of the SARS Virus S2 Protein, *Structure*, **14** (5), 889-899 (2006).

Y Deng, J Liu, Q Zheng, D Eliezer, N Kallenbach, M Lu, Antiparallel Four-Stranded Coiled Coil Specified by a 3-3-1 Hyrdrophobic Heptad Repeat, *Structure*, **14**, 247-255 (2006).

J Faraldo-Gomez, E Kutluay, V Jogini, Y Zhao, L Heginbotham, B Roux, Mechanism of Intracellular Block of the KcsA K+ Channel by Tetrabutylammonium: Insights from X-ray Crystallography, Electrophysiology and Replica-exchange Molecular Dynamics Simulations, *J. Mol. Biol.*, **365** (3), 649-662 (2006).

S Gabelli, J McLellan, A Montalvetti, E Oldfield, R Docampo, L Amzel, Structure and Mechanism of the Farnesyl Diphosphate Synthase from Trypanosoma cruzi: Implications for Drug Design, *Proteins Struc. Func. Bioinformatics*, **62** (1), 80-88 (2006).

H Gennadios, D Whittington, X Li, C Fierke, D Christianson, Mechanistic Inferences from the Binding of Ligands to LpxC, A Metal-Dependent Deacetylase, *Biochemistry*, **45**, 7940-7948 (2006).

J Guhaniyogi, V Robinson, A Stock, Crystal Structures of Beryllium Fluoride-Free and Beryllium Fluoride-Bound CheY in Complex with the Conserved C-Terminal Peptide of CheZ Reveal Dual Binding Modes Specific to CheY Conformation, *J. Mol. Biol.*, **359** (3), 624-645 (2006).

Y Guo, Z Li, S Van Vranken, H Li, A Single Point Mutation Changes in the Crystallization Behavior of Mycoplasma arthritidis-derived Mitogen, *Acta Cryst. F*, **62**, 238-241 (2006).

W Holmes, G Jogl, Crystal Structure of Inositol Phosphate Multikinase 2 and Implications for Substrate Specificity, *J. Biol. Chem.*, **281** (49), 38109-38116 (2006).

J Hu, Structural Basis for Recruitment of the Adapter Proteins APS and SH2-B to the Insulin Receptor, PhD Thesis, New York University, New York (2006).

J Hu, S Hubbard, Structural Basis for Phosphotyrosine Recognition by the Src Homology-2 Domains of the Adapter Proteins SH2-B and APS, *J. Mol. Biol.*, **361** (1), 69-79 (2006).

T Kawate, E Gouaux, Fluorescence-Detectino Size-Exclusion Chromatography for Precrystallization Screening of Integral Membrane Proteins, *Structure*, **14** (4), 673-681 (2006).

J Khan, X Tao, L Tong, Molecular Basis for the Inhibition of Human NMPRTase, a Novel Target for Anticancer Agents , *Nat. Struct. Mol. Biol.*, **13** (7), 582 (2006).

D Lim, G Gregorio, C Bingman, E Martinez-Hackert, W Hendrickson, S Goff, Crystal Structure of the Moloney Murine Leukemia Virus RNase H Domain, *J. Virology*, **80**, 8379-8389 (2006).

J Liu, Q Zheng, Y Deng, N Kallenbach, M Lu, Conformational Transition Between Four and Five-Stranded Phenylalanine Zippers Determined by a Local Packing Interaction, *J. Mol. Biol.*, **361** (1), 168-179 (2006).

C Mandel, D Gebauer, H Zhang, L Tong, A Serendipitous Discover that in situ Proteolysis is Essential for the Crystallization of Yeast CPSF-100 (Ydh1p), *Acta Cryst. F*, **62**, 1041-1045 (2006).
C Mandel, S Kaneko, H Zhang, D Gebauer, V Vethantham, J Manley, L Tong, Polyadenylation Factor CPSF-73 is the Pre-mRNA 3'-end-processing Endonuclease, *Nature*, **444**, 953 (2006).
E Martinez-Hackert, N Anikeeva, S Kalams, B Walker, W Hendrickson, Y Sykulev, Structural Basis for Degenerate Recognition of Natural HIV Peptide Variants by Cytotoxic Lymphocytes, *J. Biol. Chem.*, **281** (29), 20205-20212 (2006).
J McLellan, S Yao, X Zheng, B Geisbrecht, R Ghirlando, P Beachy, D Leahy, Structure of a Heparin-dependent Complex of Hedgehog and Ihog, *Proc Natl Acad Sci USA*, **103** (46), 17208-13 (2006).
S Olsen, J Li, A Eliseenkova, O Ibrahimi, Z Lao, F Zhang, R Linhardt, A Joyner, M Mohammadi, Structural Basis by Which Alternative Splicing Modulates the Organizer Activity of FGF8 in the Brain, *Genes Dev.*, **20**, 185-198 (2006).
H Park, H Wu, Crystal Structure of RAIDD Death Domain Implicates Potential Mechanism of PIDDosome Assembly, *J. Mol. Biol.*, **357** (2), 358-364 (2006).
C Reid, M Rushe, M Jarpe, H Van Vlijmen, B Dolinski, F Qian, T Cachero, H Cuervo, M Yanachkova, C et al., Structure Activity Relationships of Monocyte Chemoattractant Proteins in Complex with a Blocking Antibody, *Protein Eng.*, **19**, 317 (2006).
Y Shen, C Chou, G Chang, L Tong, Is Dimerization Required for the Catalytic Activity of Bacterial Biotin Carboxylase?, *Mol. Cell*, **22**, 807 (2006).
L Silvian, P Jin, P Carmillo, P Boriack-Sjodin, C Pelletier, M Rushe, B Gong, D Sah, B Pepinsky, A Rossomando, Artemin Crystal Structure Reveals Insights into Heparan Sulfate Binding, *Biochemistry*, **45**, 6801-6812 (2006).
A Stiegler, S Burden, S Hubbard, Crystal Structure of the Agrin-Responsive Immunoglobulin-like Domains 1 and 2 of the Receptor Tyrosine Kinase MuSK, *J. Mol. Biol.*, **364** (3), 424-433 (2006).
M Teplova , Y Yuan, A Phan, L Malinina, S Ilin, A Teplov, D Patel, Structural Basis for Recognition and Sequestration of UUUOH 3 ' Temini of Nascent RNA Polymerase III Transcripts by La, a Rheumatic Disease Autoantigen, *Mol. Cell*, **21**, 75-85 (2006).
L Webb, D Michalak, J Biteen, B Brunschwig, A Chan, D Knapp, H Meyer, E Nemanick, M Traub, N Lewis, High-Resolution Soft X-ray Photoelectron Spectroscopic Studies and Scanning Auger Microscopy Studies of the Air Oxidation of Alkylated Silicon(111) Surfaces, *J. Phys. Chem. B*, **110**, 23450-23459 (2006).
W Yew, A Fedorov, E Fedorov, B Wood, S Almo, J Gerlt, Evolution of Enzymatic Activities in the Enolase Superfamily: D-Tartrate Dehydratase from Bradyrhizobium japonicum, *Biochemistry*, **45**, 14598-14608 (2006).
B Yu, W Edstrom, J Benach, Y Hamuro, P Weber, B Gibney, J Hunt, Crystal structures of catalytic complexes of the oxidative DNA/RNA repair enzyme AlkB, *Nature*, **439** (7078), 879-84 (2006).
A Yunus, C Lima, Lysine Activation and Functional Analysis of E2-Mediated Conjugation in the SUMO Pathway, *Nat. Struct. Mol. Biol.*, **13** (6), 491 (2006).

Beamline X4C

Y Hsiao, G Jogl, V Esser, L Tong, Crystal Structure of Rat Carnitine Palmitoyltransferase II (CPT-II), *Biochem. Biophys. Res. Commun.*, **346** (3), 974-980 (2006).
J Khan, X Tao, L Tong, Molecular Basis for the Inhibition of Human NMPRTase, a Novel Target for Anticancer Agents , *Nat. Struct. Mol. Biol.*, **13** (7), 582 (2006).
J Liu, Q Zheng, Y Deng, C Cheng, N Kallenbach, M Lu, A Seven-Helix Coiled Coil, *Proc Natl Acad Sci USA*, **103** (42), 15457-15462 (2006).
J Liu, Y Deng, Q Zheng, C Cheng, N Kallenbach, M Lu, A Parallel Coiled-Coil Tetramer with Offset Helices, *Biochemistry*, **45**, 15224-15231 (2006).
L Silvian, P Jin, P Carmillo, P Boriack-Sjodin, C Pelletier, M Rushe, B Gong, D Sah, B Pepinsky, A Rossomando, Artemin Crystal Structure Reveals Insights into Heparan Sulfate Binding, *Biochemistry*, **45**, 6801-6812 (2006).
Q Zheng, Y Deng, J Liu, L van der Hoek, B Berkhout, M Lu, Core Structure of S2 from the Human Coronavirus NL63 Spike Glycoprotein, *Biochemistry*, **45**, 15205-15215 (2006).

Beamline X6A

A Accardi, S Lobet, C Williams, C Miller, R Dutzler, Synergism Between Halide Binding and Proton Transport in a CLC-type Exchanger, *J. Mol. Biol.*, **362** (4), 691-699 (2006).
J Adams, G Pal, Z Jia, S Smith, Mechanism of Bacterial Cell-Surface Attachment Revealed by the Structure of Cellulosomal Type II Cohesin-dockerin Complex, *Proc Natl Acad Sci USA*, **103**, 305-310 (2006).
M Adams, V Singh, B Keller, Z Jia, Structural and Biochemical Characterization of Gentisate 1,2-Dioxygenase from Escherichia coli O157:H7., *Mol. Microbiol.*, **61**, 1469-84 (2006).
M Adams, Z Jia, Modulator of Drug Activity B from Escherichia Coli: Crystal Structure of a Prokaryotic Homologue of DT-Diaphorase, *J. Mol. Biol.*, **359** (2), 455-465 (2006).
R Alvarez-Venegas, M Sadder, A Hlavacka, F Baluska, Y Xia, A Firsov, G Sarath, H Moriyama, J Dubrovsky, Z Avramova, The Arabidopsis homolog of trithorax, ATX1, binds phosphatidylinositol 5-phosphate, and the two regulate a common set of target genes., *Proc Natl Acad Sci USA*, **103**, 6049-54 (2006).
M Barreras, M Bianchet, L Ielpi, L Tong, Crystallization and Preliminary Crystallographic Characterization of GumK, A Membrane-Associated Gluocuronosyltransferase from Xanthomonas campestris Required for Xanthan Polysaccharide Synthesis, *Acta Cryst. F*, **62**, 880-883 (2006).
G Cingolani, D Andrews, S Casjens, Crystallogenesis of Bacteriophage P22 Tail Accessory Factor gp26 at Acidic and Neutral pH, *Acta Cryst. F*, **62**, 477-482 (2006).
F Ferreira, G Mendoza-Hernandez, M Castaneda-Bueno, R Aparicio, H Fischer, M Calcagno, G Oliva, Structural Analysis of N-acetylglucosamine-6-phosphate Deacetylase Apoenzyme from Escherichia coli, *J. Mol. Biol.*, **359** (2), 308-321 (2006).
S Gabelli, H Azurmendi, M Bianchet, L Amzel, A Mildva, X-ray, NMR, and Mutational Studies of the Catalytic Cycle of the GDP-Mannose Mannosyl Hydrolase Reaction, *Biochemistry*, **45**, 11290-11303 (2006).

T Holyoak, S Sullivan, T Nowak, Structural Insights into the Mechanism of PEPCK Catalysis, *Biochemistry*, **45**, 8254-8263 (2006).
H Hong, D Patel, L Tamm, B van den Berg, The Outer Membrane Protein OmpW Forms an Eight-Stranded beta-Barrel with a Hydrophobic Channel, *J. Biol. Chem.*, **281**, 7568-7577 (2006).
K Horii, M Kahn, A Herr, Structural Basis for Platelet Collagen Responses by the Immune-type Receptor Glycoprotein VI, *Blood*, **108**, 936-942 (2006).
W Hwang, Y Lin, E Santelli, J Sui, L Jaroszewski, B Stec, M Farzan, W Marasco, R Liddington, Structural Basis of Neutralization by a Human Anti-severe Acute Respiratory Syndrome Spike Protein Antibody,80R., *J. Biol. Chem.*, **281**, 34610-6 (2006).
J Jakoncic, M Di Michiel, Z Zhong, V Honkimaki, Y Jouanneau, V Stojanoff, Anomalous Diffraction at Ultra-High Energy for Protein Crystallography, *J. Appl. Cryst.*, **39**, 831-841 (2006).
J Jakoncic, Y Jouanneau, C Meyer, V Stojanoff, The Catalytic Pocket of the Ring-hydroxylating Dioxygenase from Sphingomonas CHY-1, *Biochem. Biophys. Res. Commun.*, **352**, 861-866 (2006).
D Krosky, M Bianchet, L Seiple, S Chung, L Amzel, J Stivers, Mimicking Damaged DNA with a Small Moleclue Inhibitor of Human UNG2, *Nucleic Acids Res.*, **34**, 5872-5879 (2006).
O Laptenko, S Kim, J Lee, M Starodubtseva, F Cava, J Berenguer, X Kong, S Borukhov, pH-Dependent Conformational Switch Activates the Inhibitor of Transcription Elongation, *EMBO J.*, **25** (10), 2131 (2006).
M Nicholson, B Moradi, N Seth, X Xing, G Cuny, R Stein, K Wucherpfenning, Small Molecules that Enhance the Catalytic Efficiency of HLA-DM, *J. Immunol.*, **176**, 4208 (2006).
A Olia, J Al-Bassam, D Winn-Stapley, L Joss, S Casjens, G Cingolani, Binding-induced Stabilization and Assembly of the Phage P22 Tail Accessory Factor gp4, *J. Mol. Biol.*, **363**, 558-76 (2006).
K Pant, B Crane, Nitrosyl-Heme Structures of Bacillus subtilis Nitric Oxide Synthase Have Implications for Understanding Substrate Oxidation, *Biochemistry*, **45**, 2537-2544 (2006).
N Pashkova, Y Jin, S Ramaswamy, L Weisman, Structural Basis for Myosin V Discrimination Between Distinct Cargoes, *EMBO J.*, **25**, 693-700 (2006).
P Pawelek, N Croteau, C Ng-Thow-Hing, C Khursigara, N Moiseeva, M Allaire, J Coulton, Structure of TonB in Complex with FhuA, E. Coli Outer Membrane Receptor, *Science*, **312**, 1399-1402 (2006).
H Payandeh, M Fujihashi, W Gillon, E Pai, The Crystal Structure of (S)-3-O-geranylgeranylglycerol-phosphate-synthase from Archaeoglobus fulgidus Reveals an Ancient Fold for an Ancient Enzyme., *J. Biol. Chem.*, **281**, 6070-6078 (2006).
J Prada, R Haire, M Allaire, J Jakoncic, V Stojanoff, J Cannon, G Litman, D Ostrov, Ancient Evolutionary Origin of Diversified Variable Regions Demonstrated by Crystal Structures of an Immune-Type Receptor in Amphioxus, *Nat. Immunol.*, **7** (8), 875-882 (2006).
E Schreiter, S Wang, D Zamble, C Drennan, NikR-Operator Complex Structure and the Mechanism of Repressor Activation by Metal Ions, *Proc Natl Acad Sci USA*, **103** (37), 13676-13681 (2006).
C Shao, F Zhang, M Kemp, R Lindhardt, D Waisman, J Head, B Seaton, Crystallographic Analysis of Calcium-dependent Heparin Binding to Annexin A2, *J. Biol. Chem.*, **281**, 31689-31695 (2006).
G Subbarao, B van den Berg, Crystal Structure of the Monomeric Porin OmpG, *J. Mol. Biol.*, **360** (4), 750-759 (2006).
J Sudhamsu, B Crane, Structure and Reactivity of a Thermostable Prokaryotic Nitric-oxide Synthase That Forms a Long-lived Oxy-Heme Complex, *J. Biol. Chem.*, **281** (14), 9623-9632 (2006).
Y Tang, M Poustovoitov, K Zhao, M Garfinkel, A Canutescu, R Dunbrack, P Adams, R Marmorstein, Structure of a Human ASF1a-HIRA Complex and Insights into Specificity of Histone Chaperone Complex Assembly, *Nat. Struct. Mol. Biol.*, **13** (10), 921 (2006).
Y Wang, Y Zhang, Y Ha, Crystal Structure of a Rhomboid Family Intramembrane Protease., *Nature*, **444**, 179-183 (2006).
R Williams, T Holyoak, G McDonald, C Gui, A Fenton, Differentiating a Ligand's Chemical Requirements for Allosteric Interactions from Those for Protein Binding. Phenylalanine Inhibition of Pyruvate Kinase, *Biochemistry*, **45**, 5421-5429 (2006).
J Wilson, R Kovall, Crystal Structure of the CSL-Notch-Mastermind Ternary Complex Bound to DNA, *Cell*, **124**, 985-996 (2006).
J Xi, R Liu, M Rossi, J Yang, P Loll, W Dailey, R Eckenhoff, High Resolution Features from Low Affinity Interactions: Photoactive Analogs of the Haloether Anesthetics, *ACS Chem. Biol.*, **1**, 377-384 (2006).
W Xu, S Ahmed, H Moriyama, R Chollet, The Importance of the Strictly Conserved, C-terminal Glycine Residue in Phosphoenolpyruvate Carboxylase for Overall Catalysis: Mutagenesis and Truncation of GLY-961 in the Sorghum C4 Leaf Isoform, *J. Biol. Chem.*, **281**, 17238-45 (2006).
Y Yang, J Yuan, J Ross, J Noel, E Pichersky, An Arabidopsis thaliana methyltransferase Capable of Methylating Farnesoic Acid, *Arch. Biochem. Biophys.*, **448**, 123-32 (2006).
M Yang, K Horii, A Herr, T Kirley, Calcium-dependent Dimerization of Human Soluble Calcium Activated Nucleotidase: Characterization of the Dimer Interface, *J. Biol. Chem.*, **281**, 28307-28317 (2006).

Beamline X6B

B Chapman, A Checco, R Pindak, T Siegrist, C Kloc, Dislocations and Grain Boundaries in Semiconducting Rubrene Single-Crystals, *J. Cryst. Growth*, **290** (2), 479-484 (2006).
S Jaradat, H Gleeson, N Roberts, Y Wang, The Effects of Highly Chiral Dopants on the Smectic Phases of Liquid Crystals Remarkably Wide Intermediate Phases, *J Mater. Chem.*, **16**, 3753 (2006).
M Maye, D Nykypanchuk, D van der Lelie, O Gang, A Simple Method for Kinetic Control of DNA-Induced Nanoparticle Assembly, *J. Am. Chem. Soc.*, **128**, 14020-14021 (2006).
K Subburaman, N Pernodet, S Kwak, E DiMasi, S Ge, V Zaitsev, X Ba, N Yang, M Rafailovich, Templated Biomineralization on Self-Assembled Protein Fibers, *Proc Natl Acad Sci USA*, **103** (40), 14672-14677 (2006).

Beamline X7A

E Anokhina, Y Go, Y Lee, T Vogt, A Jacobson, Chiral Three-Dimensional Microporous Nickel Aspartate with Extended Ni-O-Ni Bonding, *J. Am. Chem. Soc.*, **128**, 9957-9962 (2006).

P Barnes, M Lufaso, P Woodward, Structure Determination of A2M3+TaO6 and A2M3+NbO6 Ordered Perovskites: Octahedral Tilting and Pseudosymmetry, *Acta Cryst. B*, **62**, 384-396 (2006).

J Breger, Y Meng, Y Hinuma, S Kumar, K Kang, Y Shao-Horn, G Ceder, C Grey, Effect of High Voltage on the Structure and Electrochemistry of LiNi0.5Mn0.5O2: A Joint Experimental and Theoretical Study, *Chem. Mater.*, **18**, 4768-4781 (2006).

S Budko, T Weiner, R Ribeiro, P Canfield, Y Lee, T Vogt, Lacerda, Effect of Pressure and Chemical Substitutions on the Charge-Density-Wave in LaAgSb2, *Phys. Rev. B*, **73**, 184111 (2006).

G Gatta, Y Lee, On the Elastic Behaviour of Zeolite Mordenite: a Synchrotron Powder Diffraction Study, *Phys. Chem. Miner.*, **32**, 726-732 (2006).

J Graetz, S Chaudhuri, Y Lee, T Vogt, J Muckerman, J Reilly, Pressure-induced Structural and Electronic Changes in alpha-AlH3, *Phys. Rev. B: Condens. Matter*, **74**, 214114 (2006).

K Hirota, S Wakimoto, D Cox, Neutron and X-ray Studies of Relaxors, *J. Phys. Soc. Japan*, **75** (11), 111006-1 to 13 (2006).

J Hriljac, High-Pressure Synchrotron X-ray Powder Diffraction Studies of Zeolites, *Crystallogr. Rep.*, **12** (2), 181-193 (2006).

P Karen, A Moodenbaugh, J Goldberger, P Santhosh, P Woodward, Electronic Magnetic and Structural Properties of A2VM0O6 Perovskites (A = Ca, Sr), *J. Solid State Chem.*, **179**, 2120-2125 (2006).

Y Lee, J Hriljac, J Parise, T Vogt, Pressure-induced Hydration in Zeolite Tetranatrolite, *Am. Mineral.*, **91**, 247-251 (2006).

M Lufaso, R Macquart, Y Lee, T Vogt, H zur Loye, Pressure induced octahedral tilting distortion in Ba2YTaO6, *Chem. Commun.*, **168**, 168-170 (2006).

M Lufaso, W Gemmil, S Mugavero, Y Lee, T Vogt, H zur Loye, Compression mechanisms of symmetric and Jahn–Teller distorted octahedra in double perovskites: A2CuWO6 (A ¼ Sr, Ba), Sr2CoMoO6, and La2LiRuO6, *J. Solid State Chem.*, **179**, 3571-3576 (2006).

M Lufaso, R Macquart, Y Lee, T Vogt, H zur Loye, Pressure-Induced Phase Transition and Octahedral Tilt System Change of Ba2BiSbO6, *J. Solid State Chem.*, **179** (3), 917-922 (2006).

M Lufaso, R Macquart, Y Lee, T Vogt, H zur Loye, Structural Studies of Sr2GaSbO6, Sr2NiMoO6, and Sr2FeNbO6 using Pressure and Temperature, *J. Phys.: Condens. Matter*, **18**, 8761-8780 (2006).

B Noheda, D Cox, Bridging Phases at the Morphotropic Boundaries of Lead Oxide Solid Solutions, *Phase Transit*, **79** (1-2), 5-20 (2006).

S Park, Y Lee, M Elcombe, T Vogt, Synthesis and Structure of the Bilayer Hydrate Na0.3NiO2.1.3D2O, *Inorg. Chem.*, **45** (9), 3490-3492 (2006).

J Provis, Modelling the Formation of Geopolymers, Ph.D. Thesis, University of Melbourne, Melbourne (2006).

P Sarin, W Yoon, K Jurkschat, P Zschack, W Kriven, Quadrupole Lamp Furnace for High Temperature (up to 2050 K) Synchrotron Powder X-ray Diffraction Studies in Air in Reflection Geometry, *Rev. Sci. Instrum.*, **77**, 093906-1-093906-9 (2006).

T Vogt, J Hriljac, Y Lee, Pressure Induced Swelling in Microporous Materials, US Patent No. 7,074,386 (2006).

Beamline X7B

E Anokhina, Y Go, Y Lee, T Vogt, A Jacobson, Chiral Three-Dimensional Microporous Nickel Aspartate with Extended Ni-O-Ni Bonding, *J. Am. Chem. Soc.*, **128**, 9957-9962 (2006).

T Asthalter, I Sergueev, U Van Burck, R Dinnebier, Indentification of a Rotator Phase of Octamethyl Ferrocene and Correlations Between its Structural and Dynamical Properties, *J. Phys. Chem. Solids*, **67** (7), 1416-1422 (2006).

S Basu, P Devi, A Mati, Y Lee, J Hanson, Lanthanum Molybdenum Oxide: Low Temperature Synthesis and Characterization, *J. Mater. Res.*, **21**, 1133-1140 (2006).

M Capracotta, R Sullivan, J Martin, Sorptive Reconstruction of CuMCl4 (M = Al and Ga) Upon Small-Molecule Binding the Competitive Binding of CO and Ethylene, *J. Am. Chem. Soc.*, **128**, 13463-13473 (2006).

K Chung, H Lee, W Yoon, J McBreen, X Yang, Studies of LiMn2O4 Capacity Fading Mechanism at Elevated Temperature Using In Situ Synchrotron X-Ray Diffraction, *J. Electrochem. Soc.*, **153**, A774 (2006).

A Clearfield, A Tripathi, D Medvedev, A Celestian, J Parise, In Situ Type Study of Hydrothermally Prepared Titanates and Silicotitanates, *J. Mater. Sci.*, **41** (5), 1325-1333 (2006).

G Cruciani, Zeolites Upon Heating: Factors Governing Their Thermal Stability and Structural Chages, *J. Phys. Chem. Solids*, **67**, 1973-1994 (2006).

A Dattelbaum, J Martin, Benzen and Ethylene Binding to Copper(I)-Ziconium(IV) Chloride Materials: The Crystal Structure and Solid-State Reactivity of ((bz)2Cu)2Zr2Cl10.bz, *Polyhedron*, **25**, 349-359 (2006).

E Fujita, B Brunschwig, C Creutz, J Muckerman, N Sutin, D Szaida, R van Eldik, Transition State Characterization for the Reversible Binding of Dihydrogen to Bis(2,2'-bipyridine)rhodium(I) from Temperature- and Pressure-Dependent Experimental and Theoretical Studies, *Inorg. Chem.*, **45**, 1595-1603 (2006).

I Hassan, S Antao, J Parise, Cancrinite: Crystal Structure, Phase Transitions, and Dehydration Behavior with Temperature, *Am. Mineral.*, **91**, 1117-1124 (2006).

L Hildebrandt, R Dinnebier, M Jansen, Crystal Structure and Ionic Conductivity of Three Polymorphic Phases of Rubidium Trefluoromethyl Sulfonate, RbSO3CF3, *Inorg. Chem.*, **45** (8), 3217-3223 (2006).

E Johnson, J Post, Water in the Interlayer Region of Birnessite: Importance in Cation Exchange and Structural Stability, *Am. Mineral.*, **91**, 609-619 (2006).

D Kim, J Szanyi, J Kwak, T Szailer, J Hanson, C Wang, C Peden, Effect of Barium Loading on the Desulfation of Pt-BaO/Al2O3 Studied by H2 TPRX, TEM, Sulfur K-edge XANES, and In Situ TR-XRD, *J. Phys. Chem. B*, **110**, 10441-10448 (2006).

J Martin, C Keary, T Thornton, M Novotnak, J Knutson, J Folmer, Metallotropic Liquid Crystals Formed by Surfactant Templating of Molten Metal Halides, *Nat. Mater.*, **5**, 271 (2006).

A Martinez-Arias, D Gamarra, M Fernandez-Garcia, X Wang, J Hanson, J Rodriguez, Comparative Study on Redox Properties of Nanosized CeO2 and CuO/Ce2 Under CO/O2 , *J. Catal.*, **240** (1), 1-7 (2006).

M Nyman, A Celestian, G Holland, T Alam, J Parise, Solid-state Structural Characterization of a Rigid Framework of Lacunary Heteropolyniobates, *Inorg. Chem.*, **45** (3), 1043-1052 (2006).

J Pike, S Chan, F Zhang, X Wang, J Hanson, Foramtion of Stable Cu2O from Reduction of CuO Nanoparticles, *Appl. Catal. A*, **303** (2), 273-277 (2006).

S Ruebush, G Icopini, S Brantley, M Tien, In Vitro Enzymatic Reduction Kinetics of Mineral Oxides by Membrane Fractions from Shewanella oneidensis MR-1, *Geochim. Cosmochim. Acta*, **70** (1), 56-70 (2006).

A Setlur, W Heward, Y Gao, A Srivastava, R Chandron, M Shankar, Crystal Chemistry and Luminescence of Ce3+ -Doped Lu2CaMg2(Si,Ge)3O12 and Its Use in LED Based Lighting, *Chem. Mater.*, **18**, 3314-3322 (2006).

X Shen, Y Ding, J Hanson, M Aindow, S Suib, In situ Synthesis of Mixed-Valent Manganese Oxide Nanocrystals: An In situ Synchrotron X-ray Diffraction Study, *J. Am. Chem. Soc.*, **128** (14), 4570 (2006).

T Szailer, J Kwak, D Kim, J Hanson, C Peden, J Szanyi, Reduction of Stored NOx on Pt/Al2O3 Catalysts with H2 and CO, *J. Catal.*, **239**, 51-64 (2006).

W Yoon, J Hanson, J McBreen, X Yang, A Study on the Newly Observed Intermidate Structures During the Thermal Decomposition of Nickel-Based Layered Cathode Materials using Time-Resolved XRD, *Electrochem. Commun.*, **8** (5), 859-862 (2006).

F Zhang, C Chen, J Raitano, J Hanson, W Caliebe, S Khalid, S Chan, Phase Stability in Ceria-Zirconia Binary Oxide Nanoparticles: The Effect of the Ce3+ Concentration and the Redox Environment, *J. Appl. Phys.*, **99**, 084313 (2006).

F Zhang, C Chen, J Hanson, I Herman, S Chan, Phases in ceria-zirconia binary oxide (1-x)CeO2-xZrO2 nanoparticles: the size effects, *J. Am. Ceram. Soc.*, **80** (3), 1028-1036 (2006).

Beamline X8A

G Rochau, J Bailey, G Chandler, T Nash, D Nielsen, G Dunham, O Garcia, N Joseph, J Keister, et al., Energy Dependent Sensitivity of Microchannel Plate Detectors, *Rev. Sci. Instrum.*, **77**, 10E323 (2006).

C Sorce, J Schein, F weber, K Widmann, K Campbell, E Dewald, R Turner, O Landen, K Jacoby, et al., Soft X-ray Power Diagnostic Improvements at the Omega Laser Facility, *Rev. Sci. Instrum.*, **77**, 10E518 (2006).

Beamline X8C

J Adams, G Pal, Z Jia, S Smith, Mechanism of Bacterial Cell-Surface Attachment Revealed by the Structure of Cellulosomal Type II Cohesin-dockerin Complex, *Proc Natl Acad Sci USA*, **103**, 305-310 (2006).

M Austin, T Saito, M Bowman, S Haydock, A Kato, B Moore, R Kay, J Noel, Biosynthesis of Dictyostelium Discoideum Differentation-Inducing Factor by a Hybrid Type I Fatty Acid A-Type III polyketide synthase , *Nat. Chem. Biol.*, **2**, 494-502 (2006).

X Chu, W DePinto, D Bartkovitz, S So, B Vu, K Packman, C Lukacs, Q Ding, N Jiang, et al., Discovery of [4-Amino-2-(1-methanesulfonylpiperidin-4-ylamino)pyrimidin-5-yl](2,3-difluoro-6-methoxyphenyl)methanone (R547), A Potent and Selective Cyclin-Dependent Kinase Inhibitor with Significiant in Vivo Antitumor Activity, *J. Med. Chem.*, **49**, 6549-6560 (2006).

E Crouch, B McDonald, K Smith, T Cararella, B Seaton, J Head, Contributions of Phenylalanine 335 to Ligand Recognition by Human Surfactant Protein D: Ring Interactions with SP-D Ligands, *J. Biol. Chem.*, **281**, 18008 (2006).

N Dimasi, Crystal Structure of the C-terminal SH3 Domain of the Adaptor Protein GADS in Complex with SLP-76 Motif Peptide Reveals a Unique SH3-SH3 Interaction, *Int. J. Biochem. Cell Biol.*, **39** (1), 109-123 (2006).

A Faravelli, N Dimasi, Expression, Refolding and Crystallizations of the Grb2-like (GADS) C-Terminal SH3 Domain Complexed with a SLP-76 Motif Peptide, *Acta Cryst. F*, **F62**, 52-55 (2006).

D Fong, V Yim, M D'elia, E Brown, A Berghuis, Crystal Structure of CTP: Glycerol-3-Phosphate Cytidylyl Tranferase from Staphylococcus Aurues: Examination of Structural Basis for Kinetic Mechanism , *Biochim Biophys Acta*, **1764**, 63 (2006).

M Hung, E Rangarajan, C Munger, G Nadeau, T Sulea, A Matte, Crystal Structure of TDP-Fucosamine Acetyl Transferase (WECD) from Escherichia Coli, an Enzyme Required for Enterobacterial Common Antigen Synthesis, *J. Bacteriol.*, **188**, 5606 (2006).

N Ishiyama, C Creuzenet, W Miller, M Demendi, E Anderson, G Harauz, J Lam, A Berghuis, Structural Studies of FlaA1 from Helicobacter Pylori Reveal the Mechanism for Inverting 4,6-dehydratase Activity, *J. Biol. Chem.*, **281**, 24489-24495 (2006).

A Kim, J Rylett, B Shilton, Substrate Binding and Catalytic Mechanism of Human Choline Acetyltransferase, *Biochemistry*, **45**, 14621-14631 (2006).

G Kozlov, P Maattanen, J Schrag, S Pollack, M Cygler, B Nagar, D Thomas, K Gehring, Crystal Structure of the bb' Domains of the Protein Disulfide Isomerase ERp57, *Structure*, **14**, 1331-1339 (2006).

S Ku, P Yip, P Howell, Structure of Escherichia Coli Tryptophanase, *Acta Cryst. D*, **62**, 814-823 (2006).

C Lukacs, N Oikonomakos, R Crowther, L Hong, R Kammlott, W Levin, S Li, C Liu, D Lucas-McGady, et al., The Crystal Structure of Human Muscle Glycogen Phosphorylase A with Bound Glucose and AMP: An Intermediate Conformation with T-State and R-State Features, *Proteins: Struc. Func. Genet.*, **63**, 1123 (2006).

A Lyubimov, P Lario, I Moustafa, A Vrielink, Atomic Resolution Crystallography Reveals how Changes in pH Shape the Protein Microenvironment, *Nat. Chem. Biol.*, **2**, 259-264 (2006).

T Modoveanu, Q Liu, A Tocilj, M Watson, G Shore, K Gehring, The X-ray Structure of a BAK Homodimer Reveals an Inhibitory Zinc Binding Site, *Mol. Cell*, **24**, 677-688 (2006).

T Moldoveanu, Q Liu, J Tocilj, M Watson, G Shore, K Gehring, The X-ray Structure of a BAK Homodimer Reveals an Inhibitory Zinc Binding Site, *Mol. Cell. Bio.*, **24**, 677-688 (2006).
S Mrkobrada, L Boucher, D Tyers, F Sicheri, Structural and Functional Analysis of Saccharomyces Cerevisiae Mob1, *J. Mol. Biol.*, **362**, 430-440 (2006).
J Payandeh, E Pai, A Structural Basis for Mg(2+) Homeostasis and the CorA Translocation Cycle, *EMBO J.*, **25**, 3762-3773 (2006).
J Payandeh, E Pai, Crystallization and Preliminary X-ray Diffraction Analysis of the Magnesium Transporter CorA, *Acta Cryst. F*, **62**, 148-152 (2006).
J Pedelacq, S Cabantous, T Tran, T Terwilliger, G Waldo, Engineering and Characterization of a Superfolder Green Fluorescent Protein, *Nat. Biotechnol.*, **24**, 79-88 (2006).
E Rangarajan, A Proteau, J Wagner, M Hung, A Matte, M Cygler, Structural Snapshots of Escherichia coli Histidinol Phosphate Phosphatase along the Reaction Pathway, *J. Biol. Chem.*, **281** (49), 37930-37941 (2006).
B Rho, L Hung, J Holton, D Vigil, S Kim, M Park, T Terwilliger, j Pedelacq, Functional and Structural Characterization of a Thiol Peroxidase from Mycobacterium tuberculosis, *J. Mol. Biol.*, **361** (5), 850-863 (2006).
C Shao, F Zhang, M Kemp, R Lindhardt, D Waisman, J Head, B Seaton, Crystallographic Analysis of Calcium-dependent Heparin Binding to Annexin A2, *J. Biol. Chem.*, **281**, 31689-31695 (2006).
D Shaya, A Tocilj, Y Li, J Myette, G Venkatarman, R Sasisekharan, M Cygler, Crystal Structure of Heparinase II from Pedobacter Heparinus and its Complex with a Disaccharide Product, *J. Biol. Chem.*, **281** (2), 22 (2006).
E Sickmier, K Frato, H Shen, S Paranawithana, M Green, C Kielkopf, Structural Basis for Polypyrimidine Tract Recognition by the Essential Pre-mRNA Splicing Factor U2AF65, *Mol. Cell*, **23** (1), 49-59 (2006).
S Singh, D Christendat, Structure of Arabidopsis Dehydroquinate Dhydratase-Shikimate Dehydrogeanse and Implications for Metabolic Channeling in the Shikimate Pathway, *Biochemistry*, **45**, 7787-7796 (2006).
M Suits, N Jaffer, Z Jia, Structure of the Escherichia coli O157:H7 heme oxygenase ChuS in complex with heme and enzymatic inactivation by mutation of the heme coordinating residue His-193, *J. Biol. Chem.*, **281** (48), 36776-82 (2006).
Q Ye, X Li, A Wong, Q Wei, Z Jia, Structure of Calmodulin Bound to a Calcineurin Peptide: A New Way of Making an Old Binding Mode , *Biochemistry*, **45** (3), 738-745 (2006).

Beamline X9A

A Hoelz, J Janz, S Lawrie, B Corwin, A Lee, T Sakmar, Crystal Structure of the SH3 Domain of beta PIX in Complex with a High Affinity Peptide from PAK2, *J. Mol. Biol.*, **358** (2), 509-522 (2006).
A Ketkar, A Shenoy, U Ramagopal, S Visweswariah, K Suguna, A Structural Basis for the Role of Nucleotide Specifying Residues in Regulating the Oligomerization of the RV1625C Adenylyl Cyclase from M. Tuberculosis, *J. Mol. Biol.*, **356**, 904 (2006).
V Lamour, B Hogan, D Erie, S Darst, Crystal Structure of Thermus Aquaticus Gfh1, a Gre-factor Paralog that Inhibits rather than Stimulates transcript Cleavage, *J. Mol. Biol.*, **356**, 179-188 (2006).
Y Leduc, C Phenix, J Puttick, K Nienaber, D Palmer, L Delbaere, Crystallization, Preliminary X-ray Diffraction and Structure Solution of MosA, a Dihydrodipicolinate Synthase from Sinorhizobium Meliloti L5-30, *Acta Cryst. F*, **F62**, 49-51 (2006).
M Lilic, M Vujanac, C Stebbins , A Common Structural Motif in the Binding of Virulence Factors to Bacterial Secretion Chaperones, *Mol. Cell*, **21**, 653-664 (2006).
I Lorenz, J Marcotrigiano, T Dentzer, C Rice, Structure of the catalytic domain of the hepatitis C virus NS2-3 protease, *Nature*, **442** (7104), 831-5 (2006).
B Manjasetty, M Chance, Crystal Structure of Escherichia coli L-Arabinose Isomerase (ECAI), The Putative Target of Biological Tagatose Production, *J. Mol. Biol.*, **360** (2), 297-309 (2006).
B Manjasetty, K Bussow, M Fieber-ErdMan, Y Roske, J Gobam, C Scheich, F Gotz, F Niesen, U Heinemann, Crystal Structure of Homo Sapiens PTD012 Reveals a Zinc-Containing Hydrolase Fold, *Protein Sci.*, **15**, 914-920 (2006).
S Margarit, W Davidson, L Frego, F Stebbins, A Steric Antagonism of Actin Polymerization by a Salmonella Virulence Protein, *Structure*, **14**, 1219-1229 (2006).
E McManus, B Luisi, R Perham, Structure of a Putative Lipoate Protein Ligase from Thermoplasma acidophilum and the Mechanism of Target Selection for Post-Translational Modification, *J. Mol. Biol.*, **356** (3), 625-637 (2006).
S Patel, C Ciatto, C Chen, F Bahna, M Rajebhosale, N Arkus, I Schieren, T Jessell, B Honig, Type II Cadherin Ectodomain Structures: Implications for Classical Cadherin Specificity, *Cell*, **124** (6), 1255-1268 (2006).
G Prehna, M Ivanov, J Blisha, C Stebbins, Yersinia Virulence Depends on Mimicry of Host Rho-Family Nucleotide Dissociation Inhibitors, *Cell*, **126**, 869-880 (2006).
M Roden, D Brims, A Fedorov, T DiLorenzo, S Almo, s Nathenson, L Anovitz, D Wesolowski, Structural Analysis of H2-Db Class I Molecules Containing Two Different Allelic Forms of the type 1 Diabetes Susceptibility Factor beta-2 Microglobulin: Implications for the Mechanism Underlying Viriations in Antigen Presentation, *Mol. Immunol.*, **43** (9), 1370-1378 (2006).
T Schwartz, D Schmidt, S Brohawn, G Blobel, Homodimerization of the G Protein Srbeta in the Nucleotide-Free State Involves Proline cis/trans Isomerication in the Switch II Region, *Proc Natl Acad Sci USA*, **103** (18), 6823-6828 (2006).
V Singh, W Shi, S Almo, G Evans, R Furneaux, P Tyler, G Painter, D Lenz, S Mee, et al., Structure and Inhibition of Quorum Sensing Target from Streptococcus pneumoniae, *Biochemistry*, **45**, 12929-12941 (2006).
W Yew, A Fedorov, E Fedorov, J Rakus, R Pierce, S Almo, J Gerlt, Evolution of Enzymatic Activities in the Enolase Superfamily: L-Fuconate Dehydratase from Xanthomonas campestris, *Biochemistry*, **45**, 14582-14597 (2006).
W Yew, A Fedorov, E Fedorov, B Wood, S Almo, J Gerlt, Evolution of Enzymatic Activities in the Enolase Superfamily: D-Tartrate Dehydratase from Bradyrhizobium japonicum, *Biochemistry*, **45**, 14598-14608 (2006).

Beamline X9B

J Bielnicki, Y Devedjiev, U Derewenda, Z Dauter, A Joachimiak, Z Derewenda, B. subtilis ykuD Protein at 2.0 Angstrom Resolution: Insights into the Structure and Function of a Novel, Ubiquitous Family of Bacterial Enzymes, *Proteins: Struc. Func. Bioinformatics*, **62**, 144-151 (2006).

K Boeshans, F Liu, G Peng, W Idler, S Jang, L Marekov, L Black, B Ahvazi, Purification, Crystallization and Preliminary X-ray Diffraction Analysis of the Phage T4 Vertex Protein Gp24 and its Mutant Forms, *Protein Expr. Purif.*, **49** (2), 235-243 (2006).

J Cook, K Bencze, A Jankovic, A Crater, C Busch, P Bradley, A Stemmler, M Spaller, T Stemmler, Monomeric Yeast Frataxin is an Iron-Binding Protein, *Biochemistry*, **45**, 7767-7777 (2006).

A Costello, G Periyannan, K Yang, M Crowder, D Tierney, Site Selective Binding of Zn(II) ot Metallo-b-Lactamase L1 from Stenotrophomonas Maltophilia, *J. Biol. Inorg. Chem.*, **11**, 351-358 (2006).

A Costello, N Sharma, K Yang, M Crowder, D Tierney, X-ray Absorption Spectroscopy of the Zinc-Binding Sites in the Class B2 Metallo-B-lactamsase ImiS from Aeromonas veronii bv. sobria, *Biochemistry*, **45**, 13650-13658 (2006).

E Eren, D Kennedy, M Maroney, J Arguello, A Novel Regulatory Metal Binding Domain is Present in the C Terminus of Arabidopsis Zn2+ -ATPase HMA2, *J. Biol. Chem.*, **281**, 33881-33891 (2006).

R Franzini, R Watson, G Patra, R Breece, D Tierney, M Hendrich, C Achim, Metal Binding to Bipyridine-Modified PNA, *Inorg. Chem.*, **45**, 9798-9811 (2006).

B Frost, C Bautista, R Huang, J Shearer, Manganese Complexes of 1,3,5-triaza-7-phosphaadamantane (PTA): The First Nitrogen Bound Transition Metal Complex of PTA, *Inorg. Chem.*, **45**, 3481-3483 (2006).

J Grembecka, T Cierpicki, Y Drvedjiev, U Derewenda, B Kang, J Bushweller, Z Derewenda, The Binding of the PDZ Tandem of Syntenin to Target Proteins, *Biochemistry*, **45**, 3674-3683 (2006).

K Gunter, M Aschner, L Miller, R Eliseev, J Salter, K Andersen, T Gunter, Determining the Oxidation States of Manganese in NT2 Cells and Cultured Astrocytes, *Neurobiol. Aging*, **27** (12), 1816-26 (2006).

T Ju, R Beaulieu Goldsmith, S Chai, M Maroney, S Sondej Pochapsky, T Pochapsky, One Protein, Two Enzymes Revisited: A Structural Entropy Switch Interconverts the Two Isoforms of Acireductone Dioxygenase, *J. Mol. Biol.*, **363** (4), 823-834 (2006).

J Kaste, B Bostick, A Friedland, A Schroth, T Siccama, Fate and Speciation of Gasoline-Derived Lead in Organic Horizons of the Northeastern USA, *Soil Sci. Soc. Am. J.*, **70**, 1688-1698 (2006).

F Larsen, A Boisen, K Berry, B Moubaraki, K Murray, V McKee, R Scarrow, C McKenzie, Identification of the Dinuclear and Tetranuclear Air-Oxidized Products Derived from Labile Phenolate-Bridged Dimanganese(II) Pyridyl-Chelate Compounds, *Eur. J. Inorg. Chem.*, **2006**, 3841-3852 (2006).

R Lieberman, K Kondapalli, D Shrestha, A Hakemian, S Smith, J Telser, J Kuzelka, R Gupta, A Borovik, et al., Charactization of the Particulate Methane Monooxygenase Metal Centers in Multiple Redox States by X-ray Absorption Spectroscopy, *Inorg. Chem.*, **45** (20), 8372-8381 (2006).

Y Liu, M Cheney, J Gaudet, M Chruszcz, S Lukasik, D Suglyama, J Lary, J Cole, Z Dauter, et al., The Tetramer Structure of the Nervy Homology Two Domain, NHR2, is Critical for AML1/ETO's Activity, *Cancer Cell*, **9**, 249-260 (2006).

J Momb, P Thomas, R Breece, D Tierney, W Fast, The Quorum-Quenching Metallo-gamma-lactonase from Bacillus thuringiensis Exhibits a Leaving Group Thio Effect, *Biochemistry*, **45**, 13385-13393 (2006).

K Neupane, J Shearer, Influence of Amide/Amine vs Nis-Amide Coordination in Nickel Superoxide Dismutase, *Inorg. Chem.*, **45**, 10552-10566 (2006).

G Periyannan, A Costello, D Tierney, K Yang, b Bennett, M Crowder, Sequential Binding of Cobalt(II) to Metallo-beta-lactamase CcrA, *Biochemistry*, **45**, 1313-1320 (2006).

B Ramakrishnan, V Ramasamy, P Qasba, Structural Snapshots of Beta- 1,4Galactosyltransferase-I Along the Kinetic Pathway, *J. Mol. Biol.*, **357**, 1619-1633 (2006).

J Rohde, A Stubna, E Bominaar, E Munck, W Nam, L Que, Jr., Nonheme Oxoiron(IV) Complexed of Tris(2-pyridylmethyl)amine with cis-Monoanionic Ligands, *Inorg. Chem.*, **45** (16), 6435-6445 (2006).\

K Sekar, M Yogavel, S Kanaujia, A Sharma, D Velmurugan, M Poi, Z Dauter, M Tsai, Suggestive Evidence for the Involvement of the Second Calcium and Surface Loop in Interfacial Binding: Monoclinci and Trigonal Crystal Structures of a Quadruple Mutant of Phospholipase A2, *Acta Cryst. D*, **62**, 717-724 (2006).

K Sekar, M Yogavel, D Gayathri, D Velmurugan, R Krishna, M Poi, Z Dauter, M Dauter, M Tsai, Atomic Resolution Structure of the Double Mutant (K53,56M) of Bovine Pancreatic Phospholipase A2, *Acta Cryst. F*, **62**, 1-5 (2006).

J Shearer, L Long, A Superoxide Dismutase Maquette That Reproduces the Spectroscopic and Functional Properties of the Metalloenzyme, *Inorg. Chem.*, **45**, 2358 - 2360 (2006).

E Stone, A Costello, D Tierney, W Fast, Substrate-Assisted Cysteine Deprotonation in the Mechanism of Dimethylargininase (DDAH) from Pseudomonas aeruginosa, *Biochemistry*, **45**, 5618-5630 (2006).

J Strzalka, T Xu, A Tronin, S Wu, I Miloradovic, I Kuzmenko, T Gog, M Therien, K Blasie, Structural Studies of Amphiphilic 4-Helix Bundle Peptides Incorporating Designed Extended Chromophores for Nonlinear Optical Biomolecular Materials, *Nano Lett.*, **6** (11), 2395-2405 (2006).

A Szyk, M Maurizi, Crystal Structure at 1.9A of E. coli ClpP With a Peptide Convalently Bound at the Active Site, *J. Struct. Biol.*, **156** (1), 165-174 (2006).

D Velmurugan, V Rajakannan, D Gayathri, S Banumathi, T Yamane, Z Dauter, M Dauter, K Sekar, Ab Initio Structure Determination of the Triple Mutant (K53,56,121M) of Bovine Pancreatic Phospholipase A(2) at Atomic and High Resolution Using ACORN, *N/A*, **90** (8), 1091-1099 (2006).

Y Zhang, S Vorobiev, B Gibson, B Hao, G Dishu, V Mishra, E Yarmola, M Bubb, S Almo, F Southwick, A CapG Gain-of-Function Mutant Reveals Critical Structure and Functional Determinants for Actin Filament Severing, *EMBO J.*, **25**, 4458-4467 (2006).

Beamline X10A

A Cisneros, G Mazzanti, R Campos, A Marangoni, Polymorphic Transformation in Mixtures of High- and Low-Melting Fractions of Milk Fat, *J. Agr. Food Chem.*, **54** (16), 6030-6033 (2006).

B Coldren, H Warriner, R van Zanten, J Zasadzinski, E Sirota, Flexible Bilayers with Spontaneous Curvature Lead to Lamellar Gels and Spontaneous Vesicles, *Proc Natl Acad Sci USA*, **103** (8), 2524-2529 (2006).

B Coldren, H Warriner, R van Zanten, J Zasadzinski, Lamellar Gels and Spontaneous Vesicles in Catanionic Surfactant Mixtures, *Langmuir*, **22**, 2465-2473 (2006).

B Coldren, H Warriner, R van Zanten, J Zasadzinski, Zero Spontaneous Curvature and Its Effects on Lamellar Phase Morphology and Vesicle Size Distributions, *Langmuir*, **22**, 2472-2481 (2006).

G Tompsett, B Panzarella, W Conner, K Yngvesson, F Lu, S Suib, K Jones, S Bennett, In Situ Small Angle X-ray Scattering, Wide Angle X-ray Scattering, and Raman Spectroscopy of Microwave Synthesis, *Rev. Sci. Instrum.*, **77**, 124101 (2006).

D Walba, H Yang, R Shoemaker, P Keller, r Shao, D Coleman, C Jones, M Nakata, N Clark, Main-chain Chiral Smectic Polymers Showing a Large Electroclinic Effect in the SmA* Phase, *Chem. Mater.*, **18**, 4576-4584 (2006).

J Yoon, R Mathers, G Coates, E Thomas, Optically Transparent and High Molecular Weight Polyolefin Block Copolymers Toward Self-Assembled Photonic Band Gap Materials, *Macromolecules*, **39**, 1913 (2006).

Beamline X10B

D Dorset, S Weston, S Dhingra, Crystal Structure of Zeolite MCM-68: A New Three-Dimensional Framework with Large Pores, *J. Phys. Chem. B*, **110**, 2045-2050 (2006).

N Koch, A Vollmer, I Salzmann, B Nickel, H Weiss, J Rabe, Evidence for Temperature-Dependent Electron Band Dispersion in Pentacene, *Phys. Rev. Lett.*, **96**, 156803 (2006).

C Kostelansky, J Peitron, M Chen, W Dressick, K Sider-Lhons, D Ramaker, R Stroud, C Klug, B Zelakiewicz, T Schull, Triarylphosphine-Stabilized Platinum Nanoparticles in Three-Dimensional Nanostructured Films as Active Electrocatalysts, *J. Phys. Chem. B*, **110**, 21487-21496 (2006).

Y Sun, A Frenkel, H White, L Zhang, Y Zhu, H Xu, J Yang, T Koga, V Zaitsev, et al., Comparison of Decanethiolate Gold Nanoparticles Synthesized by One-Phase and Two-Phase Methods, *J. Phys. Chem. B*, **110**, 23022-23030 (2006).

Y Sun, A Frenkel, R Isseroff, C Shnobrun, M Forman, K Shin, T Koga, H White, L Zhang, et al., Characterization of Palladium Nanoparticles by Using X-ray Reflectivity, EXAFS, and Electron Microscopy, *Langmuir*, **22**, 807-816 (2006).

J Xavier, S Sharma, Y Seo, R Isseroff, T Koga, H White, A Ulman, K Shin, S Satija, et al., Effect of Nanoscopic Fillers on Deweting Dynamics, *Macromolecules*, **39**, 2972-2980 (2006).

Beamline X10C

J Calla, M Bore, A Datye, R Davis, Effect of Alumina and Titania on the Oxidation of CO over Au Nanoparticles Evaluted by 13C Isotopic Transient Analysis, *J. Catal.*, **238** (2), 458-467 (2006).

A Faravelli, N Dimasi, Expression, Refolding and Crystallizations of the Grb2-like (GADS) C-Terminal SH3 Domain Complexed with a SLP-76 Motif Peptide, *Acta Cryst. F*, **F62**, 52-55 (2006).

J Mathur, P Thakur, C Dodge, A Francis, G Choppin, Coordination Modes in the Formation of Ternary Complexes of Am(III), Cm(III) and Eu(III) with EDTA and NTA: TRLFS, 13C NMR, EXAFS, and Thermodynamics of the complexation. , *Inorg. Chem.*, **45**, 8026-8035 (2006).

U Skyllberg, P Bloom, J Qian, C Lin, W Bleam, Complexation of Mercury(II) in Soil Organic Matter: EXAFS Evidence for Linear Two-Coordination with Reduced Sulfur Groups, *Environ. Sci. Tech.*, **40**, 4174-4180 (2006).

P Thakur, J Mathur, C Dodge, A Francis, G Choppin, Thermodynamics and the Structural Aspects of the Ternary Complexes of Am(III), Cm(III), and Eu(III) with Ox and EDTA+Ox, *Dalton Trans.*, **2006**, 4829-4837 (2006).

Y Yang, S Lim, G Du, C Wang, D Ciuparo, Y Chen, Haller, Controlling of Physicochemical Properties of Nickel-Substituted MCM-41 by Adjustment of the Synthesis Solution pH and Tetramethylammonium Silicate Concentration, *J. Phys. Chem. B*, **110**, 5927-5935 (2006).

Beamline X11A

A Argo, J Odzak, J Goellner, F Lai, F Xiao, B Gates, Catalysis by Oxide-Supported Clusters of Iridium and Rhodium: Hydrogenation of Ethene, Propene, and Toluene, *J. Phys. Chem. B*, **110**, 1775-1786 (2006).

M Bervas, A Mansour, W Yoon, J Al-Sharab, F Badway, F Cosandey, L Klein, G Amatucci, Investigation of the Lithiation and Delithiation Conversion Mechanisms of Bismuth Fluoride Nanocomposites, *J. Electrochem. Soc.*, **153** (4), A799-A808 (2006).

T Boonfueng, L Axe, Y Xu, T Tyson, The Impact of Mn Oxide Coatings on Zn Distribution, *J. Colloid Interface Sci.*, **298** (2), 615-623 (2006).

T Boonfueng, L Axe, Y Xu, T Tyson, Nickel and Lead Sequestration in Manganese Oxide-coated Montmorillonite, *J. Colloid Interface Sci.*, **303** (1), 87-98 (2006).

E Elzinga, A Rouff, R Reeder, The Long-Term Fate of Cu2+, Zn2+, and Pb2+ Adsorption Complexes at the Calcite Surface: An X-ray Absorption Spectroscopy Study, *Geochim. Cosmochim. Acta*, **70** (11), 2715-2725 (2006).

A Frenkel, D Pease, J Budnick, P Metcalf, E Stern, P Shanthakumar, T Huang, Strain-Induced Bond Buckling and Its Role in Insulating Properties of Cr-Doped V2O3, *Phys. Rev. Lett.*, **97**, 195502-1 to 195502 - 4 (2006).

P Kenward, D Fowle, N Yee, Microbial Selenate Sorption and Reduction in Nutrient Limited Systems, *Environ. Sci. Tech.*, **40**, 3782-3786 (2006).

S Lee, J Dyer, D Sparks, N Scrivner, E Elzinga, A Multi-Scale Assessment of Pb(II) Sorption on Dolomite, *J. Colloid Interface Sci.*, **298** (1), 20-30 (2006).

S Maeng, L Axe, T Tyson, L Gladczuk, M Sosnowski, Corrosion Behavior of Magnetron Sputtered Alpha Ta Coatings on Smooth and Rough Steel Substrates, *Surf. Coat. Technol.*, **200**, 5717-5724 (2006).
S Maeng, L Axe, T Tyson, P Cote, Corrosion Hehaviour of Electrodeposited and Sputtered Cr Coatings and Sputtered Ta Coatings with Alpha and Beta Phases, *Surf. Coat. Technol.*, **200**, 57675777 (2006).
L Menard, H Xu, S Gao, R Twesten, A Harper, Y Song, G Wang, A Douglas, J Yang, et al., Metal Core Bonding Motifs of Monodisperse Icosahedral Au13 and Larger Au Monolayer-Protected Clusters as Revealed by X-ray Absorption Spectroscopy and Transmission Electron Microscopy, *J. Phys. Chem. B*, **110**, 14564-14573 (2006).
S Morrison, C Cahill, E Carpenter, V Harris, Production Scaleup of Reverse Micelle Synthesis, *Ind. Eng. Chem. Res.*, **45**, 1217-1220 (2006).
S Park, K Kang, W Yoon, A Moodenbaugh, L Lewis, T Vogt, Magnetic Spin Glass Properties of the Bi-layer Hydrate Na0.3NiO2 1.3H2O, *Solid State Commun.*, **139** (2), 60-63 (2006).
E Peltier, R Allada, A Navrotsky, D Sparks, Nickel Solubility and Precipitation in Soils: A Thermodynamic Study, *Clays and Clay Minerals*, **54** (2), 153-164 (2006).
A Scheinost, A Rossberg, D Vantelon, I Xifra, R Kretzschmar, A Leuz, H Funke, C Johnson, Quantitative Antimony Speciation in Shooting-Range Soils by EXAFS Spectroscopy, *Geochim. Cosmochim. Acta*, **70** (13), 3299-3312 (2006).
M Shultz, E Carpenter, S Morrison, S Calvin, Cation Occupancy Determination in Manganese Zinc Ferrites using Fourier Transform Infrared Spectroscopy, *J. Appl. Phys.*, **99**, 08M901 (2006).
R Swaminathan, J Woods, S Calvin, J Huth, M McHenry, Microstructural Evolution Model of the Sintering Behavior and Magnetic Properties of NiZn Ferrite Nanoparticles, *Adv. Sci. Tech.*, **45**, 2337-2344 (2006).
J Wong, E Larson, P Waide, R Frahm, Combustion Front Dynamics in the Combustion Synthesis of Refractory Metal Carbides and Di-borides using Time-Resolved X-ray Diffraction, *J. Synch. Rad.*, **13**, 326-335 (2006).
Y Xu, T Boonfueng, L Axe, S Maeng, T Tyson, Surface Complexation of Pb(II) on Amorphous Iron Oxide and Manganese Oxide: Spectroscopic and Time Studies, *J. Colloid Interface Sci.*, **299** (1-3), 28-40 (2006).

Beamline X11B

B Ravel, Y Kim, P Woodward, C Fang, Role of Local Disorder in the Dielectric Response of BaTaO2N, *Phys. Rev. B: Condens. Matter*, **73**, 184121 (2006).
A Ryser, D Strawn, M Marcus, S Fakra, J Johnson-Maynard, G Moller, Microscopically Focused Synchrotron X-ray Investigation of Selenium Speciation in Soils Developing on Reclaimed Mine Lands, *Environ. Sci. Tech.*, **40**, 462-467 (2006).
P Shanthakumar, M Balasubramanian, D Pease, A Frenkel, D Potrepka, V Kraizman, J Budnick, W Hines, X-ray Study of the Ferroelectric [Ba0.6Sr0.4][(YTa)0.03Ti0.94]O3, *Phys. Rev. B*, **74**, 174103 (2006).
M Si, V Zaitsev, M Goldman, A Frenkel, D Peiffer, E Weil, J Sokolov, M Rafailovich, Self-extinguishing Polymer/Organoclay Nanocomposites, *Polym. Degrad. Stab.*, **92** (1), 86-93 (2006).

Y Xu, T Boonfueng, L Axe, S Maeng, T Tyson, Surface Complexation of Pb(II) on Amorphous Iron Oxide and Manganese Oxide: Spectroscopic and Time Studies, *J. Colloid Interface Sci.*, **299** (1-3), 28-40 (2006).

Beamline X12A

A Bolotnikov, G Camarda, G Carini, M Fiederle, L Li, D McGregor, W McNeil, G Wright, R James, Performance Characteristics of Frisch-Ring CdZnTe Detectors, *IEEE Trans. Nucl. Sci.*, **53** (2), 607-614 (2006).
W Caliebe, I So, A Lenhard, D Siddons, Cam-driven Monochromator for QEXAFS, *20th International Conference on X-Ray and Inner-Shell Processes*, Vol 75, p. 1962-1965, sponsored by University of Melbourne (2006).
W Caliebe, I So, A Lenhard, D Siddons, Cam-Driven Monochromator for QEXAFS, *Radiat. Phys. Chem.*, **75** (11), 1962-1965 (2006).
G Camarda, A Bolotnikov, G Carini, R James, L Li, Effects of Tellurium Precipitates on Charge Collection in CZT Nuclear Radiation Detectors, *Nato Conference on Countering Nuclear and Radiological Terrorism*, p. 199-207, Springer, (2006).
G Camarda, A Bolotnikov, G Carini, Y Cui, K Kohman, L Li, R James, High Spatial-Resolution Imaging of Te Inclusions in CZT Material, *In Proceedings of SPIE Hard X-ray and Gamma-Ray Detector Physics VIII*, Vol 6319, p. 63190Z-1, sponsored by SPIE (2006).
G Carini, A Bolotnikov, G Camarda, Y Cui, H Jackson, A Burger, K Kohman, L Li, R James, Te Inclusions and Their Relationship to the Performance of CdZnTe Detectors, *In Proceedings of SPIE Hard X-ray and Gamma-Ray Detector Physics VIII*, Vol 6319, p. 631906-1, sponsored by SPIE (2006).
G Carini, A Bolotnikov, G Camarda, G Wright, R James, Y Li, Effect of Te Precipitates on the Performance of CdZnTe Detectors, *Appl. Phys. Lett.*, **88**, 143515 (2006).
G Carini, Development of CdZnTe Radiation Detectors, Ph.D. Thesis, University of Palermo, Palermo (2006).
M Chu, S Terterian, G Carini, G Camarda, A Bolotnikov, R James, D Xu, Z He, Effects of Material Improvement on CZT Detectors, *In Proceedings of SPIE Hard X-ray and Gamma-Ray Detector Physics VIII*, Vol 6319, p. 631905-1, sponsored by SPIE (2006).
A Mavroudis, A Avgeropoulos, N Hadjichristidis, E Thomas, D Lohse, Synthesis and Morphological Behavior of Model 6-Miktoarm Star Copolymers, PS(P2MP)5, of Styrene (S) and 2-Methyl-1,3-Pentadiene (P2MP), *Chem. Mater.*, **18**, 2164-2168 (2006).

Beamline X12B

M Adams, Z Jia, Modulator of Drug Activity B from Escherichia Coli: Crystal Structure of a Prokaryotic Homologue of DT-Diaphorase, *J. Mol. Biol.*, **359** (2), 455-465 (2006).
D Copeland, A Soares, A West, G Richter-Addo, Crystal Structures of the Nitrite and Nitric Oxide Complexes of Horse Heart Myoglobin, *J. Inorg. Biochem.*, **100** (8), 1413-1425 (2006).
M Groves, M Singh, G Beydaghyan, M Muller, E Sheridan, D Schneider, Design and Implementation of a simple and Inexpensive GISAXS Sample Chamber, *J. Appl. Cryst.*, **39**, 120-123 (2006).

S Kamtekar, R Ho, M Cocco, W Li, S Wenwieser, M Boocock, N Grindley, T Steitz, Implications of Structures of Synaptic Tetramers of gamma delta Resolvase for the Mechanism of Recombination, *Proc Natl Acad Sci USA*, **103** (28), 10642-10647 (2006).

J Mao, S Mukherjee, Y Zhang, R Cao, J Sanders, Y Song, Y Zhang, G Meints, Y Gao, et al., Solid-State NMR, Crystallographic, and Computational Investigation of Bisphosphonates and Farnesyl Diphosphate Synthase-Bisphosphonate Complexes, *J. Am. Chem. Soc.*, **128**, 14485-14497 (2006).

M McDonough, V Li, E Flashman, R Chowdhury, C Mohr, B Lienard, J Zondlo, N Oldham, I Clifton, et al., Cellular Oxygen Sensing: Crystal Structure of Hypoxia-Inducible Factor Prolyl Hydroxylase (PHD2), *Proc Natl Acad Sci USA*, **103** (26), 9814-9819 (2006).

S Mylavarapu, M Furgason, D Brewer, M Munson, The Structure of the Exocyst Subunit Sec6p Defines a Conserved Architecture with Diverse Roles, *Nat. Struct. Mol. Biol.*, **13** (6), 555-556 (2006).

H Pinkett, K Shearwin, S Stayrook, I Dodd, T Burr, A Hochschild, J Egan, M Lewis, The Structural Basis of Cooperative Regulation at an Alternate Genetic Switch, *Mol. Cell*, **21**, 605-615 (2006).

C Simmons, Q Liu, Q Huang, Q Hao, T Begley, P Karplus, M Stipanuk, Crystal Structure of Mammalian Cysteine dioxygenase: A Novel Mononuclear Iron Center for Cysteine Thiol Oxidation, *J. Biol. Chem.*, **281**, 18723-18733 (2006).

M Swan, D Bastia, C Davies, Crystal Structure of pi Initiator Protein-iteron Complex of Plasmid R6K: Implications for Initiation of Plasmid DNA Replication, *Proc Natl Acad Sci USA*, **103** (49), 18481-18486 (2006).

J Thompson, Z Ryan, J Salisbury, R Kumar, The Structure of the Human Centrin 2-Xeroderma Pigmentosum Group C Protein Complex, *J. Biol. Chem.*, **281**, 18746 (2006).

Z Wang, C Li, M Ellenburg, E Soistman, J Ruble, B Wright, J Ho, D Carter, Structure of Human Ferritin L Chain, *Acta Cryst. D*, **62**, 800-806 (2006).

Beamline X12C

R Agarwal, J Bonanno, S Burley, S Swaminathan, Structure Determination of an FMN Reductase from Pseudomonas aeruginosa PA01 using Sulfur Anomalous Signal, *Acta Cryst. D*, **62**, 383-391 (2006).

S Bajaj, A Schmidt, S Agah, M Bajaj, K Padmanabhan, High Resolution Structures of p-Aminobenzamidine- and Benzamidine- VIIa/Soluble Tissue Factor: Unpredicted Conformation of the 192-193 Peptide Bond and Mapping of Ca2+, Mg2+, Na+ an Zn2+ Sites in Facto VIIa, *J. Biol. Chem.*, **281**, 24873-24888 (2006).

A Balakrishna, Y Tan, H Mok, A Saxena, K Swaminathan, Crystallization and Preliminary X-ray Diffraction Analysis of Salmonella typhi PilS, *Acta Cryst. F*, **62**, 1024-1026 (2006).

M Barreras, M Bianchet, L Ielpi, L Tong, Crystallization and Preliminary Crystallographic Characterization of GumK, A Membrane-Associated Gluocuronosyltransferase from Xanthomonas campestris Required for Xanthan Polysaccharide Synthesis, *Acta Cryst. F*, **62**, 880-883 (2006).

M Bewley, V Graziano, J Jiang, E Matz, F Studier, A Pegg, C Coleman, J Flanagan, Structures of Wild-Type and Mutant Human Spermidine/Spermine N1-acetyltransferase, a Potential Therapeutic Drug Target, *Proc Natl Acad Sci USA*, **103**, 2063-8 (2006).

M Botuyan, J Lee, I Ward, J Kim, J Thompson, J Chen, G Mer, Structural Basis for the Methylation State-Specific Recognition of Histone H4-K20 by 53BP1 and Crb2 in DNA Repair, *Cell*, **127** (7), 1361-1373 (2006).

D Ceccarelli, H Song, F Poy, M Schaller, M Eck, Crystal Structure of the FERM Domain of Focal Adhesion Kinase, *J. Biol. Chem.*, **281** (1), 252-259 (2006).

W Franks, B Wylie, S Stellfox, C Rienstra, Microcrystalline U-15N-Labeled Protein by 3D Dipolar-Shift Solid-State NMR Spectroscopy, *J. Am. Chem. Soc.*, **128**, 3154-3155 (2006).

H Gennadios, D Christianson, Binding of Uridine 5'-Diphosphate in the "Basic Patch" of the Zinc Deacetylase LpxC and Implications for Substrate Binding, *Biochemistry*, **45**, 15216-15223 (2006).

Q Huai, Structure of Human Urokinase Plasminogen Activator, *Science*, **311**, 656 (2006).

S Kamtekar, R Ho, M Cocco, W Li, S Wenwieser, M Boocock, N Grindley, T Steitz, Implications of Structures of Synaptic Tetramers of gamma delta Resolvase for the Mechanism of Recombination, *Proc Natl Acad Sci USA*, **103** (28), 10642-10647 (2006).

B Kelly, B Howard, H Wang, H Robinson, W Sundquist, C Hill, Implications for Viral Capsid Assembly from Crystal Structures of HIV-1 Gag1-278 and CAN133-278, *Biochemistry*, **45** (38), 11257 -11266 (2006).

D Kumaran, J Bonnano, S Burley, S Swaminathan, Crystal Structure of Phosphatidylglycerophosphat ase (PGPase), a Putative Membrane-Bound Lipid Phosphatase, Reveals a Novel Binuclear Metal Binding Site and Two "Proton Wires", *Proteins: Struc. Func. Bioinformatics*, **64**, 851-862 (2006).

C Lawson, B Yung, A Barbour, W Zuckert, Crystal Structure of Neurotropism-Associated Variable Surface Protein 1 (VSP1) of Borrelia Turicatae, *J. Bacteriol.*, **188**, 4522 (2006).

S Lee, Y Tsai, R Mattera, W Smith, M Kostelansky, A Weissman, J Bonifacino, J Hurley, Structural Basis for Ubiquitin Recognition and Autoubiquitination by Rabex-5, *Nat. Struct. Mol. Biol.*, **13**, 264-271 (2006).

Y Liu, J Wu, J Song, J Sivaraman, C Hew, Identification of a Novel Nonstructural Protein, VP9, from White Spot Syndrome Virus: Its Structure Reveals a Ferredoxin Fold with Specific Metal Binding Sites, *J. Virology*, **80** (21), 10419-10427 (2006).

Y Liu, J Sivaraman, C Hew, Expression, purification and crystallization of a novel nonstructural protein VP9 from white spot syndrome virus., *Acta Cryst. F*, **62** (8), 802 - 804 (2006).

S Ni, F Forouhar, D Bussiere, H Robinson, M Kennedy, Crystal Structure of VC0702 at 2.0 Angstrom: Conserved Hypothetical Protein from Vibrio Cholerae, *Proteins: Struc. Func. Bioinformatics*, **63** (4), 733-741 (2006).

S Park, P Borbat, G Gonzalez-Bonet, J Bhatnagar, A Pollard, J Freed, A Bilwes, B Crane, Reconstruction of the Chemotaxis Receptor-Kinase Assembly, *Nat. Struct. Mol. Biol.*, **13** (5), 400 (2006).

K Rao, J Bonanno, S Burley, S Swaminathan, Crystal Structure of Glycerophosphodiester Phosphodiesterase from Agrobacterium tumefaciens by SAD with a Large Asymmetric Unit, *Proteins: Struc. Func. Bioinformatics*, **65**, 514-518 (2006).

J Seetharaman, D Kumaran, J Bonanno, S Burley, S Swaminathan, Crystal Structure of a Putative HTH-Type Transcriptional Regulator yxaF from Bacillus subtilis, *Proteins: Struc. Func. Bioinformatics*, **63**, 1087-1091 (2006).

J Seetharaman, K Rajashankar, V Solarzano, R Kniewel, C Lima, J Bonanno, S Burley, S Swaminathan, Crystal Structures of Two Putative Phosphoheptose, *Proteins: Struc. Func. Bioinformatics*, **63**, 1092-1096 (2006).

N Silvaggi, C Zhang, Z Lu, J Dai, D Dunaway-Mariano, K Allen, The X-ray Crystal Structures of Human {alpha}-Phosphomannomutase 1 Reveal the Structural Basis of Congenital Disorder of Glycosylation Type 1a, *J. Biol. Chem.*, **281** (21), 14918-14926 (2006).

S Sunita, H Zhenxing, J Swaathi, M Cygler, A Matte, J Sivaraman, Domain organization and crystal structure of the catalytic domain of E.coli RluF, a pseudouridine synthase that acts on 23S rRNA, *J. Mol. Biol.*, **359** (4), 998 - 1009 (2006).

F Xue, R Burnett, Capsid-like Arrays in Crystals of Chimpanzee Adenovirus Hexon, *J. Struct. Biol.*, **154** (2), 217-221 (2006).

Y Yuan, Y Pei, H Chen, T Tuschl, D Patel, A Potential Protein-RNA Recognition Event Along the RISC-Loading Pathway from the Structure of A. aeolicus Argonaute with Externally Bound siRNA, *Structure*, **14** (10), 1557-1565 (2006).

Beamline X13A

B Kirby, J Borchers, J Rhyne, K O'Donovan, S Velthuis, S Roy, C Sanchez-Hanke, T Wojtowicz, X Liu, et al., Magnetic and Chemical Nonuniformity in Ga1-xMnxAs Films as Probed by Polarized Neutron and X-ray Reflectometry, *Phys. Rev. B*, **74**, 245304 (2006).

C Sanchez-Hanke, R Gonzalez-Arrabal, J Prieto, E Andrzejewska, N Gordillo, D Boerma, R Loloee, J Skuza, R Lukaszew, Observation of Nitrogen Polarization in Fe-N Using Soft X-ray Magnetic Circular Dichorism, *J. Appl. Phys.*, **99**, 08B709 (2006).

Beamline X13B

G Cargill, III, L Moyer, G Wang, H Zhang, C Hu, W Yang, B Larson, G Ice, Thermal and Electromigration-Induced Strains in Polycrystalline Films and Conductor Lines: X-ray Microbeam Measurements and Analysis, *AIP Conference Proceedings*, Vol 817, p. 303, sponsored by AIP (2006).

G Wang, H Zhang, G Cargill III, C Hu, L Ge, A Maniatty, Thermal and Electromigration-Induced Strains in Copper Conductor Lines: X-ray Microbeam Measurements and Analysis, *Materials Research Society Spring 2006 Meeting*, Vol 914, p. 0914-F06-06, sponsored by Materials Research Society (2006).

H Yan, I Noyan, Measurement of Stress/Strain in Single-Crystal Samples using Diffraction, *J. Appl. Cryst.*, **39**, 320-325 (2006).

Beamline X14A

J Biernacki , C Parnham, T Watkins, C Hubbard, J Bai, Phase-Resolved Strain Measurements in Hydrated Ordinary Portland Cement Using Synchrotron X-rays, *J. Am. Ceram. Soc.*, **89** (9), 2853-2859 (2006).

M Deleon, Structural, Magnetic, and Transport Characteristics of Strained Lanthanum Deficient Manganite Films, Ph. D. Thesis, New Jersey Institute of Technology, Newark (2006).

S Jaradat, H Gleeson, N Roberts, Y Wang, The Effects of Highly Chiral Dopants on the Smectic Phases of Liquid Crystals Remarkably Wide Intermediate Phases, *J Mater. Chem.*, **16**, 3753 (2006).

S Kewalramani, G Dommett, K Kim, G Evmenenko, H Mo, B Stripe, P Dutta, Aggregation-governed Oriented Growth of Inorganic Crystals at an Organic Template, *J. Chem. Phys.*, **125** (22), 224713 (2006).

H Sheng, W Luo, F Alamgir, J Bai, E Ma, Atomic Packing and Short-to-Medium-Range Order in Metallic Glasses, *Nature*, **439**, 419-425 (2006).

Beamline X15A

A Antunes, A Safatle, P Barros, S Morelhao, X-ray Imaging in Advanced Studies of Ophthamic Diseases, *Med. Phys.*, **33** (7), 2338-2343 (2006).

J Brankov, M Wernick, Y Yang, J Li, C Muehleman, Z Zhong, M Anastasio, A Computed Tomography Implementation of Multiple-Image Radiography, *Med. Phys.*, **33** (2), 278 (2006).

D Connor, D Sayers, D Sumner, Z Zhong, Diffraction Enhanced Imaging of Controlled Defects Within Bone, Including Bone-Metal Gaps, *Phys. Med. Biol.*, **51** (12), 3283-3300 (2006).

M Kelly, R Beavis, D Fourney, E Schultke, C Parham, B Juurlink, Z Zhong, L Chapman, Diffraction-enhanced Imaging of the Rat Spine, *Can. Assoc. Radiol. J.*, **57**, 204-210 (2006).

G Khelashvili, J Brankov, D Chapman, M Anastasio, Y Yang, Z Zhong, M Wernick, A Physical Model of Muliple-Image Radiography, *Phys. Med. Biol.*, **51** (2), 221-236 (2006).

C Kim, M Bourham, J Doster, A Wide-Beam X-ray Source Suitable for Diffraction Enhanced Imaging Applications, *Nucl. Instrum. Meth. A*, **566** (2), 713-721 (2006).

C Muehleman, J Li, Z Zhong, J Brankov, M Wernick, Multiple-Image Radiography for Human Soft Tissue, *J. Anatomy*, **208**, 115-124 (2006).

C Muehleman, J Li, Z Zhong, Preliminayr Study on Diffraction Enhanced Radiographic Imaging for a Canine Model of Cartilage Damage, *Osteoarthr. Cartilage*, **14** (92), 882-888 (2006).

M Wernick, Y Yang, I Mondal, D Chapman, M Hasnah, C Parham, E Pisano, Z Zhong, Computation of Mass Density Images from X-ray Refraction-Angle Images, *Phys. Med. Biol.*, **51**, 1769-1778 (2006).

Z Zhang, P Fenter, L Cheng, N Sturchio, M Bedzyk, M Machesky, L Anovitz, D Wesolowski, Zn2+ and Sr2+ Adsorption at the TiO2 (110)-Electrolyte Interface: Influence of Ionic Strength, Coverage, and Anions, *J. Colloid Interface Sci.*, **295** (1), 50-64 (2006).

Z Zhang, P Fenter, S Kelly, J Catalano, A Bandura, J Kubicki, J Sofo, D Wesolowski, M Machesky, et al., Structure of Hydrated Zn2+ at the Rutile TiO2 (110)-Aqueous Solution Interface: Comparsion of X-ray Standing Wave, X-ray Absorption Spectroscopy, and Density Functional Theory Results, *Geochim. Cosmochim. Acta*, **70** (16), 4039-4056 (2006).

Beamline X15B

H Sheng, W Luo, F Alamgir, J Bai, E Ma, Atomic Packing and Short-to-Medium-Range Order in Metallic Glasses, *Nature*, **439**, 419-425 (2006).

M Vittadello, P Stallworth, F Alamgir, S Suarez, S Abbrent, C Drain, V Di Noto, S Greenbaum, Polymeric gamma-MgCl2 Nanoribbons, *Inorg. Chim. Acta*, **359** (8), 2513-2518 (2006).

Beamline X16C

J Kim, G Korshin, A Frenkel, A Velichenko, Electrochemical and XAFS Studies of Effects of Carbonate on the Oxidation of Arsenite, *Environ. Sci. Tech.*, **40**, 228-234 (2006).

P Lyman, V Shneerson, R Fung, S Parihar, H Johnson-Steigelman, E Lu, D Saldin, Structure and Stability of Sb/Au(110)-c(2x2) Surface Phase, *Surf. Sci.*, **600** (2), 424-435 (2006).

L Menard, H Xu, S Gao, R Twesten, A Harper, Y Song, G Wang, A Douglas, J Yang, et al., Metal Core Bonding Motifs of Monodisperse Icosahedral Au13 and Larger Au Monolayer-Protected Clusters as Revealed by X-ray Absorption Spectroscopy and Transmission Electron Microscopy, *J. Phys. Chem. B*, **110**, 14564-14573 (2006).

K Pokhodnya, M Bonner, J Her, P Stephens, J Miller, Magnetic Ordering (Tc=90K) Observed for Layered [FeII(TCNE-)(NCMe)2]+[FeIIICl4]- (TCNE = Tetracyanoethylene), *J. Am. Chem. Soc.*, **128**, 15592-15593 (2006).

M Sachan, N Walrath, S Majetich, K Krycka, C Kao, Interaction Effects Witin Langmuir Layers and Three-Dimensional Arrays of E-Co Nanoparticles, *J. Appl. Phys.*, **99**, 08C302 (2006).

K Sugimoto, R Dinnebier, T Schlecht, Chlorartinite, A Volcanic Exhalation Product Also Found in Industrial Magnesia Screed, *J. Appl. Cryst.*, **39**, 739-744 (2006).

Y Sun, A Frenkel, H White, L Zhang, Y Zhu, H Xu, J Yang, T Koga, V Zaitsev, et al., Comparison of Decanethiolate Gold Nanoparticles Synthesized by One-Phase and Two-Phase Methods, *J. Phys. Chem. B*, **110**, 23022-23030 (2006).

Beamline X17B1

D Anschel, B Foerster, T Yuasa, H Benveniste, Z Zhong, J Heinfeld, A Dilmanian, 9.4 T MRI Characterization of a Focal Lesion in the Rat Brain Induced by Interlaced Microbeam Radiation, *Epilepsia*, Vol 46, p. 280-281, sponsored by American Epilepsy Society and American Clinical Neurophysiology Society (2006).

G Carini, Development of CdZnTe Radiation Detectors, Ph.D. Thesis, University of Palermo, Palermo (2006).

G Carini, C Arnone, A Bolotnikov, G Camarda, R De Wames, J Dinan, J Markunas, B Raghothamachar, S Sivananthan, et al., Material Quality Characterization of CdZnTe Substrates for HgCdTe Epitaxy, *J. Electron. Mater.*, **35** (6), 1495-1502 (2006).

T Chen, A Neville, K Sorbie, Z Zhong, Using Synchrotron Radiation Wide Angle X-Ray Scattering (WAXS) to Study the Inhibition Effect of DiEthyleneTriaminePenta (MethylenePhosphonic acid) (DETPMP) on CaCO3 Scale Formation , *SPE Eighth International Symposium on Oilfield Scale*, p. Paper 100440, sponsored by SPE (2006).

T Chen, A Neville, K Sorbie, Z Zhong, Using Synchrotron Radiation Wide Angle X-Ray Scattering (WAXS) to Study the Inhibiting Effect of Polyphosphonocarboxylic Acid (PPCA) on CaCO3 Scale Formation, *CORROSION/2006*, p. Paper 06386, sponsored by NACE (2006).

T Chen, New Insights into the Mechanisms of Calcium Carbonate Mineral Scale Formation and Inhibiton, Ph.D Thesis, Heriot-Watt University, Edinburgh (2006).

F Dilimanian, Z Zhong, T Bacarian, H Benveniste, P Romanelli, R Wang, J Welwart, T Yuasa, E Rosen, D Anschel, Interlaced X-ray Microplanar Beams: A Radiosurgery Approach with Clinical Potential, *Proc Natl Acad Sci USA*, **103** (25), 9709-9714 (2006).

G Gwanmesia, J Zhang, K Darling, J Kung, B Li, L Wang, D Neuville, R Liebermann, Elasticity of Polycrystalline Pyrope (Mg3Al2Si3O12) to 9 GPa and 1000 degrees C, *Phys. Earth Planet. Interiors*, **155** (3-4), 179-190 (2006).

K Hirota, S Wakimoto, D Cox, Neutron and X-ray Studies of Relaxors, *J. Phys. Soc. Japan*, **75** (11), 111006-1 to 13 (2006).

J Jakoncic, M Di Michiel, Z Zhong, V Honkimaki, Y Jouanneau, V Stojanoff, Anomalous Diffraction at Ultra-High Energy for Protein Crystallography, *J. Appl. Cryst.*, **39**, 831-841 (2006).

B Noheda, D Cox, Bridging Phases at the Morphotropic Boundaries of Lead Oxide Solid Solutions, *Phase Transit*, **79** (1-2), 5-20 (2006).

A Phelippeau, S Pommier, T Tsakalakos, M Clavel, C Prioul, Cold Drawn Steel Wires—Processing, Residual Stresses and Ductility—Part I: Metallography and Finite Element Analyses, *Fatigue Fract. Eng. Mater. Struct.*, **29**, 201-208 (2006).

A Phelippeau, S Pommier, I Zakharchenko, R Levy-Tubiana, T Tsakalakos, M Clavel, M Croft, Z Zhong, C Prioul, Cold Drawn Steel Wires—Processing, Residual Stresses and Ductility Part II: Synchrotron and Neutron Diffraction, *Fatigue Fract. Eng. Mater. Struct.*, **29**, 255-265 (2006).

C Stock, D Ellis, I Swainson, G Xu, H Hiraka, Z Zhong, H Luo, X Zhao, D Viehland, et al., Damped Soft Phonons and Diffuse Scattering in 40% Pb(Mg1/3Nb2/3))3-60% PbTiO3, *Phys. Rev. B*, **73**, 064107 (2006).

T Tsakalakos, M Croft, N Jisrawi, R Holtz, Z Zhong, Measurement of Residual Stress Distributions by Energy Dispersive X-ray Diffraction Synchrotron Radiation, *Int. J. Offshore Polar Eng.*, **16**, 358-366 (2006).

G Xu, Z Zhong, Y Bing, Z Ye, G Shirane, Electric-Field-Induced Redistribution of Polar Nano-Regions in a Relaxor Ferroelectric, *Nat. Mater.*, **5**, 134-140 (2006).

Beamline X17B2

J Chen, L Li, T Yu, H Long, D Weidner, L Wang, M Vaughan, Do Reuss and Voigt Bounds Really Bound in High-Pressure Rheology Experiments?, *J. Phys.: Condens. Matter*, **18**, S1049-1059 (2006).

G Gwanmesia, J Zhang, K Darling, J Kung, B Li, L Wang, D Neuville, R Liebermann, Elasticity of Polycrystalline Pyrope (Mg3Al2Si3O12) to 9 GPa and 1000 degrees C, *Phys. Earth Planet. Interiors*, **155** (3-4), 179-190 (2006).

J Kung, B Li, R Liebermann, Ultrasonic Observations of Elasticity Changes Across Phase Transformations in MgSiO3 Pyroxenes, *J. Phys. Chem. Solids*, **67** (9-10), 2051-2055 (2006).

W Liu, B Li, Thermal Equation of State of (Mg0.9Fe0.1)2SiO4 Olivine, *Phys. Earth Planet. Interiors*, **157** (3-4), 188-195 (2006).

V Solozhenko, O Kurakevych, E Solozhenko, J Chen, J Parise, Equation of State of Graphite-like BC,, *Solid State Commun.*, **137** (5), 268-271 (2006).

Beamline X17B3

R Aksoy, Y Ma, E Selvi, M Chyu, A Ertas, A White, Equation of State Measurement of Molybdenum Disulfide, *J. Phys. Chem. Solids*, **67**, 1914-1917 (2006).

V Levitas, Y Ma, J Hashemi, M Holtz, N Guven, Strain-induced disorder, phase transformations and TRIP in hexagonal boron nitride under compression and shear in a rotational diamond anvil cell: in-situ X-ray diffraction study and modeling, *J. Chem. Phys.*, **125**, 044507 (2006).

Y Ma, J Liu, C Gao, A White, W Mei, J Rasty, High-pressure X-ray diffraction study of the giant dielectric constant material CaCu3Ti4O12: evidence of stiff grain surface, *American Physical Society Spring meeting*, p. #Q1.152, sponsored by American Physical Society (2006).

Y Ma, V Levitas, J Hashemi, X-ray Diffraction Measurements in a Rotational Diamond Anvil Cell, *J. Phys. Chem. Solids*, **67**, 2083-2090 (2006).

Y Ma, E Selvi, V Levitas, J Hashemi, Effect of Shear Strain on the α-ε Phase Transition of Iron: a New Approach in the Rotational Diamond Anvil Cell, *J. Phys.: Condens. Matter*, **18**, 1075 (2006).

Y Ma, J Liu, C Gao, W Mei, A White, J Rasty, High-pressure X-ray Diffraction Study of the Giant Dielectric Constant Material CaCu3Ti4O12: Evidence of Stiff Grain Surface, *Appl. Phys. Lett.*, **88**, 191903 (2006).

E Selvi, Y Ma, R Aksoy, A Ertas, A White, J Sandhu, High pressure x-ray diffraction study of tungsten disulfide, *J. Phys. Chem. Solids*, **67**, 2183-2186 (2006).

Beamline X17C

R Aksoy, Y Ma, E Selvi, M Chyu, A Ertas, A White, Equation of State Measurement of Molybdenum Disulfide, *J. Phys. Chem. Solids*, **67**, 1914-1917 (2006).

N Conil, A Kavner, Elastic Behavior and Strength of Al2O3 Fiber/Al Matrix Composite and Implications for Equation of State Measurements in the Diamond Anvil Cell, *J. Appl. Phys.*, **100**, 043517 (2006).

G Gatta, Y Lee, On the Elastic Behaviour of Zeolite Mordenite: a Synchrotron Powder Diffraction Study, *Phys. Chem. Miner.*, **32**, 726-732 (2006).

D He, T Duffy, X-ray Diffraction Study of the Static Strength of tungsten to 69 Gpa, *Phys. Rev. B*, **73**, 134106 (2006).

J Hu, H Mao, J Shu, Q Guo, H Liu, Diamond Anvil Cell Radial X-ray Diffraction Program at the National Synchrotron Light Source, *Workshop on Synergy of 21st Century High-Pressure Science and Technology*, Vol 18, p. S1091-S1096, sponsored by HPcat, APS, ANL (2006).

J Hu, H Mao, J Shu, Q Guo, H Liu, Diamond Anvil Cell Radial X-ray Diffraction Program at the National Synchrotron Light Source, *J. Phys.: Condens. Matter*, **18** (25), S1091-S1096 (2006).

F Jiang, S Speziale, T Duffy, Single-crystal Elasticity of Brucite, Mg(OH)2, to 15 Gpa by Brillouin Scattering, *Am. Mineral.*, **91**, 1893-1900 (2006).

Y Lee, J Hriljac, J Parise, T Vogt, Pressure-induced Hydration in Zeolite Tetranatrolite, *Am. Mineral.*, **91**, 247-251 (2006).

V Levitas, Y Ma, J Hashemi, M Holtz, N Guven, Strain-induced disorder, phase transformations and TRIP in hexagonal boron nitride under compression and shear in a rotational diamond anvil cell: in-situ X-ray diffraction study and modeling, *J. Chem. Phys.*, **125**, 044507 (2006).

M Lufaso, W Gemmil, S Mugavero, Y Lee, T Vogt, H zur Loye, Compression mechanisms of symmetric and Jahn–Teller distorted octahedra in double perovskites: A2CuWO6 (A ¼ Sr, Ba), Sr2CoMoO6, and La2LiRuO6, *J. Solid State Chem.*, **179**, 3571-3576 (2006).

M Lufaso, R Macquart, Y Lee, T Vogt, H zur Loye, Pressure induced octahedral tilting distortion in Ba2YTaO6, *Chem. Commun.*, **168**, 168-170 (2006).

Y Ma, J Liu, C Gao, A White, W Mei, J Rasty, High-pressure X-ray diffraction study of the giant dielectric constant material CaCu3Ti4O12: evidence of stiff grain surface, *American Physical Society Spring meeting*, p. #Q1.152, sponsored by American Physical Society (2006).

Y Ma, V Levitas, J Hashemi, X-ray Diffraction Measurements in a Rotational Diamond Anvil Cell, *J. Phys. Chem. Solids*, **67**, 2083-2090 (2006).

Y Ma, E Selvi, V Levitas, J Hashemi, Effect of Shear Strain on the α-ε Phase Transition of Iron: a New Approach in the Rotational Diamond Anvil Cell, *J. Phys.: Condens. Matter*, **18**, 1075 (2006).

Y Ma, J Liu, C Gao, W Mei, A White, J Rasty, High-pressure X-ray Diffraction Study of the Giant Dielectric Constant Material CaCu3Ti4O12: Evidence of Stiff Grain Surface, *Appl. Phys. Lett.*, **88**, 191903 (2006).

A Papandrew, M Lucas, R Stevens, I Halevy, B Fultz, M Hu, P Chow, R Cohen, M Somayazulu, Absence of Magnetism in Hcp Iron-Nickel at 11K, *Phys. Rev. Lett.*, **97**, 087202 (2006).

S Park, Y Lee, M Elcombe, T Vogt, Synthesis and Structure of the Bilayer Hydrate Na0.3NiO2.1.3D2O, *Inorg. Chem.*, **45** (9), 3490-3492 (2006).

J Provis, Modelling the Formation of Geopolymers, Ph.D. Thesis, University of Melbourne, Melbourne (2006).

W Qiu, P Baker, N Velisavljevic, Y Vohra, S Weir, Calibration of an isotopically enriched carbon-13 layer pressure sensor to 156 GPa in a diamond anvil cell, *J. Appl. Phys.*, **99**, 064906 (2006).

E Selvi, Y Ma, R Aksoy, A Ertas, A White, J Sandhu, High pressure x-ray diffraction study of tungsten disulfide, *J. Phys. Chem. Solids*, **67**, 2183-2186 (2006).
S Sen, S Gaudio, B Aitken, C Lesher, Observation of a Pressure-Induced First-Order Polyamorphic Transition in a Chalcogenide Glass at Ambient Temperature, *Phys. Rev. Lett.*, **97**, 025504 (2006).
S Speziale, S Shieh, T Duffy, High-Pressure Elasticity of Calcium Oxide: A Comparison Between Brillouin Scattering and radial X-ray Diffraction, *J. Geophys. Res.*, **111**, B02203 (2006).
F Zhang, J Lian, U Becker, R Ewing, L Wang, L Boatner, J Hu, S Saxena, Pressure-induced Structural Transitions and Phase Decomposition in the Cd2Nb2O7 Pyrochlore, *Phys. Rev. B*, **74**, 174116 (2006).

Beamline X18A

A Braun, F Huggins, K Kelly, B Mun, S Ehrlich, G Huffman, Impact of Ferrocene on the Structure of Diesel Exhaust Soot as Probed with Wide-Angle X-ray Scattering and C(1s) NEXAFS Spectroscopy, *Carbon*, **44** (14), 2904-2911 (2006).
X Chen, K Tenneti, C Li, Y Bai, R Zhou, X Wan, X Fan, Q Zhou, Design, Synthesis, and Characterization of Bent-Core Mesogen-Jacketed Liquid Crystalline Polymers, *Macromolecules*, **39**, 517-527 (2006).
K Chung, H Lee, W Yoon, J McBreen, X Yang, Studies of LiMn2O4 Capacity Fading Mechanism at Elevated Temperature Using In Situ Synchrotron X-Ray Diffraction, *J. Electrochem. Soc.*, **153**, A774 (2006).
G Liu, K Rider, W Nam, S Fonash, S Kim, Dendritic Aggregation of Oligothiophene During Desorption of 2,5-Diiodothiophene Multilayer and Topography-Induced Alignment of Oligothiophene Nanofibers, *J. Phys. Chem. B*, **110**, 20197-20201 (2006).
L Martinez-Miranda, Y Hu, Temperature and Depth Dependence of Order in Liquid Crystal Interfaces, *J. Appl. Phys.*, **99**, 113522 (2006).
H Mo, G Evmenenko, S Kewalramani, K Kim, S Ehrlich, P Dutta, Observation of Surface Layering in a Nonmetallic Liquid, *Phys. Rev. Lett.*, **96**, 096107 (2006).
G Wang, Y Ji, X Huang, X Yang, P Gouma, M Dudley, Fabrication and Characterization of Polycrystalline WO3 Nanofibers and Their Application for Ammonia Sensing, *J. Phys. Chem. B*, **110**, 23777-23782 (2006).
W Yoon, K Chung, J McBreen, X Yang, A Comparative Study on Structural Changes of LiCo1/3Ni1/3Mn1/3O2 and LiNi0.8Co0.15Al0.05O2 During First Charge using in situ XRD, *Electrochem. Commun.*, **8** (8), 1257-1262 (2006).

Beamline X18B

M Afeworki, D Dorset, G Kennedy, K Strohmaier, Synthesis and Characterization of a New Microporous Material. 1. Structure of Aluminophosphate EMM-3, *Chem. Mater.*, **18**, 1697-1704 (2006).
O Alexeev, A Siani, G Lafaye, C Williams, H Ploehn, M Amiridis, EXAFS Characterization of Dendrimer-PT Nanocomposites Used for the Preparation of Pt/gamma-Al2O3 Catalysts, *J. Phys. Chem. B*, **110**, 24903-24914 (2006).
B Anderson, J Fierro-Gonzalez, K Ramesh, C Vinod, J Niemantsverdriet, B Gates, Tricarbonyls of Low-Coordinated Au(0) Atoms in Zeolite-Supported Gold Nanoparticles: Evidence from Infrared and X-ray Absorption Spectroscopies, *Langmuir*, **22**, 4310-4314 (2006).
S Bare, G Mickelson, F Modica, A Ringwelski, N Yang, Simple Flow Through Reaction Cells for in situ Transmission and Fluorescence X-ray Absorption Spectroscopy of Heterogeneous Catalysts, *Rev. Sci. Instrum.*, **77**, 023105 (2006).
S Beauchemin, J Kwong, Impact of Redox Conditions on Arsenic Mobilization from Tailings in a Wetland with Neutral Drainage, *Environ. Sci. Tech.*, **40**, 6297-6303 (2006).
V Bhirud, J Ehresmann, P Kletnieks, J Haw, B Gates, Rhodium Complex with Ethylene Ligands Supported on Highly Dehydroxylated MgO: Synthesis, Characterization, and Reactivity, *Langmuir*, **22**, 490-496 (2006).
W Caliebe, I So, A Lenhard, D Siddons, Cam-driven Monochromator for QEXAFS, *20th International Conference on X-Ray and Inner-Shell Processes*, Vol 75, p. 1962-1965, sponsored by University of Melbourne (2006).
S Chin, O Alexeev, J Amiridis, Structure and Reactivity of Pt-Ru/SiO2 Catalysts for the Preferential Oxidation of CO Under Excess H2, *J. Catal.*, **243** (2), 329-339 (2006).
S Choi, P O'Day, N Riveria, K Mueller, S Seraphin, J Chorover, Strontium Speciation During Reactin of Kaolinite with Simulated Tank-Waste Leachate: Bulk and Microfocused EXAFS Analysis, *Environ. Sci. Tech.*, **40**, 2608-2614 (2006).
S Chotisuwan, J Wittayakun, B Gates, Pt3Ru6 Clusters Supported on gamma-Al2O3: Synthesis from Pt3Ru6(Cu)21(u3-H)(u-H)3, Structural Characterization, and Catalysis of Ethylene Hydrogenation and n-Butane Hydrogenolysis, *J. Phys. Chem. B*, **110**, 12459-12469 (2006).
A Ganjoo, G Chen, H Jain, Photoinduced Changes in the Local Structure of a-GeSe2 by in-situ EXAFS, *Phys. Chem. Glasses*, **47** (2), 177-181 (2006).
F Huggins, G Huffman, Comment on and addenda to "Arsenic in coal: a review" by Yudovich and Ketris., *Int. J. Coal Geol.*, **66**, 148-150 (2006).
R Hull, L Li, Y Xing, C Chusuei, Pt Nanoparticle Binding on Functionalized Multiwalled Carbon Nanotubes, *Chem. Mater.*, **18**, 1780-1788 (2006).
G Hutchings, M Hall, A Carley, P Landon, B Solsona, C Kiely, A Herzing, M Makkee, J Moulijn, et al., Role of Gold Cations in the Oxidation of Carbon Monoxide Catalyzed by Iron Oxide-Supported Gold, *J. Catal.*, **242** (1), 71-81 (2006).
G Jacobs, S Ricote, B Davis, Low Temperature Water-Gas Shift: Type and Loading of Metal Impacts Decomposition and Hydrogen Exchange Rates of Pseudo-stabilized Formate over Metal/ceria Catalysts, *Appl. Catal. A*, **302**, 14-21 (2006).
G Jacobs, R Keogh, B Davis, Steam Reforming of Ethanol over Pt/ceria with Co-fed Hydrogen, *J. Catal.*, **245**, 326-337 (2006).
M Keane, G Jacobs, P Patterson, Ni/SiO2 Promoted Growth of Carbon Nanofibers, *J. Colloid Interface Sci.*, **302**, 576 (2006).

D Kim, B Dunn, F Huggins, G Huffman, M Kang, J Yie, E Eyring, SBA-15-Supported Iron Catalysts for Fischer-Tropsch Production of Diesel Fuel, *Energ. Fuel*, **20**, 2608-2611 (2006).
M Kissell, An X-ray Absorption Spectroscopy Study of Arsenic Uptake and Oxidation-Reduction in the Arsenic Hyperaccumulating Fern, Pteris cretica, M.S. Thesis, Stony Brook University, Stony Brook (2006).
F Larsen, A Boisen, K Berry, B Moubaraki, K Murray, V McKee, R Scarrow, C McKenzie, Identification of the Dinuclear and Tetranuclear Air-Oxidized Products Derived from Labile Phenolate-Bridged Dimanganese(II) Pyridyl-Chelate Compounds, *Eur. J. Inorg. Chem.*, **2006**, 3841-3852 (2006).
K Lee, S Oyama, Bifunctional Nature of a SiO2-Supported Ni2P Catalyst for Hydrotreating: EXAFS and FTIR Studies, *J. Catal.*, **239** (2), 376-389 (2006).
E Maris, W Ketchie, V Oleshko, R Davis, Metal Particle Growth During Glucose Hydrogenation over Ru/SiO2 Evaluated by X-ray Absorption Spectroscopy and Electron Microscopy, *J. Phys. Chem. B*, **110** (15), 7869-7876 (2006).
S Nemana, B Gates, Surface-Mediated Synthesis and Spectroscopic Characterization of Tantalum Clusters on Silica, *Langmuir*, **22**, 8214-8220 (2006).
S Nemana, B Gates, Redox Chemisty of Tantalum Clusters on Silica Characterized by X-ray Absorption Spectroscopy, *J. Phys. Chem. B*, **110**, 17546-17553 (2006).
S Overbury, V Schwartz, D Mullins, W Yan, S Dai, Evaluation of the Au Size Effect: CO Oxidation Catalyzed by Au/TiO2, *J. Catal.*, **241** (1), 56-65 (2006).
S Pandey, A Kumar, S Khalid, A Pimpale, Electronic States of LaCoO3: Co K-edge and La L-edge X-ray Absorption Studies, *J. Phys.: Condens. Matter*, **18**, 7103-7113 (2006).
S Pandey, S Khalid, N Lalla, A Pimpale, Local Distortation in LaCoO3 and PrCO03: Extended X-ray Absorption Fine structure, X-ray Diffraction and X-ray Absorption Near Edge structure Studies, *J. Phys.: Condens. Matter*, **18**, 10617 (2006).
S Pandey, R Bindu, A Kumar, S Khalid, A Pimpale, Doping and Bond Length Contributions to Mn K-edge Shift in La1-xSrxMnO3 (x = 0 - 0.7) and Their Correlation with Electrical Transport Properties, *International Workshop on the Physics of Mesoscopic and Disordered Materials-December 4-8, 2006*, p. 88, sponsored by Indian Institute of Technology (2006).
M Pena, X Meng, G Korfiatis, C Jing, Adsorption Mechanism of Arsenic on Nanocrystalline Titanium Dioxide, *Environ. Sci. Tech.*, **40**, 1257-1262 (2006).
C Reed, Y Lee, S Oyama, Structure and Oxidation State of Silica-Supported Manganese Oxide Catalysts and Reactivity for Acetone Oxidation with Ozone, *J. Phys. Chem. B*, **110**, 4207-4216 (2006).
S Ricote, G Jacobs, M Milling, Y Ji, P Patterson, B Davis, Low temperature Water-Gas Shift: characterization and Testing of Binary Mixed Oxides of Ceria and Zirconia Promoted with Pt, *Appl. Catal. A*, **303**, 35 (2006).
A Rouff, E Elzinga, R Reeder, The Effect of Aging and pH on PB(II) Sorption Processes at the Calcite-Water Interface, *Environ. Sci. Tech.*, **40**, 1792-1798 (2006).
X Wang, J Rodriguez, J Hanson, D Gamarra, A Martinez-Arias, M Fernandez-Garcia, In Situ Studies of the Active Sites for the Water Gas Shift Reaction over Cu-CeO2 Catalysts: Complex Interaction Between Metallic Copper and Oxygen Vacancies of Ceria, *J. Phys. Chem. B*, **110**, 428-434 (2006).
J Ziegelbauer, D Gatewood, A Gulla, D Ramaker, S Mukerjee, X-Ray Absorption Spectroscopy Studies of Water Activation on an RhxSy Electrocatalyst for Oxygen Reduction Reaction Applications, *Electrochem. Solid-State Lett.*, **9** (9), A430-A434 (2006).

Beamline X19A

S Chaudhuri, J Graetz, A Ignatov, J Reilly, J Muckerman, Understanding the Role of Ti in Reversible Hydrogen Storage as Sodium Alanate: A Combined Experimental and Density Functional Theoretical Approach, *J. Am. Chem. Soc.*, **128**, 11404-11415 (2006).
W Feng, E Borguet, R Vidic, Sulfurization of a Carbon Surface for Vapor Phase Mercury Removal-II: Sulfur Forms and Mercury Uptake, *Carbon*, **44** (14), 2998-3004 (2006).
C Jing, S Liu, G Korfiatis, X Meng, Leaching Behavior of Cr(III) in Stabilized/Solidified Soil, *Chemosphere*, **64** (3), 379-385 (2006).
D Kim, J Szanyi, J Kwak, T Szailer, J Hanson, C Wang, C Peden, Effect of Barium Loading on the Desulfation of Pt-BaO/Al2O3 Studied by H2 TPRX, TEM, Sulfur K-edge XANES, and In Situ TR-XRD, *J. Phys. Chem. B*, **110**, 10441-10448 (2006).
A Leri, M Hay, A Lanzirotti, W Rao, S Myneni, Quantitative Determination of Absolute Organohalogen Concentrations in Environmental Samples by X-ray Absorption Spectroscopy, *Anal. Chem.*, **78**, 5711-5718 (2006).
Z Liu, S Wang, B McCoy, A Cady, R Pindak, W Caliebe, K Takekoshi, K Ema, H Nguyen, C Huang, Smectic-C* alpha-smectic-C* Phase Transition and Critical Point in Binary Mixtures, *Phys. Rev. E*, **74**, 030702(R) (2006).
R Maguire, D Hesterberg, A Gernat, K Anderson, M Wineland, J Grimes, Liming Poultry Manures to Kill Pathogens and Decrease Soluble Phosphorus, *J. Environ. Qual.*, **35**, 849-857 (2006).
G Murray, D Hesterberg, Iron and phosphate dissolution during abiotic reduction of ferrihydrite-boehmite mixtures, *Soil Sci. Soc. Am. J.*, **70**, 1318-1327 (2006).
V Poltavets, K Lokshin, S Dikmen, M Croft, T Egami, M Greenblatt, La2Ni2O6: A New Double T'-type Nickelate with Infinite Ni1=/2=O2 Layers, *J. Am. Chem. Soc.*, **128**, 9050-9051 (2006).
V Poltavets, M Croft, M Greenblatt, Charge Transfer, Hybridization and Local Inhomogeneity Effects in NaxCo02 Center Dot yH(2)O: An X-ray Absorpton Spectroscopy Study, *Phys. Rev. B*, **74** (12), 125103 (2006).
A Shober, D Hesterberg, J Sims, S Gardner, Characterization of Phosphorus Species in Biosolids and Manures Using XANES Spectroscopy, *J. Environ. Qual.*, **35**, 1983-1993 (2006).
U Skyllberg, P Bloom, J Qian, C Lin, W Bleam, Complexation of Mercury(II) in Soil Organic Matter: EXAFS Evidence for Linear Two-Coordination with Reduced Sulfur Groups, *Environ. Sci. Tech.*, **40**, 4174-4180 (2006).

Y Suh, M Carroll, R Levy, G Bisognin, D Salvador, M Sahiner, Implantation and Activation of High Concentrations of Phosphorus and Boron in Germanium, *Materials Research Society Fall Meeting 2005*, Vol 891, p. EE 7.20.1, sponsored by Materials Research Society (2006).

G Toevs, M Morra, M Polizzotto, D Strawn, B Bostick, S Fendorf, Metal(loid) Diagenesis in Mine-Impacted Sediments of Lake Coeur d'Alene, Idaho, *Environ. Sci. Tech.*, **40**, 2537-2543 (2006).

X Wang, J Rodriguez, J Hanson, D Gamarra, A Martinez-Arias, M Fernandez-Garcia, In Situ Studies of the Active Sites for the Water Gas Shift Reaction over Cu-CeO2 Catalysts: Complex Interaction Between Metallic Copper and Oxygen Vacancies of Ceria, *J. Phys. Chem. B*, **110**, 428-434 (2006).

S Wang, Z Liu, B McCoy, R Pindak, W Caleibe, H Nguyen, C Huang, Optical and Resonant X-Ray Diffraction Studies Confirm a SmC*F12-SmC* Liquid Crystal Sequence Reversal, *Phys. Rev. Lett.*, **96**, 097801 (2006).

L Whaley, M Lobanov, D Sehptyakov, M Croft, K Ramanujachary, S Lofland, P Stephens, J Her, G Van Tendeloo, et al., Sr3Fe5/4Mo3/4O6.9, an n = 2 Ruddlesen-Popper Phase: Synthesis and Properties, *Chem. Mater.*, **18**, 3448-3457 (2006).

W Yoon, K Chung, J McBreen, K Zaghib, X Yang, Electronic Structure of the Electrochemically Delithiated Li1-xFePO4 Electrodes Investigated by P K-edge X-ray Absorption Spectroscopy, *Electrochem. Solid-State Lett.*, **9**, A415 (2006).

F Zhang, C Chen, J Raitano, J Hanson, W Caliebe, S Khalid, S Chan, Phase Stability in Ceria-Zirconia Binary Oxide Nanoparticles: The Effect of the Ce3+ Concentration and the Redox Environment, *J. Appl. Phys.*, **99**, 084313 (2006).

F Zhao, J Lehmann, D Solomon, M Fox, S McGrath, Sulphur Speciation and Turnover in Soils: Evidence from Sulfur K-Edge XANES Spectroscopy and Isotope Dilution Studies , *Soil Biol. Biochem.*, **38** (5), 1000-1007 (2006).

Beamline X19C

G Carini, C Arnone, A Bolotnikov, G Camarda, R De Wames, J Dinan, J Markunas, B Raghothamachar, S Sivananthan, et al., Material Quality Characterization of CdZnTe Substrates for HgCdTe Epitaxy, *J. Electron. Mater.*, **35** (6), 1495-1502 (2006).

G Dhanaraj, M Dudley, D Bliss, M Callahan, M Harris, Growth and Process Induced Dislocations in Zinc Oxide Crystals, *J. Cryst. Growth*, **297** (1), 74-79 (2006).

P Konkapaka, B Raghothamachar, M Dudley, Y Makarov, M Spencer, Crystal Growth and Characterization of Thick GaN Layers Grown by Oxide Vapor Transport Technique, *J. Cryst. Growth*, **289** (1), 140-144 (2006).

S Malkova, R Stahelin, S Pingali, W Cho, M Schlossman, Orientation and Penetration Depth of Monolayer-Bound p40phox-PX, *Biochemistry*, **45**, 13566-13575 (2006).

S Pingali, T Takiue, G Luo, A Tikhonov, N Ikeda, M Aratono, M Schlossman, X-ray Studies of Surfactant Ordering and Interfacial Phases at the Water-Oil Interface, *J. Dispersion Sci. Technol.*, **27**, 715-722 (2006).

B Raghothamachar, G Dhanaraj, J Bai, M Dudley, Defect Analysis in Crystals using X-ray Topography, *Microsc. Res. Tech.*, **69**, 343-358 (2006).

J Ruggles, G Foran, H Tanida, H Nagatani, Y Jimura, I Watanabe, I Gentle, Interfacial Behavior of Tetrapyridylporphyrin Monolayer Arrays, *Langmuir*, **22**, 681-686 (2006).

A Tikhonov, Water Density in the Electric Double Layer at the Insulator/Electrolyte Solution Interface, *J. Phys. Chem. B*, **110**, 2746-2750 (2006).

A Tikhonov, X-ray Study of the Electric Double Layer at the n-Hexane/Nanocolloidal Silica Interface, *J. Chem. Phys.*, **124** (16), 164704 (2006).

A Tikhonov, H Patel, S Garde, M Schlossman, Tail Ordering Due to Headgroup Hydrogen Bonding Interactions in Surfactant Monolayers at the Water-Oil Interface, *J. Phys. Chem. B*, **110**, 19093-19096 (2006).

M Volz, M Schweizer, B Raghothamachar, M Dudley, J Szoke, S Cobb, F Szofran, X-ray Characterization of Detached-Grown Germanium Crystals, *J. Cryst. Growth*, **290** (2), 446-451 (2006).

Beamline X20A

S Gaudet, C Detarvernier, A Kellock, P Desjardins, C Lavoie, Thin Film Reaction of Transition Metals with Germanium, *J. Vac. Sci. Technol., A*, **24** (3), 474-485 (2006).

Y Gong, H Yan, I Kuskovsky, Y Gu, I Noyan, G Neumazrk, M Tamargo, Structure of Zn-Se-Te System with Submonolayer Insertion of ZnTe Grown by Migration Enhanced Epitaxy, *J. Appl. Phys.*, **99**, 064913 (2006).

I Kuskovsky, Y Gu, Y Gong, H Yan, J Lau, I Noyan, G Neumark, O Maksimov, X Zhou, et al., Mechanism for Increasing Dopant Incorporation in Semiconductors Via Doped Nanostructures, *Phys. Rev. B*, **73**, 195306 (2006).

S Larochelle, M Ramazanoglu, R Birgeneau, Effects of Disorder on a Smectic-A-nematic Phase Transition, *Phys. Rev. E*, **73**, 060702 (2006).

H Yan, I Noyan, Measurement of Stress/Strain in Single-Crystal Samples using Diffraction, *J. Appl. Cryst.*, **39**, 320-325 (2006).

Beamline X20C

S Gaudet, C Detarvernier, A Kellock, P Desjardins, C Lavoie, Thin Film Reaction of Transition Metals with Germanium, *J. Vac. Sci. Technol., A*, **24** (3), 474-485 (2006).

S Gaudet, C Lavoie, C Detavernier, P Desjardins, Germanide Phase Formation and Texture, *SiGe Technology and Device Meeting, 2006, ISTDM 2006, International*, p. 18-19, sponsored by IEEE (2006).

S Gaudet, C Detavernier, C Lavoie, P Desjardins, Reaction of Thin Ni Films with Ge: Phase Formation and Texture, *J. Appl. Phys.*, **100**, 034306 (2006).

C Lavoie, C Detavernier, C Cabral, Jr. , F d'Heurle, A Kellock, J Jordan-Sweet, J Harper, Effects of Additive Elements on the Phase Formation and Morphological Stability of Nickel Monosilicide Films, *Microelectron. Eng.*, **83** (11-12), 2042-2054 (2006).

W Leroy, C Detavernier, R van Meirhaeghe, A Kellock, C Lavoie, Solid-State Formation of Titanium Carbide and Molybdenum Carbide as Contcts for Carbon-Containing Semiconductors, *J. Appl. Phys.*, **99**, 063704 (2006).
D Mitzi, S Raoux, A Schrott, M Copel, A Kellock, J Jordan-Sweet, Solution-Based Processing of the Phase-Change Material KSb5S8, *Chem. Mater.*, **18**, 6278-6282 (2006).
K Park, Y Sung, M Toney, Structural Effect of PtRu-WO3 Alloy Nanostructures on Methanol Electrooxidation, *Electrochem. Commun.*, **8**, 359-363 (2006).
S Raoux, C Rettner, J Jordan-Sweet, V Deline, J Philipp, H Lung, Scaling properties of phase change nanostructures and thin films, *European Symposium on Phase Change and Ovonic Science*, p. 127-134, sponsored by CEA, France (2006).
H Schubert, C Hill, Structure of ATP-Bound Human ATP: Cobalamin Adenosyltransferase, *Biochemistry*, **45**, 15188-15196 (2006).
M Toney, E Marinero, J Hedstrom, Microstructural Origin of Orientation Ratio in Magnetic Recording Media, *J. Appl. Phys.*, **99**, 033907 (2006).
Y Wang, A Ozcan, k Ludwig, A Bhattacharyya, T Moustakas, L Zhou, D Smith, Complex and Incommensurate Ordering in Al0.72Ga0.28N Thin Films, *Appl. Phys. Lett.*, **88** (18), 181915 (2006).

Beamline X21

N Aliouane, D Argyriou, J Strempfer, I Zegkinoglou, S Landsgesell, M von Zimmermann, Field-Induced Linear Magnetoelastic Coupling in Multiferroic TbMnO3, *Phys. Rev. B: Condens. Matter*, **73**, 020102 (2006).
F Ashish, R Garg, J Anguita, J Krueger, Binding of Full-Length HIV-1 gp120 to CD4 Induces Structural Reorientation around the gp120 Core, *Biophys. J.*, **91**, L69-71L (2006).
R Daimant, R Sharon, W Caliebe, C Kao, M Deutsch, Structure of the Co and FeK alpha(3,4) Satellite Spectra, *J. Phys. B: At., Mol. Opt. Phys.*, **39** (3), 651-667 (2006).
R Diamant, Multiple Electron Excitations in Medium-Z Atoms , Ph.D. Thesis, Bar-Ilan Univesrity, Ramat-Gan (2006).
R Diamant, S Huotari, K Hämäläinen, R Sharon, C Kao, M Deutsch, The Evolution of Inner-shell Multielectronic X-ray Spectra from Threshold to Saturation for Low- to High-z Atoms, *Radiat. Phys. Chem.*, **75**, 1434 (2006).
M Foldvari, I Badea, S Wettig, R Verrall, M Bagonluri, Dicationic Gemini Surfactant Gene Delivery Complexes Contain Cubic-lamellar Mixed Polymorphic Phase, *NSTI Nanotechnology Conference and Trade Show, 2006*, Vol 2, p. 400-403, sponsored by Nano Science and Technology Institute (2006).
M Foldvari, I Badea, S Wettig, R Verrall, M Bagonluri, Structural Characterization of Novel Gemini Non-viral DNA, *J. Exp. Nanoscience*, **1** (2), 165-176 (2006).
V Graziano, W McGrath, L Yang, W Mangel, SARS CoV Main Proteinase: The Monomer-Dimer Equilibrium Dissociation Constant, *Biochemistry*, **45**, 14632-14641 (2006).
M Misner, Solvent Enhanced Block Copolymer Ordering in Thin Films, Ph. D Thesis, University of Massachusetts, Amherst (2006).
Z Niu, M Bruckman, V Kotakadi, J He, T Emrick, T Russell, L Yang , Q Wang, Study and Characterization of Tobacco Mosaic Virus Head-to-tail Assembly Assisted by Aniline Polymerization, *Chem. Commun.*, **2006** (28), 2019-3021 (2006).
A Ozcan, Y Wang, G Ozaydin, K Ludwig, A Bhattacharyya, T Moustakas, D Siddons, Real-time X-ray Studies of Gallium Adsorption and Desorption, *J. Appl. Phys.*, **100** (8), 084307 (2006).
M Paine, Calcium-Induced Conformational Changes in Gelsolin and Actin-Bound Gelsolin Using Small-Angle X-Ray Scattering, M. S. Thesis, UNC Charlotte, Charlotte (2006).
D Pan, W Wang, W Liu, L Yang, H Huang, Chain Packing in the Inverted Hexagonal Phase of Phospholipids: A Study by X-ray Anomalous Diffraction on Bromine-Labeled Chains, *J. Am. Chem. Soc.*, **128**, 3800-3807 (2006).
W Wang, D Pan, Y Song, W Liu, L Yang, H Huang, Method of X-ray anomalous diffraction for lipid structures, *Biophys. J.*, **91** (2), 736-743 (2006).
Y Wang, A Ozcan, G Ozaydin, K Ludwig, Jr., A Bhattacharyya, T Moustakas, H Zhou, R Headrick, P Siddons, Real-Time Synchrotron X-ray Studies of Low- and High-temperature Nitridation of c-plane Sapphire, *Phys. Rev. B*, **74**, 235304 (2006).

Beamline X22A

K Alvine, Nanoparticle Assembly and Liquids on Nanostructured , Ph.D. Thesis, Harvard University, Cambridge (2006).
S Dourdain, Structural, Porous and Mechanical Characterization of Mesoporous Silica Thin Films. Functionalization influence., Ph.D Thesis, Universite du Maine, Le Mans (2006).
A Gibaud, S Dourdain, G Vignaud, Analysis of Mesoporous Thin Films by X-ray Reflectivity, Optical Reflectivity and Grazing Incidence Small Angle X-ray Scattering, *Appl. Surf. Sci.*, **253** (1), 3-11 (2006).
X Guo, M Myers, S Xiao, M Lefenfeld, R Steiner, G Tulevski, J Tang, J Baumert, F Leibfarth, et al., Chemoresponsive Monolayer Transistors, *Proc Natl Acad Sci USA*, **103** (31), 11452-11456 (2006).
F He, B Wells, Lattice Strain in Epitaxial BaTiO3 Thin Films, *Appl. Phys. Lett.*, **88** (15), 152908 (2006).
G Kim, S Wang, A Jacobson, Z Yuan, W Donner, C Chen, L Reimus, P Brodersen, C Mims, Oxygen Exchange Kinetics of Epitaxial PrBaCo2O5+delta Thin Films, *Appl. Phys. Lett.*, **88** (2), 024103 (2006).
S Larochelle, M Ramazanoglu, R Birgeneau, Effects of Disorder on a Smectic-A-nematic Phase Transition, *Phys. Rev. E*, **73**, 060702 (2006).
M Lefenfeld, J Baumert, E Sloutskin, I Kuzmenko, P Pershan, M Deutsch, C Nuckolls, B Ocko, Direct Structural Observation of a Molecular Junction by High-Energy X-ray Reflectometry, *Proc Natl Acad Sci USA*, **103** (8), 2541-2545 (2006).
I Misirlioglu, S Alpay, F He, B Wells, Stress Induced Monoclinic Phase in Epitaxial BaTiO3 on MgO, *J. Appl. Phys.*, **99**, 104103 (2006).
C Nelson, R Kolagani, M Overby, V Smolyaninova, R Kennedy, Charge Order in Photosensitive Bi0.4Ca0.6MnO3 Films, *J. Phys.: Condens. Matter*, **18**, 997-1004 (2006).

S Park, E DiMasi, Y Kim, W Han, P Woodward, T Vogt, The Preparation and Characterization of Photocatalytically Active TiO2 Thin Films and Nanoparticles using Successive-Ionic-Layer-Adsorption-and-Reaction, *Thin Solid Films*, **515** (4), 1250-1254 (2006).
G Xu, J Li, D Viehland, Ground State Monoclinic (Mb) Phase in (110)c BiFeO3 Epitaxial Thin Films, *Appl. Phys. Lett.*, **89** (22), 222901 (2006).

Beamline X22B

K Alvine, Nanoparticle Assembly and Liquids on Nanostructured , Ph.D. Thesis, Harvard University, Cambridge (2006).
E DiMasi, S Kwak, F Amos, M Olszta, D Lush, L Gower, Complementary Control by Additivies of the Kinetics of Amorphous CaCO3 Mineralization at an Organic Interface: In-Situ Synchrotron X-ray Observations, *Phys. Rev. Lett.*, **97**, 045503 (2006).
S Dourdain, Structural, Porous and Mechanical Characterization of Mesoporous Silica Thin Films. Functionalization influence., Ph.D Thesis, Universite du Maine, Le Mans (2006).
M Fukuto, O Gang, K Alvine, P Pershan, Capillary Wave Fluctuations and Intrinsic Widths of Coupled Fluid-fluid Interfaces: An X-ray Scattering Study of a Wetting Film on Bulk Liquid, *Phys. Rev. E*, **74**, 031607 (2006).
A Gibaud, S Dourdain, G Vignaud, Analysis of Mesoporous Thin Films by X-ray Reflectivity, Optical Reflectivity and Grazing Incidence Small Angle X-ray Scattering, *Appl. Surf. Sci.*, **253** (1), 3-11 (2006).
S Kim, M Misner, L Yang, O Gang, B Ocko, T Russell, Salt Complexation in Block Copolymer Thin Films, *Macromolecules*, **39** (24), 8473-8479 (2006).
L Martinez-Miranda, Y Hu, Temperature and Depth Dependence of Order in Liquid Crystal Interfaces, *J. Appl. Phys.*, **99**, 113522 (2006).
M Maye, D Nykypanchuk, D van der Lelie, O Gang, A Simple Method for Kinetic Control of DNA-Induced Nanoparticle Assembly, *J. Am. Chem. Soc.*, **128**, 14020-14021 (2006).
M Misner, Solvent Enhanced Block Copolymer Ordering in Thin Films, Ph. D Thesis, University of Massachusetts, Amherst (2006).
E Ofer, E Sloutskin, L Tamam, B Ocko, M Deutsch, Surface Freezing in Binary Alkane-Alcohol Mixtures, *Phys. Rev. E*, **74**, 021602 (2006).
O Shpyrko, R Streitel, V Balagurusamy, A Grigoriev, M Deutsch, B Ocko, M Meron, B Lin, P Pershan, Surface Crystallization in a Liquid AuSi Alloy, *Science*, **313**, 77 (2006).
E Sloutskin , R Lynden-Bell, S Balasubramanian, M Deutsch, Comparing Simulated and X-ray-measured Surface Structure: The Case of Ionic Liquids, *J. Chem. Phys.*, **175**, 174715 (2006).
J Strzalka, T Xu, A Tronin, S Wu, I Miloradovic, I Kuzmenko, T Gog, M Therien, K Blasie, Structural Studies of Amphiphilic 4-Helix Bundle Peptides Incorporating Designed Extended Chromophores for Nonlinear Optical Biomolecular Materials, *Nano Lett.*, **6** (11), 2395-2405 (2006).
J Wang, J Leiston-Belanger, J Sievert, T Russell, Grain Rotation in Ion-Complexed Symmetric Diblock Copolymer Thin Films under an Electric Field, *Macromolecules*, **39**, 8487-8491 (2006).

Beamline X22C

A Borissov, X-ray Scattering Study of Inhomogeneous Charge-ordered States of Colossal Magnetoresistance Manganites and Chalcogenide Spinel Compounds, Ph.D. Thesis, Rutgers University, New Brunswick (2006).
F He, B Wells, Lattice Strain in Epitaxial BaTiO3 Thin Films, *Appl. Phys. Lett.*, **88** (15), 152908 (2006).
M Hucker, M Zimmermann, R Klingelar, S Kiele, J Geck, S Bakehe, J Zhang, J Hill, A Revcolevschi, et al., Undirectional Diagonal Order and Three-Dimensional Stacking of Charge Stripes in Orthorhombic Pr1.67Sr0.33NiO4 and Nd1.67Sr0.33NiO4, *Phys. Rev. Lett.*, **74**, 085112 (2006).
M Hucker, V Zimmermann, R Klingeler, S Kiele, J Geck, S Bakehe, J Zhang, J Hill, A Revcolevschi, et al., Unidirectional Diagonal Order and Three-Dimensional Stacking of Charge Stripes in Orthorhombic Pr1.67Sr0.33Ni)4 and Nd1.67Sr0.33NiO4, *Phys. Rev. B*, **74**, 085112 (2006).
G Kim, S Wang, A Jacobson, Z Yuan, W Donner, C Chen, L Reimus, P Brodersen, C Mims, Oxygen Exchange Kinetics of Epitaxial PrBaCo2O5+delta Thin Films, *Appl. Phys. Lett.*, **88** (2), 024103 (2006).
V Kiryukhin, Y Horibe, Y Hor, H Noh, S Cheong, Incommensurate Structural Correlations in the Disordered Spin-Dimer State Induced by X-Ray and Electron Irradiation in CuIr2S4, *Phys. Rev. Lett.*, **97**, 225503 (2006).
P Lyman, V Shneerson, R Fung, S Parihar, H Johnson-Steigelman, E Lu, D Saldin, Structure and Stability of Sb/Au(110)-c(2x2) Surface Phase, *Surf. Sci.*, **600** (2), 424-435 (2006).
C Nelson, R Kolagani, M Overby, V Smolyaninova, R Kennedy, Charge Order in Photosensitive Bi0.4Ca0.6MnO3 Films, *J. Phys.: Condens. Matter*, **18**, 997-1004 (2006).
Y Uozu, Y Wakabayashi, Y Ogimoto, N Takubo, H Tamuru, N Nagaosa, K Miyano, Intrinsic Colassol Magnetoresistance Effect in Thin-Film Pr0.5Sr0.5MnO3 Through Dimensionally Switching, *Phys. Rev. Lett.*, **97**, 037202 (2006).

Beamline X23A2

I Levin, E Cockayne, M Lufaso, J Woicik, J Masler, Local structures and Raman spectra in the Ca(Zr,Ti)O3 perovskite solid solutions, *Chem. Mater.*, **18**, 854 (2006).
M Shao, T Huang, P Liu, J Zhang, K Sasaki, M Vukmirovic, R Adzic, Palladium Monolayer and Palladium Alloy Electrocatalysts for Oxygen Reduction, *Langmuir*, **22**, 10409-10415 (2006).

Beamline X23B

M Altman, A Shukla, T Zubkov, G Evmenenko, P Dutta, M van der Boom, Controlling Structure from the Bottom-Up: Structural and Optical Properties of Layer-by-Layer Assembled Palladium Coordination-Based Multilayers, *J. Am. Chem. Soc.*, **128**, 7374-7382 (2006).
G Evmenenko, H Mo, S Kewalramani, P Dutta, Conformational Rearrangements in Interfacial Region of Polydimethylsiloxane Melt Films, *Polymer*, **47**, 878-882 (2006).

G Evmenenko, H Mo, S Kewalramani, P Dutta, X-ray Reflectivity Study of Ultrathin Liquid Films of diphenylsiloxane-dimethylsiloxane Copolymers, *Langmuir*, **22** (14), 6245-6248 (2006).

A Facchetti, L Beverina, M van der Boom, A Shukla, P Dutta, G Evmenenko, T Marks, G Pagani, Strategies for Electrooptic Film Fabrication. Influence of Pyrrole-Pyridine-Based Dibranched Chromophore Architecture on Covalent Self-Assembly, Thin-Film Microstructure, and Nonlinear Optical Response, *J. Am. Chem. Soc.*, **128**, 2142-2153 (2006).

Q Huang, J Li, G Evmenenko, P Dutta, T Marks, Systematic Investigation of Nanoscale Adsorbate Effects at Organic Light-Emitting diode Interfaces. Interfacial Structure-Charge Injection-Luminance Relationships, *Chem. Mater.*, **18**, 2431-2442 (2006).

H Kang, G Evmenenko, P Dutta, K Clays, K Song, T Marks, X-shaped Electro-Optic Chromophore with Remarkably Blue-Shifted Optical Absorption. Synthesis, Characterization, Linear/Nonlinear Optical Properties, Self-Assembly, and Thin Film Microstructural Characteristics, *J. Am. Chem. Soc.*, **128**, 6194-6205 (2006).

M Kieber-Emmons, J Annaraj, M Seo, K Van Heuvelen, T Tosha, T Kitagawa, T Brunold, W Nam, C Riordan, Identification of an "End-on" Nickel-Superoxo Adduct, [Ni(tmc)(O2)]+, *J. Am. Chem. Soc.*, **128**, 14230-14231 (2006).

S Morrison, C Cahill, E Carpenter, V Harris, Production Scaleup of Reverse Micelle Synthesis, *Ind. Eng. Chem. Res.*, **45**, 1217-1220 (2006).

P Pfalzer, G Obermeier, M Klemm, S Horn, M denBoer, Structural Precursor to the Metal-Insulator Transition in V2O3, *Phys. Rev. B*, **73**, 144106 (2006).

A Yang, X Zuo, C Vittoria, V Harris, Magnetism, Structure, and Cation Disbribution in MnFe2O4 Films Processed by Conventional and Alternating Target Laser Ablation Deposition, *IEEE Trans. Magn.*, **42** (10), 2870 (2006).

S Yoon, Y Chen, D Heiman, A Yang, N Sun, C Vittoria, V Harris, Room temperature magnetism in semiconducting films of ZnO doped with ferric ions, *J. Appl. Phys.*, **99**, 08M109 (2006).

Beamline X24C

C Back, U Feldman, J Weaver, J Seely, C Constantin, G Holland, R Lee, H Chung, H Scott, Absolute Time-Resolved Emission of Non-LTE L-Shell Spectra from Ti-Doped Aerogels, *J. Quant. Spectr. Rad. Trans.*, **99**, 21 (2006).

L Goray, J Seely, S Sadov, Spectral Separation of the Efficiencies of the Inside and Outside Orders of Soft X-Ray - Extreme Ultraviolet Gratings at Near Normal Incidence, *J. Appl. Phys.*, **100**, 094901 (2006).

J Hu, X Xin, J Zhao, F Yan, B Guan, J Seely, B Kjornrattanawanich, Highly Sensitive Visible-Blind Extreme Ultraviolet Ni/4H-SiC Schottky Photodiodes with Large Detection Area, *Opt. Lett.*, **31**, 1591 (2006).

B Kjornrattanawanich, D Windt, J Seely, Y Uspenskii, SiC/Tb and Si/Tb Multilayer Coatings for Extreme Ultraviolet Solar Imaging, *N/A*, **45** (8), 1765-1772 (2006).

B Kjornrattanawanich, R Korde, C Boyer, G Holland, J Seely, Temperature Dependence of the EUV Responsivity of Silicon Photodiodes, *IEEE Trans. Elect. Device*, **53**, 218 (2006).

B Kjornrattanawanich, D Windt, J Seely, Y Uspenskii, SiC/Tb and Si/Tb Multilayer Coatings for Extreme Ultraviolet Solar Imaging, *Appl. Optics-OT*, **45**, 1765 (2006).

C Korendyke, C Brown, R Thomas, C Keyser, J Davilla, R Hagood, H Hara, K Heidemann, A James, et al., Optics and Mechanisms for the Extreme-Ultraviolet Imaging Spectrometer on the Solar-B Satellite, *Appl. Optics-OT*, **45**, 8674 (2006).

M Kowalski, R Heilmann, M Schattenburg, C Chang, F Berendse, W Hunter, Near-normal-incidence Extreme-Ultraviolet Efficiency of a Flat Crystalline Anisotropically Etched Blazed Grating, *Appl. Optics-OT*, **45** (8), 1676-1679 (2006).

M Kowalski, W Hunter, T Barbee, Replication of a Holographic ion-etched Spherical Blazed Grating for use at Extreme-Ultraviolet Wavelengths: Topography, *Appl. Optics-OT*, **45** (2), 305-321 (2006).

M Kowalski, T Barbee, W Hunter, Replication of a Holographic Ion-etched Spherical Blazed Grating for use at Extreme-Ultraviolet Wavelengths: Efficiency, *Appl. Optics-OT*, **45** (2), 322-334 (2006).

C Lang, B Kent, W Paulstian, C Brown, C Keyser, M Anderson, G Case, R Chaudry, A James, et al., Laboratory Calibration of the Extreme-Ultraviolet Imaging Spectrometer for the Solar-B Satellite, *Appl. Optics-OT*, **45**, 8689 (2006).

J Seely, L Goray, B Kjornrattanawanich, M Laming, G Holland, K Flanagan, R Heilmann, C Chang, M Schattenberg, A Rasmussen, Efficiency of a Grazing-Incidence Off-Plane Grating in the Soft X-Ray Region, *Appl. Optics-OT*, **45**, 1680 (2006).

Beamline X25

R Albright, J Vazquez Ibar, C Kim, S Gruner, J Morais-Cabral, The RCK Domain of the KtrAB K+ Transporter: Multiple Conformations of an Octameric Ring, *Cell*, **126** (6), 1147-1159 (2006).

A Banerjee, W Santos, G Verdine, Structure of a DNA Glycosylase Searching for Lesions, *Science*, **311**, 1153-57 (2006).

C Barinka, G Parry, J Callahan, D Shaw, A Kuo, B Cines, A Mazar, J Lubkowski, Structural Basis of Interaction Between Urokinase-type Plasminogen Activator and its Receptor, *J. Mol. Biol.*, **363** (2), 482-495 (2006).

M Bewley, V Graziano, K Griffin, J Flanagan, The Asymmetry in the Mature Amino-Terminus of ClpP Facilitates a Local Symmetry Match in ClpAP and ClpXP Complexes, *J. Struct. Biol.*, **153**, 113-28 (2006).

N Brot, J Collet, L Johnson, T Jonsson, H Weissbach, W Lowther, The Thioredoxin Domain of Neisseria Gonorrhoeae PilB can use Electrons from DsbD to Reduce Downstream Methionine Sulfoxide Reductases, *J. Biol. Chem.*, **281**, 32668 (2006).

C Brown, Z Gu, Y Matsuka, S Olmsted, P Cleary, D Ohlendorf, C Earhart, The Structure of the Cell-Wall Protease from Streptococci that Inactivates the Human Complement Factor 5A, *Int. Congr. Ser.*, **1289**, 211-215 (2006).

M Cosgrove, K Bever, J Avalos, S Muhammad, X Zhang, C Wolberger, The Structural Basis of Sirtuin Substrate Affinity, *Biochemistry*, **45**, 7511-7521 (2006).

G Da, J Lenkart, K Zhao, R Shiekhattar, B Cairns, R Marmorstein, Structure and Function of the SWIRM Domain, a Conserved Protein Module Found in Chromatin Regulatory Complexes, *Proc Natl Acad Sci USA*, **103** (7), 2057-2062 (2006).

R Diamant, S Huotari, K Hämäläinen, R Sharon, C Kao, M Deutsch, The Evolution of Inner-shell Multielectronic X-ray Spectra from Threshold to Saturation for Low- to High-z Atoms, *Radiat. Phys. Chem.*, **75**, 1434 (2006).

R Diamant, Multiple Electron Excitations in Medium-Z Atoms , Ph.D. Thesis, Bar-Ilan Univesrity, Ramat-Gan (2006).

C Eakin, A Berman, A Miranker, A Native to Amyloidogenic Transition Regulated by a Backbone Trigger, *Nat. Struct. Mol. Biol.*, **13** (3), 202 (2006).

S Eswaramoorthy, J Bonanno, S Burley, S Swaminathan, Mechanism of Action of a Flavin-Containing Monooxygenase, *Proc Natl Acad Sci USA*, **103** (26), 9832-9837 (2006).

G Fuchs, A Stein, C Fu, K Reinisch, S Wolin, Structural and Biochemical Basis for Misfolded RNA Recognition by the Ro Autoantigen, *Nat. Struct. Mol. Biol.*, **13** (11), 1002 (2006).

S Gabelli, H Azurmendi, M Bianchet, L Amzel, A Mildva, X-ray, NMR, and Mutational Studies of the Catalytic Cycle of the GDP-Mannose Mannosyl Hydrolase Reaction, *Biochemistry*, **45**, 11290-11303 (2006).

S Gabelli, J McLellan, A Montalvetti, E Oldfield, R Docampo, L Amzel, Structure and Mechanism of the Farnesyl Diphosphate Synthase from Trypanosoma cruzi: Implications for Drug Design, *Proteins Struc. Func. Bioinformatics*, **62** (1), 80-88 (2006).

M Gill, S Strobel, J Loria, Crystallization and Characterization of the Thallium Form of the Oxytricha Nova G-Quadruplex, *Nucleic Acids Res.*, **34**, 4506-4514 (2006).

K Gupta, B Selinsky, P Loll, 2.0 Angstrom Structure of Prostaglandin H2 Synthase-1 Reconstituted with a Manganese Porphyrin Cofactor, *Acta Cryst. D*, **62**, 151-156 (2006).

Q Han, H Robinson, Y Gao, N Vogelaar, S Wilson, M Rizzi, J Li, Crystal Structures of Aedes Aegypt Alanine Glyoxylate Aminotransferase, *J. Biol. Chem.*, **281**, 37175-37182 (2006).

J Hu, C Foerster, J Skaritka, D Waterman, Novel Chamber Design for An In-Vacuum Cryo-Cooled Mini-Gap Undulator, *4th International Workshop on Mechanical Engineering Design of Synchrotron Radiation Equipment & Instrumentation*, Vol 1, p. 8, sponsored by Japan Synchrotron Radiation Research Institute and MEDSI-06 (2006).

G Hu, G Lin, M Wang, L Dick, R Xu, C Nathan, H Li, Structure of the Mycobacterium tuberculosis proteasome and mechanism of inhibition by a peptidyl boronate, *N/A*, **59** (5), 1417-1428 (2006).

Q Huai, Structure of Human Urokinase Plasminogen Activator, *Science*, **311**, 656 (2006).

Q Huai, Y Sun, H Wang, D MacDonald, R Aspiotis, H Robinson, Z Huang, H Ke, Enantiomer Discrimintation Illustrated by the High Resolution Crystal Structures of Type 4 Phosphodiesterase, *J. Med. Chem.*, **49**, 1867-1873 (2006).

K Juznedelov, V Lamour, G Patikoglou, M Chlenov, S Darst, K Severinov, Recombinant Thermus aquaticus RNA Polymerase for Structural Studies, *J. Mol. Biol.*, **359** (1), 110-121 (2006).

S Kamtekar, A Berman, J Wang, J Lazaro, M Vega, L Blanco, M Salas, T Steitz, The 29 DNA Polymerase: Protein-Primer Structure Suggests a Model of the Initiation to Elongation Transition, *EMBO J.*, **25** (6), 1335 (2006).

S Kang, K Hoke, B Crane, Solvent Isotope Effects on Interfacial Protein Electron Transfer in Crystals and Electode Films, *J. Am. Chem. Soc.*, **128**, 2346-2355 (2006).

B Kelly, B Howard, H Wang, H Robinson, W Sundquist, C Hill, Implications for Viral Capsid Assembly from Crystal Structures of HIV-1 Gag1-278 and CAN133-278, *Biochemistry*, **45** (38), 11257 -11266 (2006).

H Kleinman, B Ford, J Keller, N Carpino, N Nassar, Crystallization and Initial Crystal Characterization of the C-terminal Phosphoglycerate Mutase Homology Domain of Sts-1, *Acta Cryst. F*, **62**, 218-220 (2006).

V Lamour, B Hogan, D Erie, S Darst, Crystal Structure of Thermus Aquaticus Gfh1, a Gre-factor Paralog that Inhibits rather than Stimulates transcript Cleavage, *J. Mol. Biol.*, **356**, 179-188 (2006).

W Lane, S Darst, The Structural Basis for Promoter –35 Element Recognition by the Group IV ? Factors, *PLoS Biol.*, **4**, e269 (2006).

O Laptenko, S Kim, J Lee, M Starodubtseva, F Cava, J Berenguer, X Kong, S Borukhov, pH-Dependent Conformational Switch Activates the Inhibitor of Transcription Elongation, *EMBO J.*, **25** (10), 2131 (2006).

C Lawson, B Yung, A Barbour, W Zuckert, Crystal Structure of Neurotropism-Associated Variable Surface Protein 1 (VSP1) of Borrelia Turicatae, *J. Bacteriol.*, **188**, 4522 (2006).

Z Li, R Cao, M Wang, M Myers, Y Zhang, R Xu, Structure of a BMI-1-Ring1B Polycomb Group Ubiquitin Ligase Complex, *J. Biol. Chem.*, **281**, 20643 (2006).

Y Liu, J Sivaraman, C Hew, Expression, purification and crystallization of a novel nonstructural protein VP9 from white spot syndrome virus., *Acta Cryst. F*, **62** (8), 802 - 804 (2006).

H Losey, A Ruthenburg, G Verdine, Crystal Structure of Staphylococcus aureus tRNA Adenosine Deaminase TadA in Complex with RNA, *Nat. Struct. Mol. Biol.*, **13** (2), 153 (2006).

P Meyer, M Suh, P Ye, M Zhang, J Fu, Phasing RNA Polymerase II Using Intrinsically Bound Zn Atoms: An Updated Structural Model, *Structure*, **14** (6), 973-82 (2006).

H Moroder, C Kreutz, K Lang, A Serganov, R Micura, Synthesis, Oxidation Behavior, Crystallization and Structure of 2'-Methylseleno Guanosine Containing RNAs, *J. Am. Chem. Soc.*, **128**, 9909-9918 (2006).

A Napoli, C Lawson, R Ebright, H Berman, Indirect Readout of DNA Sequence at the Primary-kink Site in the CAP-DNA Complex: Recognition of Pyrimidine-Purine and Purine-Purine Steps, *J. Mol. Biol.*, **357** (1), 173-183 (2006).

M Neiditch, M Federle, A Pompeani, R Kelly, D Swem, P Jeffrey, B Bassler, F Hughson, Ligand-Induced Asymmetry in Histidine Sensor Kinase Complex Regulates Quorum Sensing, *Cell*, **126** (6), 1095-1108 (2006).

K Pant, B Crane, Nitrosyl-Heme Structures of Bacillus subtilis Nitric Oxide Synthase Have Implications for Understanding Substrate Oxidation, *Biochemistry*, **45**, 2537-2544 (2006).

S Park, P Borbat, G Gonzalez-Bonet, J Bhatnagar, A Pollard, J Freed, A Bilwes, B Crane, Reconstruction of the Chemotaxis Receptor-Kinase Assembly, *Nat. Struct. Mol. Biol.*, **13** (5), 400 (2006).

S Park, B Lowder, A Bilwes, D Blair, B Crane, Structure of FliM Provides Insight into Assembly of the Switch Complex in the Bacterial Flagella Motor, *Proc Natl Acad Sci USA*, **103** (32), 11886-11891 (2006).

H Pinkett, K Shearwin, S Stayrook, I Dodd, T Burr, A Hochschild, J Egan, M Lewis, The Structural Basis of Cooperative Regulation at an Alternate Genetic Switch, *Mol. Cell*, **21**, 605-615 (2006).

K Rao, J Bonanno, S Burley, S Swaminathan, Crystal Structure of Glycerophosphodiester Phosphodiesterase from Agrobacterium tumefaciens by SAD with a Large Asymmetric Unit, *Proteins: Struc. Func. Bioinformatics*, **65**, 514-518 (2006).

P Sanghani, W Davis, L Zhai, H Robinson, Structure-Function Relationships in Human Glutathione-Dependent Formaldehyde Dehydrogenase. Role of Glu-67 and Arg-368 in the Catalytic Mechanism, *Biochemistry*, **45**, 4819-4830 (2006).

A Serganov, A Polonskaia, A Phan, R Breaker, D Patel, Structural Basis for Gene Regulation by a Thiamine Pyrophosphate-Sensing Riboswitch, *Nature*, **441**, 1167-1171 (2006).

J Sudhamsu, B Crane, Structure and Reactivity of a Thermostable Prokaryotic Nitric-oxide Synthase That Forms a Long-lived Oxy-Heme Complex, *J. Biol. Chem.*, **281** (14), 9623-9632 (2006).

S Sunita, H Zhenxing, J Swaathi, M Cygler, A Matte, J Sivaraman, Domain organization and crystal structure of the catalytic domain of E.coli RluF, a pseudouridine synthase that acts on 23S rRNA, *J. Mol. Biol.*, **359** (4), 998 - 1009 (2006).

M Teplova , Y Yuan, A Phan, L Malinina, S Ilin, A Teplov, D Patel, Structural Basis for Recognition and Sequestration of UUUOH 3 ' Temini of Nascent RNA Polymerase III Transcripts by La, a Rheumatic Disease Autoantigen, *Mol. Cell*, **21**, 75-85 (2006).

K Terry, P Casey, L Beese, Conversion of Protein Farnesyltransferase to a Geranylgeranyltransferase, *Biochemistry*, **45**, 9746-9755 (2006).

G Tian, S Xiang, R Noiva, W Lennarz, H Schindelin, The Crystal Structure of Yeast Protein Disulfide Isomerase Suggests Cooperativity Between Its Active Sites, *Cell*, **124** (1), 61-73 (2006).

J Tokarski, J Newitt, C Chang, J Cheng, M Wittekind, S Kiefer, K Kish, F Lee, R Borzilerri, et al., The Structure of Dasatinib (BNS-354825) Bound to Activated ABL Kinase Domain Elucidates its Inhibitory Activity Against Imatinib-Resistant ABL Mutants, *Cancer Res.*, **66**, 5790-5797 (2006).

F Valiyaveetil, M Sekedat, R MacKinnon, T Muir, Structural and Functional Consequences of an Amide-to-Ester Substitution in the Selectivity Filter of a Potassium Channel, *J. Am. Chem. Soc.*, **128**, 11591-11599 (2006).

R Van Waardenburg, D Duda, C Lancaster, B Schulman, M Bjornsti, Distinct Functional Domains of UBC9 Dictate Cell Survival and Resistance to Genotoxic Stress, *Mol. Cell. Bio.*, **26**, 4958 (2006).

J Wally, P Halbrooks, C Vonrhein, M Rould, S Everse, A Mason, S Buchanan, The Crystal Structure of Iron-free Human Serum Transferrin Provides Insight into Inter-lobe Communication and Receptor Binding, *J. Biol. Chem.*, **281** (34), 24934-24944 (2006).

Y Xing, Y Xu, Y Chen, P Jeffrey, Y Chao, Z Lin, Z Li, S Strack, J Stock, Y Shi, Structure of Protein Phosphatase 2A Core Enzyme Bound to Tumor-Inducing Toxins, *Cell*, **127**, 341-353 (2006).

H Xu, H Beernink, M Rould, S Morrical, Crystallization and Preliminary X-ray Analysis of Bacteriophasge T4 UvsY Recombination Mediator Protein, *Acta Cryst. F*, **62**, 1013-1015 (2006).

X Zhou, G Zhao, J Truglio, L Wang, G Li, W Lennarz, H Schindelin, Structural and Biochemical Studies of the C-Terminal Domain of Mouse Peptide-N-glycanase Identify it as a Mannose-Binding Module, *Proc Natl Acad Sci USA*, **103**, 17214-17219 (2006).

J Zimmer, W Li, T Rapoport, A Novel Dimer Interface and Conformational Changes Revealed by an X-ray Structure of B. subtilis SecA, *J. Mol. Biol.*, **364**, 259-265 (2006).

Beamline X26A

Y Arai, A Lanzirotti, S Sutton, M Newville, J Dyer, D Sparks, Spatial and Temporal Variability of Arsenic Solid-State Speciation in Historically Lead Arsenate Contaminated Soils, *Environ. Sci. Tech.*, **40** (3), 673-679 (2006).

D Brownlee, P Tsou, J Aléon, C Alexander, T Araki, S Bajt, G Baratta, R Bastien, P Bland, et al., Comet 81P/Wild 2 Under a Microscope, *Science*, **314** (5806), 1711 - 1716 (2006).

J Cempirek, M Novak, A Ertl, J Hughes, G Rossman, M Dyar, Fe-bearing Olenite with Tetrahedrally Coordinated Al from an Abyssal Pegmatite at Kutná Hora, Czech Republic: Structure, Crystal Chemistry, Optical and XANES Spectra, *Can. Mineral*, **44** (1), 23-30 (2006).

M Corriveau, Characterization of Arsenic-bearing Near-surface and Airborne Particulates from Gold-mine Tailings in Nova Scotia, Canada, M.Sc. Thesis, Queen's University , Kingston (2006).

G Flynn, J Borg, P Bleuet, F Brenker, S Brennan, C Daghlian, Z Djouadi, T Ferroir, J Gallien, P Gillet, Chemical Analysis of Wild-2 Samples Returned by Stardust, *Lunar and Planetary Science* , Vol XXXVII, p. 1217, sponsored by Lunar and Planetary Institute (2006).

G Flynn, A Lanzirotti, S Sutton, Chemical Compositions of Large Cluster IDP's, *Lunar and Planetary Science* , Vol XXXVII, p. 1216, sponsored by Lunar and Planetary Institute (2006).

G Flynn, P Bleuet, J Borg, J Bradley, F Brenker, S Brennan, J Bridges, D Brownlee, E Bullock, et al., Elemental Compositions of Comet 81P/Wild 2 Samples Collected by Stardust, *Science*, **314** (5806), 1731 - 1735 (2006).

E Hendy, A Lanzirotti, T Rasbury, J Lough, Synchrotron u-XRF Mapping of Elemental Distributions Across Coral Skeleton Micro-Architecture, *Geochim. Cosmochim. Acta*, **70** (18, supplement 1), 246 (2006).

H Jamieson, S Walker, C Andrade, Application of Synchrotron-based Micro-analysis to Mine Waste Miineralogy, *Geochim. Cosmochim. Acta*, **70** (18), A289 (2006).

K Jones, H Feng, E Stern, U Neuhausler, J Osan, N Marinkovic, Z Song, Properties of New York/New Jersey Harbor Sediments, *Acta Phys. Pol. A*, **109** (3), 279-286 (2006).

J Kaste, B Bostick, A Friedland, A Schroth, T Siccama, Fate and Speciation of Gasoline-Derived Lead in Organic Horizons of the Northeastern USA, *Soil Sci. Soc. Am. J.*, **70**, 1688-1698 (2006).
S Kim, T Punshon, A Lanzirotti, L Li, J Alonso, J Ecker, J Kaplan, M Guerinot, Localization of Iron in Arabidopsis Seed Requires the Vacuolar Membrane Transporter VIT1, *Science*, **314** (5803), 1295-1298 (2006).
A Lanzirotti, S Sutton, Synchrotron X-ray Microbeam Techniques in Assessing Metal Bioavailability in the Environment, *Geochim. Cosmochim. Acta*, **70** (18, supplement 1), 343 (2006).
A Leri, M Hay, A Lanzirotti, W Rao, S Myneni, Quantitative Determination of Absolute Organohalogen Concentrations in Environmental Samples by X-ray Absorption Spectroscopy, *Anal. Chem.*, **78**, 5711-5718 (2006).
R Martin, S Naftel, S Macfie, K Jones, H Feng, C Trembley, High Variability of the Metal Content of Tree Growth Rings as Measured by Synchrotron Micro X-ray Fluorescence Spectrometry, *X-Ray Spectrom.*, **35**, 57-62 (2006).
C Martinez, K Bazilevskaya, A Lanzirotti, Zinc coordination to multiple ligand atoms in organic-rich surface soils, *Environ. Sci. Tech.*, **40**, 5688-5695 (2006).
L Miller, Q Wang, T Telivala, R Smith, A Lanzirotti, J Miklossy, Synchrotron-based Infrared and X-ray Imaging Shows Focalized Accumulation of Cu and Zn Co-localized With Beta-amyloid Deposits in Alzheimer's Disease, *J. Struct. Biol.*, **155** (1), 30-37 (2006).
P Poussart, S Myneni, A Lanzirotti, Tropical dendrochemistry: A novel approach to estimate age and growth from ringless trees, *Geophys. Res. Lett.*, **33** (17), L17711 (2006).
R Reeder, A Lanzirotti, Accessing User Facilities and Making your Research Experience Successful, *Elements*, **2**, 31-36 (2006).
R Reeder, M Schoonen, A Lanzirotti, Metal Speciation and Its Role in Bioaccessibility and Bioavailability, *Medical Mineralogy and Geochemistry*, p. 59-113, Mineralogical Society of America, Washington (2006).
S Sutton, User Research Facilities in the Earth Sciences, *Elements*, **2**, 7-8 (2006).
S Walker, The Solid-Phase Speciation of Arsenic in Roasted and Weathered Sulfides at the Giant Gold Mine, Yellowknife, NWT. Application of Synchrotron MicroXANES and MicroXRD at the Grain Scale., Ph.D. Thesis, Queen's University, Kingston (2006).
C Weisener, S Crowe, D Fowle, J Roberts, Spectroscopic Investigation of the Microbial Controls on Trace Element Mobility in Iron Rich Equatorial Lacustrine Sediments, *Geochim. Cosmochim. Acta*, **70** (18), A695 (2006).
M Zolensky, P Bland, J Bradley, A Brearley, S Brennan, J Bridges, D Brownlee, A Butterworth, Z Dai, D Ebel, Mineralogy and Petrology of Comet Wild2 Nucleus Samples, *Lunar and Planetary Science* , Vol XXXVII, p. 1203, sponsored by Lunar and Planetary Institute (2006).
M Zolensky, T Zega, H Yano, S Wirick, A Westphal, M Weisberg, I Weber, J Warren, M Velbel, et al., Mineralogy and Petrology of Comet 81P/Wild 2 Nucleus Samples, *Science*, **314** (5806), 1735 - 1739 (2006).

Beamline X26C

M Bewley, V Graziano, J Jiang, E Matz, F Studier, A Pegg, C Coleman, J Flanagan, Structures of Wild-Type and Mutant Human Spermidine/Spermine N1-acetyltransferase, a Potential Therapeutic Drug Target, *Proc Natl Acad Sci USA*, **103**, 2063-8 (2006).
J Connelly, P Yuan, H Hsu, Z Li, R Xu, R Sternglanz, Structure and Function of the Saccharomyces Cerevisiae Sir3 BAH Domain, *Mol. Cell. Bio.*, **26**, 3256 (2006).
E Enemark, L Joshua-Tor, Mechanism of DNA Translocation in a Replicative Hexameric Helicase, *Nature*, **442**, 270-275 (2006).
A Feldman, J Lee, B Delmas, M Paetzel, Crystal Structure of a Novel Viral Protease with a Serine/Lysine Catalytic Dyad Mechanism, *J. Mol. Biol.*, **358**, 1378 (2006).
B Ford, V Hornak, H Kleinman, N Nassar, Structure of a Transient Intermediate for GTP Hydrolysis of Ras, *Structure*, **14** (3), 427-436 (2006).
D Gallagher, N Smith, S Kim, A Heroux, H Robinson, P Reddy, Structure of the Class IV Adenylyl Cyclase Reveals a Novel Fold, *J. Mol. Biol.*, **362** (1), 114-122 (2006).
A Ghosh, P Sridhar, S Leshchenko, A Hussain, J Li, A Kovalevsky, D Walters, J Wedelind, V Grum-Tokars, et al., Structure-Based Design of Novel HIV-1 Protease Inhibitors to Combat Drug Resistance, *J. Med. Chem.*, **49** (17), 5252-5261 (2006).
P Haenzelmann, H Schindelin, Binding of 5'-GTP to the C-terminal FeS Cluster of the Radical S-Adenosylmethionine Enzyme MoaA Provides Insights into its Mechanism, *Proc Natl Acad Sci USA*, **103**, 6829-6834 (2006).
Q Huai, Y Sun, H Wang, D MacDonald, R Aspiotis, H Robinson, Z Huang, H Ke, Enantiomer Discrimintation Illustrated by the High Resolution Crystal Structures of Type 4 Phosphodiesterase, *J. Med. Chem.*, **49**, 1867-1873 (2006).
Y Huang, J Fang, M Bedford, Y Zhang, R Xu, Recognition of Histone H3 Lysine-4 Methylation by the Double Tudor Domain of JMJD2A, *Science*, **312**, 748 (2006).
Y Huang, M Myers, R Xu, Crystal Structure of the HP1-EMSY Complex Reveals an Unusual Mode of HP1 Binding, *Structure*, **14** (4), 703-712 (2006).
S Kamtekar, A Berman, J Wang, J Lazaro, M Vega, L Blanco, M Salas, T Steitz, The 29 DNA Polymerase: Protein-Primer Structure Suggests a Model of the Initiation to Elongation Transition, *EMBO J.*, **25** (6), 1335 (2006).
R Kanai, K Kar, K Anthony, L Gould, M Ledizet, E Fikrig, W Marasco, R Koski, Y Modis, Crystal Structure of West Nile Virus Envelope Glycoprotein Reveals Viral Surface Epitopes, *J. Virology*, **80**, 11000-11008 (2006).
E Kim, N Schrader, B Smolinsky, C Bedet, C Vannier, G Schwartz, H Schindelin, Deciphering the Structural Framework of Glycine Receptor Anchoring by Gephyrin, *EMBO J.*, **25**, 1385-1395 (2006).
H Kleinman, B Ford, J Keller, N Carpino, N Nassar, Crystallization and Initial Crystal Characterization of the C-terminal Phosphoglycerate Mutase Homology Domain of Sts-1, *Acta Cryst. F*, **62**, 218-220 (2006).

S Komeda, T Moulaei, K Kruger Woods, M Chikuma, N Farrell, L Williams, A Third Mode of DNA Binding: Phosphate Clamps by a Polynuclear Platinum Complex, *J. Am. Chem. Soc.*, **128**, 16092-16103 (2006).

S Lawrence, K Luther, H Schindelin, J Ferry, Structural and Functional Studies Suggest a Catalytic Mechanism for the Phosphotransacetylase from Methanosarcina Thermophila, *J. Bacteriol.*, **188**, 1143 (2006).

T Mallett, J Wallen, P Karplus, H Sakai, T Tsukihara, A Claiborne, Structure of Coenzyme A-Disulfide Reductase from Staphylococcus aureus at 1.54 Angstrom Resolution, *Biochemistry*, **45**, 11278-11289 (2006).

A Nagpal, M Valley, P Fitzpatrick, A Orville, Crystal Structures of Nitroalkane Oxidase: Insights into the Reaction Mechanism of a Covalent Complex of the Flavoenzyme Trapped During Turnover, *Biochemistry*, **45**, 1138-1150 (2006).

K Natarajan, A Hicks, J Mans, H Robinson, R Guan, R Mariuzza, D Margulies, Crystal Structure of the Murine Cytomegalovirus MHC-I Homolog m144, *J. Mol. Biol.*, **358**, 157-171 (2006).

P Pena, F Davrazou, X Shi, K Walter, V Verhusha, O Gozani, R Zhao, T Kutateladze, Molecular Mechanism of Histone H3K4me3 Recognition by Plant Homeodomain of ING2, *Nature*, **442**, 100 (2006).

F Reyes-Turcu, J Horton, J Mullally, A Heroux, X Cheng, K Wilkinson, The Ubiquitin Binding Domain ZnF UBP Recognizes the C-Terminal Diglycine Motif of Unanchored Ubiquitin, *Cell*, **124** (6), 1197-1208 (2006).

I Schoenhofen, V Lunin, J Julien, Y Li, E Ajamian, A Matte, M Cygler, J Brisson, A Aubry, et al., Structural and Functional Characterization of PseC, an Aminotransferase Involved in the Biosynthesis of Pseudaminic Acid, an Essential Flagellar Modification in Helicobacter Pylori, *J. Biol. Chem.*, **281** (13), 8907-8916 (2006).

T Sullivan, J Truglio, M Boyne, P Novichenok, X Zhang, C Stratton, H Li, T Kaur, A Amin, et al., High Affinity Inha Inhibitors with Activity Against Drug-Resistant Strains of Mycobacterium Tuberculosis, *ACS Chem. Biol.*, **1**, 43 (2006).

G Tian, S Xiang, R Noiva, W Lennarz, H Schindelin, The Crystal Structure of Yeast Protein Disulfide Isomerase Suggests Cooperativity Between Its Active Sites, *Cell*, **124** (1), 61-73 (2006).

L Tremblay, D Dunaway-Mariano, K Allen, Structure and Activity Analyses of Escherichia coli K-12 NagD Provide Insight into the Evolution of Biochemical Function in the Haloakanoic Acid Dehlogenase Superfamily, *Biochemistry*, **45**, 1183-1193 (2006).

J Truglio, E Karakas, B Rhau, H Wang, M DellaVecchia, B Van Houten, C Kisker, Structural Basis for DNA Recognition and Processing by UvrB, *Nat. Struct. Mol. Biol.*, **13** (4), 360 (2006).

A VanDemark, M Blanksma, E Ferris, A Heroux, C Hill, T Formosa, The Structure of the yFACT Pob3-M Domain, Its Interaction with the DNA Replication Factor RPA, and a Potential Role in Nucleosome Deposition, *Mol. Cell*, **22**, 363-374 (2006).

J Wally, P Halbrooks, C Vonrhein, M Rould, S Everse, A Mason, S Buchanan, The Crystal Structure of Iron-free Human Serum Transferrin Provides Insight into Inter-lobe Communication and Receptor Binding, *J. Biol. Chem.*, **281** (34), 24934-24944 (2006).

S Xiang, E Kim, J Connelly, N Nassar, J Kirsch, Winking, G Schwartz, H Schindelin, The Crystal Structure of Cdc42 in Complex with Collybisin II, a Gephyrin-Interacting Guanine Nucleotide Exchange Factor, *J. Mol. Biol.*, **359** (1), 35-46 (2006).

X Zhou, G Zhao, J Truglio, L Wang, G Li, W Lennarz, H Schindelin, Structural and Biochemical Studies of the C-Terminal Domain of Mouse Peptide-N-glycanase Identify it as a Mannose-Binding Module, *Proc Natl Acad Sci USA*, **103**, 17214-17219 (2006).

Beamline X27A

J Ablett, C Kao, R Reeder, Y Tang, A Lanzirotti, X27A - A New Hard X-ray Micro-Spectroscopy Facility at the National Synchrtron Light Source, *Nucl. Instrum. Meth. A*, **562**, 487-494 (2006).

Beamline X27B

A Bolotnikov, M Black, G Camarda, G Carini, Y Cui, K Kohman, L Li, M Salomon, R James, The Effect of Te Precipitates on Characteristics of CdZnTe Detectors, *Proceedings of Hard X-ray and Gamma-Ray Detector Physics VIII*, Vol 6319, p. 631903-1, sponsored by SPIE (2006).

G Camarda, A Bolotnikov, G Carini, R James, L Li, Effects of Tellurium Precipitates on Charge Collection in CZT Nuclear Radiation Detectors, *Nato Conference on Countering Nuclear and Radiological Terrorism*, p. 199-207, Springer, (2006).

G Camarda, A Bolotnikov, G Carini, Y Cui, K Kohman, L Li, R James, High Spatial-Resolution Imaging of Te Inclusions in CZT Material, *In Proceedings of SPIE Hard X-ray and Gamma-Ray Detector Physics VIII*, Vol 6319, p. 63190Z-1, sponsored by SPIE (2006).

G Carini, A Bolotnikov, G Camarda, Y Cui, H Jackson, A Burger, K Kohman, L Li, R James, Te Inclusions and Their Relationship to the Performance of CdZnTe Detectors, *In Proceedings of SPIE Hard X-ray and Gamma-Ray Detector Physics VIII*, Vol 6319, p. 631906-1, sponsored by SPIE (2006).

M Chu, S Terterian, G Carini, G Camarda, A Bolotnikov, R James, D Xu, Z He, Effects of Material Improvement on CZT Detectors, *In Proceedings of SPIE Hard X-ray and Gamma-Ray Detector Physics VIII*, Vol 6319, p. 631905-1, sponsored by SPIE (2006).

Beamline X27C

M Birnkrant, H McWilliams, C Li, L Natarajan, V Tondiglia, R Sutherland, P Lloyd, T Bunning, On the Structure of Holographic Polymer-dispersed Polyethylene Glycol, *Polymer*, **47** (24), 8147-8154 (2006).

J Buckley, P Cebe, D Cherdack, J Crawford, B Ince, M Jenkins, J Pan, M Reveley, N Washington, N Wolchover, Nanocomposites of Poly(vinylidene Fluoride) with Organically Modified Silicate, *Polymer*, **47** (7), 2411-2422 (2006).

X Chen, C Burger, D Fang, D Ruan, L Zhang, B Hsiao, B Chu, X-ray Studies of Regenerated Cellulose Fibers Wet Spun from Cotton Linter Pulp in NaOH/Thiourea Aqueous Solutions, *Polymer*, **47** (8), 2839-2848 (2006).

X Chen, K Tenneti, C Li, Y Bai, R Zhou, X Wan, X Fan, Q Zhou, Design, Synthesis, and Characterization of Bent-Core Mesogen-Jacketed Liquid Crystalline Polymers, *Macromolecules*, **39**, 517-527 (2006).

X Chen, C Burger, D Fang, I Sics, X Wang, W He, R Somani, K Yoon, B Hsiao, B Chu, In-Situ X-ray Deformation Study of Fluorinated Mulitwalled Carbon Nanotube and Fluorinated Ethylene-Propylene Nanocomposite Fibers, *Macromolecules*, **39**, 5427-5437 (2006).

T Chung, R Ho, J Kuo, J Tsai, B Hsiao, I Sics, Trilayer Crystalline Lamellar Morphology Under Confinement, *Macromolecules*, **39**, 2739-2742 (2006).

D Dillon, K Tenneti, C Li, F Ko, I Sics, B Hsiao, On the Structure and Morphology of Polyvinylidene Fluoride-nanoclay Nanocomposites, *Polymer*, **47** (5), 1678-1688 (2006).

T Fornes, J Baur, Y Sabba, E Thomas, Morphology and Properties of Melt-Spun Polycarbonate Fibers Containing Single- and Multi-Wall Carbon Nanotubes, *Polymer*, **47** (5), 1704-1714 (2006).

M Gelfer, C Burger, B Hsiao, S D'Andrea, A Fadeev, Highly-Ordered Layered Organo-Mineral Materials Prepared via Reactions of n-Alkylphosphonic Acids with Apatite, *J. Colloid Interface Sci.*, **295** (2), 388-392 (2006).

S Hofmann, C Wong Po Foo, F Rossetti, M Textor, G Vunjak-Novakovic, D Kaplan, H Merkle, L Meinel, Silk Fibroin as an Organic Polymer for Controlled Drug Delivery, *J. Controlled Release*, **111** (1-2), 219-227 (2006).

P Huang, Y Guo, R Quirk, J Ruan, B Lotz, E Thomas, B Hsiao, C Avila-Orta, I Sics, S Cheng, Confined Cylinders Constructed by a Poly(ethylene oxide)-b-polystyrene Diblock Copolymer and a Blend of Poly(ethylene Oxide)-b-Polystyrene and Polystyrene, *Polymer*, **47** (15), 5457-5466 (2006).

D Kawakami, S Ran, C Burger, C Avila-Orta, I Sics, B Chu, B Hsiao, T Kikutani, Superstructure Evolution in Poly(ethylene terephthalate) During Uniaxial Deformation Above Glass Transition Temperature, *Macromolecules*, **39**, 2909-2920 (2006).

A Kelarakis, K Yoon, R Somani, I Sics, X Chen, B Hsiao, B Chu, Relationship Betwen Structure and Dynamic Mechanical Properties of a Carbon Nanofiber Reinforced Elastomeric Nanocomposite, *Polymer*, **47** (19), 6797-6807 (2006).

L Korley, B Pate, E Thomas, P Hammond, Effect of the Degree of Soft and Hard Segment Ordering on the Morphology and Mechanical Behavior of Semicrystalline Segmented Polyurethanes, *Polymer*, **47** (9), 3073-3082 (2006).

C Krishnan, J Chen, C Burger, B Chu, Polymer-Assisted Growth of Molybdenum Oxide Whiskers via a Sonochemical Process, *J. Phys. Chem. B*, **110**, 20182-20188 (2006).

L Liu, B Hsiao, S Ran, B Fu, S Toki, F Zuo, A Tsou, B Chu, In Situ WAXD Study of Structure Changes During Uniaxial Deformation of Ethylene-based Semicrystalline Ethylene-Propylene Copolymer, *Polymer*, **47** (8), 2884-2893 (2006).

Y Liu, H Nie, R Bansil, M Steinhart, J Bang, T Lodge, Kinetics of Disorder-to-fcc Phase Transition via an Intermediate bcc State, *Phys. Rev. E*, **73**, 061803 (2006).

M Mondeshki, G Milhov, R Graf, H Spiess, K Mullen, P Papadopoulos, A Gitsas, G Floudas, Self-Assembly and Molecular Dynamics of Peptide-Functionalized Polyphenylene Dendrimers, *Macromolecules*, **39**, 9605-9613 (2006).

C Osuji, C Chao, C Ober, C Thomas, Supramolecular Microphase Separation in a Hydrogen-Bonded Liquid Crystalline Comb Copolymer in the Melt State , *Macromolecules*, **39** (9), 3114 (2006).

J Ouyang, Y Pan, S Zhou, S Goh, Supramolecular Assembled C60-Containing Carboxylated Poly(dimethylsiloxane) Composites, *Polymer*, **47** (17), 6140-6148 (2006).

K Page, F Landis, A Phillips, R Moore, SAXS Analysis of the Thermal Relaxation of Anisotropic Morphologies in Oriented Nafion Membranes, *Macromolecules*, **39**, 3939-3946 (2006).

J Park, E Thomas, Frustrated Crystallization of a Rod-Coil Block Copolymer from Its Liquid Crystalline State , *Macromolecules*, **39** (14), 4650 (2006).

R Somani, L Yang, B Hsiao, Effects of High Molecular Weight Species on Shear-Induced Orientation and Crystallization of Isotactic Polypropylene, *Polymer*, **47** (15), 5657-5668 (2006).

L Sun, J Ginorio, L Zhu, I Sics, L Rong, B Hsiao, Phase Transitions and Honeycomb Morphology in an Incompatiable Blend of Enantiomeric Polylactide Block Copolymers, *Macromolecules*, **39** (24), 8203-8206 (2006).

S Toki, B Hsiao, S Kohjiya, M Tosaka, A Tosaka, A Tsou, S Datta, Synchrotron X-ray Studies of Vulcanized Rubbers and Thermoplastic Elastomers, *Rubber Chem. Technol.*, **79** (3), 460 (2006).

S Toki, I Sics, C Burger, D Fang, L Liu, B Hsiao, S Datta, A Tsou, Structure Evolution During Cyclic Deformation of an Elastic Propylene-Based Ethylene-Propylene Copolymer, *Macromolecules*, **39**, 3588-3597 (2006).

Z Wang, Z Xia, Z Yu, E Chen, H Sue, C Han, B Hsiao, Lamellar Formation and Relaxatin in Simple Sheared Poly(ethylene terephthalate) by Small-Angle X-ray Scattering, *Macromolecules*, **39**, 2930-2939 (2006).

S Xu, J Gu, B Belknap, H White, L Yu, Structural Characterization of the Binding of Myosin*ADP*Pi to Actin in Permeabilized Rabbit Psoas Muscle, *Biophys. J.*, **91**, 3370-3382 (2006).

S Xu, D Martyn, J Zaman, L Yu, X-ray Diffraction Studies of the Thick Filament in Permeabilized Myocardium from Rabbit, *Biophys. J.*, **91**, 3768-3775 (2006).

L Yang, R Somani, I Scis, B Hsiao, R Kolb, D Lohse, The Role of High Molecular Weight Chains in Flow-Induced Crystallization Precursor Structures, *J. Phys.: Condens. Matter*, **18**, S2421-S2436 (2006).

J Yoon, R Mathers, G Coates, E Thomas, Optically Transparent and High Molecular Weight Polyolefin Block Copolymers Toward Self-Assembled Photonic Band Gap Materials, *Macromolecules*, **39**, 1913 (2006).

F Zuo, J Keum, L Yang, R Somani, B Hsiao, Thermal Stability of Shish-Induced Shish-Kebab Precursor Structure from High Molecular Weight Polyethylene Chains, *Macromolecules*, **39** (6), 2209 (2006).

Beamline X28C

T Adilakshmi, R Lease, S Woodson, Hydroxyl Radical Footprinting in vivo: Mapping Macromolecular Structures with Synchrotron Radiation, *Nucleic Acids Res.*, **34** (8), e64 (2006).

L Kwok, I Scherbakova, J Lamb, H Park, K Andresen, H Smith, M Brenowitz, L Pollack, Concordant Exploration of the Kinetics of RNA Folding from Global and Local Perspectives, *J. Mol. Biol.*, **355**, 282-293 (2006).

A Laederach, I Shcherbakova, M Liang, M Brenowitz, R Altman, Local Kinetic Measures of Macromolecular Structure Reveal Partitioning Among Multiple Parallel Pathways from the Earliest Steps in the Folding of a Large RNA Molecule, *J. Mol. Biol.*, **358**, 1179-1190 (2006).

T Nguyenle, M Laurberg, M Brenowitz, H Noller, Following the Dynamics of Changes in Solvent Accessiblity of 16 S and 23 S RRNA During Ribsomal Subunit Assocaition Using Synchrotron-Generated Hydroxyl Radicals, *J. Mol. Biol.*, **359** (5), 1235-1248 (2006).

I Shcherbakova, S Mitra, R Beer, M Brenowitz, Fast Fenton Footprinting: A Laboratory-Based Method for the Time-Resolved Analysis of DNA, RNA and Proteins, *Nucleic Acids Res.*, **34**, e48 (2006).

K Takamoto, M Chance, Protein-protein Interactions using Radiolytic Footprinting, *Annu. Rev. Bioph. Biom.*, **35**, 251-275 (2006).

Beamline X29A

S Alam, C Langelier, F Whitby, S Koirala, H Robinson, C Hill, W Sundquist, Structural Basis for Ubiquitin Recognition by the Human ESCRT-II EAP45 GLUE Domain, *Nat. Struct. Mol. Biol.*, **13** (11), 1029-1030 (2006).

W Barton, D Tzvetkova-Robev, E Miranda, M Kolev, K Rajashankar, J Himanen, D Nikolov, Crystal Structures of the Tie2 Receptor Ectodomain and the Angiopoietin-2–Tie2 Complex, *Nat. Struct. Mol. Biol.*, **13**, 524-532 (2006).

G Buchko, S Ni, H Robinson, E Welsh, H Pakrasi, M Kennedy, Characterization of two Potentially Universal Turn Motifs that Shape the Repeated VFive-Residues Fold - Crystal Structure of a Lumenal Pentapeptide Repeat Protein from Cyanothece 51142, *Protein Sci.*, **15**, 2579-2595 (2006).

E Cao, U Ramagopal, A Fedorov, E Fedorov, Q Yan, J Lary, J Cole, S Nathenson, S Almo, NTB-A Receptor Crystal Structure: Insights into Homophilic Interactions in the Signaling Lymphocytic Activation Molecule Receptor Family, *Immunity*, **25**, 559-570 (2006).

Y Chao, Y Xing, Y Chen, Y Xu, Z Lin, Z Li, P Jeffrey, J Stock, Y Shi, Structure and Mechanism of the Phosphotyrosyl Phosphatase Activator, *Mol. Cell*, **23**, 535-546 (2006).

D Copeland, A Soares, A West, G Richter-Addo, Crystal Structures of the Nitrite and Nitric Oxide Complexes of Horse Heart Myoglobin, *J. Inorg. Biochem.*, **100** (8), 1413-1425 (2006).

J Cordero-Morales, L Cuello, Y Zhao, V Jogini, D Cortes, B Roux, E Perozo, Molecular Determinants of Gating at the Potassium-Channel Selectivity Filter, *Nat. Struct. Mol. Biol.*, **13** (4), 311 (2006).

E Enemark, L Joshua-Tor, Mechanism of DNA Translocation in a Replicative Hexameric Helicase, *Nature*, **442**, 270-275 (2006).

L Esser, X Gong, S Yang, L Yu, C Yu, D Xia, Surface-Modulated Motion Switch: Capture and Release of Iron-Sulfur Protein in the Cytochrome bc1 Complex, *Proc Natl Acad Sci USA*, **103**, 13045-13050 (2006).

S Fisher, L Govindasamy, N Boyle, M Agbandje-McKenna, D Silverman, G Blackburn, R McKenna, X-ray Crystallographic Studies Reveal That the Incorporation of Spacer Groups in Carbonic Anhydrase Inhibitors Causes Alternate Binding Modes, *Acta Cryst. F*, **62**, 618 (2006).

C Fisher, N Beglova, s Blacklow, Structure of an LDLR-RAP Complex Reveals a General Mode for Ligand Recognition by Lipoprotein Receptors , *Mol. Cell*, **22**, 277-283 (2006).

H Gill, W Boron, Preliminary X-ray Diffraction Analysis of the Cytoplasmic N-terminal Domain of the Na/HCO3 Cotransporter NBCe1-A, *Acta Cryst. F*, **62**, 534-537 (2006).

H Gill, W Boron, Expression and Purification of the Cytoplasmic N-Terminal Domain of the Na/HCO3 Cotransporter NBCe1-A: Structural Insights from the a Generalized Approach, *Protein Expr. Purif.*, **49** (2), 228-234 (2006).

G Hu, G Lin, M Wang, L Dick, R Xu, C Nathan, H Li, Structure of the Mycobacterium tuberculosis proteasome and mechanism of inhibition by a peptidyl boronate, *N/A*, **59** (5), 1417-1428 (2006).

W Hwang, Y Lin, E Santelli, J Sui, L Jaroszewski, B Stec, M Farzan, W Marasco, R Liddington, Structural Basis of Neutralization by a Human Anti-severe Acute Respiratory Syndrome Spike Protein Antibody,80R., *J. Biol. Chem.*, **281**, 34610-6 (2006).

C Johnston, E Lobanova, A Shavkunov, J Low, J Ramer, R Blasesius, Z Fredericks, F willard, B Kuhlman, et al., Minimal Determinants for Binding Activated G alpha from the Structure of a G alpha i1-Peptide Dimer, *Biochemistry*, **45**, 11390-11400 (2006).

J Kim, V Malashkevich, S Roday, M Lisbin, V Schramm, S Almo, Structural and Kinetic Characterization of Escherichia coli TadA, the Wobble-Specific tRNA Deaminase, *Biochemistry*, **45**, 6407-6416 (2006).

Y Leduc, C Phenix, J Puttick, K Nienaber, D Palmer, L Delbaere, Crystallization, Preliminary X-ray Diffraction and Structure Solution of MosA, a Dihydrodipicolinate Synthase from Sinorhizobium Meliloti L5-30, *Acta Cryst. F*, **F62**, 49-51 (2006).

I Lorenz, J Marcotrigiano, T Dentzer, C Rice, Structure of the catalytic domain of the hepatitis C virus NS2-3 protease, *Nature*, **442** (7104), 831-5 (2006).

J Lu, D Ho, N Vogelaar, C Kraml, S Bernhard, N Byme, L Kim, R Pascal, Jr., Synthesis, Structure, and Resolution of Exceptionally Twisted Pentacenes, *J. Am. Chem. Soc.*, **128**, 17043-17050 (2006).

B Manjasetty, A Turnbull, K Bussow, M Chance, Recent Advances in Protein Structure Analysis , *Recent Research Developments in Biochemistry*, p. 47-71, Transworld Research Network, Trivandrum (2006).

B Manjasetty, M Chance, Crystal Structure of Escherichia coli L-Arabinose Isomerase (ECAI), The Putative Target of Biological Tagatose Production, *J. Mol. Biol.*, **360** (2), 297-309 (2006).

S Margarit, W Davidson, L Frego, F Stebbins, A Steric Antagonism of Actin Polymerization by a Salmonella Virulence Protein, *Structure*, **14**, 1219-1229 (2006).

G Meinke, P Bullock, A Bohm, Crystal Structure of the Simian Virus 40 Large T-Antigen Origin-Binding Domain, *J. Virology*, **80**, 4304 (2006).
S Mylavarapu, M Furgason, D Brewer, M Munson, The Structure of the Exocyst Subunit Sec6p Defines a Conserved Architecture with Diverse Roles, *Nat. Struct. Mol. Biol.*, **13** (6), 555-556 (2006).
D Nair, R Johnson, L Prakash, S Prakash, A Aggarwal, Hoogsteen Base Pair Formation Promotes Synthesis Opposite the 1, N6-Ethenodeoxyadenosine Lesion by Human DNA Polymerase 1, *Nat. Struct. Mol. Biol.*, **13** (7), 619 (2006).
Y Nam, P Silz, L Song, J Aster, S Blacklow, Structural Basis for Cooperativity in Recruitment of MAML Co-activators to Notch Transcription Complexes, *Cell*, **124**, 973-983 (2006).
J Nandakumar, S Shuman, C Lima, RNA Ligase Structures Reveal the Basis for RNA Specificity and Conformational Changes that Drive Ligation Forward, *Cell*, **127** (1), 71-84 (2006).
W Nguitragool, C Miller, Uncoupling of a CLC Cl-/H+ exchange transporter by polyatomic anions, *J. Mol. Biol.*, **362**, 682-690 (2006).
X Pan, S Eathiraj, D Lambright, TBC-Domain GAPs for Rab GTPases Accelerate GTP Hydrolysis by a Dual-Finger Mechanism, *Nature*, **442**, 303-306 (2006).
P Pawelek, N Croteau, C Ng-Thow-Hing, C Khursigara, N Moiseeva, M Allaire, J Coulton, Structure of TonB in Complex with FhuA, E. Coli Outer Membrane Receptor, *Science*, **312**, 1399-1402 (2006).
G Prehna, M Ivanov, J Blisha, C Stebbins, Yersinia Virulence Depends on Mimicry of Host Rho-Family Nucleotide Dissociation Inhibitors, *Cell*, **126**, 869-880 (2006).
E Rangarajan, G Nadeau, Y Li, J Wagner, M Hung, J Schrag, M Cygler, A Matte, The structure of the exopolyphsophatase (PPX) from Escherchia coli O157: H7 suggests a binding mode for long polyphosphate chains, *J. Mol. Biol.*, **359** (5), 1249-1260 (2006).
A Ruthenburg, W Wang, D Graybosch, H Li, D Allis, D Patel, G Verdine, Histone H3 Recogntion and Presentation by the WDR5 Module of the MLL1 Complex, *Nat. Struct. Mol. Biol.*, **13** (8), 704 (2006).
M Safo, T Ko, F Musayev, Q Zhao, A Wang, G Archer, Structure of the MecI Repressor from Staphylococcus aureus in Complex with the Cognate DNA Operator of mec, *Acta Cryst. F*, **62**, 320-324 (2006).
P Sanghani, W Davis, L Zhai, H Robinson, Structure-Function Relationships in Human Glutathione-Dependent Formaldehyde Dehydrogenase. Role of Glu-67 and Arg-368 in the Catalytic Mechanism, *Biochemistry*, **45**, 4819-4830 (2006).
I Schoenhofen, V Lunin, J Julien, Y Li, E Ajamian, A Matte, M Cygler, J Brisson, A Aubry, et al., Structural and Functional Characterization of PseC, an Aminotransferase Involved in the Biosynthesis of Pseudaminic Acid, an Essential Flagellar Modification in Helicobacter Pylori, *J. Biol. Chem.*, **281** (13), 8907-8916 (2006).
E Schreiter, S Wang, D Zamble, C Drennan, NikR-Operator Complex Structure and the Mechanism of Repressor Activation by Metal Ions, *Proc Natl Acad Sci USA*, **103** (37), 13676-13681 (2006).
D Shaya, A Tocilj, Y Li, J Myette, G Venkatarman, R Sasisekharan, M Cygler, Crystal Structure of Heparinase II from Pedobacter Heparinus and its Complex with a Disaccharide Product, *J. Biol. Chem.*, **281** (2), 22 (2006).
Y Shen, C Chou, G Chang, L Tong, Is Dimerization Required for the Catalytic Activity of Bacterial Biotin Carboxylase?, *Mol. Cell*, **22**, 807 (2006).
W Shi, H Robinson, M Sullivan, D Abel, J Toomey, L Berman, D Lynch, G Rosenbaum, G Rakowsky, et al., Beamline X29: A Novel Undulator Source for X-ray Crystallography, *J. Synch. Rad.*, **13**, 365-372 (2006).
M Suits, N Jaffer, Z Jia, Structure of the Escherichia coli O157:H7 heme oxygenase ChuS in complex with heme and enzymatic inactivation by mutation of the heme coordinating residue His-193, *J. Biol. Chem.*, **281** (48), 36776-82 (2006).
H Wang, Y Liu, Q Huai, J Cai, R Zoraghi, S Francis, J Corbin, H Robinson, Z Xin, et al., Multiple Conformations of Phosphodiesterase-5: Implications for Enzyme Function and Drug Developement, *J. Biol. Chem.*, **281**, 21469 (2006).
Y Xu, Y Xing, Y Chen, Y Chao, Z Lin, E Fan, J Yu, S Strack, P Jeffrey, Y Shi, Structure of the Protein Phosphatase 2A Holoenzyme, *Cell*, **127**, 1239-1251 (2006).
W Yew, A Fedorov, E Fedorov, J Rakus, R Pierce, S Almo, J Gerlt, Evolution of Enzymatic Activities in the Enolase Superfamily: L-Fuconate Dehydratase from Xanthomonas campestris, *Biochemistry*, **45**, 14582-14597 (2006).
Y Yuan, Y Pei, H Chen, T Tuschl, D Patel, A Potential Protein-RNA Recognition Event Along the RISC-Loading Pathway from the Structure of A. aeolicus Argonaute with Externally Bound siRNA, *Structure*, **14** (10), 1557-1565 (2006).
H Zhu, J Nandakumar, J Aniukwu, L Wang, M Glickman, C Lima, S Shuman, Atomic Structure and Nonhomologous End-Joining Function of the Polymerase Component of Bacterial DNA Ligase D, *Proc Natl Acad Sci USA*, **103** (6), 1711-1716 (2006).

Beamline X29B

H Wang, Y Liu, Q Huai, J Cai, R Zoraghi, S Francis, J Corbin, H Robinson, Z Xin, et al., Multiple Conformations of Phosphodiesterase-5: Implications for Enzyme Function and Drug Developement, *J. Biol. Chem.*, **281**, 21469 (2006).

NSLS STAFF

J Ablett, C Kao, R Reeder, Y Tang, A Lanzirotti, X27A - A New Hard X-ray Micro-Spectroscopy Facility at the National Synchrtron Light Source, *Nucl. Instrum. Meth. A*, **562**, 487-494 (2006).
D Anschel, B Foerster, T Yuasa, H Benveniste, Z Zhong, J Heinfeld, A Dilmanian, 9.4 T MRI Characterization of a Focal Lesion in the Rat Brain Induced by Interlaced Microbeam Radiation, *Epilepsia*, Vol 46, p. 280-281, sponsored by American Epilepsy Society and American Clinical Neurophysiology Society (2006).

D Arena, E Vescovo, C Kao, Y Guan, W Bailey, Weakly Coupled Motion of Individual Layers in Ferromagnetic Resonance, *Phys. Rev. B*, **74**, 064409 (2006).

I Baek, W Kim, E Vescovo, H Lee, Effect of Ni Concentration on Quantum-well States of the Alloy System Ag/Fe1-xNix: A Spin- and angle-Resolved Photoemission Study, *Phys. Rev. B*, **74**, 113302 (2006).

J Beaujour, J Lee, A Kent, K Krycka, C Kao, Magnetization Damping in Ultrathin Polycrystalline Co Films: Evidence for Nonlocal Effects, *Phys. Rev. B*, **74**, 214405 (2006).

J Bengtsson, A Control Theory Approach for Dynamic Aperture, *Proceedings of EPAC 2006, Edinburgh, Scotland*, p. 3478-3480, sponsored by EPAC (2006).

A Blednykh, Trapped Modes in Tapered Vacuum Chambers for a Mini-Gap Undulator Magnet, *Nucl. Instrum. Meth. A*, **565** (2), 380-393 (2006).

A Blednykh, S Krinsky, B Podobedov, J Wang, Transverse Impedance of Small-gap Undulators for NSLS-II, *EPAC2006*, p. 2970, sponsored by EPAC (2006) (2006).

J Brankov, M Wernick, Y Yang, J Li, C Muehleman, Z Zhong, M Anastasio, A Computed Tomography Implementation of Multiple-Image Radiography, *Med. Phys.*, **33** (2), 278 (2006).

L Brewer, M Othon, Y Gao, B Hazel, W Buttrill, Z Zhong, Comparison of Diffraction Methods for Measurement of Surface Damage in Superalloys, *J. Mater. Res.*, **21** (7), 1775-1781 (2006).

Y Cai, P Chow, O Restrepo, Y Takano, H Kito, H Ishii, C Chen, K Liang, C Chen, et al., Low-Energy Charge-Density Excitations in MgB2: Striking Interplay Between Single-Particle and Collective Behavior for Large Momenta, *Phys. Rev. Lett.*, **97**, 176402-4 (2006).

W Caliebe, I So, A Lenhard, D Siddons, Cam-driven Monochromator for QEXAFS, *20th International Conference on X-Ray and Inner-Shell Processes*, Vol 75, p. 1962-1965, sponsored by University of Melbourne (2006).

W Caliebe, I So, A Lenhard, D Siddons, Cam-Driven Monochromator for QEXAFS, *Radiat. Phys. Chem.*, **75** (11), 1962-1965 (2006).

B Chapman, A Checco, R Pindak, T Siegrist, C Kloc, Dislocations and Grain Boundaries in Semiconducting Rubrene Single-Crystals, *J. Cryst. Growth*, **290** (2), 479-484 (2006).

D Connor, D Sayers, D Sumner, Z Zhong, Diffraction Enhanced Imaging of Controlled Defects Within Bone, Including Bone-Metal Gaps, *Phys. Med. Biol.*, **51** (12), 3283-3300 (2006).

R Daimant, R Sharon, W Caliebe, C Kao, M Deutsch, Structure of the Co and FeK alpha(3,4) Satellite Spectra, *J. Phys. B: At., Mol. Opt. Phys.*, **39** (3), 651-667 (2006).

G Decker, M Borland, D Horan, A Lumpkin, N Sereno, B Yang, S Krinsky, Transient Bunch Compression using Pulsed Phase Modulation in High-Energy Electron Storage Rings, *Phys. Rev. ST AB*, **9**, 120702 (2006).

F Dilimanian, Z Zhong, T Bacarian, H Benveniste, P Romanelli, R Wang, J Welwart, T Yuasa, E Rosen, D Anschel, Interlaced X-ray Microplanar Beams: A Radiosurgery Approach with Clinical Potential, *Proc Natl Acad Sci USA*, **103** (25), 9709-9714 (2006).

E DiMasi, S Kwak, F Amos, M Olszta, D Lush, L Gower, Complementary Control by Additivies of the Kinetics of Amorphous CaCO3 Mineralization at an Organic Interface: In-Situ Synchrotron X-ray Observations, *Phys. Rev. Lett.*, **97**, 045503 (2006).

T Ellis, K Park, M Ulrich, S Hulbert, J Rowe, Interaction of Metallophthalocyanines (Mpc, M=Co, Ni) on Au(001): Ultraviolet Photoemission Spectroscopy and Low Energy Electron Diffraction Study, *J. Appl. Phys.*, **100**, 093515-10 (2006).

R Fiorito, A Shkvarunets, T Watanabe, V Yakimenko, D Snyder, Interference of Diffraction and Transition Radiation and Its Application as a Beam Divergence Diagnostic, *Phys. Rev. ST AB*, **9** (5), 052802 (2006).

Y Guan, W Bailey, C Kao, E Vescovo, D Arena, Comparison of Time-Resolved X-ray Magnetic Circular Dichroism Measurements in Reflectino and Transmission for Layer-Specific Precessional Dynamics Measurements, *J. Appl. Phys.*, **99**, 08J305 (2006).

K Gunter, M Aschner, L Miller, R Eliseev, J Salter, K Andersen, T Gunter, Determining the Oxidation States of Manganese in NT2 Cells and Cultured Astrocytes, *Neurobiol. Aging*, **27** (12), 1816-26 (2006).

D Hill, D Arena, R Bartynski, P Wu, G Saraf, Y Lu, I Wielunski, R Gateau, J Dvorak, et al., Room Temperature Ferromagnetism in MN Ion Implanted Epitaxial ZnO Films, *Phys. Status Solidi (a)*, **203** (15), 3836-3843 (2006).

J Hu, C Foerster, J Skaritka, D Waterman, Novel Chamber Design for An In-Vacuum Cryo-Cooled Mini-Gap Undulator, *4th International Workshop on Mechanical Engineering Design of Synchrotron Radiation Equipment & Instrumentation*, Vol 1, p. 8, sponsored by Japan Synchrotron Radiation Research Institute and MEDSI-06 (2006).

J Jakoncic, Y Jouanneau, C Meyer, V Stojanoff, The Catalytic Pocket of the Ring-hydroxylating Dioxygenase from Sphingomonas CHY-1, *Biochem. Biophys. Res. Commun.*, **352**, 861-866 (2006).

J Jakoncic, M Di Michiel, Z Zhong, V Honkimaki, Y Jouanneau, V Stojanoff, Anomalous Diffraction at Ultra-High Energy for Protein Crystallography, *J. Appl. Cryst.*, **39**, 831-841 (2006).

Y Jouanneau, C Meyer, J Jakoncic, V Stojanoff, J Gaillard, Characterization of a Naphthalene Dioxygenase Endowed with an Exceptionally Broad Substrate Specificity Toward Polycyclic Aromatic Hydrocarbons, *Biochemistry*, **45**, 12380-12391 (2006).

M Kelly, R Beavis, D Fourney, E Schultke, C Parham, B Juurlink, Z Zhong, L Chapman, Diffraction-enhanced Imaging of the Rat Spine, *Can. Assoc. Radiol. J.*, **57**, 204-210 (2006).

G Khelashvili, J Brankov, D Chapman, M Anastasio, Y Yang, Z Zhong, M Wernick, A Physical Model of Muliple-Image Radiography, *Phys. Med. Biol.*, **51** (2), 221-236 (2006).

C Kinane, A Suszka, C Marrows, B Hickey, D Arena, J Dvorak, T Charlton, S Langridge, Soft x-ray resonant magnetic scattering from an imprinted magnetic domain pattern , *Appl. Phys. Lett.*, **89**, 092507 (2006).

B Kirby, J Borchers, J Rhyne, K O'Donovan, S Velthuis, S Roy, C Sanchez-Hanke, T Wojtowicz, X Liu, et al., Magnetic and Chemical Nonuniformity in Ga1-xMnxAs Films as Probed by Polarized Neutron and X-ray Reflectometry, *Phys. Rev. B*, **74**, 245304 (2006).

D Koller, G Ediss, L Mihaly, G Carr, Infrared Measurements of Possible IR Filter Materials, *Int. J. Infrared Millimeter Waves*, **27** (6), 835-846 (2006).

S Kramer, S Krinsky, J Bengtsson, Comparison of Double Bend and Triple Bend Achromatic Lattice Structures for NSLS-II, *Proceedings of EPAC 2006, Edinburgh, Scotland*, p. 3484-3486, sponsored by EPAC (2006).

S Kramer, J Bengtsson, Optimizing the Dynamic Aperture for Triple Bend Achromatic Lattices, *Proceedings of EPAC 2006, Edinburgh, Scotland*, p. 3481-3483, sponsored by EPAC (2006).

A Kretlow, Q Wang, J Kneipp, P Lasch, M Beekes, L Miller, D Naumann, FTIR-Microspectroscopy of Prion-Infected Nervous Tissue, *Biochim Biophys Acta*, **1758**, 948-959 (2006).

S Krinsky, J Bengtsson, S Kramer, Consideration of a Double Bend Achromatic Lattice for NSLS-II, *Proceedings of EPAC 2006, Edinburgh, Scotland*, p. 3487-3489, sponsored by EPAC (2006).

S Krinsky, Y Li, Statistical Analysis of the Chaotic Optical Field from a Self-Amplified Spontaneous-Emission Free-Electron Laser, *Phys. Rev. E*, **73**, 066501 (2006).

H Lee, I Baek, E Vescovo, Spin Reorientation Transition in Fe-Rich Alloy Films on W(110): The Role of Magnetoelastic Anisotropy and Structural Transition, *Appl. Phys. Lett.*, **89**, 112516 (2006).

H Lee, I Baek, S Kim, E Vescovo, Electronic and Magnetic Properties in Fe-Based Fe1-xNix, Fe1-xCox, and Fe1-xVx Films on W(110), *Surf. Sci.*, **600**, 4137-4142 (2006).

Z Liu, S Wang, B McCoy, A Cady, R Pindak, W Caliebe, K Takekoshi, K Ema, H Nguyen, C Huang, Smectic-C* alpha-smectic-C* Phase Transition and Critical Point in Binary Mixtures, *Phys. Rev. E*, **74**, 030702(R) (2006).

H Liu, M Quijada, D Romero, D Tanner, A Zibold, G Carr, H Berger, L Forro, L Mihaly, et al., Drude Behavior in the Far-Infrared Conductivity of Cuprate Superconductors, *Ann. Phys.*, **15** (7), 606-618 (2006).

J Miklossy, A Kis, A Radenovic, L Miller, L Forro, R Martins, K Reiss, N Darbinian, P Darekar, et al., Beta-Amyloid Deposition and Alzheimer's Type Changes Induced by Borrelia Spirochetes, *Neurobiol. Aging*, **27**, 228-236 (2006).

L Miller, P Dumas, Chemical Imaging of Biological Tissue with Synchrotron Infrared Light, *Biochim Biophys Acta*, **1758** (7), 846-57 (2006).

L Miller, Q Wang, T Telivala, R Smith, A Lanzirotti, J Miklossy, Synchrotron-based Infrared and X-ray Imaging Shows Focalized Accumulation of Cu and Zn Co-localized With Beta-amyloid Deposits in Alzheimer's Disease, *J. Struct. Biol.*, **155** (1), 30-37 (2006).

H Mo, G Evmenenko, S Kewalramani, K Kim, S Ehrlich, P Dutta, Observation of Surface Layering in a Nonmetallic Liquid, *Phys. Rev. Lett.*, **96**, 096107 (2006).

C Muehleman, J Li, Z Zhong, J Brankov, M Wernick, Multiple-Image Radiography for Human Soft Tissue, *J. Anatomy*, **208**, 115-124 (2006).

C Muehleman, J Li, Z Zhong, Preliminayr Study on Diffraction Enhanced Radiographic Imaging for a Canine Model of Cartilage Damage, *Osteoarthr. Cartilage*, **14** (92), 882-888 (2006).

C Nelson, R Kolagani, M Overby, V Smolyaninova, R Kennedy, Charge Order in Photosensitive Bi0.4Ca0.6MnO3 Films, *J. Phys.: Condens. Matter*, **18**, 997-1004 (2006).

Z Niu, M Bruckman, V Kotakadi, J He, T Emrick, T Russell, L Yang , Q Wang, Study and Characterization of Tobacco Mosaic Virus Head-to-tail Assembly Assisted by Aniline Polymerization, *Chem. Commun.*, **2006** (28), 2019-3021 (2006).

A Ozcan, Y Wang, G Ozaydin, K Ludwig, A Bhattacharyya, T Moustakas, D Siddons, Real-time X-ray Studies of Gallium Adsorption and Desorption, *J. Appl. Phys.*, **100** (8), 084307 (2006).

S Pandey, A Kumar, S Khalid, A Pimpale, Electronic States of LaCoO3: Co K-edge and La L-edge X-ray Absorption Studies, *J. Phys.: Condens. Matter*, **18**, 7103-7113 (2006).

S Pandey, S Khalid, N Lalla, A Pimpale, Local Distortation in LaCoO3 and PrCO03: EXAFS, X-ray Diffraction and X-ray Absorption Near Edge structure Studies, *J. Phys.: Condens. Matter*, **18**, 10617 (2006).

S Pandey, R Bindu, A Kumar, S Khalid, A Pimpale, Doping and Bond Length Contributions to Mn K-edge Shift in La1-xSrxMnO3 (x = 0 - 0.7) and Their Correlation with Electrical Transport Properties, *International Workshop on the Physics of Mesoscopic and Disordered Materials-December 4-8, 2006*, p. 88, sponsored by Indian Institute of Technology (2006).

S Park, E DiMasi, Y Kim, W Han, P Woodward, T Vogt, The Preparation and Characterization of Photocatalytically Active TiO2 Thin Films and Nanoparticles using Successive-Ionic-Layer-Adsorption-and-Reaction, *Thin Solid Films*, **515** (4), 1250-1254 (2006).

P Pawelek, N Croteau, C Ng-Thow-Hing, C Khursigara, N Moiseeva, M Allaire, J Coulton, Structure of TonB in Complex with FhuA, E. Coli Outer Membrane Receptor, *Science*, **312**, 1399-1402 (2006).

A Phelippeau, S Pommier, T Tsakalakos, M Clavel, C Prioul, Cold Drawn Steel Wires—Processing, Residual Stresses and Ductility—Part I: Metallography and Finite Element Analyses, *Fatigue Fract. Eng. Mater. Struct.*, **29**, 201-208 (2006).

A Phelippeau, S Pommier, I Zakharchenko, R Levy-Tubiana, T Tsakalakos, M Clavel, M Croft, Z Zhong, C Prioul, Cold Drawn Steel Wires—Processing, Residual Stresses and Ductility Part II: Synchrotron and Neutron Diffraction, *Fatigue Fract. Eng. Mater. Struct.*, **29**, 255-265 (2006).

I Pinayev, T Shaftan, Synchrotron Radiation Monitor for NSLS Booster, *Beam Instrumentation Workshop 2006: Twelfth Beam Instrumentation Workshop*, Vol 868, p. 428-434, sponsored by AIP (2006).

I Pinayev, Lepton Beam Emittance Instrumentation, *Beam Instrumentation Workshop 2006: Twelfth Beam Instrumentation Workshop*, Vol 868, p. 112, sponsored by AIP (2006).

B Podobedov, S Krinsky, Transverse impedance of elliptical cross-section tapers, *EPAC2006*, p. 2973, sponsored by EPAC (2006).

B Podobedov, S Krinsky, Transverse Impedance of Axially Symmetric Tapered Structures, *Phys. Rev. ST AB*, **9** (5), 054401 (2006).

J Prada, R Haire, M Allaire, J Jakoncic, V Stojanoff, J Cannon, G Litman, D Ostrov, Ancient Evolutionary Origin of Diversified Variable Regions Demonstrated by Crystal Structures of an Immune-Type Receptor in Amphioxus, *Nat. Immunol.*, **7** (8), 875-882 (2006).

M Ruppel, D Burr, L Miller, Chemical Makeup of Microdamaged Bone Differs from Undamaged Bone, *Bone*, **39** (2), 318-324 (2006).

A Rusydi, P Abbamonte, H Eisaki, Y Fujimaki, G Blumberg, S Uchida, G Sawatzky, Quantum Melting of the Hole Crystal in the Spin Ladder of Sr14-xCaxCu24O41, *Phys. Rev. Lett.*, **97**, 016403 (2006).

C Ryan, D Siddons, G Moorhead, P Dunn, R Kirkham, A Dragone, G De geronimo, R Hough, B Etschmann, The Next Generation of Synchrotron Fluorescence Imaging for Geological Applications, *Geochim. Cosmochim. Acta*, **70** (18), A550 (2006).

M Sachan, N Walrath, S Majetich, K Krycka, C Kao, Interaction Effects Witin Langmuir Layers and Three-Dimensional Arrays of E-Co Nanoparticles, *J. Appl. Phys.*, **99**, 08C302 (2006).

G Sainz, J Jakoncic, L Sieker, V Stojanoff, N Sanishvilli, M Asso, P Bertrand, J Armengaud, Y Jouanneau, Structrue of a [2Fe-2S] Ferredoxin from Rhodobacter capsulatus likely Involved in Fe-S Cluster Biogenesis and Conformational Changes Observed upon Reduction, *J. Biol. Inorg. Chem.*, **11**, 235-246 (2006).

C Sanchez-Hanke, R Gonzalez-Arrabal, J Prieto, E Andrzejewska, N Gordillo, D Boerma, R Loloee, J Skuza, R Lukaszew, Observation of Nitrogen Polarization in Fe-N Using Soft X-ray Magnetic Circular Dichorism, *J. Appl. Phys.*, **99**, 08B709 (2006).

T Shaftan, J Bengtsson, S Kramer, Control of Dynamic Aperture with Insertion Devices, *Proceedings of EPAC 2006, Edinburgh, Scotland*, p. 3490-3492, sponsored by EPAC (2006).

W Shi, H Robinson, M Sullivan, D Abel, J Toomey, L Berman, D Lynch, G Rosenbaum, G Rakowsky, et al., Beamline X29: A Novel Undulator Source for X-ray Crystallography, *J. Synch. Rad.*, **13**, 365-372 (2006).

V Struzhkin, H Mao, J Lin, R Hemley, J Tse, Y Ma, M Hu, P Chow, C Kao, Valence Band X-Ray Emission Spectra of Compressed Germanium, *Phys. Rev. Lett.*, **96**, 137402 (2006).

K Subburaman, N Pernodet, S Kwak, E DiMasi, S Ge, V Zaitsev, X Ba, N Yang, M Rafailovich, Templated Biomineralization on Self-Assembled Protein Fibers, *Proc Natl Acad Sci USA*, **103** (40), 14672-14677 (2006).

T Tanabe, J Ablett, L Berman, D Harder, S Hulbert, M Lehecka, G Rakowsky, J Skaritka, A Deyhim, et al., X-25 Cryo-ready In-vacuum Undulator at The NSLS, *International Conference on Synchrotron Radiation Instrumentation*, Vol 879, p. 283-286, sponsored by PAL/JASRI (2006).

T Tsakalakos, M Croft, N Jisrawi, R Holtz, Z Zhong, Measurement of Residual Stress Distributions by Energy Dispersive X-ray Diffraction Synchrotron Radiation, *Int. J. Offshore Polar Eng.*, **16**, 358-366 (2006).

E Vescovo, Reply to “Comment on ‘Oxidation of the Fe(110) Surface: An Fe3O4(111)/Fe(110) Bilayer’”, *Phys. Rev. B*, **74**, 026406 (2006).

E Vescovo, Reply to “Comment on `Oxidation of the Fe(110) surface: An Fe3O4(111)/Fe(110) bilayer’ “, *Phys. Rev. B: Condens. Matter*, **74**, 26406 (2006).

E Vescovo, Spin-Resolved Photoemission Studies of Magnetic Films, *Modern Techniques for Characterizing Magnetic Materials* , p. 600, Kluwer Academic Pub, New York (2006).

F Wang, D Cheever, M Farkhondeh, W Franklin, E Ihloff, J van der Laan, B McAllister, R Milner, C Tschalaer, et al., Coherent THz Synchrotron Radiation from a Storage Ring with High-Frequency RF System, *Phys. Rev. Lett.*, **96**, 064801 (2006).

S Wang, Z Liu, B McCoy, R Pindak, W Caleibe, H Nguyen, C Huang, Optical and Resonant X-Ray Diffraction Studies Confirm a SmC*F12-SmC* Liquid Crystal Sequence Reversal, *Phys. Rev. Lett.*, **96**, 097801 (2006).

W Wang, D Pan, Y Song, W Liu, L Yang, H Huang, Method of X-ray anomalous diffraction for lipid structures, *Biophys. J.*, **91** (2), 736-743 (2006).

Y Wang, A Ozcan, G Ozaydin, K Ludwig, Jr., A Bhattacharyya, T Moustakas, H Zhou, R Headrick, P Siddons, Real-Time Synchrotron X-ray Studies of Low- and High-temperature Nitridation of c-plane Sapphire, *Phys. Rev. B*, **74**, 235304 (2006).

T Watanabe, D Liu, J Murphy, J Rose, T Shaftan, T Tsang, X Wang, L Yu, P Sprangle, Experimental Characterization of Seeded FEL Amplifier at the NSLS SDL, *The 27th International Conference on Free Electron Lasers*, Vol , p. 98, sponsored by APS, LBNL, LNL, LCLS, SLAC and UCLA (2006).

T Watanabe, D Liu, J Murphy, J Rose, T Shaftan, T Tanabe, T Tsang, X Wang, L Yu, et al., Design Study of a Compact Megawatt Class FEL Amplifier Based on the VISA Undulator, *The 27th International Conference on Free Electron Lasers*, Vol , p. 320, sponsored by APS, LBNL, LNL, LCLS, SLAC and UCLA (2006).

T Watanabe, D Liu, J Murphy, J Rose, T Shaftan, T Tsang, X Wang, L Yu, Y Shen, et al., An Experimental Test of Superradiance in a Single Pass Seeded FEL, *The 27th International Conference on Free Electron Lasers*, Vol , p. 526, sponsored by APS, LBNL, LNL, LCLS, SLAC and UCLA (2006).

M Wernick, Y Yang, I Mondal, D Chapman, M Hasnah, C Parham, E Pisano, Z Zhong, Computation of Mass Density Images from X-ray Refraction-Angle Images, *Phys. Med. Biol.*, **51**, 1769-1778 (2006).

P Wu, G Saraf, Y Lu, D Hill, R Gateau, L Wielunski, R Bartynski, D Arena, J Dvorak, et al., Ferromagnetism in Fe-Implanted a-plane ZnO Films, *Appl. Phys. Lett.*, **89**, 012508 (2006).

D Xiang, S Park, J Park, Y Parc, X Wang, Reduction of Thermal Emittance by using P-polarized Laser at Oblique Incidence, *Nucl. Instrum. Meth. A*, **562** (1), 48-52 (2006).

L Xie, J Jacobsen, B Busa, L Donahue, L Miller, C Rubin, S Judex, Low-Level Mechanical Vibrations can Reduce Bone Resorption and Enhance Bone Formation in the Growing Skeleton, *Bone*, **39** (5), 1059-1056 (2006).

G Xu, Z Zhong, Y Bing, Z Ye, G Shirane, Electric-Field-Induced Redistribution of Polar Nano-Regions in a Relaxor Ferroelectric, *Nat. Mater.*, **5**, 134-140 (2006).

S Yoon, Y Chen, A Yang, T Goodrich, X Zuo, D Arena, K Ziemer, C Vittoria, V Harris, Oxygen-defect-induced Magnetism to 880 K in Semiconducting Anatase TiO2-delta Films, *J. Phys.: Condens. Matter*, **18** (27), L355-L361 (2006).

F Zhang, C Chen, J Raitano, J Hanson, W Caliebe, S Khalid, S Chan, Phase Stability in Ceria-Zirconia Binary Oxide Nanoparticles: The Effect of the Ce3+ Concentration and the Redox Environment, *J. Appl. Phys.*, **99**, 084313 (2006).